Fall 2016

Testing and Analysis of an Exergetically Efficient 4 K to 2 K Helium Heat Exchanger

Peter N. Knudsen
Old Dominion University, knudsen@frib.msu.edu

TESTING AND ANALYSIS OF AN EXERGETICALLY EFFICIENT 4 K TO 2 K HELIUM HEAT EXCHANGER

by

Peter N. Knudsen
B.S. December 1990, Colorado State University
M.S. May 2008, Old Dominion University

A Dissertation Submitted to the Faculty of
Old Dominion University in Partial Fulfillment of the
Requirements for the Degree of

DOCTOR OF PHILOSOPHY

MECHANICAL ENGINEERING

OLD DOMINION UNIVERSITY
December 2016

Approved by:

Ayodeji Demuren (Director)

Arthur Taylor (Member)

Venkatarao Ganni (Member)

ABSTRACT

TESTING AND ANALYSIS OF AN EXERGETICALLY EFFICIENT 4 K TO 2 K HELIUM HEAT EXCHANGER

Peter N. Knudsen
Old Dominion University, 2016
Director: Ayodeji Demuren

Modern experimental nuclear physics programs that utilize advanced superconducting devices require refrigeration below the lambda temperature of helium (2.1768 K) and involve sub-atmospheric helium at some point in the process. They typically operate between 1.8 and 2.1 K (16 to 40 mbar) and can require refrigeration ranging from tens to thousands of watts. These processes are very energy intensive, requiring roughly 850 W/W even for large and well-designed refrigerators, though they can easily require much more. Adiabatic expansion of sub-cooled liquid helium to these sub-atmospheric pressures will result in a two-phase mixture with a large liquid to vapor density ratio. Since there are no practical expanders to handle this condition, a counter flow heat exchanger is used to cool the super-critical helium supply using the returning sub-atmospheric helium. Typically, the super-critical helium exiting this 4.5 K to 2-K counter flow heat exchanger is throttled across an expansion valve to a sub-atmospheric pressure. This is a substantial irreversibility, typically 13 percent of the enthalpy difference between the load supply and return. A significant process improvement is theoretically obtainable by handling the exergy loss across the expansion valve supplying the flow to the load in a simple but different manner. The exergy loss can be minimized by allowing the supply flow pressure to decrease to a sub-atmospheric pressure concurrent with heat exchange with the sub-atmospheric flow from the load. This dissertation work encompasses testing of a practical implementation using a Collin's type heat exchanger to investigate the overall performance, as

well as, the optimum selections of independent process parameters and how this affects the heat exchanger size distribution. The thermodynamics of heat exchange with a significant pressure drop for a non-ideal fluid are investigated, in regards to an equivalent expansion efficiency pseudo-property, a practical process expansion efficiency equivalence and an overall 2-K system performance improvement expectation. Theoretically predicted optimum independent process parameters are compared to those measured.

Grace – *proper noun*

Being found by unmerited favor

…given without cause or predisposition of deserving it,

past, present or future

…without expectation of return from the receiver

or, of the receiver to pay it forward

As it is found in,

The Gospel According to St. John, Chapter 1, verses 14, 16 and 17

ACKNOWLEDGEMENTS

"And He is before all things, and in Him all things hold together." (excerpt from, *The Epistle of Paul the Apostle to the Colossians, Chapter 1, verse 17*). It is my acknowledgement, first and foremost, that it is the God "…who did not spare his own Son *(Jesus)* but gave him up for us all…" (excerpt from, *The Epistle of Paul the Apostle to the Romans, Chapter 8, verse 32*, parenthesis added) who has indeed held me and my family together through this work, in every manner possible that there is to be held together. Lest, that be interpreted as an upwardly inclined journey with a few setbacks to make it more interesting, it is more like the climax in Twister (1996, Helen Hunt, Bill Paxton). Because the work is coincident with life, as many who have traveled this way can attest, there is much more than the intellectual obstacles encountered. It is impossible to describe to someone who has never come to the end of one's self what it is to be rescued by Another, when every means by which they can do so has failed. And that this rescue was by Grace.

I would like to thank Dr. Venkatarao Ganni for his tenacious and unwavering confidence, support, guidance, and for his insight; which is truly a gift. His family has been involved with farming. And although I am not, there are two attributes that are most pertinent here of one who is; careful, intentional and persistent patience, and faith to plant something so small and insignificant. This dissertation would not have been possible without him being who he is. I am also grateful to my advisor Dr. Demuren for his patience and guidance in this work, and to Dr. Taylor for serving on my committee.

This work would have also not been possible without the investment made by Dr. Fabio Casagrade at MSU-FRIB and the help of my colleagues at Jefferson Lab and MSU-FRIB; Robert

Norton, Sasa Radovic, Buddy Carlton, Roland Evans, Mike Beizer, John Barber, Mat Wright, Nate Laverdure, Corey Butler, Paul Stewart, Scott Thompson, Isaac Snowberg, Jay Noble, Willy Berkley, Dan Oprisko and his crew, Kelly Dixon, Jonathan Creel, Dr. Dave Meekins, Shelly Jones and Mark Shuptar. To them, I am indebted.

My family has labored with me, although not the specific tasks required for this work, but nonetheless. They have sacrificed and endured with me through this long journey. Perhaps, some might say this is expected. But, it would be remiss to not acknowledge the love and support of my wife Bonni, and my children, Brad and Elizabeth.

NOMENCLATURE

Symbols

A_c	Cross-sectional area, in^2
C_V	Valve flow coefficient, $gpm/psi^{1/2}$
C_p	Specific heat at constant pressure, J/g-K
h	Specific enthalpy, J/g
I	Irreversibility, W
i	Current, A or mA
L	Length, in
$\dot{m}$	Mass flow rate, g/s
NTU	Heat exchanger number of transfer units, non-dimensional
P	Power, W
p	Pressure, Pa, atm, or bar
q	Heat transfer, W or mW
R	Specific gas constant, J/g-K; or, resistance (electrical), Ω
s	Specific entropy, J/g-K
T	Temperature, K
T_0	Reference temperature (e.g., 300 K), K
(UA)	Heat exchanger net thermal rating, W/K
V	Voltage, V or mV
v	Specific volume, ℓ/g or cm^3/g
x	Quality (of vapor), non-dimensional

β	Volume expansivity, K^{-1}
ΔX	Change (difference) in variable 'X', units same as 'X'
δx	Accuracy of variable 'x', same units as variable 'x'
δ_x	Accuracy of variable 'x' relative to the current value, non-dimensional
ε	Heat exchanger effectiveness, non-dimensional; or, specific physical exergy, J/g
ε_x	Accuracy of variable 'x', based upon current value, non-dimensional
K	Thermal conductivity integral (with respect to the temperature), W/in
λ	Latent heat, J/g; or, axial conduction parameter, non-dimensional
η	Efficiency (various definitions), non-dimensional
ρ	Resistivity, μΩ·in

Abbreviations

ASTM	American Society for Testing and Materials
AWG	American Wire Gauge
CBX	Cold Box
CEBAF	Continuous Electron Beam Accelerating Facility (also, JLab)
CP	Critical Point
CTF	Cryogenic Test Facility (at Jefferson Lab)
DAM	Double Aluminized Mylar (PET)
EDM	Extensible Display Manager (an interactive graphical user interface builder and execution engine for EPICS)
ETP	Electrolytic Tough-Pitch (copper)
FRIB	Facility for Rare Isotope Beams (at MSU)

HX	Heat Exchanger
IPS	Inch Pipe Size (also, NPS)
JLab	Jefferson Lab
JT	Joule-Thompson (throttling) valve
MSU	Michigan State University
NIST	National Institute of Standards and Technology
OD	Outside Diameter
OHFC	Oxygen Free High Conductivity (copper)
PET	Polyethylene Terephthalate
PFA	Perfluoroalkoxy Alkane
PID	Proportional, Integral and Differential
PLC	Programmable Logic Controller
RHP	Reversible Heat Pump
RRR	Residual Resistance Ratio
RTD	Resistance Temperature Diode
SNS	Spallation Neutron Source (at Oak Ridge National Lab)
SRF	Super-conducting Radio Frequency
TCL	Transposed Critical Line
TL	Temperature Level

Subscripts

CE	Cold-end (of heat exchanger)
(h)	High pressure, supercritical, supply stream

htr	Heater
k	Index or heat in-leak
(l)	Low and/or sub-atmospheric stream
L	Load (refrigeration); same as the "*R*" subscript
R	Refrigeration load
TL	Transfer-line (distribution)
WE	Warm-end (of heat exchanger)

TABLE OF CONTENTS

LIST OF TABLES

LIST OF FIGURES

1. INTRODUCTION AND BACKGROUND

Cryogenic refrigeration generally refers to systems that provide cooling at a temperature less than -150 °C, which usually involves working fluids that have a normal boiling point that are less than the same temperature. Although the process cycles used in cryogenics depart significantly from a vapor compression cycle common to building and home refrigeration systems, undergraduate thermodynamics adequately provides the foundation to examine cryogenic process cycles. However, from a thermodynamic point of view, the crucial feature that may not be fully appreciated is the energy intensiveness of these processes. This is even more imperative for 4.5 K helium cryogenic systems, since the minimum input power required for every watt of cooling is inversely proportional to the absolute temperature. So, by the time we get to sub-atmospheric helium systems, which provide refrigeration below 4.5 K, a throughout appreciation of this feature becomes essential. To roughly quantify these qualitative statements, a normal home refrigeration system requires around 0.25 W (of input power) for every 1 W of cooling provided; this what is defined as the (real) inverse coefficient of performance (which will be discussed more thoroughly later). Large (load capacity) cryogenic helium systems tend to be more efficient than smaller ones (Green 2008), and a large 4.5 K helium refrigerator could be designed to around 250 W/W. A large 2-K (say, 31 mbar at the load) helium refrigerator will require over three times the input power for the same cooling, or around 850 W/W, though it is not uncommon to find 1000 W/W (for large systems) (Knudsen and Ganni 2015).

But why and for what are such low temperatures needed, and why helium? Regarding the former question, helium refrigerators that operate at 4.5 K or below are essential to particle

accelerators that use super-conducting technology (Lebrun and Tavian 2015, Ganni and Fesmire 2012, Wagner 2002). Practical superconductors for magnets in particle accelerators typically use Nb-Ti, which has a transition temperature of around 9.6 K, or Nb_3Sn, which has a transition temperature of 18.1 K. These transition, or 'critical', temperatures are at zero magnetic field and zero current density. These three variables form a three-dimensional surface with the current density decreasing with both increasing temperature and increasing magnetic field, such that for given current density, the critical magnetic field decreases with increasing temperature; as an example refer to (Bottura 1999). For superconducting cavities, the BCS losses (i.e., the conductor surface losses due to Cooper pair inertia) increase exponentially with temperature (Lebrun and Tavian, Cooling with superfluid helium 2015). The later question is answered by a cursory examination of various fluids, in that helium is the only fluid that will not freeze[1] at the temperatures required to operate these superconductors. Figure 1.1 shows the phase diagram for helium-4. Helium-4, with the "4" denoting the atomic number (i.e., the number of neutrons), is the second most abundant element in the observable universe, although it is somewhat rare here on Earth and at present a nonrenewable resource. However, it is many orders of magnitude more abundant than Helium-3, which is the only other stable isotope. The lambda temperature (2.172 K at 50 mbar) is the demarcation between 'normal' helium (sometimes called helium-I) and 'superfluid' helium (sometimes called helium-II). It is actually a second order (liquid) phase transition, in which the helium-II exhibits varying degrees of superfluidity (i.e., part of it behaving as a quantum fluid). This property is desirable at the load (i.e., magnet and/or cavity), but not within the helium refrigerator.

[1] Actually helium has a solid phase at very high pressures; i.e., around 25 bar below 1.5 K

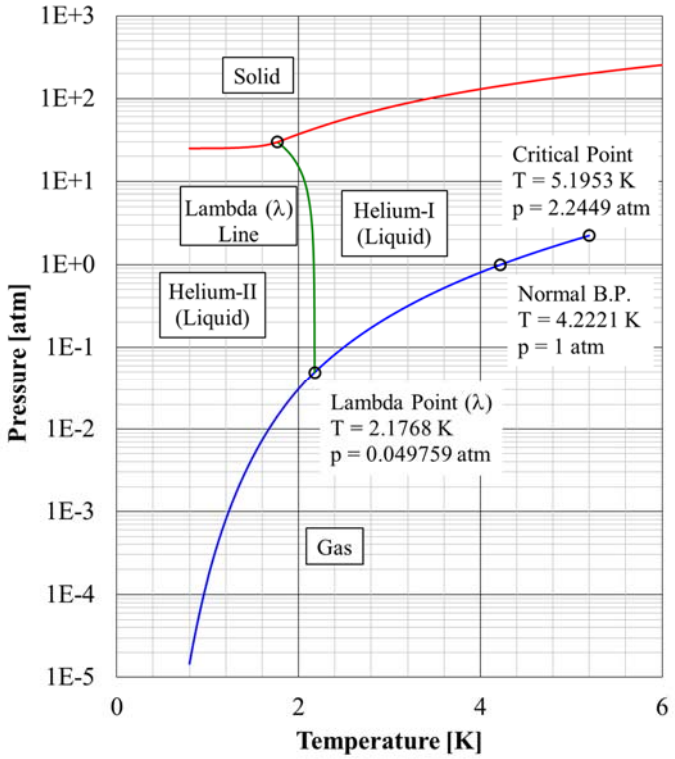

Figure 1.1. Helium-4 phase diagram

The demarcation of what is termed a 4.5 K helium refrigeration process intends to separate between a process that does not require the working fluid (i.e., helium) to be sub-atmospheric at some point in the process path and one that does. The boiling point for liquid helium at atmospheric pressure is 4.222 K. However, due to a finite pressure drop, the refrigeration load is adsorbed isothermally by the two-phase helium at a pressure higher than an atmosphere; normally about 1.25 bar, which corresponds to a saturation temperature of 4.453 K, or roughly 4.5 K.

It is common practice to refer to a process the *produces liquid helium* (at a saturation pressure slightly above one atmosphere) as a (4.5 K) 'helium refrigerator'. When it is returned

as a saturated vapor (or close to it), it is (an isothermal) refrigeration load[2]. When it is returned at higher temperature, it is a liquefaction load between that temperature and 4.5 K. Sometimes papers can refer to this as a non-isothermal refrigeration load, but a liquefaction load is more descriptive. A process whose only load is one that returns the helium (or requires make-up helium) at near ambient temperature is termed a liquefier. As an example, plants operated by industrial gas suppliers usually function as liquefiers since the goal is to accumulate liquid product for sale[3]. Typically for super-conducting particle accelerators, the helium refrigerator(s) being used has several different kinds of simultaneous loads; both isothermal refrigeration and liquefaction loads, as well as higher temperature non-isothermal refrigeration loads. For additional background information, the reader is referred to Appendix A.

1.1 Theory and Motivation – Exergy Preservation Below 4.5-K

Energy can neither be created nor destroyed. It is conserved. This is the axiom of the first law of thermodynamics. However, energy has differing degrees quality, or conversely, disorder. That is, some forms of energy are more readily convertible so as to extract work, even if the process, equipment and/or technology does not presently exist. This quality of energy has also been described as availability (Van Wylen and Sonntag 1985). For example, consider an isothermal compression process of a real fluid that can be adequately approximated as an ideal gas for the mechanical equation of state and a constant specific heat for the thermal equation of

[2] 4.5 K helium refrigerators often provide refrigeration to a load well above 4.5 K. These are termed (radiation) 'shield' loads and are typically used to reduce heat in-leak from ambient temperature to the 4.5 K (or lower) by reducing the temperature potential to the 4.5 K (or lower). These loads are often termed 'non-isothermal refrigeration' loads.

[3] This is true even if the liquid is warmed to ambient temperature, compressed and delivered as a high pressure gas, since it is more economical to store the helium as a liquid until needed (as a gas) and the liquefaction process serves as a highly effective purification process.

state (Callen 1985, 66, 289). This process increases the availability of the fluid by an amount equal to, $(\Delta h - T_0 \cdot \Delta s) = T_0 \cdot R \cdot \ln(p_f/p_i)$, where, Δh [J/g] is the change in enthalpy (= 0), T_0 [K] is the ambient temperature (or ambient wet bulb temperature), Δs [J/g-K] is the change in entropy, R [J/g-K] is the specific gas constant, p_f [Pa] the final (discharge) pressure, and p_i [Pa] the initial (suction) pressure. That is, it has been transformed from being less ordered to more ordered, more available for work to be extracted from it. The compressor system for cryogenic refrigerators is what provides the availability to the cold box; which then lowers the temperature of the working fluid, and then delivers cooling to the (cryogenic) load. Isothermal compression is the ideal compression process for large refrigeration systems using a process of (approximately) isobaric cooling and adiabatic expansion and/or isenthalpic throttling.

A highly useful quantity to describe the availability of a fluid for a flowing process (steady or unsteady) is physical exergy; $\varepsilon = h - T_0 \cdot s$ (Kotas 1985). Exergy is universal standard of quality for energy (Kotas 1985). What makes physical exergy so useful is that when applied to a real process, it is equal to the amount of lost work incurred, so that every watt of input power can be accounted, whether it is used usefully or not. It is equal to the theoretical minimum input power required for a process, or conversely, the maximum power that can be obtained from a process. This is indicative in its units being the same as energy (or power). The irreversibility is the product of the entropy production and the ambient temperature. And the entropy production is the net transport of entropy associated with the flow of matter across the control boundary, the rate of change of entropy within the control boundary, and the entropy associated with the reversible transfer of heat (Kotas 1985, 263-266). For steady flow without the presence of reversible heat transfer, the entropy production is just the net increase in the entropy associated with the flow of matter across the control boundary. For example, consider

an adiabatic expansion process that has an isentropic efficiency less than unity. The irreversibility, or lost work, due to the non-isentropic process is equal to the rectangular area in temperature-entropy (*T*-*s*) coordinates with a height equal to the ambient temperature, and a width equal to the increase in entropy. In the case of an equal stream mass flow counter-flow heat exchanger with negligible stream pressure drop and no heat in-leak, the irreversibility due to a finite stream temperature difference is the rectangular area in the *T*-*s* coordinates with height equal to the ambient temperature and width equal to the entropy difference at the cold-end minus the warm-end. If the fluid can be approximated as an ideal gas with a constant specific heat, introducing a transformed variable, $\tau = T_0 \cdot \ln(T)$, the exergy loss is simply, $I = \dot{m} \cdot C_p \cdot \left(\Delta\tau_{hl,WE} - \Delta\tau_{hl,CE}\right)$; where $\Delta\tau_{hl} = \tau_h - \tau_l$ and 'WE' is the warm-end, likewise for 'CE'. Which is an interesting equation, since the warm end minus the cold-end enthalpy flux is, $\dot{m} \cdot C_p \cdot \left(\Delta T_{hl,WE} - \Delta T_{hl,CE}\right) = 0$; where $\Delta T_{hl} = T_h - T_l$. Again, as another example, the exergy loss due to heat in-leak is proportional to the inverse Carnot coefficient of performance, $(T_0/T - 1)$. Which, of course is also equal to the minimum specific power (i.e., input power per 1 W of cooling) required for a reversible heat pump operating between T_0 and T.

Since cryogenic process are substantially below ambient temperature, the effect of a given irreversibility comprises a larger fraction of the overall process availability than for the same irreversibility occurring in a process near or above ambient temperature. Therefore, as the temperature of the (cryogenic) load decreases, it becomes increasing important to preserve the exergy for useful work, that is, to minimize the lost work in the cold box and distribution system to preserve it for the intended cryogenic load cooling.

This becomes even more important for helium refrigerators supporting a sub-atmospheric load, since below 4.5 K there is no work extracted from the supply to the (sub-atmospheric) load. However, for larger plants (Knudsen and Ganni 2012) the returning sub-atmospheric steam is used to cool the supply stream; or 'recover its refrigeration'. The reader is referred to Appendix A for more details and some historical excepts. It is worthwhile to examine several configurations of this 4.5 K to 2 K refrigeration recovery to gain an appreciation of its importance. The designers of the early 2-K helium refrigerators (Baldus and Sellmaier 1967, Collins and Streeter 1967, Daus and Ewald 1975, Sellmaier, Glatthaar and Klien 1970) (refer to Appendix A) recognized that for the high pressure supply (which was 12 to 30 bar), it was critical to successively lower this pressure with heat exchange (lowering the temperature of the supply stream) from the returning sub-atmospheric stream to achieve the desired cooling capacity. For modern large helium refrigerators which use an expansion stage in the range of 8 to 5 K, the supply pressure is typically lowered to just above the critical pressure to ensure flow stability (Knudsen, Ganni and Than 2012). For such systems, there are four basic arrangements to examine (Knudsen and Ganni 2015). Figure 1.2 shows arrangements 1 to 3 and Figure 1.3 shows two variations of arrangement 4. Table 1.1 shows a comparison for each of these arrangements for the same mass flow rate, supply pressure, supply temperature, load pressure, cold-end stream temperature difference and heat in-leaks. These are not absolute or limiting values necessarily, but are chosen to be representative and consistent for comparison. Arrangement 1 depicts the case with no refrigeration recovery, providing a load enthalpy flux of 12.7 J/g. Compared to the maximum possible enthalpy flux, which is the latent heat of 23.4 J/g (at 0.031 bar), this is 54% of the maximum possible.

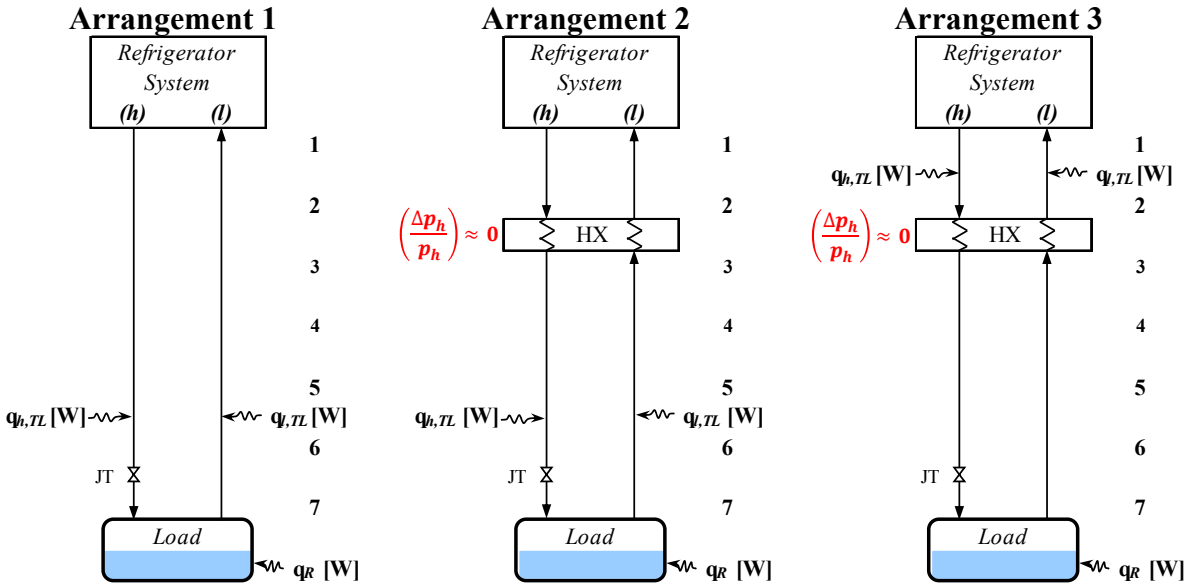

Figure 1.2. 4.5 to 2 K cold end arrangements 1 to 3

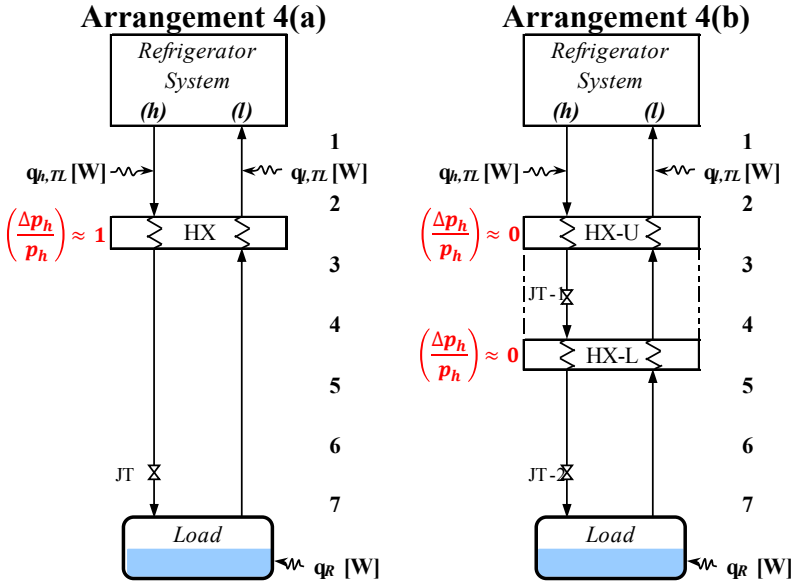

Figure 1.3. 4.5 to 2 K cold end arrangements 4(a) and 4(b)

Table 1.1. Process parameters and results for arrangements 1 to 4

Symbol	Description	Units	1	2	3(i)	3(ii)	4(a)	4(b)
$\dot{m}$	Mass flow rate (§)	[g/s]	5	5	5	5	5	5
$p_{h,1}$	Supply pressure from refrigerator	[bar]	3.0	3.0	3.0	1.4	3.0	3.0
$T_{h,1}$	Supply temperature from refrigerator	[K]	4.5	4.5	4.5	4.5	4.5	4.5
$p_{h,4}$	Intermediate *(h)* stream pressure	[bar]	3.0	3.0	3.0	1.4	0.20	0.20
$T_{l,1}$	Return temperature to refrigerator	[K]	2.3	3.4	3.7	3.9	4.0	4.0
$p_{l,7}$	Load return pressure	[bar]	0.031	0.031	0.031	0.031	0.031	0.031
$T_{l,7}$	Load return temperature (‡)	[K]	2.0	2.0	2.0	2.0	2.0	2.0
$\Delta T_{hl,5}$	Stream temperature diff. on HX cold end	[K]	N/A	0.20	0.20	0.20	0.20	0.20
$\Delta h_{lh,7}$	Load enthalpy flux	[J/g]	12.7	18.7	20.0	21.1	21.9	21.9
$q_{h,TL}$	*(h)* stream transfer line heat in-leak	[W]	2.5	2.5	2.5	2.5	2.5	2.5
$q_{l,TL}$	*(l)* stream transfer line heat in-leak	[W]	10	10	10	10	10	10
q_R	Load	[W]	63.7	93.6	100	105	109	109
NTU	HX no. transfer units	[-]	N/A	3.3	3.6	3.8	4.1	5.1

Notes: (‡) Load temperature is saturation temperature at load pressure
(§) *(h)* stream mass flow is equal to *(l)* stream mass flow

Arrangement 2 is how CEBAF was designed (Chronis, et al. 1996), before recognizing the importance of the temperature level that the distribution heat in-leak is adsorbed, and provides a load enthalpy flux of 18.7 J/g (which is 80% of the maximum possible). Arrangement 3 can have two variations; one for large systems like SNS that have a super-critical supply pressure (~3 bar to the load; i.e., cryo-modules) and one for smaller systems that supply sub-cooled liquid to the intended load (say, ~1.4 bar to the load). The super-critical load supply provides a load enthalpy flux of 20.0 J/g (which is 85% of the maximum possible). However, the saturated liquid load supply provides a load enthalpy flux of 21.1 J/g (90% of the maximum possible). Arrangement 4(a) involves lowering the supply stream pressure and exchanging heat with the returning sub-atmospheric stream and provides a load enthalpy flux of 21.9 J/g (94% of the maximum possible). There are a number of variations on this, encompassing varying degrees of practicality. As can be seen in Table 1.1, arrangement 1 supports the smallest load because none of the enthalpy of the returning sub-atmospheric stream is used to cool the supply stream; i.e.,

there is no counter-flow heat exchange. Arrangement 2 is better, but the 4.5 K to 2 K heat exchanger is not located properly with respect to the heat in-leak. This should be apparent from the second law, since the heat in-leak is being adsorbed at a lower temperature than if the heat exchanger were located close to the load. Arrangement 3 addresses the fundamental thermodynamic issue not handled properly in arrangement 2. Arrangement 4(a) incorporates an idea not exploited in the other arrangements, which is, significantly reducing the supply stream pressure while being cooled by the returning sub-atmospheric stream. The difference between arrangement 4(a) and 4(b) is that in the former case, the supply stream pressure drop is occurring concurrently with heat exchange; while in the latter case, it occurs in a step-wise manner. That is, between two heat exchanger sections using an intermediate throttling (or JT) valve. Both arrangement 4(a) and 4(b) support the same load (i.e., have the same load enthalpy flux), but arrangement 4(b) requires a longer heat exchanger (i.e., higher *NTU*'s).

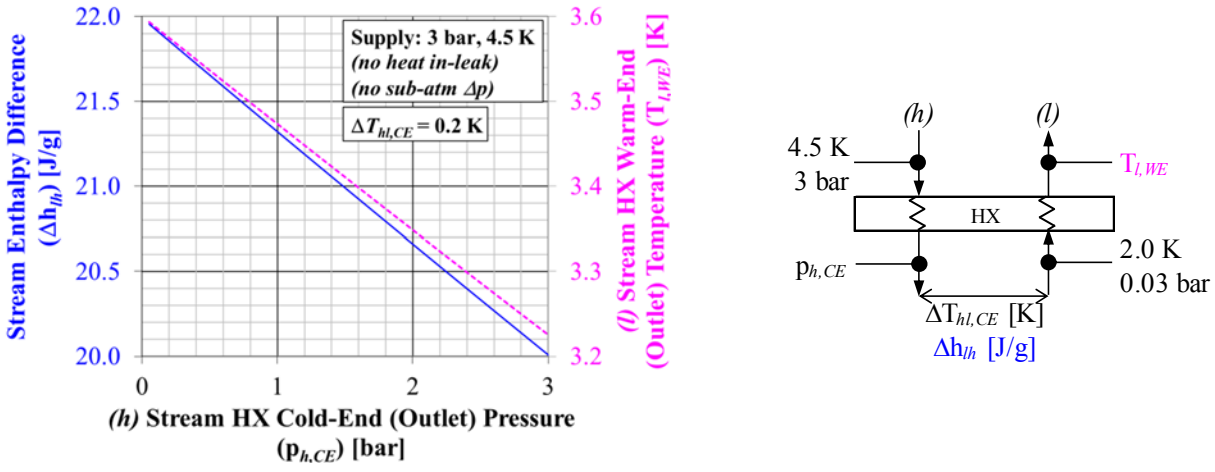

Figure 1.4. Effect of the load supply stream pressure drop through the 4.5 to 2 K heat exchanger

The purpose for presenting arrangement 4(b) is that, although it requires more heat exchanger surface area than arrangement 4(a) for the same load and the same supply and return process conditions, it is more practical. The geometry required to result in a large supply stream pressure drop (say, 2.8 bar) would be prohibitive during temperature transients. This includes cool-down (say, from 300 K), warm-up and operational variances. And, it would assume that the pressure drop could be accurately designed for the specified load and that the actual process conditions and the actual load are precisely known. So, this would impose the requirement that the construction of the heat exchanger *(h)* stream pressure drop be adjustable. But this would seem to be more amendable to arrangement 4(b). This arrangement (4(b)) is comprised of an 'upper' and 'lower' heat exchanger (HX-U and HX-L, respectively), and an additional valve (JT-1) in between these heat exchangers. The pressure downstream of the additional valve (JT-1) is the "intermediate pressure". Note that 'upper' and 'lower' are descriptive of the temperature 'level' and that these may be separate units or a single unit with an intermediate tap (for JT-1).

It should be noted that although this comparison was done for equal mass flows, it could have been done for equal loads. That is, rather than the objective of a load reduction for the same mass flow, the objective of a mass flow reduction for the same load could have also been examined. However, the load enthalpy flux does not change between these two objectives. Figure 1.4 explores the results of arrangement 4(a) bit further, showing the (sub-atmospheric) return stream to supply stream enthalpy difference vs. the supply stream cold end outlet pressure, assuming a 3 bar 4.5 K condition at the warm end and a cold end stream temperature difference of 0.2 K. It should be recalled that for equal mass flow on the supply and return streams (and no heat in-leak), the stream enthalpy difference will be the same at the warm-end and the cold-end of the heat exchanger. One might wonder about two seemingly arbitrary parameters; the cold-

end stream temperature difference of 0.2 K and the supply stream intermediate pressure at the heat exchanger cold-end of 0.2 bar. As previously mentioned, helium undergoes a second order phase transition below what is known as the lambda temperature; which is about 2.173 K. This second liquid phase, also called superfluid helium, exhibits properties of a quantum fluid (Van Sciver 2012). The particular property pertinent for a heat exchanger is the fluid's unusually high thermal conductivity. Superfluid helium can have an effective thermal conductivity one to three orders of magnitude greater than commercially pure copper (RRR = 100); although its thermal conductivity depends on the heat flux. So, if the supply temperature drops to the lambda temperature, then it will no longer cool and from that point to the outlet the heat exchanger surface area is not useful for heat transfer. Regarding the other seemingly arbitrary parameter, although the saturation pressure at 2.2 K is 52.1 mbar, and in theory the pressure could be reduced further from 0.2 bar, the heat exchanger length would be completely impractical.

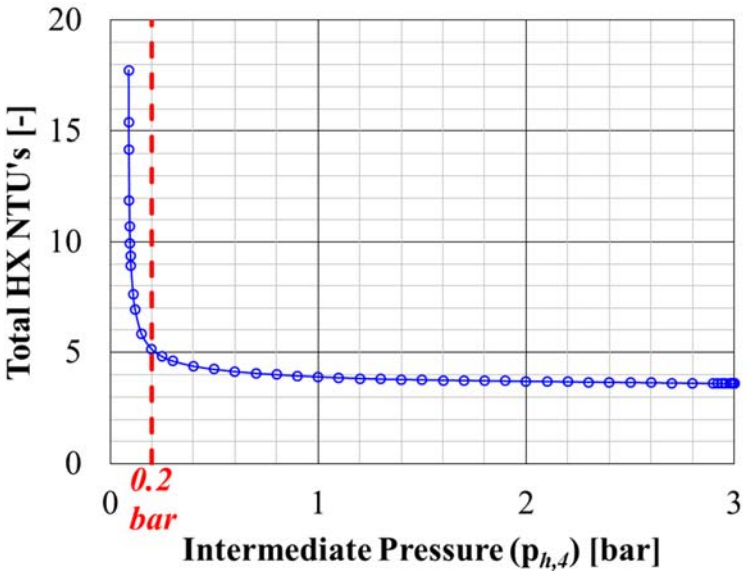

Figure 1.5. Total (lower and upper) heat exchanger *NTU*'s vs. *(h)* stream outlet pressure

The selection of 0.2 bar corresponds to approximately 5.2 *NTU*'s, which is still reasonable. This can be seen clearly in Figure 1.5 (which is applicable for arrangement 4(b)). Figure 1.6 shows the fraction of the total *NTU*'s and duty carried by the upper heat exchanger for arrangement 4(b). Both Figure 1.5 and 1.6 are solutions based upon the given process conditions and a minimization of total heat exchanger *NTU*'s.

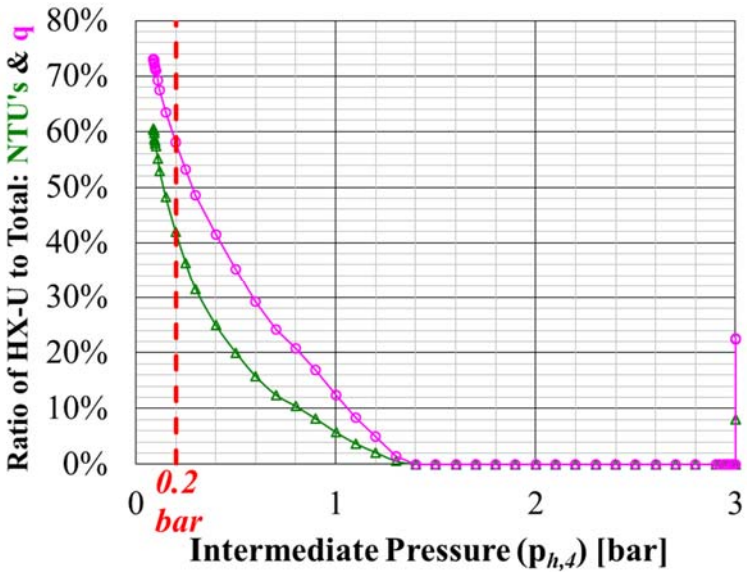

Figure 1.6. Ratio of upper heat exchanger *NTU*'s to total *NTU*'s and duty to total duty vs. *(h)* stream outlet pressure

A useful diagram to show the heat transfer with pressure drop process is the pressure – enthalpy diagram. This diagram is typically used in commercial refrigeration but not for 4.5 K (or 2 K) helium refrigeration. The later encompasses large changes in temperature and several adiabatic expansion stages, so the temperature – entropy (*T-s*) diagram is more appropriate. However, the processes in Figures 1.2 and 1.3 do not encompass a large temperature range.

And, the heat exchange between 4.5 K and 2 K, as previously mentioned, has not incorporated the use of adiabatic expansion and is focused on the two-phase and liquid/vapor dome region. Figure 1.7 shows the pressure – enthalpy diagram for arrangement 4(a) and 4(b); the former labeled as "Δp Across HX" and the latter as "Δp Across JT". Points "A" to "B" represent the warm-end and cold-end, respectively, for the *(h)* stream in arrangement 3(i) (see Table 1.1). Points "A" to "C" represent the warm-end and cold-end, respectively, of the heat exchanger for the *(h)* stream in arrangement 4(a) and 4(b).

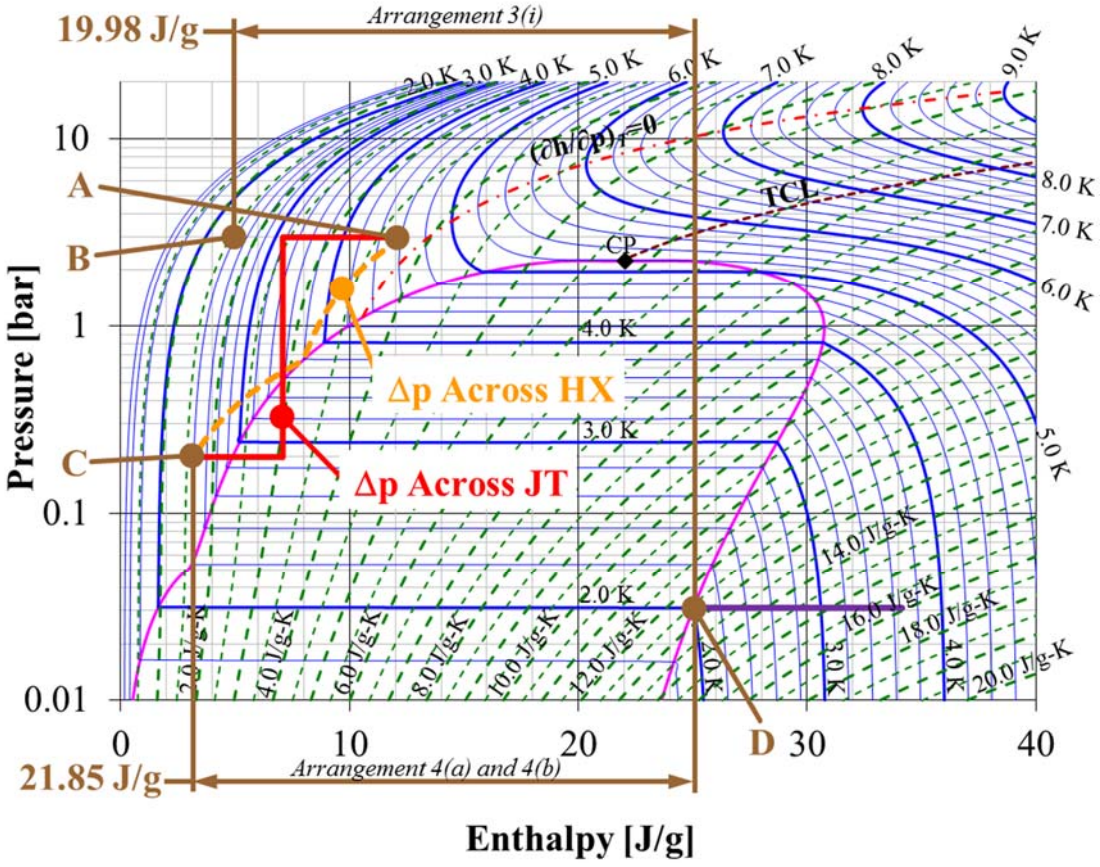

Figure 1.7. Helium pressure-enthalpy diagram for arrangements 4(a) and 4(b) [4]

[4] The process points are as follows: "A" = 3 bar, 4.5 K; "B" = 3 bar, 2.2 K; "C" = 0.2 bar, 2.2 K; "D" = 0.031 bar, 2.0 K

1.2 Scope and Goals of the Dissertation

1. Investigate the viability of using a counter-flow heat exchanger to minimize exergy losses between the supply from a 4.5-K helium refrigerator and the return from a nominal 2-K sub-atmospheric heat load by incorporating a large pressure drop across the supply stream. This is to encompass examining the:
   a. Configuration selection
   b. Heat exchanger type selection
   c. Performance of a Collins-type heat exchanger under such conditions
   d. Optimum intermediate pressure; theory vs. measured
   e. Cold-end supply to return stream temperature difference 'pinch'

The previous paragraph discussed the practical considerations in employing a process that has a significant pressure drop in the supply stream of the heat exchanger. Two separate heat exchangers with an intermediate JT valve on the supply stream in between the 'upper' and 'lower' (the connotation here is in the sense of temperature level) units is considered as the best practical method for this investigation (see item "a" above).

Testing has been conducted to quantitatively examine the performance of a single wrap Collins-type heat exchanger supplying a sub-atmospheric load. This heat exchanger is a simple, but effective and robust design; largely unaffected by the effects of flow distribution[5]. It is actually a cross-flow configuration for each tube coil (~360 degrees), but is overall counter-flow. In fact, it can be shown theoretically that this configuration is a very effective counter-flow heat exchanger. Physically, the Collins-type heat exchanger consists of a mandrel with closed ends,

[5] Unlike multi-pass, multi-layer heat exchangers; refer to Fleming, (1967).

with finned tubing wrapped helically onto it, enclosed by an outer shell. The higher pressure supply stream is inside the tube and the sub-atmospheric stream flows around the finned tubing in the annular region between mandrel and shell to minimize the pressure drop. The tubing and fins should be OFHC or ETP copper, with the fins either soldered or brazed to the tube. The pitch between adjacent coils (for a single tube pass) is the same as the fin diameter. The low helix angle assures a long conduction path along the tubing and therefore minimizing the effect of axial conduction. The mandrel should be evacuated, or at least filled with an insulation like crumpled PET (or some such similar insulation) to prevent natural convection within the mandrel. Incorporating a solid braid nylon (or PET) rope is essential for good performance, to foremost prevent the sub-atmospheric flow from bypassing the finned tubing either on the mandrel outside or the shell inside. It also increases the heat transfer (and pressure drop) by forcing the flow to follow the fin tubing contour. The mandrel and shell have a relatively thin wall (~0.120 inches or less) and being constructed of 304 or 316 stainless steel minimize axial conduction. The Collins-type heat exchanger has demonstrated a long history (referring to Appendix A) of being an effective and robust design to both scientific laboratories and to industry (see item “b” above).

2. Investigate the pseudo-adiabatic expansion nature of pressure drop with heat transfer in particular and on the overall refrigeration process. This is to encompass the analysis and evaluation of the:
    a. Thermodynamic nature of the phenomenon
    b. Equivalent isentropic efficiency of pressure drop with heat transfer
    c. Overall process efficiency improvement; trade-off between higher load capacity and higher discharge temperature from the cryogenic compression process

For a real fluid, near or below its critical point, when heat is removed from the supply stream at successively lower pressures, this can have the same effect as an adiabatic expansion, although no work is being extracted. For example, heat exchange between a warmer supply stream and the colder return gas, where the heat removed from supply stream occurs as its pressure decreases in either a continuous or step-wise (discontinuous) manner. This is a phenomenon of a real pure fluid and is useful to understand, especially in applications where work extraction is not practical, or has not been developed. There are two aspects to be examined; a thermodynamic and a practical process equivalent adiabatic expansion efficiency for heat exchange with pressure drop. It is also of interest to get an idea of how this cold-end effect impacts the overall helium refrigeration process. That is, if this is providing a certain performance benefit locally at the cold-end (4.5 to 2 K), how does this translate into the overall refrigerator performance? Both the perspective of a reduction in input power for the same load performance, and the perspective of a load performance increase for the same input power is of interest.

2. EXPERIMENTAL SET-UP

2.1 Research Facility – Cryogenic Test Facility

The Cryogenic Test Facility (CTF) is the first location at Jefferson Lab to have an operational 2-K helium plant. Its original purpose was to support SRF Niobium cavity testing and single cryo-module testing (CEBAF 1988). The main components of the helium refrigeration system are Mycom screw compressors which supply a Koch model 2200 (4.5 K) cold box with a cryogenic distribution system to the vertical cavity and horizontal cryo-module testing areas, and a vacuum pumping system to produce the sub-atmospheric helium. Figure B.1 in Appendix B shows a basic flow diagram for the CTF. The Mycom screw compressors are a series 2016C compound type (meaning that they are a two stage compressor driven by the same shaft) with 298 kW (400 Hp) induction motor and are capable of roughly 55 g/s (CEBAF 1987). The Koch model 2200 (cold box 2 in Figure B.1) is capable of 590 W of 4.5 K refrigeration or about 5.4 g/s of liquefaction (4.5 K to 300 K), but is also capable of supplying 9.3 g/s of helium with it returning at roughly 24 K (Koch Process Systems 1989). It has two stages of expansion comprised of Koch M1600 dual cylinder reciprocating expansion engines (high pressure to low pressure stream). Helium returned from the vertical cavity test area is warmed by heat transfer to the environment before reaching the vacuum pumping system. However, helium from the horizontal cryo-module test area returns through the cryogenic distribution system. This allows the refrigeration of the return gas to be partially recovered. This is done using cold box 4 (see Figure B.1) by counter flow heat exchange with a slip stream of flow from the compressor discharge which is then injected at roughly 24 K and 1.2 bar to cold box 2. The CTF can support a 180 W 2-K refrigeration load, and is presently limited by the distribution system. The vacuum

pumping system is comprised of two separate sets of a Kinney KMBD-8000 lobe (roots) blower and Kinney KLRC-2100S liquid ring pump, which have a capacity of ~9.7 g/s per set (Knudsen, Process study for the design of small scale 2 Kelvin refrigeration systems 2008, 60). Flow from the vacuum pumping system can go to either (or both) the compressor suction or the purifier, but it is best to send the full flow through the purifier to maximize the system availability. The purifier design quite similar to that used by FermiLab in the 1980's, adequate for less than approx. 1000 ppm (by volume) contamination and consisting of an ambient temperature molecular-sieve bed (for removing moisture) and an activated carbon bed at liquid nitrogen temperature (approx. 80 K; for removing air constituents). The present purifier only has sufficient capacity to handle the flow from a single blower-ring pump set.

The apparatus used for testing the 4.5 K to 2 K heat exchanger performance was installed in the horizontal cryo-module test area, next to what is called the junction box, which has a number of distribution system (cold) connections. JLab uses a mechanical cryogenic coupling connection, first developed for a few small sizes at Fermi Lab, which are nicknamed 'bayonets'. These are commonly used to connect between equipment and the distribution, and between different distribution sections. They offer the advantage of a physical disconnection, although they introduce a small heat in-leak (as compared to if there were no mechanical connection and a cryogenic valve was used). These are similar to ones provided by the cryogenic industry (PHPK Technologies n.d.), except that the tolerance between male and female tubes is not as tight and an ambient temperature valve (not a cryogenic valve) is used to close off the female end. This offers a significant advantage of being able to install and remove these couplings without warming the adjoining piping, although at a slightly higher heat in-leak penalty. The warm valve on the female end is significantly less expensive than the cryogenic valve that would be required

if this type of coupling was not used. JLab uses 1 in., 1-1/2 in., 2 in., 3-1/8 in., 5-3/16 in. and 9-1/4 in. sizes, which is the outside diameter of the female (inner) tube. The test apparatus used a 1-1/2 in. size bayonet connection for the supply, and a 3-1/8 in. size bayonet connection for the sub-atmospheric return. So, vacuum jacketed piping with 'male' cryogenic couplings at each end are used to connect from the junction box 'female' cryogenic couplings to the test apparatus. This interconnecting vacuum jacketed piping is usually in the shape of a disproportionate and upside-down "U", since the bayonets must be oriented vertically (which also usually facilities installation and removal too) to ensure a stable density gradient in the small annular gap between male and female inner tubes. A vacuum jacketed interconnecting piping assembly, (usually) comprised of male bayonet ends, is known as a 'u-tube'. Between the junction box in the horizontal test area (or 'cave', as it is referred to) and valve box in the CTF itself is approximately 55 ft. of vacuum jacketed transfer line. Figure 2.1 shows the cross-section of this line which carries super-critical helium ("2K SUPPLY"), sub-atmospheric helium ("2K RETURN"), helium cool-down, and a helium shield supply and return. This basic idea is used extensively at JLab, SNS and (in the near future at) MSU-FRIB.

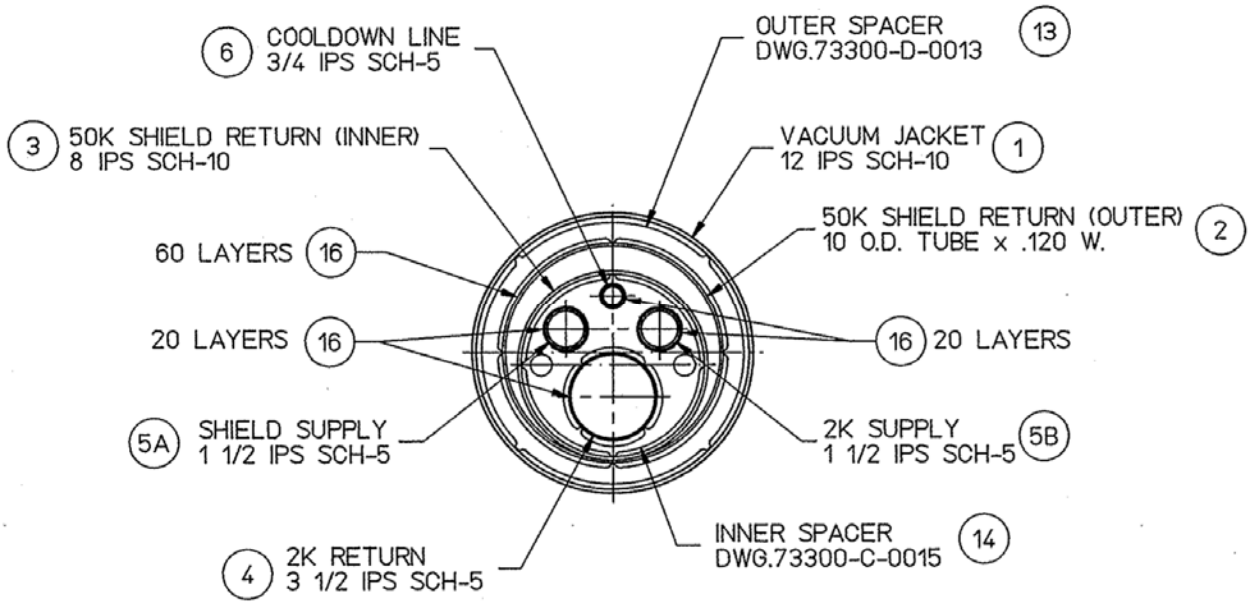

Figure 2.1. CTF valve box to junction box cryogenic transfer-line cross-section

The valve box in CTF (itself) has an aluminum brazed-plate-fin type 4.5 K to 2 K heat exchanger ("2K SC" in Figure C.7 in Appendix C). However, there is considerable heat in-leak to it and to the distribution line from the horizontal test area, so except at high mass flows (> ~6 g/s), the supply temperature at the junction box is usually around 5 to 5.5 K. Although, this is undesirable in general, it enabled the desired test to be done. Appendix C includes EDM screen snap-shots (not during HX testing) of the CTF system for reference with Figures B.1 and B.2. Referring to Figure C.9, the test apparatus supply was connected to the junction box on the line with the flow element CFI2452. And, the sub-atmospheric return was connected to the junction box on the line with the diode CTD2450V.

2.2 Test Apparatus and Supporting Hardware

Referring to Figure B.2 and Figure C.9, an 'upper' and a 'lower' Collins-type heat exchanger ("HX2471" and "HX2472", respectively), JT valves ("EV2471" and "EV2473"), liquid vessel ("V2473") and interconnecting piping were supported from the top 24 IPS flange. As in Figure 1.3, these are "HX-U", "HX-L", "JT-1", JT-2" and "Load", respectively. All of the equipment and instrumentation shown 'inside' the outer 'square' (see Figure B.2) were surrounded by a cylindrical copper radiation shield with a (flat) top and a bottom. The top shield had a number of through holes to accommodate the penetrations through the top flange for piping and instrumentation. This cylindrical copper radiation shield was hung from the top flange, so that the entire assembly can be removed or installed into the 24 in. diameter vacuum can. Four copper braids brazed to the sub-atmospheric 2 IPS piping on the warm-end of the upper heat exchanger before exiting the apparatus were connected to the copper shield for a thermal anchor. The original design for this was modified to shorten the length of the copper braids, more evenly distribute them and provide less thermal resistance at conduction contact joints.

Forty layers of super-insulation were used on the outside of the copper radiation shield, 10 layers were used on the inside, and 20 layers were used on all the internal piping and components. The super-insulation is comprised of 1 ply of crinkled double-aluminized Mylar (DAM) and 1 ply of Reemay. The DAM is 0.25 mill polyester with a 500 Angstrom aluminum coating on both sides. The Reemay is a filtration grade spunbonded 100% polyester (style #2250). Although it is important to keep the insulation as 'fluffy' as possible, when it is compacted, but not compressed, 40 layers is about 3/8 in. The blanket layers are held together (loosely) by a clothes (plastic) 'tag', applied using a 'tagging gun'. A thicker (non-aluminized)

Mylar sheet is incorporated on the outside of the blanket to provide rigidity. Adjoining blankets are either butted and taped (using Mylar tape), with some compression (to account for shrinkage from contraction as it is cooled), or they are joined 'warm' layer to 'warm' layer and 'cold' layer to 'cold' layer.

The supply line was either a 1/2 in. outside diameter (OD) tube (with a 0.035 in. wall, if 304 stainless steel, otherwise, a 0.049 in. wall for the heat exchanger copper tube) or a 1/2 IPS sch. 10 pipe. The sub-atmospheric line was a 2 IPS sch. 10 pipe. Instrument lines (for pressure) were 1/4 in. OD tubing with a 0.035 in. wall. Except for some parts of the heat exchangers and the thermal relief valves, all 'wetted' piping and components were made of 304/304L or 316/316L grade stainless steel. The 24 IPS vacuum shell and flanges were also 304/304L stainless steel.

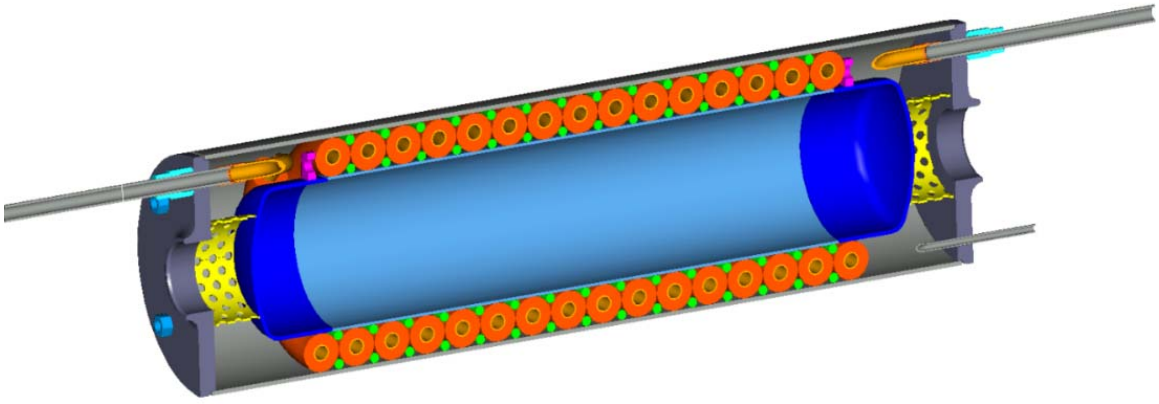

Figure 2.2. Cross-section of Collins-type heat exchanger (upper and lower are similar)

The liquid vessel is a 31 in. long (head-to-head) 6 in. OD tube with a 0.083 in. wall thickness (~13.1 liter 'water' volume). The supply line is shielded to prevent spray from being entrained using a 'half-pipe' guard. Four Chromalox 1-1/2 in. wide, 6 in. diameter, two-piece,

HB-6040 band heaters are attached to the outside of the liquid vessel, over 2 in. wide, 0.018 in. thick ETP copper sheet. Tension is maintained using Bellville washers. Additionally, stud-posts are welded to the vessel to allow (304 stainless steel) flat plate strips to be fastened on top of the heaters. An RTD is attached to a copper block which is brazed to the vessel, and serves as a high temperature shut-off to protect the heaters. Several layers of aluminum foil backed fiberglass are wrapped over the heaters to protect the super-insulation. Only two of the four band heater are used at any one time; the other two serve as back-ups.

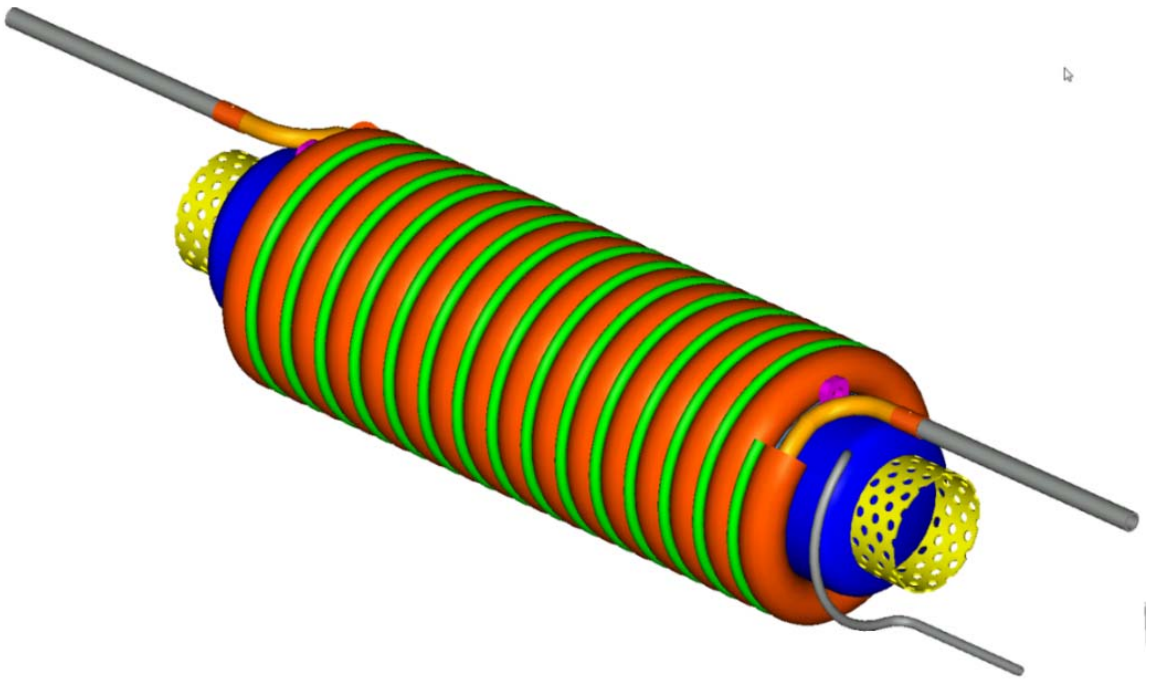

Figure 2.3. Collins-type heat exchanger, mandrel, fin-tube with nylon rope assembly (before being inserted into the shell)

The heat exchangers are a Collins-type (see Figures 2.2 and 2.3), copper tube with soldered copper fins, wound helically around a 4 IPS (4.5 in. OD) Sch. 10 304/304L stainless

steel mandrel, with a pitch equal to the fin diameter. Nylon rope (the bright green in Figures 2.2 and 2.3) is wrapped such that the gap between the fins and the mandrel and between the fins and the shell is filled. The mandrel and fin-tube with nylon rope assembly is inserted into a 7 in. OD tube with a 0.125 in. wall thickness, and the end plates are attached. The mandrel is exposed to the same pressure the vacuum space is at, by way of a 1/4 in. OD tube. Geometric details for these heat exchangers are given in Chapter 3.

The JT valves (EV2471 and EV2473 in Figure B.2) are a JLab design, which have been modified from an original Fermi Lab design, and are used extensively at JLab. The intermediate JT (EV2471) has a wide open flow coefficient (C_V) of 0.32 (at 9/16 inch travel) and the JT to the liquid vessel (EV2473) has a wide open C_V of 3.0 (at 9/16 inch travel). These valves use electric (motor-gear driven) actuators, which are also a JLab design.

Table 2.1. Micro Motion (model #CMF025M) Coriolis mass flow accuracy

Mass Flow Rate [g/s]	**Mass Flow Accuracy [%]**
10.000	0.350
9.010	0.350
8.020	0.350
7.030	0.350
6.040	0.350
5.050	0.350
4.060	0.350
3.070	0.350
2.080	0.363
1.090	0.694
0.100	7.560

2.2.1 Mass Flow Measurement

In the supply u-tube connecting the Junction Box to port "D1" on the test apparatus (refer to Figure B.2), a Micro Motion (model #CMF025M) Coriolis mass flow meter was installed within the vacuum jacketed piping. A Cermaseal type feed-through on the piping vacuum jacket was necessary for the 9-wire from the flow meter (sensor) to the Model 1700 transmitter, but no other special modifications were required. This flow meter was a standard commercial product, well suited and rated for helium cryogenic service, and did not need any of the special modifications required for earlier developmental units (Serio 2007). There are only two set-up items that require special attention. First is to effectively disable the resistance temperature diode (RTD) on the (mass flow) sensor which is used to compensate for changes in Young's modulus with respect to temperature. Below approximately 20 K, Young's modulus for 304/316 stainless steel is essentially constant due to an intrinsic magnetic transition (Ledbetter 1981). The second is to ensure that when the flow meter is calibrated for zero flow, that there is in fact zero flow and it is at the operating temperature (i.e., ~4.5 to 5.5 K, in this case). At first thought this second item may seem trivial, but all valves leak, and that is even truer in cryogenics. Table 2.1 shows the mass flow accuracy for the flow meter, provided by Micro Motion. Figure 2.4 shows the interpolation used for the Micro Motion accuracy data. So, even at the lowest mass flow measured, which was 1.513 g/s in Test #25 (2-Jan-15 19:20 30 W 0.2 atm), the mass flow measurement accuracy should about 0.5%. The 4-20 mA signal from the Model 1700 transmitter was sent to an Allen Bradley 1756-IF16 ControlLogix current analog input module, and scaled to 0 - 18.1 g/s (by the PLC). This input module has a resolution of 16 bits (0-65535) at 0 to 20.5 mA, and a calibrated accuracy (at 25 °C) of better than 0.15% of the range (0 to 20 mA).

Additionally, there is the resolution due to the archiver, which had a dead-band of 0.01 g/s per Appendix D, since it was used to obtain the average reading for the mass flow.

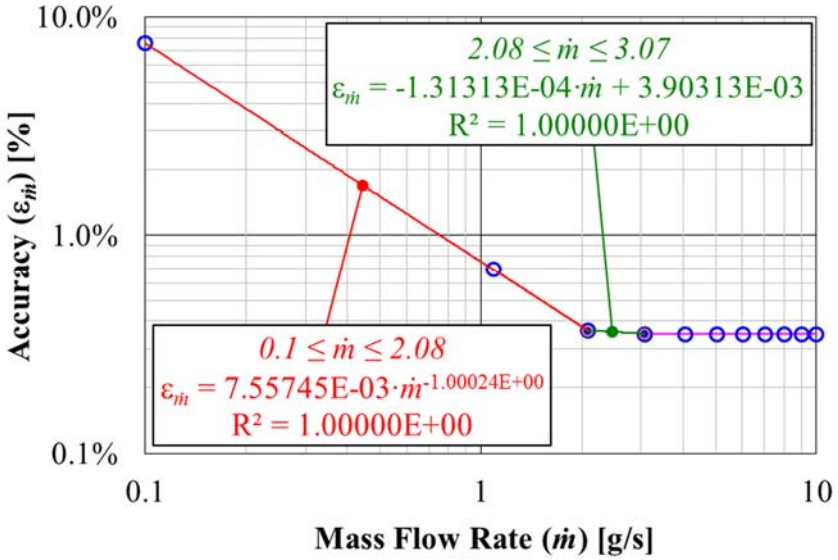

Figure 2.4. Interpolation of Coriolis mass flow accuracy

In general, the accuracies for each measurement can be based on the full range (of the variable) and/or the current value; e.g.,

$$\delta x = \sum_k \nu_k \cdot \Delta x_k + \sum_j \varepsilon_j \cdot x \qquad \text{(Eq. 2.1)}$$

where, first summation term is based on a selected range, Δx_i, of the variable (which is 'x', in this case). Often, the 'selected' range is the full range, $\Delta x_i = x_{max,i} - x_{min,i}$. Also, for the 'selected' range, it may be necessary to convert units from another variable 'y' to 'x'; i.e., $\Delta x_i = \beta \cdot \Delta y_i$. The second summation is the accuracy based on the current value only. So, the total accuracy of measurement 'x' is,

$$\delta_x = \frac{\delta x}{x} = \sum_k \frac{\nu_k \cdot \Delta x_k}{x} + \sum_j \varepsilon_j \qquad \text{(Eq. 2.2)}$$

Note that the first summation term is larger at values of 'x' that are closer to $x_{min,i}$; i.e., at the low end of the range. Where the second summation term is a constant (contribution to the total measurement accuracy).

In this instance, $x = \dot{m}$, with the units in [g/s], and,

$$\delta_{\dot{m}} = \frac{\delta \dot{m}}{\dot{m}} = \frac{\beta \cdot (\nu_1 \cdot \Delta y_1 + \nu_2 \cdot \Delta y_2) + \nu_3 \cdot \Delta x_3}{\dot{m}} + \varepsilon_{\dot{m}} \qquad \text{(Eq. 2.3)}$$

where, $\varepsilon_{\dot{m}}$ is per Figure 2.4. For the lowest mass flow measured, $\varepsilon_{\dot{m}} = 0.005$, as stated previously; so, we have,

$$\delta_{\dot{m}} = \frac{\left(\frac{18.1\ g/s}{16\ mA}\right) \cdot \left\{\frac{20.5\ mA}{65535} + (0.0015) \cdot (20\ mA)\right\} + (1) \cdot (0.01\ g/s)}{\dot{m}} + 0.005 \qquad \text{(Eq. 2.4)}$$

$$\delta_{\dot{m}} = \frac{0.0443\ g/s}{\dot{m}} + 0.005 \qquad \text{(Eq. 2.5)}$$

The overall mass flow measurement accuracy will be better than this since the meter accuracy of 0.5% is being applied for the all flow rates (contrary to Table 2.1). At the lowest flow rate, $\dot{m} \cong$ 1.5 g/s, the accuracy is about, 3.5% (0.052 g/s); at the highest flow rate tested, $\dot{m} \cong 5.0$ g/s, the accuracy is about, 1.2% (i.e., 0.062 g/s). This accuracy model assumed the worst possible situation that all of the inaccuracies combine, rather than cancel. Perhaps, a more realistic error estimate would be to take the largest term,

$$\tilde{\delta}_{\dot{m}} = \frac{0.0339}{\dot{m}} \qquad \text{(Eq. 2.6)}$$

2.2.2 Heat Load Measurement

The power supply for the liquid vessel heater was a Sorensen-Ametek DLM 150-4 (i.e., DLM 600 Series) with a M130 option, rated for an output voltage of 0-150 VDC and a current of 0-4 A. The M130 option allows remote control and programming via. Ethernet (16 bit, IEEE 802.3 compliant) and was operated from an Allen Bradley PLC. This is a very sophisticated (and expensive) DC power supply that monitors what it is providing. The basic path is as follows:

(a) User inputs (via. HMI to PLC) the requested power (in Watts)

(b) PLC calculates the voltage based upon a given heater resistance

(c) PLC sends the request via Ethernet to the power supply

(d) Power supply outputs the voltage requested and measures the current supplied

(e) Power supply reports the current back to the PLC through the Ethernet connection

(f) PLC multiplies the voltage (requested) by the current (read-back) to get the power

The specifications for this unit state that it has a programming accuracy of 0.1% of the maximum voltage (150 V), a read-back accuracy of 0.25% of the maximum current (4 A), and a load regulation accuracy of 0.005% of the maximum voltage plus 2 mV. So, these are 150 mV, 10 mA, and 9.5 mV, respectively. The resolution for programming and read-back is 16 bit, or approximately 0.002% of the full scale, which is 3 mV and 0.08 mA, respectively. So, the total (programmed) voltage and current (read-back) accuracy is 159.5 mV and 10 mA, respectively. The power is,

$$P = i \cdot V \qquad \text{(Eq. 2.7)}$$

And the power accuracy is found as follows,

$$(P + \delta P) = (V + \delta V) \cdot (i + \delta i) \qquad \text{(Eq. 2.8)}$$

Neglecting second order terms, and substituting, $i = V/R$, with R the total resistance (heater and wire), this simplifies to,

$$\delta_P = \frac{\delta P}{P} = \frac{\delta V}{V} + \frac{\delta i}{i} = \delta_V + \delta_i \quad \text{(Eq. 2.9)}$$

So, the power accuracy is the sum of the voltage and current accuracies (to the first order). Further substituting in,

$$\delta_V = \frac{\delta V}{V} = \sum_k \frac{\nu_{V,k} \cdot \Delta V_k}{V} + \sum_j \varepsilon_{V,j} \quad \text{(Eq. 2.10)}$$

$$\delta_i = \frac{\delta i}{i} = \sum_k \frac{\nu_{i,k} \cdot \Delta i_k}{(V/R)} + \sum_j \varepsilon_{i,j} \quad \text{(Eq. 2.11)}$$

Per the Chromalox catalogue, the heater has a nominal resistance of, $R = (240)^2/400 = 144\ \Omega$. While this value is likely not accurate, it is not necessary for it to be since the current is measured. So, using the accuracies previously listed,

$$\delta_V = \frac{\{(0.001) \cdot (150) + (0.00005) \cdot (150) + 0.002\}}{V} + 0 = \frac{0.1595}{V} \quad \text{(Eq. 2.12)}$$

$$\delta_i = \frac{(0.0025) \cdot (4)}{(V/R)} = \frac{1.44}{V} \quad \text{(Eq. 2.13)}$$

$$\delta_P = \frac{1.5995}{V} = \frac{1.5995}{\sqrt{P \cdot R}} = \frac{0.133}{\sqrt{P}} \quad \text{(Eq. 2.14)}$$

So, for the lowest (nominal) power setting, $P = 30$ W, the PLC would calculate a required voltage of, $V = \sqrt{P \cdot R} = 65.73$ V, which corresponds to a power accuracy of, $\delta_P = 2.4\%$. For a power setting, $P = 100$ W, the PLC would calculate a required voltage of, $V = \sqrt{P \cdot R} = 120$V, which corresponds to a power accuracy of, $\delta_P = 1.3\%$.

As with the mass flow, this accuracy model assumed the worst possible situation that all of the inaccuracies combine, rather than cancel. So again, perhaps, a more realistic error estimate would be to take the largest term (which is the current read-back),

$$\tilde{\delta}_P = \frac{0.120}{\sqrt{P}} \qquad \text{(Eq. 2.15)}$$

A more precise and complicated accuracy model could be used. However, it was deemed unnecessary for the present work.

Although the precise resistance of the heater and the wiring does not affect the aforementioned accuracy, it does affect the actual power reading. The wire used within the vacuum was a 16 AWG Omega HTTG-1CU. This is a high temperature lead wire comprised of a 26x30 stranded, 7% nickel plated copper conductor, wrapped with PFA tape, two PFA glass sleeves and a treated PFA glass braid. Per ASTM B355 (Standard Specification for Nickel-Coated Soft or Annealed Copper Wire), this is a class 7 conductor with a resistivity of 0.74593 μΩ·in and a density of 8.89 g/cm^3. There is some variability between a single solid conductor with a given AWG size and a stranded conductor with the same AWG size. But the stranding increases the equivalent nominal diameter. For a 16 AWG 26x30 stranded conductor, the nominal diameter is 0.0589 in (as compared to a 16 AWG solid conductor with a diameter of 0.0508 in.). The resistance of a 55 in. length (which was used) of this wire is,

$$R_w = \frac{\rho_w}{(A_c/L)} = \frac{(0.74593)\cdot(10)^{-6}}{\left[\frac{\pi}{4}(0.0589)^2/55\right]} = 0.01506\ \Omega \qquad \text{(Eq. 2.16)}$$

The wire used outside of the vacuum was 12 AWG (i.e., say, a nominal diameter of 0.102 in). So, assuming that the length of this larger diameter wire is no longer than (55·(0.102/0.0589)^2 =) 165 in., which was the case since the power supply was located with 3 feet of the test apparatus, the total wire resistance would be less than four times R_w, or, 0.06024 Ω. The fraction of power dissipated by the wires is the ratio of the wire resistance to the total resistance, which is roughly, 100·(0.06024 / 144) = 0.042%. Consequently, this effect can be ignored.

2.2.3 Other Instrumentation

The accuracy of remaining instrumentation to be mentioned is not important from the aspect of determining the load enthalpy flux, as will be discussed in Chapter 4. The pressure measurement used for CPI2472 (downstream of the intermediate JT) is a MKS DMB13T. This is a digital capacitance manometer, with a range of 1000 Torr. The specifications for this device state that the combined non-linearity, hysteresis, and repeatability is 0.25% of the reading and that it has a measurement resolution of 0.001% of full scale (on digital output). This is more than sufficiently accurate.

The pressure measurement used for CPI2474 (vessel vapor pressure) is a MKS DMB12T. This is a digital capacitance manometer, with a range of 100 Torr. The specifications for this device do not provide an accuracy explicitly, but it can be implied that it is no worse than the 1000 Torr range unit (which was 0.25% of the reading). It has a measurement resolution of 0.001% of full scale (on digital output). The vessel pressure was not lower than 30 mbar, and this corresponds to an accuracy of 0.075 mbar and a measurement resolution of 0.0013 mbar. This is sufficiently accurate.

The pressure measurement used for CPI2470 (supply to upper heat exchanger), CPI2472DEV (high range device, downstream of intermediate JT), and CPI2474DEV (high range device, vessel vapor pressure) is a GE-UNIK PTX-5072, 4-20 mA output, 2-wire. The specifications for this device stated that it has combined non-linearity, hysteresis, and repeatability of ± 0.2% full scale best straight line. The full scale is 17 atm (250 psia), so that for an operating pressure of about 2.8 atm, this is an accuracy of approximately 1%. This is more than adequate for the one location that this was needed for analysis (i.e., CPI2470). The use of the device at the other locations was just for operational visibility.

The differential pressure measurement used for the sub-atmospheric stream upper and lower heat exchanger pressure drop is a Rosemount 1151DP3S. Presently this product is discontinued by Emerson Process Management. This measurement was used only as an indicator that there may be two-phase in the sub-atmospheric return, and so its accuracy is irrelevant. However, the specifications are ±0.0785% of the calibrated span (which can be from 1:1 to 10:1 of the upper range limit, which is 30 in. H_2O).

The differential pressure measurement used for the vessel liquid level is a Rosemount 3051CD1, which has an upper range limit of 25 in. H_20 and an accuracy of ±0.10% of the span for spans that are less than a ratio of 15 to 1. A completely full vessel filled with liquid at 2 K would have a differential pressure of about 4.5 in. H_2O. This is sufficiently accurate, but unfortunately, this measurement was not stable. As such the super-conducting liquid level probe was used.

An American Magnetics super-conducting liquid level probe was used to measure the liquid level in the vessel. It uses a small Niobium-Titanium wire for the sensing element, which is super-conducting in the liquid helium (i.e., no electrical resistance), but 'normally' conducting in the vapor. A nominal current of 75 mA (DC) is supplied and so the output voltage will vary depending on the length of the element that is immersed. The probe used in the liquid vessel had an active length of 28 in. This unit has two 'on' modes; continuous and sample-and-hold. Although, this super-conducting probe is widely used. The manufacturer specifies no accuracy for the measurement.

The temperature measurements were made using 4-wire Lakeshore DT-670-SD silicon diodes. The "Band A" standard curve for these provides an accuracy of ±0.25 K between 2 and 100 K. Their reproducibility is stated to be ±0.010 K. No matter how accurate a diode is (or can

be) calibrated, the key to the accuracy is in the installation. This measurement is extremely sensitive to the effect of heat in-leak through the wires. It is crucial to properly anchor the wire to the process line (that is cold). There is some question in the case of this apparatus as to how well this was done, and in light of the testing, it is clear that this did affect the accuracy of these measurements. However, this was irrelevant for the primary test measurement goal, which was the load enthalpy flux (which will be discussed in a later in Chapter 4).

Accuracy of the temperatures affects the heat exchanger performance analysis. However, it believed that at least their behavior is consistent. The diodes themselves were essentially mounted in-stream, although not directly exposed to the helium. A standard design that JLab has used for many years is a copper bulb, brazed to a 1/2 in. OD 304 stainless steel tube. The primary and back-up diodes (item 3 in Figure 2.5) are epoxied to a brass stand-off or bobbin (item 1 or 9 in Figure 2.5). The brass set screw (item 2 in Figure 2.5) facilitates the installation into the copper diode receiver (item 1 in Figure 2.6). Item 3 in Figure 2.6 is a 304 stainless steel 1/2 in. OD tube (0.035 in. wall thickness) silver brazed to the copper diode receiver. These are then installed into an appropriate size pipe tee. It is important that the wires coming out of the 1/2 in. OD tube be shielded from thermal radiation, then properly thermally anchored to the process line close to the tee.

The wiring from the diodes was routed through the vacuum into air using a Ceramaseal feed-through, then connected to a CryoCon 18 (Cryogenic Control Systems, Inc. n.d.). This unit can handle up to eight diodes, has the calibration curve built-in, and provides a variety of interface protocols. Figures 2.7 to 2.9 provide an idea of the internal configuration of the test apparatus.

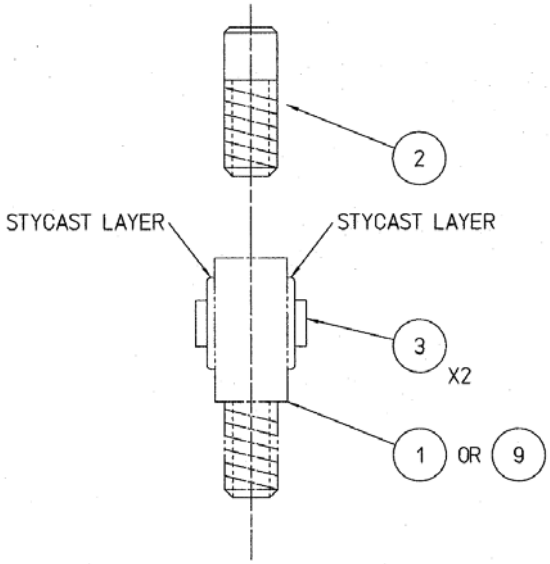

Figure 2.5. Diode mounting on brass stand-off (or bobbin)

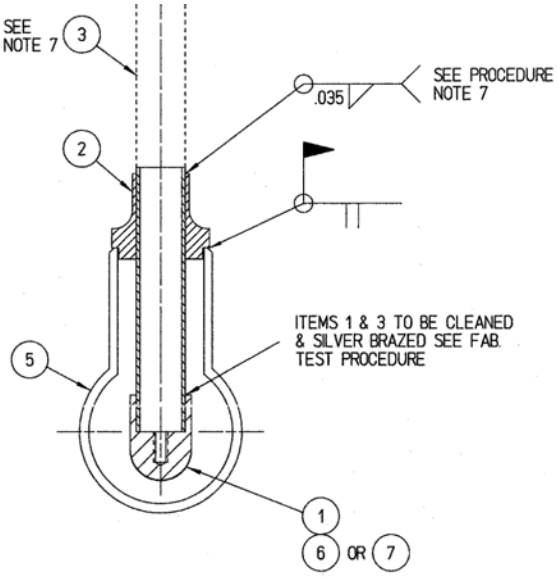

Figure 2.6. Tee for diode installation

2.3 Data Acquisition and Archival

All measurements were archived as per the parameters listed in Appendix D. Although the data can be 'dumped' at a 1 second sample, this must be done while running the plot tool during testing. If that plot is closed or the data being collected by it exceeds its specified buffer size, the data being taken by that plot tool is lost. Unfortunately, the request for a higher sample time for the archiver was not accomplished prior to testing. However, what is contained in the archiver is sufficient for test analysis.

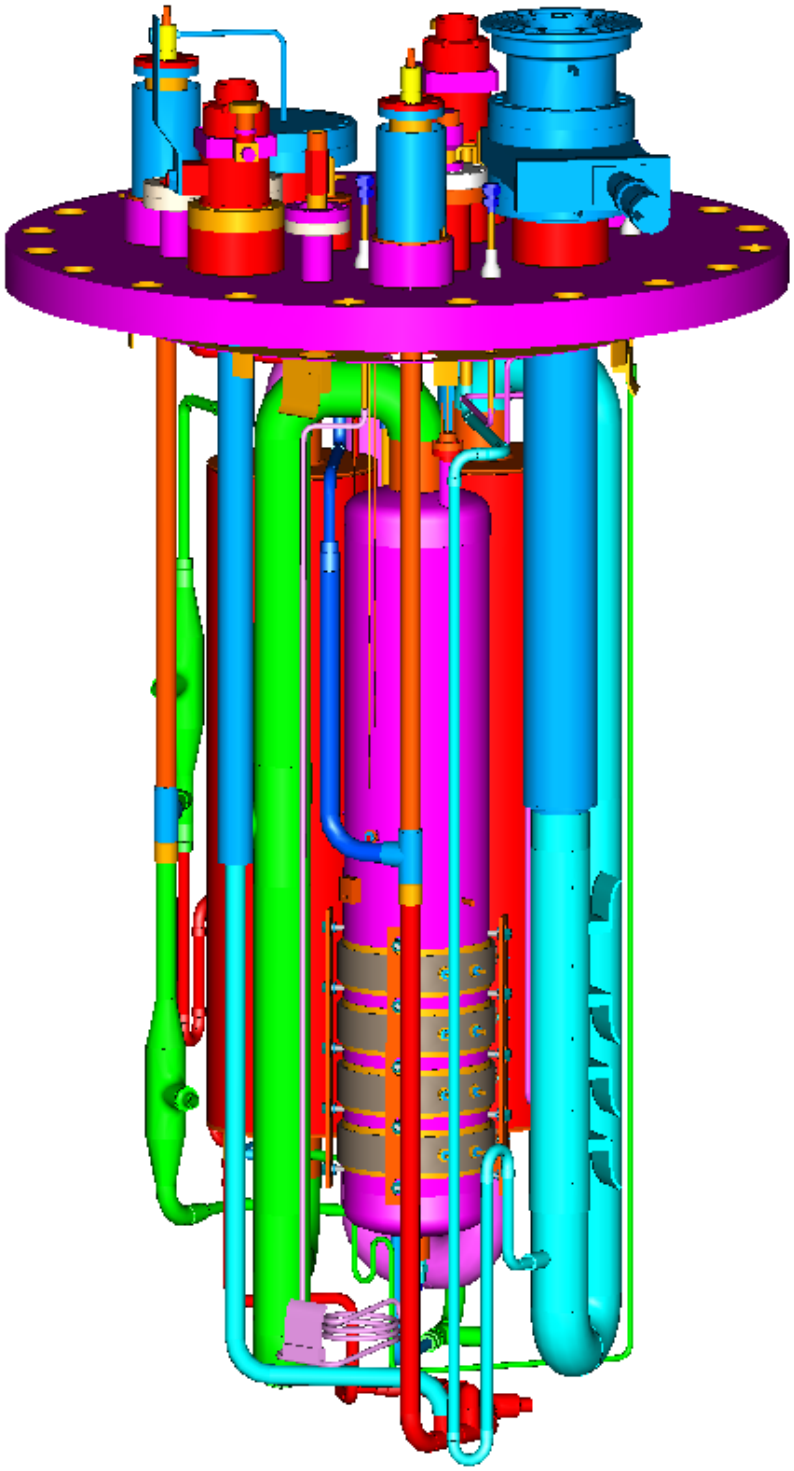

Figure 2.7. Internals of heat exchanger test apparatus, view of liquid vessel in front

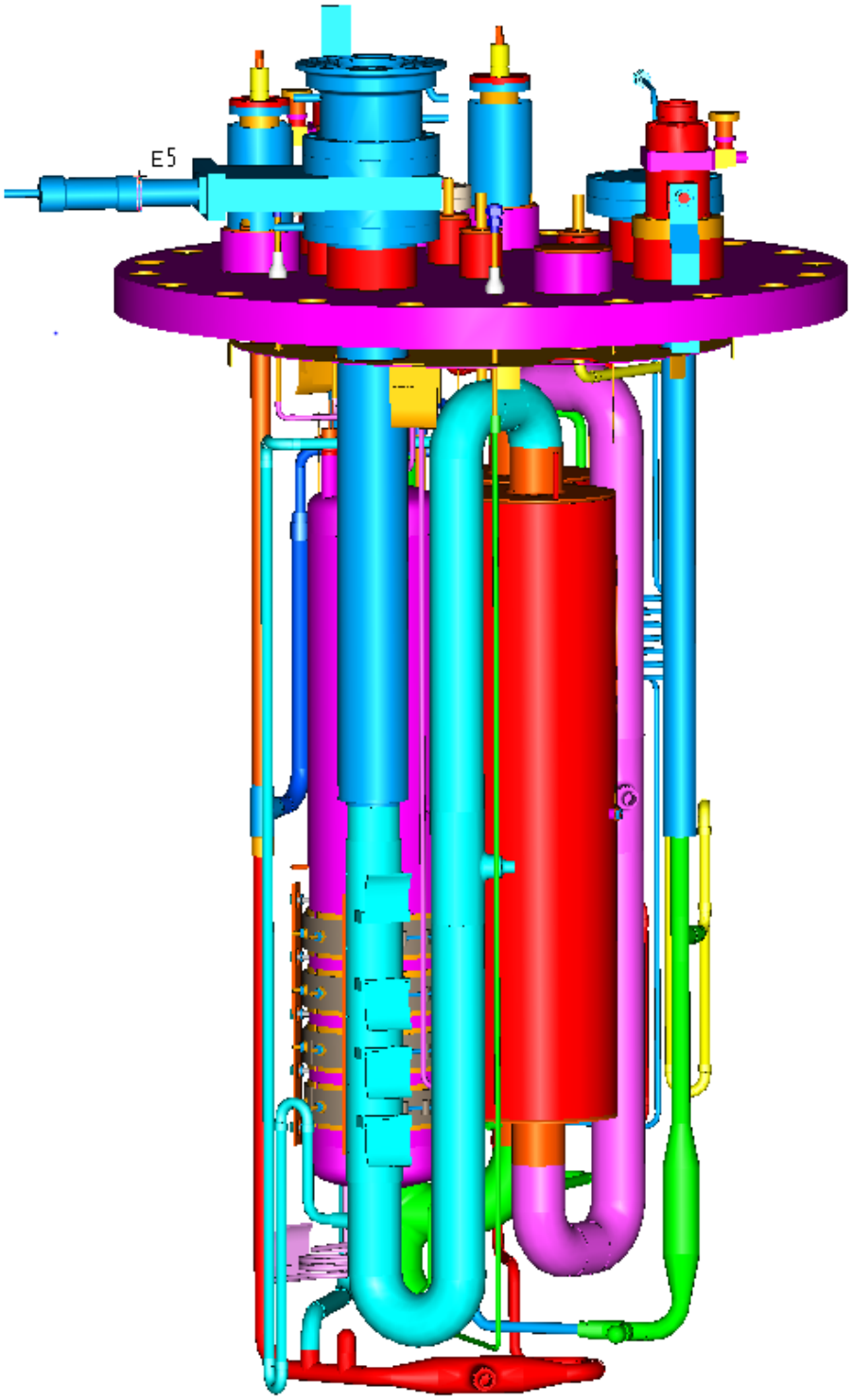

Figure 2.8. Internals of heat exchanger test apparatus, view of upper heat exchanger and connections on 2 IPS pipe for thermal anchoring of copper shield (not shown)

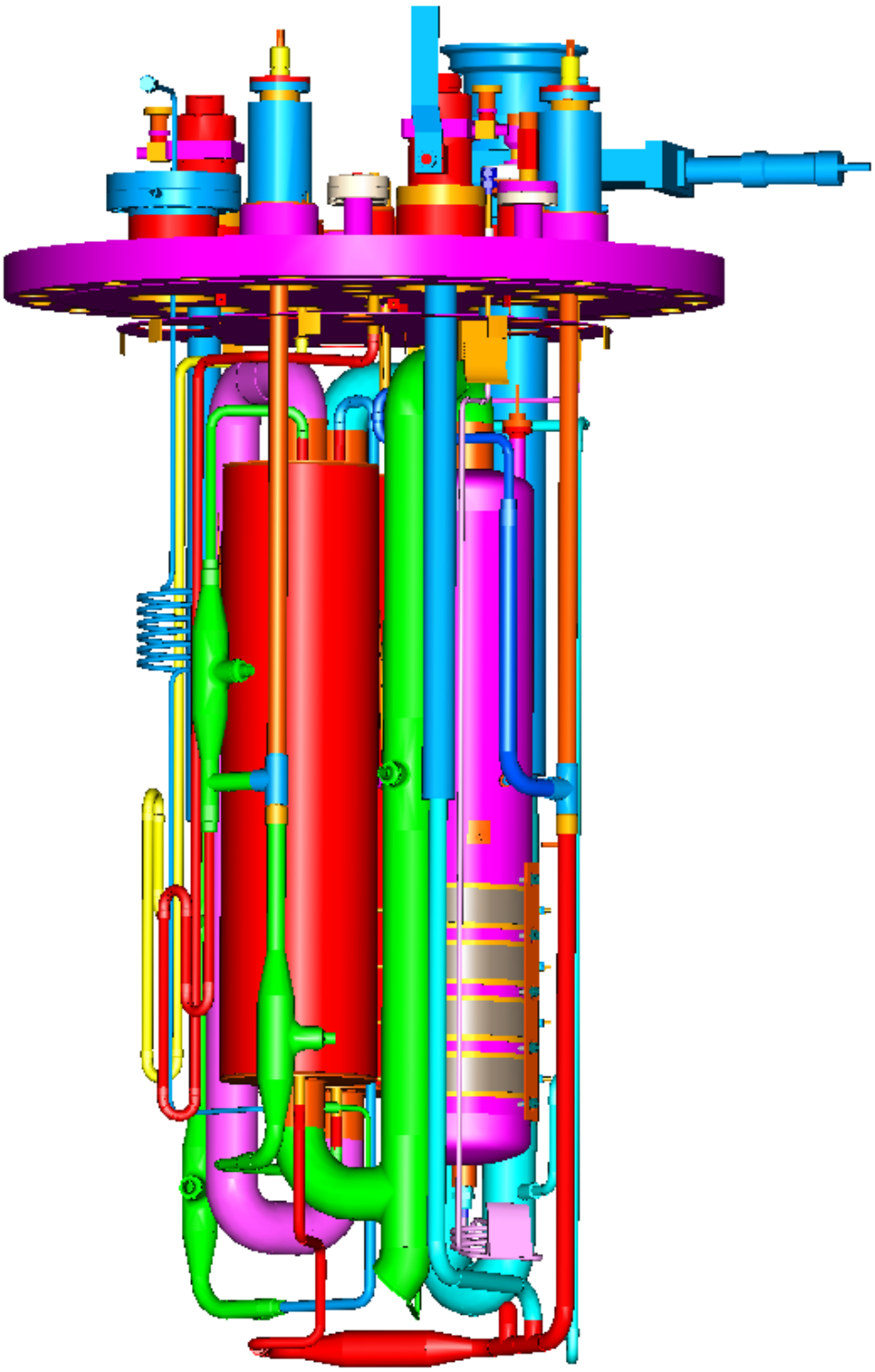

Figure 2.9. Internals of heat exchanger test apparatus, view of lower heat exchanger to left

3. PROCESS THERMODYNAMICS

3.1 Equivalent Pseudo-Adiabatic Expansion

The basic idea why the supply stream can cool to a lower temperature by lowering its pressure in-between and/or concurrent with heat exchange is shown in the pressure – enthalpy diagram already presented in Chapter 1. This provides a qualitative understanding, but a more quantitative one will now be investigated. Figure 3.1 is a pressure-enthalpy diagram (as in Figure 1.7 previously presented), showing constant temperature and entropy curves, which will be useful to refer to as this is discussed further. Note that "CP" is the critical point (2.2746 bar, 5.1953 K) and "TCL" is the transposed critical line (the locus of specific heat maxima; see (V. Arp 1972))

3.2 Pseudo-Fluid Property

Let's consider two fluid process paths; the first is a constant entropy process from pressure, p_1, to pressure, p_2. The second is a constant temperature process from pressure, p_1 to pressure, p_2. As shown in Figure 3.2, in the liquid and super-critical region, near the two-phase region of a pure fluid, there are three cases for these two process paths. Of course, for an ideal gas, the constant temperature lines are coincident with the constant enthalpy lines (which are vertical lines parallel to the *y*-axis in a pressure- enthalpy plot) and on a logarithmic pressure (*y*-) axis, the constant entropy lines are logarithmic, with the entropy decreasing as the pressure increases for a constant enthalpy. However, the area of interest is far from where the fluid behavior would approximated as an ideal gas.

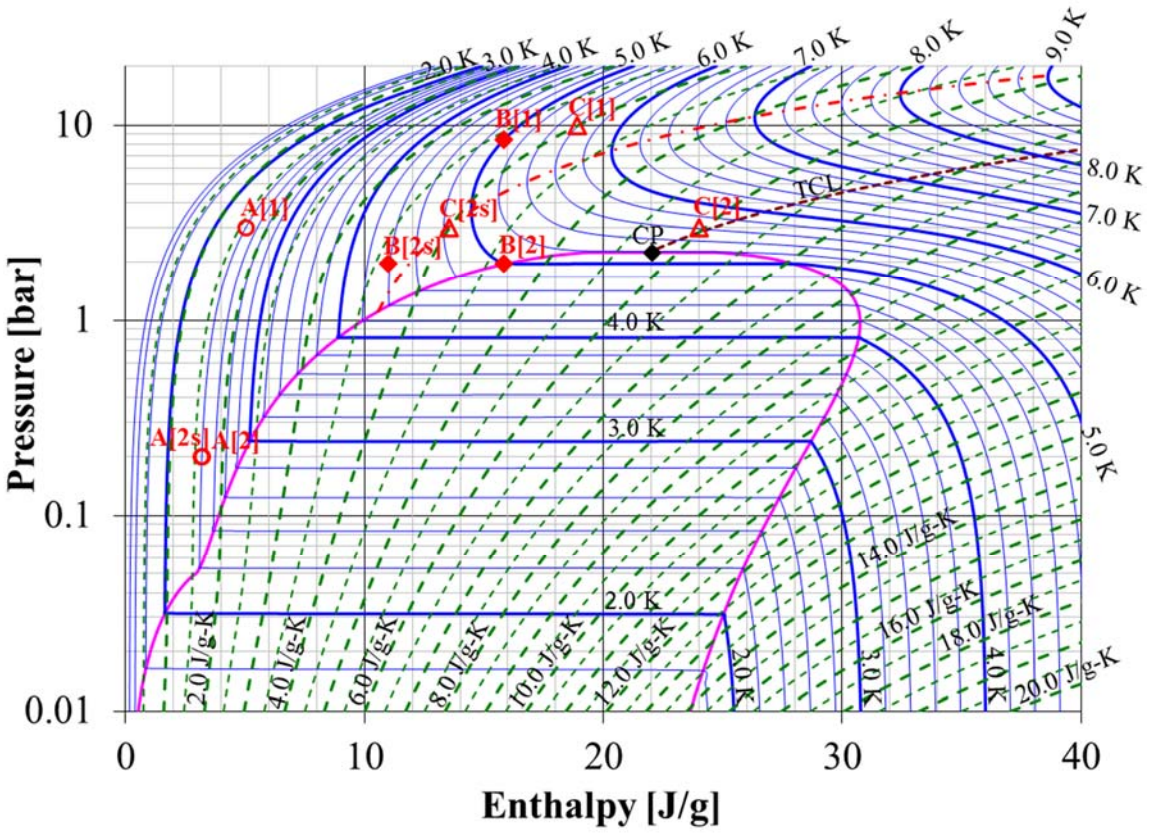

Figure 3.1. Pressure – enthalpy diagram for helium in the two-phase region

Referring to Figure 3.2, starting at point 1, if we following a constant enthalpy path from p_1 to p_2, obviously we have an isenthalpic process and the isentropic and polytropic (or as it is sometimes called, 'small-stage') efficiency of this expansion is zero. If we follow a constant entropy path from p_1 to p_2 (points 1 to 2s), obviously we have an isentropic process and the isentropic and polytropic efficiency is unity. If we follow a constant temperature path from p_1 to p_2 (points 1 to 2s), obviously we have an isothermal process. The reason for establishing these three process paths is that we would like to know the equivalent isentropic and polytropic

expansion efficiency of the isothermal process (with respect to the isentropic process). As it turns out, this can be labeled as a pseudo-thermodynamic property, seemingly dependent only on the start and end points (point 1 and 2); that is, it is path independent. However, the implied path is an isothermal one, hence the use of 'pseudo'.

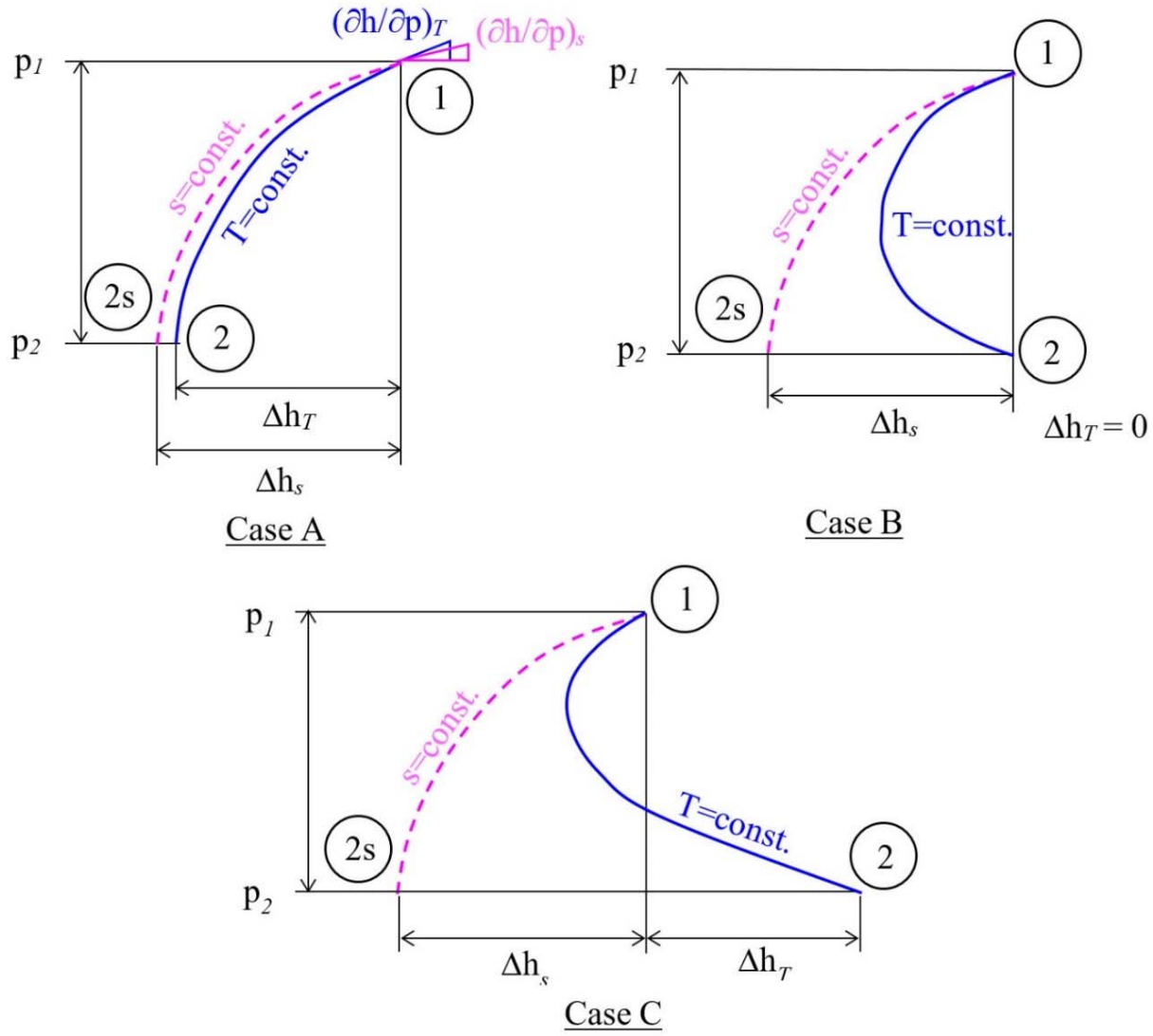

Figure 3.2. Constant entropy and constant temperature lines on a pressure-enthalpy diagram

Using Maxwell's relations we know that,

$$\left(\frac{\partial h}{\partial p}\right)_s = v \qquad \text{(Eq. 3.1)}$$

$$\left(\frac{\partial h}{\partial p}\right)_T = v(1 - T \cdot \beta) \qquad \text{(Eq. 3.2)}$$

These are the inverse of the 'slopes' for the isentropic and isothermal process paths. The former is always greater than zero. The latter requires that, $\beta < T^{-1}$ for it to be greater than zero (note that for an ideal gas, $\beta = T^{-1}$). Referring to Figure 3.2, if the latter becomes negative at some point along the (isothermal) path, then it is turning 'away from' the isentropic path. The line where $(\partial h/\partial p)_T$ is equal to zero is shown in Figure 3.1 as the dashed red line above the transposed critical line. The enthalpy change for the isentropic and isothermal paths can be found by integrating these relations,

$$\Delta h_s = \int_{p_1}^{p_2} v \cdot dp \qquad \text{(Eq. 3.3)}$$

$$\Delta h_T = \int_{p_1}^{p_2} v(1 - T \cdot \beta) \cdot dp \qquad \text{(Eq. 3.4)}$$

Further, since the enthalpy change in consideration is the isothermal path enthalpy change, Δh_T, the isentropic efficiency is,

$$\eta_s = \frac{\Delta h}{\Delta h_s} = \frac{\Delta h_T}{\Delta h_s} \qquad \text{(Eq. 3.5)}$$

The polytropic efficiency is defined as,

$$\eta_p = \frac{dh}{v \cdot dp} \qquad \text{(Eq. 3.6)}$$

So, since, $\Delta h = \Delta h_T$ (for the isothermal path),

$$\Delta h_T = \eta_p \int_{p_1}^{p_2} v \cdot dp \qquad \text{(Eq. 3.7)}$$

And, solving for the polytropic efficiency, noting that the integral is the isentropic enthalpy change,

$$\eta_p = \frac{\Delta h_T}{\Delta h_s} \qquad \text{(Eq. 3.8)}$$

which shows that, for the isothermal path,

$$\eta = \eta_p = \eta_s \qquad \text{(Eq. 3.9)}$$

So, this equivalent efficiency (isentropic or polytropic) is like a thermodynamic property, in that only the start and end points need to be evaluated; i.e., (p_1, T) and (p_2, T). However, it is for an isothermal process, so we will call it a pseudo-property.

Returning to Figure 3.2, in the two-phase region (though not two-phase), it is clear that when the isentropes and isotherms are similar to case A, the equivalent efficiency will be $0 < \eta < 1$. When they are similar to case B, the equivalent efficiency will be $\eta = 0$, that is, equal to an isenthalpic process. When they are similar to case C, the equivalent efficiency will be worse than an isenthalpic process; i.e., $\eta < 0$. An example for each of these three cases in plotted on Figure 3.1; where, for example, "B[1]" is case B: point 1, "B[2]" is case B: point 2 and "B[2s]" is case B: point 2s. Note that points "A[2]" and "A[2s]" are practically coincident. Table 3.1 provides the numerical values for these points shown on Figure 3.1.

Perhaps, the process 'path' for these can be elucidated by referring back to Figure 1.4 in Chapter 1. In this figure we fixed the *(h)* stream temperature at the heat exchanger (cold-end) outlet, and varied the outlet pressure from 3 bar down to 52.1 mbar. This is like the 'path' for the "T=const." in Figure 3.2; specifically like case A for the inlet conditions given in Figure 1.4.

Table 3.1. Numerical values for points 1, 2, and 2s in cases A, B, and C in figure 3.2

	Case A	Case B	Case C	
T	2.200	5.000	5.600	[K]
$\mathbf{p}_1$	3.000	8.449	10.000	[bar]
$\mathbf{h}_1$	5.024	15.846	18.916	[J/g]
$\mathbf{s}_1$	1.618	3.627	3.995	[J/g-K]
$(\partial \mathbf{h}/\partial \mathbf{p})_{T,1}$	0.006451	0.004101	0.003498	[m^3/kg]
$\mathbf{p}_{2,min}$	0.053	1.960	N/A	[bar]
$\mathbf{p}_2$	0.200	1.960	3.000	[bar]
$\mathbf{h}_2$	3.188	15.846	23.999	[J/g]
$(\partial \mathbf{h}/\partial \mathbf{p})_{T,2}$	0.006673	-0.0458	-0.15458	[m^3/kg]
$\Delta \mathbf{p}_{max}$	2.947	6.489	N/A	[bar]
$\Delta \mathbf{p}$	2.800	6.489	7.000	[bar]
$\Delta \mathbf{h}_T$	1.836	0.000	-5.083	[J/g]
$\mathbf{h}_{2s}$	3.146	10.996	13.525	[J/g]
$\Delta \mathbf{h}_s$	1.878	4.850	5.390	[J/g]
η_s (= η_p)	97.8%	0.0%	-94.3%	[-]

3.3 Equivalent Process Comparison

Referring to Figure 3.3, consider a counter-flow heat exchanger in-line with a refrigeration load applied to a saturated liquid bath. In one case a Joule-Thompson valve (i.e., isenthalpic expansion) supplies the bath and the supply stream has a non-zero pressure drop concurrent with counter-flow heat exchange with the saturated vapor leaving the bath. Assuming steady conditions, the supply and return mass flow are equal. And assuming negligible heat in-leak to the heat exchanger, the return minus supply stream enthalpy difference at the heat exchanger warm-end and cold-end are equal. The refrigeration load is simply the product of this stream enthalpy difference (at either warm-end or cold-end) and the mass flow.

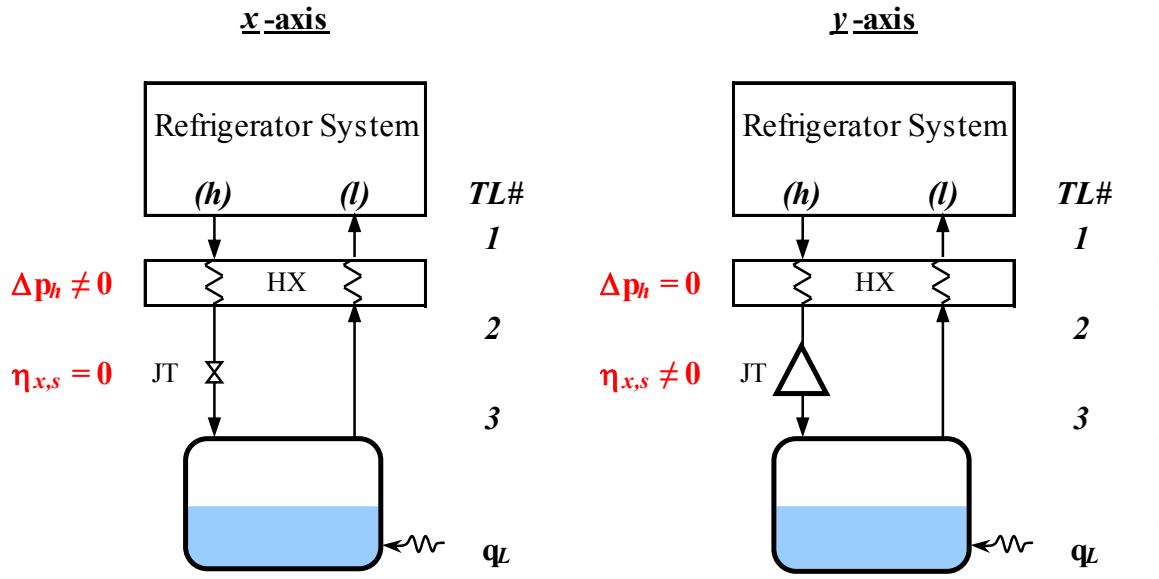

Figure 3.3. Process model diagrams for equivalent process comparison [6]

In a second, equivalent case, an expander supplies (two-phase flow to) the liquid bath and the supply stream has a zero (or negligible) pressure drop through the heat exchanger. For both the first and second cases, the refrigeration load (q_L) is taken as the same, as well as the supply stream condition ($p_{h,1}, T_{h,1}$) at the heat exchanger inlet and the bath pressure ($p_{l,3}$). Additionally, it will be assumed that the heat exchanger cold-end stream temperature difference ($\Delta T_{hl,2}$) is the same for both cases, so that the supply stream cold end (exit) temperature ($T_{h,2}$) is known. In the case of a sub-atmospheric helium bath at a saturation temperature below lambda, the cold-end of the heat exchanger has the smallest stream temperature difference (i.e., where it 'pinches'). And, it will be assumed that the supply stream will not be cooled below lambda, since the very high thermal conductivity of the super-fluid will keep its temperature essentially constant.

[6] "*x*-axis" case (figure on right): no work extraction and non-zero *(h)* stream pressure drop; "*y*-axis" case (figure on left): non-zero work extraction and zero *(h)* stream pressure drop

An equivalent isentropic expander efficiency in the second case can be found for a given supply stream heat exchanger pressure drop in the first case. This a practical load process equivalence, in the sense that it gives a direct comparison that pressure drop with heat exchange (for the supply stream) has on the load process that in terms of its 'apparent' effect; i.e., pseudo-expansion. The result of this analysis is shown in Figure 3.4 and Table 3.2. The supply condition ($p_{h,1}, T_{h,1}$) was taken as 3 bar and 4.5 K; the liquid bath pressure ($p_{l,3}$) was taken as 0.031 bar; and, the heat exchanger cold-end *(h)* to *(l)* stream temperature difference ($\Delta T_{hl,2}$) was taken as 0.2 K.

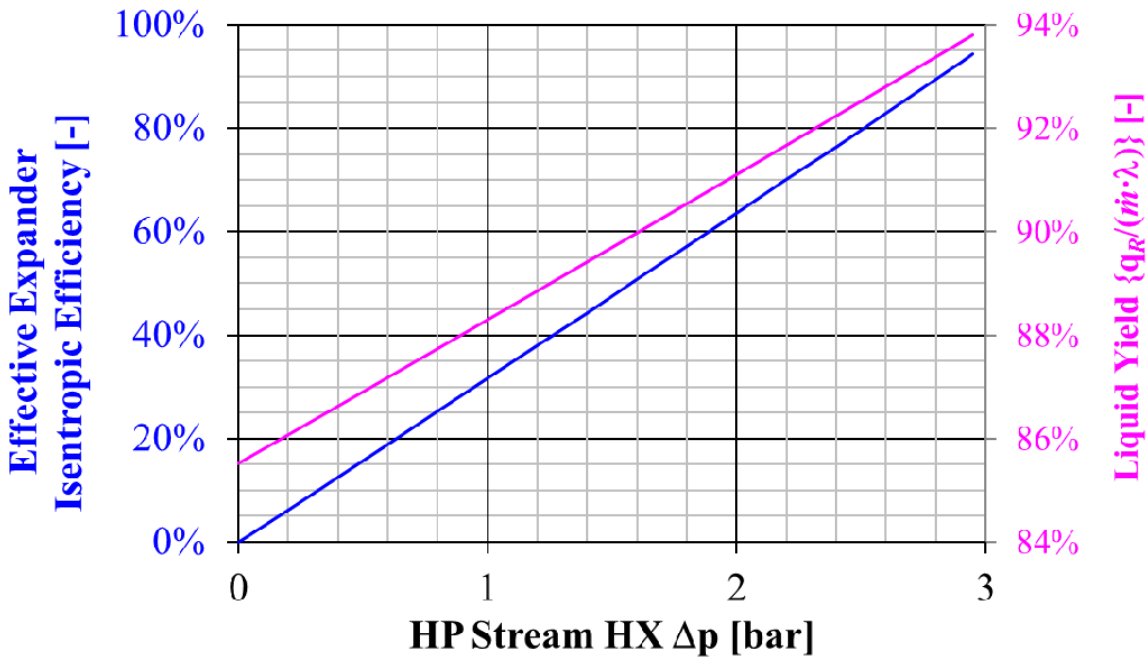

Figure 3.4. Results for equivalent process comparison [7]

[7] Heat exchanger pressure drop in "*x*-axis" case (no work extraction) vs. equivalent expander isentropic expander efficiency in "*y*-axis" case (no heat exchanger pressure drop)

Note that a heat exchanger with a pressure drop of 2.8 bar (i.e., 0.2 bar *(h)* stream pressure upstream of the JT valve) has an equivalent isentropic efficiency of 89.5%. This figure (3.4) also shows on the right-hand *y*-axis the liquid yield $(1 - x)$; i.e., the amount of liquid available to be boiled-off due to the load, where 'q_L' is the refrigeration load [W], '$\dot{m}$' is the mass flow [g/s], and 'λ' is the latent heat [J/g].

Table 3.2. Equivalent isentropic expansion efficiency, liquid yield, load enthalpy flux and *(l)* stream exit temperature at heat exchanger warm-end

$\Delta p_{h,HX}$ [bar]	$\eta_{x,s}$ [-]	(1-*x*) [-]	$\Delta h_{lh,3}$ [J/g]	$T_{l,1}$ [K]
0.0	0.0%	85.5%	20.01	3.225
0.2	6.3%	86.1%	20.14	3.249
0.4	12.6%	86.6%	20.27	3.274
0.6	18.9%	87.2%	20.40	3.298
0.8	25.3%	87.7%	20.53	3.323
1.0	31.6%	88.3%	20.66	3.348
1.2	38.0%	88.9%	20.79	3.372
1.4	44.4%	89.4%	20.93	3.397
1.6	50.8%	90.0%	21.06	3.422
1.8	57.2%	90.5%	21.19	3.447
2.0	63.6%	91.1%	21.32	3.472
2.2	70.1%	91.7%	21.45	3.497
2.4	76.5%	92.2%	21.59	3.522
2.6	83.0%	92.8%	21.72	3.548
2.8	89.5%	93.4%	21.85	3.573
2.9	92.8%	93.7%	21.92	3.586
2.947	94.3%	93.8%	21.95	3.592

So, why use an expansion process at all, if the 'expansion' (i.e., pressure drop) in the supply stream is accomplishing such a high efficiency equivalent adiabatic expansion? Although, the load capacity increase is real (or conversely, the mass flow reduction for the same

load), there is no work extraction (in the case of non-zero pressure drop in the supply stream through the heat exchanger) and the effect of this is a bit subtle. Figure 3.5 shows the temperature of the sub-atmospheric *(l)* stream exiting the warm-end of the heat exchanger vs. the *(l)* stream heat exchanger pressure drop. For example, using the previous numbers with a heat exchanger with a pressure drop of 2.8 bar (i.e., 0.2 bar *(h)* stream pressure upstream of the JT valve), which has an equivalent isentropic efficiency of 89.5%, the *(l)* stream temperature exiting the warm-end of the heat exchanger is 3.573 K, or 10.8% higher than if the *(h)* stream heat exchanger pressure drop were zero (and zero work extraction). As will be discussed next, the effect of this elevated *(l)* stream temperature on the overall process (specifically the 4.5 K refrigerator) is significant.

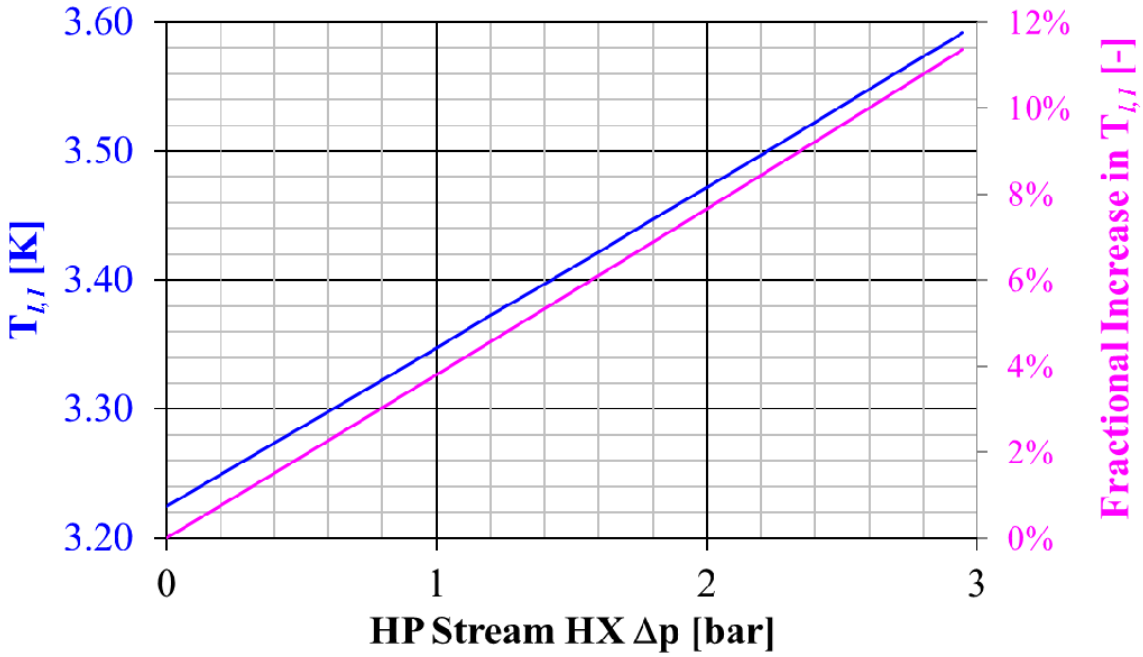

Figure 3.5. Sub-atmospheric *(l)* stream exit temperature at the warm-end of the heat exchanger vs. the *(h)* stream heat exchanger pressure drop

3.4 Effect on the Overall Helium Refrigeration Process

Although using the pressure drop available in the *(h)* stream in the counter-flow heat exchange with the sub-atmospheric load return stream to harness the pseudo-fluid property of an equivalent expansion efficiency increases the load capacity (for the same mass flow rate to the load, or conversely decreases the mass flow rate to the load for a given load), it comes with a penalty since it is not work extraction.

Referring to Figure 3.6, there are five major components to a 2 K system that uses (only) cryogenic-cold compression (i.e., no ambient temperature vacuum pumps) to process the sub-atmospheric flow from the load. In Figure 3.6, the "compressors" are typically oil cooled rotary screw compressors which operate in ambient conditions, unlike the cold compressors in the "2-K CBX". The "4.5 K CBX" (CBX = cold box), which uses the availability given by the compressors, produces refrigeration at nominally 4.5 K. It houses counter-flow heat exchangers and (usually) turbines, among other items. The supply from it is typically around 3 bar and 4.5K, although in smaller refrigerators the supply pressure (and temperature) can be somewhat higher (~12 bar) or, conversely, sometimes even lower (~1.4 bar). The distribution carries the helium supply to the load. As discussed previously, it is best to locate the 4.5 to 2 K heat exchanger at the load. The flow from the load is conveyed back through the distribution to the "2-K CBX". This houses the (cryogenic-)cold compressors, which are typically centrifugal machines. For large size sub-atmospheric helium refrigerators (approx. 1 kW at 2 K or greater) it is practically advantageous to use cold compressors to bring the sub-atmospheric helium back to positive pressure. The number of stages depends on the mass flow and the total pressure ratio (i.e., the ratio of the positive pressure ~1.2 bar to the load sub-atmospheric pressure, say ~0.031

bar for 2 K). The discharge from the 2-K CBX is injected into the 4.5 K CBX, which recovers the refrigeration from that temperature upward.

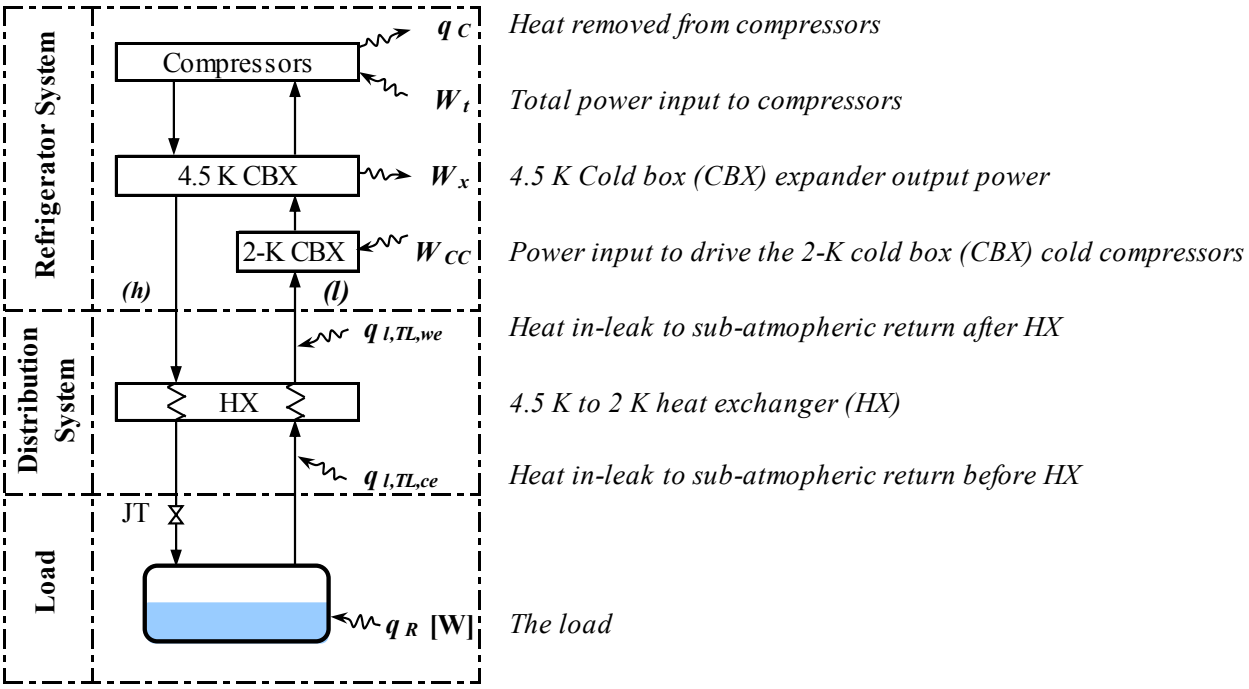

Figure 3.6. General arrangement of a sub-atmospheric (nominally 2 K) helium refrigerator system that uses full cold compression (no vacuum pumps)

So, an elevated temperature of the sub-atmospheric *(l)* stream returning from the load affects the suction temperature of the first cold compressor stage. And, consequently, the discharge temperature from the cold compressors being injected to the 4.5 K refrigerator is elevated. This effect has less consequence on a system which does not use cold compression. That is, one where the sub-atmospheric stream refrigeration is recovered by heat exchange with the supply stream and ambient temperature vacuum pumps are used to process the helium from the load. However, for the same capacity as a system that uses cold compressors, these type of

(nominal) 2-K systems are significantly less efficient and require more space for the equipment (Knudsen and Ganni, Process options for nominal 2-K helium refrigeration system design 2012).

Although the 4.5 K cold box typically handles several different kinds of loads (non-isothermal shield load, 4.5 K liquefaction, 4.5 K refrigeration, cold compressor load, etc.), for simplicity consider a 4.5 K cold box that only handles the load from the cold compressors (as shown in Figure 3.6). The question is, for a given 4.5 to 2-K heat exchanger *(h)* stream pressure drop, what is the net effect on the input power to the 'warm' helium compressors ('W_t' in Figure 3.6)? Examining all the process options for this would be a dissertation in itself. So, instead a specific cold-end process condition will be assumed and the effect of the cold compressor discharge temperature on the input power to the (warm) compressor system will be evaluated. There are three approaches of analysis that were used, from relatively simple to complex:

(a) Simplified 'Carnot-Step' analysis

(b) 'Carnot-Step' analysis (non-simplified), incorporating models for 4.5 to 2 K heat exchanger, distribution, cold compressors and warm compressors

(c) Full process cycle model

Refer to Appendices E to G for more details on each of these approaches and the results obtained. In all cases a baseline load of approximately 5100 W was used, with a pressure at the load of 31 mbar, 2 mbar pressure drop in the sub-atmospheric stream of the 4.5 K to 2 K heat exchanger, 2 mbar pressure drop from this heat exchanger (through the distribution) to the cold compressor suction, 500 W of heat in-leak to the sub-atmospheric stream going back to the cold compressors, five stages of cold compressors with an adiabatic efficiency of 70% each, a 3 bar 4.5 K supply from the 4.5 K cold box, 0.1 bar pressure drop in the supply stream from the 4.5 K cold box to the 4.5 K to 2 K heat exchanger (through the distribution), and a 0.2 K stream

temperature difference at the cold-end of the 4.5 K to 2 K heat exchanger. Table 3.3 presents the overall results, which indicate that the overall process would greatly benefit from incorporating a significant pressure drop in the supply stream of the 4.5 K to 2 K heat exchanger. However, as presented later (Table 4.1), there can be applications where the capacity increase is of greater importance than any potential input power savings.

Table 3.3. Summary of results of various analyses examining the effect of an elevated cold compressor discharge on the overall refrigeration process

Analysis Method	**Input power reduction for the same load: 4.5 K to 2 K HX pressure drop of 2.7 bar compared to 0 bar pressure drop**	**Load increase for same input power: 4.5 K to 2 K HX pressure drop of 2.7 bar compared to 0 bar pressure drop**
Simplified 'Carnot-Step'	4.2%	4.4%
Non-Simplified 'Carnot-Step'	2.8%	3.0%
Full Process Cycle	5.0%	6.1%

3.5 Process Model for Evaluation of Experimental Data

3.5.1 Process Model Description

The process model used to analyze the test data employs real fluid (helium) properties; namely, using HePak v.3.40 (Horizon Technologies n.d.). This software, commercialized by Horizon Technologies (Littleton, CO), uses code developed by NIST (formerly NBS) employees who researched and analyzed helium-I and helium-II properties. It is valid from 0.8 K to 1500 K

and up to 1000 bar, including the saturated liquid/vapor mixtures and the superfluid region. Thermodynamic and thermal transport properties are also available. It uses a single equation of state for all the thermodynamic properties, which is the Helmholtz energy, and is comprised of two additive components; the ideal and real gas contributions (for a non-helium example see Jacobsen (A new fundamental equation for thermodynamic property correlations 1986)). This formulation is an improvement from the 32 term modified Weber-Benedict-Ruben (MWBR) equation of state, also known as the 32 term Jacobsen equation (Jacobsen 1972), which was combined with a real gas specific heat equation to obtain thermodynamic properties (see for example, Younglove (Thermophysical properties of fluids. I. argon, ethylene, parahydrogen, nitrogen, nitrogen trifluoride and oxygen 1982)). The former is like the 'mechanical' ideal gas or Van der Waal state equation (but more complicated) and the later a 'thermal' equation. Unlike the Helmholtz energy equation of state, both of these are needed since neither one by itself is a true equation of state (Callen 1985). Arp and McCarty (Thermodynamic properties of helium-4 from 0.8 to 1500 K with pressures to 2000 MPa, TN 1334 1998) successfully integrated the normal and superfluid state equations into the 32 term Jacobsen equation. Later, (Arp and McCarty 1998) successfully converted the 32 term Jacobsen equation (and specific heat equation) to the Helmholtz formulation (the details of this work were never published), which is the foundation of the HePak code.

Referring to Figure 3.7, the output structure of the process model is as follows:

A. Test #, date, time, nominal heat load and nominal intermediate pressure
B. Stream and temperature level (TL#) matrix for the process, containing temperature (T in K), pressure (p in atm), enthalpy (h in J/g), stream temperature difference (ΔT_{hl} in K), *(l)* minus *(h)* stream enthalpy difference (Δh_{lh} in J/g), and *(h)* stream quality (x_h in %).

Stream information is by column; TL# are by row. *(h)* is the supply stream, *(l)* is the return (sub-atmospheric) stream. Increasing TL# indicates colder temperatures.

C. Diagram of process that matches the stream and TL# matrix.

D. Stream and temperature level (TL#) matrix for the diode measurements, average diode temperature and fractional error to the calculated value.

E. Heat exchanger data: *(h)* stream pressure drop (Δp_h in atm), *(l)* stream pressure drop (Δp_l in atm), heat in-leak (q_k in W), duty (q in W), ratio of heat exchanger duty to total (both heat exchangers) duty (in %), duty check (i.e., *(h)* stream duty must equal *(l)* stream duty), net thermal rating ((UA) in W/K), ratio of heat exchanger net thermal rating to total (sum of both heat exchangers) (in %), number of transfer units (NTU), ratio of heat exchanger NTU's to total (sum of both heat exchangers) (in %).

F. Heat exchanger pressure drop estimates (reported results from another sheet): *(h)* stream pressure drop (Δp_h in atm), *(l)* stream pressure drop (Δp_l in atm), fractional error to current input (in block "E"), *(h)* stream heat exchanger duty (q_h in W), *(l)* stream heat exchanger duty (q_l in W), duty calculated from '*HX_Anal*' code (q in W). See Figures J.2 and J.3 for a sample calculation of *(h)* and *(l)* stream pressure drop.

G. Inputs: measured mass flow rate ($\dot{m}$ in g/s), zero offset for mass flow measurement ($\delta\dot{m}$ in g/s), liquid vessel heat input ($q_{L,htr}$ in W, i.e., power read-back from PLC), and *(l)* stream quality leaving vessel ($x_{l,6}$ in %).

H. Plot of heat exchanger cooling curve: *(h)* stream temperature profile, *(l)* stream temperature profile, and *(h)* to *(l)* stream temperature difference; vs. % total *NTU*'s.

I. JT-1 valve flow coefficient and percent open estimates.

J. Vessel (liquid) accumulation inputs (not used for steady state).

In general a light yellow cell indicates an input (from the user). Regarding the stream and temperature level matrix, the convention used herein for variable nomenclature is, for example, the temperature of the *(h)* stream at TL#1 is denoted as $T_{h,1}$; equivalently it can be referred to as the temperature at (h, 3). The process model output for all test cases is included in Appendix Q following the designation in block "A" (Figure 3.7).

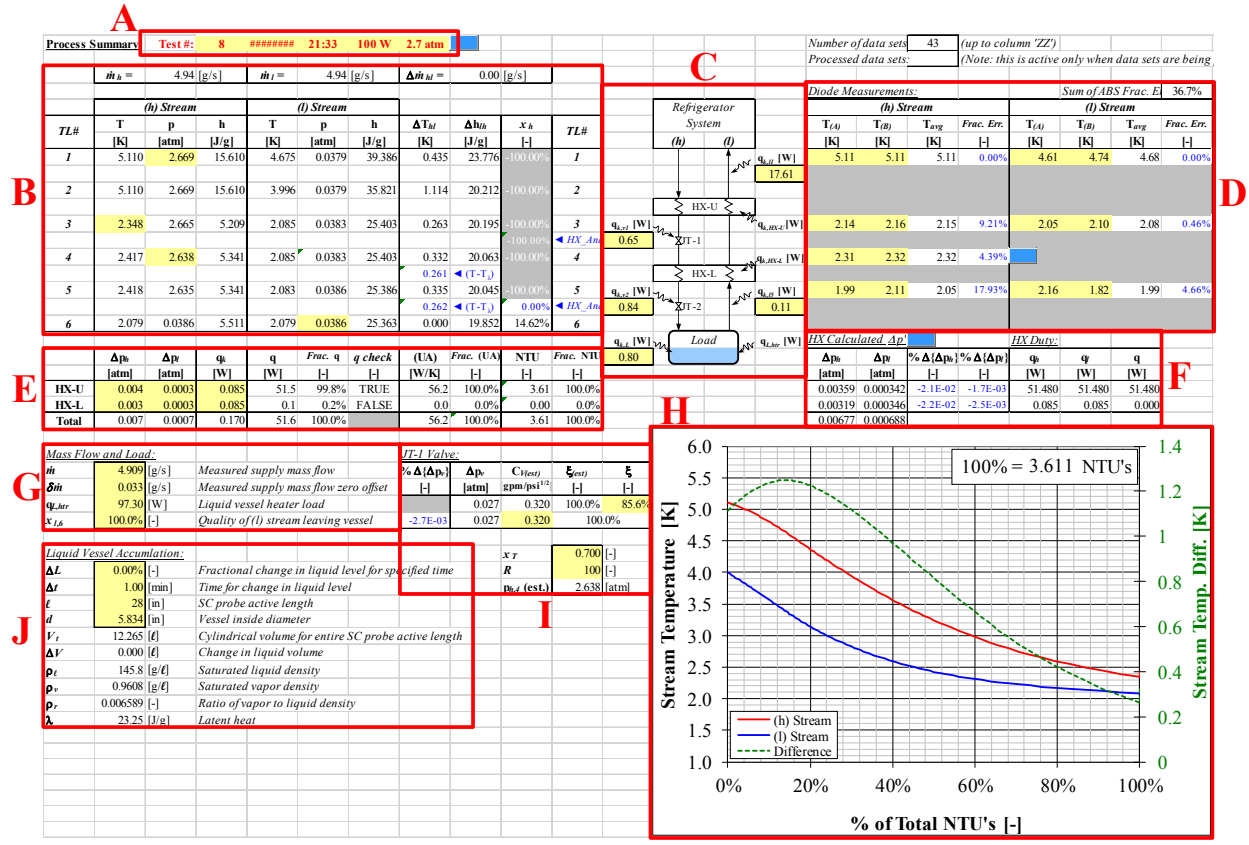

Figure 3.7. Output structure of process model [8]

The model assumes that the following are known (specified):

1. Mass flow; $\dot{m}$ [g/s]

[8] This figure is just to show the various areas in the process model output; refer to Appendix Q for details of the output.

2. Heater heat (to liquid vessel); $q_{L,htr}$ [W]
3. All heat in-leaks (liquid vessel, JT valves, heat exchangers);

   $q_{k,L}, q_{k,v1}, q_{k,v2}, q_{k,HX-U}, q_{k,HX-L}, q_{k,l}$ [W]
4. Supply pressure and temperature; $p_{h,1}$ [atm], $T_{h,1}$ [K]
5. Liquid vessel pressure; $p_{h,6}$ [atm]
6. Supply stream temperature at the cold-end of the upper heat exchanger; $T_{h,3}$ [K]
7. Heat exchanger stream pressure drops; $\Delta p_{h,HX-U}, \Delta p_{h,HX-L}, \Delta p_{l,HX-U}, \Delta p_{l,HX-L}$[atm]

The model uses the mass flow and heater heat plus heat in-leak (to the liquid vessel) to calculate the enthalpy flux to the load. Using the vessel (vapor) pressure, the return enthalpy from the load can be found (as the saturated vapor at that pressure). This and the load enthalpy flux yields the supply enthalpy to the load. To determine the conditions on the warm-end of the lower heat exchanger and the cold-end of the upper heat exchanger, in principle any one of the three temperatures ($T_{h,3}, T_{h,4}$ or $T_{l,3} = T_{l,4}$) could be used. However, the conditions to warm-end supply to the lower heat exchanger (h, 4) could be (and many times are) two-phase. Since temperature and enthalpy are poor independent variables for a real fluid, this leaves $T_{h,3}$ and $T_{l,3}$ (and the former was chosen for the model). However, the value used for $T_{h,3}$ can certainly be adjusted to match a given (specified) value for $T_{l,3}$. With the conditions in between the heat exchangers (now) determined, the conditions at the warm-end of the upper heat exchanger can be determined. All process model sheets, including a plot of the 4.5 to 2 K heat exchanger cooling curve, are included in Appendix Q. Input for these sheets was taken (in part) from the data in Appendix P; except for the mass flow as previously mentioned. The process model uses an integrated cooling curve calculation for the heat exchanger (as described in para. 3.5.2), that can

handle a two-phase fluid, and pressure drop estimates for the supply (tube-side) and sub-atmospheric return (shell-side).

3.5.2 Heat Exchanger Cooling Curve Code

The fundamental assumption in the code that calculates the heat exchanger cooling curves is that there are two temperature streams. A '*(h)*' stream which is being cooled (or is at constant temperature), and a '*(l)*' stream that is being warmed (or is at constant temperature). There can be more than one '*(h)*' stream and likewise, there can be more than one '*(l)*' stream. But all the *(h)* streams are at the same temperature at every point, and likewise for the *(l)* streams. So, if the *(h)* stream is two-phase at any point, there must be only one *(h)* stream; likewise for the *(l)* streams. This is checked upon entry to the code at the boundaries (i.e., warm-end and cold-end) and as the internal temperatures are being calculated. It can handle four configurations:

1. Counter-flow – the convention is the *(h)* and *(l)* stream mass flows are positive in this configuration.
2. Parallel flow – the convention is the *(h)* stream mass flow is positive and the *(l)* stream mass flow is negative for this configuration.
3. Constant *(l)* stream temperature cooling – the *(h)* stream mass flow must be positive and the inputs for the *(l)* stream are permissible but irrelevant, except for the inlet temperature (which is constant from inlet to outlet). This is a boiler.
4. Constant *(h)* stream temperature cooling – the *(l)* stream mass flow must be positive and the inputs for the *(h)* stream are permissible but irrelevant, except for the inlet temperature (which is constant from inlet to outlet). This is a condenser.

The *(h)* stream must always have a positive mass flow input. But the *(l)* stream may be either (as described above). The inlet can be specified to be two-phase for either or both *(h)* and *(l)* streams. And, one of the outlet conditions may be specified to be two-phase. Either the warm-end or the cold-end *(h)* to *(l)* stream difference is given (i.e., non-zero and non-negative), but not both. If the outlet is specified as two-phase, the stream temperature difference that is given (warm or cold-end) determines the meaning of this input. The BOILER=TRUE designation in the code can signify either a constant *(l)* or constant *(h)* stream temperature; i.e., configuration 3 or 4. The *(h)* to *(l)* stream temperature difference that is provided determines which is assumed; i.e., a warm-end stream temperature difference is a constant temperature *(h)* stream (condenser) or configuration 4, and a cold-end temperature difference is a constant temperature *(l)* stream (boiler) or configuration 3. For either configurations 3 or 4, the non-constant temperature stream may be specified as two-phase. However, there is an interesting situation that the code will exit with an error (indicating that the *(l)* stream is cooling); namely, when the *(l)* stream is two-phase and experiencing a pressure drop. This is not a problem for the *(h)* stream, which will cool under this condition. But thermodynamics demands that a pure fluid that is two-phase and has its pressure lowered requires the removal of heat (cooling). This was encountered when examining the effect of two-phase in the sub-atmospheric return. However, since the *(l)* stream pressure drop is usually quite small in most situations, this can be circumvented be specifying zero pressure drop.

The code subdivides a selected stream by its enthalpy into 'N' sub-divisions, from index, $i = 0$ (the warm-end) to $i = N$ (the cold-end). This selected stream is the first stream (in sequential input order) whose inlet or exit conditions is two-phase; otherwise, the first *(h)* stream is selected. This selected stream is the 'marching' stream. The sub-division can be by equal

increments (DT_Type = TRUE), or by an equal ratio between steps (DT_Type = FALSE); although by enthalpy and not temperature. In this way, since the conditions at '*i*-1' are known, and all but one are known at '*i*', the unknown can be calculated by an energy balance. However, for more than one stream (e.g., if there are two *(l)* streams, or two *(h)* streams, and these are the unknown), this must be done by iteration since the enthalpy of the two streams are not necessarily equal (unless they are the same fluid and at the same pressure), although the temperature is equal. This calculation is handled in the 'HX_T1" code and is foundational to the cooling curve code. A heat in-leak, 'qLK' may be input and is distributed equally with respect to the 'marching' stream enthalpy.

The 'HX_Anal' routine checks user input and sets-up the input needed for the 'HX_UA_NTU' routine, which actually performs the sub-division and ensuing integration. The 'HX_T_out' routine is used by the 'HX_UA_NTU' routine to calculate the unknown outlet temperature. 'HX_Anal' returns the outlet temperatures, duty, thermal rating *(UA)*, *NTU*'s and the outlet qualities. It should be noted that the convention used for the value of the quality, other than the obvious when it is two-phase (i.e., between 0 and 1), is to assign a value of 3 if the fluid pressure and temperature are equal or greater than critical. Or, assign a value of -1 if the fluid pressure is equal or greater than critical but the temperature is less than critical. Otherwise, if it is not two-phase, and the fluid pressure is less than critical it will assign a value equal to the enthalpy minus the saturated liquid enthalpy, divided by the latent heat. So, in this case, the quality will be less than zero in some continuous manner or greater than one in some continuous manner.

The 'HX-T1' code relies upon a simple energy balance and initially employs the Newton-Raphson method. If this puts the solution outside of the valid temperature bounds, then a mid-

point is selected and the Newton-Raphson method continues. If it is deemed not to be converging, in that the objective function is not successively decreasing, it will attempt to switch to the bi-section method as long as it determines that the solution has been bounded. If not, it will exit on an error. This 'HX_T1' code can handle a two-phase condition and returns the result of the calculated quality.

A listing of the cooling curve code, 'HX_T1' and the 'HX_Anal' code is provided in Appendix H and I, respectively. It is written in Visual Basic (for Applications; i.e., VBA).

3.5.3 Static Heat In-Leak

There are eight locations to consider the static heat in-leak to the test apparatus from ambient temperature:

1. To the *(h)* stream, upstream of the inlet to the upper heat exchanger
    a. 1-1/2 in. JLab style bayonet ("D1")
    b. Line from RV2470
2. To the *(h)* stream, in between the lower and upper heat exchanger
    a. EV2471
    b. Line from RV2472
3. To the *(h)* stream, in between the outlet of the lower heat exchanger and the vessel
    a. Line from 1-1/2 in. JLab style bayonet ("D2")
    b. EV2473
4. To the liquid vessel
    a. Heater wires
    b. Line from high side of DP2473

c. Liquid level probe

d. Radiation

e. Support wires

5. To the *(l)* stream, upstream of the inlet to the lower heat exchanger

    a. Line from 1/4 in. capped port; two places

    b. Line from high side of DP2476

6. To the *(l)* stream, downstream of the outlet of the upper heat exchanger

    a. 3-1/8 in. JLab style bayonet

    b. Line from RV2477

    c. Shield load

7. To the upper heat exchanger

    a. Radiation

    b. Support wires

8. To the lower heat exchanger

    a. Radiation

    b. Support wires

Except for 4(c), 4(d), 7(a), and 8(a), all of these heat in-leaks are due to conduction through piping, tubing, braid, and wires. For the shield load, 6(c), the radiation intercepted by the copper in between the vacuum shell and inner piping and components, is conducted via. copper braided straps to the sub-atmospheric 2 IPS line exiting the test can through the 3-1/8 in. bayonet “D4” connection. Heat in-leak to this location should not affect CTD2477. However, CTD2477 was observed to be higher than CTD2470 (the supply stream inlet temperature to the test can) in many instances during conditions known to be steady, which could have been due to

the location of the diode wire thermal anchor. However, this diode (CTD2477) is not used for the thermal calculations, so the heat in-leak calculations are not presented. Likewise, the heat in-leak to location #1 should not affect CTD2470 since it is sufficiently downstream of the heat in-leaks due to the 1-1/2" bayonet-coupling and the connection to RV2470; so, heat in-leak calculations are not presented for this location.

Table 3.4. Super-conducting probe heat in-leak

Variable	Value	Unit	Description
L	76.2	[cm]	*Active and exposed length of probe*
ξ	65.0%	[-]	*Liquid level*
L_G	26.7	[cm]	*Length of probe exposed to vapor (normal conducting, resistive zone), = (1-ξ)·L*
v_{nrz}	20.0	[cm/s]	*Normal resistive zone propagation velocity*
Δt	1.33	[s]	*Time for normal resistive zone to propagate to liquid (surface), = L_G / v*
i	0.0750	[A]	*Wire current*
R_{htr}	5.00	[Ω]	*Heater resistance (at top of probe)*
q_{htr}	0.0281	[W]	*Power produced by heat (at top of probe), = $i^2 \cdot R_{htr}$*
R_{nrz}	4.55	[Ω/cm]	*Wire (Nb-Ti) normal resistive zone resistance per unit length at 20 K*
q_{nrz}	0.341	[W]	*Power produced during propagation of normal resistive zone to liquid, = $i^2 \cdot R_{nrz} \cdot L_G / 2$*
q_t	0.369	[W]	*Total power produced until normal resistive zone propagation reaches liquid, = $q_{htr} + q_{nrz}$*

The heat in-leak from the liquid level probe, 4(c), is due to the heat generated by current flow in the normal resistive (non-superconducting) part of the Niobium-Titanium (Nb-Ti) wire. The AMI Model 135 has a feature that automatically senses when the resistive zone reaches the liquid helium, which prevents the current from being on 100% of the time, even when switched

to the 'continuous sample' mode. Consequently, the heat in-leak is linear with respect to the probe length exposed to the vapor and in this specific installation, it turns out to be about 1 W at 0% liquid level (and about 0 W at 100% liquid level). Table 3.4 shows a sample calculation for a liquid level of 65%, which was a low end value during testing (i.e., but a 'high-end' estimate for heat in-leak).

In the case of conduction heat in-leak, there is a temperature gradient from ambient to the cold temperature. The thermal conductivity cannot be assumed a constant, as it varies considerably. The solution is found by integrating the material thermal conductivity with respect to temperature (which it is a function of), so that the heat in-leak is found by simply multiplying the integrated thermal conductivity, K [W/in], by a 'shape factor'. In this case the appropriate shape factor is the cross-sectional area (perpendicular to the heat flow) divided by the conduction length; i.e., (A_c/L) [in^2/in]. Stainless steel 304 and 316 are commonly used for piping, tubing and structural supports as it does not become brittle at cryogenic temperatures (even below 4.5K), while maintaining its strength. It also provides a relatively good thermal (conduction) resistance, is easy to machine and weld, and is also, relatively inexpensive (say, as compared to Invar). CryoComp, ver. 5.0 (Eckels Engineering, Inc. n.d.) was used to determine the integrated thermal conductivity of 304 stainless steel and copper (wire). This software also has a great many other materials and material properties available. Ambient temperature was assumed to be 300 K. There are two important comments regarding the value for the integrated thermal conductivity. The first is that for metals (pure and alloy), the difference between 300 to ~6 K and 300 to ~2 K is negligible. The second is that for pure metals, the thermal conductivity is highly dependent on the residual resistance ratio, or 'RRR', and increases with increasing RRR (see for example, (Hust and Lankford 1984)). For typical copper conductors, the RRR is

typically 60 to 100, consequently, the integrated thermal conductivity is 4300 to 5000 W/in. The RRR does not govern the integrated thermal conductivity for alloys. So, the integrated thermal conductivity for 304 stainless steel (SST) is 78.0 W/in from 300 to 4.5 K. Table 3.5 summarizes the pertinent conduction heat in-leaks. All items in Table 3.5, except 4(a) (i.e., the heater wire) which is copper, are 304 stainless steel.

Table 3.5. Test apparatus conduction heat in-leaks

Location #	**Description**	**Shape Factor [in^2/in]**	**Heat In-Leak [mW]**
2(a)	Tube: 3/4 in. OD x 0.028 in. wall x 22 in. long, in parallel with, Tube: 7/8 in. OD x 0.035 in. wall x 22 in. long	7.09E-03	553
2(b)	Tube: 1/2 in. OD x 0.035 in. wall x 40-1/2 in. long	1.26E-03	98.5
3(a)	Male Tube: 1-1/2 in. OD x 0.035 in. wall x 25-1/4 in. long, in series with, Pipe: 1/2 IPS Sch. 10 x 22-3/4 in. long	3.68E-03	287
3(b)	Same as 2(a)	7.09E-03	553
4(a)	Wire: (8 ea.) 16 AWG (0.0508 in. dia.) x 55 in. long	2.95E-04	1268
4(b)	Tube: 1/4 in. OD x 0.035 in. wall x 43-3/4 in. long	5.40E-04	42.1
4(e)	Wire: (4 ea.) 0.024 in. dia. X 21-1/4 in. long	8.52E-05	6.64
5(a)	Tube: 1/4 in. OD x 0.035 in. wall x 45 in. long, in parallel with, Tube: 1/4 in. OD x 0.035 in. wall x 34 in. long	1.22E-03	95.2
5(b)	Tube: 1/4 in. OD x 0.035 in. wall x 94-3/4 in. long	2.50E-04	19.5
7(b)	Same as 4(e)	8.52E-05	6.64
8(b)	Same as 4(e)	8.52E-05	6.64

The estimate for the radiation heat flux [W/m^2] to the heat exchangers and vessel are based upon (Barron, Cryogenic systems 1985, 34-36) and experience from actual systems (to adjust the parameters) and is shown in Table J.1 in Appendix J. Radiation heat in-leak to the piping is neglected. As indicated in Figure 4.13, the shield temperature was believed to be around 33 K, which is estimated to result in a heat flux of 0.194 W/m^2. The surface area for the Collins-type heat exchangers is 680.4 in^2 (each) and for the vessel, 640.9 in^2. So, the heat in-leak due to radiation is about 85.2 mW to the heat exchangers (each) and 80.2 mW to the vessel.

As discussed in Chapter 4.1, the total heat in-leak to the liquid vessel was measured by a boil-off test (in fact, several tests), which indicated a value of about 0.80 W. This value is considerably lower than the sum of 4(a) through 4(d), which is 1.77 W. This would indicate that the heater wires were, in effect, thermally anchored, causing the heat in-leak difference (of roughly 1 W) to go elsewhere (than into the vessel liquid).

3.5.4 Collins Heat Exchanger (How Counter-Flow Is It?)

Collins-type heat exchangers are overall counter flow heat exchangers and can be quite effective. However, due to the low angle helical wrap, the sub-atmospheric (or lower pressure) flow approaches the supply (i.e., higher pressure) stream in a cross-flow manner. This flow configuration has been labeled as cross-counter flow (Hausen 1983), and can approach pure counter flow if sufficient passes are used. For the Collins-type heat exchanger, the sub-atmospheric (shell side) flow is not required to be well mixed after passing over each coil-wrap and will likely tend to follow the direction imparted by the fins; which forms a high angle helix. Obviously, the actual degree of mixing in a real Collins-type heat exchanger will be somewhere in between unmixed and well-mixed in between each coil. Appendix K contains the derivation

of the case where the sub-atmospheric (shell side) is well-mixed in between each coil, with a compact closed form result.

It should be stated that the author developed the solution for the well mixed case and later found that this had been already done (Hausen 1983, 232-248). However, the author believes that the approach use herein, although less compact than (Hausen 1983), is more easily followed. The results assuming constant stream capacity for a well-mixed and an unmixed sub-atmospheric flow are quite close. A comparison is included in Appendix L (with a description in the latter part of Appendix K) for the case of balanced flow (i.e., equal stream capacities) and was done using Mathematica, such that an analytical solution for the unmixed case is found for the cases of 1 to 5 coils. Balanced flow demands the highest heat exchanger effectiveness. A solution for more than 5 coils is easily obtainable given sufficient computational time. As can be seen, the unmixed solution complexity grows quickly and so far, defies a compact solution (per the literature surveyed and as attempted by the author).

3.5.5 Shell and Tube Pressure Drop Estimates

In Collins-type heat exchangers, the pressure drop (and heat transfer) through the tube is well established by literature. Consideration must be given to the aspect of the coil geometry which results in a secondary flow induced by the centrifugal force (because the coil is curved). Additional non-dimensional numbers such as the Dean number, or the helical number are introduced into the friction factor and heat transfer correlations. However, the tube used in the heat exchanger for the test apparatus contained a twisted copper ‘tape’ (strip, or ‘turbulator’). It was assumed that any effect due to the much wider radius of the coil would be nullified by the short twist radius of the tape. The correlation found in Ebadian and Dong (Forced convection,

internal flow in ducts n.d.) was used for this analysis, and the average pressure drop calculated at the warm-end and cold-end conditions was used. Table J.2 shows a typical calculation, and in this particular case, the one for test #33 (80 W 0.2 atm 31-Dec-14 19:36).

While there has been extensive research done on banks of finned tubes in cross-flow (for example, see Rabas and Taborek (Survey of turbulent forced-convection heat transfer and pressure drop characteristics of low-finned tube banks in cross-flow 1987)), very little predictive tools exist for the design and analysis of a Collins-type heat exchanger; specifically the shell side. Collins used these extensively (for example, Collins (Refrigeration at temperatures below the boiling point of helium 1968)); however, he did not publish any correlations regarding his designs. Pressure drop tests were conducted at JLab for these heat exchangers, and this data was used for the pressure drop estimates (Hasan and Knudsen 2016). Appendix M is a survey of known pressure drop and heat transfer correlations for the shell side of the Collins-type heat exchanger. Table J.3 presents the calculations that follow the method given by Hasan and Knudsen (Shell-side pressure drop measurement in a Collins-type 4.5K-2K heat exchanger, JLAB-TN-16-036 2016) for test #33 (80 W 0.2 atm 31-Dec-14 19:36). As will be observed in Appendix M there exists a number of definitions for the free flow area, heat transfer surface area, and hydraulic radius from which the correlations for fraction factor and heat transfer are based.

3.5.6 Axial Conduction

The general definition of heat exchanger effectiveness is the actual duty (i.e., total heat transferred between the cooling and warming streams) divided by the maximum possible duty. For the case of constant stream capacities, this is the condition where the minimum capacity stream outlet temperature reaches the maximum capacity stream inlet temperature (which would

require an infinite heat exchanger length). However, for the case of variable specific heat, the maximum possible duty condition could be one such that the stream temperature difference at a particular end (either warm or cold end) creates an internal stream temperature 'pinch'; that is, the difference is zero somewhere along the heat exchanger length, but not necessarily at one of the ends.

The thermal conductivity integral for a (solid) material is,

$$\mathrm{K} = \int_{T_1}^{T_2} k(T) \cdot dT \qquad \text{(Eq. 3.11)}$$

where, T_1 and T_2, are the temperatures of the heat exchanger material at the cold and warm ends, respectively; and, $k(T)$ is the material thermal conductivity (which is a function of temperature). So, if the thermal conductivity of the heat exchanger material does not vary greatly between the two ends, it makes sense to define an integrated average thermal conductivity,

$$\bar{k} = \frac{\mathrm{K}}{\Delta T} \qquad \text{(Eq. 3.10)}$$

where, $\Delta T = T_2 - T_1$.

The one-dimensional heat conduction through a material with $k(T)$ and cross-sectional area A_c, and length L, with one end at temperature T_2, and the other at T_1, is,

$$q_c = \mathrm{K} \cdot \frac{A_c}{L} = \frac{\bar{k} \cdot A_c}{L} \cdot \Delta T \qquad \text{(Eq. 3.12)}$$

The heat exchanger material axial conduction parameter is (Kays and London 1998),

$$\lambda = \frac{\bar{k} \cdot A_c}{L \cdot C_{min}} = \frac{q_c}{C_{min} \cdot \Delta T} = \frac{q_c}{q_{max}} \qquad \text{(Eq. 3.13)}$$

where, q_{max}, is the maximum possible heat exchanger duty, if T_1 and T_2 are taken as the stream inlet temperatures (for counter-flow heat exchange). So, λ is really the heat exchanger ineffectiveness, $(1-\varepsilon)$, due to the axial conduction through the heat exchanger material.

Table 3.6. Collins heat exchanger material axial conduction between 6 K and 2 K

	A_c [in^2]	**L [in]**	**K [W/in]**	**q [mW]**
Coil	0.06943	283.3	0.7777	0.191
Twisted Tape	0.006030	283.3	64.24	1.367
Shell	2.700	18.00	0.02400	3.600
Mandrel	1.152	18.00	0.02400	1.536
Total				6.694

Referring to Table 3.6, for the Collin's heat exchanger tested, the material conduction heat transfer can be conservatively estimated by assuming, $T_1 = 2$ K and $T_2 = 6$ K (i.e., as if the entire, temperature span occurred over the upper or lower heat exchanger). The coil is a ½ in. OD x 0.049 in. wall tube, composed of 16 coils with a mean diameter of 5.625 in. and a pitch (equal to the fin outside diameter) of 1.125 in. It is made of C122 phosphorous-deoxidized annealed copper (refer to Powell, et al. (Low temperature thermal conductivity of some commercial coppers 1957)). The twisted tape tube insert is a 0.335 in wide by 0.018 in. thick strip, twisted on a helical pitch of 8 (360°) turns per foot. It is presumably made of C110 (electrolytic-tough-pitch, with a 'RRR' of 100, to be conservative). Due to the helix, its length is greater than the tube length, but is taken as being the same (which is conservative). The shell is

a 7 in. OD x 0.125 in. thick wall tube, made of ASTM A269-304/304L stainless steel. And, the mandrel is a 4 IPS sch. 5 pipe (i.e., 4.500 in. OD x 0.083 in. thick wall), made of ASTM A312-TP304/304L. The effective length for both shell and mandrel is taken as the coil height (which is 16 times the pitch of 1.125 in, or 18 in.). With the exception of the coil material, the integrated thermal conductivities were obtained using CryoComp (version 5.1 for Windows). The reference for the coil integrated thermal conductivity was previously given by Powell, et al. (Low temperature thermal conductivity of some commercial coppers 1957).

The lowest duty testing was around 20 W, so keeping with the initial assumption for the axial conduction estimate, this gives an axial conduction parameter of, $\lambda \cong 0.00034$. Kroeger (Performance deterioration in high effectiveness heat exchangers due to axial heat conduction effects 1966) considered the effect of axial conduction on the heat exchanger effectiveness. Although his analysis was for constant (not variable) capacity streams, we can still ascertain whether the axial conduction in this case is significant to the heat exchanger performance). Taking the worst case of a balanced flow (i.e., stream capacities are equal), the fractional deterioration in heat exchanger effectiveness is roughly equal to the axial conduction parameter. That is, if the effectiveness of the heat exchanger without axial heat conduction is ε, and the difference between this and a heat exchanger which has axial heat conduction is $\delta\varepsilon$, then the ratio $(\delta\varepsilon/\varepsilon) \approx \lambda$. Or, in this case, $(\delta\varepsilon/\varepsilon) \approx 0.034\%$. Further, keeping in mind that for unbalanced flow, the effect of axial conduction decreases, we will take note that for this application of supercritical or saturated liquid helium at around 4.5 to 6 K and sub-atmospheric helium (16 to 41 mbar) at similar temperatures, the flow is unbalanced. In particular, the sub-atmospheric stream will tend to have a higher specific heat (and so, a higher capacity rate, since supply and return mass flow rates are the same). That is why, the heat exchanger will 'pinch'

(have a minimum stream temperature difference) at or toward the cold end. Also, since we are only expecting a maximum *NTU* of around 5, the effectiveness of this heat exchanger is less than 95% (and more like 90%). Therefore, we can neglect the effect of axial heat conduction through the heat exchanger material.

4. EXPERIMENTAL RESULTS AND ANALYSIS

4.1 Load Enthalpy Flux

The load enthalpy flux measurement requires:

1. Steady conditions (no depletion or accumulation of mass; nothing is warming and cooling with respect to a fixed spatial position)
2. Mass flow rate measurement
3. Heat load measurement into the liquid vessel; this consists of two parts, (a) heater and (b) heat in-leak

Steady conditions are obtained by ensuring a constant vessel liquid level and pressure, and heat exchanger temperatures (i.e., they are not changing significantly with respect to time). Of course, in reality, there are small variations, but they should be small and the moving average constant. Since the supply flow is a dense fluid [9], and the heat exchanger, piping and vessel material specific heat capacity is quite low [10], it took several hours to transition from each data point and establish steady conditions (i.e., at each heater and intermediate pressure setting). It was necessary to manually adjust valves since the PID loop control is not sensitive enough to establish a steady condition required for measurement, keeping in mind that no more than a 10% flow variation was expected for a given heat load as the intermediate pressure was varied. Also, although the Coriolis mass flow measurement is not dependent on the process fluid pressure or temperature, it was observed even during 'steady' conditions to vary a little. This is summarized

[9] Density at 2.8 bar and 5 K is 116 g/ℓ, compared to 120 g/ℓ for saturated liquid at 1.25 bar; but the fluid is still compressible, with an isothermal compressibility of 0.084 bar^{-1}, as compared to 0.00036 bar^{-1} for liquid nitrogen at 1.4 bar and 80 K, or 0.000045 bar^{-1} for water at 1 bar and 300 K.

[10] 304 stainless steel heat capacity is ~0.0024 J/g-K at 5 K vs. 0.48 J/g-K at 300 K.

in Appendix N, showing the minimum, average, maximum and standard deviation during the 'steady' condition period. The red rows are the reduced data (refer to further paragraphs). The average value is used in the process model calculations.

The heat in-leak to the liquid vessel was measured by (sub-atmospheric) boil-off tests. These tests were accomplished by filling the vessel at a sub-atmospheric condition, then shutting both JT valves (to ensure no leakage) and logging the liquid level vs. time (while maintaining a sub-atmospheric condition). The plots of liquid level vs. time and heat in-leak calculations are given in Appendix O. A 'middle' section of the vessel was selected to assure a cylindrical geometry. The slope was calculated using both a linear (least squares) regression (using Rscript) and just the start and end points. The latter was used for the heat in-leak calculation, since the linear regression will be slightly affected by the occasional 'step change' type behavior of the super-conducting liquid level probe. Also, the higher of the two values is used (0.80 W as opposed to 0.77 W).

Knowing the total heat input to the liquid vessel, comprised of the heater heat ($q_{L,htr}$) and the heat in-leak ($q_{k,L}$), and knowing the mass flow ($\dot{m}$), the enthalpy flux (to the liquid vessel) is found,

$$\Delta h_{lh,6} = \left(q_{L,htr} + q_{k,L}\right)/\dot{m} \qquad \text{(Eq. 4.1)}$$

This is the crucial part of the test. Note that the mass flow is the measured value corrected by the flow offset, discussed in paragraph 4.3. It is also of interest to roughly quantify the performance of the upper and lower heat exchangers, so that further insight into the test results may be possible. As mentioned previously, it is recognized that the diode measurements are not highly accurate, but are expected to be consistent.

The accuracy of the vessel heater and the Coriolis mass flow meter were derived and discussed in Chapter 2. They were found to be approximately,

$$\delta_{\dot{m}} = \frac{0.0443\ g/s}{\dot{m}} + \varepsilon_{\dot{m}} \qquad \text{(Eq. 4.2)}$$

$$\delta_P = \frac{0.133}{\sqrt{P}} \qquad \text{(Eq. 4.3)}$$

The heat in-leak 'accuracy' can be roughly quantified by difference between the two measurements presented, which is, 0.03 W. So, the total heat load accuracy is about,

$$\delta_q = \delta_P + \delta_k = \frac{0.133}{\sqrt{P}} + \frac{0.03}{P} \qquad \text{(Eq. 4.4)}$$

For the range of (nominal) heat loads tested (i.e., 30 to 100 W), the heat in-leak term is about 2.2% to 4.0% of the total heat accuracy. Temporarily adopting a slightly less cumbersome notion, the accuracy of the enthalpy flux can be expressed as,

$$\Delta h + \delta(\Delta h) = \frac{(q + \delta q)}{(\dot{m} - \delta\dot{m})} = \frac{q \cdot (1 + \delta_q)}{\dot{m} \cdot (1 - \delta_{\dot{m}})} \qquad \text{(Eq. 4.5)}$$

Using a Taylor series expansion for the term in the denominator, neglecting second order terms, and simplifying,

$$\delta_{\Delta h} = \frac{\delta(\Delta h)}{\Delta h} = \delta_{\dot{m}} + \delta_q = \left(\frac{0.0443}{\dot{m}} + \varepsilon_{\dot{m}}\right) + \left(\frac{0.133}{\sqrt{P}} + \frac{0.03}{P}\right) \qquad \text{(Eq. 4.6)}$$

So, at the test extremes; $\dot{m} = 1.5$ g/s, $q = 30$ W, and, $\dot{m} = 5.0$ g/s, $q = 100$ W, the load enthalpy flux accuracy ranges from (3.5% + 2.5% =) 6.0% at the low mass flow end to (1.2% + 1.4% =) 2.6% at the high mass flow end. However, as discussed in Chapter 2, it is unlikely that all of the inaccuracies would combine, rather than cancel. So, using the alternate equations presented in Chapter 2,

$$\tilde{\delta}_{\Delta h} = \tilde{\delta}_{\dot{m}} + \tilde{\delta}_q = \frac{0.0339}{\dot{m}} + \frac{0.120}{\sqrt{P}} \qquad \text{(Eq. 4.7)}$$

In this case, the load enthalpy accuracy ranges from (2.3% + 2.2% =) 4.5% (at the low mass flow end) to (0.7% + 1.2% =) 1.9% (at the high mass flow end).

4.2 Testing and Data

The test data are organized by nominal heat load (30, 40, 60, 80, 100 or 120 W) and by the nominal intermediate pressure; that is, the approximate set point value as indicated by CPI2472DEV (i.e., the 'high' range transducer). "Low" (see Appendix N) for the nominal intermediate pressure indicates that the intermediate pressure was allowed to go as low as the back-pressure would allow (i.e., an intermediate pressure set point was not imposed by the valve control loop).

The vessel (vapor) pressure, CPI2474 (which is the low range transducer), is assumed accurate. Below (but not including) a set point for CPI2472DEV of 1.3 atm, CPI2472 was used for the intermediate pressure; which cannot read above 1.31 atm. CPI2472DEV was noted to be greater than CPI2470 for cases were there was no imposed pressure drop across CEV2471 (JT-1); i.e., nominal 2.7 atm intermediate pressure cases. CPI2470 seemed more consistent with the supply pressure profile at the CTF. As such CPI2472DEV was only used for the nominal 1.3 atm intermediate pressure cases. For the nominal 2.7 atm cases, the pressure at (h, 4) was taken as CPI2470 minus the estimated pressure drop through the upper heat exchanger.

The differential pressure measurement across the upper and lower heat exchangers for the sub-atmospheric stream was not reliable, nor accurate.

The liquid vessel had a super-conducting liquid level probe and a differential pressure measurement for the liquid level. The lower tap (to the liquid vessel) must be designed to ensure that a stable meniscus can form. Some amount of heat in-leak (very small for helium) is required to allow this to occur and the heat in-leak can be from a lower temperature source (like a thermal shield) rather than ambient (300 K). In this case, the heat in-leak was anchored by the shield

(~33 K) and was too high to allow a stable meniscus. So, the super-conducting liquid level probe was used.

Although the diodes located on the sub-atmospheric line downstream of the upper heat exchanger (CTD2477) should have not been significantly influence by the thermal anchoring connections to the copper radiation shield, they appeared to be affected more than anticipated. This measurement was not used (or needed) in evaluating the heat exchanger performance.

The original configuration for the thermal anchoring of the copper shield was modified to result in shorter copper braid lengths and to distribute them more evenly on the copper shield. However, the diode installed on the copper shield (CTD2479) failed and was not functional during testing. Prior to these modifications, the apparatus was cooled down for some initial check-outs, and the shield temperature during cool-down was measured.

In practice, it was found that it was difficult to establish a stable measurement below 30 W due to the CTF distribution system. At high loads, the limit on the liquid-vapor separation in the vessel was reached, such that a stable measurement could be taken for 100 W, but it became much more difficult at 120 W. At loads greater than 120 W, and certainly by 145 W, the supply temperature would cool-down to ~2.7 K (as indicated by CTD2470).

4.3 Data Analysis and Reduction

The process model results for the test data in Appendix P is presented in Appendix Q. The flow offset ($\delta\dot{m}$) was adjusted to 0.0325 g/s so that the *(h)* stream outlet temperature from the lower heat exchanger is not below lambda. The controlling test condition for this was the nominal 80 W and 0.2 atm intermediate pressure (31-Dec-14 19:36) test (#33); which was the most negative uncorrected (minus 0.018 K). This offset was previously reported by Knudsen

and Ganni (Testing of a 4 K to 2 K heat exchanger with an intermediate pressure drop 2015) as 0.0277 g/s because the data were only partially analyzed. It is still within the range of one sigma of the mass flow variation.

In some instances, the temperature at (*h*, 3) (which is a process model input) was adjusted so that there would not be a negative heat exchanger duty (which is not plausible for steady conditions).

The nominal 120 W and 2.7 intermediate pressure test (30-Dec-14 13:15, test #9) was neglected since the model predicts heat exchanger temperature cross-overs which is only possible during cool-down. And, the plot of the test data would seem to indicate that steady conditions were not prevalent.

The nominal 40 W and 60 W tests at a (nominal) 0.3 atm intermediate pressure (7-Feb-15 15:25 and 21:0, and test #23 and #24, respectively) were neglected since the mass flow is not consistent with the other test data and would result in an enthalpy flux greater than physically possible; 27.4 J/g for test #23 and 24.9 J/g for test #24. Over the all tests, the range of measured vessel pressure varies from 0.0316 to 0.0391 atm, with a maximum latent heat of 23.4 J/g. This result was most likely due to a zero drift or loss in zero calibration between the December/January tests and these February tests. So, the data from these three tests were disregarded (#9, #23, #24), leaving 40 tests.

As mentioned, to calculate the heat exchanger thermal rating and *NTU*'s, one of the temperatures at (*h*, 3), (*h*, 4) or (*l*, 3) is assumed to be correct, but the temperature at (*h*, 4) is a poor choice since it can be two-phase. So, for all selected tests (40) the two remaining cases were examined. If the (average) diode temperature at (*h*, 3) is assumed to be correct, the process model results show that the average total (sum) absolute value of the fractional error between

model and measured (average) diode temperatures is 31.1% with a standard deviation of 16.7%. That is, the population of the sum of absolute value of the fractional error between the seven diode measurements to what the model predicts for the forty data sets. And, if the average diode temperature at (l, 3) is assumed to be correct, this average is 33.1% with a standard deviation of 18.9%. This would seem to indicate that the model tends to agree well with either assumption. However, for all further analysis of the heat exchanger performance, it was assumed that the average diode temperature at (h, 3) was correct.

For the 40 selected tests, Figure 4.1 shows the calculated load enthalpy flux vs. the actual intermediate pressure; Figure 4.2 shows the calculated load enthalpy flux vs. the *(h)* stream temperature at the cold-end (outlet) of the lower heat exchanger; Figure 4.3 shows the calculated load enthalpy flux vs. the total heat exchanger *(UA)*; and Figure 4.4 shows the calculated load enthalpy flux vs. the total *NTU*'s. From these it is apparent that tests #3, #4, #6, #11, #15-#17, #22, #29, #30, #32 and #35 lay outside of the rest of the results. Appendix R contains a more detailed comparison of these cases. Keeping in mind that it has been assumed for the process calculations that the tests were at steady state, the common differences that the low performing tests exhibited (i.e., tests #3/#4 , #6, #11, #22, #29/#30, #32, and #35) as compared to the tests that match theoretical expectations (i.e., tests #5, #7, #12, #19, #31, #33, and #37, respectively) is as follows:

a. Much greater (>) lower heat exchanger (HX-L) cold-end *(h)* to *(l)* stream temperature difference ($\Delta T_{hl,5}$); over 100% greater in all cases (i.e., 0.33 to 1.40 K greater). This is also true of the lower heat exchanger (HX-L) warm-end stream temperature difference ($\Delta T_{hl,4}$) and the upper heat exchanger (HX-U) cold end stream temperature difference

($\Delta T_{hl,3}$). The upper heat exchanger (HX-U) warm-end stream temperature difference ($\Delta T_{hl,2}$) is also higher but by a lesser, but still significant, amount (8% to 121%).

b. Much lower total net thermal rating (UA) and total number of transfer units (NTU's); i.e., 27 to 67% less for the (UA), and 49% to 84% less for the NTU's.

Additionally, for the test cases with an intermediate pressure ($p_{h,4}$) around 1.3 to 2.6 atm, the lower heat exchanger essentially carried the entire duty; as opposed to the higher performing tests, it was the opposite. At lower intermediate pressures this was not observed from the process calculation results. And, for the test cases with an intermediate pressure ($p_{h,4}$) around 0.4 atm and less, the *(h)* stream quality ($x_{h,5}$) entering the lower heat exchanger (HX-L) for the low performing tests was (calculated to be) two-phase; as opposed to a single phase liquid for the higher performing tests. It is strongly believed that the test conditions at each measurement were at a steady condition, as far as could be observed from the instruments. Plots of process data for each test are in Appendix P. The most straight forward possibilities for the low performing tests include filling (i.e., mass accumulation) and/or additional heat (in-leak or otherwise). These would exhibit the large stream temperature differences observed and the apparent low performing heat exchangers (i.e., (UA) and NTU's). Appendix S examines these possibilities for test case #29. Namely, (i) filling of the vessel (although, as stated it is believed that the conditions were steady for all test cases), (ii) additional heat into the vessel with the temperature at (h, 3) matched to the average measured value and (iii) additional heat into the vessel with the temperature at (h, 5) and (l, 3) matched to the average measured values. All of these low performing tests occurred during a time before the higher performing ones; i.e., Dec. 20 to Dec. 29 vs. Dec. 29 to Jan 17. In fact, it was during testing on Dec. 29th that the first test (#4 29-Dec-

14, 60 W, 2.7 atm) exhibited the low performance, and the following tests did not. Since it is not reasonable for the heat exchanger (total) performance to either be as low as calculated or spuriously increase in a substantial manner, these tests, including #15 to #17, will be disregarded from further analysis. On this basis, the test data set was reduced to exclude these tests; so that the test data set now being considered is #'s 1, 2, 5, 7, 8, 10, 12-14, 18-21, 25, 26-28, 31, 33, 34, 36-39, and 40-43 (i.e., 28 of the original 43 tests).

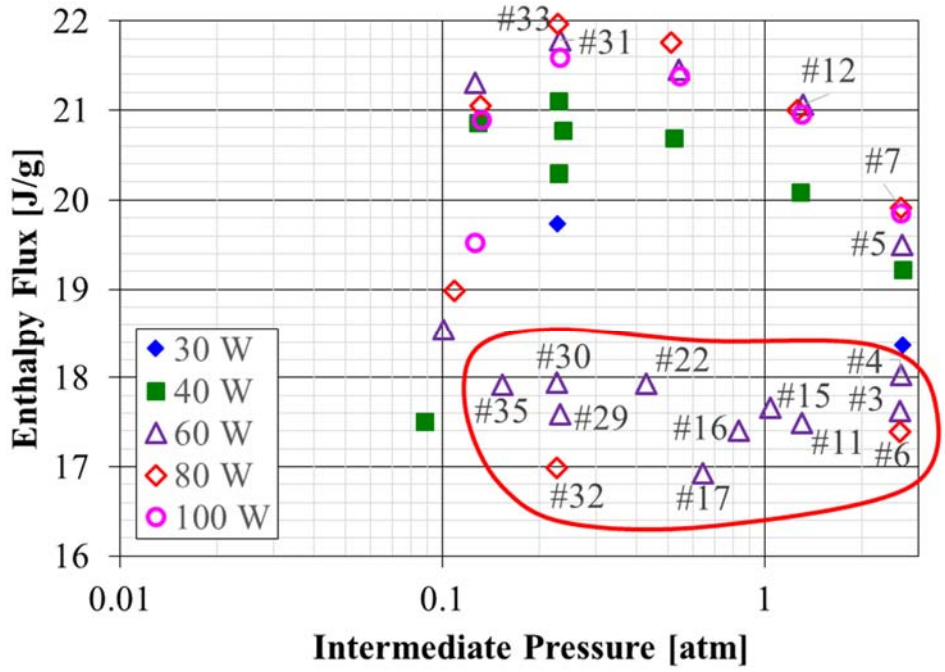

Figure 4.1. Load enthalpy flux vs. intermediate pressure

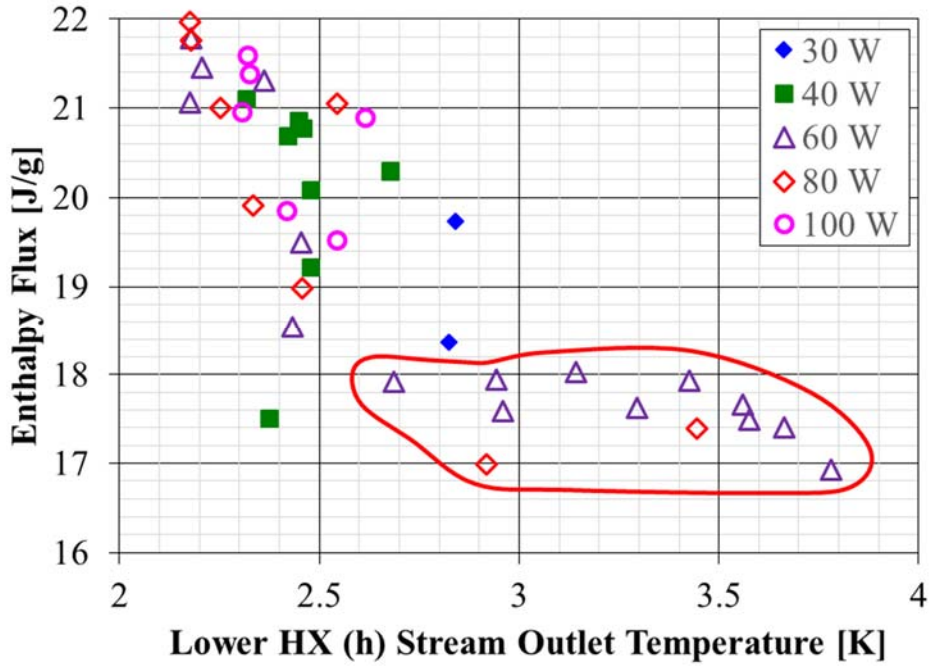

Figure 4.2. Load enthalpy flux vs. *(h)* stream temperature at outlet of lower heat exchanger

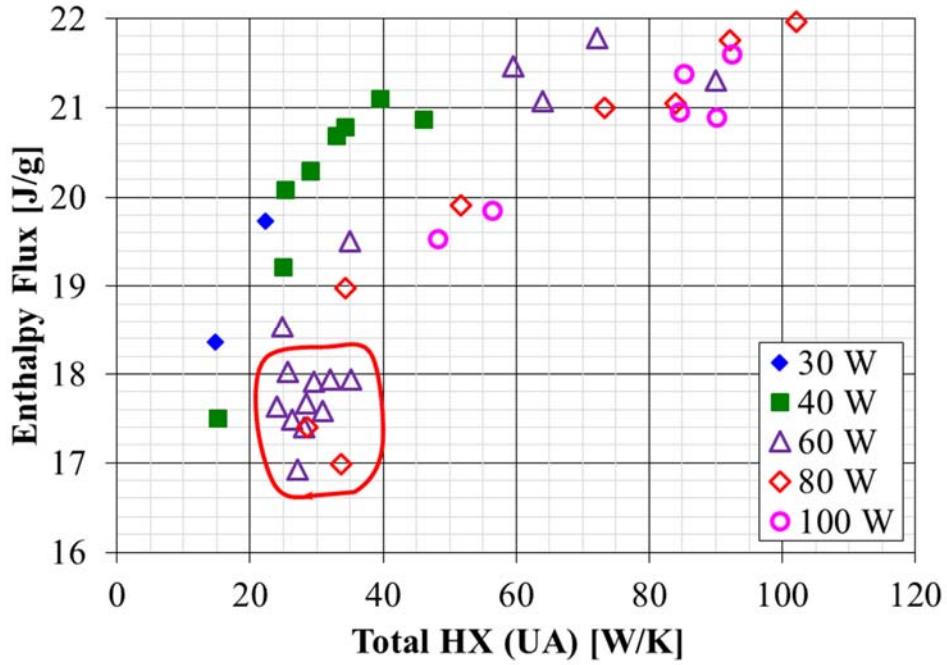

Figure 4.3. Load enthalpy flux vs. total (upper + lower) heat exchanger *(UA)*

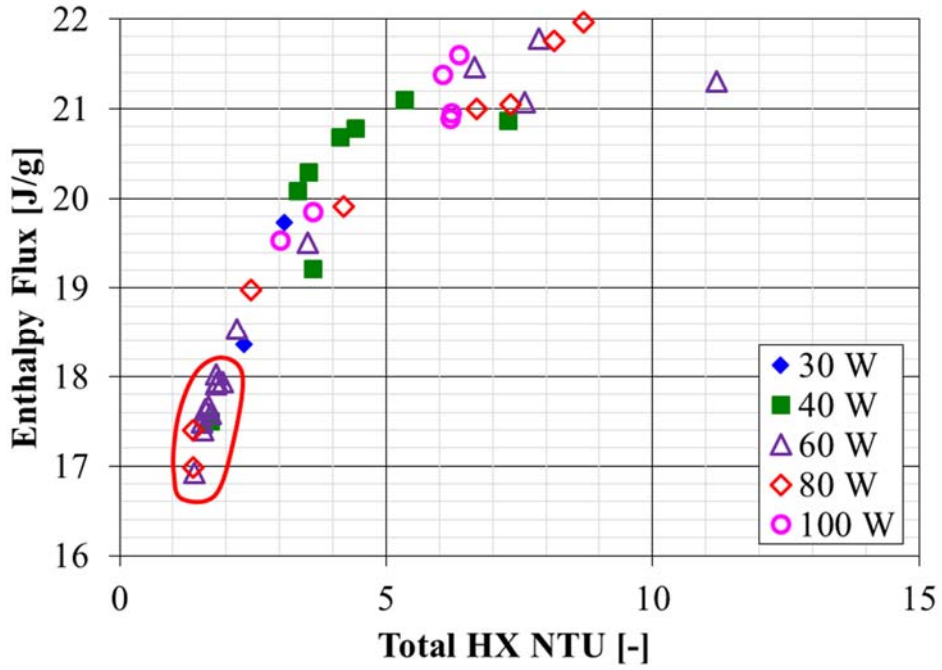

Figure 4.4. Load enthalpy flux vs. total (upper + lower) heat exchanger *NTU's*

Figure 4.5 shows the load enthalpy flux vs. intermediate pressure for the aforementioned 28 test cases. It is observed that as theoretically anticipated, the enthalpy flux increases as the intermediate pressure decreases down to a certain point; in this case, around 0.23 atm. However, rather than leveling off at the peak enthalpy flux, it sharply decreases to a value even lower that the no imposed pressure drop case (i.e., ~2.7 atm). In Figure 4.5, test #26 appears to be inconsistent with the other data and overall trend. Test #27 seems to follow the overall trend the best (see also, Figures 4.6 through 4.8), but test #28 is plausible.

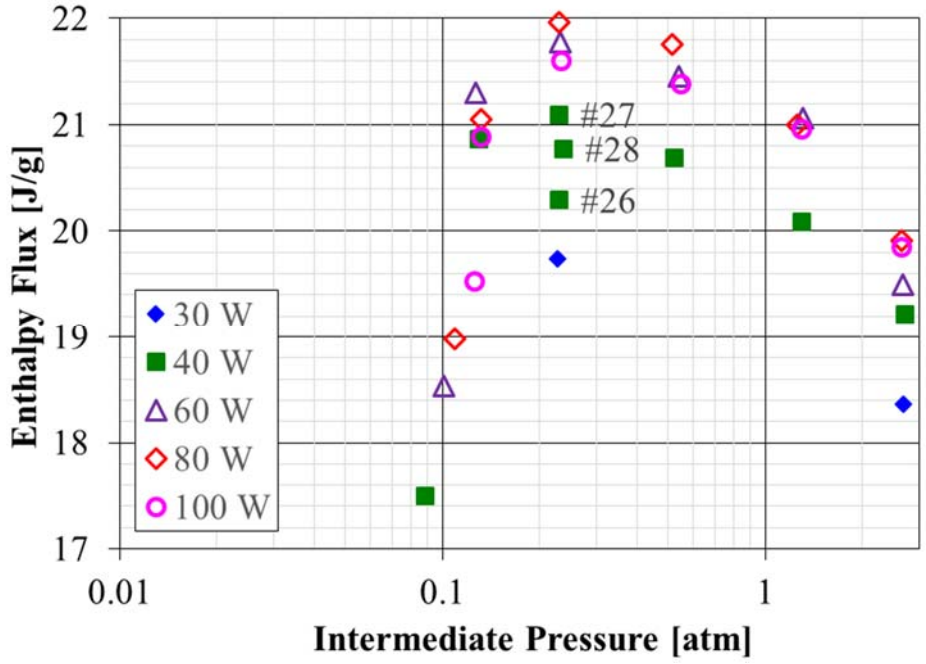

Figure 4.5. Load enthalpy flux vs. intermediate pressure for reduced data

For all the nominal 0.1 atm intermediate pressure tests (#36 - #39) it appears that the load enthalpy flux is beginning to drop-off after the peak at the nominal 0.2 atm intermediate pressure tests (#25, #27, #31, #33, #34). This matched the initial prediction (see Chapter 1, Figure 1.5). However, the analysis done in Chapter 1 was posed from the perspective of the heat exchanger sizing. That is, for given process conditions, the heat exchanger (UA) and/or NTU requirement was determined. For the testing, there is a given 'size' for the heat exchanger (i.e., surface area). So, the pertinent issue is how the (UA) is used in the two heat exchanger sections and how the overall heat transfer coefficient (U) changes. From Figure 1.5, it is clear that the total (UA) and NTU requirement increases rapidly below 0.2 atm. Further, from Figure 1.6, it is clear that the upper heat exchanger bears a rapidly increasing and a majority of this total. Figure 4.6 shows the upper heat exchanger (UA) vs the intermediate pressure, Figure 4.7 the lower heat exchanger

(UA) vs the intermediate pressure, and Figure 4.8 the total (UA) vs. intermediate pressure. Additionally, it should be noted from the process model results that the temperature at (h, 3) was increased above the average measured value for all of the "Low" intermediate pressure test cases (i.e., #40 to #43) and, except for test #1 (30 W), all of the nominal "2.7 atm" cases (i.e., #2, #5, #7, and #8) in order make the lower heat exchanger duty non-negative [11]. From Figures 4.6 to 4.8, as the intermediate pressure decreases from a nominal "2.7 atm", the (UA) increases for both heat exchangers down to a nominal "0.2 atm", then rapidly decreases. It is possible that this degradation in heat exchanger performance was due to a two-phase effect with a very low driving pressure difference.

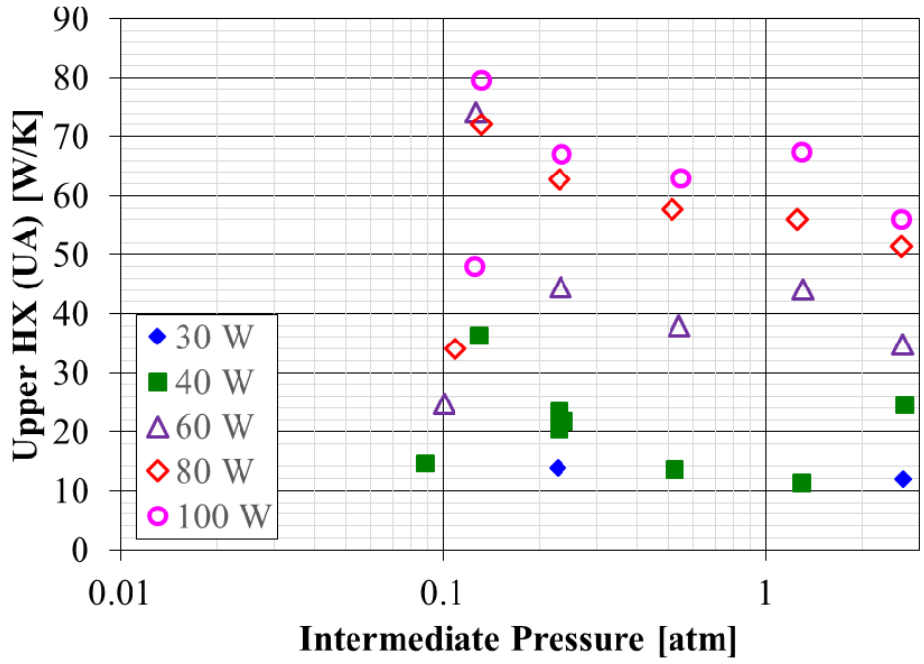

Figure 4.6. Upper heat exchanger net thermal rating vs. intermediate pressure

[11] Negative duty being when the *(h)* stream is cooled and the *(l)* stream is warmed.

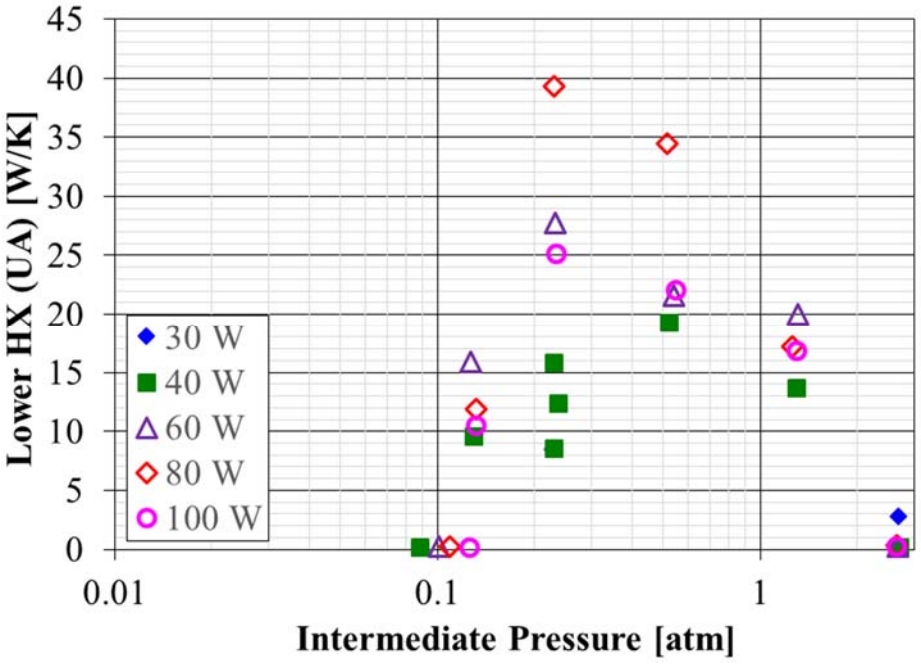

Figure 4.7. Lower heat exchanger net thermal rating vs. intermediate pressure

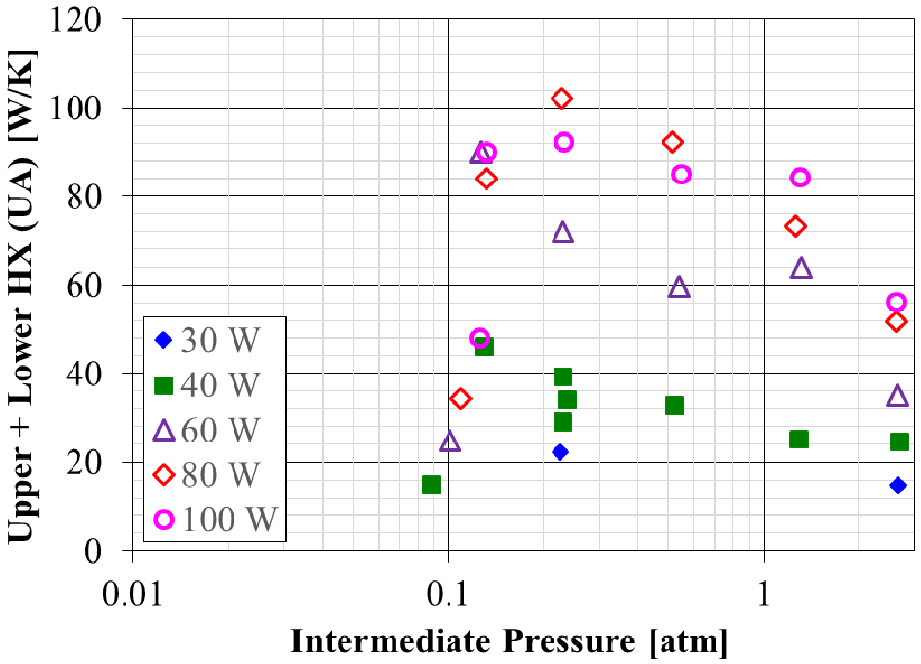

Figure 4.8. Total (upper + lower) net thermal rating vs. intermediate pressure

Figure 4.9 shows the quality of the *(h)* stream at the outlet of the lower heat exchanger. Note the convention used for the quality. Also, notice that as the intermediate pressure falls below the nominal "0.2 atm" cases, although the upper heat exchanger comprises a greater portion of the total (UA), the (UA) of the lower heat exchanger goes to zero at the "Low" test cases. But the overall heat exchanger (UA) degradation also certainly contributed to the performance drop-off shown in Figure 4.5, in addition to the effect indicated in Figure 1.5 of Chapter 1.

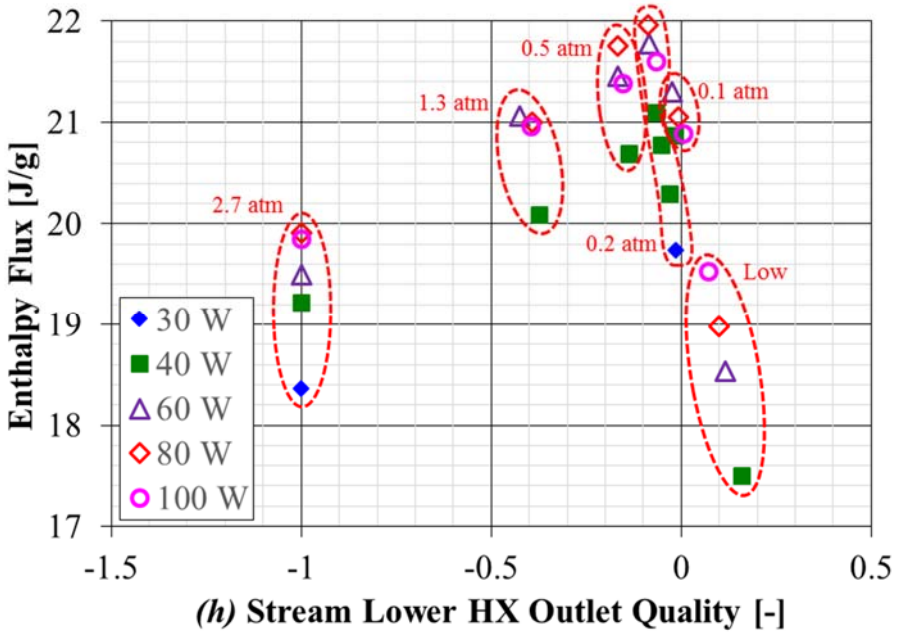

Figure 4.9. *(h)* stream lower heat exchanger outlet quality [12]

[12] Given (p, h), the convention for quality is, $x = 3$ if $p \geq p_c$ and $T \geq T_c$; $x = -1$ if $p \geq p_c$ and $T < T_c$; otherwise, $x = \big(h - h_{l,sat}(T)\big)/\big(h_{v,sat}(T) - h_{l,sat}(T)\big)$ with $T = T_{sat}(p)$

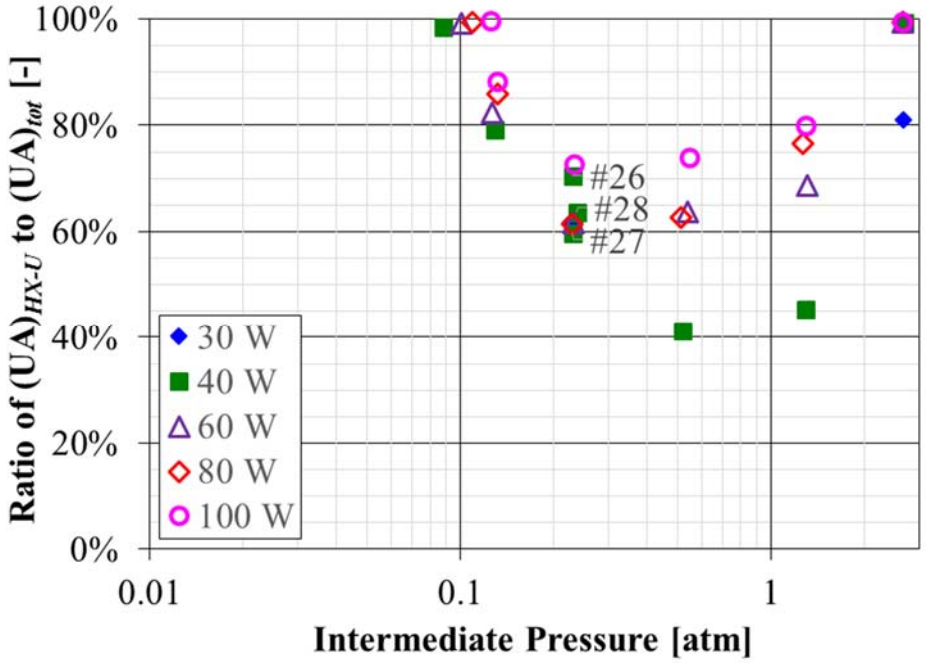

Figure 4.10. Ratio of upper heat exchanger net thermal rating to total vs. intermediate pressure

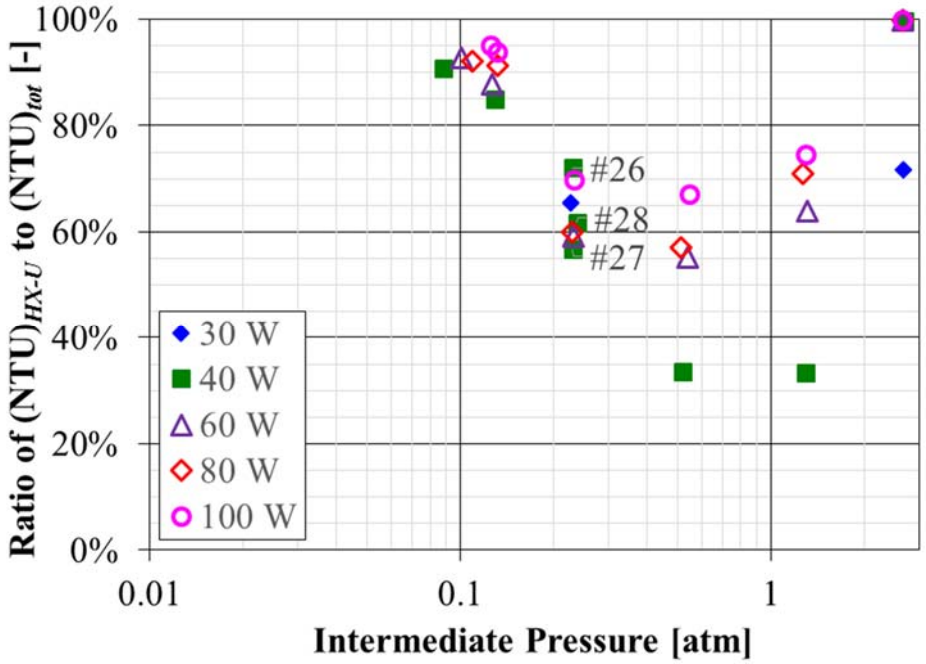

Figure 4.11. Ratio of upper heat exchanger *NTU*'s to total vs. intermediate pressure

As shown in Figure 4.10, plotting the ratio of the upper heat exchanger (UA) to the total (UA) vs. the intermediate pressure can provide some insight into the design sizing for a specified intermediate pressure. Likewise, as shown in Figure 4.11, the ratio of the upper heat exchanger NTU's to the total NTU's vs. the intermediate pressure shows a similar behavior, as would be expected.

Figure 4.12 shows the total (upper plus lower) heat exchanger (UA) vs. the adjusted mass flow rate. The dashed ellipses show the nominal heat load groupings. The (UA) normally scales with the mass flow to some exponent. In fact, the nominal "2.7 atm" and "Low" test cases would appear to behave in this manner over the whole mass flow range. However, the "0.5 atm", "0.2 atm", and "0.1 atm" test cases appear to either have a peak and then slightly decrease, or just taper off (in their increase); given the temperature measurement uncertainties, further cannot be said with confidence. For a fixed heat exchanger size (i.e., surface area), one would expect the performance to taper as the design flow is exceeded.

Likewise, Figure 4.13 shows the total heat exchanger NTU's vs. the adjusted mass flow rate, with the dashed ellipses showing the nominal heat load groupings. A similar behavior as described for the total (UA) is evident. However, it appears for the "0.5 atm", "0.2 atm", and "0.1 atm" test cases that they reach a peak and then decrease.

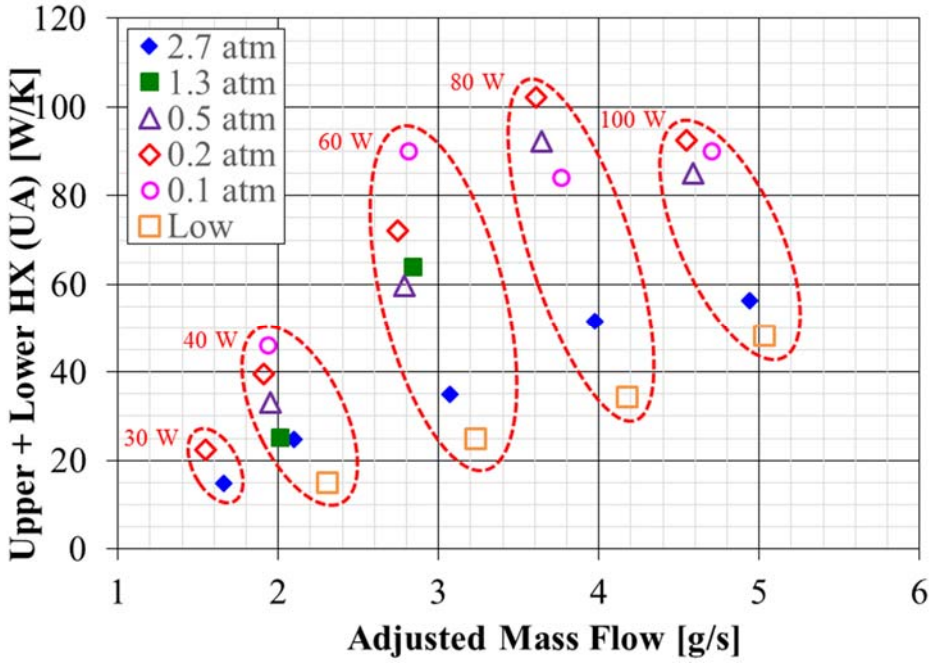

Figure 4.12. Total heat exchanger net thermal rating vs. (adjusted) mass flow rate

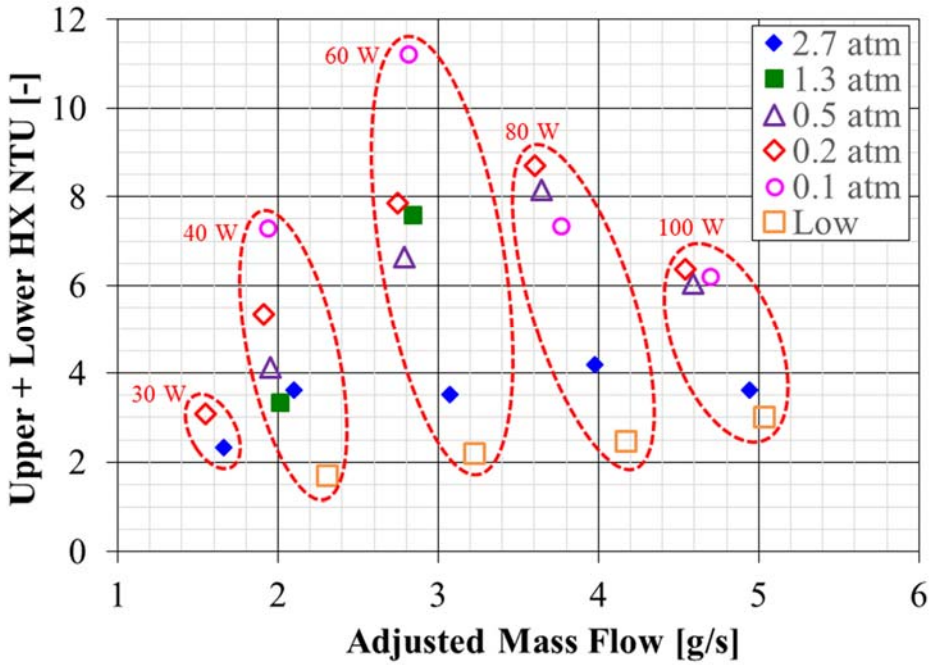

Figure 4.12. Total heat exchanger *NTU's* vs. (adjusted) mass flow rate

Figure 4.14 shows a cool-down profile of the copper radiation shield prior to modifications (done to improve it). A temperature of about 33 K was reached after around 78 hours. It is believed that the shield temperature would have been colder than this, and consequently would result in a higher heat in-leak to the point where the copper braids were anchored on the 2 IPS sub-atmospheric line.

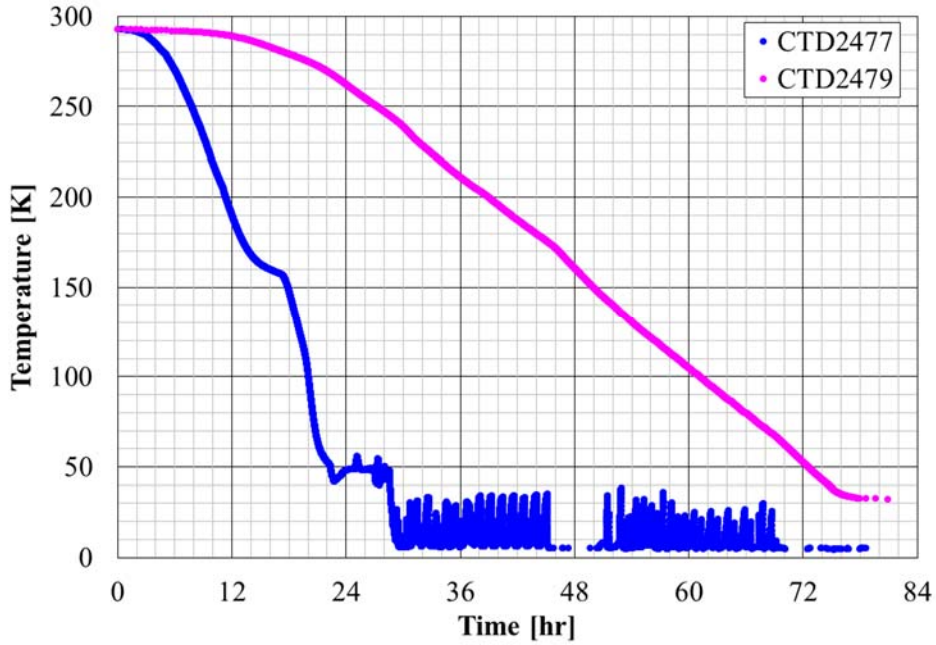

Figure 4.14. Cool-down temperature profile of copper radiation shield prior to modifications [13]

[13] CTD2477 [K] – *(l)* stream temperature exiting upper heat exchanger warm-end, CRD2479 [K] – copper shield temperature

4.4 Summary

Overall, it is observed that the load enthalpy flux increases from the (nominal) 2.7 atm intermediate pressure to the peak at the 0.2 atm intermediate pressure as shown in Table 4.1. After this peak, the performance of the heat exchanger for this process rapidly diminishes due to an effective loss in the heat transfer surface area. These testing data establish experimentally the performance range of this particular Collins heat exchanger for a wide range of intermediate pressures.

Table 4.1. Increase in load enthalpy flux between 2.7 and 0.2 atm nominal intermediate pressure for various nominal heat loads

Nominal Heat Load	Increase in Load Enthalpy between 2.7 and 0.2 atm Nominal Intermediate Pressures
30 W	7.51%
40 W	9.77%
60 W	11.7%
80 W	10.3%
100 W	8.80%

5. DISCUSSION AND CONCLUSIONS

The following are the contributions of this work:

1. The viability of using a counter-flow heat exchanger together, but not necessarily concurrent, with a significant pressure drop in the supply steam to increase the capacity to a sub-atmospheric, nominally 2 K load, has been confirmed experimentally:
    a. Optimum performance was confirmed experimentally and was found to result in an increase in enthalpy flux to the load of around 7.5% to almost 12%, depending on the load
    b. Approximate performance envelope was ascertained using a Collins-type heat exchanger
    c. Experimentally confirmed the theoretical prediction for the optimum intermediate pressure, being around 0.2 atm
    d. Found that such a heat exchanger is capable of a very tight stream temperature difference ‘pinch’ at the cold end; with the exiting supply temperature very close to lambda

    The Collins-type heat exchanger used proved to be quite robust and, as presented, demonstrated a good and wide range performance.
2. The pseudo-adiabatic expansion nature of pressure drop with heat transfer in particular and on the overall refrigeration process was theoretically investigated:
    a. The pseudo-(thermo)property termed an ‘equivalent efficiency’ was developed, which provides a direct comparison of the performance gained by pressure drop with heat exchange to that gained by adiabatic expansion.

b. A practical process equivalence was developed between pressure drop with heat exchange and an adiabatic expansion process which provides a qualitative and quantitative understanding in a real process application.

c. The overall 2-K helium refrigeration process efficiency improvement trade-off between higher load capacity and higher discharge temperature from the cryogenic compression process was investigated. This estimate showed that the overall process for a large system could provide a capacity increase of around 6% for the same input power, or, around 5% power reduction for the same 2 K load capacity.

5.1 Outlook and Suggestions for Further Work

1. Further work is needed to develop and test a passive back-pressure device, rather than use an actively controlled JT valve (as was done for the testing presented in this work). Operation with two JT valves, though certainly demonstrated to be workable, would not be a robust implementation given its complexity.
2. Regarding the testing performed for this work, there are several aspects that could be further studied by additional testing and analysis:
   a. Re-create the conditions that initially produced poor performance, but yet were obtained ostensibly at steady conditions; with later tests at the same load and process conditions producing good performance in line with theoretical expectations.
   b. Understand the performance degradation below the nominally 0.2 atm intermediate pressure to a greater degree, quantitatively and qualitatively.
   c. Understand the total heat exchanger performance vs. mass flow more precisely.

Before performing such testing, the issues with the temperature instrumentation must addressed to provide higher fidelity measurements.

3. The development of a wet, two-phase expander, although not likely not have an adiabatic efficiency much higher than 65%, would likely provide an equal input power reduction for the same load (or capacity increase for the same input power) as utilizing the pressure drop in the supply stream to the load with counter-flow heat exchange. It would also have the benefit of keeping the first cold compressor stage small for large plants (i.e., 18 kW of equivalent 4.5 K refrigeration or larger). However, it is a rotating machine and therefore adds reliability risk (or additional capital investment and maintenance for redundancy). The process study touched on in Chapter 3 would be a first step in evaluating the anticipated benefit of such a development.
4. Considerable work is needed to more systematically characterize the heat transfer and pressure drop of the Collins type heat exchanger in terms of Colburn '*j*' and Fanning friction factors. As discussed, the information available for determining these factors is limited and not easily compared, since the basis for determining them varies considerably. Consideration for manufacturing variances and the effect that these have on the performance characteristics is crucial. This could, and probably should, combine experimental and (fluid) computational work to ensure that the scope is feasible for realistic funding. Unfortunately, the need for such a heat exchanger too often presents itself without the resources to further an understanding of their performance.

REFERENCES

Agapov, N. N., V. I. Batin, A. B. Davydov, H. G. Khodzhibagian, A. D. Kovalenko, G. A. Perestoronin, I. I. Sergeev, V. L. Stulov, and V. N. Udut. 2002. "More effective wet turboexpander for the nuclotron helium refrigerator." *Advances in Cryogenic Engineering.* AIP. 280-287.

Arp, V. D., and R. D. McCarty. 1998. *Thermodynamic properties of helium-4 from 0.8 to 1500 K with pressures to 2000 MPa, TN 1334.* Technical Note, National Institute of Standards and Technology (NIST), National Institute of Standards and Technology (NIST).

Arp, V. 1972. "Forced flow, single-phase helium cooling systems." Edited by K. D. Timmerhaus. *Advances in Cryogenic Engineering.* Springer. 342-351.

Baldus, W. 1971. "Helium-II refrigerator for 300 W at 1.8 K." Edited by K. D. Timmerhaus. *Advancesin Cryogenic Engineering.* Springer. 163-170.

Baldus, W., and A. Sellmaier. 1967. "A continuous helium II refrigerator." Edited by K. D. Timmerhaus. *Advances in Cryognenic Engineering.* Springer. 434-440.

Barron, R. F. 1999. *Cryogenic heat transfer.* Philadelphia, Pennsylvania: Taylor and Francis.

—. 1985. *Cryogenic systems.* 2nd. Oxford University Press.

Bottura, L. 1999. *A practical fit for the critical surface of NbTi, LHC project report 358.* Geneva: CERN, LHC Division. Accessed 11 4, 2016. https://cdsweb.cern.ch/record/411159/files/lhc-project-report-358.pdf.

Brown, E. H. 1960. "Expansion engines for hydrogen liquefiers." *Journal of Research of the National Bureau of Standards* (National Bureau of Standards) 64C (1): 25-36.

Byrns, R. A. 1984. *Large helium refrigerators and liquefiers, LBL-15167.* Lawrence Berkeley Laboratory, Lawrence Berkeley Laboratory.

Callen, H. B. 1985. *Thermodynamics and an introduction to thermostatistics.* 2nd. New York: Wiley.

Casagrande, F., I. Campisi, P. Gurd, D. Hatfield, M. Howell, D. Stout, H. Strong, et al. 2006. "SNS cryogenic systems commissioning." *Advances in Cryogenic Engineering.* Keystone, Colorado: AIP. 1436-1443.

CEBAF. 1988. *CEBAF design handbook: Chapter 11 "Cryogenics".* Newport News, Virginia: CEBAF.

—. 1987. "Specification for the cryogenic test facility two-stage compression systems, 7-86-001A." Newport News, Virginia, March 2.

CERN. 2014. *CERN-2004-003 Chapter 11: Cryogenics.* LHC Design Report, Geneva: CERN.

Chorowski, M., W. Erdt, Ph. Lebrun, G. Riddone, L. Serio, L. Tavian, U. Wagner, and R. van Weelderen. 1998. "A simplified cryogenic distribution scheme for the large hadron collider." *Advances in Cryogenic Engineering.* Springer. 395-402.

Chronis, W. C., D. M. Arenius, B. S. Bevins, V. Ganni, D. H. Kashy, M. M. Keesee, T. R. Reid, and J. D. Wilson. 1996. "Procurement and commissioning of the CHL refrigerator at CEBAF." Edited by P. Kittel. *Advances in Cryogenic Engineering.* Springer. 641-648.

Claudet, G., G. Bon Mardion, B. Jager, and G. Gistau. 1986. "Design of the cryogenic system for the TORE SUPRA tokamak." *Cryogenics* 26: 443-449.

Collins, S. C. 1947. "A helium cryostat." *Review of Scientific Instruments* 18 (3): 157-167.

—. 1968. "Refrigeration at temperatures below the boiling point of helium." *Proceedings of the 1968 Summer Study on Superconducting Devices and Accelerators Part I, BNL-50155(C-55).* 59-66.

Collins, S. C., and M. H. Streeter. 1967. "Refrigerator for 1.8 K." *Proceedings of the 1st International Cryogenic Engineering Conference.* Heywood-Temple Industrial Publications. 215-217.

Collins, S. C., and R. L. Cannaday. 1958. *Expansion machines for low temperature processes.* Oxford University Press.

Collins, S. C., R. W. Stuart, and M. H. Streeter. 1967. "Closed-cycle refrigeration at 1.85 K." *Review of Scientific Instruments* 38 (11): 1654-1657.

Croft, A. J., and P. B. Tebby. 1970. "The design of finned-tube cryogenic heat exchangers." *Cryogenics* 236-238. doi:10.1016/0011-2275(70)90108-6.

Cryogenic Control Systems, Inc. n.d. *Temperature monitor selection guide.* Accessed June 4, 2016. http://cryocon.com/TMSelectGuide.php.

Daly, E. F., V. Ganni, C. H. Rhode, W. J. Schneider, K. M. Wilson, and M. A. Wiseman. 2002. "Spallation neutron source cryomodule heat loads and thermal design." *Advances in Cryogenic Engineering.* Madison, Wisonsin: AIP. 531-539.

Daus, W., and R. Ewald. 1975. "A refrigeration plant with 300 W capacity at 1.8 K." *Cryogenics* 591-598. doi:10.1016/0011-2275(75)90068-5.

de Bruyn Ouboter, R. 2009. "Cryogenics at the end of the first half of the 20th century (1880-1940)." *Journal of Physics: Condensed Matter* (IOP) 21 (16). doi:10.1088/0953-8984/21/16/164221.

Ebadian, M. A., and Z. F. Dong. n.d. "Forced convection, internal flow in ducts." Chap. 5 in *Handbook of Heat Transfer*, edited by W. M. Rohsenow, J. P. Hartnett and Y. I. Cho, 102-104. Mc-Graw-Hill.

Eckels Engineering, Inc. n.d. "CryoComp." Accessed May 31, 2016. http://www.eckelsengineering.com.

ESDU 73031. 2000. *Convective heat transfer during crossflow of fluids over plain tube banks.* London: IHS.

ESDU 84016. 2000. *Low-fin staggered tube banks: heat transfer and pressure loss for turbulent single-phase crossflow.* London: IHS.

Fleming, R. B. 1967. "The effect of flow distribution in parallel channels of counterflow heat exchangers." Edited by K. D. Timmerhaus. *Advances in Cryogenic Engineering.* Springer. 352-362.

Ganni, V. 2009. *Design and optimization of helium refrigeration and liquefaction systems.* Oak Park, Illinois: Cryogenic Society of America.

Ganni, V., and J. Fesmire. 2012. "Cryogenic for superconductors: refrigeration, delivery and preservation of the cold." *Advances in Cryogenic Engineering.* Melville, New York: AIP. 15-27. doi:10.1063/1.4706901.

Ganni, V., and P. Knudsen. 2014. "Helium refrigeration considerations for cryomodule design." *AIP Conference Proceedings - Advances in Cryogenic Engineering.* Melville, New York: AIP. 1814-1821. doi:10.1063/1.4860928.

—. 2010. "Optimal design and operation of helium refrigeration systems using the Ganni cycle." *Advances in Cryogenic Engineering.* Melville, New York: AIP. 1057-1071. doi:10.1063/1.3422267.

Ganni, V., D. M. Arenius, B. S. Bevins, W. C. Chronis, J. D. Creel, and J. D. Wilson, Jr. 2002. "Design, fabrication, commissioning, and testing of a 250 g/s helium cold compressor system." *Advances in Cryogenic Engineering.* Melville, New York: AIP. 288-304.

Ganni, V., P. Knudsen, D. Arenius, and F. Casagrande. 2014. "Application of JLab 12 GeV helium refrigeration system for the FRIB accelerator at MSU." *Advances in Cryogenic Engineering.* Melville, New York: AIP. 323-328. doi:10.1063/1.4860718.

Ganni, V., P. Knudsen, J. Creel, D. Arenius, F. Casagrande, and M. Howell. 2008. "Screw compressor characteristics for helium refrigeration systems." *AIP Conference Proceedings - Advances in Cryogenic Engineering.* Melville, New York: AIP. 309-315. doi:10.1063/1.2908562.

Ganni, V., R. Moore, and P. Winn. 1986. "Capacity upgrade of the Excell helium liquefier plant by the addition of a wet engine." *Advances in Cryogenic Engineering.* Springer. 699-707.

Gilbert, N., P. Roussel, G. Riddone, R. Moracchioli, and L. Tavian. 2006. "Performance assessment of 239 series helium sub-cooling heat exchangers for the large hadron collider." *Advances in Cryogenic Engineering.* AIP. 523-530.

Gistau, G. M., and G. Claudet. 1984. "The design of the helium refrigerator for TORE SUPRA." *Proceedings of the 10th International Cryogenic Engineering Conference.* Otaniemi, Finland: Butterworth. 288-291.

—. 1986. "The TORE SUPRA 300 W – 1.75 K refrigerator." *Advances in Cryogenic Engineering.* Cambridge, Massachusetts: Springer. 607-615.

Green, M. A. 2008. "The cost of helium refrigerators and coolers for superconducting devices as a function of cooling at 4 K." *API Conference Proceedings.*

Gruehagen, H., and U. Wagner. 2004. "Measured performance of four new 18 kW at 4.5 K helium refrigerators for the LHC cryogenic system." *Proceeding of the 20th International Cryogenic Engineering Conference.* Beijing, China: Elsevier. 991-994.

Gupta, P. K., P. K. Kush, and A. Tiwari. 2009. "Experimental research on heat transfer coefficients from cryogenic cross-counter-flow finned-tube heat exchangers." *International Journal of Refrigeration* 20: 960-972.

Gupta, P. K., P. K. Kush, and A. Tiwari. 2010. "Experimental studies on pressure drop characteristics of cryogenic cross-counter flow coiled finned tube heat exchangers." *Cryogenics* 20: 257-265.

Haberstroh, Ch. 2009. "Helium refrigerators for SC Accelerators." *SRF Tutorial.* Dresden, Germany. 41. Accessed 10 17, 2016. https://accelconf.web.cern.ch/accelconf/SRF2009/CONTENTS/Tutorials/ch_haberstroh_cryo_tutorial.pdf.

Hasan, N., and P. Knudsen. 2016. *Shell-side pressure drop measurement in a Collins-type 4.5K-2K heat exchanger, JLAB-TN-16-036.* Tech Note, Newport News, Virginia: Jefferson Lab.

Hausen, H. 1983. *Heat transfer in counterflow, parallel flow and cross flow.* London: McGraw-Hill.

Horizon Technologies. n.d. "Horizon Technologies." Accessed May 30, 2016. http://www.htess.com.

Hust, J. G., and A. B. Lankford. 1984. *Thermal conductivity of aluminum, copper, iron, and tungsten for temperatures from 1 K to the melting point, NBSIR 84-3007.* Springfield, Virginia: U.S. Department of Commerce, National Technical Information Service.

Jacobsen, R. T. 1986. "A new fundamental equation for thermodynamic property correlations." *Advances in Cryogenic Engineering.* Springer. 1161-1168.

Jacobsen, R. T. 1972. *The thermodynamic properties of nitrogen from 65 to 2000 K with pressures to 10000 Atm.* PhD Thesis, Washington State University, Washington State University.

Johnson, R. W., and S. C. Collins. 1970. "Hydraulically operated two-phase helium expansion engine." Edited by K. D. Timmerhaus. *Advances in Cryogenic Engineering.* Springer. 171-177.

Kapitza, P. 1934. "The liquefaction of helium by an adiabatic method." *Proceeding of the Royal Society of London. Series A Mathematical and Physcial Sciences* 189-211.

Kays, W. M., and A. L. London. 1998. *Compact heat exchangers.* Malabar, Florida: Krieger.

Knudsen, P. 2008. *Process study for the design of small scale 2 Kelvin refrigeration systems.* MSc Thesis, Old Dominon University, Norfolk, Virginia: Old Dominon University, Appendix B.

Knudsen, P., and V. Ganni. 2012. "Process options for nominal 2-K helium refrigeration system design." *AIP Conf. Proc. 1434.* Spokane, Washington: AIP. 800-813. doi:10.1063/1.4706993.

—. 2006. "Simplified helium refrigerator cycle analysis using the ‘Carnot Step’." *Advances in Cryogenic Engineering.* AIP. 1977-1986.

Knudsen, P., and V. Ganni. 2015. "Testing of a 4 K to 2 K heat exchanger with an intermediate pressure drop." *IOP Conf. Ser.: Mater. Sci. Eng. IOP Conference Series: Materials Science and Engineering* 012105.

Knudsen, P., V Ganni, K. Dixon, R. Norton, and J. Creel. 2016. "Performance testing of Jefferson Lab 12 GeV helium screw compressors." *IOP Conference Series: Materials Science and Engineering.* IOP. 012072. doi:10.1088/1757-899X/90/1/012072.

Knudsen, P., V. Ganni, and R. Than. 2012. "Options for cryogenic load cooling with forced flow helium circulation." *Advances in Cryogenic Engineering.* AIP. 790-799.

Knudsen, P., V. Ganni, N. Hasan, K. Dixon, R. Norton, and J. Creel. 2016. "Modifications to JLab 12 GeV refrigerator and wide range mix mode performance testing results." *Proceedings of the 26th International Cryogenic Engineering Conference.* New Delhi, India: IOP Conference Series.

Koch Process Systems. 1989. "Operational and maintenance manual for CEBAF cryogenic test facility cold box and expansion engine modules." Westborough, Massachusetts: Koch Process Systems, April.

Kotas, T. J. 1985. *The exergy method of thermal plant analysis.* London: Butterworths.

Kroeger, P. G. 1966. "Performance deterioration in high effectiveness heat exchangers due to axial heat conduction effects." *Advances in Cryogenic Engineering.* Springer. 363-372.

Kroptschot, R. H., B. W. Birmingham, and D. B. Mann. 1968. *Technology of liquid helium NBS monograph 111.* U.S. Department of Commerce, National Bureau of Standards.

Lebrun, Ph., and L. Tavian. 2015. "Cooling with superfluid helium." *CERN Yellow Report CERN-2014-005* 453-476.

Lebrun, Ph., L. Serio, L. Tavian, and R. van Weelderen. 1998. "Cooling strings of superconducting devices below 2 K: the helium II bayonet heat exchanger." Edited by P. Kittel. *Advances in Cryogenic Engineering.* Springer. 419-426.

Ledbetter, H. M. 1981. "Stainless-steel elastic constants at low temperature." *Journal of Applied Physics* 52 (3): 1587-1589.

Mann, D. B., W R. Bjorklund, J. Macinko, and M. J. Hiza. 1960. "Design, construction, and performance of a laboratory size helium liquefier." Edited by K. D. Timmerhaus. *Advances in Cryogenic Engineering.* Springer. 346-353.

McAshan, M. 1980. *Stanford superfluid refrigerator.* Cryogenic Workshop, Fermi Lab, 36-38.

Onnes, H. K. 1909. "The liquefaction of helium." *Royal Netherlands Academy of Arts and Sciences (KNAW)* 11: 268-185.

Peterson, T. 1989. "Status: large-scale subatmospheric cryogenic systems." *Particle Accelerator Conference.* Chicago, Illinois: IEEE. 1769-1773.

PFR Engineering Systems. 1976. *Heat transfer and pressure drop characteristics of dry tower extended surfaces, part II: Data analysis and correlations.* Marina del Rey, California: PFR Engineering Systems.

PHPK Technologies. n.d. *Cryogenic and high vacuum products.* Accessed June 4, 2016. http://www.phpk.com/couplings.html.

Pickard, G. L., and F. E. Simon. 1948. "A quantitative study of the expansion method for liquefying helium." *Proceedings of the Physcial Society* 60 (341): 405-413.

Powell, R. L., H. M. Roder, and W. M. Rogers. 1957. "Low temperature thermal conductivity of some commercial coppers." *Journal of Applied Physics* 28 (11): 1282-1288.

Quack, H. 1980. "Turbines as ‘wet’ expanders in helium refrigerators." *Proceedings of the 8th International Cryogenic Engineering Conference.* Genova, Italy: IPC Science and Technology. 343-347.

Rabas, T. J., and J. Taborek. 1987. "Survey of turbulent forced-convection heat transfer and pressure drop characteristics of low-finned tube banks in cross-flow." *Heat Transfer Engineering* 8 (2): 49-62. doi:10.1080/01457638708962793.

Roussel, P., A. Bezaguet, H. Bieri, R. Devidal, B. Jager, R. Moracchioli, P. Seyfert, and L. Tavian. 2002. "Performance tests of industrial prototype subcooling helium heat exchangers for the large hadron collider." *Advances in Cryogenic Engineering.* AIP. 1429-1436.

Roussel, P., A. Girard, B. Jager, B. Rousset, P. Bonnay, F. Millet, and P. Gully. 2006. "The 400 W at 1.8 K test facility at CEA-Grenoble." *Advances in Cryogenic Engineering.* AIP. 1420-1427.

Schwettman, H. A., P. B. Wilson, J. M. Pierce, and W. M. Fairbanks. 1964. "The application of superconductivity to electron linear accelerators." *International Advances in Cryogenic Engineering.* Columbus, Ohio: Plenum Press. 88-97.

Scott, R. B. 1959. *Cryogenic engineering.* D. van Nostrand.

Sellmaier, A., R. Glatthaar, and E. Klien. 1970. "Helium refrigerator with a capacity of 300 W at 1.8 K." *Proceedings of the 3rd International Cryogenic Engineering Conference.* Berlin: Illiffe Science and Technology Publications. 310-314.

Serio, L. 2007. *A cryogenic helium mass flowmeter for the Large Hadron Collider.* PhD Thesis, Cranfield University, Cranfield University.

Shah, R., and D. Sekulic. 2003. *Fundamentals of heat exchanger design.* Hoboken, New Jersey: John Wiley & Sons.

Smith, Jr., J. L. 2002. "50 years of helium liquefaction at the MIT cryogenic engineering laboratory." *Advances in Cryogenic Engineering.* AIP. 213-224.

—. 1985. "A tribute to Samuel C. Collins: September 28, 1898 – June 19, 1984." *Advances in Cryogenic Engineering.* Springer. 1-11.

Steel, A. J., S. Bruzzi, and M. E. Clarke. 1976. "A 300 W 18K refrigerator and distribution system for the CERN superconducting RF particle separator." *6th International Cryogenic Engineering Conference.* Grenoble, France: BOC Ltd. 58-61.

Tavian, L. 2012. "Large-scale 2-K cryoplant experience." *Workshop on superconducting linear accelerator technology for a next generation light source.* Fermi Lab.

Trepp, Ch. 1966. "A large scale helium liquefier." *Liquid Helium Technology Proceedings of the International Institute of Refrigeration.* 215-226.

—. 1961. "Refrigeration systems below 25 K with turboexpanders." *Advances in Cryogenic Engineering.* Ann Arbor, Michigan: Springer. 251-261.

Trumpler, P. R., and B. F. Dodge. 1947. "The design of ribbon-packed exchangers for low temperature air separation plants." *Transactions of the American Institute of Chemical Engineers* 43 (2): 75-84.

Van Sciver, S. W. 2012. *Helium cryogenics.* New York: Springer.

Van Wylen, G. J., and R. E. Sonntag. 1985. *Fundamentals of classical thermodynamics.* 3rd. New York: Wiley.

von der Nuell, W. T. 1952. "Single-stage radial turbines for gaseous substances with high rotative and low specific speed." *Transactions of the American Society of Mechanical Engineers (ASME)* 74: 499-515.

Wagner, U. 2002. *Cryogenics for particle accelerators and detectors: refrigeration.* Divisional, Geneva: LHC Division CERN.

Younglove, B. A. 1982. "Thermophysical properties of fluids. I. argon, ethylene, parahydrogen, nitrogen, nitrogen trifluoride and oxygen." *Journal of Physical and Chemical Reference Data* 11, Sup. 1, App. E: 1-11.

Zukauskas, A. 1989. "Heat transfer and flow over finnned tubes." Chap. 14 in *High-Performance Single-Phase Heat Exchangers*, translated by J. Karni. Hemisphere.

APPENDIX A – ADDITIONAL BACKGROUND INFORMATION

A.1. Processes and Cycles for Refrigeration and Liquefaction

Refrigeration can be accomplished by quite a number of processes. Among those that use recuperative heat exchange, there are,

a. Pre-cooled system which uses two working fluids, one being used to pre-cool the other
b. Cascade system which is an extension of a pre-cooled system employing multiple stages of pre-cooling
c. Joule-Thompson (JT) effect
d. Adiabatic expansion (work extraction)

These are all familiar from a first year thermodynamics class and it is not uncommon to find the combination of several of these used in a 4.5 K helium refrigerator. Undergraduate textbooks present the Carnot cycle to students, a reversible cycle operating between two constant temperature reservoirs. Operating as a refrigerator (as opposed to a heat pump), the process steps are reversible constant temperature adsorption of heat (over an infinitely small temperature difference) from the cold temperature reservoir (being refrigerated), followed by isentropic compression, reversible constant temperature rejection of heat (over an infinitely small temperature difference) to the high (ambient) temperature reservoir, isentropic expansion who's work output is used to partially power the compression step, then returning to the first step. To analyze this cycle, we required the concept of an absolute temperature scale and the inequality of Clausius; namely, $(Q_H/Q_L) = (T_H/T_L)$ and $\oint(dQ/T) \leq 0$, respectively, where the subscript "*H*" denotes the high temperature reservoir and "*L*" denotes the low temperature reservoir. Of course the 'inequality' of Clausius is an equality only if the process path is reversible. Using these we

can show that the best performance we can ever hope for of a heat pump operating between the constant temperature reservoirs T_H and T_L, is $(T_H/T_L - 1)$. That is, this is the lowest possible input power per watt of cooling provided, also known as the inverse coefficient of performance (COP_{inv}). For helium this is 70 W/W. Interestingly a helpful analogy can be made using the equality of Clausius. In an ideal electrical transformer, the power is conserved; i.e., $P = V \cdot i$, where V is the voltage and i is the current. In an ideal heat engine, the entropy is conserved, $S = Q/T$. Ideally electrical energy can be transformed without degrading that energy. Even, ideally mechanical energy can be transformed into electrical energy without degrading the availability of that energy; and visa-versa. However, even ideally, heat energy cannot be transformed between different temperatures without degrading that heat energy. So, the Carnot cycle is the 'standard bearer', in that it serves the purpose of telling us the absolute best performance possible for a refrigeration (or power) cycle; although, practically, we know that even if nearly ideal components were developed, the process rates will asymptotically approach zero as the efficiency approaches the Carnot efficiency.

Regarding the Carnot cycle, it is stated that, "…this is the most efficient cycle that can operate between two constant temperature reservoirs." (Van Wylen and Sonntag 1985, 171). As will be explained shortly, this is somewhat misleading. To promote the suggestion that this 'square' cycle is the standard bearer, the ideal vapor compression cycle is usually compared to it. Some effort is made to avoid this ennobling when power and refrigeration cycles are discussed. The key is that the cycle processes must be reversible, which we learned from undergraduate thermodynamics requires that heat transfer take place across an infinitely small temperature difference. And, that compression or expansion be isentropic; that there be no friction (mechanical and fluid), etc. So, actually, assuming that the individual process steps are reversible (however,

currently impractical they may be; like reversible isothermal expansion), the Stirling cycle (isochors and isotherms) and Ericsson cycle (isobars and isotherms) are also 'Carnot' cycles; refer to Figure A.1. The Brayton cycle could be also be a 'Carnot' cycle, as long as the thermal reservoirs are not isothermal. This may sound strange, but is not uncommon in cryogenics. A common variant of the (reverse) Brayton cycle, involving isentropic expansion and isothermal compression (rather than isentropic compression) forms the essential process step basis for nearly all large refrigerators and most small refrigerators supporting a non-isothermal refrigeration load {see Figure A.2, Knudsen and Ganni (Simplified helium refrigerator cycle analysis using the 'Carnot Step' 2006)). This could equally be called a variant to an Ericsson cycle. In fact, there are an infinite number of such (yet to be named?) 'Carnot' cycles.

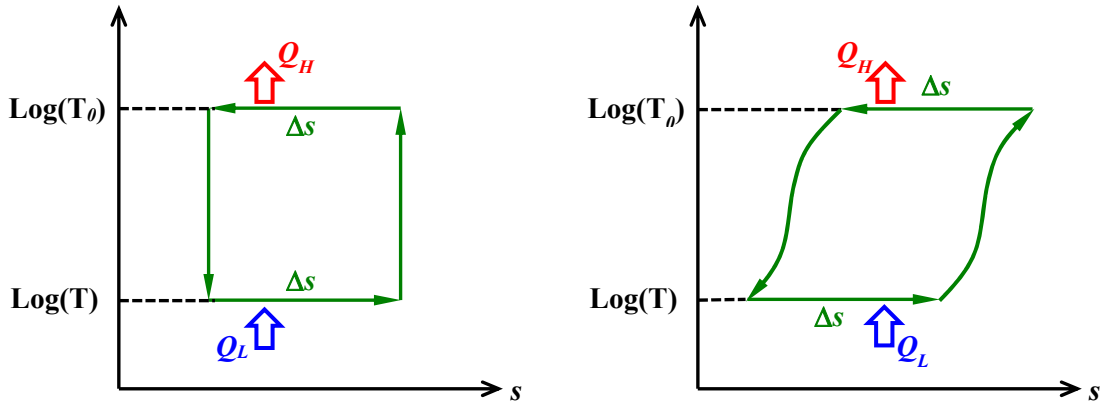

Figure A.1. Traditional Carnot cycle and an equivalent 'Carnot' cycle with isothermal reservoirs

So, if the 'squareness' is not the defining (visual) characteristic for a (closed) cycle, what qualifies it as a 'Carnot', or a 'standard bearer', cycle? To start we should notice that what does not occur in the 'square' Carnot cycle is heat transfer between the working fluid itself at different process points in the cycle. Recalling the Clausius (in)equality, if there is heat transfer to (from)

the fluid, its entropy increases (decreases). It is straight-forward to show that balanced (equal mass flow in both streams) counter-flow heat exchange is reversible as long as the entropy difference between the two process conditions is the same at every temperature where the heat transfer (between the working fluid at different process conditions) is occurring.

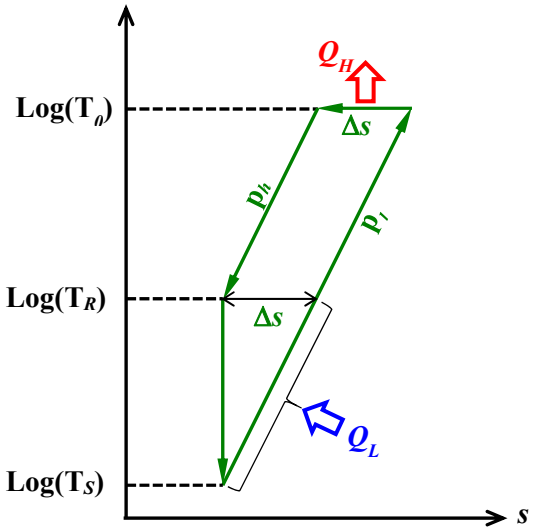

Figure A.2. Modified Brayton (or Ericsson) cycle with non-isothermal reservoir

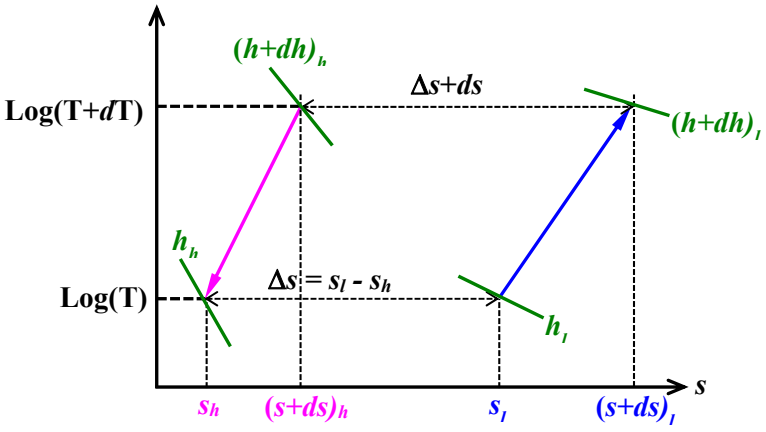

Figure A.3. Balanced counter-flow heat exchange occurring reversibly

Referring to Figure A.3, with $\dot{m} = \dot{m}_h = \dot{m}_l$, according to the first law of thermodynamics, the net (specific) work output is $dw_{net} - dq_{sur} = (dh_h - dh_l)$; where the heat transfer in from the surroundings (or another thermal reservoir) is q_{sur}. The net (physical) exergy flux is, $d\varepsilon = (dh_h - dh_l) - T_0 \cdot (ds_h - ds_l)$. If the process is reversible, then, $dw_{rev(net)} = dw_{net} = d\varepsilon = (dh_h - dh_l) + dq_{sur}$. So, $dq_{sur} = -T_0 \cdot (ds_h - ds_l)$. For a cryogenic process, $dq_{sur} \geq 0$, which requires, $ds_l \geq ds_h$. That is, for non-zero dq_{sur} we would expect Δs to increase as the temperature increases. It is more plausible to require, $dq_{sur} = 0$, then $ds_l = ds_h$, which means that Δs is constant with respect to the temperature; that is, the entropy difference at every temperature is the same. However, in general, if $dq_{sur} \neq 0$, the process path required for $dw_{rev(net)} = 0$, is $d\varepsilon_h = d\varepsilon_l$. Otherwise, there could be reversible compression or expansion occurring, concurrent with the balanced counter-flow heat exchange. In any case, this greatly expands the 'picture' of what a 'Carnot' cycle could look like.

An ideal cycle, as opposed to a 'Carnot' (standard bearer) cycle, requires more input power if it is a refrigerator, or provides less output power if it is a heat engine. However, it uses ideal (reversible) components; i.e., isentropic compression and/or expansion and the heat exchange between the working fluid itself occurs at the same entropy difference for every temperature that the heat transfer is occurring. However, the heat transfer to the surroundings is not necessarily reversible. Consequently, it will be less efficient than a Carnot cycle. So, in general to analyze a cycle, is it necessary to develop its 'Carnot' cycle in order to ascertain how efficient it is as compared to the thermodynamic limit? Process cycles used in industry and in cryogenics can be quite complex, so this becomes a non-academic question. The answer is 'yes' and it is done employing the concept of exergy (or reversible work as it is called in some older textbooks).

However, before discussing this, several basic measures of efficiency must be established. The term efficiency generally indicates some sort of comparison ratio with a value that is between zero and one. In cryogenic refrigeration cycles, there are two commonly used 'efficiencies'; namely, the exergetic efficiency, also known as the efficiency as compared to 'Carnot', and inverse coefficient of performance. The former is the ratio of the exergy provided for an end use (the 'load') to either the exergy, or the actual (or equivalent) input power, supplied to a process to produce the exergy provided. For example, the overall exergetic efficiency is the ratio of the exergy provided to the load to the total (equivalent) electric input power. The cold box efficiency is the ratio of the exergy provided to the load to the exergy provided to the cold box (from the compressor system). The compressor system exergetic efficiency is the ratio of the exergy provided to the cold box to the total electric input power (to the compressors). The inverse coefficient of performance is the ratio of either total electrical input power or the exergy provided to a particular sub-system (e.g., compressor system, cold box) supplied to the process to produce the load to the load itself (not the load exergy). Figure A.4 and Table A.1 show these typical efficiency definitions and calculations for a helium cryogenic system.

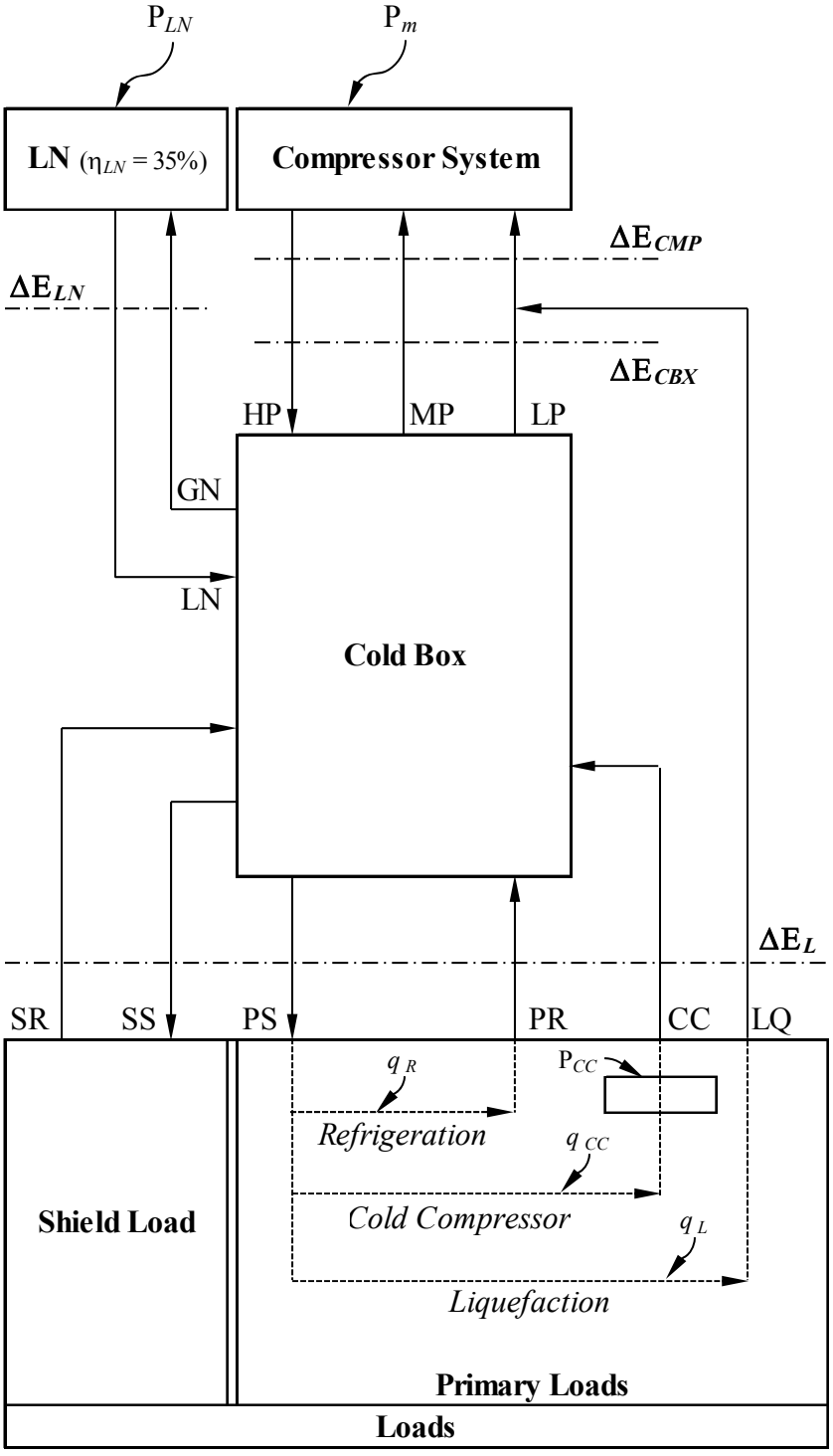

Figure A.4. Cold box system and associated mass, energy and exergy fluxes

Table A.1. Variables and symbol definition for cold box system fluxes

Stream	Description
HP	*High pressure supply stream to cold-box*
MP	*Recycle return stream to compressor system*
LP	*Load return stream to compressor system*
LN	*Liquid nitrogen*
GN	*Gaseous nitrogen (vent to atmosphere)*
SS	*Shield supply*
SR	*Shield return*
PS	*Primary supply*
PR	*Primary (refrigeration) return*
CC	*Cold compressor (or target) return*
LQ	*Liquefaction return (~1 atm, ~300 K)*

Variable	Definition	
$COP_{inv,act}$	*Actual inverse coefficient of performance*	$= P_{tot} / q_{R,eq}$
$COP_{inv,ideal}$	*Ideal inverse coefficient of performance*	$= (\Delta E_{CBX} + \Delta E_{LN}) / q_{R,equiv}$
η_{SYS}	*Overall system exergetic (percent of Carnot) efficiency*	$= \Delta E_L / P_{tot}$
η_{CMP}	*Overall compressor system efficiency*	$= \Delta E_{CBX} / P_m$
η_{CBX}	*Cold box efficiency (including LN)*	$= \Delta E_L / (\Delta E_{CBX} + \Delta E_{LN})$
η'_{CBX}	*Cold box efficiency (excluding LN)*	$= \Delta E_L / \Delta E_{CBX}$
η_{LN}	*LN system exergetic (percent of Carnot) efficiency*	
$q_{R,eq}$	*Equivalent 4.5-K refrigeration load for a load exergy of* ΔE_L	
P_{tot}	*Total equivalent input power*	$= P_m + P_{LN} + P_{CC}$
P_m	*Electrical power input to compressors*	
P_{LN}	*Equivalent input power for LN system*	$= \Delta E_{LN} / \eta_{LN}$
P_{CC}	*Input power to cold compressors*	
ΔE_{CBX}	*Cold box warm-end exergy flux*	
ΔE_{LN}	*LN exergy flux*	
ΔE_L	*Load exergy flux*	

Employing the concept of exergy, the task of ascertaining the cycle exergetic efficiency does not require the development of a 'Carnot' cycle (for example, Kotas (The exergy method of thermal plant analysis 1985)). The exergy method will simply provide the maximum work output possible under reversible process conditions, or conversely, the minimum work input possible

under reversible process conditions. Here, we recall the thermodynamics principle of path independence, that fluid properties such as enthalpy and entropy are state, not path, dependent variables (unlike work and heat transfer). Specific physical exergy is an intrinsic variable and is equal to the maximum amount of work possible when a process stream is brought from its initial state to the environmental state by physical processes involving only thermal interaction with the environment, and is defined as, $\varepsilon = h - T_0 \cdot s$, where h is the enthalpy, T_0 is the zero exergy reference (environmental) temperature and s is the entropy (Kotas 1985). Physical exergy is not appropriate for a non-flowing control volume process. Extrinsic physical exergy is obtained by multiplying by the mass flow rate; i.e., $\mathrm{E} = \dot{m} \cdot \varepsilon$. The exergy associated with heat transfer is, $\dot{W}_{rev,min} = q \cdot (T_0/T - 1)$, which brings us back to the familiar 'square' Carnot cycle efficiency, and is the minimum input power required to provide q cooling (since we are discussing refrigeration) at a temperature T (Kotas 1985, 34, 35). Figure A.5 shows the inverse coefficient of performance ($COP_{inv} = \left(\dot{W}_{rev,min}/q\right) = T_0/T - 1$) vs. the load temperature (T) and emphasizes the previous point of the energy intensiveness required by 4.5 K and 2 K helium refrigeration systems.

We have discussed refrigeration cycles which are (usually) closed cycles. However, like the combustion cycles typically discussed in undergraduate thermodynamic texts, liquefaction cycles can be 'open' cycles; that is, mass leaves the cycle and is replenished. A liquefier can be thought of as a refrigeration process that is successively cooling the mass flow (to be liquefied) from ambient to the final (liquid) temperature. Using this idea, one can think of a number of reversible heat pumps (RHP's i.e., Carnot refrigeration cycles) operating between ambient temperature and successively colder temperatures.

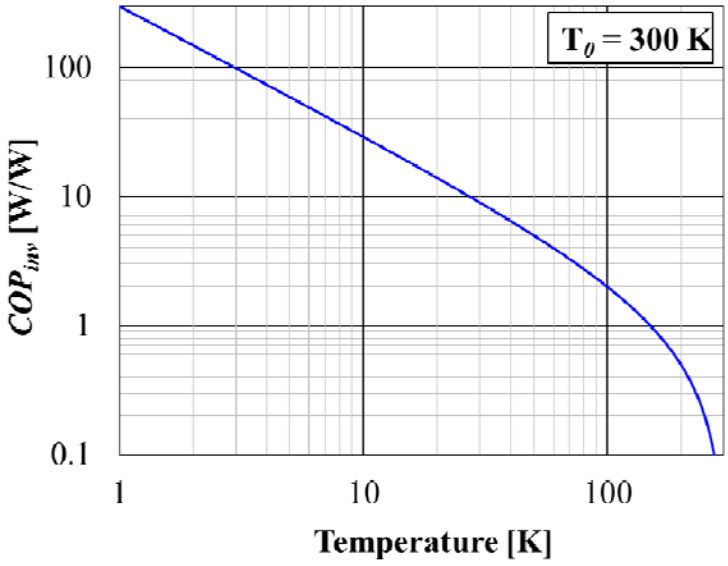

Figure A.5. Inverse coefficient of performance as a function of the load temperature

Of course, it would take an infinite number of these RHP's, each cooling the mass flow to be liquefied over an infinitesimal temperature span. More commonly in introductory textbooks on cryogenic systems, the Carnot liquefier is introduced (Barron, Cryogenic systems 1985), consisting of two process steps: reversible isothermal compression (of the feed gas at 1 atm and 300 K), and adiabatic isentropic expansion, producing 100 percent liquid. This of course is an impractical cycle for helium, even if the components that were used operated reversibly, since a (minimum) pressure ratio of approx. 718,200 would be required. An analysis of the Carnot liquefier shows that the reversible work per unit mass liquefied is, $w_{rev} = (T_0 \cdot \Delta s - \Delta h)$; where, T_0 is the ambient temperature (of the make-up gas), Δs is the entropy difference between the make-up gas (1 atm, 300 K) and the saturated liquid produced, and Δh is the enthalpy difference occurring in the adiabatic isentropic expansion. Note that $(T_0 \cdot \Delta s)$ is the heat rejected by the isothermal compression to ambient, which is equal to the isothermal compression work, and Δh is

the adiabatic isentropic work extracted, both per unit mass flow of the feed gas. Of course, this is easily obtainable just using an exergy analysis. The reversible input power required per 1 g/s of liquid helium produced would be 6.84 kW. Table A.2 shows the required input power per 1 g/s of liquid produced for other selected fluids.

Table A.2. Specific liquefaction input power [(W/(g/s)] for various fluids [14]

Name	Symbol	R #	T_{sat} at p_0 [K]	COP_{inv} [W/W]	Δh [J/g]	$(T_0 \cdot \Delta s)$ [J/g]	w_{rev} [J/g]
Refrigerant-11	CCl_3F	R-11	296.78	0.01	183.2	185.2	2.0
n-Butane	C_4H_{10}	R-600	272.64	0.10	432.0	473.0	41.0
Iso-Butane	C_4H_{10}	R-600a	261.53	0.15	429.4	487.7	58.3
Refrigerant-124	C_2HF_4Cl	R-124	261.11	0.15	192.8	219.2	26.5
Refrigerant-134A	$C_2H_2F_4$	R-134a	246.85	0.22	260.5	311.6	51.0
Refrigerant-12	CCl_2F_2	R-124	243.40	0.23	199.3	241.5	42.2
Ammonia	NH_3	R-717	239.81	0.25	1501.9	1861.1	359.2
Refrigerant-22	$CHClF_2$	R-22	234.33	0.28	274.9	348.0	73.1
Propane	C_3H_8	R-290	231.07	0.30	533.8	675.1	141.3
Refrigerant-125	C_2HF_5	R-125	225.01	0.33	220.6	283.6	63.0
Refrigerant-32	CH_2F_2	R-32	221.47	0.35	446.1	591.9	145.7
Ethane	C_2H_6	R-170	184.55	0.63	670.2	1021.6	351.4
Ethylene	C_2H_4	R-1150	169.24	0.77	662.3	1088.8	426.4
Xenon	Xe		165.04	0.82	118.5	204.7	86.2
Krypton	Kr	R-784	119.77	1.50	153.6	340.5	186.9
Methane	CH_4	R-50	111.69	1.69	914.0	2006.3	1092.3
Oxygen	O_2	R-732	90.19	2.33	406.1	1041.3	635.2
Argon	Ar	R-740	87.28	2.44	273.7	751.2	477.5
Carbon Monoxide	CO		81.62	2.68	444.1	1200.9	756.8
Nitrogen	N_2	R-728	77.31	2.88	433.6	1203.4	769.8
Neon	Ne	R-720	27.09	10.07	368.6	1705.1	1336.5
Deuterium	D		23.66	11.68	2271.4	9132.4	6861.0
Hydrogen	H_2	R-702	20.28	13.80	4455.3	17028.1	12572.8
Helium-4	He	R-704	4.22	70.05	1563.5	8402.9	6839.4

[14] Also, the inverse coefficient of performance for each has been included. Note: p_0 = 1 atm, the pressure of the 300K feed gas

Neither of these two cycle models (infinite cascade of RHP's and Carnot liquefier) for a liquefier have a practical cycle counter-part (i.e., one using practical, irreversible components). Modern liquefiers use multiple expansion stages, often with more than two pressure levels, consisting of a superposition of modified (reverse) Brayton cycles. They are 'modified', in that the compression step is isothermal (at ambient temperature) rather than isentropic. Also, typically, the coldest stage is a JT stage, since turbo-machinery is usually employed for the adiabatic expansion and a reliable turbo-expander capable of a two-phase discharge has not yet been developed. As it turns out, assuming an ideal gas[15], this superposition of modified (reverse) Brayton cycles using adiabatic-isentropic expansion, reversible-isothermal compression, and perfect counter-flow heat exchange, has an exergetic efficiency (and input power per unit cooling provided) the same as the Carnot liquefier and an infinite cascade of RHP's (Knudsen and Ganni, Simplified helium refrigerator cycle analysis using the 'Carnot Step' 2006). The actual load on helium refrigerators is usually some combination of both isothermal refrigeration and liquefaction, and often, also a non-isothermal refrigeration load. In addition, due to heat in-leaks, finite counter-flow heat exchanger stream-to-stream temperature differences and the high pressure stream (being cooled) having a higher specific heat (C_p) than the lower pressure stream(s), this arrangement is used for both refrigeration and liquefaction. This arrangement, which we shall refer to as a Collins type cycle (except that there can be more than two expansion stages and more than two pressure levels), minimizes the magnitude of the pressure level for the high pressure stream (recall the Carnot liquefier), but at the cost of additional mass flow in the cycle. A pure isothermal refrigeration load, negating the other factors mentioned (i.e., heat in-leaks, finite stream ΔT's,

[15] Helium is essentially an ideal gas down to 15 to 20 K.

higher C_p for high pressure stream), actually benefits from not expanding from the high pressure back to the returning lower pressure stream (as in the Collins type cycle). Rather, simply expanding the high pressure stream to overcome the latent heat as the liquid vapor dome is approached is more efficient (Ganni, Design and optimization of helium refrigeration and liquefaction systems 2009).

Three final comments should be made. Recall from thermodynamics that any given cycle is independent of the working fluid. The selection of the working fluid is based upon practical considerations of real-components used in the cycle. Second, vapor compression refrigeration is not used in cryogenics because of the severe operating conditions that would be imposed due to the very large temperature change that the working fluid undergoes (recall the Carnot liquefier). Lastly, it is important to realize that JT stages do not 'produce' refrigeration since the throttling process is isenthalpic (i.e., work is not extracted, even though the fluid 'expands'). The yield of the JT stage is dependent on the availability given to it by the (ambient) compressors and by efficiency of the turbines 'above' it (i.e., those operating at a higher temperature). It can only 'yield' based upon what it is given, not from 'its own merits'.

A.2. Selected History Overview

The purpose for this selected overview is to:

1. Introduce those less familiar to helium cryogenics some of the history of these systems. In particular, to early (historically important) systems which did not use a JT (or 'wet') expander at the cold-end of the refrigerator and to key sub-atmospheric helium systems (i.e., those maintaining a load temperature below the normal boiling point at 4.5 K) used for large accelerator projects.

2. Highlight instances recognized by investigators/researchers of the effect of pressure drop concurrent with counter-flow heat exchange.
3. Highlight the history of expanders used in a two-phase regime. As mentioned previously, this is pertinent since the present investigation involves heat exchange between 4.5 and (nominally) 2-K, rather than work extraction. Expanding into the two-phase regime for 2-K systems is not the same as at 4.5 K, since the saturated liquid to vapor density ratio is 5.7 at 1.25 bar (4.45 K) and is 185 at 31 mbar (2.00 K).

This overview is separated into two sections: 4.5 K helium systems and nominally 2-K (sub-atmospheric) helium systems. This is also chronological. 4.5 K refrigeration is discussed since this technology is foundational to 2-K refrigeration. More sections and sub-sections are possible, but they are not pertinent; such as milli-Kelvin refrigeration (e.g., dilution and adiabatic demagnetization systems), and regenerative cryo-coolers (e.g., Stirling, Gifford-McMahon, pulse tube, etc.), among others.

A.2.1. Normal Helium Refrigeration

For helium refrigerators, liquid nitrogen is commonly used in the US to pre-cool the helium to around 80 K in an open (pre-cooler) cycle; i.e., the nitrogen is vented. Before the development of S.C. Collin's 1946 liquefier (and subsequent ones), hydrogen was used in a pre-cooler system or a cascade system, that usually also included liquid nitrogen. Typically the hydrogen would be at a reduced pressure (approx. 0.072 atm, or 14 K), as in (Scott 1959, 58). After the hydrogen pre-cooler stage, there would be a JT stage, comprising a counter-flow heat exchanger followed by a throttling valve on the high pressure supply stream. The discharge pressure from the ambient

temperature compressor would typically be considerably higher than modern helium refrigerators. For example, the NBS Cryogenic Engineering Laboratory Helium Liquefier had a supply pressure of 30 atm (426 psig) (Mann, et al. 1960). H. Kamerlingh Onnes (see Figure A.6), who was the first to liquefy a tea cup (60 mL) of helium on July 10, 1908, used a similar process, except liquid air was used instead of liquid nitrogen and the helium was compressed to 100 atm (1455 psig) (de Bruyn Ouboter 2009, Onnes 1909). These were processes amenable to continuous operation. The Simon expansion liquefier (Pickard and Simon 1948) was commonly used to batch produce small amounts of liquid helium, and also required liquid nitrogen, liquid hydrogen and high pressure helium, but uses a different process (Scott 1959).

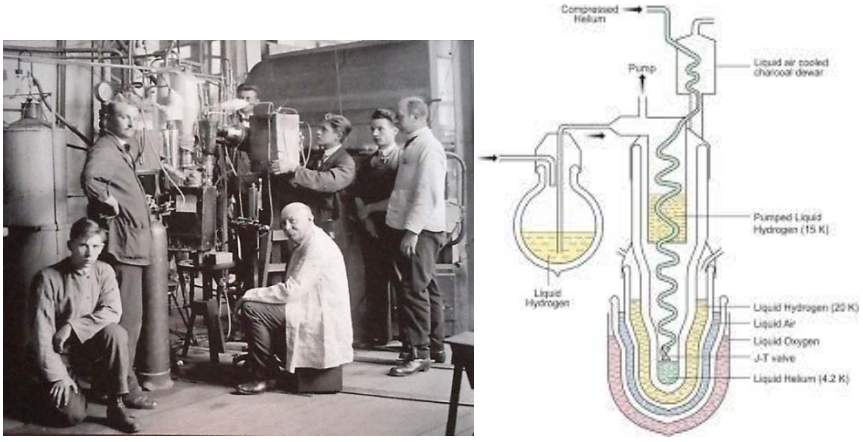

Figure A.6. Onnes helium liquefier [16]

[16] (Left) Heike Kamerlingh Onnes with his apparatus that produced the first liquid helium in 1908; (right) schematic of apparatus (courtesy of Peter Kes, Leiden University, Kamerlingh Onnes Laboratory)

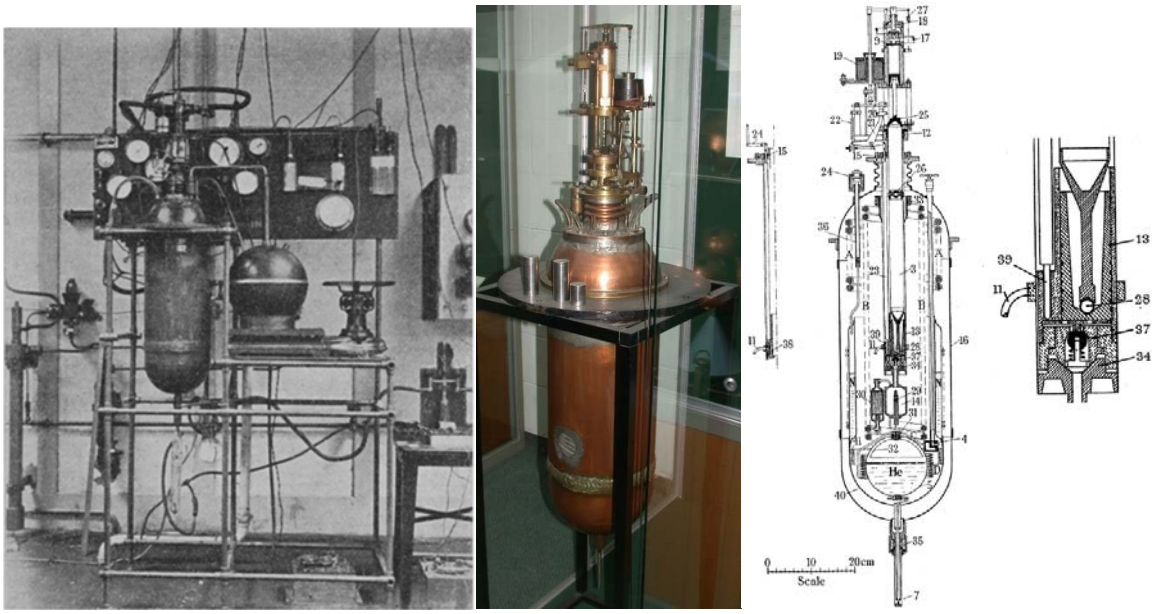

Figure A.7. Kapitza helium liquefier [17]

Although Kapitza was the first to use an expansion engine (of his design) to produce liquid helium (see Figure A.7) (Kapitza 1934), it was not until the development of S.C. Collin's 1946 liquefier with its flexible rod piston expanders (see Figure A.8) (Collins, A helium cryostat 1947, Collins and Cannaday, Expansion machines for low temperature processes 1958) at MIT and the subsequent commercialization by Arthur D. Little (ADL), Inc. (Kroptschot, Birmingham and Mann 1968) that helium cycles using work extraction became common place. The ADL Collins Helium Cryostat, as it became known, made liquid helium readily available to low temperature physics labs all over the world (Smith, Jr., 50 years of helium liquefaction at the MIT cryogenic engineering laboratory 2002). Collins (A helium cryostat 1947) would continue to test new ideas and refine existing ones throughout his career at MIT, and after retiring and continuing his work

[17] (Left) from (Kapitza 1934, Figure 4)); (middle) picture at Cavendish Lab, London, http://www-outreach.phy.cam.ac.uk/camphy/museum/area7/images/cabinet1_1.jpg; (right) from (Kapitza 1934, Figure 3)

at ADL, where he designed and built the Model 2000 and the highly successful and well known Model 1400 helium liquefiers. These would use a piston-displacer expander consisting of a 3 inch diameter solid phenolic-plastic bar with the seal, a Buna rubber O-ring, at the warm end. In 1970, a 'wet' expander, discharging two-phase helium, was successfully developed (Johnson and Collins 1970) and implemented commercially (Ganni, Moore and Winn, Capacity upgrade of the Excell helium liquefier plant by the addition of a wet engine 1986), increasing liquid production by approx. 30% without any additional process/equipment changes.

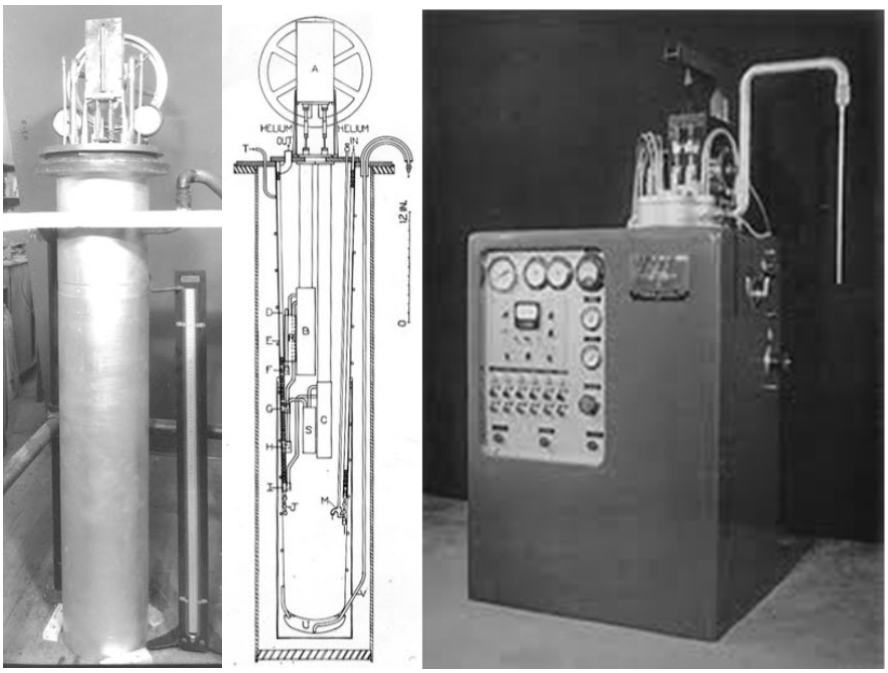

Figure A.8. S.C. Collins helium liquefiers [18]

[18] (Left and middle) 1946 Collins helium liquefier, http://web.mit.edu/hmtl/www/liquidhelium.pdf, accessed 19-Oct-2016, Figure 2(a) and 2(b), respectively; (right) Collins ADL commercial helium liquefier, https://www.tut.fi/smg/tp/kurssit/DEE-54030/2015-2016/Kryogeniikan-historiaa.pdf, accessed 16-Oct-2016, slide 11)

The 1946 liquefier had two stages of expanders and a final (cold) JT stage. This basic arrangement of two expansion stages (without liquid nitrogen pre-cooling) and a final (cold-end) JT stage is what is known as the Collins (helium liquefaction) cycle (Barron, Cryogenic systems 1985) and is still used in the Linde (formerly Koch/CTI) Model 1400 and 1600 helium liquefiers. The significance of the Collins cycle is that unless liquid nitrogen pre-cooling (or another fluid providing a lower temperature) is used, a practical helium liquefier requires at least two expansion stages. There is a maximum number of expansion stages that can be implemented for a given compressor discharge pressure and expander efficiency (Knudsen and Ganni, Simplified helium refrigerator cycle analysis using the 'Carnot Step' 2006, Trepp, Refrigeration systems below 25 K with turboexpanders 1961). As it turns out, there is an optimum temperature to 'locate' each expansion step (Knudsen and Ganni, Simplified helium refrigerator cycle analysis using the 'Carnot Step' 2006) and an optimum design mass flow for each expander. It is important to realize that although the arrangement in the Collins cycle has the expansion steps from the high pressure stream (recycled) to the low pressure stream, that the expansion step can also occur without 'recycling' the expansion flow back to the return (lower pressure) stream. As long as there is a counter-flow heat exchanger (exchanging heat between the high pressure stream(s) being cooled and the return stream(s)) in between the expansion stages, then it is its own (expansion) stage. In modern helium refrigerators, this is quite commonly done in the cooling stage just 'above' (i.e., higher in temperature level) the final (JT) stage, in which the high pressure is dropped down to just above helium's critical pressure (i.e., usually around 3 bar) to ensure a stable supply stream to the load (i.e., to cool a super-conducting device). Confusingly, this stage is usually called a 'JT-expander' or 'wet-expander' stage (Knudsen, Ganni and Than, Options for cryogenic load cooling with forced flow helium circulation 2012).

By the 1960's oil bearing radial in-flow turbines (with an oil brake) had been developed for helium refrigerators and self-acting (or dynamic) gas bearing radial in-flow turbines (with a variable brake) were being developed (Trepp, Refrigeration systems below 25 K with turboexpanders 1961, Trepp, A large scale helium liquefier 1966). By the 1970's self-acting gas bearings with variable brakes and static gas bearings with fixed brakes were in use (Byrns 1984). These turbines use a fixed nozzle and as long as an appropriate cycle is used (Ganni and Knudsen, Optimal design and operation of helium refrigeration systems using the Ganni cycle 2010) with the self-acting variable brake design, this does not cause un-due adiabatic efficiency loss when the plant is operated at an off-as-designed condition. However, radial in-flow turbines with adjustable guide vanes and an oil bearing have been used for a very large helium refrigerator (Byrns 1984). Radial in-flow turbines are the proper choice for helium refrigerators (Brown 1960, von der Nuell 1952), offering excellent reliability (no wear and being adequately robust) and modern designs offering good adiabatic efficiency (up to 88% for a non-JT expander with a pressure ratio of around 2.5 to 3). They are used even for small refrigerators only producing 2 g/s (liquefaction, or equivalently, 200 W of 4.5 K refrigeration), though the turbine wheel sizes are quite small (~15 mm wheel diameters; see Figure A.9). (Haberstroh 2009) offers a concise pictorial view of the 'evolution of helium plant technology'; see Figure A.10.

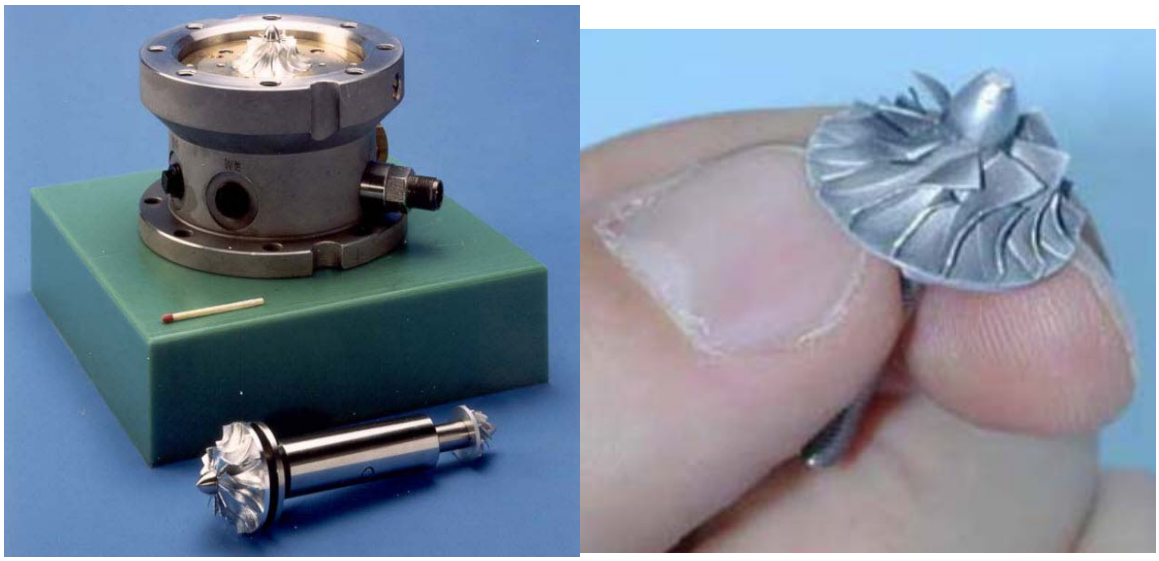

Figure A.9. Dynamic gas bearing turbo-expander [19]

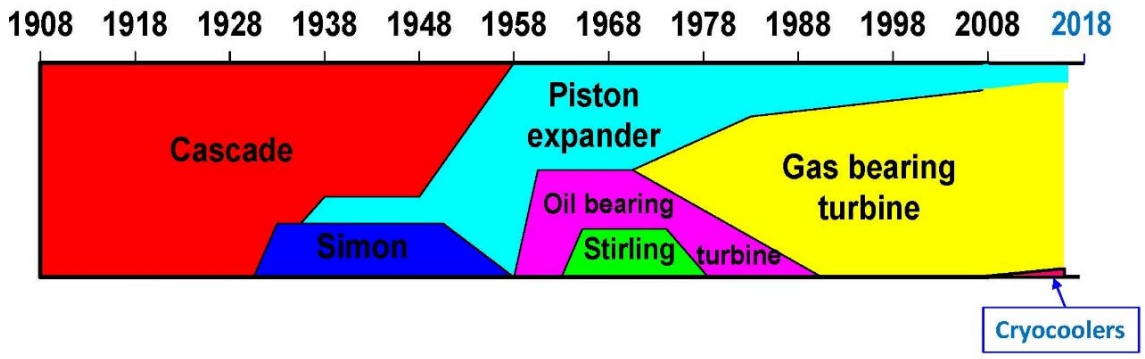

Figure A.10. "Evolution of helium plant technology" [20]

[19] Courtesy of Linde Kryrotechnik, Pfungen, Switzerland
[20] Courtesy of Ch. Haberstroh, TU Dresden

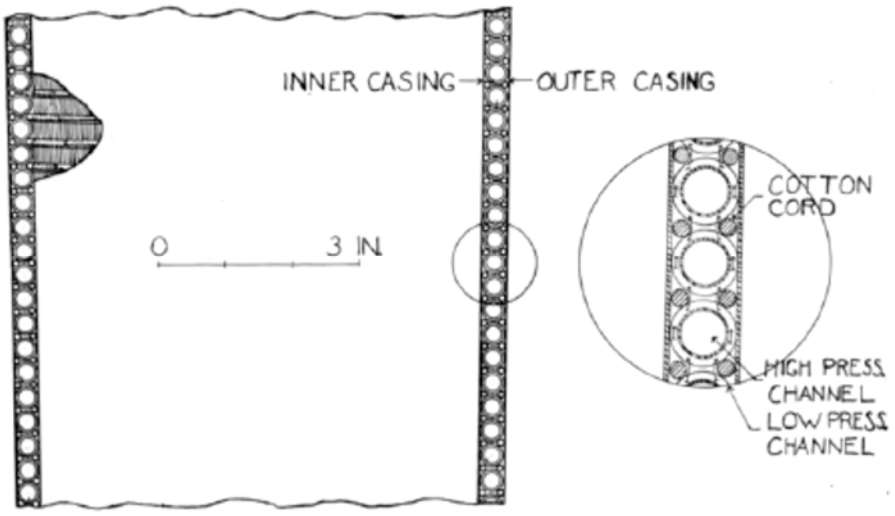

Figure A.11. 1946 Collins helium liquefier heat exchanger [21]

The heat exchanger used in the 1946 Collins liquefier consisted of tubing, with spiral finning made of edge-wound copper ribbon, that was helically wound on a conical mandrel and enclosed on the outside by a larger diameter conical shell (see Figure A.11 and Collins (1947, Figure 10)). The high pressure helium flows inside the tubing. Cotton cord is used to seal the gap between the fins and the conical shells, which forces the low pressure helium to flow through the fins, rather than the annular gap and open spaces that would otherwise be present if the cord was not used. The use of the conical shells allowed easy assembly and a tight fit (from a wedge action). This counter-flow heat exchanger design offers a significant improvement to the Giauque-Hampson heat exchanger (Kroptschot, Birmingham and Mann 1968) with high surface area per unit volume and minimizes the effect of improper flow distribution which can easily and significantly degrade the performance (Fleming 1967). Later this basic design would be used for

[21] http://web.mit.edu/hmtl/www/liquidhelium.pdf, accessed 16-Oct-2016, Figure 3.

the highly successful Linde (formerly Koch/CTI) Model 1400 and 1600 helium liquefiers, except using cylindrical shells (and solid braided nylon rope) which would be cylindrically 'nested' (see Figure A.12), with the coldest heat exchanger being the inner most one and a vacuum gap in between each successive heat exchanger 'layer'. These are known today as Collins heat exchangers, although Collins also developed during World War II a coaxial tube heat exchanger with an edge-wound helix of copper ribbon soft soldered to the outside tube that surrounds it and the inner tube that it surrounds (Trumpler and Dodge 1947); these are sometimes referred to as Collins-Joy-tube heat exchangers (Smith, Jr., A tribute to Samuel C. Collins: September 28, 1898 – June 19, 1984 1985). Interestingly, prior to the Model 2000, in Collins' designs, the heat exchangers and expanders were housed within the dewar, such that they were surrounded with the low pressure (approx. 1 atmosphere) helium and would have an temperature gradient from ambient at the top plate to 4.5 K near the saturated vapor.

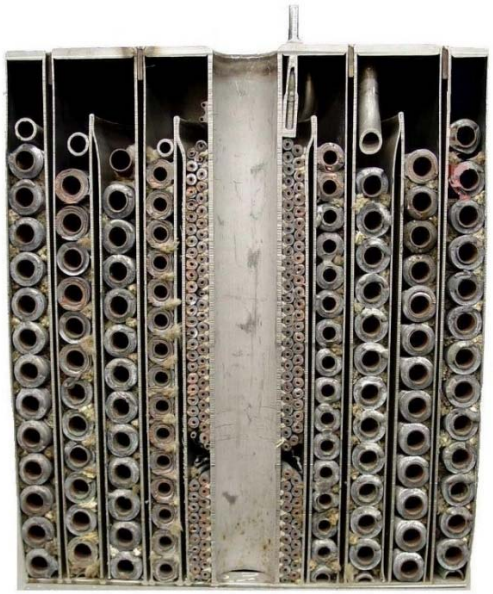

Figure A.12. Linde model 1400 helium liquefier heat exchanger [22]

[22] Courtesy of Linde Group, Tulsa, Oklahoma

A.2.2. Helium Refrigeration Below 4.5 K

In 1967 S.C. Collins tested an experimental helium refrigerator capable of 10 W at 2 K (Collins and Streeter, Refrigerator for 1.8 K 1967, Collins, Stuart and Streeter, Closed-cycle refrigeration at 1.85 K 1967). It consisted of an Arthur D. Little (ADL) – Collins type ('standard') liquefier, which used two reciprocating expanders and liquid nitrogen pre-cooling, a 300 to 2 K heat exchanger and vacuum pumps (Figure 6 in Smith, Jr. (A tribute to Samuel C. Collins: September 28, 1898 – June 19, 1984 1985) shows Collins' process design). The expanders were Collins' piston-displacer type design. The heat exchanger recovering the sub-atmospheric 2 K helium refrigeration was composed of a stack of tightly wound spirals of finned tubing, wound from inside to outside, then from the outside to the inside, forming successive 'pancake' layers, with the high pressure helium (being cooled) inside the tube and the sub-atmospheric helium flowing perpendicular to the 'pancakes' in an overall counter-flow configuration (see Figure A.13). The 'pancake' layers were enclosed within a tight fitting shell, whose diameter varied in steps; with smallest diameter section at the coldest end and the largest diameter section at the warmest end. The capacity of this test apparatus was limited by the vacuum pumps. The 300 to 80 K section was pre-cooled using liquid nitrogen and the 80 K to 7 K section of this heat exchanger was imbalanced, with more sub-atmospheric flow. Below 7 K the flow was balanced, with 15 atm helium injected at 7 K from the ADL-Collins liquefier and three Joule-Thompson valves (see Figure 6 in Smith, Jr., (1985)), each with an intermediate heat exchanger section and the last (fourth) valve supplying the 2 K load. It was noted that, "If only the final expansion valve is used the high pressure stream cannot adsorb all of the refrigeration available in the outgoing vapor." (Collins and Streeter, Refrigerator for 1.8 K 1967, 215) This experimental refrigerator was intended as a proof of concept demonstration for a 300 W 1.85 K refrigerator to be built for

the Stanford Linear Accelerator (SLAC) (Schwettman, et al. 1964) and was the first non-batch production of refrigeration below 4.5 K.

Figure A.13. 'Pancake' heat exchanger section used by S.C. Collins for experimental 1.8 K helium refrigerator [23]

The SLAC 1.8 K helium refrigerator, designed by S.C. Collins and manufactured by 500 Inc. (a subsidiary of Arthur D. Little, Inc., Cambridge, Massachusetts) (Collins, Refrigeration at temperatures below the boiling point of helium 1968) was capable of 330 W at 1.9 K (McAshan 1980). This refrigerator supported the first linear accelerator using super-conducting radio frequency cavities. It was similar to the experimental one (in a scaled sense), except that a portion of the high pressure flow through the 'pancake' heat exchanger (see Figure A.14) at 16 K was routed to the low pressure (return) stream of the 4.5 K refrigerator such that the second (and last) expansion engine effectively provided cooling between 16 and 8 K; at which point 15 atm flow at

[23] http://web.mit.edu/hmtl/www/liquidhelium.pdf, accessed 16-Oct-2016, Figure 6(a)

8 K was injected to the 'pancake' heat exchanger. Only two Joule-Thompson valves in between heat exchanger sections were used with a final (third) JT valve to the 1.9 K load in the original design. Later a wet expander, presumably similar to Johnson and Collins (Hydraulically operated two-phase helium expansion engine 1970) was used as reported by McAshan (Stanford superfluid refrigerator 1980). This is the only known use of a wet expander used in a 2-K (1.8 K) helium refrigerator. However, there are no known references or data (published or unpublished) describing more details as to its performance. The refrigerator system by 1980 had been operated for more than 30,000 hours. At the time of this writing, it has been decommissioned for many years.

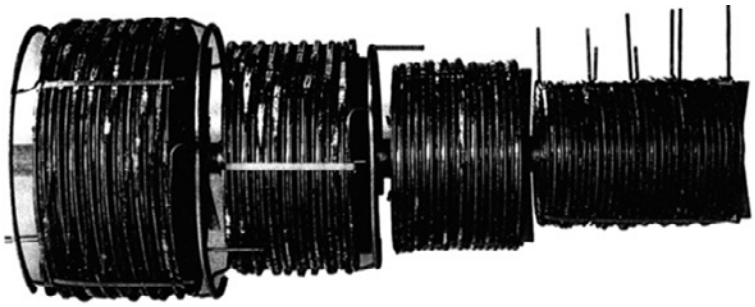

Figure A.14. SLAC 1.8 K helium refrigerator low pressure 'pancake' heat exchanger [24]

In 1967, Linde AG built a 1.8 K helium refrigerator capable of 28-32 W (Baldus and Sellmaier, A continuous helium II refrigerator 1967, Peterson 1989). This machine used a standard 4.5 K liquefier (capable of approx. 55 liter per hour), incorporating a LN pre-cooler consuming

[24] Approx. 7 ft. tall with 4 sections (300 to 80 K, 80 to 16 K, 16 to 7 K, 7 to 1.8 K) and upper-warmest section diameter approx. 2.7 ft. (shown horizontal, but installed vertically, warm-end on top).

~10 lph, and a four stage, oil lubricated, air-cooled compressor supplying the 4.5 K liquefier ~5 g/s at 30 atm. The liquefier used a Doll-Eder reciprocating expander operating between 24 to 12K. About 40% of the compressor mass flow was provided to the 1.8 K refrigeration recovery, which was separate from the standard 4.5 K liquefier. However, a portion of the high pressure flow from the 1.8 K refrigeration recovery was cooled by the 4.5 K liquefier reciprocating expander and re-injected downstream of an intermediate JT valve. A 3000 m^3/hr capacity, two-stage vacuum pumping system comprised of a rotary pump and a roots (blower) pump brought the sub-atmospheric flow to positive pressure and supplied the 4.5 K liquefier compressor. The power consumption was around 76 kW. It was noted by the authors that (in the 1.8 K refrigeration recovery), "It is known, however, that, with decreasing temperature of the pressurized gas, the pressure must be reduced because of the change in specific heat of the pressurized gas near saturation. There are two possibilities of reducing the pressure, either with valves, as is done here at higher temperatures with valves V1 or V5 (see Figure 1 in Baldus and Sellmaier (A continuous helium II refrigerator 1967)), or by making use of the pressure drop in the heat exchanger (18) itself. The latter solution of this problem has the advantage of greater simplicity in operation, because otherwise more than three valves would be necessary. On the other hand, the latter solution needs a very exact calculation of the pressure drop, an exact fabrication, and comprehensive experiments." (Baldus and Sellmaier, A continuous helium II refrigerator 1967, 436). The counter-flow heat exchanger as describe (item 18 in Figure 1 of Baldus and Sellmaier (A continuous helium II refrigerator 1967)) indicates a pressure drop of ~5 atm to 3 atm, spanning 5 to 1.8 K, and yielding ~85% liquid yield.

In 1969 Linde AG built a 1.8 K (16.6 mbar) 300 W (nominal) helium refrigerator for the Nuclear Research Centre, Karlsruhe (Germany) (Baldus, Helium-II refrigerator for 300 W at 1.8

K 1971, Sellmaier, Glatthaar and Klien 1970) based upon the experience gained from the 1.8 K 30 W refrigerator (Baldus and Sellmaier, A continuous helium II refrigerator 1967). This plant had an integrated 4.5 K liquefier and 2-K refrigeration recovery. It had three process streams, high pressure, low pressure (~1 atm) and sub-atmospheric. It did not use liquid nitrogen pre-cooling and had two expansion steps, each using an oil-bearing Linde turbine. The sub-atmospheric heat exchanger was a cross-counter flow type, using wound smooth copper coil tube. The compressor was a plastic-ring, dry-type, water-cooled, three stage machine, capable of 3000 m^3/h displacement (at 1 bar) and supplying 150 g/s at 20 bar to the liquefier and 1.8 K refrigeration recovery. The vacuum pumping system used eight stages of a dry (oil-free) water cooled, roots (blower) pumps capable of 10 m^3/s at room temperature and 10 mbar. Its capacity was measured to be 340 W at 1.8 K and required 520 kW of input power to the compressors and 170 kW of input power to the vacuum pumps (i.e., an inverse coefficient of performance of ~2 kW/W). It was noted by the authors that, "For effective heat transfer, three additional expansion valves…are provided to increase the specific heat of helium by lowering the pressure in the individual gas stream. In principle, it would be possible to make use of the pressure drop in the heat exchangers, thus avoiding the installation of the expansion valves. This would, however, mean a loss in flexibility, especially with respect to the combined operation of the plant, where, at reduced refrigeration performance, helium is simultaneously liquefied" (Sellmaier, Glatthaar and Klien 1970, 311).

A 370 W 1.8 K helium refrigerator was built by Messer Griesheim for the Nuclear Research Centre in Karlsruhe (Germany) in 1972 (Daus and Ewald 1975). It used one reciprocating expansion stage, also made by Messer Griesheim, which incorporated power regeneration of the fly wheel. The 4.5 K refrigerator and 1.8 K refrigeration recovery were integrated and the helium is pre-cooled from 300 to 80 K by nitrogen. A nitrogen cryo-generator re-liquefies the nitrogen

vapor. Aluminum brazed plate-fin heat exchangers are used for the 4.5 K (i.e., positive pressure) portion of the refrigerator. Unidirectional cross-counter flow, coil-fin tube heat exchangers are used for the 1.8 K refrigeration (i.e., sub-atmospheric) refrigeration recovery. The authors provide some pressure drop and heat transfer data for the shell side of these heat exchangers. These heat exchangers do not use a rope/cord seal to fill the gap between the circular fins. Between 4.5 K and 1.8 K the authors note that, "After passing E8 *(the heat exchanger just above the 4.5 to 1.8 K heat exchanger)*, the helium is brought down to a temperature level of 1.8 K by a triple process of alternating cooling and expansion." (italics text added) (Daus and Ewald 1975, 592). The sub-atmospheric helium (at near ambient temperature) exiting the cold box is compressed from 11 mbar to 0.47 bar by four stages of roots vacuum pumps that can handle 18.5 g/s; adequate for the 16.4 g/s returning from the 1.8 K load. A dry reciprocating piston compressor compresses the helium to 1.1 bar, then three further stages compress this and the 4.5 K refrigerator recycle flow to 20 bar. These can handle 55 g/s which is adequate for the 50 g/s supply required to the cold box. The total electrical input power required is stated to be 436 kW.

In 1976 BOC Limited built a 300 W 1.8 K helium refrigerator for a superconducting RF particle separator built at GfK Karlsruhe and to be used at CERN (Steel, Bruzzi and Clarke 1976). The 4.5 K and 2 K cold box were integrated and it could use liquid nitrogen. It used three BOC gas lubricated turbines, two in the upper (warmer) expansion step and one in the lower (colder) expansion step. Evidently, the preferred method for overall plant stability in controlling the turbines was to modulate the inlet valve to maintain a given inlet temperature. The warm compressor was a three stage, dry, reciprocating type (Sulzer Brothers), and has a discharge pressure of 12.7 bar, delivering 150 g/s. Six stages of roots (BOC-Edwards) vacuum pumps, which were water-cooled and oil lubricated, were used to process the sub-atmospheric helium from 11.3

mbar to 1 bar at 19 g/s, which was fed to the suction of the warm compressors (i.e., there was no purifier). The total input power was about 600 kW. From 10 K to ambient temperature, the refrigeration of the sub-atmospheric stream was recovered using a wound copper tube heat exchanger (with the high pressure inside the tubes and the sub-atmospheric flow outside the tubes, between the shell and mandrel) that has a 850 mm outside (shell) diameter and splits the high pressure into 11 tube passes. All other heat exchangers were aluminum brazed plate-fin type, including the 4.5 to 1.8 K heat exchanger and the one spanning from ~4 to 10 K. The authors cited, "The present process of sub-cooling liquid at atmospheric pressure is much simpler than the one previously used [1-4] which employs multiple expansion of high pressure gas. As there is only one stage of expansion process control is much easier. The design of exchanger 6 is also greatly simplified, as there is no phase change and the temperature profile is continuous and monotonic."[25] (Steel, Bruzzi and Clarke 1976, 58). Their method took saturated liquid from the 4.4 K 1.2 bar bath, counter-flow heat exchanged with the 1.8 K sub-atmospheric helium and then throttled (they used the term 'expanded') to the sub-atmospheric load (16.7 mbar).

The Tore Supra refrigerator was built by Air Liquide for the CEA (France) around 1986 and was designed to provide 300 W at 1.75 K (13.7 mbar saturation pressure) (Claudet, et al. 1986, Gistau and Claudet, The design of the helium refrigerator for TORE SUPRA 1984, Gistau and Claudet, The TORE SUPRA 300 W – 1.75 K refrigerator 1986). The 4.5 K and 2 K cold boxes were integrated and it had three (Air Liquid, static gas bearing) turbines. Two were used for expansion steps and a third was used for an 80 K helium shield. The warm compressors were oil lubricated screw compressors (STAL, Sweden) and comprised of two stages with two compressors

[25] References 1-4 in are the previously discussed papers by (Baldus and Sellmaier, A continuous helium II refrigerator 1967, Collins, Stuart and Streeter, Closed-cycle refrigeration at 1.85 K 1967, Daus and Ewald 1975, Sellmaier, Glatthaar and Klien 1970). And, "exchanger 6" is the 4.5 to 1.8 K heat exchanger.

for each stage, discharging at 18 bar and delivering 251 g/s to the cold box. It used mixed compression for the sub-atmospheric helium from the 1.75 K load. That is, the sub-atmospheric helium is partially pressurized (but still sub-atmospheric) using cold (centrifugal) compressors, the refrigeration is recovered to ambient temperature, and then warm vacuum pumps pressurize the helium to positive pressure. The two stages of cold compressors, manufactured by Air Liquid, processed 14 g/s from 13 to 80 mbar, discharging at around 15 K. It is unclear what type of heat exchanger was used for the sub-atmospheric helium between 15 K and ambient temperature; but it may have been an aluminum-stainless steel plate type manufactured by DATE (France). All other heat exchangers were the aluminum brazed plate-fin type. There were two vacuum pumps in series. The first processed 14 g/s from 64 to 660 mbar and the second processed 57 g/s from 660 mbar to 1.05 bar. The second handled more flow to maintain a liquid bath at 4.0 K. These were oil liquid ring pumps developed by Alsthom Atlantique Neyrtec (France) and used the same oil as the warm compressors. The 4.5 – 1.8 K heat exchanger counter-flowed 1.2 bar saturated liquid (which was also sent to the tokamak coil current leads) with the 1.8 K sub-atmospheric return from the load (at 14 g/s). The refrigerator used a Koch Process Systems 'wet' (two-phase) reciprocating helium expander, discharging into a positive pressure helium bath. This project was considered important in the development of centrifugal cold compressors for 2 K (and 1.8 K) helium systems. And, although it did not use full cold compression (i.e., from the sub-atmospheric load pressure to ~1 bar), it was the 'scaling' basis for CEBAF.

The continuous electron beam accelerator facility (CEBAF) at Thomas Jefferson National Accelerator Facility (known as JLab) is the first superconducting linear accelerator (LINAC) to intentionally and successfully use full cold compression; meaning a series of cryogenic centrifugal compressors raise the sub-atmospheric pressure (at around 32 mbar) returning from the load

(which are super-conducting niobium cavities housed in 'cryo-modules') to a positive pressure then inject this flow into the 4.5 K cold box (at around 30 K, 1.2 bar). The original design used four stages supplied by Air Liquide with wheels ranging from 13.7 to 5.6 inches in diameter, specified to run at 116 to 565 Hz (from biggest to smallest diameter) and compress the helium from 28 mbar at 3.32 K to 1.19 bar at 29 K (i.e., a total pressure ratio of 42.5 and overall adiabatic efficiency of 45%). The original process design was done by CVI (Columbus, Ohio) and was specified for 4820 W at 2.0 K (237 g/s processed by the cold compressors), plus a modest liquefaction load (10 g/s) and non-isothermal shield load (12 kW between 35 and 52 K) (Chronis, et al. 1996). The 4.5 to 2 K heat exchanger, which recovered the refrigeration from the returning sub-atmospheric helium flow from the LINAC to cool the super-critical 4.5 K helium supply to the LINAC, was housed within the 2 K cold box. This was a large brazed aluminum plate fin heat exchanger (core size 17 in. wide x 12 in. high x 60 in. long for 1.4 kW of duty). It was not recognized at the time that the location of this heat exchanger increased the load on the 4.5 K cold box since the distribution heat leak is adsorbed at a colder temperature than if the heat exchanger was located within the cryo-module (i.e., close to the load). Many hardware changes were made to the cold box system, including changing all of the warm compressors to a larger frame size and adding a liquid helium sub-cooler. After three years of effort, the supplier was unable to commission the 2-K system and this responsibility was assumed by JLab staff in 1994. After changing the supplier's control philosophy for both cold compressor and 4.5 K cold box operation, the 2 K system was successfully commissioned four months later. The two major lessons learned from this experience was (1) the original process design is likely not the optimum condition to operate the as-built equipment and (2) the most stable method to control the cold compressors is to adjust the speed of the last stage based upon the mass flow required for the intended load (plus

some margin) with the other (lower) stage speeds following at a set 'gear' ratio. Regarding the last lesson learned, it should be noted that the LINAC pressure is controlled using electric heat compensation. Regarding, the 'first lesson learned', the next logical question is, 'what is the optimum process condition to operate the actual system at'? The solution is actually quite simple and is addressed using the patented Floating Pressure process (Ganni and Knudsen, Optimal design and operation of helium refrigeration systems using the Ganni cycle 2010) developed in 1992 during the Super-Conducting Super Collider (SSC) project. In 2000 a new 2 K cold box was built and commissioned (Ganni, Arenius, et al. 2002) which incorporated 5 stages of cold compressors, with the first four the same as the original and the fifth the same as the fourth stage. Commissioning took only a few weeks and the new cold box operated with a much wider range of stability, greatly improving the system availability. This design also used a larger (brazed aluminum plate fin) 4.5 to 2 K heat exchanger which had a lower sub-atmospheric stream pressure drop and higher effectiveness. Even for 6 GeV operation[26], only 215 g/s of cold compressor flow was required. For the 12 GeV upgrade the original 2-K cold box was modified to incorporate the changes implemented in the 2-K cold box commissioned in 2000. This was commissioned in 2013 for the 12 GeV upgrade in just a few weeks. The pressure stability at the load (the vapor pressure within the cavities) is better than 0.1 mbar. This is an important requirement for a continuous electron beam accelerator using superconducting radio-frequency niobium cavities operating below lambda (i.e., around 2 K).

Air Liquide built a 1.8 K refrigerator for CEA-Grenoble, which achieved 370 W, used liquid nitrogen pre-cooling, and a mixed compression process for the sub-atmospheric helium

[26] CEBAF was originally designed for 4 GeV.

returning from the load (Roussel, Girard, et al. 2006). Two stages of cold compressors were used to process 19.6 g/s of helium from 14.5 mbar and 3.53 K to 44.6 mbar and 15.2 K. An oil ring pump processed the helium to a positive pressure to feed two screw compressors, discharging at 72 g/s and 16 bar. The cold box integrated the 4.5 K and 2K cold boxes and used brazed aluminum plate fin heat exchangers for the sub-atmospheric helium, except for the 4 K to 2 K heat exchanger which was a stainless steel plate heat exchanger manufactured by DATE (France). Saturated liquid helium at 1.25 bar was supplied to this heat exchanger (in counter-flow with the sub-atmospheric helium). Notably, a KPS 'wet' reciprocating expander was used to expand the supercritical helium to 1.25 bar.

The 4.5 K refrigerator for the Spallation Neutron Source (SNS) at Oak Ridge, Tennessee, was built by Linde Kryotechnik. The 2-K cold box design was very similar to JLab's, except that it (1) only used 4 stages of cold compressors, (2) did not house a 4.5 K to 2 K heat exchanger, and (3) did not use a liquid nitrogen shield. The SNS system was designed for 2.4 kW at 2.1 K (43 mbar) and so its design only required 120 g/s of cold compressor flow, which was rough half of JLab's. Like JLab, this process used 'full cold compression' (rather than mixed; some cold and some warm sub-atmospheric to positive pressure compression). The importance of the location for the 4.5 K to 2 K heat exchanger was properly recognized (Daly, et al. 2002). As such, these were located within the 'end-can' of the cryo-modules. The liquid nitrogen shield developed a significant leak into the cold box during commissioning. However, since the temperature of the sub-atmospheric helium returning to the 2-K cold box was 4 K instead of 2 K, it was not needed. The 2 K system was commissioned in 2005 after roughly 4 weeks of cumulative concentrated effort (Casagrande, et al. 2006). This was the second full cold compression process to be built and successfully commissioned.

Eight plants with a capacity each of about 2.4 kW at 1.8 K were installed for CERN's 27 km circumference Large Hadron Collider (LHC) (CERN 2014). Four of these plants were upgraded from the LEP (Large Electron-Positron) collider project and four were new. The 4.5 K and 2 K cold boxed were provided by two teams; Linde Kryotechnik with IHI (Japan, formerly, Ishikawajima-Harima Heavy Industries), and Air Liquide. IHI provided the cold compressors to Linde Kryotechnik's sub-atmospheric cold box. A mixed compression process for the sub-atmospheric helium is used. The Air Liquide 2-K cold box uses three stages of cold compressors and two single stage (Kaeser) warm compressors with a single turbine stage injected into the (Air Liquide) 4.5 K cold box. The Linde-IHI 2-K cold box uses four stages of cold compressors and a two-stage (Mycom) warm compressor with two turbine stages, the last injected into the (Linde) 4.5 K cold box. Both of these process 124 g/s at 15 mbar and 4 K from the sub-atmospheric load and inject the same 124 g/s of helium at 1.3 bar and 20 K into their respective 4.5 K cold box. Although this process configuration allows for a 3 to 1 turn down (Tavian 2012), it does not provide a sub-atmospheric load pressure stability any better than ±0.3 mbar. This is not a continuous beam machine and this is acceptable for magnet strings, since the magnets are surrounded by pressurized superfluid helium (at ~ 1 bar) which is cooled via superfluid conduction using a unique helium II bayonet heat exchanger design (Lebrun, Serio, et al. 1998). Each magnet cell (107 m long) has its own 4.5 K to 2 K heat exchanger, which are a stainless steel plate type and were manufactured by DATE (France) (Chorowski, et al. 1998, Gilbert, et al. 2006, Roussel, Bezaguet, et al. 2002) .

Notably, the Air Liquid 4.5 K cold box uses a 'wet' turbo-expander (T8) that discharges two-phase helium into the helium sub-cooler (which operates at around 1.25 bar) (Gruehagen and Wagner 2004). The LHC magnet "cells", which are cooled to 1.8 K, contain and steer the hadron

beam. Sixteen superconducting radio-frequency cavities (in four cryo-modules), which are cooled to 4.5 K (i.e., not sub-atmospheric) and operate at 400 MHz, focus and accelerate the beam, providing 2 MV each; that is, 16 MV per beam (there are two beams going in opposite directions).

The cryogenic system for the FRIB project at Michigan State University (MSU) is using a refrigerator with an equivalent capacity (roughly 18 kW of 4.5 K refrigeration) and very similar design to the JLab's 12 GeV cold box (Ganni, Knudsen and Arenius, et al. 2014). The 2-K cold box design is planned to be similar to the SNS project, with the 4.5 to 2 K heat exchangers distributed within the cryo-modules in the LINAC. However, it is planned to use 5 stages of cold compressors with considerably smaller wheel diameters than used for JLab (or SNS). Linde has provided the 4.5 K cold box, Air Liquide is providing the cold compressors and the 2-K cold box is planned to be assembled at MSU. The 4.5 K to 2 K heat exchangers are a single wrap Collins type designed by JLab and manufactured by Ability Engineering Technology. Two different sizes are required for the cryo-modules.

There are three other instances, not already mentioned, found in literature that used a 'wet' helium expander. A Koch Process System (KPS)/CTI reciprocating expander was installed as an upgrade to the Bureau of Mines Excell helium liquefier, increasing its capacity by 30% (Ganni, Moore and Winn, Capacity upgrade of the Excell helium liquefier plant by the addition of a wet engine 1986). As already mentioned, the Tore Supra and CEA-Grenoble refrigerators used the same type of expander. Sulzer Brother's (now Linde Kryotechnik) reported that their turbines have worked successfully as 'wet' expanders (discharging to a positive pressure), but that the gain in doing so was negligible as compared to incorporating a JT valve in series with the expander and an intermediate HX (Quack 1980). A two-phase (outlet) turbo-expander (discharging to a positive

pressure) was developed and used on a Russian KGU-1600/4.5 helium refrigerator (1600 W at 4.5 K) in 2002 (Agapov, et al. 2002).

Of all of these, only the KPS 'wet' expander used at SLAC discharged to a sub-atmospheric pressure. Unfortunately, no additional information was found either in literature or through direct sources. The refrigerator has been decommissioned for many years.

APPENDIX B – FLOW DIAGRAMS

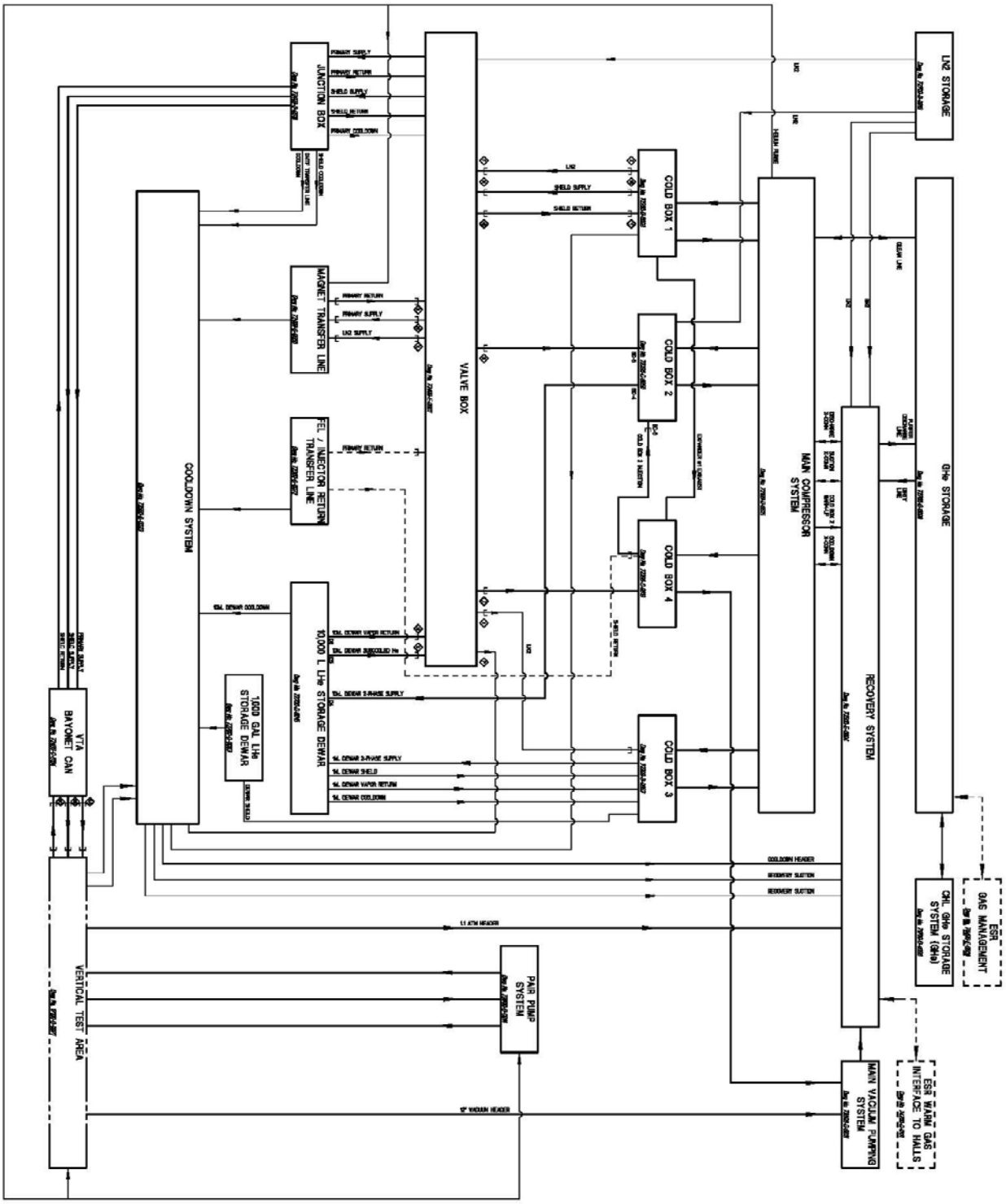

Figure B.1. Jefferson Lab Cryogenic Test Facility (CTF) block flow diagram

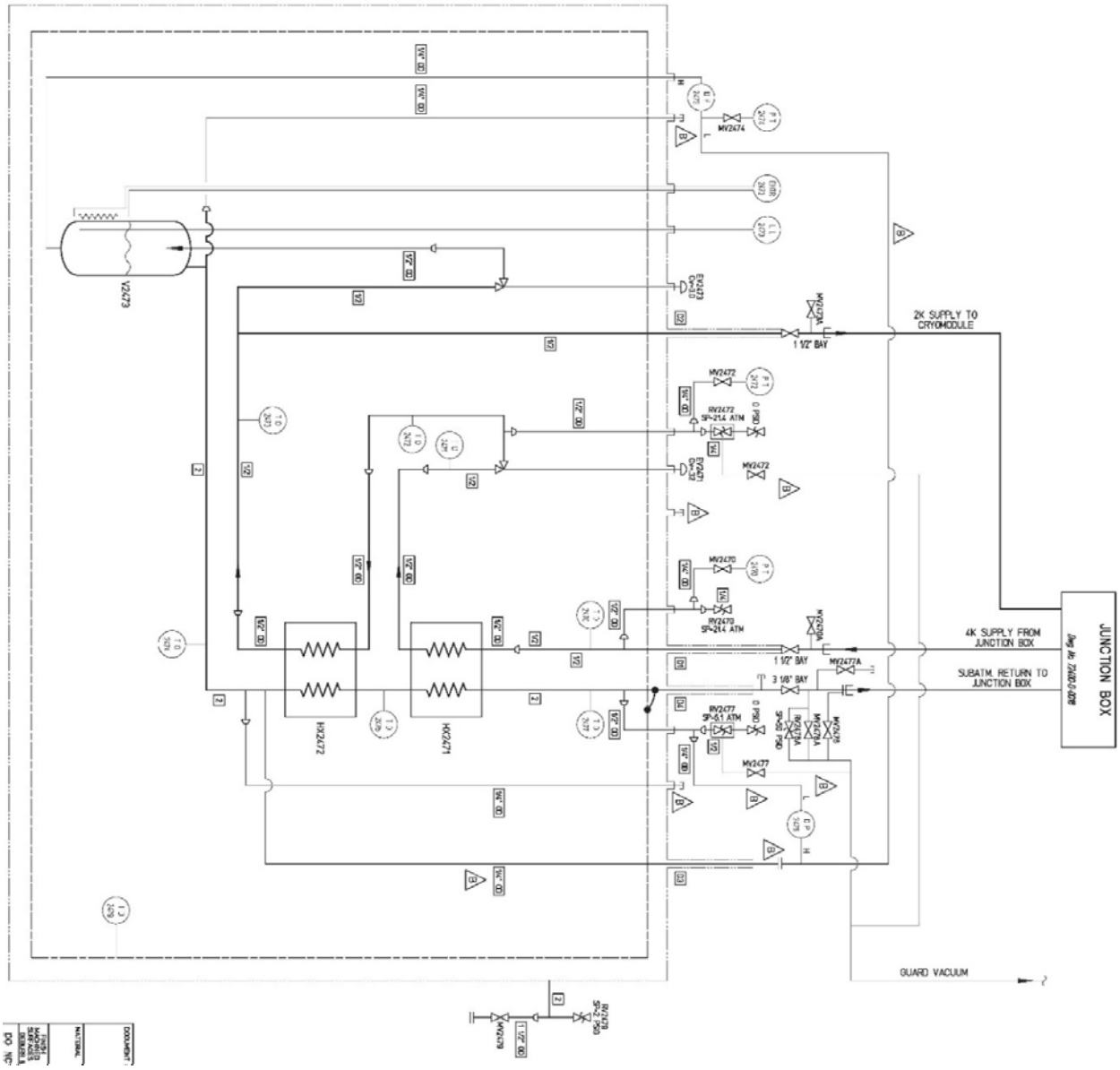

Figure B.2. Test apparatus flow diagram

APPENDIX C – CTF SYSTEM EDM SCREEN SNAP-SHOTS

Note: These were not taken during testing.

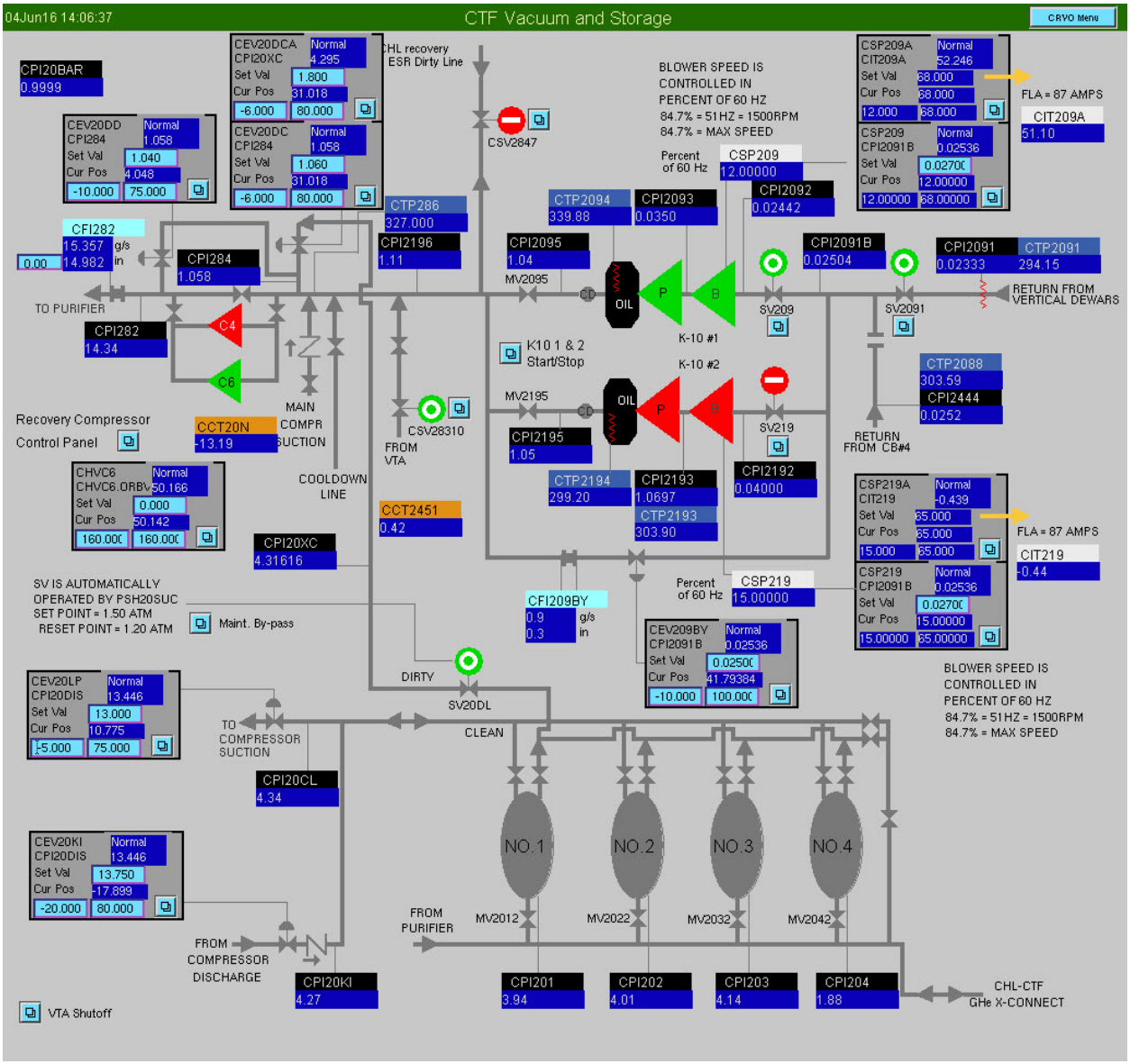

Figure C.1. EDM screen for the CTF vacuum pumping system, gas storage and purifier compressors

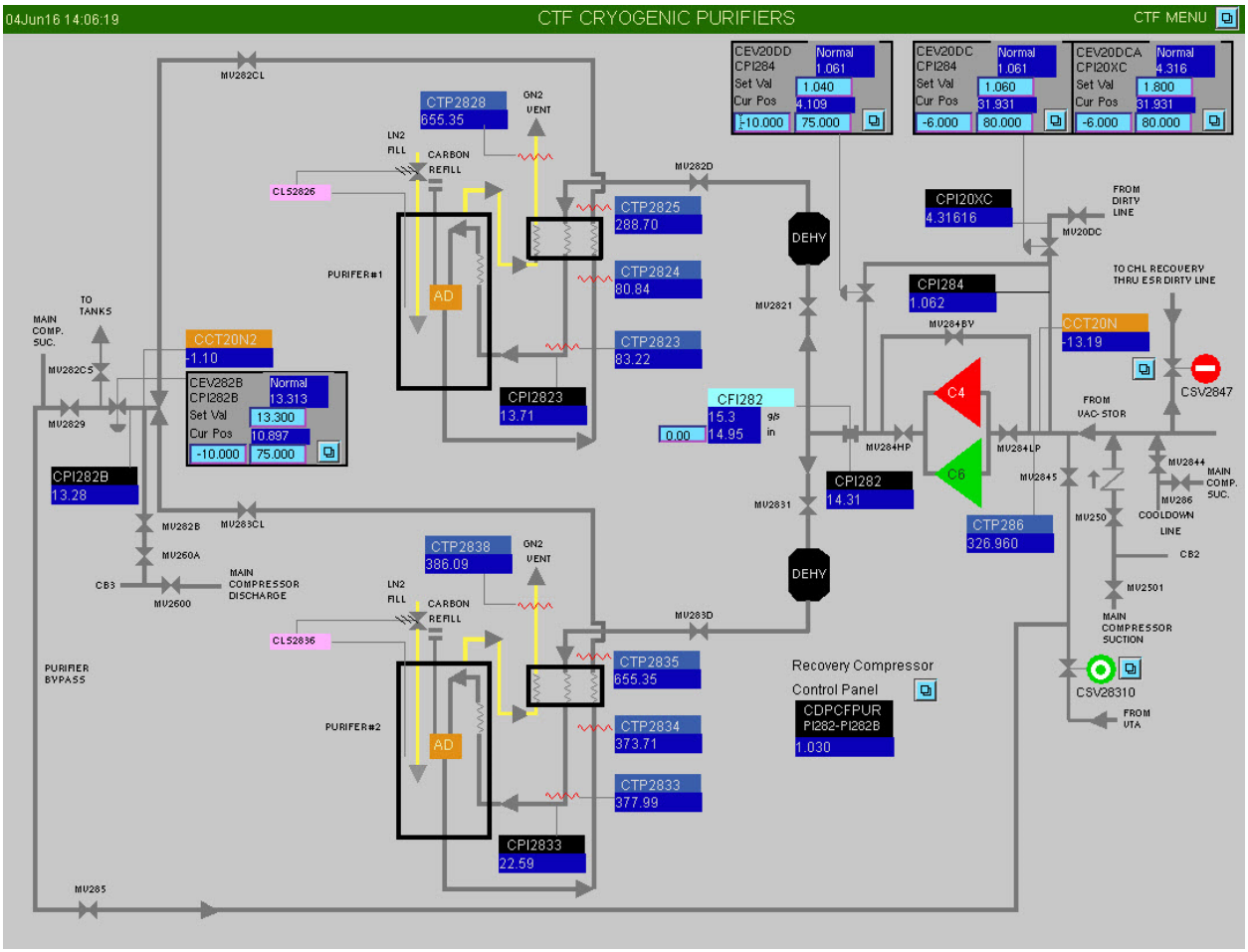

Figure C.2. EDM screen for the CTF purifier compressors and purifier

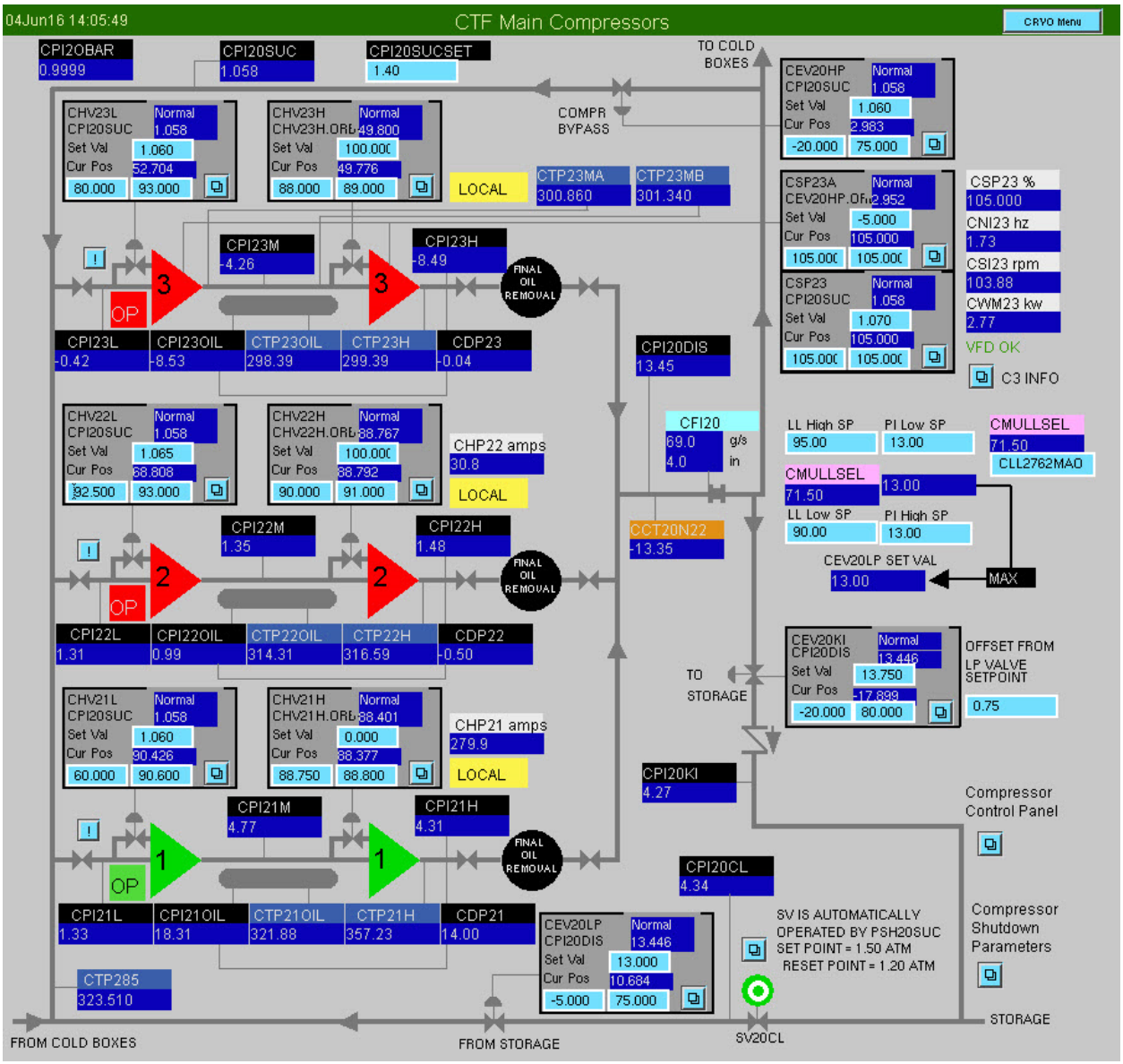

Figure C.3. EDM screen for the CTF (main warm Mycom) compressors

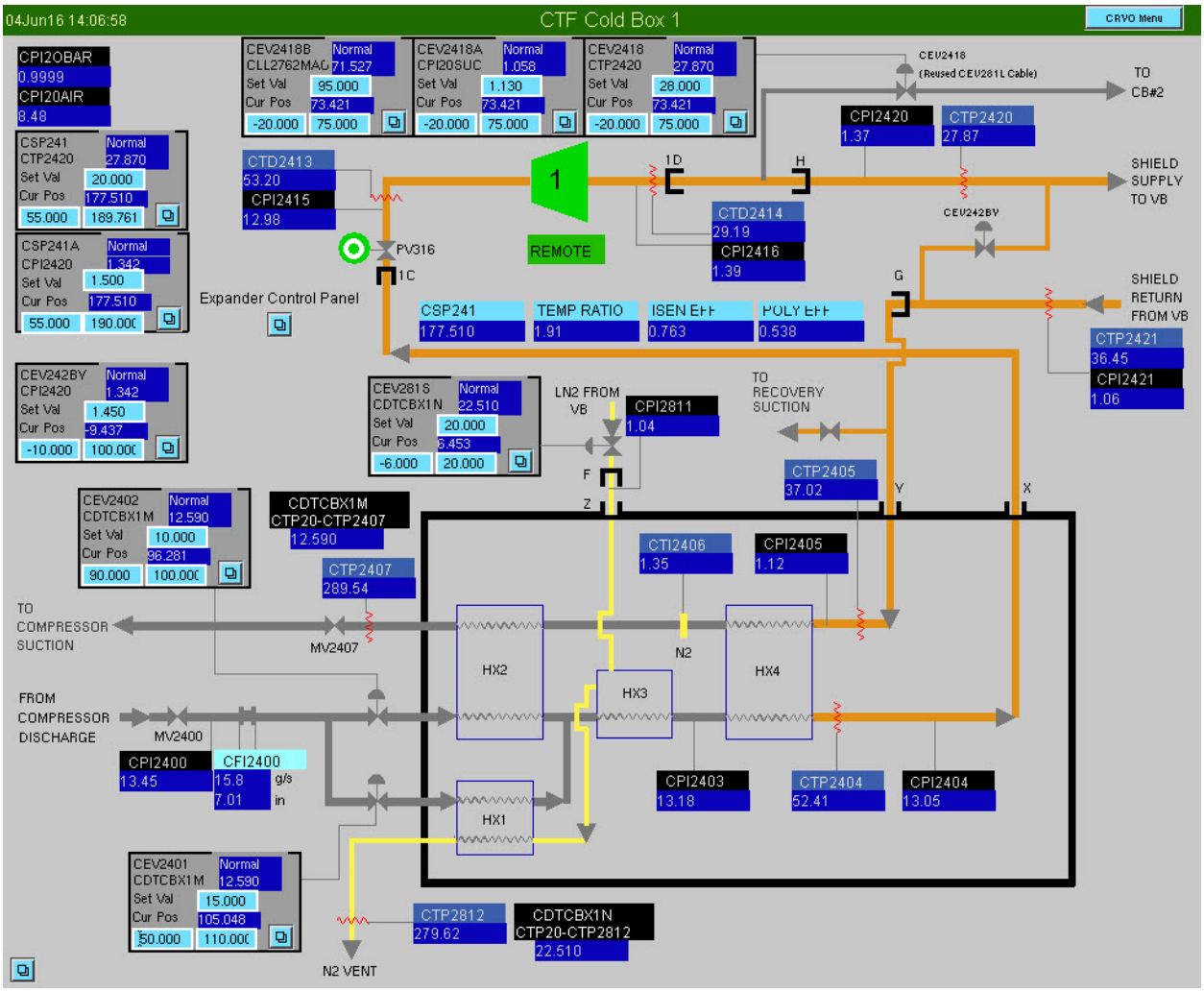

Figure C.4. EDM screen for the CTF cold box 1 (CB1), the shield refrigerator using a (Koch M1600 dual stage) reciprocating expander

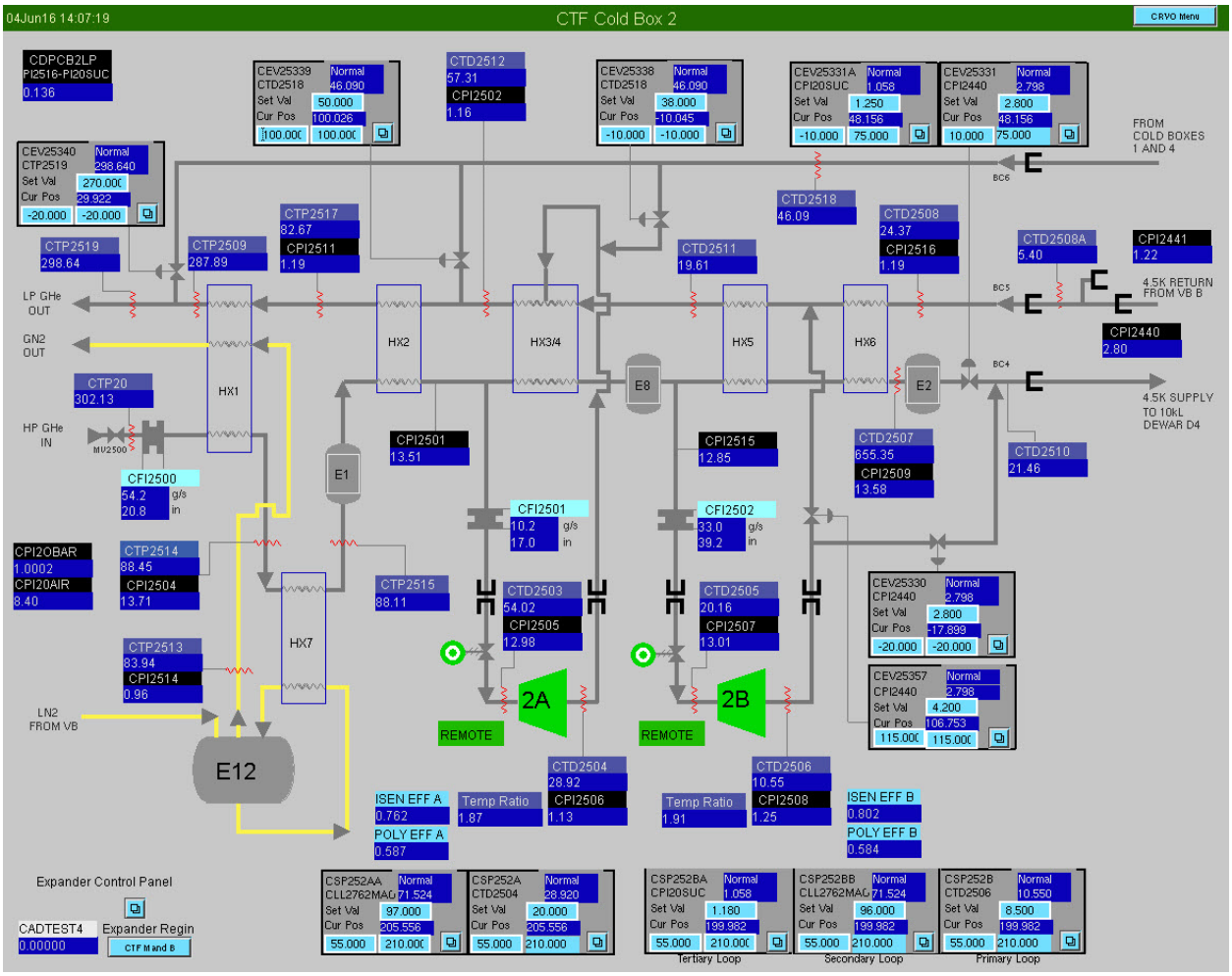

Figure C.5. EDM screen for the CTF cold box 2 (CB2), the main 4.5 K refrigerator (Koch model 2200) using two (Koch M1600 dual stage) reciprocating expanders

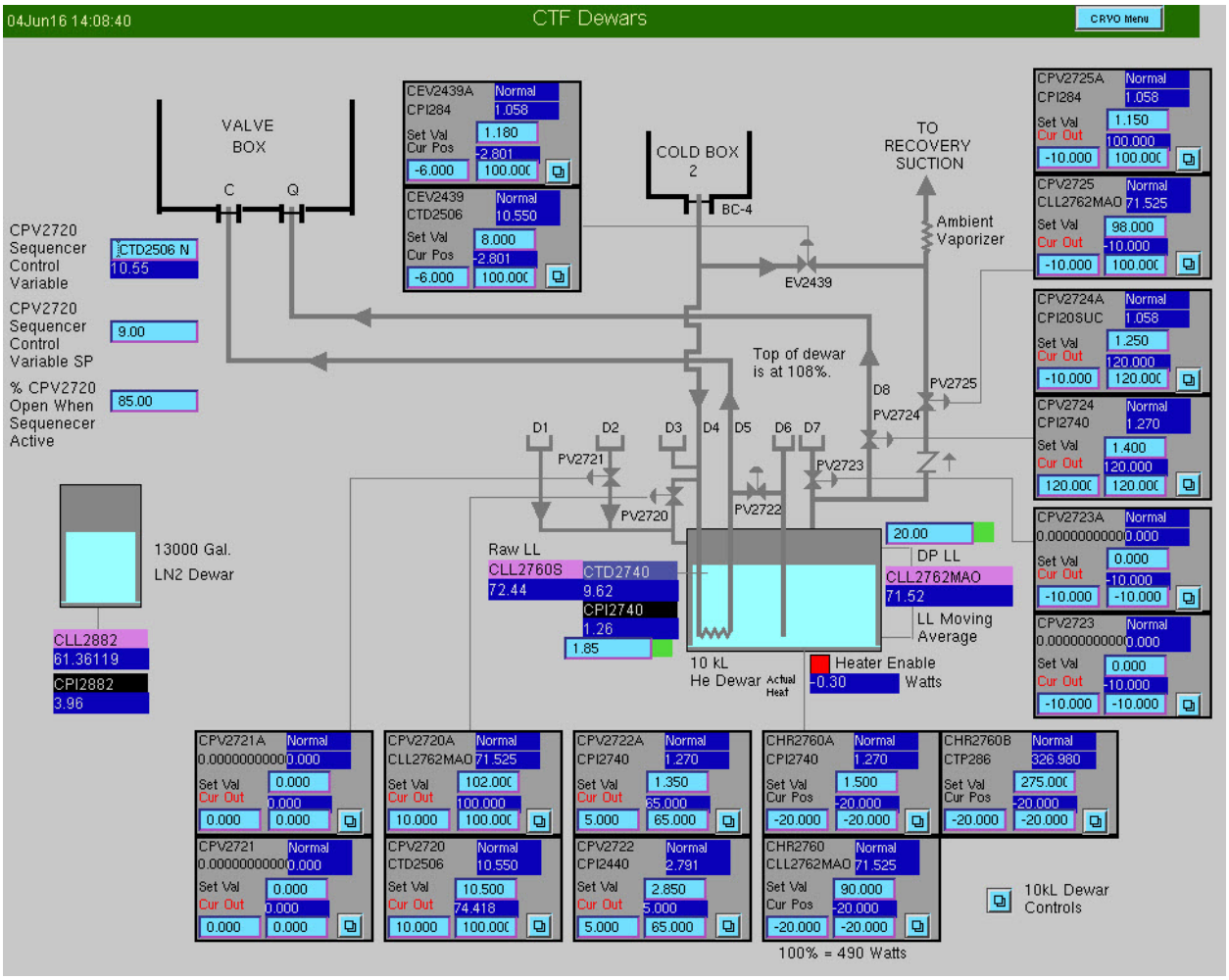

Figure C.6. EDM screen for the CTF 10,000 liter liquid helium dewar with sub-cooling coil for helium supply

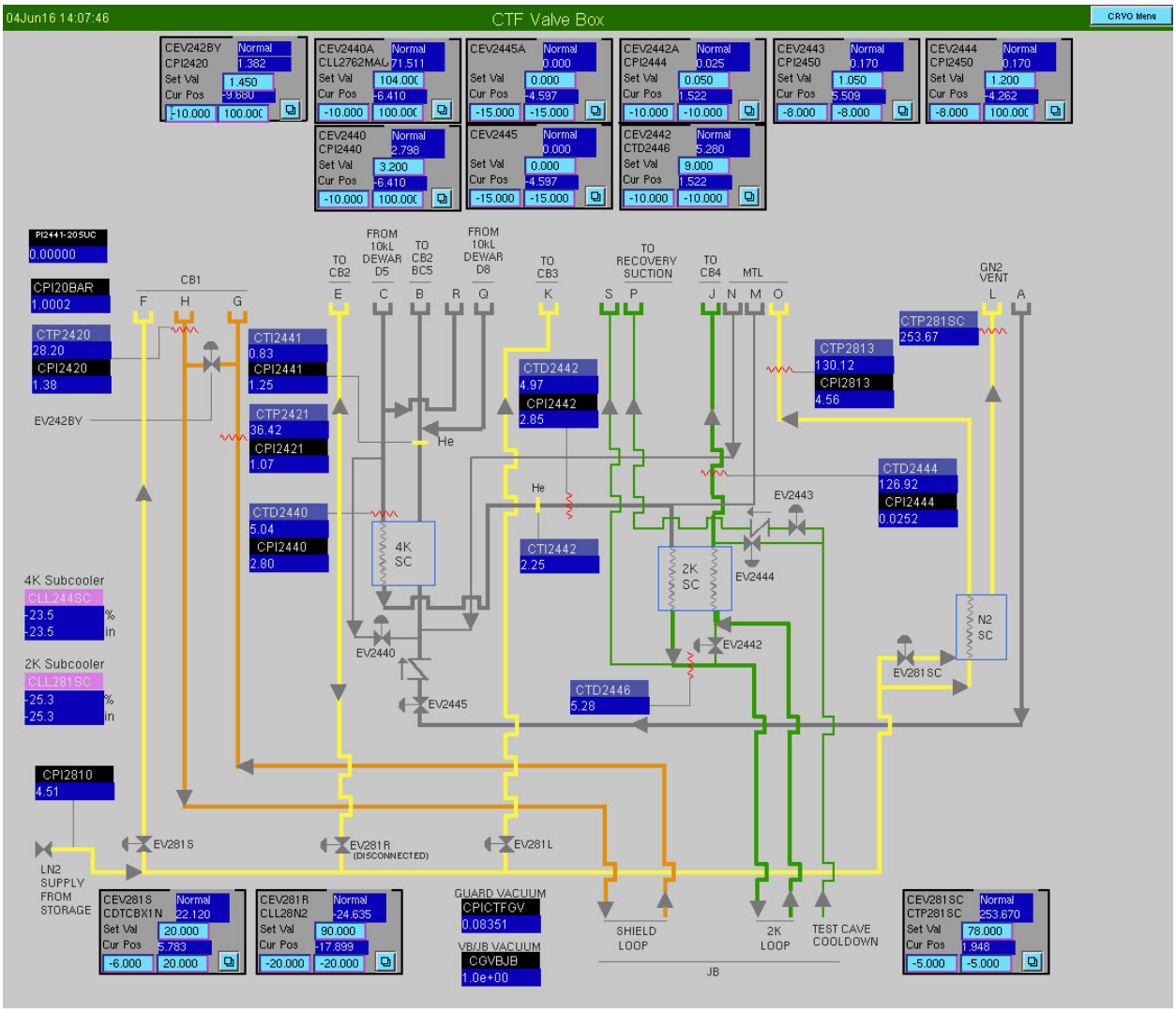

Figure C.7. EDM screen for the CTF valve box

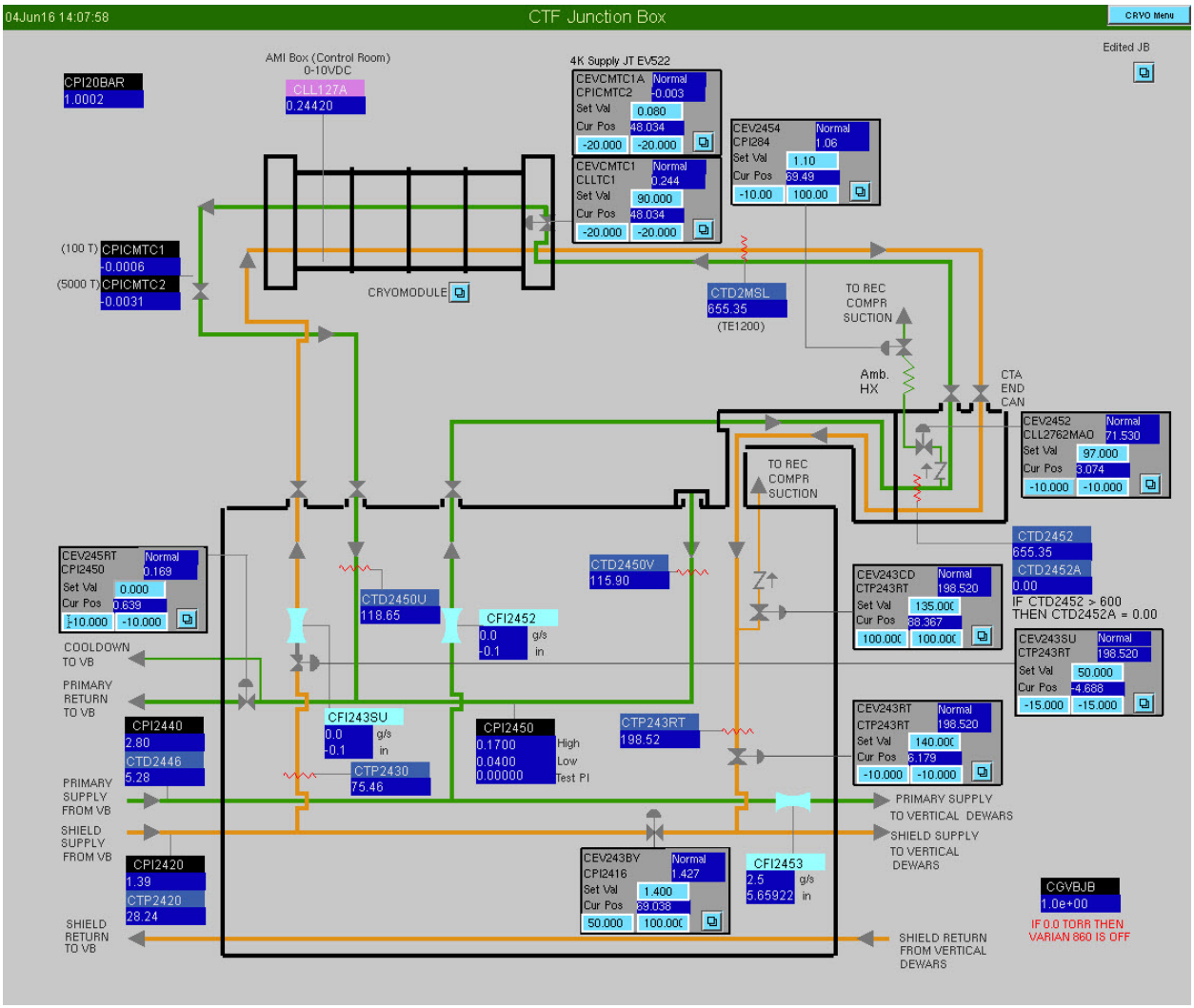

Figure C.8. EDM screen for the CTF junction box, located in the horizontal test area

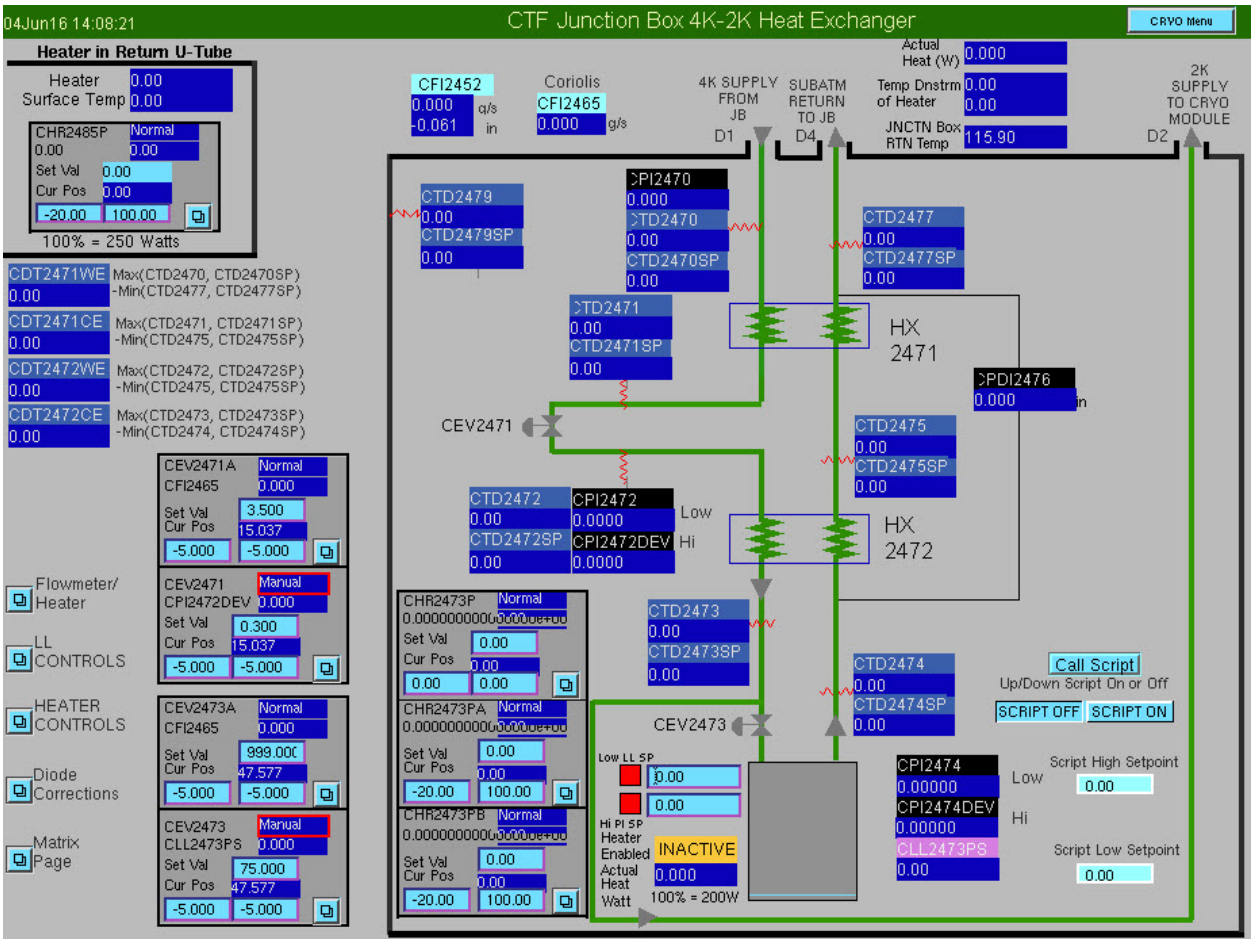

Figure C.9. EDM screen for the CTF HX test can apparatus (not active)

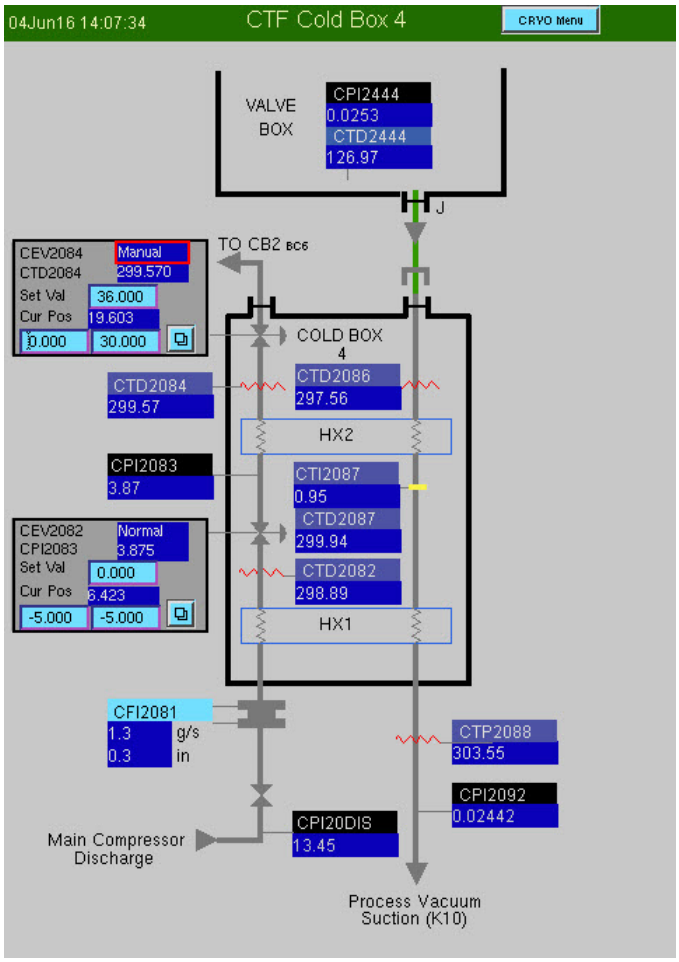

Figure C.10. EDM screen for cold box 4 in the CTF

APPENDIX D – PROCESS SIGNAL ARCHIVER INFORMATION

Table D.1. Process signal archiver information

Signal	Units	Dead Band [Units]	Max. Rate [sec]
CTD2440	K	0.01	*None*
CTD2450V	K	0.01	*None*
CTD2470	K	0.1	10
CTD2471	K	0.01	10
CTD2472	K	0.01	10
CTD2473	K	0.1	10
CTD2474	K	0.1	10
CTD2475	K	0.1	10
CTD2477	K	0.1	10
CTD2487	K	0.01	*None*
CTD2470SP	K	0.1	10
CTD2471SP	K	0.1	10
CTD2472SP	K	0.1	10
CTD2473SP	K	0.1	10
CTD2474SP	K	0.1	10
CTD2475SP	K	0.1	10
CTD2477SP	K	0.1	10
CTD2487SP	K	0.01	*None*
CDT2471WE	K	0.1	*None*
CDT2471CE	K	0.1	*None*
CDT2472WE	K	0.1	*None*
CDT2472CE	K	0.1	*None*
CPI2440	Atm	0.01	
CPI2470	Atm	0.01	10
CPI2472	Atm	0.1	10
CPI2472DEV	Atm	*None*	10
CPI2474	Atm	0.000025	*None*
CPI2474DEV	Atm	*None*	10
CPDI2473	Atm	0.1	10
CPDI2476	Atm	0.1	10
CFI2452	g/s	0.01	10
CFI2452C	g/s	0.01	*None*
CFI2465	g/s	0.01	*None*
CLL2473PS	%	0.2	*None*
CWM2473C	W	0.2	10
CHR2473P.ORBV	%	0.1	*None*
CEV2471.ORBV	%	0.1	*None*
CEV2473.ORBV	%	0.1	*None*

APPENDIX E – SIMPLIFIED 'CARNOT-STEP' ANALYSIS

The 'Carnot-Step' analysis (simplified and non-simplified) is explained in Knudsen and Ganni (Simplified helium refrigerator cycle analysis using the 'Carnot Step' 2006). The crucial points pertinent here are:

(a) Counter-flow isobaric heat exchange between *(h)* and *(l)* stream(s), with work extraction from the *(h)* to *(l)* stream(s) – usually only one *(h)*, or supply, stream, but many times there are two *(l)* streams, one at a higher pressure level than the other; the higher one, often referred to as the recycle stream, has a pressure that varies with the load (i.e. it 'floats') and the other remains constant and is from the load (or from the 4.5 K sub-cooler bath in the case of a 2 K refrigerator), this is the 'load-return' stream

(b) Expansion step 'unit'; *(h)* and *(l)* streams are 'pinched' (relative to inside the expansion step 'unit') at warm and cold-ends; it includes an upper heat exchanger, lower heat exchanger and an expander; extracting work by expanding from the high supply pressure drawn from between the upper and lower heat exchangers, to the low pressure stream at the cold-end of the lower heat exchanger

(c) As a liquefier, the mass flow difference between the *(h)* and *(l)* streams at the expansion step 'unit' boundaries is equal to the mass flow supporting the liquefaction load and is called the 'unbalance'. Conversely, as a refrigerator, this difference is zero, and is called 'balanced'. The expansion steps provide the cooling required by the 'unbalanced' flow (which is both due to the mass flow difference and that the specific heat for the *(h)* stream is higher than the *(l)* stream), the finite temperature difference between *(h)* and *(l)* streams at the expansion step 'unit' boundaries and heat in-leak.

(d) If helium could be assumed to be an ideal gas with constant specific heat (which is a reasonable assumption down to ~20 K), the heat exchangers were perfect (i.e., no *(h)* to *(l)* temperature difference at the expansion step 'unit' boundaries), and the expanders operated isentropically (i.e., 100% adiabatic efficiency), the process described in (a) and (b) has the same efficiency has a Carnot liquefier.

(e) The main process parameters are (using the nomenclature in Knudsen and Ganni (Simplified helium refrigerator cycle analysis using the 'Carnot Step' 2006)):

1. Total pressure ratio, $\Gamma = p_h/p_l$, between the *(h)* and *(l)* streams; the pressure drop along the *(h)* stream and along the *(l)* stream is usually small and assumed to be zero in the Carnot-Step analysis
2. Total temperature ratio between the *(h)* stream entering the cold box and the *(l)* stream returning from the (4.5 K) load; $\Theta = T_{h,0}/T_{l,N}$
3. Number of expansion step 'units', N; this is not necessarily the same as the number of expanders
4. Ratio of the *(h)* to *(l)* stream temperature difference to the *(l)* stream temperature at the expansion step 'unit' boundaries; $\tau_i = \Delta T_{hl,i}/T_{l,i}$
5. Expansion step adiabatic efficiency, $\eta_{X,i}$; equal to the expander adiabatic efficiency if the expansion step has a single expander, or equal to the 'string' adiabatic efficiency if there is more than one (which do not have a heat exchanger between them)
6. Liquefaction ('unbalanced') mass flow, $\dot{m}_L$, and the refrigeration ('balanced') mass flow, $\dot{m}_R$

7. Expansion step ‘unit’ temperature ratio, θ_i; i.e., the temperature ratio between the *(h)* stream at the warm-end of the expansion step ‘unit’ and the *(l)* stream at the cold-end of the expansion step ‘unit’; this is found knowing (2), (3) and (4) above
8. Expander temperature ratio, $\theta_{X,i}$; this is equal to or less than the expansion step ‘unit’ temperature ratio, and is found knowing (1) and (5) above
9. There is a maximum number of (integer) expansion steps possible for a given total pressure and temperature ratio and expansion step adiabatic efficiency; and, the number of (integer) expansion stages, total temperature ratio, expansion step ‘unit’ temperature ratio and ratio of the *(h)* to *(l)* stream temperature difference to the *(l)* stream temperature at the expansion step ‘unit’ boundaries are related (by a single equation)

For equal expander adiabatic efficiencies (in each expansion step ‘unit’), equal *(h)* to *(l)* stream temperature difference to *(l)* stream temperature ratios at the expansion step ‘unit’ boundaries, and a few additional factors (that have a less significant effect; these are discussed in detail in Knudsen and Ganni (Simplified helium refrigerator cycle analysis using the ‘Carnot Step’ 2006), the expansion step ‘unit’ temperature ratio and expander mass flow that yields a minimum compressor mass flow (for a given total pressure ratio between the *(h)* to *(l)* stream) are ones that are equal for each expansion step ‘unit’.

Let’s return to the idea of an ‘unbalanced’ vs. a ‘balanced’ expansion step and consider the load imposed by the cold compressors. Between the warm-end of the expansion step where the cold compressor discharge is injected to the 4.5 K cold box *(l)* stream (usually 20 to 35 K) and the cold-end of the coldest expansion step supplying the load (4.5 K) the 4.5 K cold box expansion steps are ‘unbalanced’ by an amount equal to the cold compressor mass flow. The expansion steps above the temperature where the cold compressor discharge is injected to the *(l)* stream of the 4.5

K cold box are ‘balanced’; assuming that the only load being supported is the cold compressor load.

For the simplified ‘Carnot-Step’ analysis, the heat exchangers are assumed to be perfect and the expander adiabatic efficiency is the same for each expansion step ‘unit’ but less than unity. Only the ‘unbalanced’ section of the cold box between the cold compressor discharge injection down to the 4.5 K supply will be considered since the rest (warmer part) is ‘balanced’ and does not need work extraction (since the heat exchangers are perfect). Following the nomenclature in Knudsen and Ganni (Simplified helium refrigerator cycle analysis using the ‘Carnot Step’ 2006), noting that the refrigeration load mass flow is zero ($\dot{m}_R = 0$) and the liquefaction flow is equal to the cold compressor flow, the compressor mass flow is,

$$\dot{m}_C = \dot{m}_L + \dot{m}_R + \sum_{i=1}^{N} \dot{m}_{X,i} = \dot{m}_L \cdot \left(1 + \beta_{r,0} \cdot N\right) \qquad \text{(Eq. E.1)}$$

$$\beta_{r,0} = \frac{\Theta^{1/N} - 1}{\theta_X - 1} \qquad \text{(Eq. E.2)}$$

$$\theta_X = \left[1 - \eta_X \cdot \left(1 - \Gamma^{-\phi}\right)\right]^{-1} \qquad \text{(Eq. E.3)}$$

where, $\phi = (\gamma - 1)/\gamma$, and γ is the ratio of specific heats; and approx. 0.4 for helium. The compressor input power, assuming an ideal gas is,

$$\dot{W}_{C,m} = \dot{m}_C \cdot \frac{\phi \cdot C_p \cdot T_S \cdot \ln \Gamma}{\eta_m \cdot \eta_i} \qquad \text{(Eq. E.4)}$$

where, C_p - specific heat (at constant pressure)

T_S - compressor suction pressure

η_i - isothermal efficiency

η_m - motor efficiency

Although the isothermal efficiency is a function of the pressure ratio (and the stage type and built-in volume ratio), it will be taken as constant for this simple analysis. Likewise, the (induction) motor efficiency is a function of the percent to full load that it is operating at, but it will also be taken as constant. So, the compressor mass flow is proportional to the input power for a given (specified) total pressure ratio.

The cold compressor total temperature ratio (Θ_{CC}, from first stage suction, $T_{CC,S}$, to last stage discharge, $T_{CC,D}$) is related to the total (cold compressor) pressure ratio (Γ_{CC}), the adiabatic efficiency per stage (η_{CC}, assumed to be equal for each stage), and the number of stages (N_{CC}) by,

$$\Theta_{CC} = \frac{T_{CC,D}}{T_{CC,S}} = \frac{\left[\Gamma_{CC}{}^{(\phi/N_{CC})} - 1\right]}{\eta_{CC}} + 1 \qquad \text{(Eq. E.5)}$$

with,

$$\Theta = \frac{T_{h,0}}{T_{l,N}} = \frac{T_{CC,D}}{T_{PS}} \qquad \text{(Eq. E.6)}$$

where, $T_{h,0} = T_{CC,D}$, since the *(h)* to *(l)* stream temperature difference is zero with perfect heat exchangers, and, $T_{l,N} = T_{PS}$, which is the "primary supply" temperature (4.5 K). So,

$$\Theta = \frac{T_{CC,S}}{T_{PS}} \cdot \Theta_{CC} \qquad \text{(Eq. E.7)}$$

Since this analysis is being used to see how an increased cold compressor suction temperature affects the input power (or, for this analysis, how it affects the compressor mass flow), we can introduce the following 'perturbing' variables, α and ω, as follows,

$$T_{CC,S} = (1 + \alpha) \cdot T_{CC,S}{}^{*} \qquad \text{(Eq. E.8)}$$

$$\dot{m}_L = \frac{\dot{m}_L{}^{*}}{(1 + \omega)} \qquad \text{(Eq. E.9)}$$

where, the asterisk super script (*) is the baseline case, with no heat exchanger *(h)* stream pressure drop through the 4.5 to 2 K heat exchanger. Since α and ω should be much less than 1, the following approximations can be used,

$$(1+\alpha)^{1/N} \cong 1 + \frac{\alpha}{N} \quad \text{(Eq. E.10)}$$

$$(1+\omega)^{-1} \cong 1 - \omega \quad \text{(Eq. E.11)}$$

So,

$$\dot{m}_C = (1+\omega) \cdot \dot{m}_L{}^* \cdot B \quad \text{(Eq. E.12)}$$

$$B = \left\{ 1 + \frac{\left[\left(1+\frac{\alpha}{N}\right) \cdot (\Theta^*)^{1/N} - 1\right]}{(\theta_X - 1)} \cdot N \right\} \quad \text{(Eq. E.13)}$$

and,

$$\dot{m}_C{}^* = \dot{m}_L{}^* \cdot B^* \quad \text{(Eq. E.14)}$$

$$B^* = \left\{ 1 + \frac{\left[(\Theta^*)^{1/N} - 1\right]}{(\theta_X - 1)} \cdot N \right\} \quad \text{(Eq. E.15)}$$

The ratio of the compressor mass flow between the 'perturbed' case and the baseline (*) is then,

$$\frac{\dot{m}_C}{\dot{m}_C{}^*} = (1-\omega) \cdot (1+\tilde{\alpha}) \quad \text{(Eq. E.16)}$$

where,

$$\tilde{\alpha} = A \cdot \alpha \quad \text{(Eq. E.17)}$$

$$A = \frac{(\Theta^*)^{1/N}}{\{(\theta_X - 1) + [(\Theta^*)^{1/N} - 1] \cdot N\}} \quad \text{(Eq. E.18)}$$

We will need to address one more issue before working with actual numbers. The return distribution heat in-leak to the sub-atmospheric flow is significant factor to consider. And, although, it does not contribute directly to the load (in the sub-atmospheric liquid bath), it does affect the first stage cold compressor suction temperature. This increases the final cold compressor discharge temperature. It also increases the wheel size of the first stage, since the volume flow is greater (for a given mass flow). This will not be discussed further, but it is important to consider

that this will tend to lower the tip speed (due to stresses and roto-dynamics) and the pressure ratio that can be developed (by way of the tip speed Mach number being lower). The effect of the return transfer-line heat in-leak can be considered as follows. The enthalpy increase in the sub-atmospheric stream from the outlet of the 4.5 to 2 K heat exchanger to the first stage cold compressor suction is,

$$C_p \cdot \Delta T_{RTL} \cong \Delta h_{RTL} = \frac{q_{k,RTL}}{\dot{m}_L} \qquad \text{(Eq. E.19)}$$

where, ΔT_{RTL} is the temperature increase, $q_{k,RTL}$ is the return distribution (transfer-line) heat in-leak, and, as in what has been done so far, $\dot{m}_L$ is the flow from the load which is equal to the cold compressor mass flow. The load (q_L), cold compressor mass flow, and load enthalpy flux (Δh_{lh}) are related by,

$$q_L = \dot{m}_L \cdot \Delta h_{lh} \qquad \text{(Eq. E.20)}$$

The baseline case where there is no supply stream pressure drop across the 4.5 to 2 K heat exchanger has a nominal load enthalpy flux (as presented earlier) of about, $\Delta h_{lh}{}^{*} = 20$ J/g, where as before, the asterisk (*) is denoting the baseline case. Also, from Chapter 1 (Figure 1.4), the load enthalpy flux for a non-zero supply stream 4.5 K to 2 K heat exchanger pressure drop is,

$$\Delta h_{lh} = (1 + \omega) \cdot \Delta h_{lh}{}^{*} \qquad \text{(Eq. E.21)}$$

$$\omega \cong \nu \cdot \Delta p_{h,HX} \qquad \text{(Eq. E.22)}$$

where, $\nu \approx 1/30$ (for $\Delta p_{h,HX}$ units of bar or atm), and $0 \leq \omega \leq \sim 0.1$. Note that this coefficient is easily found by plotting the pressure drop across the 4.5 K to 2 K heat exchanger vs. the stream difference enthalpy flux (Δh_{lh}). Then taking zero pressure drop as the baseline ($\Delta p_{h,HX} = 0$), determine the percent increase in stream Δh_{lh} from the baseline; so, ν is the slope of this line.

Combining these, we have,

$$\Delta T_{RTL} = \frac{q_{k,RTL}}{q_L} \cdot \left(1 + \nu \cdot \Delta p_{h,HX}\right) \cdot \frac{\Delta h_{lh}{}^{*}}{C_p} \qquad \text{(Eq. E.22)}$$

As an example of a system with a large 2 K load, $q_L = 5100$ W, and $q_{k,RTL} = 500$ W. Assume that the 4.5 K cold box supplies 4.5 K at 3 bar, but there is a (supply) stream pressure drop of 0.1 bar. We will take the 4.5 K to 2 K heat exchanger cold end stream temperature difference as 0.2 K, the pressure at the 2 K load as 31 mbar and the sub-atmospheric pressure drop back to the cold compressor suction as 4 mbar (i.e., 2 mbar across the 4.5 K to 2 K heat exchanger and 2 mbar through the distribution line back to the cold compressor suction).

So, for the baseline case, $\Delta p_{h,HX} = 0$ bar (i.e., no supply stream pressure drop across the 4.5 K to 2 K heat exchanger), $\Delta h_{lh}{}^{*} = 20.08$ J/g, and, $\Delta T_{RTL} = 0.3785$ K; where, $C_p = 5.200$ J/g-K. If, if $\Delta p_{h,HX} = 2.7$ bar (so that the supply stream outlet pressure is 0.2 bar), $\Delta h_{lh}{}^{*} = 21.85$ J/g, and, $\Delta T_{RTL} = (0.3785) \cdot (1.090) = 0.4126$ K. So, for the baseline case, $T_{CC,S}{}^{*} = 3.2774 + 0.3785 = 3.656$ K; where the temperature of the sub-atmospheric stream leaving the 4.5 K to 2 K heat exchanger is $T((32-2)mbar, h(2.9\ bar, T_{sat}(1.25\ bar) + 0.1\ K) + \Delta h_{lh})$. And, for the case where, $\Delta p_{h,HX} = 2.7$ bar, $T_{CC,S} = 3.6135 + 0.4126 = 4.026$ K; although, the effect of the ~10% increase in ΔT_{RTL} due to the lower flow in the non-baseline case could be neglected. So, $\alpha = \frac{4.026}{3.656} - 1 = 0.1012$.

Assuming some reasonable values for the cold compressors, $\Gamma_{CC} = \frac{1.200}{0.027} = 44.44$, $N_{CC} = 5$, $\eta_{CC} = 70.0\%$, then $\Theta_{CC} = 7.763$, and $T_{CC,D} = 27.96$ K. So, for the 4.5 K cold box, $\Theta^{*} = (0.8004) \cdot (7.763) = 6.214$.

Assuming some reasonable values for the 4.5 K cold box, $\Gamma = \frac{17.50}{1.250} = 14.00$, $\eta_X = 82.0\%$ and $N = 3$ (i.e., the number of expansion steps between the cold compressor discharge injection

and the 4.5 K primary supply to the load; not the number of expansion steps for the entire 4.5 K cold box), then, $\theta_X = 2.149$.

So, $A = 0.5017$, and, $\tilde{\alpha} = (0.5017) \cdot (0.1012) = 0.05077$

And, $\omega = \frac{21.85}{20.08} - 1 = 0.08815$, which gives, $\frac{\dot{m}_C}{\dot{m}_C{}^*} = (1 - 0.08815) \cdot (1 + 0.05077) = 0.9581$.

So, from this simplified Carnot-Step analysis we would expect a 4.2% reduction in input power for the same load, or the reciprocal for the increase in capacity for the same input power, i.e., 4.4%. The effect of the cold compressor input power is not considered, but is quite small compared to the total input power (~1%) and varies little between the base-line and non-baseline cases (less than 10%).

APPENDIX F – NON-SIMPLIFIED 'CARNOT-STEP' ANALYSIS

This analysis does not neglect the heat exchanger *(h)* to *(l)* stream finite temperature difference, includes the effect if the *(h)* stream specific heat is different than the *(l)* stream and includes heat in-leak. The cold compressor total temperature ratio is calculated essentially the same as the previous analysis, but is included into the total input power. And, the effect of the return distribution (transfer-line) heat in-leak on the sub-atmospheric return from the load to the first stage cold compressor suction was essentially done the same. However, the real-fluid cooling curve analysis was included for the 4.5 to 2 K heat exchanger. And, an ideal gas model was used for the warm compressors, including the pressure ratio and 'stage type' influence on the isothermal efficiency (Ganni, Knudsen and Creel, et al. 2008), but using a constant motor efficiency. The compressor arrangement was selected as a first (low pressure) stage followed by a second (high pressure) stage, so that the 4.5 K cold box was essentially a two stream, *(h)* and *(l)*, type. The inter-stage pressure was adjusted to give a minimum input power; though, for an actual process it would be dictated by the selected compressor displacements and their volumetric efficiencies. No effort was made to model around selected or known equipment sizes, but the total 2 K load is consistent with an 18 kW equivalent 4.5 K refrigerator, and a realistic distribution pressure drop and heat in-leak was used. Table F.1 presents a summary of process parameters selected and results. Table F.2 presents the fractional differences of the two non-baseline cases with respect to the baseline. Tables F.3 to F.5 present the detailed calculations sheets which follow the nomenclature given in Knudsen and Ganni (Simplified helium refrigerator cycle analysis using the 'Carnot Step' 2006).

This analysis only predicts an input power reduction of 2.8% for the same load if there is a 2.7 bar pressure drop in the supply stream through the 4.5 K to 2 K heat exchanger (with the supply upstream of the JT to the load at 0.20 bar). And, it predicts a 3.0% capacity increase for the same input power if the same is used. This is less than the 4.2% and 4.4%, respectively, predicted by the simplified Carnot-Step analysis (see Appendix E).

Table F.1. Non-simplified 'Carnot-Step' analysis process parameters and results

		Baseline No HX Δp	Same Load with HX Δp	Same Input Power with HX Δp
4.5-2K HX cold-end supply press. (upstream of JT)	[bar]	2.90	0.20	0.20
CC mass flow (same as the flow to the load)	[g/s]	254.0	233.4	240.4
2-K load	[W]	5100	5100	5254
Load enthalpy flux	[J/g]	20.08	21.85	21.85
CC discharge temperature (to 4.5 K cold box)	[K]	28.35	31.24	31.17
Total (equivalent) input power	[kW]	3978	3868	3978
Supply mass flow to cold box (from compressors)	[g/s]	1059	1029	1059
Number of cold compressor stages	[-]	5	5	5
Adiabatic efficiency for each stage	[-]	70%	70%	70%
Supply pressure from 4.5 K cold box	[bar]	3.00	3.00	3.00
Supply temperature from 4.5 K cold box	[K]	4.55	4.55	4.55
Sub-atmospheric load pressure	[bar]	0.0310	0.0310	0.0310
4.5-2K HX cold-end (h) minus (l) stream temperature difference	[K]	0.20	0.20	0.20
Compressor high pressure discharge pressure	[bar]	18.5	18.5	18.5
Supply pressure from compressors to cold box	[bar]	18.0	18.0	18.0
First stage compressor suction pressure	[bar]	1.05	1.05	1.05
First stage compressor suction temperature	[K]	300	300	300
Distribution supply heat in-leak	[W]	0	0	0
Distribution sub-atmospheric return heat in-leak	[W]	500	500	500
Distribution supply flow pressure drop	[bar]	0.10	0.10	0.10
Distribution sub-atmospheric return pressure drop	[bar]	0.002	0.002	0.002
4.5-2K HX supply pressure drop	[bar]	0.00	2.70	2.70
4.5-2K HX sub-atmospheric return pressure drop	[bar]	0.002	0.002	0.002

Table F.2. Non-simplified 'Carnot-Step' analysis - fractional difference between non-baseline and baseline cases

		Fractional Difference to Baseline	
		Same Load with HX Δp	**Same Input Power with HX Δp**
CC mass flow (same as the flow to the load)	[g/s]	-8.1%	-5.4%
2-K load	[W]	0.0%	3.0%
Load enthalpy flux	[J/g]	8.8%	8.8%
CC discharge temperature (to 4.5 K cold box)	[K]	10.2%	9.9%
Total (equivalent) input power	[kW]	-2.8%	0.0%
Supply mass flow to cold box (from compressors)	[g/s]	-2.8%	0.0%

Table F.3. Non-simplified 'Carnot-Step' analysis - detailed calculations for baseline with no heat exchanger pressure drop

4 K to 2K HX Pressure Drop vs. CC Injection Temperature - Carnot Step Analysis										
Zero 4.5-2K HX Dp - Baseline										
$C_{p,l}$	5.200	[J/g-K]	*Specific heat at constant pressure for (l) stream*							
ϕ	0.400	[-]	*= (γ - 1)/ γ*							
Transfer-line and Cryo-module 4 K to 2 K HX										
	(h) Stream			*(l) Stream*						
	p	**T**	**h**	**p**	**T**	**h**	**ΔT_{hl}**			
	[atm]	**[K]**	**[J/g]**	**[atm]**	**[K]**	**[J/g]**	**[K]**			
CBX	2.96	4.55	12.03	0.0266	3.65	34.08		*Cold box*		
HX WE	2.86	4.56	12.03	0.0286	3.28	32.11	1.276	*Warm-end of CM HX*		
HX CE	2.86	2.20	4.95	0.0306	2.00	25.03	0.200	*Cold-end of CM HX*		
	(h) Stream	*(l) Stream*								
$q_{k,TL}$	0	500	[W]	*Transfer-line heat in-leak*						
Δp_{TL}	0.10	0.0020	[atm]	*Transfer-line pressure drop*						
Δp_{HX}	0.00	0.0020	[atm]	*HX pressure drop*						
2 K Load										
Δh_{lh}	20.08	[J/g]	*Supply enthalpy flux*							
$\dot{m}$	254.0	[g/s]	*Helium mass flow to load*							
q	5100	[W]	*2 K heat load (static & dynamic)*							
COP_{inv}	780.0	[W/W]	*Inverse coefficient of performance*							
Cold Compressor Train										
p_S	0.0266	[atm]	*First stage CC suction pressure*							
p_D	1.18	[atm]	*Last stage CC discharge pressure*							
Γ	44.44	[-]	*Total CC train pressure ratio*							
N	5	[-]	*Number of CC stages in train*							
η_C	70.0%	[-]	*Adiabatic efficiency of each (individual) CC*							
Θ	7.763	[-]	*Total CC train temperature ratio*							
T_S	3.65	[K]	*First stage CC suction temperature*							
T_D	28.35	[K]	*Last stage CC discharge temperature*							
$\eta_{cc,m}$	95.0%	[-]	*Cold compressor motor efficiency*							
$W_{cc,m}$	34.3	[kW]	*Total cold compressor motor power input*							

Table F.3. Continued

Cold Box												
4.5 K to CC Injection			*CC Injection to 300 K*									
p_h	17.27		17.76	[atm]	*Expansion step inlet pressure*							
p_l	1.23		1.18	[atm]	*Expansion step exit pressure*							
Γ	14.00		15.00	[-]	*Expansion step pressure ratio*							
η_x	82.0%		85.0%	[-]	*Adiabatic efficiency of expansion step*							
θ_x	2.149		2.285	[-]	*Expansion step temperature ratio*							
N	3		3	[-]	*Number of expansion steps*							
$T_{h,4}$ ($T_{h,1}$)	29.77		300.00	[K]	*(h) stream warm-end temperature*							
$T_{l,7}$ ($T_{l,4}$)	4.50		28.35	[K]	*(l) stream cold-end temperature*							
Θ	6.616		10.581	[-]	*Total temperature ratio*							
τ	0.050		0.015	[-]	*Ratio of stream temp. diff. to (l) stream at HX pinch point*							
θ_{hl}	1.050		1.015	[-]	*Ratio of (h) to (l) stream temperature at HX pinch point*							
θ	1.939		2.217	[-]	*Expansion stage temperature ratio*							
ε_k	0.050		0.050	[-]	*Non-dimensional expansion stage heat load*							
α	1.050		1.000	[-]	*Ratio of (h) to (l) stream* C_p							
f	0.087		0.018	[-]	*(h) stream mass flow multiplier*							
g	0.897		1.234	[-]	*Mass flow imbalance multiplier*							
h	1.154		1.270	[-]	*Expansion step mass flow multiplier*							
k	1.067		1.252	[-]	*= h - f*							
$\dot{m}_L$	254.0		0.0	[g/s]	*Mass flow imbalance (liquefaction)*							
$\dot{m}_R$	0.0		1015.2	[g/s]	*Refrigeration mass flow from cold-end of (l) stream*							
$\dot{m}_{LR}$	254.0		1015.3	[g/s]	*Total load mass flow,* $= \dot{m}_L + \dot{m}_R$							
ν_L	1.000		0.000	[-]	$= \dot{m}_L / \dot{m}_{LR}$							
$\beta_{r,0}$	0.922		0.014	[-]	*Ratio of final expander to total load flow*							
β_r	1.081		1.014	[-]	*Ratio of sucessive expansion step mass flows*							
$\dot{m}_{h,4}$ ($\dot{m}_{h,1}$)	1015		1059	[g/s]	*(h) stream mass flow at warm-end*							
Compressors:												
T_S	300.0	[K]	*Suction temperature*									
η_m	95.0%	[-]	*Motor efficiency*									
	HP		**LP**									
$\dot{m}$	1059		1059	[g/s]	*Mass flow*							
Δp_S	0.05		0.197	[atm]	*Suction pressure drop*							
Δp_D	0.49		0.099	[atm]	*Discharge pressure drop*							
p_S	4.65		1.04	[atm]	*Suction pressure*							
p_D	18.26		4.79	[atm]	*Discharge pressure*							
Γ	3.930		4.626	[-]	*Pressure ratio*							
η_i	52.5%		50.0%	[-]	*Isothermal efficiency*							
w_i	854.1		955.8	[W/(g/s)]	*Specific isothermal work*							
W_m	1814		2130	[kW]	*Motor input power*							
W_{tot}	3978			[kW]	*Total input power*							

Table F.4. Non-simplified 'Carnot-Step' analysis - detailed calculations for same load with heat exchanger pressure drop

4 K to 2K HX Pressure Drop vs. CC Injection Temperature - Carnot Step Analysis										
Non-Zero 4.5-2K HX Dp - Same Load										
$C_{p,l}$	5.200	[J/g-K]	*Specific heat at constant pressure for (l) stream*							
ϕ	0.400	[-]	*= (γ - 1)/ γ*							
Transfer-line and Cryo-module 4 K to 2 K HX										
	(h) Stream			*(l) Stream*						
	p	**T**	**h**	**p**	**T**	**h**	**ΔT_{hl}**			
	[atm]	**[K]**	**[J/g]**	**[atm]**	**[K]**	**[J/g]**	**[K]**			
CBX	2.96	4.55	12.03	0.0266	4.02	36.03		*Cold box*		
HX WE	2.86	4.56	12.03	0.0286	3.62	33.88	0.940	*Warm-end of CM HX*		
HX CE	0.20	2.20	3.17	0.0306	2.00	25.03	0.200	*Cold-end of CM HX*		
	(h) Stream	*(l) Stream*								
$q_{k,TL}$	0	500	[W]	*Transfer-line heat in-leak*						
Δp_{TL}	0.10	0.0020	[atm]	*Transfer-line pressure drop*						
Δp_{HX}	2.66	0.0020	[atm]	*HX pressure drop*						
2 K Load										
Δh_{lh}	21.85	[J/g]	*Supply enthalpy flux*							
$\dot{m}$	233.4	[g/s]	*Helium mass flow to load*							
q	5100	[W]	*2 K heat load (static & dynamic)*							
COP_{inv}	758.4	[W/W]	*Inverse coefficient of performance*							
Cold Compressor Train										
p_S	0.0266	[atm]	*First stage CC suction pressure*							
p_D	1.18	[atm]	*Last stage CC discharge pressure*							
Γ	44.44	[-]	*Total CC train pressure ratio*							
N	5	[-]	*Number of CC stages in train*							
η_C	70.0%	[-]	*Adiabatic efficiency of each (individual) CC*							
Θ	7.763	[-]	*Total CC train temperature ratio*							
T_S	4.02	[K]	*First stage CC suction temperature*							
T_D	31.24	[K]	*Last stage CC discharge temperature*							
$\eta_{cc,m}$	95.0%	[-]	*Cold compressor motor efficiency*							
$W_{cc,m}$	34.8	[kW]	*Total cold compressor motor power input*							

Table F.4. Continued.

Cold Box												
4.5 K to CC Injection			*CC Injection to 300 K*									
p_h	17.27		17.76	[atm]	*Expansion step inlet pressure*							
p_l	1.23		1.18	[atm]	*Expansion step exit pressure*							
Γ	14.00		15.00	[-]	*Expansion step pressure ratio*							
η_x	82.0%		85.0%	[-]	*Adiabatic efficiency of expansion step*							
θ_x	2.149		2.285	[-]	*Expansion step temperature ratio*							
N	3		3	[-]	*Number of expansion steps*							
$T_{h,4}$ ($T_{h,1}$)	32.80		300.00	[K]	*(h) stream warm-end temperature*							
$T_{l,7}$ ($T_{l,4}$)	4.50		31.24	[K]	*(l) stream cold-end temperature*							
Θ	7.288		9.605	[-]	*Total temperature ratio*							
τ	0.050		0.015	[-]	*Ratio of stream temp. diff. to (l) stream at HX pinch point*							
θ_{hl}	1.050		1.015	[-]	*Ratio of (h) to (l) stream temperature at HX pinch point*							
θ	2.003		2.147	[-]	*Expansion stage temperature ratio*							
ε_k	0.050		0.050	[-]	*Non-dimensional expansion stage heat load*							
α	1.050		1.000	[-]	*Ratio of (h) to (l) stream* C_p							
f	0.093		0.017	[-]	*(h) stream mass flow multiplier*							
g	0.958		1.165	[-]	*Mass flow imbalance multiplier*							
h	1.154		1.270	[-]	*Expansion step mass flow multiplier*							
k	1.061		1.253	[-]	*= h - f*							
$\dot{m}_L$	233.4		0.0	[g/s]	*Mass flow imbalance (liquefaction)*							
$\dot{m}_R$	0.0		989.3	[g/s]	*Refrigeration mass flow from cold-end of (l) stream*							
$\dot{m}_{LR}$	233.4		989.3	[g/s]	*Total load mass flow,* $= \dot{m}_L + \dot{m}_R$							
ν_L	1.000		0.000	[-]	$= \dot{m}_L / \dot{m}_{LR}$							
$\beta_{r,0}$	0.990		0.013	[-]	*Ratio of final expander to total load flow*							
β_r	1.088		1.013	[-]	*Ratio of sucessive expansion step mass flows*							
$\dot{m}_{h,4}$ ($\dot{m}_{h,1}$)	989		1029	[g/s]	*(h) stream mass flow at warm-end*							
Compressors:												
T_S	300.0	[K]	*Suction temperature*									
η_m	95.0%	[-]	*Motor efficiency*									
	HP		**LP**									
$\dot{m}$	1029		1029	[g/s]	*Mass flow*							
Δp_S	0.05		0.197	[atm]	*Suction pressure drop*							
Δp_D	0.49		0.099	[atm]	*Discharge pressure drop*							
p_S	4.65		1.04	[atm]	*Suction pressure*							
p_D	18.26		4.79	[atm]	*Discharge pressure*							
Γ	3.930		4.626	[-]	*Pressure ratio*							
η_i	52.5%		50.0%	[-]	*Isothermal efficiency*							
w_i	854.1		955.8	[W/(g/s)]	*Specific isothermal work*							
W_m	1763		2070	[kW]	*Motor input power*							
W_{tot}	3868			[kW]	*Total input power*							

Table F.5. Non-simplified 'Carnot-Step' analysis - detailed calculations for same input power with heat exchanger pressure drop

4 K to 2K HX Pressure Drop vs. CC Injection Temperature - Carnot Step Analysis										
Non-Zero 4.5-2K HX Dp - Same Input Power										
$C_{p,l}$	5.200	[J/g-K]	*Specific heat at constant pressure for (l) stream*							
ϕ	0.400	[-]	*= (γ - 1)/ γ*							
Transfer-line and Cryo-module 4 K to 2 K HX										
	(h) Stream			*(l) Stream*						
	p	**T**	**h**	**p**	**T**	**h**	**ΔT_{hl}**			
	[atm]	**[K]**	**[J/g]**	**[atm]**	**[K]**	**[J/g]**	**[K]**			
CBX	2.96	4.55	12.03	0.0266	4.01	35.96		*Cold box*		
HX WE	2.86	4.56	12.03	0.0286	3.62	33.88	0.940	*Warm-end of CM HX*		
HX CE	0.20	2.20	3.17	0.0306	2.00	25.03	0.200	*Cold-end of CM HX*		
	(h) Stream	*(l) Stream*								
$q_{k,TL}$	0	500	[W]	*Transfer-line heat in-leak*						
Δp_{TL}	0.10	0.0020	[atm]	*Transfer-line pressure drop*						
Δp_{HX}	2.66	0.0020	[atm]	*HX pressure drop*						
2 K Load										
Δh_{lh}	21.85	[J/g]	*Supply enthalpy flux*							
$\dot{m}$	240.4	[g/s]	*Helium mass flow to load*							
q	5254	[W]	*2 K heat load (static & dynamic)*							
COP_{inv}	757.1	[W/W]	*Inverse coefficient of performance*							
Cold Compressor Train										
p_S	0.0266	[atm]	*First stage CC suction pressure*							
p_D	1.18	[atm]	*Last stage CC discharge pressure*							
Γ	44.44	[-]	*Total CC train pressure ratio*							
N	5	[-]	*Number of CC stages in train*							
η_C	70.0%	[-]	*Adiabatic efficiency of each (individual) CC*							
Θ	7.763	[-]	*Total CC train temperature ratio*							
T_S	4.01	[K]	*First stage CC suction temperature*							
T_D	31.14	[K]	*Last stage CC discharge temperature*							
$\eta_{cc,m}$	95.0%	[-]	*Cold compressor motor efficiency*							
$W_{cc,m}$	35.7	[kW]	*Total cold compressor motor power input*							

Table F.5. Continued

Cold Box												
4.5 K to CC Injection			*CC Injection to 300 K*									
p_h	17.27		17.76	[atm]	*Expansion step inlet pressure*							
p_l	1.23		1.18	[atm]	*Expansion step exit pressure*							
Γ	14.00		15.00	[-]	*Expansion step pressure ratio*							
η_x	82.0%		85.0%	[-]	*Adiabatic efficiency of expansion step*							
θ_x	2.149		2.285	[-]	*Expansion step temperature ratio*							
N	3		3	[-]	*Number of expansion steps*							
$T_{h,4}$ ($T_{h,1}$)	32.70		300.00	[K]	*(h) stream warm-end temperature*							
$T_{l,7}$ ($T_{l,4}$)	4.50		31.14	[K]	*(l) stream cold-end temperature*							
Θ	7.267		9.633	[-]	*Total temperature ratio*							
τ	0.050		0.015	[-]	*Ratio of stream temp. diff. to (l) stream at HX pinch point*							
θ_{hl}	1.050		1.015	[-]	*Ratio of (h) to (l) stream temperature at HX pinch point*							
θ	2.001		2.149	[-]	*Expansion stage temperature ratio*							
ε_k	0.050		0.050	[-]	*Non-dimensional expansion stage heat load*							
α	1.050		1.000	[-]	*Ratio of (h) to (l) stream* C_p							
f	0.093		0.017	[-]	*(h) stream mass flow multiplier*							
g	0.956		1.167	[-]	*Mass flow imbalance multiplier*							
h	1.154		1.270	[-]	*Expansion step mass flow multiplier*							
k	1.061		1.253	[-]	*= h - f*							
$\dot{m}_L$	240.4		0.0	[g/s]	*Mass flow imbalance (liquefaction)*							
$\dot{m}_R$	0.0		1017.3	[g/s]	*Refrigeration mass flow from cold-end of (l) stream*							
$\dot{m}_{LR}$	240.4		1017.4	[g/s]	*Total load mass flow,* $= \dot{m}_L + \dot{m}_R$							
ν_L	1.000		0.000	[-]	$= \dot{m}_L / \dot{m}_{LR}$							
$\beta_{r,0}$	0.988		0.013	[-]	*Ratio of final expander to total load flow*							
β_r	1.087		1.013	[-]	*Ratio of sucessive expansion step mass flows*							
$\dot{m}_{h,4}$ ($\dot{m}_{h,1}$)	1017		1059	[g/s]	*(h) stream mass flow at warm-end*							
Compressors:												
T_S	300.0	[K]	*Suction temperature*									
η_m	95.0%	[-]	*Motor efficiency*									
	HP		**LP**									
$\dot{m}$	1059		1059	[g/s]	*Mass flow*							
Δp_S	0.05		0.197	[atm]	*Suction pressure drop*							
Δp_D	0.49		0.099	[atm]	*Discharge pressure drop*							
p_S	4.65		1.04	[atm]	*Suction pressure*							
p_D	18.26		4.79	[atm]	*Discharge pressure*							
Γ	3.930		4.626	[-]	*Pressure ratio*							
η_i	52.5%		50.0%	[-]	*Isothermal efficiency*							
w_i	854.1		955.8	[W/(g/s)]	*Specific isothermal work*							
W_m	1813		2129	[kW]	*Motor input power*							
W_{tot}	3978			[kW]	*Total input power*							

APPENDIX G – FULL PROCESS CYCLE MODEL

The process cycle model used for the 12 GeV upgrade at JLab (P. Knudsen, V. Ganni and N. Hasan, et al. 2016) and for the FRIB refrigerator at MSU (Ganni, Knudsen and Arenius, et al. 2014), was used to evaluate the effect of the cold compressor discharge temperature on the overall process. Since the 2-K load is around the maximum capacity of the 12 GeV and FRIB plants and the dominate load in the actual refrigerators, this analysis was straight forward to accomplish; i.e., there was no need for process configuration studies. And, this process model has been well validated. As can be seen between Table F.1 in Appendix F and Table G.1, the main process parameters are the same between this analysis and the non-simplified 'Carnot-Step' analysis. The full cycle model uses,

- Real fluid properties for all calculations
- Integrated cooling curve calculations for heat exchanger thermal rating *(UA)*, *NTU's* and effectiveness
- Turbine expander flow coefficient modeling
- Real warm compressor isothermal and volumetric efficiency estimates and real induction motor efficiency estimates (P. Knudsen, V. Ganni, et al. 2016)

However, no effort was made to model around selected or known equipment sizes. But, the same compressor displacement size was used for the baseline and non-baseline cases. Table G.2 presents the fractional differences of the two non-baseline cases with respect to the baseline. Tables G.3 to G.5 contain the detailed calculations of the process cycle.

This analysis predicts an input power reduction of 5.0% for the same load if there is a 2.7 bar pressure drop in the supply stream through the 4.5 K to 2 K heat exchanger (with the supply

upstream of the JT to the load at 0.20 bar). And, it predicts a 6.1% capacity increase for the same input power if the same is used. The difference between these results and the ones predicted using the previous analysis (in Appendix F) is this model's ability to simulate the components of cold box (and compressor system) in more detail. Note the fractional differences in Tables F.2 and Table G.2 for the supply mass flow from the warm compressors to the cold box is minus 2.8% and minus 7.0%, respectively, for the same load and for the case of 2.7 bar *(h)* stream pressure drop in the 4.5 K to 2 K heat exchanger. And, it is 0% and minus 3.1%, respectively, for the same input power and for the case of 2.7 bar *(h)* stream pressure drop in the 4.5 K to 2 K heat exchanger. This indicates that the full cycle process model has more flexibility in the cold box system modeling.

Table G.1. Full cycle process model parameters and results

		Baseline No HX Δp	Same Load with HX Δp	Same Input Power with HX Δp
4.5-2K HX cold-end supply press. (upstream of JT)	[bar]	2.90	0.20	0.20
CC mass flow (same as the flow to the load)	[g/s]	254.5	233.8	248.0
2-K load	[W]	5109	5109	5420
Load enthalpy flux	[J/g]	20.08	21.84	21.84
CC discharge temperature (to 4.5 K cold box)	[K]	28.37	30.88	30.70
Total (equivalent) input power	[kW]	3575	3396	3575
Supply mass flow to cold box (from compressors)	[g/s]	1023	951.4	991.4
Number of cold compressor stages	[-]	5	5	5
Adiabatic efficiency for each stage	[-]	70%	70%	70%
Supply pressure from 4.5 K cold box	[bar]	3.00	3.00	3.00
Supply temperature from 4.5 K cold box	[K]	4.56	4.54	4.54
Sub-atmospheric load pressure	[bar]	0.0310	0.0310	0.0310
4.5-2K HX cold-end (h) minus (l) stream temperature difference	[K]	0.20	0.20	0.20
Compressor high pressure discharge pressure	[bar]	18.5	17.8	18.0
Supply pressure from compressors to cold box	[bar]	18.0	17.3	17.5
First stage compressor suction pressure	[bar]	1.06	1.04	1.04
First stage compressor suction temperature	[K]	300	300	300
Distribution supply heat in-leak	[W]	0	0	0
Distribution sub-atmospheric return heat in-leak	[W]	500	500	500
Distribution supply flow pressure drop	[bar]	0.10	0.10	0.10
Distribution sub-atmospheric return pressure drop	[bar]	0.002	0.002	0.002
4.5-2K HX supply pressure drop	[bar]	0.00	2.70	2.70
4.5-2K HX sub-atmospheric return pressure drop	[bar]	0.002	0.002	0.002

Table G.2. Full process cycle model – fractional difference between non-baseline and baseline cases

		Fractional Difference to Baseline	
		Same Load with HX Δp	**Same Input Power with HX Δp**
CC mass flow (same as the flow to the load)	[g/s]	-8.1%	-2.6%
2-K load	[W]	0.0%	6.1%
Load enthalpy flux	[J/g]	8.7%	8.7%
CC discharge temperature (to 4.5 K cold box)	[K]	8.9%	8.2%
Total (equivalent) input power	[kW]	-5.0%	0.0%
Supply mass flow to cold box (from compressors)	[g/s]	-7.0%	-3.1%

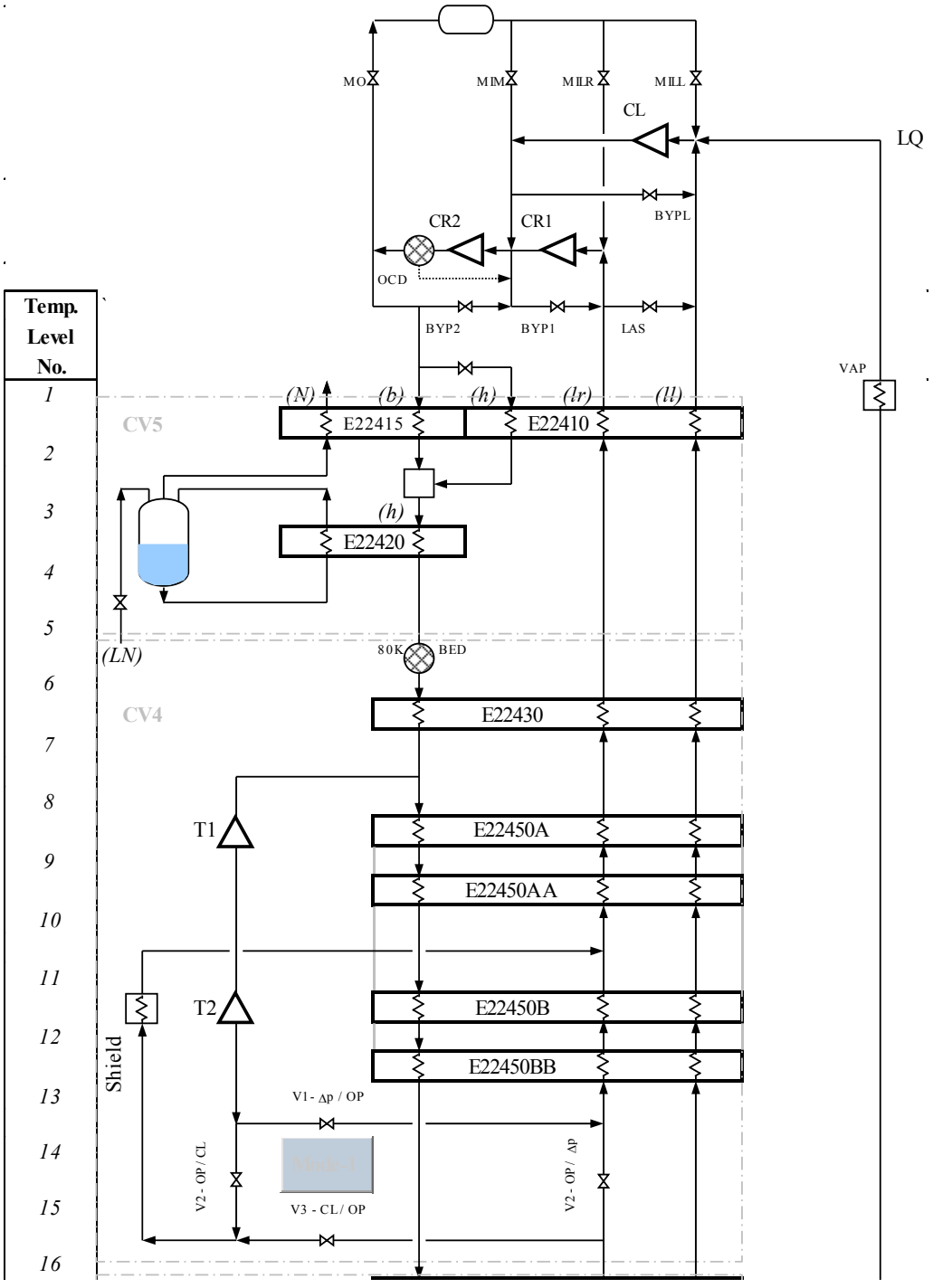

Figure G.1. Diagram of the 4.5 K cold box used for the full process cycle model in the evaluation of the effect of the cold compressor discharge temperature on the overall 2 K refrigeration process

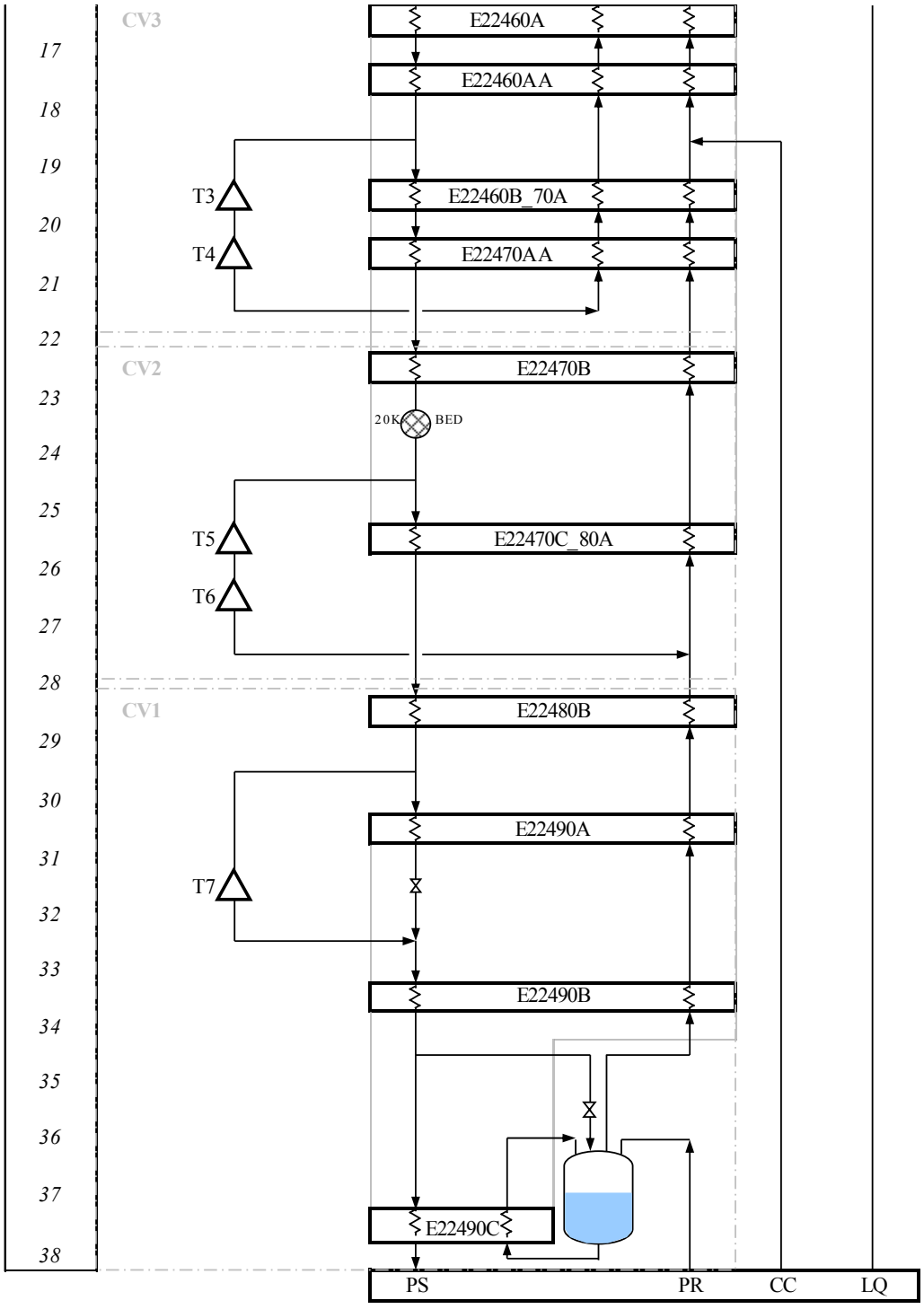

Figure G.1. Continued.

Table G.3. Full cycle process model – baseline, zero heat exchanger pressure drop

Design: Overview: Baseline (Zero HX Dp)

E.B. Violation	NO	X.B. Violation?	NO	M.B. Violation?	NO

Loads:

	w [g/s]	Supply p [atm]	Supply T [K]	Return p [atm]	Return T [K]	T_{sat} [K]	Δp [atm]	q [kW]	E_L [kW]	*Frac* E_L [-]
Shield	0.0	2.29	27.45	2.04	55.00		0.250	0.00	0.0	0.0%
4K Ref.	0.0	2.96	4.56	1.242	4.46	4.460		0.00	0.0	0.0%
4K Liq.	0.0	2.96	4.56	1.094	300.00				0.0	0.0%
S.A.	254.5	2.96	4.56	1.19	28.37			38.24	1127.7	100.0%

Total Load Carnot Work:	1127.7	[kW]
Total Carnot Efficiency:	31.85%	
Total Equiv. Input Power	3575	[kW]

Compressors:

	N_c [-]	w_c [g/s]	w_{byp} [g/s]	p_S [atm]	p_D [atm]	p_r [-]	T_S [K]	T_D [K]	η_v [-]	η_i [-]	P_m [kW]	$E_{c,iso}$ [kW]
1st Load	2	566.6	0.1	1.044	4.85	4.65	300.00	305.00	86.2%	50.0%	1149.5	543.3
1st Recycle	1	456.6	0.0	1.81	4.85	2.68	300.00	305.00	87.5%	55.6%	529.1	281.1
2nd Recycle	1	1023.1	0.0	4.71	18.26	3.88	313.00	305.00	78.8%	52.6%	1720.4	868.3

Total Input Power:	3399.0	[kW]
Effective Compr. Sys. Eff.:	48.0%	

LN Pre-Cooling:

w_{LN} [g/s]	Q [gph]	Supply p [atm]	Supply T [K]	Vent p [atm]	Vent T [K]	$\Delta T_{hN,1}$ [K]	q [kW]	E_c [kW]	η_{LN2} [-]	COP_{INV} [-]
71.5	92.1	3.95	91.18	1.05	299.06	5.98	28.84	49.5	35.0%	4.90

Equiv. LN_2 P.C. Input Power:	141.3	[kW]
Availability to Coldbox	1631.4	[kW]
Cold Box Efficency:	69.1%	

Control Volumes:

	HP Stream (*h*) T [K]	HP p [atm]	HP w [g/s]	LR Stream (*lr*) T [K]	LR p [atm]	LR w [g/s]	LL Stream (*ll*) T [K]	LL p [atm]	LL w [g/s]	ΔT_{hl} [K]	$(\Delta T_{hl}/T_l)$ [-]	Σq_{LK} [W]
T.L. #												
1	305.03	17.76	1023.1	298.76	1.86	456.6	298.76	1.09	566.6	6.274	2.10%	
CV5												445
5	80.13	17.38	1023.1	78.94	1.97	456.6	78.94	1.13	566.6	1.184	1.50%	
CV4												590
16	27.86	17.28	938.4	27.45	2.04	456.6	27.45	1.18	566.6	0.412	1.50%	
CV3												175
22	13.78	17.27	566.6				13.50	1.21	312.1	0.283	2.10%	
CV2												165
28	5.55	17.27	282.7				5.38	1.24	28.2	0.167	3.10%	
CV1												295
38	4.56	2.96	254.5				4.46	1.24	0.0	0.100	2.24%	

Expanders:

#	w_x [g/s]	Δp_i [atm]	p_i [atm]	p_o [atm]	p_r [-]	T_i [K]	T_o [K]	T_r [-]	Δh_x [J/g]	η_x [-]	W_x [kW]	ϕ_x [-]
T1	84.7	0.15	17.13	6.26	2.73	53.14	38.22	1.39	79.96	85.0%	6.78	22.0
T2	84.7	0.00	6.26	2.29	2.73	38.22	27.45	1.39	56.46	85.0%	4.78	50.5
T3	371.8	0.15	17.13	5.94	2.89	27.43	19.27	1.42	42.46	85.0%	15.79	68.1
T4	371.8	0.00	5.94	2.06	2.89	19.27	13.50	1.43	28.89	85.0%	10.74	162.5
T5	283.9	0.15	17.12	4.61	3.72	13.71	8.71	1.57	21.02	85.0%	5.97	32.6
T6	283.9	0.00	4.61	1.24	3.72	8.71	5.38	1.62	12.22	85.0%	3.47	93.4
T7	282.7	0.15	17.12	2.96	5.78	5.46	4.788	1.14	8.25	82.0%	2.33	18.1

Total Expander Work:	49.86	[kW]

Table G.3. Continued

Heat Exchangers:

		W.E.	*C.E.*				*(Calc.)*	*(Proj.)*		*Ref.*
		($\Delta T_{hl}/T_l$)	**($\Delta T_{hl}/T_l$)**	**q_h**	**NTU**	**ε**	**(UA)**	**$(UA)_P$**	**% Δ(UA)**	**$(UA)_{ref}$**
	HX #	**[-]**	**[-]**	**[kW]**	**[-]**	**[-]**	**[kW/K]**	**[W/K]**	**[-]**	**[W/K]**
CV5	*E22410*	2.1%	4.4%	1168.00	48.14	98.5%	252.61	245.25	0.0%	3965.89
	E22415	2.0%	5.5%	16.67	36.98	98.1%	2.76	2.76	0.0%	386.22
	E22420	5.5%	2.6%	12.17	0.76	53.2%	4.07	4.07	0.0%	63.69
CV4	*E22430*	1.5%	3.1%	145.75	20.28	95.9%	107.87	107.87	0.0%	1686.33
	E22450A	3.1%	2.0%	74.92	13.72	95.2%	69.07	69.07	**0.0%**	1108.50
	E22450AA	2.0%	2.0%	**0.00**	0.00	**0.0%**	0.00	0.00	0.0%	0.00
	E22450B	2.0%	1.5%	53.67	19.50	96.1%	101.18	101.19	**0.0%**	1624.11
	E22450BB	1.5%	1.5%	0.00	0.00	0.5%	0.01	0.00	0.0%	0.00
CV3	*E22460A*	1.5%	1.6%	0.63	0.31	23.8%	1.50	4.02	**0.0%**	66.11
	E22460AA	1.6%	3.7%	1.67	1.28	66.4%	2.51	0.00	0.0%	0.00
	E22460B_70	3.7%	2.1%	47.02	37.36	98.2%	130.66	110.73	0.0%	2756.44
	E22470AA	2.1%	2.1%	**0.00**	**N/D**	**N/D**	**N/D**	0.00	0.0%	0.00
CV2	*E22470B*	2.1%	2.9%	0.27	0.49	36.6%	0.83	0.83	0.0%	22.38
	E22470C_80	2.9%	3.1%	14.10	13.05	**98.9%**	19.89	19.89	0.0%	653.21
CV1	*E22480B*	3.1%	16.0%	0.15	1.77	82.2%	0.37	0.37	**0.0%**	31.10
	E22490A	16.0%	**0.0%**	0.00	**N/D**	**N/D**	**N/D**			
	E22490B	2.1%	7.2%	0.06	1.24	73.1%	0.33	0.33	**0.0%**	27.86
	E22490C	7.2%	2.2%	0.49	1.16	80.4%	2.55	2.55	0.0%	91.95
	Min.	1.5%	1.5%	**0.00**		**0.0%**		0.00	**0.0%**	0.00
	Max.	16.0%	16.0%			**98.9%**		245.25	0.0%	3965.89
	Total			1535.58	159.07		696.22	668.93		
MIN ($\Delta T_{hl}/T_l$)		1.5%			**ε_{max}**	98.5%				
			300-80K	1196.84	48.90		259.45			
			80-35K	274.34	53.51		278.13			
			35-4.5K	64.39	56.66		158.63			

Sub-Coolers:

	w_{JT}	**w_{BO}**	**p**	**T**	**$\Delta T_{hl,CE}$**	***x***
	[g/s]	**[g/s]**	**[atm]**	**[K]**	**[K]**	**[-]**
SC-LN	71.5	61.6	1.099	78.13	2.00	13.9%
SC-He	28.2	25.5	1.242	4.46	0.10	9.4%

$\phi_{x,D}$	**% $\Delta\phi_x$**
[-]	**[-]**
22.0	0.0%
50.5	0.0%
68.1	0.0%
162.5	0.0%
32.6	0.0%
93.4	0.0%
18.1	0.0%

T2 Outlet ΔT:

($T_{lr,16} - T_{x2,o}$)

[K]
0.000

(h) - (x) at TL=10:

$\Delta T_{hx,10}$
[K]
0.000

T4 Outlet ΔT:

($T_{ll,22} - T_{x4,o}$)

[K]
0.000

(h) - (l) at TL=31:

$\Delta T_{hl,31}$
[K]
0.000

T6 Outlet ΔT:

($T_{ll,28} - T_{x6,o}$)

[K]
0.000

T7 Bypass:

$\xi_{h7,b}$
[-]
0.00%

Table G.3. Continued

Process Summary — *Baseline (Zero HX Dp)*

$\dot{m}_{h,0}$ = 254.46 [g/s] — *(h) Stream*; $\dot{m}_{u,8}$ = 254.46 [g/s] — *(u) Stream*

TL#	T [K]	p [atm]	h [J/g]	T [K]	p [atm]	h [J/g]	TL#
0	4.560	2.961	12.07	28.367	1.192	162.34	*0*
1				28.367	1.192	162.34	*1*
				-2.2E-11		*-2.0E-11*	
2				3.658	0.0266	34.11	*2*
3				3.658	0.0266	34.11	*3*
4				3.658	0.0266	34.11	*4*
5				3.288	0.0286	32.14	*5*
6	4.565	2.862	12.07	3.288	0.0286	32.14	*6*
	Downstream of HX			*3.4E-07*		*1.9E-07*	
7	2.197	2.862	4.95	1.997	0.0306	25.03	*7*
8	1.997	0.031	4.95	1.997	0.0306	25.03	*8*

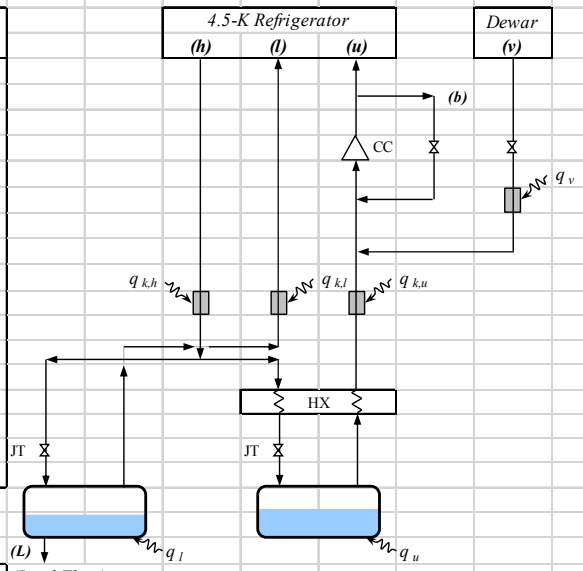

$\dot{m}_v$ = 0.00 [g/s] — *(v) Stream*; $\dot{m}_l$ = 0.00 [g/s] — *(l) Stream*

TL#	T [K]	p [atm]	h [J/g]	T [K]	p [atm]	h [J/g]	TL#
0	4.549	1.342	30.36	4.460	1.242	30.53	*0*
2	2.950	0.027	30.36	4.460	1.242	30.53	*8*
3	2.950	0.027	30.36				

$\dot{m}_L$	0.00	[g/s]	*Lead flow*	Δh_{lh}	18.469	[J/g]	*4.5-K load enthalpy flux*
q_l	0	[W]	*4.5-K load*	Δh_{uh}	20.079	[J/g]	*2-K load enthalpy flux*
q_u	5109	[W]	*2-K load*	$COP_{inv,2K}$	699.7	[W/W]	2-K inverse coefficient of performance

	Transfer-Line			*Dewar*	*HX*			
	(h)	*(l)*	*(u)*	*(v)*	*(h)*	*(u)*		
Δp	0.10	0.000	0.0020	1.315	0.00	0.0020	[atm]	*Pressure drop*
q_k	0.0	0.0	500.0	0.0	0.0		[W]	*Heat in-leak*

Cold Compressors:

$\dot{m}_{CC}$ = 254.46 [g/s] — ξ_b = 0.0% [-]

Stage #	p [atm]	T [K]	h [J/g]	T_r [-]	p_r [-]	Q [ℓ/s]	η_s [-]	Dh_s [J/g]	W_{cc} [kW]	η_m [-]	$W_{cc,m}$ [kW]
5	1.192	28.367	162.34	1.507	2.139	124.5	70.0%	34.76	12.6362	95.0%	13.301
4	0.557	18.823	112.68	1.507	2.139	176.0	70.0%	23.00	8.3596	95.0%	8.800
3	0.261	12.493	79.83	1.506	2.139	249.2	70.0%	15.23	5.5346	95.0%	5.826
2	0.122	8.293	58.07	1.506	2.139	352.9	70.0%	10.09	3.6669	95.0%	3.860
1	0.057	5.506	43.66	1.505	2.139	500.3	70.0%	6.69	2.4314	95.0%	2.559
0	0.027	3.658	34.11			709.7					
Total		24.71	128.23	7.754	44.737		52.6%		32.629		34.346

Table G.4. Full cycle process model – same load, non-zero heat exchanger pressure drop

Design: Overview: Non-Zero HX Dp - Same Load

E.B. Violation	NO	X.B. Violation?	NO	M.B. Violation?	NO

Loads:

	w [g/s]	Supply p [atm]	Supply T [K]	Return p [atm]	Return T [K]	T_{sat} [K]	Δp [atm]	q [kW]	E_L [kW]	*Frac* E_L [-]
Shield	0.0	2.06	38.20	1.81	55.00		0.250	0.00	0.0	0.0%
4K Ref.	0.0	2.96	4.54	1.222	4.44	4.442		0.00	0.0	0.0%
4K Liq.	0.0	2.96	4.54	1.074	300.00				0.0	0.0%
S.A.	233.8	2.96	4.54	1.17	30.88			38.23	1068.0	100.0%

Total Load Carnot Work:	1068.0	[kW]
Total Carnot Efficiency:	31.77%	
Total Equiv. Input Power	3396	[kW]

Compressors:

	N_c [-]	w_c [g/s]	w_{byp} [g/s]	p_S [atm]	p_D [atm]	p_r [-]	T_S [K]	T_D [K]	η_v [-]	η_i [-]	P_m [kW]	$E_{c,iso}$ [kW]
1st Load	2	557.9	3.6	1.024	4.53	4.42	300.00	305.00	86.5%	50.2%	1090.0	517.4
1st Recycle	1	397.1	0.0	1.57	4.53	2.88	300.00	305.00	87.5%	55.4%	495.2	261.8
2nd Recycle	1	951.4	0.0	4.38	17.57	4.01	313.00	305.00	78.7%	52.4%	1644.9	826.9

Total Input Power:	3230.0	[kW]
Effective Compr. Sys. Eff.:	47.7%	

LN Pre-Cooling:

w_{LN} [g/s]	Q [gph]	Supply p [atm]	Supply T [K]	Vent p [atm]	Vent T [K]	$\Delta T_{hN,1}$ [K]	q [kW]	E_c [kW]	η_{LN2} [-]	COP_{INV} [-]
66.5	85.6	3.95	91.18	1.05	299.06	5.98	26.81	46.0	35.0%	4.90

Equiv. LN_2 P.C. Input Power:	131.4	[kW]
Availability to Coldbox	1542.3	[kW]
Cold Box Efficency:	69.2%	

Control Volumes:

	HP Stream (*h*) T [K]	HP p [atm]	HP w [g/s]	LR Stream (*lr*) T [K]	LR p [atm]	LR w [g/s]	LL Stream (*ll*) T [K]	LL p [atm]	LL w [g/s]	ΔT_{hl} [K]	$(\Delta T_{hl}/T_l)$ [-]	Σq_{LK} [W]
T.L. #												
1	305.03	17.07	951.4	298.76	1.62	397.1	298.76	1.07	554.3	6.274	2.10%	
CV5												445
5	80.13	16.69	951.4	78.94	1.74	397.1	78.94	1.11	554.3	1.184	1.50%	
CV4												590
16	38.77	16.59	915.1	38.20	1.81	397.1	38.20	1.16	554.3	0.573	1.50%	
CV3												175
22	14.79	16.58	554.3				14.50	1.19	320.5	0.290	2.00%	
CV2												165
28	5.98	16.58	272.5				5.88	1.22	38.7	0.100	1.70%	
CV1												295
38	4.54	2.96	233.8				4.44	1.22	0.0	0.100	2.25%	

Expanders:

#	w_x [g/s]	Δp_i [atm]	p_i [atm]	p_o [atm]	p_r [-]	T_i [K]	T_o [K]	T_r [-]	Δh_x [J/g]	η_x [-]	W_x [kW]	ϕ_x [-]
T1	36.3	0.15	16.44	5.81	2.83	75.44	53.72	1.40	115.89	85.0%	4.20	11.6
T2	36.3	0.00	5.81	2.06	2.83	53.72	38.20	1.41	81.45	85.0%	2.95	27.5
T3	360.9	0.15	16.44	5.47	3.00	30.12	20.92	1.44	48.22	85.0%	17.40	72.0
T4	360.9	0.00	5.47	1.82	3.00	20.92	14.50	1.44	32.55	85.0%	11.75	178.2
T5	281.8	0.15	16.43	4.48	3.67	14.75	9.39	1.57	23.29	85.0%	6.56	35.8
T6	281.8	0.00	4.48	1.22	3.67	9.39	5.88	1.60	13.91	85.0%	3.92	102.4
T7	272.5	0.15	16.43	2.96	5.55	5.78	4.955	1.17	8.07	82.0%	2.20	18.1

Total Expander Work:	48.99	[kW]

Table G.4. Continued

Heat Exchangers:

		W.E.	*C.E.*				*(Calc.)*	*(Proj.)*		*Ref.*
		$(\Delta T_{hl}/T_l)$	$(\Delta T_{hl}/T_l)$	q_h	NTU	ε	(UA)	$(UA)_P$	% Δ(UA)	$(UA)_{ref}$
	HX #	[-]	[-]	[kW]	[-]	[-]	[kW/K]	[W/K]	[-]	[W/K]
CV5	*E22410*	2.1%	4.4%	1086.14	48.11	98.5%	234.76	227.92	0.0%	3849.89
	E22415	2.0%	5.5%	15.49	36.96	98.1%	2.57	2.57	0.0%	374.95
	E22420	5.5%	2.6%	11.32	0.76	53.2%	3.79	3.79	0.0%	61.85
CV4	*E22430*	1.5%	1.8%	23.84	3.87	80.3%	19.14	19.14	0.0%	312.52
	E22450A	1.8%	1.6%	41.88	7.37	89.1%	35.42	35.42	0.0%	585.22
	E22450AA	1.6%	1.6%	**0.00**	0.00	**0.0%**	0.00	0.00	0.0%	0.00
	E22450B	1.6%	1.5%	135.92	37.88	98.0%	184.52	184.52	0.0%	3048.77
	E22450BB	1.5%	1.5%	0.00	0.00	0.0%	0.00	0.00	0.0%	0.00
CV3	*E22460A*	1.5%	3.3%	41.48	11.71	93.8%	55.95	57.44	**0.0%**	960.11
	E22460AA	3.3%	5.6%	1.88	0.79	50.6%	1.49	0.00	0.0%	0.00
	E22460B_70.	5.6%	2.0%	50.42	26.64	98.0%	89.96	76.24	0.0%	1913.19
	E22470AA	2.0%	2.0%	**0.00**	**N/D**	**N/D**	**N/D**	0.00	0.0%	0.00
CV2	*E22470B*	2.0%	2.4%	0.14	0.26	22.5%	0.45	0.45	0.0%	12.26
	E22470C_80.	2.4%	1.7%	15.24	17.55	**99.3%**	27.60	27.60	0.0%	910.03
CV1	*E22480B*	1.7%	18.1%	0.27	2.75	91.6%	0.71	0.71	0.0%	52.20
	E22490A	18.1%	**0.0%**	0.00	**N/D**	**N/D**	**N/D**			
	E22490B	1.5%	10.2%	0.15	2.09	87.4%	0.69	0.69	0.0%	50.49
	E22490C	10.2%	2.3%	0.64	1.51	85.6%	2.68	2.68	**0.0%**	101.47
	Min.	1.5%	1.5%	**0.00**		**0.0%**		0.00	**0.0%**	0.00
	Max.	18.1%	18.1%			**99.3%**		227.92	0.0%	3849.89
	Total			1424.82	161.30		659.74	639.18		
MIN $(\Delta T_{hl}/T_l)$		1.5%			ε_{max}	98.5%				

300-80K	1112.95	48.87	241.12
80-35K	201.63	49.12	239.08
35-4.5K	110.24	63.31	179.54

Sub-Coolers:

	w_{JT}	w_{BO}	p	T	$\Delta T_{hl,CE}$	x
	[g/s]	[g/s]	[atm]	[K]	[K]	[-]
SC-LN	66.5	57.2	1.099	78.13	2.00	13.9%
SC-He	38.7	33.4	1.222	4.44	0.10	13.5%

$\phi_{x,D}$	% $\Delta\phi_x$
[-]	[-]
11.6	0.0%
27.5	0.0%
72.0	0.0%
178.2	0.0%
35.8	0.0%
102.4	0.0%
18.1	0.0%

T2 Outlet ΔT: $(T_{lr,16} - T_{x2,o})$

[K]
0.000

(h) - (x) at TL=10: $\Delta T_{hx,10}$

[K]
13.000

T4 Outlet ΔT: $(T_{ll,22} - T_{x4,o})$

[K]
0.000

(h) - (l) at TL=31: $\Delta T_{hl,31}$

[K]
0.000

T6 Outlet ΔT: $(T_{ll,28} - T_{x6,o})$

[K]
0.000

T7 Bypass: $\xi_{h7,b}$

[-]
0.00%

Table G.4. Continued

Process Summary — *Non-Zero HX Dp - Same Load*

$\dot{m}_{h,0}$ = 233.80 [g/s] — *(h) Stream*; $\dot{m}_{u,8}$ = 233.80 [g/s] — *(u) Stream*

TL#	T [K]	p [atm]	h [J/g]	T [K]	p [atm]	h [J/g]	TL#
0	4.542	2.961	11.98	30.884	1.172	175.49	*0*
1				30.884	1.172	175.49	*1*
				2.5E-09		*2.3E-09*	
2				4.013	0.0266	35.97	*2*
3				4.013	0.0266	35.97	*3*
4				4.013	0.0266	35.97	*4*
5				3.608	0.0286	33.83	*5*
6	4.547	2.862	11.98	3.608	0.0286	33.83	*6*
	Downstream of HX			*3.1E-07*		*1.8E-07*	
7	2.197	0.197	3.17	1.997	0.0306	25.03	*7*
8	1.997	0.031	3.17	1.997	0.0306	25.03	*8*

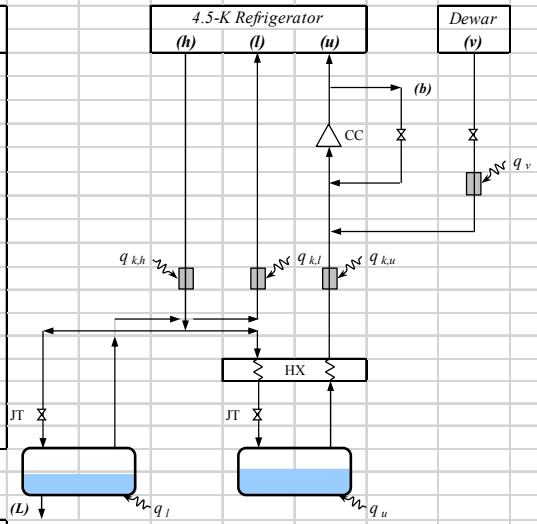

$\dot{m}_v$ = 0.00 [g/s] — *(v) Stream*; $\dot{m}_l$ = 0.00 [g/s] — *(l) Stream*

TL#	T [K]	p [atm]	h [J/g]	T [K]	p [atm]	h [J/g]	TL#
0	4.532	1.322	30.40	4.442	1.222	30.56	*0*
2	2.957	0.027	30.40	4.442	1.222	30.56	*8*
3	2.957	0.027	30.40				

(L) (Lead Flow)

$\dot{m}_L$	0.00 [g/s]	*Lead flow*	Δh_{lh}	18.584 [J/g]	*4.5-K load enthalpy flux*	
q_l	0 [W]	*4.5-K load*	Δh_{uh}	21.853 [J/g]	*2-K load enthalpy flux*	
q_u	5109 [W]	*2-K load*	$COP_{inv,2K}$	664.6 [W/W]	2-K inverse coefficient of performance	

	Transfer-Line			*Dewar*	*HX*			
	(h)	*(l)*	*(u)*	*(v)*	*(h)*	*(u)*		
Δp	0.10	0.000	0.0020	1.295	2.66	0.0020	[atm]	*Pressure drop*
q_k	0.0	0.0	500.0	0.0	0.0		[W]	*Heat in-leak*

Cold Compressors:

$\dot{m}_{CC}$ = 233.80 [g/s] — ξ_b = 0.0% [-]

Stage #	p [atm]	T [K]	h [J/g]	T_r [-]	p_r [-]	Q [ℓ/s]	η_s [-]	Dh_s [J/g]	W_{cc} [kW]	η_m [-]	$W_{cc,m}$ [kW]
5	1.172	30.884	175.49	1.505	2.131	126.6	70.0%	37.73	12.6030	95.0%	13.266
4	0.550	20.526	121.58	1.504	2.131	178.9	70.0%	25.01	8.3542	95.0%	8.794
3	0.258	13.645	85.85	1.504	2.131	252.8	70.0%	16.59	5.5415	95.0%	5.833
2	0.121	9.071	62.15	1.504	2.131	357.6	70.0%	11.01	3.6779	95.0%	3.872
1	0.057	6.032	46.42	1.503	2.131	506.0	70.0%	7.31	2.4426	95.0%	2.571
0	0.027	4.013	35.97			716.5					
Total		26.87	139.52	7.696	43.996		52.7%		32.619		34.336

Table G.5. Full cycle process model – same input, non-zero heat exchanger pressure drop

Design: Overview: Non-Zero HX Dp - Same Input Power

E.B. Violation	NO	X.B. Violation?	NO	M.B. Violation?	NO

Loads:

	w [g/s]	Supply p [atm]	Supply T [K]	Return p [atm]	Return T [K]	T_{sat} [K]	Δp [atm]	q [kW]	E_L [kW]	*Frac* E_L [-]
Shield	0.0	2.03	39.30	1.78	55.00		0.250	0.00	0.0	0.0%
4K Ref.	0.0	2.96	4.54	1.222	4.44	4.442		0.00	0.0	0.0%
4K Liq.	0.0	2.96	4.54	1.074	300.00				0.0	0.0%
S.A.	248.0	2.96	4.54	1.17	30.70			40.32	1130.8	100.0%

Total Load Carnot Work:	1130.8	[kW]
Total Carnot Efficiency:	31.96%	
Total Equiv. Input Power	3575	[kW]

Compressors:

	N_c [-]	w_c [g/s]	w_{byp} [g/s]	p_S [atm]	p_D [atm]	p_r [-]	T_S [K]	T_D [K]	η_v [-]	η_i [-]	P_m [kW]	$E_{c,iso}$ [kW]
1st Load	2	603.5	3.3	1.024	4.71	4.60	300.00	305.00	86.2%	50.1%	1214.0	574.3
1st Recycle	1	391.2	0.0	1.55	4.71	3.03	300.00	305.00	87.4%	55.1%	515.1	270.9
2nd Recycle	1	991.4	0.0	4.56	17.76	3.89	313.00	305.00	78.8%	52.6%	1672.5	843.8

Total Input Power:	3401.7	[kW]
Effective Compr. Sys. Eff.:	47.7%	

LN Pre-Cooling:

	w_{LN} [g/s]	Q [gph]	Supply p [atm]	Supply T [K]	Vent p [atm]	Vent T [K]	$\Delta T_{hN,1}$ [K]	q [kW]	E_c [kW]	η_{LN2} [-]	COP_{INV} [-]
	69.2	89.2	3.95	91.18	1.05	299.06	5.98	27.94	47.9	35.0%	4.90

Equiv. LN_2 P.C. Input Power:	136.9	[kW]
Availability to Coldbox	1623.5	[kW]
Cold Box Efficency:	69.6%	

Control Volumes:

	HP Stream (*h*) T [K]	HP p [atm]	HP w [g/s]	LR Stream (*lr*) T [K]	LR p [atm]	LR w [g/s]	LL Stream (*ll*) T [K]	LL p [atm]	LL w [g/s]	ΔT_{hl} [K]	$(\Delta T_{hl}/T_l)$ [-]	Σq_{LK} [W]
T.L. #												
1	305.03	17.27	991.4	298.76	1.60	391.2	298.76	1.07	600.2	6.274	2.10%	
CV5												445
5	80.13	16.89	991.4	78.94	1.72	391.2	78.94	1.11	600.2	1.184	1.50%	
CV4												590
16	39.91	16.79	957.0	39.30	1.79	391.2	39.30	1.16	600.2	0.609	1.55%	
CV3												175
22	15.26	16.78	600.2				14.89	1.19	352.2	0.372	2.50%	
CV2												165
28	6.16	16.78	293.2				6.05	1.22	45.2	0.109	1.80%	
CV1												295
38	4.54	2.96	248.0				4.44	1.22	0.0	0.100	2.25%	

Expanders:

#	w_x [g/s]	Δp_i [atm]	p_i [atm]	p_o [atm]	p_r [-]	T_i [K]	T_o [K]	T_r [-]	Δh_x [J/g]	η_x [-]	W_x [kW]	ϕ_x [-]
T1	34.4	0.15	16.64	5.82	2.86	78.17	55.46	1.41	121.11	85.0%	4.17	11.0
T2	34.4	0.00	5.82	2.03	2.86	55.46	39.30	1.41	84.83	85.0%	2.92	26.5
T3	356.8	0.15	16.64	5.47	3.04	31.14	21.56	1.44	50.37	85.0%	17.97	71.6
T4	356.8	0.00	5.47	1.80	3.04	21.56	14.89	1.45	33.90	85.0%	12.10	178.8
T5	307.0	0.15	16.63	4.51	3.69	15.19	9.66	1.57	24.36	85.0%	7.48	39.4
T6	307.0	0.00	4.51	1.22	3.69	9.66	6.05	1.60	14.58	85.0%	4.48	113.3
T7	293.2	0.15	16.63	2.96	5.62	5.92	5.015	1.18	8.26	82.0%	2.42	19.4

Total Expander Work:	51.53	[kW]

Table G.5. Continued.

Heat Exchangers:

		W.E.	*C.E.*				*(Calc.)*	*(Proj.)*		*Ref.*
		$(\Delta T_{hl}/T_l)$	$(\Delta T_{hl}/T_l)$	q_h	NTU	ε	(UA)	$(UA)_P$	% Δ(UA)	$(UA)_{ref}$
	HX #	[-]	[-]	[kW]	[-]	[-]	[kW/K]	[W/K]	[-]	[W/K]
CV5	*E22410*	2.1%	4.4%	1131.82	48.13	98.5%	244.71	237.58	**0.0%**	3915.04
	E22415	2.0%	5.5%	16.14	36.96	98.1%	2.68	2.68	0.0%	381.21
	E22420	5.5%	2.6%	11.79	0.76	53.2%	3.95	3.95	**0.0%**	62.87
CV4	*E22430*	1.5%	1.7%	10.65	1.68	63.6%	8.63	8.63	**0.0%**	137.51
	E22450A	1.7%	1.6%	33.63	5.59	85.7%	28.05	28.05	**0.0%**	451.71
	E22450AA	1.6%	1.6%	0.00	0.00	0.0%	0.00	0.00	0.0%	0.00
	E22450B	1.6%	1.5%	160.13	40.76	98.1%	207.14	207.14	**0.0%**	3335.29
	E22450BB	1.5%	1.6%	0.00	0.00	0.0%	0.00	0.00	0.0%	0.00
CV3	*E22460A*	1.6%	3.3%	45.24	11.64	93.7%	58.13	58.68	0.0%	954.85
	E22460AA	3.3%	4.1%	0.61	0.29	24.3%	0.55	0.00	0.0%	0.00
	E22460B_70.	4.1%	2.5%	56.15	30.80	97.8%	110.46	93.61	**0.0%**	2265.08
	E22470AA	2.5%	2.5%	**0.00**	0.00	**0.0%**	0.00	0.00	0.0%	0.00
CV2	*E22470B*	2.5%	3.1%	0.28	0.36	28.6%	0.68	0.68	0.0%	17.29
	E22470C_80.	3.1%	1.8%	16.98	16.62	**99.3%**	28.62	28.62	0.0%	897.74
CV1	*E22480B*	1.8%	19.4%	0.34	2.81	91.7%	0.83	0.83	0.0%	56.26
	E22490A	19.4%	**0.0%**	0.00	**N/D**	**N/D**	**N/D**			
	E22490B	1.5%	11.2%	0.20	2.22	88.6%	0.84	0.84	0.0%	56.62
	E22490C	11.2%	2.3%	0.74	1.61	86.6%	2.88	2.88	0.0%	105.47
	Min.	1.5%	1.5%	**0.00**		**0.0%**		0.00	**0.0%**	0.00
	Max.	19.4%	19.4%			**99.3%**		237.58	0.0%	3915.04
	Total			1484.71	163.25		698.15	674.18		
	MIN $(\Delta T_{hl}/T_l)$	1.5%			ε_{max}	98.5%				

300-80K	1159.75	48.88	251.33
80-35K	204.42	48.02	243.82
35-4.5K	120.54	66.34	203.00

Sub-Coolers:

	w_{JT}	w_{BO}	p	T	$\Delta T_{hl,CE}$	x
	[g/s]	[g/s]	[atm]	[K]	[K]	[-]
SC-LN	69.2	59.6	1.099	78.13	2.00	13.9%
SC-He	45.2	38.4	1.222	4.44	0.10	14.9%

$\phi_{x,D}$	% $\Delta\phi_x$
[-]	[-]
11.0	0.0%
26.5	0.0%
71.6	0.0%
178.8	0.0%
39.4	0.0%
113.3	0.0%
19.4	0.0%

T2 Outlet ΔT: $(T_{lr,16} - T_{x2,o})$

[K]
0.000

(h) - (x) at TL=10: $\Delta T_{hx,10}$

[K]
16.000

T4 Outlet ΔT: $(T_{ll,22} - T_{x4,o})$

[K]
0.000

(h) - (l) at TL=31: $\Delta T_{hl,31}$

[K]
0.000

T6 Outlet ΔT: $(T_{ll,28} - T_{x6,o})$

[K]
0.000

T7 Bypass: $\xi_{h7,b}$

[-]
0.00%

Table G.5. Continued.

Process Summary — *Non-Zero HX Dp - Same Input Power*

$\dot{m}_{h,0}$ = 248.00 [g/s] — *(h) Stream*; $\dot{m}_{u,8}$ = 248.00 [g/s] — *(u) Stream*

TL#	T [K]	p [atm]	h [J/g]	T [K]	p [atm]	h [J/g]	TL#
0	4.542	2.961	11.98	30.703	1.172	174.54	*0*
1				30.703	1.172	174.54	*1*
				4.4E-09		*4.1E-09*	
2				3.989	0.0266	35.85	*2*
3				3.989	0.0266	35.85	*3*
4				3.989	0.0266	35.85	*4*
5				3.608	0.0286	33.83	*5*
6	4.547	2.862	11.98	3.608	0.0286	33.83	*6*
	Downstream of HX			*3.1E-07*		*1.8E-07*	
7	2.197	0.197	3.17	1.997	0.0306	25.03	*7*
8	1.997	0.031	3.17	1.997	0.0306	25.03	*8*

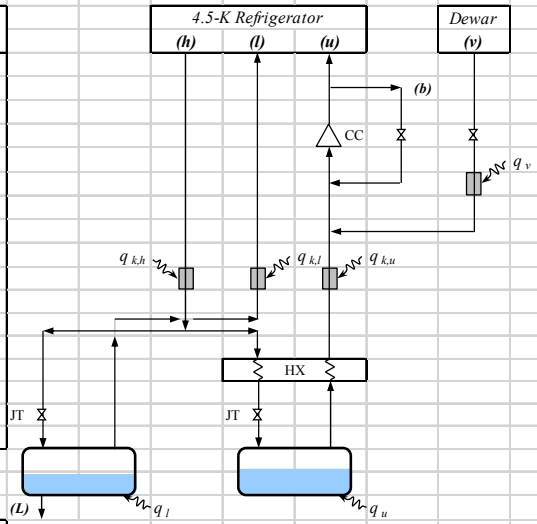

$\dot{m}_v$ = 0.00 [g/s] — *(v) Stream*; $\dot{m}_l$ = 0.00 [g/s] — *(l) Stream*

TL#	T [K]	p [atm]	h [J/g]	T [K]	p [atm]	h [J/g]	TL#
0	4.532	1.322	30.40	4.442	1.222	30.56	*0*
2	2.957	0.027	30.40	4.442	1.222	30.56	*8*
3	2.957	0.027	30.40				

(L) (Lead Flow)

$\dot{m}_L$	0.00 [g/s]	*Lead flow*	Δh_{lh}	18.584 [J/g]	*4.5-K load enthalpy flux*	
q_l	0 [W]	*4.5-K load*	Δh_{uh}	21.853 [J/g]	*2-K load enthalpy flux*	
q_u	5420 [W]	*2-K load*	$COP_{inv,2K}$	659.6 [W/W]	2-K inverse coefficient of performance	

	Transfer-Line			*Dewar*	*HX*			
	(h)	*(l)*	*(u)*	*(v)*	*(h)*	*(u)*		
Δp	0.10	0.000	0.0020	1.295	2.66	0.0020	[atm]	*Pressure drop*
q_k	0.0	0.0	500.0	0.0	0.0		[W]	*Heat in-leak*

Cold Compressors:

$\dot{m}_{CC}$ = 248.00 [g/s] — ξ_b = 0.0% [-]

Stage #	p [atm]	T [K]	h [J/g]	T_r [-]	p_r [-]	Q [ℓ/s]	η_s [-]	Dh_s [J/g]	W_{cc} [kW]	η_m [-]	$W_{cc,m}$ [kW]
5	1.172	30.703	174.54	1.505	2.131	133.5	70.0%	37.51	13.2895	95.0%	13.989
4	0.550	20.406	120.95	1.504	2.131	188.6	70.0%	24.86	8.8091	95.0%	9.273
3	0.258	13.565	85.43	1.504	2.131	266.6	70.0%	16.49	5.8432	95.0%	6.151
2	0.121	9.018	61.87	1.504	2.131	377.0	70.0%	10.95	3.8782	95.0%	4.082
1	0.057	5.997	46.23	1.503	2.131	533.6	70.0%	7.27	2.5756	95.0%	2.711
0	0.027	3.989	35.85			755.5					
Total		26.71	138.69	7.696	43.996		52.7%		34.396		36.206

APPENDIX H – HX_T1 VBA CODE LISTING

```
HX_Module - 1

Option Explicit
' P. Knudsen, (c) 2016

Const maxIter As Integer = 100              ' max. no. of iterations
Const NSD As Integer = 15                   ' no. signifigant digits
Const maxTol As Double = 5 * 10 ^ (-NSD)    ' max. iteration tolerance

Type HX_CC_Type
    Nh As Integer       ' # (h) streams
    Nl As Integer       ' # (l) streams; if Boiler is TRUE, this must be 1
    FID() As Integer    ' fluid ID #
    w() As Double       ' [g/s] stream mass flow rate
    p() As Double       ' [atm] stream pressure
    T() As Double       ' [K] (h) & (l) stream temperatures
    DT() As Double      ' [K] (h) & (l) stream temp. diff bet. sub-div. 'i-1' & 'i'
    DTh1() As Double    ' [K] (h) minus (l) stream temp. diff. at sub-div. 'i'
    x() As Double       ' [-] stream quality
    h() As Double       ' [J/g] stream enthalpy
    DH() As Double      ' (l) stream duty for sub-div. 'i'
    Dq() As Double      ' (h) stream duty for sub-div. 'i'
    EBF() As Double     ' energy balence fraction for each sub-div. 'i'
    DTLM() As Double    ' log mean temp. diff. for sub-div. 'i'
    CC() As Double      ' capacity rate
    CRs() As Double     ' element (Cl/Ch)
    Cmin() As Double    ' [W/K] minimum stream capacity rate
    theta() As Double   ' element (1-CRs)*(DUA)/C
    DUA() As Double     ' [W/K] (UA) for sub-div. 'i'
    DNtu() As Double    ' [-] Ntu for sub-div. 'i'
    q_tot As Double     ' [W] total duty
    UA_tot As Double    ' [W/K] total (UA)
    Ntu_tot As Double   ' [-] total Ntu's
    qLK As Double       ' [W] total leak heak
    DT_type As Boolean  ' TRUE - (h) stream constant enthalpy difference for each sub-div.;
                        ' FALSE - (h) stream constant enthalpy ratio for each sub-div.
                        ' Note: Dp_Type not used when DT_Type is used; i.e.,
                        '       when DT_Type is used, Dp_Type is automatically assumed.
    Dp_Type As Boolean  ' TRUE - constant Dp for each sub-div.;
                        ' FALSE - constant press. ratio for each sub-div.
    Boiler As Boolean   ' ? (l) stream a boiler (constant temperature)
    TPS() As Boolean    ' is the stream two-phase at sub-div. 'i'?
    MFE_tol As Double   ' max. allowed fractional error tolerance
End Type

Public Function HX_T1(ParamArray inpv() As Variant) As Double

'  This function calculates the inlet or outlet stream temperature of a two
'  or more stream HX.  If the result is 2-phase, the result is negative with
'  the integer part the stream number and the fractional part the quality.
'
'  Inputs:  FID1, FID2, etc. - fluid ID # for stream #1, #2, etc.
'           w1, w2, etc.     - [g/s] mass flow rate for stream #1, #2, etc.
'           p1, p2, etc.     - [atm] inlet/outlet pressure for stream #1, #2, etc.
'           DT12, DT13, etc. - [K] stream #1 minus stream #2 temperature, etc.
'           T_10             - [K] initial guess for stream #1 temperature
'           H0               - [W] HX duty + sum of enthalpies leaving/entering HX
'           Note: w1*h1 + w2*h2 + ... = H0, with h1(p1,T1), h2(p2,T2), etc.
'                 so, the objective function is,
'                 HT(T1) = 0 = -H0 + w1*h1 + w2*h2 + ...

    Const max_eps_ratio = 0.9

    Dim n As Integer          ' no. of input fluid streams; must be >= 2
    Dim m As Integer          ' used to det. if there are any unwanted extra arguments in 'inpv'
    Dim i As Integer          ' index
    Dim j As Integer          ' index
    Dim c As Integer          ' iteration counter
    Dim kv As Integer         ' stream number whose HTv < 0 and is closest to zero
    Dim kl As Integer         ' stream number whose HTl > 0 and is closest to zero
    Dim n_OK As Integer       ' # streams w/ acceptable inputs
    Dim FID() As Integer      ' fluid ID no. of stream 'i'
    Dim sgn_HTl As Integer     ' [-] sign of (HT + HTl)
```

```
HX_Module - 2

    Dim sgn_HTv As Integer    ' [-] sign of (HT + HTv)
    Dim sgn_HT As Integer
    Dim sgn_HT_old As Integer
    Dim sgn_HT_LB As Integer
    Dim sgn_HT_UB As Integer

    Dim w() As Double         ' [g/s] mass flow of stream 'i'
    Dim wT As Double          ' [g/s] total mass flow of 2-phase stream(s)
    Dim p() As Double         ' [atm] inlet/outlet pressure of stream 'i'
    Dim T() As Double         ' [K] temperature of unknown stream 'i'
    Dim Ti As Double          ' [K] stream 'i' temperature; used for single stream calc.
    Dim Ts() As Double        ' [K] saturation temperature
    Dim DT_1i() As Double     ' [K] stream #1 - stream 'i' temperature difference
    Dim T_10 As Double        ' [K] initial guess for stream #1 temperature
    Dim T1_old As Double
    Dim T1_LB As Double
    Dim T1_UB As Double
    Dim DT1 As Double         ' [K] difference between old and new T(1)
    Dim T_ll() As Double      ' [K] lower temperature limit of stream 'i'
    Dim DT_LL As Double       ' [K] difference between T_LL(i) and T(i)
    Dim DTLL_max As Double    ' [K] the maximum (most positive) DT_LL for all valid streams
    Dim hi As Double          ' [J/g] stream 'i' enthalpy; used for single stream calcuation
    Dim hl() As Double        ' [J/g] saturated liquid enthalpy of stream 'i'
    Dim hv() As Double        ' [J/g] saturated vapor enthalpy of stream 'i'
    Dim HT As Double          ' [W] HX energy balence (which should be = 0)
    Dim HT_old As Double
    Dim HT_LB As Double
    Dim HT_UB As Double
    Dim HTl As Double         ' [W] used to see if solution is in 2-phase
    Dim HTv As Double         ' [W] used to see if solution is in 2-phase
    Dim DHTl As Double        ' [W] = HT + HTl
    Dim DHTv As Double        ' [W] = HT + HTv
    Dim DHTl_min As Double    ' [W] the minimum DHTl
    Dim DHTv_min As Double    ' [W] the minimum DHTv
    Dim H0 As Double          ' [W] HX duty + sum of enthalpies leaving/entering HX
    Dim h_min As Double       ' [J/g] lowest allowable enthalpy; used for single stream calc.
    Dim DH_DT1 As Double      ' [W/K] gradient of H function w/ respect to T1
    Dim x As Double           ' [-] quality of two phase stream
    Dim eps As Double         ' fractional change in T1
    Dim eps_old As Double
    Dim R_eps As Double
    Dim ERN As Double

    Dim SF As Boolean         ' solution found?
    Dim EMI As Boolean        ' exceeded max. iterations?
    Dim inp_OK() As Boolean   ' inputs for stream #i OK?
    Dim IA As Boolean         ' input array?
    Dim soln_bound As Boolean
    Dim N_method As Boolean
    Dim converging As Boolean

    Dim break As Boolean
    Dim xx As Double

    ' Actual # input parameters is Ubound(inpv) + 1 [since inpv(0) is the 1st parameter
    ' value]. So, for 'N' fluid streams (whose temperature we need), there must be,
    ' 3*N + (N-1) + 2 = 4*N + 1, number of input parameters; i.e., Ubound(inpv) mod 4
    ' must be zero & N = Ubound(inpv)/4 must be >= 1 for there to be a valid number
    ' of input parameters.
    '
    ' When this function is called from another VBA procedure, 'inpv' is an array vs.
    ' when it is called from an Excel worksheet it is a series of parameters; e.g.,
    '
    '   'inpv' is an array (IA=True)    'inpv' is a list of params (IA=False)
    '   ----------------------------    -------------------------------------
    '   inpv(0)(0)      FID1            inpv(0)      FID1
    '   inpv(0)(1)      FID2            inpv(1)      FID2
    '   inpv(0)(N)      w1              inpv(N)      w1
    '   inpv(0)(N+1)    w2              inpv(N+1)    w2
    '   inpv(0)(2*N)    p1              inpv(2*N)    p1
    '   inpv(0)(2*N+1)  p2              inpv(2*N+1)  p2
```

```
HX_Module - 3

    '   inpv(0)(3*N)    DT12            inpv(3*N)    DT12
    '   inpv(0)(4*N-1)  T_10            inpv(4*N-1)  T_10
    '   inpv(0)(4*N)    H0              inpv(4*N)    H0

    n = UBound(inpv) / 4
    m = UBound(inpv) Mod 4
    IA = False  ' assume not an input array (as if called from a worksheet)
    If (n = 0) Then
        n = UBound(inpv(0)) / 4
        m = UBound(inpv(0)) Mod 4
        IA = True  ' could be an input array from another function
    End If

    If ((n < 1) Or (m <> 0)) Then
        ERN = -0.1  ' missing no. req'd inputs
        GoTo errLbl
    End If

    ReDim FID(1 To n) As Integer
    ReDim w(1 To n) As Double
    ReDim p(1 To n) As Double
    ReDim T(1 To n) As Double
    ReDim Ts(1 To n) As Double
    ReDim DT_1i(1 To n) As Double
    ReDim T_ll(1 To n) As Double
    ReDim hl(1 To n) As Double
    ReDim hv(1 To n) As Double
    ReDim inp_OK(1 To n) As Boolean

    ' obtain input from parameter array
    DT_1i(1) = 0#
    For i = 1 To n
        If IA Then
            FID(i) = CInt(inpv(0)(i - 1))
            w(i) = CDbl(inpv(0)(n + i - 1))
            p(i) = CDbl(inpv(0)(2 * n + i - 1))
            ' Note: DT_1i(1) is not used and S/B zero.
            If ((n <> 1) And (i <> n)) Then
                DT_1i(i + 1) = CDbl(inpv(0)(3 * n + i - 1))
            End If
        Else
            FID(i) = CInt(inpv(i - 1))
            w(i) = CDbl(inpv(n + i - 1))
            p(i) = CDbl(inpv(2 * n + i - 1))
            ' Note: DT_1i(1) is not used and S/B zero.
            If ((n <> 1) And (i <> n)) Then
                DT_1i(i + 1) = CDbl(inpv(3 * n + i - 1))
            End If
        End If
    Next i
    If IA Then
        T_10 = CDbl(inpv(0)(4 * n - 1))
        H0 = CDbl(inpv(0)(4 * n))
    Else
        T_10 = CDbl(inpv(4 * n - 1))
        H0 = CDbl(inpv(4 * n))
    End If

    ' Establish for each stream whether the input is valid; and if so, the
    ' lower temperature limit.  Not all streams are required to have valid input.
    For i = 1 To n
        inp_OK(i) = ((FID(i) >= 1) And (FID(i) <= 38) And (p(i) > 0#) And (Abs(w(i)) > maxTol))
        If inp_OK(i) Then T_ll(i) = T_L_limit(FID(i))
    Next i

    ' at least one of the streams must be 'OK' to continue
    n_OK = 0
    For i = 1 To n
        If inp_OK(i) Then n_OK = n_OK + 1
    Next i
```

```
HX_Module - 4

    If (n_OK = 0) Then
        ERN = -0.2  ' must have at least one valid stream
        GoTo errLbl
    End If

    ' If there is only one stream w/ valid inputs, then no iteration is
    ' required for the solution.  Find which single stream is valid first.
    'If (n_OK = 1) Then
    '    For j = 1 To N
    '        If inp_OK(j) Then i = j
    '    Next j

    '    hi = H0 / w(i)
    '    h_min = (h_pT(FID(i), p(i), T_LL(i)))
    '    If (hi > h_min) Then
    '        Ti = T_ph(FID(i), p(i), hi)
    '        T(1) = Ti + DT_1i(i)
    '    Else
    '        T(1) = T_LL(i)
    '    End If
    '    HX_T1 = T(1)
    '    Exit Function
    'End If

    ' If there is more than one stream w/ valid inputs, then iteration is req'd
    ' Note that it does not matter if stream #1 does not have valid input.  Its
    ' temperature is simply used as the reference for all the other (valid stream)
    ' temperatures.
    T(1) = T_10  ' the initial guess for stream #1

    ' Check initial guess to see that it does not result in one of the other
    ' stream temperatures being below its lower limit.  If it does, then find
    ' which stream is the furthest below its lower limit; set it to its lower
    ' limit, and adjust the other (valid) stream temperatures accordingly.
    DTLL_max = 0#
    j = 0
    For i = 2 To n
        If inp_OK(i) Then
            T(i) = T(1) - DT_1i(i)
            DT_LL = T_ll(i) - T(i)
            If (DT_LL > DTLL_max) Then
                DTLL_max = DT_LL
                j = i
            End If
        End If
    Next i

    If (j <> 0) Then
        T(j) = T_ll(j)
        T(1) = T(j) + DT_1i(j)
        For i = 2 To n
            If ((i <> j) And inp_OK(i)) Then T(i) = T(1) - DT_1i(i)
        Next i
    End If

    ' calculate saturation temperature and enthalpies for streams whose pressure
    ' is less than critical.
    For i = 1 To n
        If inp_OK(i) Then
            If (p(i) < (0.9995 * p_crit(FID(i)))) Then
                Ts(i) = Tsat_p(FID(i), p(i))
                hl(i) = hl_p(FID(i), p(i))
                hv(i) = hv_p(FID(i), p(i))
            End If
        End If
    Next i

    ' To visualize what this section is doing, the plot of temperature [T(1)] vs.
    ' the objective function (HT, or HTV & HTl in this section) has a positive
    ' slope, except at phase transitions where it is discontinous (i.e., takes a
    ' vertical jump).  If the lower temperature limit and/or initial guess are not
```

HX_Module - 5

```
    ' chosen close to the solution (HT=0, or HTv, HTl = 0 in this section), Newton's
    ' method may not converge; especially depending on the derivative of the slope
    ' (i.e., the curvature).  The purpose this section is to see if the solution is
    ' in the 2-phase region, or to modify the lower temperature limit and/or initial
    ' temperature (solution) guess to as to avoid Newton's method from 'bouncing
    ' back and forth' across one or more 2-phase (vertical jumps) transitions.

    kv = 0  ' if this stays zero, then the temperature lower limit stays the same
    kl = 0  ' if this stays zero, then the initial guess stays the same
    For j = 1 To n
        If (inp_OK(j) And (Ts(j) > 0#)) Then
            HT = -H0
            HTv = 0#
            HTl = 0#
            For i = 1 To n
                If inp_OK(i) Then
                    ' Note: if eps < maxTol then stream 'i' saturation
                    ' temperature is essentially the same as stream 'j'
                    eps = Abs(1# - Ts(i) / Ts(j))
                    If ((i = j) Or (eps < maxTol)) Then
                        HTv = HTv + w(i) * hv(i)
                        HTl = HTl + w(i) * hl(i)
                    Else
                        HT = HT + w(i) * h_pT(FID(i), p(i), Ts(j))
                    End If
                End If
            Next i

            DHTv = HT + HTv
            DHTl = HT + HTl
            sgn_HTv = Sgn(DHTv)
            sgn_HTl = Sgn(DHTl)
            If ((sgn_HTv <> sgn_HTl) Or (sgn_HTv = 0) Or (sgn_HTl = 0)) Then
                ' solution is in the 2-phase region
                ' and can be found without iteration
                x = -DHTl / (HTv - HTl)
                ' this if...then should not be necessary; it is for checking
                If ((x >= 0#) And (x <= 1#)) Then
                    ' returned result:
                    ' integer part - stream number
                    ' fractional part - quality
                    HX_T1 = -(CDbl(j) + x)
                Else
                    ERN = -0.3  ' why did this happen?  soln S/B two-phase...
                    GoTo errLbl
                End If
                GoTo exitLbl
            End If

            ' Look to see if HTv is negative and close to zero (i.e., the solution).
            ' Will use the saturated vapor temperature as temperature lower limit
            ' instead, if found.
            If (sgn_HTv < 0) Then
                DHTv = -DHTv
                If (j = 1) Then
                    kv = 1
                    DHTv_min = DHTv
                End If
                If (j <> 1) Then
                    If (DHTv < DHTv_min) Then
                        kv = j
                        DHTv_min = DHTv
                    End If
                End If
            End If

            ' Look to see of HTl is positive and close to zero (i.e., the solution).
            ' Will use the saturated liquid temperature as the initial guess, if found.
            If (sgn_HTl > 0) Then
                If (j = 1) Then
                    kl = 1
```

HX_Module - 6

```
                    DHT1_min = DHT1
                End If
                If (j <> 1) Then
                    If (DHT1 < DHT1_min) Then
                        k1 = j
                        DHT1_min = DHT1
                    End If
                End If
            End If

        End If
    Next j

    ' Check to see if the lower temperature limits should be adjusted.
    If (kv <> 0) Then
        For i = 1 To n
            T_l1(i) = Ts(kv)
        Next i
    End If

    ' Check to see of the initial temperature guess should be adjusted.
    If (k1 <> 0) Then
        T(1) = Ts(k1) - maxTol
        For i = 2 To n
            If inp_OK(i) Then T(i) = T(1) - DT_1i(i)
        Next i
    End If

    ' iterate to determine T(1)
    c = 0
    T1_old = T(1)
    eps_old = 1#
    N_method = True  ' initially use Newton's method
    Do
        If (N_method And (c <> 0)) Then
            HT_old = HT
            sgn_HT_old = sgn_HT
        End If

        HT = -H0
        If N_method Then DH_DT1 = 0#
        For i = 1 To n
            If inp_OK(i) Then
                HT = HT + w(i) * h_pT(FID(i), p(i), T(i))
                If N_method Then DH_DT1 = DH_DT1 + w(i) * Cp_pT(FID(i), p(i), T(i))
            End If
        Next i

        sgn_HT = Sgn(HT)

        If (N_method And (c <> 0)) Then
            soln_bound = (sgn_HT * sgn_HT_old = -1)  ' has solution been bounded?
        Else
            soln_bound = True  ' i.e., not defined yet
        End If

        If (N_method And (c >= 2)) Then
            converging = (Abs(HT) < Abs(HT_old))
            If (c >= 10) Then converging = converging And (R_eps < max_eps_ratio)
        Else
            converging = True  ' i.e., not defined yet
        End If

        If N_method Then
            If ((c >= 3) And Not (converging)) Then
                If soln_bound Then
                    N_method = False
                    If (sgn_HT = 1) Then
                        T1_LB = T1_old
                        HT_LB = HT_old
                        sgn_HT_LB = sgn_HT_old
```

HX_Module - 7

```
                    Else
                        T1_UB = T1_old
                        HT_UB = HT_old
                        sgn_HT_UB = sgn_HT_old
                    End If
                Else
                    ERN = -0.4  ' solution is not converging & cannot bracket it
                    GoTo errLbl
                End If
            End If
        End If

        If N_method Then  ' Newton's method
            DT1 = -HT / DH_DT1
            T1_old = T(1)
            T(1) = T1_old + DT1
        Else  ' bi-section method
            ' determine whether T(1) is a new lower or upper bound
            If (sgn_HT = 1) Then
                T1_UB = T(1)
                HT_UB = HT
                sgn_HT_UB = sgn_HT
            End If
            If (sgn_HT = -1) Then
                T1_LB = T(1)
                HT_LB = HT
                sgn_HT_LB = sgn_HT
            End If

            T(1) = 0.5 * (T1_UB + T1_LB)  ' compute new value
            DT1 = T(1) - T1_LB
            If (DT1 < 0#) Then
                ERN = -0.5  ' why did this happen?
                GoTo errLbl
            End If
        End If

        For i = 2 To n
            If inp_OK(i) Then T(i) = T(1) - DT_1i(i)
        Next i

        ' Check to see if the updated value of T(1) puts any of the valid
        ' stream temperatures below their lower limit.
        ' Note: It is only necessary to be concerned about one of the
        ' valid stream temperature going below their lower bound
        ' if using Newton's method.
        j = 0
        DTLL_max = 0#
        If N_method Then
            For i = 1 To n
                If inp_OK(i) Then
                    DT_LL = T_ll(i) - T(i)
                    If (DT_LL > DTLL_max) Then  ' look for stream furthest below LL
                        DTLL_max = DT_LL
                        j = i
                    End If
                End If
            Next i

            If (j <> 0) Then
                ' adjust the stream who is the furthest below its lower limit
                ' to a value equal to the average between its lower limit
                ' and its previous value.
                T(j) = 0.5 * (T_ll(j) + (T1_old - DT_1i(j)))
                T(1) = T(j) + DT_1i(j)
                For i = 2 To n
                    If ((i <> j) And inp_OK(i)) Then T(i) = T(1) - DT_1i(i)
                Next i
            End If
        End If
```

```
HX_Module - 8

        If (N_method And (j <> 0)) Then DT1 = T(1) - T1_old

        If (c <> 0) Then eps_old = eps
        eps = DT1 / T(1)
        SF = (Abs(eps) < maxTol) Or (HT = 0#)
        R_eps = Abs(eps / eps_old)
        c = c + 1
        EMI = (c >= maxIter)
    Loop Until (SF Or EMI)

    If SF Then
        HX_T1 = T(1)
    Else
        ERN = -0.6  ' exceeded max. no. iterations w/ no soln. found
        GoTo errLbl
    End If
    GoTo exitLbl

errLbl:
    HX_T1 = ERN

exitLbl:
End Function
```

APPENDIX I – HX_ANAL VBA CODE LISTING

```
HX_Analysis - 1

Option Explicit
' P. Knudsen, (c) 2016

Const maxIter As Integer = 100            ' max. no. of iterations
Const NSD As Integer = 12                 ' no. signifigant digits
Const maxTol As Double = 5 * 10 ^ (-NSD)  ' max. iteration tolerance

Const h As Integer = 1                    ' (h) stream index
Const l As Integer = 2                    ' (l) stream index

Const FID_min As Integer = 1              ' lowest FID #
Const FID_max As Integer = 33             ' highest FID #


Public Function HX_Anal(rr As Integer, n As Integer, n_h As Integer, n_l As Integer, _
                        Th_0 As Double, Tl_N As Double, DThl_0 As Double, DThl_N As Double, _
                        qLK As Double, DT_type As Boolean, Boiler As Boolean, _
                        MFE_tol As Double, ParamArray HX_arg() As Variant) As Variant

'   The fundamental assumption in this function is that the heat exchanger is a two TEMPERATURE
'   stream HX.  That is, there may be more than two streams, but all the (h) streams are at the same
'   temperature, and likewise the (l) streams.  There can be only one (h) stream if it is two-phase
'   at any point, and likewise for the (l) stream.  This requirement is implicit for a two temperature
'   stream HX.
'   There are four possible configurations (note that the (h) stream mass flow is allways +),
'   (1) counter flow:  + (h) stream and + (l) stream mass flow, either DThl_0 or DThl_N may be specified
'                      If the optional outlet quality 'x_e' is input, then
'                          if DThl_0 > 0, it is the (l) stream outlet quality
'                          if DThl_N > 0, it is the (h) stream outlet quality
'                      Note: for this configuration the (h) stream is being cooled; (l) stream is being warmed
'
'   Note: Counter flow with - (h) stream and - (l) stream mass flow is redundant to configuration (1), and is
'         not considered a proper input.  If this is the case, user should reverse the (h) and (l) stream inputs.
'
'   (2) parallel flow: + (h) stream and - (l) stream mass flow, either DThl_0 or DThl_N may be specified
'                      Note: 'Tl_N' is not the (l) stream inlet temperature; it is the outlet temperature.
'                      If the optional outlet quality 'x_e' is input, then
'                          if DThl_0 > 0, it is the (l) stream outlet quality (at T(l, N) not T(l, 0))
'                          if DThl_N > 0, it is the (h) stream outlet quality
'                      Note: (h) stream is being cooled; (l) stream is being warmed
'
'   Note: Parallel flow with (-) (h) stream and (+) (l) stream flow is redundant to configuration (2), and is
'         not consdiered a proper input.  If this is the case, user should switch the 'warm-end' and 'cold-end' i
nputs.
'
'   (3) Constant (l) stream temperature cooling (h) stream:
'                      (l) stream is a constant temperature 'boiler'; 'boiler' input = TRUE
'                      + (h) stream mass flow, Tl_0 = Tl_N (constant), DThl_N must be specified
'                      If the optional outlet quality 'x_e' is input, even though DThl_N will not be used (since
'                      both cannot be specified) it must be input and > 0 (and DThl_0 < 0).
'                      Note: the 'boiler' option does not require property evaluation of the (l) stream
'                            (so the FID is not checked, the flow is set to zero, the inlet pressure value does
'                            not matter and the pressure drop is set to zero).
'
'   (4) Constant (h) stream temperature heating (l) stream:
'                      (h) stream is a constant temperature 'condenser'; 'boiler' input = TRUE
'                      + (l) stream mass flow, Th_0 = Th_N (constant), DThl_0 must be specified
'                      If the optional outlet quality is input, even though DThl_0 will not be used (since
'                      both cannot be specified) it must be input and > 0 (and DThl_N < 0).
'                      Note: the 'boiler' option does not require property evaluation of the (h) stream
'                            (so the FID is not checked, the flow is zet to zero, the inlet pressure value does
'                            not matter and the pressure drop is set to zero).
'
'   Additional notes:
'   (a) Configurations (3) and (4) are both designated as a 'boiler'.
'   (b) Depending on the configuration, specify either DThl_0 or DThl_N as > 0 and the other < 0, so that it is
'       clear which configuration is intended.
'   (c) The 'warm-end' is at sub-division 0 and the 'cold-end' is at sub-division N.
'
'   Inputs:
'
'                                  Variable    Description
'   ---------------------------------------------------------------------------------------------
'                   RR          RESERVED
'                   N           # HX sub-divisions (for integration)
'                   Nh          # (h) streams; streams i = 1 to Nh
'                   Nl          # (l) streams; streams i = (Nh+1) to (Nh+Nl)
'                   Th_0        [K] 'warm-end' temperature for (h) stream(s)
'                   Tl_N        [K] 'cold-end' temperature for (l) stream(s)
'                   DThl_0      [K] 'warm end' (h) to (l) stream temp. diff.
'                   DThl_N      [K] 'cold end' (h) to (l) stream temp. diff.
```

HX_Analysis - 2

```
'                   qLK         [W] total heat leak
'                   DT_Type     type of HX DT; i.e., TRUE - normal DT, FALSE - temp. ratio
'                   Boiler      either (h) or (l) stream is a constant temperature stream
'                   MFE_tol     [-] max. fractional error for temp. field or sub-div. energy balence
'
'   j for HX_arg(j) Variable    Description
'   ---------------------------------------------------------------------------------------------
'   (k-1)           FID(i)      stream 'i' fluid ID no.
'   (k+Ns-1)        w(i)        [g/s] mass flow rate for stream 'i'
'   (k+2*Ns-1)      p(i)        [atm] inlet pressure for stream 'i';
'                               indicates (negative of) inlet quality if between 0 and -1
'   (k+3*Ns-1)      Dph(i)      [atm] (h) stream total pressure drop
'   (k+3*Ns+Nh-1)   Dpl(i)      [atm] (l) stream total pressure drop
'   (k+4*Ns)        x_e         [-] optional - outlet quality
'
'   Note:   k = 1 to Ns, with Ns = Nh + Nl
'           k = 1 to Nh, are the (h) streams
'           k = (Nh+1) to Ns, are the (l) streams
'           There should be at least a total of 0..(4*Ns-1) arguments in HX_arg().
'
'           If the inlet is two-phase, p(i) is a negative number between 0 and -1 (inclusive).
'           This is taken as the negative of the inlet quality.
'           Note that for parallel flow, this is the pressure for the (l) stream at i=0, not i=N
'
'           x_e is the quality of the applicable outlet stream; it may be 0 to 1.
'
'           Convention for quality, given (p, h):
'             x =  3; (p >= pc) and (T >= Tc), where T = T_ph(p,h)
'             x = -1; (p >= pc) and (T <  Tc), where T = T_ph(p,h)
'             x = {h - hl(T)}/{hv(T) - hl(T)}; otherwise, where T = Tsat(p)

    Dim HX As HX_CC_Type

    Dim wh_T As Double          ' [g/s] sum of (h) stream mass flow rates
    Dim wl_T As Double          ' [g/s] sum of (l) stream mass flow rates
    Dim p_I As Double           ' [atm] stream inlet pressure
    Dim Dp As Double            ' [atm] stream pressure drop
    Dim x_e As Double           ' [-] outlet quality

    Dim Narg As Integer         ' no. input array arguments
    Dim ERN As Integer          ' error #
    Dim Ns As Integer           ' no. of streams
    Dim k As Integer            ' stream index no.
    Dim sign_wh As Integer      ' sign of (h) stream
    Dim sign_wl As Integer      ' sign of (0) stream
    Dim sign_wh0 As Integer     ' sign of first (h) stream
    Dim sign_wl0 As Integer     ' sign of first (l) stream

    Dim h_boiler As Boolean     ' (h) stream is condensing at const. temp. Th_0
    Dim l_boiler As Boolean     ' (l) stream is boiling at const. temp. Tl_0
    Dim xe_given As Boolean     ' has the optional argument for an outlet quality been given?
    Dim TP_h As Boolean         ' one (h) stream is two-phase at the inlet (this is not used if h_boiler is TRUE)
    Dim TP_l As Boolean         ' one (l) stream is two-phase at the inlet (this is not used if l_boiler is TRUE)

    Dim start_time As Single    ' calculation start time
    Dim stop_time As Single     ' calculation stop time
    Dim calc_time As Single     ' = stop_time - start_time


    ' The basic goal 'HX_Anal' is to check the input, and extract it to set-up the 'HX' variable; this
    ' includes everything at the warm-end and cold-end except for the enthalpies, unspecified qualities,
    ' and the unknown outlet temperature.  The 'HX_UA_NTU' routine will handle the rest.

    start_time = Timer
    If (n < 1) Then
        ERN = 1
        GoTo errLbl
    End If

    ' reserve HX_arg(0)
    Narg = UBound(HX_arg)

    With HX
        .Nh = n_h
        .Nl = n_l
        If ((.Nh < 1) Or (.Nl < 1)) Then
            ERN = 2  ' must have at least one (h) and one (l) stream
            GoTo errLbl
        End If

        Ns = .Nh + .Nl
```

```
HX_Analysis - 3

        If (Narg < (4 * Ns - 1)) Then
            ERN = 3  ' insuffient number of arguments
            GoTo errLbl
        End If
        ReDim .FID(1 To Ns) As Integer
        ReDim .w(1 To Ns) As Double
        ReDim .p(1 To Ns, 0 To n) As Double
        ReDim .T(1 To 2, 0 To n) As Double
        ReDim .DT(1 To 2, 1 To n) As Double
        ReDim .x(1 To Ns, 0 To n) As Double
        ReDim .h(1 To Ns, 0 To n) As Double
        ReDim .DH(1 To n) As Double
        ReDim .EBF(1 To n) As Double
        ReDim .DThl(0 To n) As Double
        ReDim .DTLM(1 To n) As Double
        ReDim .Cmin(1 To n) As Double
        ReDim .Dq(1 To n) As Double
        ReDim .DUA(1 To n) As Double
        ReDim .DNtu(1 To n) As Double
        ReDim .TPS(1 To Ns, 0 To n) As Boolean
    End With

    With HX
        If (Th_0 < Tl_N) Then
            ' (h) warm-end temperature must be > (l) stream cold-end temperature
            ' otherwise the meaning of the sign for DThl_0 or DThl_N becomes more difficult
            ERN = 4
            GoTo errLbl
        End If

        If (((DThl_0 <= 0#) And (DThl_N <= 0#)) Or ((DThl_0 > 0#) And (DThl_N > 0#))) Then
            ERN = 5  ' both stream temperature differences cannot be <= 0 or > 0
            GoTo errLbl
        End If

        If (qLK < 0#) Then qLK = 0#

        ' Note: If (Boiler = TRUE) and (DThl_0 > 0) then (h) stream is condensing at const. temp. Th_0
        '       If (Boiler = TRUE) and (DThl_N > 0) then (l) stream is boiling at const. temp. Tl_0
        h_boiler = (Boiler And (DThl_0 > 0#))  ' DThl_0 is the 'pinch' point for a 'h_boiler'
        l_boiler = (Boiler And (DThl_N > 0#))  ' DThl_N is the 'pinch' point for a 'l_boiler'
        If ((h_boiler And (.Nh > 1)) Or (l_boiler And (.Nl > 1))) Then
            ERN = 6 ' If Boiler=TRUE can only have one constant temperture stream
            GoTo errLbl
        End If

        x_e = 3#  ' will set exit quality in 'HX_UA_NTU' routine
        xe_given = (Narg = (4 * Ns))
        If xe_given Then x_e = CDbl(HX_arg(4 * Ns))
        If ((x_e < 0#) Or (x_e > 1#)) Then
            xe_given = False  ' disregard x_e provided
            x_e = 3#  ' will set exit quality in 'HX_UA_NTU' routine
        End If

        .T(h, 0) = Th_0
        .T(l, n) = Tl_N
        .DThl(0) = DThl_0
        .DThl(n) = DThl_N
        .qLK = qLK
        .DT_type = DT_type
        .Boiler = Boiler

        wh_T = 0#
        wl_T = 0#
        TP_h = False
        TP_l = False
        For k = 1 To Ns
            .FID(k) = CInt(HX_arg(k - 1))  ' the 'boiler' stream does not need a valid FID
            .w(k) = CDbl(HX_arg(k + Ns - 1))
            p_i = CDbl(HX_arg(k + 2 * Ns - 1))
            Dp = CDbl(HX_arg(k + 3 * Ns - 1))

            ' Check that, (a) the sum of the mass flow for the (h) or (l) temperature streams is not zero,
            ' (b) the mass flow for the (h) stream is not < 0 and,
            ' (c) the signs of the (l) streams do not change.
            If (k = 1) Then sign_wh0 = Sgn(.w(k))
            If (k = (.Nh + 1)) Then sign_wl0 = Sgn(.w(k))
            If (k > .Nh) Then
                sign_wl = Sgn(.w(k))
                If ((sign_wl = sign_wl0) Or (sign_wl = 0)) Then
                    wl_T = wl_T + .w(k)
```

```
HX_Analysis - 4

                Else  ' (sign_wl <> sign_wl0) and (sign_wl <> 0)
                    ERN = 7  ' all the signs for the mass flow must be the same or zero (but not all zero)
                    GoTo errLbl
                End If
            Else
                sign_wh = Sgn(.w(k))
                If (sign_wh < 0) Then
                    ERN = 8 ' a negative mass flow for the (h) stream is not a valid input
                    GoTo errLbl
                End If
                wh_T = wh_T + .w(k)
            End If

            If ((h_boiler And (k <= .Nh)) Or (l_boiler And (k > .Nh))) Then
                ' boiler stream does not need to have a valid FID, mass flow rate, inlet pressure,
                ' quality or pressure drop
                .w(k) = 0#
                Dp = 0#
                ' if a boiler, even though this is not used, make it positive to prevent confusion
                If (p_i <= 0#) Then p_i = maxTol
                ' If a valid FID is given for the boiler stream and the the temperature is between the
                ' lower limit and critical pressure, make the pressure equal to the saturation pressure
                If ((.FID(k) >= FID_min) And (.FID(k) <= FID_max)) Then
                    If ((k <= .Nh) And (.T(h, 0) <= T_crit(.FID(k))) And _
                        (.T(h, 0) > T_L_limit(.FID(k)))) Then p_i = psat_T(.FID(k), .T(h, 0))

                    If ((k > .Nh) And (.T(l, n) <= T_crit(.FID(k))) And _
                        (.T(l, n) > T_L_limit(.FID(k)))) Then p_i = psat_T(.FID(k), .T(l, n))
                End If

                .p(k, 0) = p_i
                .p(k, n) = p_i
            Else  ' not a boiler stream
                If ((.FID(k) < FID_min) Or (.FID(k) > FID_max)) Then
                    ERN = 9  ' fluid ID number is not valid
                    GoTo errLbl
                End If

                If (k > .Nh) Then
                    If ((.T(l, n) < T_L_limit(.FID(k))) Or (.T(l, n) > T_U_limit(.FID(k)))) Then
                        ERN = 10 ' cold-end (l) stream temperature is not within temperature bounds for fluid
                        GoTo errLbl
                    End If
                Else
                    If ((.T(h, 0) < T_L_limit(.FID(k))) Or (.T(h, 0) > T_U_limit(.FID(k)))) Then
                        ERN = 11  ' warm-end (h) stream temperature is not within temperature bounds for fluid
                        GoTo errLbl
                    End If
                End If

                If (p_i < -1#) Then
                    ERN = 12  ' pressure cannot be < -1
                    GoTo errLbl
                End If

                If (Dp < 0#) Then
                    ERN = 13  ' pressure drop cannot be < 0
                    GoTo errLbl
                End If

                If ((p_i >= -1#) And (p_i <= 0#)) Then
                    If (k <= .Nh) Then  ' (h) stream
                        If TP_h Then
                            ERN = 14  ' there can be only one two-phase (h) stream
                            GoTo errLbl
                        Else
                            TP_h = True  ' (h) stream is two-phase at the inlet
                        End If

                        If (.T(h, 0) > T_crit(.FID(k))) Then
                            ERN = 15 ' (h) stream inlet designated as two-phase at the inlet, but temperature is
above critical
                            GoTo errLbl
                        End If

                        .x(k, 0) = -p_i
                        .p(k, 0) = psat_T(.FID(k), .T(h, 0))
                    Else  ' (k > .Nh) i.e., (l) stream
                        If TP_l Then
                            ERN = 18  ' there can be only one two-phase (l) stream
                            GoTo errLbl
```

HX_Analysis - 5

```
                        Else
                            TP_l = True  ' (l) stream is two-phase at the inlet
                        End If

                        If (sign_wl >= 0) Then
                            If (.T(l, n) > T_crit(.FID(k))) Then
                                ERN = 19 ' (l) stream inlet designated as two-phase at the inlet, but temperature
 is above critical
                                GoTo errLbl
                            End If

                            .x(k, n) = -p_i
                            .p(k, n) = psat_T(.FID(k), .T(l, n))
                        Else  ' negative (l) stream mass flow -> parallel flow
                            If (.T(l, 0) > T_crit(.FID(k))) Then
                                ERN = 22 ' (l) stream inlet designated as two-phase at the inlet, but temperature
 is above critical
                                GoTo errLbl
                            End If

                            .x(k, 0) = -p_i
                            .p(k, 0) = psat_T(.FID(k), .T(l, 0))
                        End If
                    End If  ' (k > .Nh) i.e., (l) stream
                Else  ' inlet is not specified as two-phase
                    If (k <= .Nh) Then  ' (h) stream
                        .p(k, 0) = p_i
                        .x(k, 0) = 3#
                    Else  ' (l) stream
                        If (sign_wl >= 0) Then
                            .p(k, n) = p_i
                            .x(k, n) = 3#
                        Else  ' negative (l) stream mass flow -> parallel flow
                            .p(k, 0) = p_i
                            .x(k, 0) = 3#
                        End If
                    End If  ' (l) stream
                End If  ' inlet is not specified as two-phase

                If (k <= .Nh) Then  ' check if outlet quality is specified for (h) stream
                    .p(k, n) = .p(k, 0) - Dp
                    If (.DThl(n) > 0#) Then
                        If xe_given Then  ' (h) stream outlet is specified as being two-phase
                            If (.Nh > 1) Then
                                ERN = 25  ' there can only be one two-phase (h) stream
                                GoTo errLbl
                            End If

                            If ((.p(k, n) > p_crit(.FID(k))) Or (.p(k, n) < p_L_limit(.FID(k)))) Then
                                ERN = 26  ' two-phase outlet pressure is greater then critical pressure or less t
han lower limit
                                GoTo errLbl
                            Else
                                .x(k, n) = x_e
                                .DThl(n) = Tsat_p(.FID(k), .p(k, n)) - .T(l, n)
                                If (.DThl(n) <= 0#) Then
                                    ERN = 27 ' cold-end stream temperature difference is <= 0
                                    GoTo errLbl
                                End If
                            End If
                        Else
                            .x(k, n) = x_e  ' set to default value
                        End If  ' xe_given
                    End If  ' (h) stream and cold end DT is specified
                Else  ' check if outlet quality is specified for (l) stream
                    If (sign_wl >= 0) Then
                        .p(k, 0) = .p(k, n) - Dp
                        If (.DThl(0) > 0#) Then
                            If xe_given Then  ' (l) stream outlet is specified as being two-phase
                                If (.Nl > 1) Then
                                    ERN = 28  ' there can only be one two-phase (l) stream
                                    GoTo errLbl
                                End If

                                If ((.p(k, 0) > p_crit(.FID(k))) Or (.p(k, 0) < p_L_limit(.FID(k)))) Then
                                    ERN = 29  ' two-phase outlet pressure is greater then critical pressure or le
ss than lower limit
                                    GoTo errLbl
                                Else
                                    .x(k, 0) = x_e
                                    .DThl(0) = .T(h, 0) - Tsat_p(.FID(k), .p(k, 0))
```

HX_Analysis - 6

```
                                    If (.DThl(0) <= 0#) Then
                                        ERN = 30  ' cold-end stream temperature difference is <= 0
                                        GoTo errLbl
                                    End If
                                End If
                            Else
                                .x(k, 0) = x_e  ' set to default value
                            End If
                        End If  ' (1) stream and not parallel flow and warm end DT specified
                    Else  ' negative (1) stream mass flow -> parallel flow
                        .p(k, n) = .p(k, 0) - Dp
                        If (.DThl(0) > 0#) Then
                            If xe_given Then  ' (1) stream outlet is specified as being two-phase
                                If (.Nl > 1) Then
                                    ERN = 31  ' there can only be one two-phase (1) stream
                                    GoTo errLbl
                                End If

                                If ((.p(k, n) > p_crit(.FID(k))) Or (.p(k, n) < p_L_limit(.FID(k)))) Then
                                    ERN = 32  ' two-phase outlet pressure is greater then critical pressure or le
ss than lower limit
                                    GoTo errLbl
                                Else
                                    .x(k, n) = x_e
                                    .DThl(n) = .T(h, n) - Tsat_p(.FID(k), .p(k, n))
                                    If (.DThl(n) <= 0#) Then
                                        ERN = 33 ' cold-end stream temperature difference is <= 0
                                        GoTo errLbl
                                    End If
                                End If
                            Else
                                .x(k, n) = x_e  ' set to default value
                            End If
                        Else
                            .x(k, n) = x_e
                        End If
                    End If  ' negative (1) stream mass flow -> parallel flow
                End If  ' check if outlet quality is specified for (1) stream
            End If  ' not a boiler stream
        Next k

        If .Boiler Then
            If (((Abs(wl_T) < maxTol) And h_boiler) Or ((Abs(wh_T) < maxTol) And l_boiler)) Then
                ERN = 34  ' if it is a 'boiler', there cannot be zero or negative mass flow for the non-boiler st
ream
                GoTo errLbl
            End If
        Else
            If ((wh_T < maxTol) Or (Abs(wl_T) < maxTol)) Then
                ERN = 35  ' mass flow cannot be zero for a non-boiler
                GoTo errLbl
            End If
        End If

        If (MFE_tol <= 0#) Then MFE_tol = maxTol
        If (MFE_tol >= 0.5) Then
            ERN = 36
            GoTo errLbl
        End If
        .MFE_tol = MFE_tol
    End With

    Call HX_UA_NTU(HX, ERN)
    If (ERN <> 0) Then
        GoTo errLbl
    End If

    stop_time = Timer
    calc_time = stop_time - start_time
    ' store results in a string separated by a single space
    HX_Anal = CStr(calc_time) & " " & CStr(HX.T(h, n)) & " " & CStr(HX.T(1, 0)) & " " _
              & CStr(HX.q_tot) & " " & CStr(HX.UA_tot) & " " & CStr(HX.Ntu_tot) & " " _
              & CStr(HX.x(h, n)) & " "


    If (sign_wl0 >= 0) Then
        HX_Anal = HX_Anal & CStr(HX.x(HX.Nh + 1, 0))
    Else  ' parallel flow; outlet quality is at HX cold-end
        HX_Anal = HX_Anal & CStr(HX.x(HX.Nh + 1, n))
    End If
```

```
HX_Analysis - 7

    GoTo exitLbl

errLbl:
    HX_Anal = "Error: #" & Trim(CStr(ERN))

exitLbl:
End Function


Public Sub HX_T_out(HX As HX_CC_Type, h_stream As Boolean, i1 As Integer, i0 As Integer, _
                    Dq0 As Double, ERN As Integer)

' This subroutine is used by 'HX_UA_NTU' to obtain either the cold end temperature for the (h)
' temperature stream or the warm end (l) temperature stream.
' Inputs:
'   HX       - heat exchanger parameters; output is T, h, and x
'   h_stream - solving for a (h) stream?
'   i1       - index being solved for
'   i0       - previous/known index
'   Dq0      - passed as an input; if solving for the (h) stream temperature, it is the
'              (l) stream duty minus the heat in-leak; if solving for the (l) stream
'              temperature, it is the (h) stream duty
'              returned as the duty of the stream being solved for
'   ern      - error number (if any)

    Dim htp As Double           ' two-phase enthalpy for specified
    Dim x As Double             ' quality o two-phase stream being solve for
    Dim H0 As Double            ' [W] used for forming HX_T1 argument list
    Dim eps As Double           ' fractional difference or error

    Dim Ns As Integer           ' no. of streams
    Dim n As Integer            ' no. of HX sub-divisions for integration
    Dim nts As Integer          ' either # (h) sreams or (l) streams
    Dim k_min As Integer        ' lowest index of stream type being solved for
    Dim k_max As Integer        ' highest index of stream type being solved for
    Dim s1 As Integer           ' temperature stream being solved for; (h) stream = 1, (l) stream = 2
    Dim s2 As Integer           ' the other stream
    Dim j As Integer
    Dim j0 As Integer           ' warm-end index
    Dim j1 As Integer           ' cold end index
    Dim k As Integer            ' stream index no.
    Dim r As Integer            ' stream number of 2-phase stream


    ERN = 0
    With HX
        If .Boiler Then
            ERN = 1000  ' boiler stream is constant temperature by definition
            GoTo errLbl
        End If

        n = UBound(.DThl)
        Ns = .Nh + .Nl
        If ((i1 < 0) Or (i0 < 0) Or (i1 > n) Or (i0 > n)) Then
            ERN = 1001 ' temperature level indices out of bounds
            GoTo errLbl
        End If

        If h_stream Then
            s1 = h
            s2 = l
            k_min = 1
            k_max = .Nh
            nts = .Nh
        Else  ' (l) stream
            s1 = l
            s2 = h
            k_min = .Nh + 1
            k_max = Ns
            nts = .Nl
        End If

        ReDim inpv(0 To 4 * nts) As Variant
        ' form input argument list for function HX_T1
        j = 0
        For k = k_min To k_max
            inpv(j) = .FID(k)
            If ((s1 = h) And (.w(k) < 0#)) Then
                ERN = 1002  ' (h) stream mass flow must be >= 0
                GoTo errLbl
            End If
```

```
HX_Analysis - 8

            inpv(j + nts) = .w(k)
            inpv(j + 2 * nts) = .p(k, i1)
            j = j + 1
        Next k
        j = 3 * nts
        For k = 1 To (nts - 1)
            inpv(j) = 0#  ' temperature offsets (for same temperature streams)
            j = j + 1
        Next k
        inpv(j) = .T(s2, i1)
        j = j + 1

        ' sign structure required for HX_T1
        ' Solve For    H0
        ' ------------------------------------------------------------------
        ' T(h,i-1)     Sum{w(h)*h(h,i)}   + DH(i) - qk(i) = Sum{w(h)*h(h,i-1)}
        ' T(h,i)       Sum{w(h)*h(h,i-1)} - DH(i) + qk(i) = Sum{w(h)*h(h,i)}
        ' T(l,i-1)     Sum{w(l)*h(l,i)}   + Dq(i)         = Sum{w(l)*h(l,i-1)}
        ' T(l,i)       Sum{w(l)*h(l,i-1)} - Dq(i)         = Sum{w(l)*h(l,i)}
        ' Note: Dq(i), (h) stream duty between 'i-1' and 'i'
        '       DH(i), (l) stream duty between 'i-1' and 'i'
        ' So, Dq0 is passed as {DH(i) - qk(i)} if solving for a (h) stream and,
        '     Dq(i) if solving for a (l) stream
        If (i1 < i0) Then ' solving for a 'warm-end' temperature
            H0 = Dq0
        Else  ' solving for a 'cold-end' temperature
            H0 = -Dq0
        End If
        For k = k_min To k_max
            H0 = H0 + .w(k) * .h(k, i0)
        Next k
        inpv(j) = H0
        ' now calculate (s1) stream temperature at 'i1'
        .T(s1, i1) = HX_T1(inpv)
        If ((.T(s1, i1) <= 0#) And (.T(s1, i1) > -1#)) Then
            ERN = 1003  ' unable to calculate (s1) stream temperature at 'i1'
            GoTo errLbl
        End If
        x = 3#
        If (.T(s1, i1) <= -1#) Then
            ' solution is 2-phase; so returned result is,
            ' integer part - stream number passed to HX_T1 that is 2-phase
            ' decimal part - quality of stream (0 to 1)
            r = Abs(Fix(.T(s1, i1)))  ' stream number in 'HX_T1'
            If ((nts > 1) Or (r <> 1)) Then
                ERN = 1004  ' there can only be one two-phase (s1) stream
                GoTo errLbl
            End If
            x = Abs(r + .T(s1, i1))   ' quality of stream (s1) at 'i1'
            r = r + (k_min - 1)       ' actual stream number
            .T(s1, i1) = Tsat_p(.FID(r), .p(r, i1))
            For k = k_min To k_max
                If (k <> r) Then
                    If (.p(k, i1) < p_crit(.FID(k))) Then
                        ' if eps < maxTol, then stream (k) is adequately close
                        ' to stream (s1) to be considered 2-phase as well.
                        eps = Abs(1# - Tsat_p(.FID(k), .p(k, i1)) / .T(s1, i1))
                        If (eps < maxTol) Then
                            .TPS(k, i1) = True
                            ERN = 1005  ' there can only be one two-phase (s1) stream
                            GoTo errLbl
                        End If
                    End If
                End If
            Next k
        End If
        .DThl(i1) = .T(h, i1) - .T(l, i1)
        If (.DThl(i1) <= 0#) Then
            ERN = 1006  ' calculated warm end DThl <= 0
            GoTo errLbl
        End If
        ' establish the warm-end; j0 = warm-end, j1 = cold-end
        If (i0 < i1) Then
            j0 = i0
            j1 = i1
        Else
            j0 = i1
            j1 = i0
        End If
        Dq0 = 0#
        ' if the (s1) stream is two-phase, there is only one and this loop will not execute
```

```
HX_Analysis - 9

        For k = k_min To (k_max - 1)
            .h(k, i1) = h_pT(.FID(k), .p(k, i1), .T(s1, i1))
            H0 = H0 - .w(k) * .h(k, i1)
            .x(k, i1) = x_ph(.FID(k), .p(k, i1), .h(k, i1))
            .TPS(k, i1) = ((.x(k, i1) >= 0#) And (.x(k, i1) <= 1#))
            Dq0 = Dq0 + .w(k) * (.h(k, j0) - .h(k, j1))
        Next k
        If (Abs(.w(k_max)) >= .MFE_tol) Then
            ' Note: if (s1) stream at 'i1' is two phase it will computed here
            .h(k_max, i1) = H0 / .w(k_max)
            .x(k_max, i1) = x_ph(.FID(k), .p(k_max, i1), .h(k_max, i1))
            ' and this should be equal to,
            If ((x >= 0#) And (x <= 1#)) Then
                htp = hl_p(.FID(k_max), .p(k_max, i1)) + x * Dhvl_p(.FID(k_max), .p(k_max, i1))
                eps = Abs(htp / .h(k_max, i1) - 1#)
                If (eps > .MFE_tol) Then
                    ERN = 1007  ' calculation of (s1) stream enthalpy at 'i1' not match
                    GoTo errLbl
                End If
            End If
            .TPS(k_max, i1) = ((.x(k_max, i1) >= 0#) And (.x(k_max, i1) <= 1#))
        Else
            If (nts = 1) Then
                ERN = 1008 ' single (s1) stream flow cannot be zero, unless a boiler stream
                GoTo errLbl
            End If
            .h(k_max, i1) = 0#
        End If
        Dq0 = Dq0 + .w(k_max) * (.h(k_max, j0) - .h(k_max, j1))
    End With
    GoTo exitLbl

errLbl:

exitLbl:
End Sub


Public Sub HX_UA_NTU(HX As HX_CC_Type, ERN As Integer)
'   This subroutine calculates the (UA), Ntu's and q_tot for 'HX'

    Const Tsat_tol As Double = 0.000001  ' amount to add to saturation temperature (to separate vapor and liquid)
    Const DT_tol As Double = 0.000001    ' tolerance for stream temperature change

    Dim inpv() As Variant       ' input argument list for function HX_T1

    Dim Dpi As Double           ' [atm] stream pressure drop per sub-division (i.e., DT_Type = TRUE)
    Dim pri As Double           ' [-] stream pressure ratio per sub-division (i.e., DT_Type = FALSE)
    Dim H0 As Double            ' [W] used for forming HX_T1 argument list
    Dim Dhc As Double           ' [J/g] inlet to exit enthalpy difference of stream 'c'
    Dim Dhi As Double           ' [J/g] used if DT_Type is TRUE; stream 'c' enthalpy diff. for each sub-div.
    Dim hri As Double           ' [-] used if DT_Type is FALSE; stream 'c' enthalpy ratio for each sub-div.
    Dim q_h As Double           ' [W] total duty for (h) streams
    Dim q_l As Double           ' [W] total duty for (l) streams
    Dim qLK_s As Double         ' [W] sum of qLK from sub-division 0 to 'i'
    Dim DqLKi As Double         ' [W] used if DT_Type is TRUE; heat leak per sub-div.
    Dim qLK_Dhc As Double       ' [W/(J/g)] used if DT_Type is FALSE; heat leak per stream 'c' enthalpy diff.
    Dim C_h As Double           ' [W/K] (h) stream capacity rate
    Dim C_l As Double           ' [W/K] (l) stream capacity rate
    Dim x As Double             ' [-] quality
    Dim DThl_r As Double        ' [-] = DThl(i-1) / DThl(i)
    Dim eps As Double           ' fractional difference or error
    Dim Dq0 As Double           ' [W] temporary variable for calculating stream duty

    Dim Ns As Integer           ' no. of streams
    Dim n As Integer            ' no. of HX sub-divisions for integration
    Dim s As Integer            ' temperature stream number of stream 'c'; (h) stream = 1, (l) stream = 2
    Dim c As Integer            ' stream being used for enthalpy spacing
    Dim c_min As Integer        ' if 'c' is a (h) stream, = 1; else = .Nh+1 for a (l) stream
    Dim c_max As Integer        ' if 'c' is a (h) stream, = .Nh; else = Ns for a (l) stream
    Dim ci As Integer           ' iteration counter
    Dim i As Integer            ' HX sub-division index
    Dim j As Integer
    Dim k As Integer            ' stream index no.
    Dim k_min As Integer        ' Opposite of 'c' stream; if 'c' is a (h) stream, = 1; else = .Nh+1 for a (l) stre
am
    Dim k_max As Integer        ' Opposite of 'c' stream; if 'c' is a (h) stream, = .Nh; else = Ns for a (l) strea
m
    Dim r As Integer            ' stream number opposite of 's'
    Dim nTPS As Integer         ' no. of two-phase streams
    Dim sign_wl0 As Integer     ' sign of first non-zero (l) stream mass flow
```

```
HX_Analysis - 10

    Dim TPS_found As Boolean   ' 2-phase stream found?
    Dim Dhc_zero As Boolean    ' is (h) stream enthalpy drop zero?
    Dim DTh_zero As Boolean    ' is DTh zero?
    Dim DTl_zero As Boolean    ' is DTl zero?
    Dim DThl_r_one As Boolean  ' is DThl ratio = 1?
    Dim h_boiler As Boolean    ' (h) stream is condensing at const. temp. Th_0
    Dim l_boiler As Boolean    ' (l) stream is boiling at const. temp. Tl_0


    ERN = 0
    With HX
        n = UBound(.DThl)
        Ns = .Nh + .Nl

        h_boiler = (.Boiler And (.DThl(0) > 0#))  ' DThl_0 is the 'pinch' point for a 'h_boiler'
        l_boiler = (.Boiler And (.DThl(n) > 0#))  ' DThl_N is the 'pinch' point for a 'l_boiler'

        ' set-up pressure profile first
        If .DT_type Then  ' i.e., normal temp. diff.
            For k = 1 To Ns
                Dpi = (.p(k, 0) - .p(k, n)) / CDbl(n)
                For i = 1 To (n - 1)
                    If ((h_boiler And (k <= .Nh)) Or (l_boiler And (k > .Nh))) Then
                        .p(k, i) = .p(k, n)
                    Else
                        .p(k, i) = .p(k, i - 1) - Dpi
                    End If
                Next i
            Next k
        Else  ' i.e., use pressure ratio
            For k = 1 To Ns
                pri = (.p(k, 0) / .p(k, n)) ^ (-1# / CDbl(n))
                For i = 1 To (n - 1)
                    If ((h_boiler And (k <= .Nh)) Or (l_boiler And (k > .Nh))) Then
                        .p(k, i) = .p(k, n)
                    Else
                        .p(k, i) = .p(k, i - 1) * pri
                    End If
                Next i
            Next k
        End If

        ' determine (l) stream flow direction if not a 'l_boiler'
        If Not l_boiler Then
            k = .Nh
            Do
                k = k + 1
                sign_wl0 = Sgn(.w(k))
            Loop Until ((sign_wl0 <> 0) Or (k >= Ns))
            If (sign_wl0 = 0) Then
                ERN = 100  ' (l) stream mass flow cannot be zero
                GoTo errLbl
            End If
        End If

        ' obtain (h) stream warm-end and (l) stream cold-end enthalpies & qualities
        For k = 1 To Ns
            If ((k <= .Nh) And (Not h_boiler)) Then  ' (h) stream inlets
                If ((.x(k, 0) >= 0#) And (.x(k, 0) <= 1#)) Then
                    If (k > 1) Then
                        ERN = 101  ' there can only be one two-phase (h) stream
                        GoTo errLbl
                    End If
                    .h(k, 0) = hl_p(.FID(k), .p(k, 0)) + .x(k, 0) * Dhvl_p(.FID(k), .p(k, 0))
                Else
                    .h(k, 0) = h_pT(.FID(k), .p(k, 0), .T(h, 0))
                    .x(k, 0) = x_ph(.FID(k), .p(k, 0), .h(k, 0))
                End If
            End If

            If ((k > .Nh) And (Not l_boiler)) Then  ' (l) stream inlets
                If ((.x(k, n) >= 0#) And (.x(k, n) <= 1#)) Then
                    If (k > (.Nh + 1)) Then
                        ERN = 102  ' there can only be one two-phase (l) stream
                        GoTo errLbl
                    End If
                    .h(k, n) = hl_p(.FID(k), .p(k, n)) + .x(k, n) * Dhvl_p(.FID(k), .p(k, n))
                Else
                    .h(k, n) = h_pT(.FID(k), .p(k, n), .T(l, n))
                    .x(k, n) = x_ph(.FID(k), .p(k, n), .h(k, n))
```

```
HX_Analysis - 11

                End If
            End If
        Next k

        If (.DThl(0) <= 0#) Then
            If (.DThl(n) <= 0#) Then
                ERN = 103  ' both warm-end & cold-end DThl's provided are LTE 0
                GoTo errLbl
            End If
            ' this can be counter-flow, parallel flow or a 'l_boiler'
            If h_boiler Then
                ERN = 104  ' specifying the cold end DThl not allowed for an 'h_boiler'
                GoTo errLbl
            End If
            ' cold end DThl was specified; determine (h) stream cold end temperature
            For k = 1 To .Nh
                If ((.x(k, n) >= 0#) And (.x(k, n) <= 1#)) Then
                    If (.Nh > 1) Then
                        ERN = 105  ' cannot have more than one two-phase (h) stream
                        GoTo errLbl
                    End If
                    .h(k, n) = hl_p(.FID(k), .p(k, n)) + .x(k, n) * Dhvl_p(.FID(k), .p(k, n))
                    .T(h, n) = Tsat_p(.FID(k), .p(k, n)) + Tsat_tol
                    .DThl(n) = .T(h, n) - .T(l, n)
                    If (.DThl(n) <= 0#) Then
                        ERN = 106 ' cold-end stream temperature difference is <= 0
                        GoTo errLbl
                    End If
                Else
                    .T(h, n) = .T(l, n) + .DThl(n)
                    .h(k, n) = h_pT(.FID(k), .p(k, n), .T(h, n))
                    .x(k, n) = x_ph(.FID(k), .p(k, n), .h(k, n))
                End If
            Next k
            If (Not l_boiler) Then
                H0 = 0#
                For k = 1 To .Nh
                    If (.w(k) < 0#) Then
                        ERN = 107  ' (h) stream mass flow must be >= 0
                        GoTo errLbl
                    End If
                    H0 = H0 + .w(k) * (.h(k, 0) - .h(k, n))
                Next k
                H0 = H0 + .qLK  ' total (h) stream duty
                ' obtain (l) stream warm end temperature
                Call HX_T_out(HX, False, 0, n, H0, ERN)
                If (ERN <> 0) Then GoTo errLbl
            Else  ' l_boiler = true
                For i = 0 To (n - 1)
                    .T(l, i) = .T(l, n)
                Next i
                .DThl(0) = .T(h, 0) - .T(l, 0)
            End If
        Else  ' warm end DThl was specified
            ' this can be counter-flow, parallel flow or a 'h_boiler'
            If l_boiler Then
                ERN = 108  ' specifying the warm end DThl not allowed for an 'l_boiler'
                GoTo errLbl
            End If
            ' determine (l) stream warm end temperature
            For k = (.Nh + 1) To Ns
                If ((.x(k, 0) >= 0#) And (.x(k, 0) <= 1#)) Then
                    If (.Nl > 1) Then
                        ERN = 109  ' cannot have more than one two-phase (l) stream
                        GoTo errLbl
                    End If
                    .h(k, 0) = hl_p(.FID(k), .p(k, 0)) + .x(k, 0) * Dhvl_p(.FID(k), .p(k, 0))
                    .T(l, 0) = Tsat_p(.FID(k), .p(k, 0)) + Tsat_tol
                    .DThl(0) = .T(h, 0) - .T(l, 0)
                    If (.DThl(0) <= 0#) Then
                        ERN = 110 ' cold-end stream temperature difference is <= 0
                        GoTo errLbl
                    End If
                Else
                    .T(l, 0) = .T(h, 0) - .DThl(0)
                    .h(k, 0) = h_pT(.FID(k), .p(k, 0), .T(l, 0))
                    .x(k, 0) = x_ph(.FID(k), .p(k, 0), .h(k, 0))
                End If
            Next k
            If (Not h_boiler) Then
                H0 = 0#
```

HX_Analysis - 12

```
                For k = (.Nh + 1) To Ns
                    H0 = H0 + .w(k) * (.h(k, 0) - .h(k, n))
                Next k
                ' before the next step, 'H0' is the (l) stream duty
                H0 = H0 - .qLK
                ' obtain (h) stream cold end temperature
                Call HX_T_out(HX, True, n, 0, H0, ERN)
                If (ERN <> 0) Then GoTo errLbl
            Else  ' h_boiler = true
                For i = 1 To n
                    .T(h, i) = .T(h, 0)
                Next i
                .DThl(n) = .T(h, n) - .T(l, n)
            End If
        End If

        ' check to see that (h) streams are being cooled & (l) streams are being heated
        ' for parallel flow, the (l) stream ass flow is negative and the warm-end minus
        ' cold-end enthalpy difference is negative; so 'q_l' is >= 0
        ' for a boiler, no check between (h) and (l) streams can be done
        If .Boiler Then
            If h_boiler Then
                q_h = 0#
            Else  ' l_boiler = true
                q_l = 0#
            End If
        Else
            q_h = .qLK
            If (q_h < 0#) Then
                ERN = 111  ' heat in-leak cannot be < 0
                GoTo errLbl
            End If
            q_l = 0#
        End If

        For k = 1 To Ns
            If ((k <= .Nh) And (Not h_boiler)) Then _
                q_h = q_h + .w(k) * (.h(k, 0) - .h(k, n))
            If ((k > .Nh) And (Not l_boiler)) Then _
                q_l = q_l + .w(k) * (.h(k, 0) - .h(k, n))
        Next k

        If .Boiler Then
            eps = 1#
            If (h_boiler And (q_l >= 0#)) Then eps = 0#
            If (l_boiler And (q_h >= 0#)) Then eps = 0#
        Else
            If (q_h < maxTol) Then
                If (q_l < maxTol) Then
                    eps = 0#
                Else
                    eps = 1#
                End If
            Else
                eps = Abs(1# - q_l / q_h)
            End If
        End If

        If ((q_h < 0#) Or (q_l < 0#)) Then
            ERN = 112  ' duty cannot be < 0
            GoTo errLbl
        End If
        If (eps > .MFE_tol) Then
            ERN = 113  ' (h) and (l) stream duty do not match
            GoTo errLbl
        End If

        ' determine two-phase stream condition for warm-end and cold-end for each stream
        For k = 1 To Ns
            If (((k <= .Nh) And (Not h_boiler)) Or ((k > .Nh) And (Not l_boiler))) Then
                .TPS(k, 0) = ((.x(k, 0) >= 0#) And (.x(k, 0) <= 1#))
                .TPS(k, n) = ((.x(k, n) >= 0#) And (.x(k, n) <= 1#))
            End If
        Next k

        ' find a non-boiler two-phase stream or use the first non-boiler stream
        If h_boiler Then
            ' at the HX warm end look for either the first two-phase (l) stream,
            ' or if not found just use the first (l) stream
            c = .Nh
            Do
```

HX_Analysis - 13

```
            c = c + 1
        Loop Until (.TPS(c, 0) Or .TPS(c, n) Or (c >= Ns))
        If Not (.TPS(c, 0) Or .TPS(c, n)) Then c = .Nh + 1
    Else
        ' at the HX warm end look for either the first two-phase (h) stream,
        ' or if not found just use the first (h) stream
        c = 0
        If l_boiler Then
            c_max = .Nh
        Else
            c_max = Ns
        End If
        Do
            c = c + 1
        Loop Until (.TPS(c, 0) Or .TPS(c, n) Or (c >= c_max))
        If Not (.TPS(c, 0) Or .TPS(c, n)) Then c = 1
    End If

    If (c <= .Nh) Then  ' 'c' is a (h) stream
        s = h
        r = l
        c_min = 1
        c_max = .Nh
        k_min = .Nh + 1
        k_max = Ns
    Else  ' 'c' is a (l) stream
        s = l
        r = h
        c_min = .Nh + 1
        c_max = Ns
        k_min = 1
        k_max = .Nh
    End If  ' c <= .Nh

    ' establish enthalpy spacing using stream 'c'
    Dhc = .h(c, 0) - .h(c, n)
    eps = Dhc / Abs(.h(c, 0))
    Dhc_zero = (eps < maxTol)
    If Dhc_zero Then Dhc = 0#
    If .DT_type Then
        Dhi = Dhc / CDbl(n)
        DqLKi = .qLK / CDbl(n)
    Else
        hri = (.h(c, 0) / .h(c, n)) ^ (-1# / CDbl(n))
        If Not (Dhc_zero) Then
            qLK_Dhc = .qLK / Dhc
        Else
            qLK_Dhc = 0#
            DqLKi = .qLK / CDbl(n)
        End If  ' not Dhc_zero
    End If  ' .DT_type

    ' march thru each sub-division (integration)
    ' beginning at warm-end and moving toward to cold-end
    ' this will check the number of two-phase (h) streams and (l) streams
    .UA_tot = 0#
    .Ntu_tot = 0#
    .q_tot = 0#
    qLK_s = 0#
    For i = 1 To n
        ' Don't recalculate stream values already calculated at i = N.
        ' This is a good energy balence check.
        If (i <> n) Then
            ' perform appropriate enthalpy spacing depending on .DT_Type
            If .DT_type Then
                .h(c, i) = .h(c, i - 1) - Dhi
            Else
                .h(c, i) = .h(c, i - 1) * hri
                If (Not Dhc_zero) Then DqLKi = qLK_Dhc * (.h(c, i - 1) - .h(c, i))
            End If
            .x(c, i) = x_ph(.FID(c), .p(c, i), .h(c, i))
            .T(s, i) = T_ph(.FID(c), .p(c, i), .h(c, i))

            ' obtain enthalpy and quality of other streams of the same type as 'c'
            For k = c_min To c_max
                If (k <> c) Then
                    .h(k, i) = h_pT(.FID(k), .p(k, i), .T(s, i))
                    .x(k, i) = x_ph(.FID(k), .p(k, i), .h(k, i))
                End If
            Next k
            ' count the number of 2-phase streams of the same type as the 'c' stream
```

HX_Analysis - 14

```
                nTPS = 0
                For k = c_min To c_max
                    .TPS(k, i) = ((.x(k, i) >= 0#) And (.x(k, i) <= 1#))
                    If .TPS(k, i) Then nTPS = nTPS + 1
                Next k
                If (nTPS > 1) Then
                    ERN = 116  ' only one two-phase (c) stream allowed
                    GoTo errLbl
                End If
                ' if 'c' stream is two-phase, look for streams of the same type as the 'c'
                ' stream that are almost two-phase
                If .TPS(c, i) Then
                    For k = c_min To c_max
                    If (k <> c) Then
                        If (.p(k, i) < p_crit(.FID(k))) Then
                            ' if eps < maxTol, then stream (k) is adequately close
                            ' to stream (s) to be considered 2-phase as well
                            eps = Abs(1# - Tsat_p(.FID(k), .p(k, i)) / .T(s, i))
                            If (eps < maxTol) Then
                                ERN = 117  ' there can only be one two-phase (s) stream
                                GoTo errLbl
                            End If
                        End If
                    End If
                    Next k
                End If
            End If  ' i <> N

            If Not .DT_type Then DqLKi = qLK_Dhc * (.h(c, i - 1) - .h(c, i))

            ' Duty of 's' type streams
            If (s = h) Then
                Dq0 = DqLKi
            Else
                Dq0 = 0#
            End If
            For k = c_min To c_max
                Dq0 = Dq0 + .w(k) * (.h(k, i - 1) - .h(k, i))
            Next k
            ' Note: 's' stream, which is same type as the 'c' stream cannot be a boiler
            If (s = h) Then
                .Dq(i) = Dq0
            Else
                .DH(i) = Dq0
            End If

            If (i <> n) Then
                If (Not .Boiler) Then
                    ' obtain cold-end temperature for stream opposite 'c' at 'i'
                    If (r = h) Then Dq0 = Dq0 - DqLKi
                    Call HX_T_out(HX, (r = h), i, i - 1, Dq0, ERN)
                    If (r = h) Then Dq0 = Dq0 + DqLKi
                    ' note that 'HX_T_out' will generate an error if more than one stream is two-phase
                    ' and it will determine .TPS state and the .DThl(i)
                    If (ERN <> 0) Then GoTo errLbl
                Else  ' .Boiler = TRUE and 'r' stream is the boiler
                    .T(r, i) = .T(r, i - 1)
                    .DThl(i) = .T(h, i) - .T(l, i)
                    .EBF(i) = 0#
                End If

                ' count the number of 2-phase streams of the opposite type as the 'c' stream
                nTPS = 0
                For k = k_min To k_max
                    If .TPS(k, i) Then nTPS = nTPS + 1
                Next k
                If (nTPS > 1) Then
                    ERN = 118  ' only one two-phase opposite (c) stream allowed
                    GoTo errLbl
                End If
            Else  ' i = N
                ' Duty of 'r' type streams
                If (r = h) Then
                    DqLKi = .qLK - qLK_s
                    Dq0 = DqLKi
                Else
                    Dq0 = 0#
                End If
                If Not .Boiler Then
                    For k = k_min To k_max
                        Dq0 = Dq0 + .w(k) * (.h(k, i - 1) - .h(k, i))
```

```
HX_Analysis - 15

                Next k
            End If
        End If

        ' Check energy balance of HX between 0 to 'i' and 'i' to 'N'
        If ((Not .Boiler) And (i <> n)) Then
            ' Duty of 'h' and 'l' type streams between 0 and 'i'
            If .DT_type Then
                q_h = i * DqLKi
            Else
                q_h = qLK_Dhc * (.h(c, 0) - .h(c, i))
            End If
            q_l = 0#
            For k = 1 To Ns
                If (k <= .Nh) Then
                    q_h = q_h + .w(k) * (.h(k, 0) - .h(k, i))
                Else
                    q_l = q_l + .w(k) * (.h(k, 0) - .h(k, i))
                End If
            Next k
            If ((q_h <= 0#) Or (q_l <= 0#)) Then
                ERN = 119
                GoTo errLbl
            End If
            If (Not ((q_h <= .MFE_tol) And (q_l <= .MFE_tol)) And (Abs(1# - q_l / q_h) > .MFE_tol)) Then
                ERN = 120
                GoTo errLbl
            End If

            ' Duty of 'h' and 'l' type streams between 'i' and 'N'
            If .DT_type Then
                q_h = (n - i) * DqLKi
            Else
                q_h = qLK_Dhc * (.h(c, i) - .h(c, n))
            End If
            q_l = 0#
            For k = 1 To Ns
                If (k <= .Nh) Then
                    q_h = q_h + .w(k) * (.h(k, i) - .h(k, n))
                Else
                    q_l = q_l + .w(k) * (.h(k, i) - .h(k, n))
                End If
            Next k
            If ((q_h <= 0#) Or (q_l <= 0#)) Then
                ERN = 121
                GoTo errLbl
            End If
            If (Not ((q_h <= .MFE_tol) And (q_l <= .MFE_tol)) And (Abs(1# - q_l / q_h) > .MFE_tol)) Then
                ERN = 122
                GoTo errLbl
            End If
        End If

        ' Note that an (l) stream that is two-phase and has pressure drop will COOL.
        ' This can generate errors 123 to 126.
        .DT(s, i) = .T(s, i - 1) - .T(s, i)
        If ((s = l) And (.w(s) < 0#)) Then  ' parallel flow
            If (.DT(s, i) > DT_tol) Then
                ERN = 123  ' (l) stream in parallel flow must warm; how did this happen?
                GoTo errLbl
            End If
        Else
            If (.DT(s, i) < -DT_tol) Then
                ERN = 124  ' streams must cool; except for an (l) stream and parallel flow; how did his happe
n?
                GoTo errLbl
            End If
        End If

        .DT(r, i) = .T(r, i - 1) - .T(r, i)
        If ((r = l) And (.w(r) < 0#)) Then   ' parallel flow
            If (.DT(r, i) > DT_tol) Then
                ERN = 125  ' (l) stream in parallel flow must warm; how did this happen?
                GoTo errLbl
            End If
        Else
            If (.DT(r, i) < -DT_tol) Then
                ERN = 126  ' streams must cool; except for an (l) stream and parallel flow; how did his happe
n?
                GoTo errLbl
            End If
```

```
            End If

            ' assign duty of 'r' stream type
            If Not .Boiler Then
                ' 'Dq0' now has the duty for the stream type opposite of 'c' for the sub-dic.
                If (r = l) Then
                    .DH(i) = Dq0
                Else
                    .Dq(i) = Dq0
                End If
            Else
                ' Duty of boiler stream cannot be independently calculated
                If (r = h) Then
                    .Dq(i) = .DH(i)
                Else
                    .DH(i) = .Dq(i)
                End If
            End If

            DTh_zero = (.DT(h, i) < maxTol)
            DTl_zero = (Abs(.DT(l, i)) < maxTol)
            ' .DH(i) and .Dq(i) cannot be independently calculated for a boiler
            If (Not .Boiler) Then
                If (DTh_zero And DTl_zero) Then
                    .EBF(i) = 0#
                Else
                    If (.Dq(i) < maxTol) Then
                        If (.DH(i) < maxTol) Then
                            .EBF(i) = 0#
                        Else
                            ERN = 127  ' (h) duty zero, but (l) duty non-zero
                            GoTo errLbl
                        End If
                    Else
                        .EBF(i) = Abs(1# - .DH(i) / .Dq(i))
                    End If

                    If (.EBF(i) > .MFE_tol) Then
                        ERN = 128  ' (h) duty <> (l) duty for segment 'i'
                        GoTo errLbl
                    End If
                End If
            End If

            DThl_r = (.DThl(i - 1) / .DThl(i))
            DThl_r_one = (Abs(1# - DThl_r) < maxTol)
            If (DTh_zero And DTl_zero) Then
                ' no heat transfer
                .Cmin(i) = -1#    ' i.e., undefined
            Else
                If (DTl_zero Or l_boiler) Then
                    ' C_l is undefined
                    C_h = .Dq(i) / .DT(h, i)
                    .Cmin(i) = C_h
                Else
                    If (DTh_zero Or h_boiler) Then
                        ' C_h is undefined
                        C_l = .DH(i) / .DT(l, i)
                        .Cmin(i) = C_l
                    Else
                        C_h = .Dq(i) / .DT(h, i)
                        C_l = sign_wl0 * .DH(i) / .DT(l, i)
                        If (C_l < C_h) Then
                            .Cmin(i) = C_l
                        Else
                            .Cmin(i) = C_h
                        End If
                    End If
                End If
            End If

            If ((.Cmin(i) <= 0#) Or DThl_r_one) Then
                ' no duty for this segment
                .DUA(i) = 0#
                .DNtu(i) = 0#
            Else
                .DTLM(i) = (.DThl(i - 1) - .DThl(i)) / Log(DThl_r)
                .DUA(i) = .Dq(i) / .DTLM(i)
                .DNtu(i) = .DUA(i) / .Cmin(i)
            End If
```

HX_Analysis - 17

```
            .q_tot = .q_tot + .Dq(i)
            .UA_tot = .UA_tot + .DUA(i)
            .Ntu_tot = .Ntu_tot + .DNtu(i)
            qLK_s = qLK_s + DqLKi
        Next i
    End With

    GoTo exitLbl

errLbl:
    With HX
        .UA_tot = 0#
        .Ntu_tot = 0#
        .q_tot = 0#
    End With

exitLbl:
End Sub
```

APPENDIX J – MISCELLANEOUS CALCULATIONS

Table J.1. Radiation flux estimate for heat in-leak from copper shield (at 33 K) to internals (at ~2 to 5 K)

T_h	33	[K]	*Warm boundary temperature*
T_c	2	[K]	*Cold boundary temperature*
T_{LM}	11.06	[K]	*Log-mean temperature (use as an average temperature),* $= \Delta T / ln(T_h/T_c)$
ΔT	31	[K]	*Temperature difference,* $= T_h - T_c$
k_S	0.0773	[W/m-K]	*Separator material thermal conductivity (for Dacron, [1]),* $= f(T_{LM})$
t_S	0.0035	[in]	*Thickness of separator*
n_S	2	[-]	*Number of separator plys used*
C	0.008	[-]	*Separator solid conductance material constant*
f	0.072	[-]	*Ratio of separator density to density of solid material*
h_C	0.2504	[W/m^2-K]	*Solid conductance for separator material (for Dacron, [1]),* $= C \cdot f \cdot k_S / t_S$
ε	0.00323	[-]	*Emissivity of radiation shields, (for DAM, [2])* $= 6.51x10^{-4} (T_{LM})^{2/3}$
$(N/\Delta x)$	60	[layer/in]	*Layer density*
k_a	0.1060	[mW/m-K]	*Apparent thermal conductivity of well evacuated MLI*
			$= [(h_C + \sigma \cdot \varepsilon \cdot (T_h^2 + T_c^2) \cdot (T_h + T_c) / (2 - \varepsilon)] / (N/\Delta x)$
N	40	[layers]	*Number layers used*
Δx	0.667	[in]	*Thickess of MLI,* $= N / (N/\Delta x)$
q''	0.194	[W/m^2]	*Heat flux through MLI,* $= k_a \cdot (\Delta T/\Delta x)$

Table J.2. Tube with twisted tape insert, pressure drop estimate for test #33

	Upper HX		Lower HX			
	WE	**CE**	**WE**	**CE**		
$\dot{m}$	3.61	3.61	3.61	3.61	[g/s]	*Mass flow rate*
p	2.66	2.658	0.229	0.226	[atm]	*Pressure*
T	5.15	2.725	2.98	2.18	[K]	*Temperature*
h	16.02	5.99	6.14	3.07	[J/g]	*Enthalpy*
x	-100.0%	-100.0%	4.3%	-8.7%	[-]	*Quality*
2-Phase?	FALSE	FALSE	TRUE	FALSE		*Is flow two-phase?*
ρ	107.93	148.96	60.13	146.52	[g/ℓ]	*Density*
μ	2.860	3.640	3.097	2.520	[μPa-s]	*Dynamic viscosity*
d	0.402	0.402	0.402	0.402	[in]	*Inside diameter*
A_c	0.1269	0.1269	0.1269	0.1269	[in^2]	*Free flow cross-sectional area*
G	44.04	44.04	44.04	44.04	[kg/s-m^2]	*Mass flux*
Re	157222	123529	145189	178481	[-]	*Reynold's number*
l	0.750	0.750	0.750	0.750	[in]	*Twisted tape pitch (180 turn)*
δ	0.018	0.018	0.018	0.018	[in]	*Twisted tape thickness*
X_L	1.866	1.866	1.866	1.866	[-]	*= l/d*
(δ/d)	0.0448	0.0448	0.0448	0.0448	[-]	
S_w	63517	49906	58656	72106	[-]	*Swirl parameter,* $= Re / (X_L^{1/2} \cdot (\pi/(\pi - 4 \cdot \delta/d)) \cdot (1+(\pi / 2 \cdot X_L)^2))$
Turbulent?	TRUE	TRUE	TRUE	TRUE		*Is flow turbulent?*
f	0.009821	0.010432	0.010019	0.009515	[-]	*Fanning friction factor*
Eu	8.99	6.51	16.13	6.62	[-]	*Euler number*
L	283.3	283.3	283.3	283.3	[in]	*Flow length*
ζ	27.69	29.41	28.24	26.82	[-]	*Flow resistance*
Δp_f	0.002455	0.00189	0.004496	0.001752	[atm]	*Pressure drop due to friction*
$\Delta p_{f,avg}$	0.00217		0.00312		[atm]	*Average friction factor*
Δp_m	-4.89E-05		-0.00019		[atm]	*Pressure drop due to change in momentum*
Δp	0.00212		0.00294		[atm]	*Total pressure drop*

Table J.3. Shell side pressure drop estimate for test #33

	Upper HX		Lower HX			
D_c	5.625		5.625		[in]	*Coil mean diameter*
d_o	0.500		0.500		[in]	*Tube outside diameter*
d_f	1.125		1.125		[in]	*Fin diameter*
t	0.018		0.018		[in]	*Fin thickness*
n	9		12		[fins/in]	*Fin density*
N_c	16		16		[-]	*Number of coils*
$A_{c(p)}$	9.255		8.659		[in^2]	*Projected free flow cross-sectional area (as if the coil had no helix angle)*
A_s'	116.4		147.0		[in^2/in]	*Average heated perimeter*
r_h	0.07950		0.05891		[in]	*Hydrualic radius*
	WE	**CE**	**WE**	**CE**		
$\dot{m}$	3.606	3.606	3.606	3.606	[g/s]	*Mass flow*
G	0.6040	0.6040	0.6456	0.6456	[kg/s-m^2]	*Mass flux*
p	0.0362	0.0363	0.0363	0.0364	[atm]	*Pressure*
T	4.49	2.60	2.60	2.06	[K]	*Temperature*
ρ	0.3961	0.7016	0.7016	145.7601	[g/ℓ]	*Density*
μ	1.141	0.667	0.667	1.668	[μPa-s]	*Dynamic Viscosity*
Re	4277	7313	5792	2316	[-]	*Reynold's number*
f	0.2800	0.2800	0.2800	0.2800	[-]	*Fanning friction factor*
ζ	63.39	63.39	85.56	85.56	[-]	*Flow resistance*
Eu	0.4604	0.2600	0.2970	0.0014	[-]	*Euler number*
Δp	0.000288	0.000163	0.000251	0.000001	[atm]	*Frictional pressure drop*
Δp_{avg}	0.000225		0.000126			

APPENDIX K – COLLINS COIL FIN-TUBE HEAT EXCHANGER EFFECTIVENESS

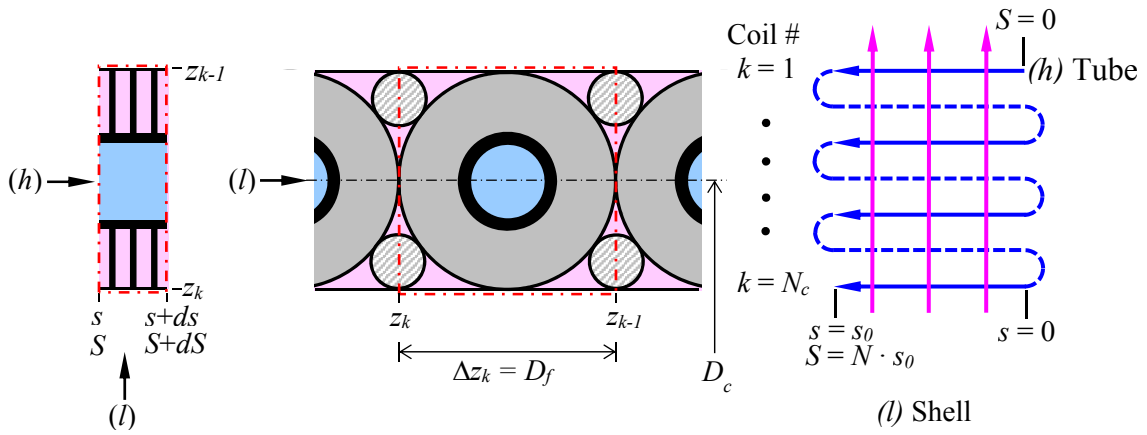

Figure K.1. Geometry for single pass, single wrap Collins coil fin-tube heat exchanger

Referring to Figure K.1, the energy balance for coil 'k' between positions S and $S + dS$ is,

$$\dot{m}_h \cdot C_{p,h} \cdot T_h - \dot{m}_h \cdot C_{p,h} \cdot (T_h + dT_h) - \left(k_w \cdot A_w \cdot \frac{dT_w}{ds}\right)_s + \left(k_w \cdot A_w \cdot \frac{dT_w}{ds}\right)_{s+ds} + d\dot{m}_l \cdot C_{p,l} \cdot T_{l,k} - d\dot{m}_l \cdot C_{p,l} \cdot T_{l,k-1} = 0 \qquad \text{(Eq. K.1)}$$

where, 'S' is the total curve length along the tube center-line and 's' is the relative curve length for coil 'k'. This simplifies to,

$$-C_h \cdot \frac{dT_h}{dS} + \frac{d}{dS}\left(k_w \cdot A_w \cdot \frac{dT_w}{dS}\right) - \frac{dC_l}{dS} \cdot \left(T_{l,k-1} - T_{l,k}\right) = 0 \qquad \text{(Eq. K.2)}$$

where,

$$C_h = \dot{m}_h \cdot C_{p,h} \qquad \text{(Eq. K.3)}$$

$$\frac{dC_l}{dS} = C_{p,l} \cdot \frac{d\dot{m}_l}{dS} \qquad \text{(Eq. K.4)}$$

If the wall conduction term is neglected,

$$-C_h \cdot \frac{dT_h}{dS} = \frac{dC_l}{dS} \cdot \Delta T_{l,k} \qquad \text{(Eq. K.5)}$$

$$\Delta T_{l,k} = T_{l,k-1} - T_{l,k} \qquad \text{(Eq. K.6)}$$

The total arc length '*S*', relative curve length '*s*', axial position '*z*' and coil '*k*' are related as follows,

$$S = s_0 \cdot (k-1) + s \quad \text{(Eq. K.7)}$$

$$z = D_f \cdot (k-1) + s \cdot \sin\phi \quad \text{(Eq. K.8)}$$

$$\sin\phi = \frac{D_f}{s_0} \quad \text{(Eq. K.9)}$$

$$\tan\phi = \frac{D_f}{\pi \cdot D_c} \quad \text{(Eq. K.10)}$$

$${s_0}^2 = (\pi \cdot D_c)^2 + {D_f}^2 \quad \text{(Eq. K.11)}$$

$$(k-1) = \left\lfloor \frac{S}{s_0} \right\rfloor \quad \text{(Eq. K.12)}$$

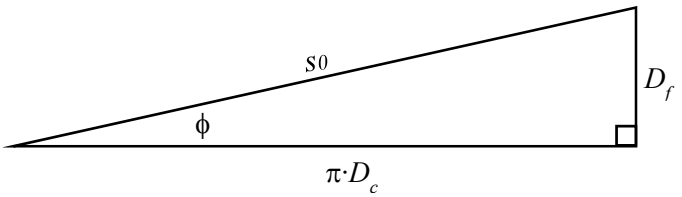

Figure K.2. Helical coil tube geometry for single pass and single wrap

where, D_f is the fin diameter, D_c is the coil mean diameter, and ϕ is the coil helix angle. Although, we could treat T_l as a function of the (total) arc length '*S*', this becomes ambiguous when we are considering a specific coil '*k*'; as such, position '*S*' will be denoted using both '*s*' and '*k*'.

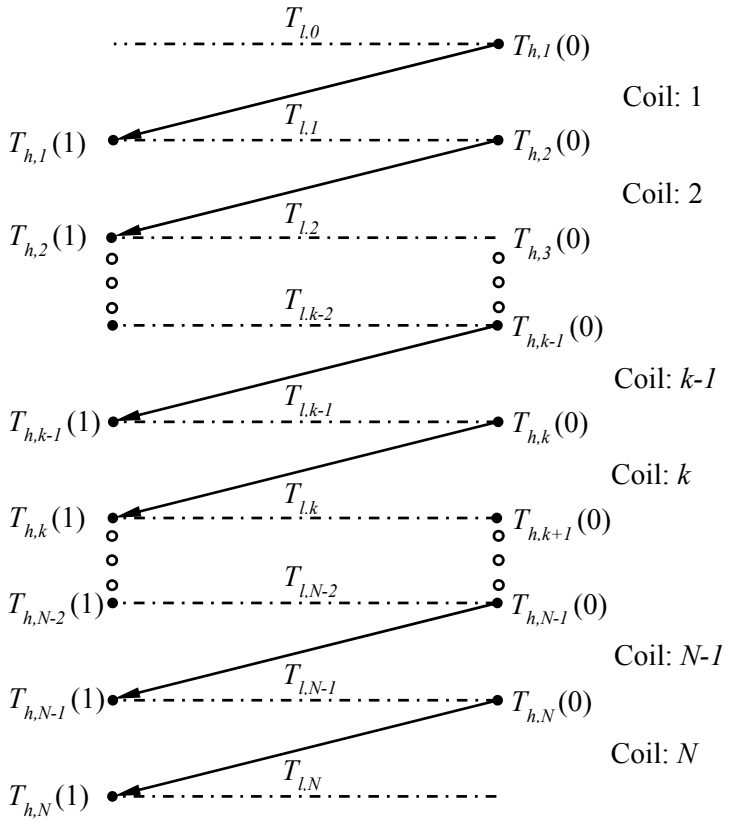

Figure K.3. Index structure for cross-counter flow helical coil geometry

Note that the *(h)* stream undergoes an infinitesimal temperature change and the *(l)* stream undergoes a finite temperature change. The *(l)* stream duty for coil '*k*' at position '*s*' is,

$$\delta q_{l,(s,k)} = dC_l \cdot \left(T_{l,(s,k-1)} - T_{l,(s,k)}\right) = d(UA)_{(s,k)} \cdot \Delta T_m \qquad \text{(Eq. K.13)}$$

where, ΔT_m is an appropriate 'mean' temperature difference between *(h)* and *(l)* streams. If T_h and C_l are assumed constant over the heat transfer area from z_k and z_{k-1}, we will temporarily treat the differential quantities as finite, between z_k and $z \leq z_{k-1}$ (i.e., as if they were constant for coil '*k*' between $0 \leq s \leq s_0$),

$$C_l \cdot dT_l = d(UA)_k \cdot (T_h - T_l) \qquad \text{(Eq. K.14)}$$

$$C_l \cdot d(T_h - T_l) = d(UA) \cdot (T_h - T_l) \qquad \text{(Eq. K.15)}$$

Integrating between, $T_{l,k}$ and $T_l \leq T_{l,k-1}$,

$$N_l = \frac{(UA)}{C_l} = -\ln\left(\frac{T_h - T_l}{T_h - T_{l,k}}\right) \quad \text{(Eq. K.16)}$$

Strictly, this is true only at position '*S*'. N_l is the *NTU*'s based on the *(l)* stream. So, solving for the temperature T_l,

$$T_l = T_{l,(s,k)} + \left(T_h - T_{l,(s,k)}\right) \cdot \left(1 - e^{-N_{l,(s,k)}}\right) \quad \text{(Eq. K.17)}$$

Also, the temperature change of the *(l)* stream across coil '*k*' (at position '*s*') is,

$$\Delta T_{l,k} = T_{l,k-1} - T_{l,k} = \left(T_h - T_{l,k}\right) \cdot \left(1 - e^{-N_{l,k}}\right) \quad \text{(Eq. K.18)}$$

Reintroducing the differential quantities, the number of *(l)* stream *NTU*'s for coil '*k*' (at position '*s*') is,

$$N_{l,k} = \frac{(UA)_k}{C_l} \quad \text{(Eq. K.19)}$$

Across coil '*k*' (at position '*s*'), the appropriate 'mean' temperature difference is the integrated average temperature difference,

$$\Delta T_m \cdot \int_0^{N_{l,k}} d\xi = \Delta T_m \cdot N_{l,k} = \int_0^{N_{l,k}} (T_h - T_l) \cdot d\xi \quad \text{(Eq. K.20)}$$

And, recalling C_l was assumed to be constant,

$$d\xi = \frac{d(UA)}{C_l} \quad \text{(Eq. K.21)}$$

$$\Delta T_m \cdot N_{l,k} = \int_0^{N_{l,k}} \left\{T_h - \left[T_{l,k} + \left(T_h - T_{l,k}\right) \cdot \left(1 - e^{-\xi}\right)\right]\right\} \cdot d\xi \quad \text{(Eq. K.22)}$$

$$\Delta T_m \cdot N_{l,k} = \left(T_h - T_{l,k}\right) \cdot \int_0^{N_{l,k}} e^{-\xi} \cdot d\xi = \left(T_h - T_{l,k}\right) \cdot \left(1 - e^{-N_{l,k}}\right) = \Delta T_{l,k} \quad \text{(Eq. K.23)}$$

So,

$$\Delta T_m = \frac{\Delta T_{l,k}}{N_{l,k}} = \frac{\left(T_h - T_{l,k}\right) \cdot \left(1 - e^{-N_{l,k}}\right)}{N_{l,k}} \quad \text{(Eq. K.24)}$$

Reintroducing the differential quantities, the *(l)* stream *NTU*'s for coil '*k*' at position '*s*' is,

$$N_{l,(s,k)} = \frac{d(UA)_{(s,k)}/dS}{dC_{l,k}/dS} \quad \text{(Eq. K.25)}$$

However, if the (UA) and C_l are constant for coil '*k*' between $0 \leq s \leq s_0$, then this is just the previous result of, $N_{l,k} = (UA)_k/C_{l,k}$, which is the *(l)* stream *NTU*'s for coil '*k*'.

The *(h)* stream duty for coil '*k*' at position '*s*' is,

$$\delta q_{h,(k,s)} = -C_{h,k} \cdot dT_h = d(UA)_{(s,k)} \cdot \Delta T_m \quad \text{(Eq. K.26)}$$

We define,

$$dN_{h,(s,k)} = \frac{d(UA)_{(s,k)}}{C_{h,k}} \quad \text{(Eq. K.27)}$$

Note that at position '*S*' (i.e., (*s, k*)), $N_{l,(s,k)}$ is not a differential quantity since there is a finite temperature change, but at position '*S*', $dN_{h,(s,k)}$ is a differential quantity because the temperature change is a differential. However, we can define the gradient,

$$\frac{dN_{h,(s,k)}}{dS} = \frac{d(UA)_{(s,k)}/dS}{C_{h,k}} \quad \text{(Eq. K.28)}$$

Since, $\delta q_{h,(k,s)} = \delta q_{l,(s,k)}$, the relationship between $N_{h,(s,k)}$ and $N_{l,(s,k)}$ is,

$$N_{l,(s,k)} = \frac{C_{h,k}}{\left(dC_{l,k}/dS\right)} \cdot \left(\frac{dN_{h,(s,k)}}{dS}\right) \quad \text{(Eq. K.29)}$$

For coil '*k*',

$$\frac{dC_{l,k}}{dS} = \frac{C_{l,k}}{s_0} \quad \text{(Eq. K.30)}$$

So,

$$N_{l,(s,k)} = s_0 \cdot C_{hl,k} \cdot \left(\frac{dN_{h,(s,k)}}{dS}\right) \quad \text{(Eq. K.31)}$$

with,

$$C_{hl,k} = \frac{C_{h,k}}{C_{l,k}} \quad \text{(Eq. K.32)}$$

And, for coil 'k' between $0 \leq s \leq s_0$, in an integrated average sense,

$$N_{h,(s,k)} = \frac{(UA)_k}{C_{h,k}} \quad \text{(Eq. K.33)}$$

where,

$$(UA)_k = \int_0^{s_0} \left(\frac{d(UA)_{(s,k)}}{ds} \right) \cdot ds \quad \text{(Eq. K.34)}$$

Similarly, we can define for coil 'k' between $0 \leq s \leq s_0$, in an integrated average sense,

$$N_{l,k} = \frac{1}{s_0} \int_0^{s_0} N_{l,(s,k)} \cdot ds = \frac{1}{s_0 \cdot C_{l,k}} \int_0^{s_0} \left(\frac{d(UA)_{(s,k)}}{ds} \right) \cdot ds \quad \text{(Eq. K.35)}$$

So, for coil 'k', the relationship between $N_{l,k}$ and $N_{h,k}$ is simply,

$$N_{l,k} = C_{hl,k} \cdot N_{h,k} \quad \text{(Eq. K.36)}$$

The equation for the *(h)* stream duty at position '*S*' is,

$$\frac{dT_h}{dS} = -\left(\frac{dN_{h,(s,k)}}{dS} \right) \cdot \left(T_h - T_{l,k} \right) \cdot \frac{\left(1 - e^{-N_{l,(s,k)}} \right)}{N_{l,(s,k)}} \quad \text{(Eq. K.37)}$$

Substituting in the expression for $\left(dN_{h,(s,k)}/dS \right)$, and, for coil '$k$', we can switch from the differential 'dS' to 'ds',

$$\frac{dT_h}{ds} = -\left(T_h - T_{l,k} \right) \cdot \frac{\left(1 - e^{-N_{l,(s,k)}} \right)}{s_0 \cdot C_{hl,k}} \quad \text{(Eq. K.38)}$$

Let, $s = s_0 \cdot \chi$, such that, $0 \leq \chi \leq 1$, so,

$$\frac{\partial T_h}{\partial \chi} = -\left(T_h - T_{l,k} \right) \cdot \Lambda_{(\chi,k)} \quad \text{(Eq. K.39)}$$

with,

$$\Lambda_{(\chi,k)} = \frac{(1 - e^{-N_{l,(\chi,k)}})}{C_{hl,k}} \quad \text{(Eq. K.40)}$$

So, the temperature profile for each coil 'k' is,

$$\frac{\partial T_{h,k}}{\partial \chi} + \Lambda_{(\chi,k)} \cdot T_{h,k} = \Lambda_{(\chi,k)} \cdot T_{l,k} \quad \text{(Eq. K.41)}$$

Assuming that Λ is not a function of 'χ', the solution to this differential equation is,

$$T_{h,k}(\chi) = \frac{\int \upsilon_k \cdot \Lambda_k \cdot T_{l,k} \cdot d\chi + B_k}{\upsilon_k} \quad \text{(Eq. K.42)}$$

$$\Lambda_k = \frac{(1 - e^{-N_{l,k}})}{C_{hl,k}} \quad \text{(Eq. K.43)}$$

$$\upsilon_k = e^{\Lambda_k \cdot \chi} \quad \text{(Eq. K.44)}$$

with, B_k an integration constant. For coil, $k = N$, the *(l)* stream temperature inlet (upstream) can be considered uniform (i.e., not a function of χ), so,

$$T_{h,N}(1) = \frac{T_{l,N} \cdot \upsilon_N(1) + B_N}{\upsilon_N(1)} \quad \text{(Eq. K.45)}$$

with,

$$\upsilon_N(1) = e^{\Lambda_N} \quad \text{(Eq. K.46)}$$

$$B_N = \left(T_h(1) - T_{l,N}\right) \cdot \upsilon_N(1) \quad \text{(Eq. K.47)}$$

So,

$$T_{h,N}(\chi) = \frac{T_{l,N} \cdot \upsilon_N + \left(T_{h,N}(1) - T_{l,N}\right) \cdot \upsilon_N(1)}{\upsilon_N} \quad \text{(Eq. K.48)}$$

or,

$$T_{h,N}(\chi) = T_{l,N} + \left(T_{h,N}(1) - T_{l,N}\right) \cdot e^{\Lambda_N(1-\chi)} \quad \text{(Eq. K.49)}$$

At $\chi = 0$ for coil 'N', this is equal to $\chi = 1$ at coil '$N - 1$',

$$T_{h,N}(0) = T_{h,N-1}(1) = T_{l,N} + \left(T_{h,N}(1) - T_{l,N}\right) \cdot \upsilon_N(1) \quad \text{(Eq. K.50)}$$

Previously, it was found that,

$$\Delta T_{l,N} = T_{l,N-1} - T_{l,N} = C_{hl,N} \cdot \Lambda_N \cdot \left(T_{h,N} - T_{l,N}\right) \quad \text{(Eq. K.51)}$$

with,

$$T_{l,N-1} = C_{hl,N} \cdot \Lambda_N \cdot \left(T_{h,N} - T_{l,N}\right) + T_{l,N} \quad \text{(Eq. K.52)}$$

Substituting in the expression for $T_{h,N}$, and simplifying,

$$T_{l,N-1} = T_{l,N} + C_{hl,N} \cdot \Lambda_N \cdot \left(T_{h,N}(1) - T_{l,N}\right) \cdot e^{\Lambda_N(1-\chi)} \quad \text{(Eq. K.53)}$$

The mixed temperature is found by obtaining the integrated average, remembering that $T_{l,N}$, is a constant,

$$\bar{T}_{l,N-1} = \int_0^1 T_{l,N-1} \cdot d\chi = \left[T_{l,N} \cdot \chi - C_{hl,N} \cdot \left(T_{h,N}(1) - T_{l,N}\right) \cdot e^{\Lambda_N(1-\chi)}\right]_0^1 \quad \text{(Eq. K.54)}$$

$$\begin{aligned} \bar{T}_{l,N-1} &= T_{l,N} - C_{hl,N} \cdot \left(T_{h,N}(1) - T_{l,N}\right) \cdot (1 - e^{\Lambda_N}) \\ &= T_{l,N} - C_{hl,N} \cdot \left(T_{h,N}(1) - T_{l,N}\right) \cdot \left(1 - \upsilon_N(1)\right) \end{aligned} \quad \text{(Eq. K.55)}$$

The *(h)* stream temperature effectiveness for coil 'N' is defined as,

$$P_{h,N} = \frac{T_{h,N}(0) - T_{h,N}(1)}{T_{h,N}(0) - \bar{T}_{l,N}} \quad \text{(Eq. K.56)}$$

The *(l)* stream temperature effectiveness for coil 'N' is defined as,

$$P_{l,N} = \frac{\bar{T}_{l,N-1} - \bar{T}_{l,N}}{T_{h,N}(0) - \bar{T}_{l,N}} \quad \text{(Eq. K.57)}$$

For coils $k < N$, if $C_{hl,k} = C_{hl}$ (i.e., it does not vary between each coil),

$$P_{h,k} = \frac{T_{h,k}(0) - T_{h,N}(1)}{T_{h.k}(0) - \bar{T}_{l.N}} \quad \text{(Eq. K.58)}$$

$$P_{l,k} = C_{hl} \cdot P_{h,k} = \frac{\bar{T}_{l,k-1} - \bar{T}_{l,N}}{T_{h,k}(0) - \bar{T}_{l,N}} \quad \text{(Eq. K.59)}$$

Substituting in the expression for $T_{h,N}(0)$, and simplifying for $P_{h,N}$,

$$P_{h,N} = \frac{(\upsilon_N(1) - 1)}{\upsilon_N(1)} = 1 - e^{-\Lambda_N} \quad \text{(Eq. K.60)}$$

and,

$$\left(\frac{1}{1 - P_{h,N}}\right) = \upsilon_N(1) = e^{\Lambda_N} \quad \text{(Eq. K.61)}$$

So, in general, the process is,

1. Integrate the indefinite integral, solving for $T_{h,k}(\chi)$
2. Using the known (or initially specified) value for $T_{h,k}(1)$, solve for the integration constant B_k, which permits a complete solution for $T_{h,k}(\chi)$
3. Evaluate $T_{h,k}(\chi)$ at $\chi = 0$, to obtain $T_{h,k}(0)$
4. Solve (algebraically) for $T_{l,k}(\chi)$

5. If needed, integrate $T_{l,k}(\chi)$ between $0 \leq \chi \leq 1$, to obtain $\bar{T}_{l,k}$
6. If needed, calculate $P_{h,k}$ and/or $P_{l,k}$

The process is repeated for each coil from, $k = N - 1$ to $k = 1$, for a $T_{l,k}$ which is a function of 'χ' (i.e., is not well mixed in between coils) and $N_{h,k}$, $N_{l,k}$, and $C_{hl,k}$ that vary for each coil (but are not a function of 'χ'). And, assuming these are known, a closed form (although, perhaps complicated) solution can be obtained. If we assume that, $\Lambda_k = \Lambda$, $C_{hl,k} = C_{hl}$ and $T_{l,k} = \bar{T}_{l,k}$ (i.e., the *(l)* stream temperature is well mixed in between each coil), for coil $k < N$,

$$T_{h,k}(\chi) = \frac{\int \upsilon \cdot \Lambda \cdot \bar{T}_{l,k} \cdot d\chi + B_k}{\upsilon} = \frac{\Lambda \cdot \bar{T}_{l,k} \cdot \int \upsilon \cdot d\chi + B_k}{\upsilon} = \frac{\bar{T}_{l,k} \cdot \upsilon + B_k}{\upsilon} \quad \text{(Eq. K.62)}$$

$$T_{h,k}(1) = T_{h,k+1}(0) = \frac{\bar{T}_{l,k} \cdot \beta + B_k}{\beta} \quad \text{(Eq. K.63)}$$

$$B_k = \left(T_{h,k+1}(0) - \bar{T}_{l,k}\right) \cdot \beta \quad \text{(Eq. K.64)}$$

with,

$$\upsilon = e^{\Lambda \cdot \chi} \quad \text{(Eq. K.65)}$$

$$\beta = \upsilon(1) = e^{\Lambda} \quad \text{(Eq. K.66)}$$

$$\Lambda = \frac{(1 - e^{-N_l})}{C_{hl}} \quad \text{(Eq. K.67)}$$

so,

$$T_{h,k}(\chi) = \bar{T}_{l,k} + \left(T_{h,k+1}(0) - \bar{T}_{l,k}\right) \cdot \tilde{\upsilon} = T_{h,k+1}(0) \cdot \tilde{\upsilon} + \bar{T}_{l,k} \cdot (1 - \tilde{\upsilon}) \quad \text{(Eq. K.68)}$$

where,

$$\tilde{\upsilon} = \beta \cdot \upsilon^{-1} = e^{\Lambda(1-\chi)} \quad \text{(Eq. K.69)}$$

$$\beta = \tilde{\upsilon}(0) = \upsilon(1) \quad \text{(Eq. K.70)}$$

and,

$$T_{h,k}(0) = \bar{T}_{l,k} + \left(T_{h,k+1}(0) - \bar{T}_{l,k}\right) \cdot \beta = T_{h,k+1}(0) \cdot \beta + \bar{T}_{l,k} \cdot (1 - \beta) \quad \text{(Eq. K.71)}$$

Recalling that,

$$T_{h,k}(1) = T_{h,k+1}(0) \quad \text{(Eq. K.72)}$$

also,

$$T_{l,k-1} = \bar{T}_{l,k} + C_{hl} \cdot \Lambda \cdot \left(T_{h,k}(1) - \bar{T}_{l,k}\right) \cdot \tilde{v} \quad \text{(Eq. K.73)}$$

$$\bar{T}_{l,k-1} = \int_0^1 T_{l,k-1} \cdot d\chi = \left[\bar{T}_{l,k} \cdot \chi - C_{hl} \cdot \left(T_{h,k}(1) - \bar{T}_{l,k}\right) \cdot \tilde{v}\right]_0^1 \quad \text{(Eq. K.74)}$$

$$\bar{T}_{l,k-1} = \bar{T}_{l,k} - C_{hl} \cdot \left(T_{h,k}(1) - \bar{T}_{l,k}\right) \cdot (1 - \beta) \quad \text{(Eq. K.75)}$$

and, the *(h)* stream effectiveness between coil '*N*' and coil '*k*' is,

$$P_{h,k} = \frac{T_{h,k}(0) - T_{h,N}(1)}{T_{h,k}(0) - \bar{T}_{l,N}} \quad \text{(Eq. K.76)}$$

$$\left(\frac{1}{1 - P_{h,k}}\right) = \frac{T_{h,k}(0) - \bar{T}_{l,N}}{T_{h,N}(1) - \bar{T}_{l,N}} \quad \text{(Eq. K.77)}$$

Noting that,

$$\left(\frac{1}{1 - P_{h,N}}\right) = \beta = e^{\Lambda} \quad \text{(Eq. K.78)}$$

The *(l)* stream effectiveness between coil '*N*' and coil '*k*' is,

$$P_{l,k} = C_{hl} \cdot P_{h,k} = \frac{\bar{T}_{l,k-1} - \bar{T}_{l,N}}{T_{h,k}(0) - \bar{T}_{l,N}} \quad \text{(Eq. K.79)}$$

We can adopt some more simple notations to elucidate the pattern for '*N*' coils. Let,

$$x_k = T_{h.k+1}(0) = T_{h.k}(1) \quad \text{(Eq. K.80)}$$

$$y_k = \bar{T}_{l.k} \quad \text{(Eq. K.81)}$$

$$r = C_{hl} \quad \text{(Eq. K.82)}$$

$$\alpha = -r \cdot (1 - \beta) \quad \text{(Eq. K.83)}$$

So, with x_N and y_N known/specified, the recursive relations are,

$$x_k = \beta \cdot x_{k+1} + (1 - \beta) \cdot y_{k+1} \quad \text{(Eq. K.84)}$$

$$y_k = \alpha \cdot x_{k+1} + (1 - \alpha) \cdot y_{k+1} \quad \text{(Eq. K.85)}$$

and,

$$\left(\frac{1}{1-P_{h,k}}\right)=\frac{x_{k-1}-y_N}{x_N-y_N} \qquad \text{(Eq. K.86)}$$

Expanding and simplifying these equations for 1 to 5 coils yields the following:

N	$\left[\mathbf{1}/\left(\mathbf{1}-\boldsymbol{P}_{\boldsymbol{h,1}}\right)\right]$
1	$+\beta$
2	$-\beta^2\cdot(r-1)+2\beta\cdot r-r$
3	$+\beta^3\cdot(r-1)^2-3\beta^2\cdot(r-1)\cdot r+3\beta\cdot r^2-r\cdot(1+r)$
4	$-\beta^4\cdot(r-1)^3+4\beta^3\cdot(r-1)^2\cdot r-6\beta^2\cdot(r-1)\cdot r^2+4\beta\cdot r^3-r\cdot(1+r+r^2)$
5	$+\beta^5\cdot(r-1)^4-5\beta^4\cdot(r-1)^3\cdot r+10\beta^3\cdot(r-1)^2\cdot r^2-10\beta^2\cdot(r-1)\cdot r^3+5\beta\cdot r^4-r\cdot(1+r+r^2+r^3)$

This is sufficient to inductively arrive at the following formula,

$$\left(\frac{1}{1-P_{h,1}}\right)=\sum_{k=1}^{N}\binom{N}{k+1}\cdot(-1)^{(k+1)}\cdot\beta^k\cdot(r-1)^{(k-1)}\cdot r^{(N-k)} - \sum_{k=1}^{N} r^{(k-1)}+1 \qquad \text{(Eq. K.87)}$$

where,

$$\binom{N}{k+1}=\frac{N!}{(k+1)!\cdot(N-k-1)!} \qquad \text{(Eq. K.88)}$$

If $r\neq 1$, we can multiply by $(r-1)$ and then adjust the first summation index to begin at $i=0$,

$$\left(\frac{r-1}{1-P_{h,1}}\right)=-\sum_{k=0}^{N}\left[\binom{N}{k}\cdot(-1)^k\cdot\beta^k\cdot(r-1)^k\cdot r^{(N-k)}\right]+r^N - (r-1)\cdot\left\{\sum_{k=1}^{N} r^{(k-1)}-1\right\} \qquad \text{(Eq. K.89)}$$

where,

$$\binom{N}{k}=\frac{N!}{k!\cdot(N-k)!} \qquad \text{(Eq. K.90)}$$

The first summation term is recognized as a binomial series and the second summation a geometric series. Substituting the closed form expressions for these finite summations, we have,

$$\left(\frac{r-1}{1-P_{h,1}}\right) = -[r-\beta\cdot(r-1)]^N + r^N - (r-1)\cdot\left[\left(\frac{r^N-1}{r-1}\right)-1\right] \qquad \text{(Eq. K.91)}$$

Dividing through by $(r-1)$, and simplifying,

$$\left(\frac{1}{1-P_{h,1}}\right) = \frac{-[r-\beta\cdot(r-1)]^N + r}{r-1} = \frac{\mathrm{Z}^{-N}-r}{1-r} \qquad \text{(Eq. K.92)}$$

where,

$$\mathrm{Z} = \frac{1-P_{h,N}}{1-r\cdot P_{h,N}} \qquad \text{(Eq. K.93)}$$

or, solving for the *(h)* stream effectiveness,

$$P_{h,1} = \frac{1-\mathrm{Z}^N}{1-r\cdot\mathrm{Z}^N} \qquad \text{(Eq. K.94)}$$

This solution is the same as presented in (Barron, Cryogenic heat transfer 1999), which does not provide either a reference or a derivation.

If $r = 1$, many of the terms in the initial summation become zero, so that,

$$\begin{aligned}\left(\frac{1}{1-P_{h,1}}\right) &= \binom{N}{N-1}\cdot\beta\cdot r^{(N-1)} - \left(\sum_{k=1}^{N} r^{(k-1)} - 1\right) \\ &= N\cdot\beta - (N-1) = N\cdot(\beta-1)+1\end{aligned} \qquad \text{(Eq. K.95)}$$

Or, solving for the *(h)* stream effectiveness,

$$P_{h,1} = \frac{N\cdot P_{h,N}}{1+(N-1)\cdot P_{h,N}} \qquad \text{(Eq. K.96)}$$

This configuration has been referred to as cross-counter flow heat exchange, because the shell flow is cross flow over each coil, but is overall counter flow to the tube flow. Now that a compact and closed form relationship has been derived, assuming constant stream capacities and uniform net thermal rating, (UA), with the shell flow well mixed in between each coil, we would like to compare this to the case where the shell flow is not mixed in between each coil. In a Collins-type heat exchanger, the actual condition will be somewhere in between these two extremes. As

mentioned previously, although the case where the shell flow is unmixed between each coil can be obtained in close form, a compact solution is not known. Therefore, we will utilize Mathematica's formidable capabilities to obtain the (lengthy) closed form solution for the unmixed shell flow and compare to the compact solution assuming a well-mixed shell flow between coils. The following table describes the variables used for the Mathematica code (see Appendix L).

Table K.1. Mathematica code variable list and description

Variable	Description
tt1	Array of 't1' for each coil
tt1m	Array of 't1m' for each coil
tt1i	Array of 'tt1' at s = 0 for each coil
tt1im	Array of 'tt1m' at s = 0 for each coil
tt2	Array of 't2' for each coil
tt2a	Array of 't1a' for each coil
tt2m	Array of 't2m' for each coil
tt2am	Array of 't2am' for each coil
t1	Unmixed *(l)* stream (shell) flow case: *(h)* stream temperature profile as a function of arc length for coil 'k'
t1i	Unmixed *(l)* stream (shell) flow case: *(h)* stream temperature at s = 0 for coil 'k'
t1m	Mixed *(l)* stream (shell) flow case: *(h)* stream temperature profile as a function of arc length for coil 'k'
t1im	Mixed *(l)* stream (shell) flow case: *(h)* stream temperature at s = 0 for coil 'k'
t2	Unmixed *(l)* stream (shell) flow case: *(l)* stream temperature profile as a function of arc length for coil 'k'
t2m	Mixed *(l)* stream (shell) flow case: *(l)* stream temperature profile as a function of arc length for coil 'k'
t2a	Unmixed *(l)* stream (shell) flow case: *(l)* stream integrated average temperature for coil 'k'
t2am	Mixed *(l)* stream (shell) flow case: *(l)* stream integrated average temperature for coil 'k'
t1ce	*(h)* stream temperature at cold-end of heat exchanger (k = N)
t2ce	*(l)* stream temperature at cold-end of heat exchanger (k = N)
t10	't1i' with variable substitution
t10m	't1im' with variable substitution
t20	't2a' with variable substitution
t20m	't2am' with variable substitution
i	Coil index
k	Coil number; k = 1 is the warm-end, k = N is the cold-end
nk	Number of coils
s	Arc length along *(h)* stream tube center-line for coil 'k'
L	= {1 - exp(-r·Nh)}/r
b	= exp(L)
r	Ratio of *(h)* to *(l)* stream capacity; same for all coils
Nh	Total heat exchanger *(h)* stream *NTU*'s

Table K.1. Continued

s1	Function for *(h)* stream temperature profile for coil 'k'
cc	Array of 'c' for each coil
ccm	Array of 'cm' for each coil
c	Unmixed *(l)* stream (shell) flow case: integration constants for *(h)* stream temperature profile for coil 'k'
cm	Mixed *(l)* stream (shell) flow case: integration constants for *(h)* stream temperature profile for coil 'k'
p1	Unmixed *(l)* stream (shell) flow case: current (from 'N' to 'k') coil *(h)* stream effectiveness
p1m	Mixed *(l)* stream (shell) flow case: current (from 'N' to 'k') coil *(h)* stream effectiveness
p1mcs	Compact solution of 'p1m'
p1cs	Compact solution for cross-counter flow *(h)* stream effectiveness
p1cf	Counter-flow *(h)* stream effectiveness
p1xf	Cross-flow {*(h)* stream mixed, *(l)* stream unmixed, across coil} *(h)* stream effectiveness
pp	Array of '(1-1/ip1)'
ppm	Array of '(1-1/ip1m)'
ip	Unmixed *(l)* stream (shell) flow case: inverse of one minus *(h)* stream effectiveness for 'k' coils
ipm	Mixed *(l)* stream (shell) flow case: inverse of one minus *(h)* stream effectiveness for 'k' coils
ip1mcs	Compact solution of inverse of one minus *(h)* stream effectiveness for 'k' coils for mixed *(l)* stream case
ip1	Unmixed *(l)* stream (shell) flow case: current (from 'N' to 'k') coil inverse of one minus *(h)* stream effectiveness
ip1m	Mixed *(l)* stream (shell) flow case: current (from 'N' to 'k') coil inverse of one minus *(h)* stream effectiveness
ddp	Difference between unmixed and mixed solution for *(h)* stream effectiveness
ddpm	Difference between mixed non-compact and mixed compact solution of *(h)* stream effectiveness
dpmcs	Difference between mixed compact solutions: a check
dpxf	Difference between mixed compact solution for a single coil to cross-flow over a single coil: a check

The code itself is rather intuitive and does not require further explanation to understand. The description of what follows is in reference to Appendix L. The term “mixed” specifically distinguishes the cross-counter flow case where the *(l)* stream (shell side) fluid is well mixed in between each coil vs. the case of “unmixed” where it is not. Obviously, in the latter case the *(l)* stream is a function of the arc length position as it approaches each coil, where for the former case it is not. The first (text) output is for the equations of $1/\left(1-P_{h,1}\right)$ for the ‘unmixed’ and ‘mixed’ cases for the stated number of coils (only up to five is shown). The second (figure) output shows curves of the difference of the *(h)* stream effectiveness between cross-counter flow for the case of

unmixed *(l)* stream flow and mixed *(l)* stream flow in between the coils vs. the total *(h)* stream *NTU*'s. Each curve corresponds to the stated number of coils ('*k*'). As can been seen the difference increases as the *(h)* stream total *NTU*'s increases, but at a diminishing rate. The next three (figure) outputs are checks. The first of the three shows the difference between the algebraic solution for the mixed case (calculated by Mathematica) and the derived compact solution, presented in the form of, $1/\left(1-P_{h,1}\right)$ (but labelled in the code as, 'ip1mcs'). The second of the three is the difference between the compact solution for the *(h)* stream effectiveness and as calculated from 'ip1mcs'. The third is the difference between the compact solution for the *(h)* stream effectiveness for a single coil and for pure cross-flow (with the *(h)* stream 'mixed' and the *(l)* stream 'unmixed', as termed and labelled in the literature; for example, see Shah and Sekulic (Fundamentals of heat exchanger design 2003, 145, Table 3.6, Equ. II.3.1). The error for these three should be very small, which as shown, is true. The fifth figure shows curves for the *(h)* stream effectiveness vs. the total *(h)* stream *NTU*'s for the pure counter flow case, pure cross-flow case and the cross-counter flow case if the *(l)* stream is well-mixed in between coils. Note that the case for a single coil cross-counter flow ($k = 1$) precisely overlaps the cross-flow case, as expected. The sixth and last figure shows a three-dimensional surface of the *(h)* stream effectiveness vs the *(h)* stream total *NTU*'s and the *(h)* to *(l)* stream capacity ratio for the cross-counter flow case with the *(l)* stream well-mixed in between each coil and for five coils.

APPENDIX L – MATHEMATICA ANALYSIS OF COLLINS HEAT EXCHANGER EFFECTIVENESS

```
(* Collins HX Effectiveness - Cross-Counter Flow *)
(* P. Knudsen, 30-July-2016 *)
s1[s_, s2_, c_] := (L Integrate[s2 Exp[L s], s] + c) / Exp[L s]

Clear[t1ce, t2ce, b, i, L, Nh, k, nk, r];
Clear[tt1, tt1m, tt1i, tt1im, tt2, tt2m, tt2a, tt2am, cc, ccm, pp, ppm, ddp, ddpm];
Clear[t10, t10m, t20, t20m, p1, p1m, ip1, ip1m, ip1mcs];

nk = 5;

tt1 = Array[t1, nk]; tt1i = Array[t1i, nk + 1]; tt1i[[nk + 1]] = t1ce;

tt1m = Array[t1m, nk]; tt1im = Array[t1im, nk + 1]; tt1im[[nk + 1]] = t1ce;

tt2 = Array[t2, nk, 0]; tt2[[nk]] = t2ce; tt2a = Array[t2a, nk, 0]; tt2a[[nk]] = t2ce;
pp = Array[p, nk]; cc = Array[c, nk];

tt2m = Array[t2m, nk, 0]; tt2m[[nk]] = t2ce; tt2am = Array[t2am, nk, 0]; tt2am[[nk]] = t2ce;
ppm = Array[pm, nk]; ccm = Array[cm, nk];

ddp = Array[dp, nk]; ddpm = Array[dpm, nk];

ip1mcs = (r - (r + (1 - r) Exp[(1 - Exp[-r Nh]) / r]) ^k) / (r - 1);

For[i = nk, i > 0, i--, tt1[[i]] = s1[s, tt2[[i]], cc[[i]]];
 tt1m[[i]] = s1[s, tt2m[[i]], ccm[[i]]];
 cc[[i]] = c[i] /. Solve[(tt1[[i]] /. s → 1) - tt1i[[i + 1]] == 0, c[i]][[1]];
 ccm[[i]] = cm[i] /. Solve[(tt1m[[i]] /. s → 1) - tt1im[[i + 1]] == 0, cm[i]][[1]];
 tt1[[i]] = Simplify[tt1[[i]] /. c[i] → cc[[i]]];
 tt1m[[i]] = Simplify[tt1m[[i]] /. cm[i] → ccm[[i]]];
 tt2[[i - 1]] = Simplify[-r D[tt1[[i]], s] + tt2[[i]]];
 tt2m[[i - 1]] = Simplify[-r D[tt1m[[i]], s] + tt2m[[i]]];
 tt1i[[i]] = Simplify[tt1[[i]] /. s → 0];
 tt1im[[i]] = Simplify[tt1m[[i]] /. s → 0];
 tt2a[[i - 1]] = Simplify[Integrate[tt2[[i - 1]], {s, 0, 1}]];
 tt2am[[i - 1]] = Simplify[Integrate[tt2m[[i - 1]], {s, 0, 1}]];
 tt2m[[i - 1]] = tt2am[[i - 1]];
 k = nk - i + 1;
 Print["Coil #: ", k];
 t10 = Simplify[TrigToExp[tt1i[[i]]] /. Exp[(a_ L | L)] → b^a];
 t10m = Simplify[TrigToExp[tt1im[[i]]] /. Exp[(a_ L | L)] → b^a];
 t20 = Simplify[TrigToExp[tt2a[[i - 1]]] /. Exp[(a_ L | L)] → b^a];
 t20m = Simplify[TrigToExp[tt2am[[i - 1]]] /. Exp[(a_ L | L)] → b^a];
 p1 = (t10 - t1ce) / (t10 - t2ce);
 p1m = (t10m - t1ce) / (t10m - t2ce);
 ip1 = Simplify[1 / (1 - p1)];
 ip1m = Simplify[1 / (1 - p1m)];
 Print["Unmixed 1/(1-P1)=", ip1];
 Print["Mixed 1/(1-P1)=", ip1m];
 ip1 = ip1 /. b → Exp[L];
 ip1m = ip1m /. b → Exp[L];
 ip1 = ip1 /. L → (1 - Exp[-r Nh]) / r;
 ip1m = ip1m /. L → (1 - Exp[-r Nh]) / r;
 pp[[i]][Nh_, r_] := Evaluate[(1 - 1 / ip1)];
 ppm[[i]][Nh_, r_] := Evaluate[(1 - 1 / ip1m)];
 ddp[[i]][Nh_, r_] := Evaluate[(1 - 1 / ip1) - (1 - 1 / ip1m)];
 ddpm[[i]][Nh_, r_] := Evaluate[(1 - 1 / ip1m) - (1 - 1 / ip1mcs)];
 Print[];]
```

Coil #: 1

Unmixed $1/(1-P1)=b$

Mixed $1/(1-P1)=b$

Coil #: 2

Unmixed $1/(1-P1)=b\left(b-L^2\,r\right)$

Mixed $1/(1-P1)=-b^2\,(-1+r)-r+2\,b\,r$

Coil #: 3

Unmixed $1/(1-P1)=\frac{1}{2}\,b\left(2\,b^2-4\,b\,L^2\,r+L^2\,r\left(-2+2\,L\,r+L^2\,r\right)\right)$

Mixed $1/(1-P1)=b^3\,(-1+r)^2-3\,b^2\,(-1+r)\,r+3\,b\,r^2-r\,(1+r)$

Coil #: 4

Unmixed $1/(1-P1)=\frac{1}{6}\,b\left(6\,b^3-18\,b^2\,L^2\,r+12\,b\,L^2\,r\left(-1+L\,r+L^2\,r\right)-L^2\,r\left(6-12\,L\,r+6\,L^2\,(-1+r)\,r+6\,L^3\,r^2+L^4\,r^2\right)\right)$

Mixed $1/(1-P1)=-b^4\,(-1+r)^3+4\,b^3\,(-1+r)^2\,r-6\,b^2\,(-1+r)\,r^2+4\,b\,r^3-r\left(1+r+r^2\right)$

Coil #: 5

Unmixed $1/(1-P1)=$

$$\frac{1}{24}\,b\left(24\,b^4-96\,b^3\,L^2\,r+36\,b^2\,L^2\,r\left(-2+2\,L\,r+3\,L^2\,r\right)-16\,b\,L^2\,r\left(3-6\,L\,r+3\,L^2\,(-2+r)\,r+6\,L^3\,r^2+2\,L^4\,r^2\right)+L^2\,r\left(-24+72\,L\,r+36\,L^2\,(1-2\,r)\,r+24\,L^3\,(-3+r)\,r^2+12\,L^5\,r^3+L^6\,r^3+12\,L^4\,r^2\,(-1+3\,r)\right)\right)$$

Mixed $1/(1-P1)=b^5\,(-1+r)^4-5\,b^4\,(-1+r)^3\,r+10\,b^3\,(-1+r)^2\,r^2-10\,b^2\,(-1+r)\,r^3+5\,b\,r^4-r\left(1+r+r^2+r^3\right)$

```
Plot[Evaluate[Table[ddp[[i]][Nh / (nk - i + 1), 0.99999], {i, nk}]],
 {Nh, 0, 10}, AxesLabel → {Nh, Difference},
 PlotLegends → {"k=5", "k=4", "k=3", "k=2", "k=1"}, AspectRatio → 0.8372]
```

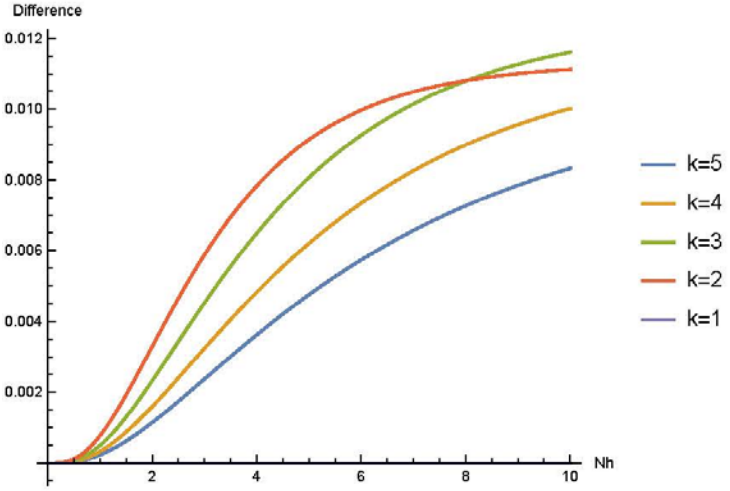

Figure L.1. Difference between unmixed and mixed cases for *(h)* stream effectiveness vs. *(h)* stream *NTU*'s

```
Plot[Evaluate[Table[ddpm[[i]][Nh / (nk - i + 1), 0.99999], {i, nk}]], {Nh, 0, 10},
 AxesLabel → {Nh, Error}, PlotLegends → {"k=5", "k=4", "k=3", "k=2", "k=1"},
 PlotRange → {{0, 10}, {-0.0000000001, 0.0000000001}}, AspectRatio → 0.8372]
```

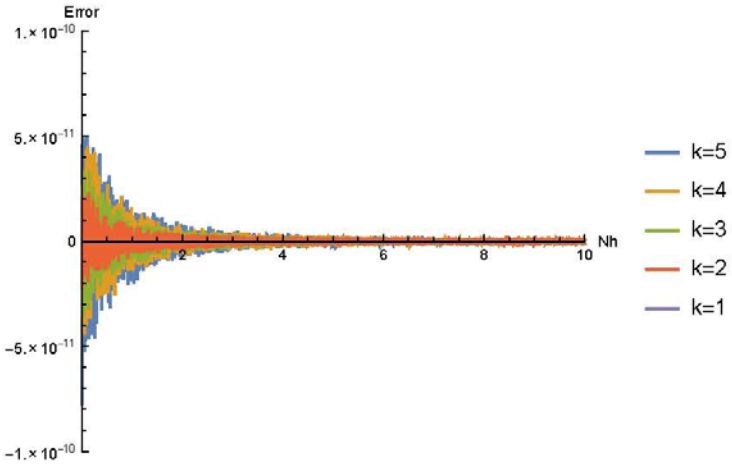

Figure L.2. Difference between algebraic solution for the mixed case, as calculated by Mathematica, and the derived compact solution vs. *(h)* stream *NTU*'s

```
Clear[p1xf, pxf, z, zz, k, p1m, dpmcs];
p1xf = 1 - Exp[-(1 - Exp[-r Nh]) / r];
zz = (1 - pxf) / (1 - r pxf);
p1m = (1 - z^k) / (1 - r z^k);
p1m = p1m /. z → zz;
p1m = p1m /. pxf → p1xf;
dpmcs[k_, Nh_, r_] := Evaluate[p1m - (1 - 1 / ip1mcs)]
Plot[Evaluate[Table[dpmcs[i, Nh / i, 0.99999], {i, nk}]], {Nh, 0, 10},
 AxesLabel → {Nh, Error}, PlotLegends → {"k=1", "k=2", "k=3", "k=4", "k=5"},
 PlotRange → {{0, 10}, {-0.0000000001, 0.0000000001}}, AspectRatio → 0.8372]
```

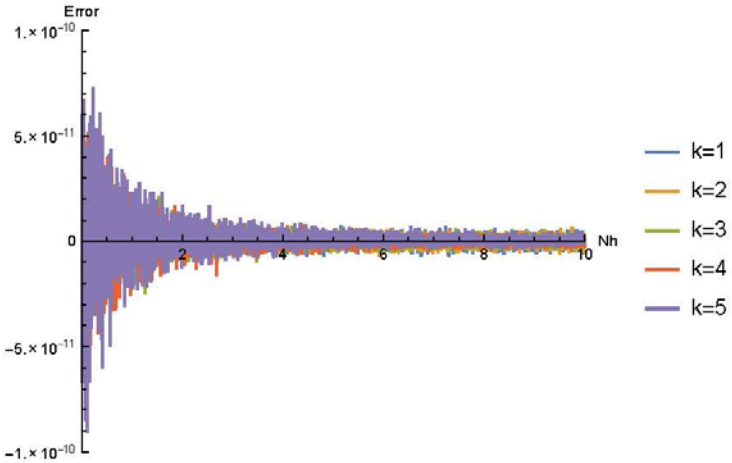

Figure L.3. Difference between the compact solution for the *(h)* stream effectiveness and as calculated from 'ip1mcs' vs. *(h)* stream *NTU*'s

```
Clear[dpxf];
dpxf[Nh_, r_] := Evaluate[p1xf - (1 - 1 / (ip1mcs /. k → 1))];
Plot[Evaluate[dpxf[Nh, 0.99999]], {Nh, 0, 10}, AxesLabel → {Nh, Error}, AspectRatio → 0.8372]
```

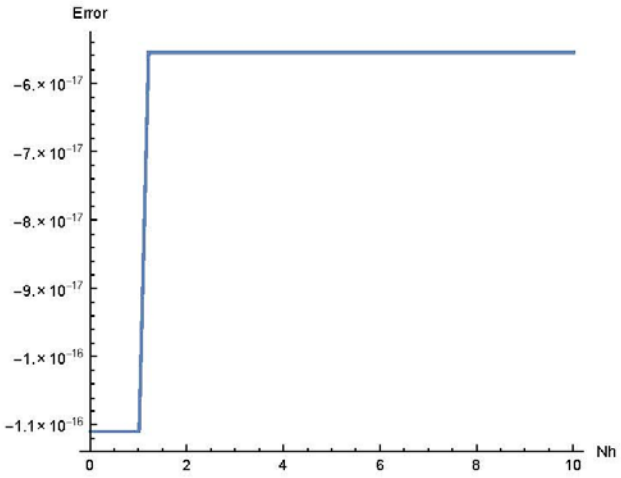

Figure L.4. Difference between compact solution for the *(h)* stream effectiveness for a single coil and for pure cross-flow vs. *(h)* stream *NTU*'s

```
Clear[p1xf];
p1xf[Nh_, r_] := 1 - Exp[- (1 - Exp[- r Nh]) / r];
Clear[p1cs];
p1cs[k_, Nh_, r_] := Evaluate[(1 - 1 / ip1mcs)];
Clear[p1cf];
p1cf[Nh_, r_] := If[r == 1, Nh / (1 + Nh), (1 - Exp[- Nh (1 - r)]) / (1 - r Exp[- Nh (1 - r)])];
Plot[Evaluate[{p1cf[Nh, 0.99999], p1xf[Nh, 0.99999], Table[p1cs[i, Nh / i, 0.99999], {i, nk}]}],
 {Nh, 0, 10}, PlotRange → {{0, 10}, {0, 1}}, AxesLabel → {Nh, Effectiveness},
 PlotLegends → {"Counter-Flow", "Cross-Flow", "Mixed: k=1",
   "Mixed: k=2", "Mixed: k=3", "Mixed: k=4", "Mixed: k=5"}, AspectRatio → 0.8372]
```

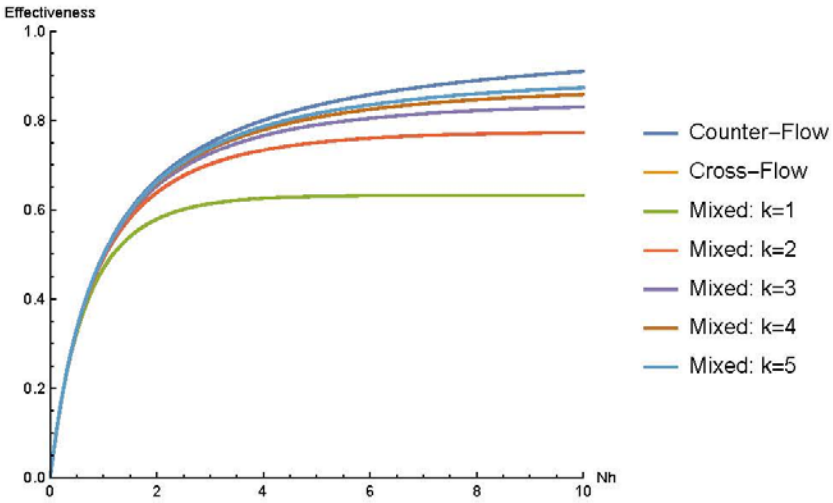

Figure L.5. *(h)* stream effectiveness vs. *(h)* stream *NTU*'s for pure counter flow, pure cross-flow and for the case if the *(l)* stream is well mixed in between coils

```
k = 5;
Plot3D[plcs[k, Nh / k, r], {Nh, 0, 10}, {r, 0.5, 2}, AxesLabel → {Nh, r, Effectiveness}]
```

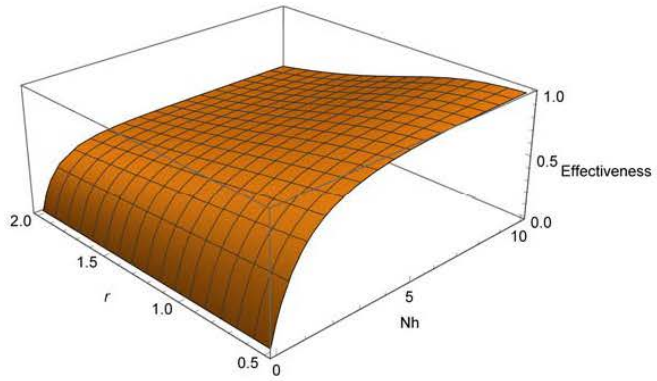

Figure L.6. *(h)* stream effectiveness for the case if the *(l)* stream is well mixed in between coils vs. *(h)* stream *NTU*'s and the *(h)* to *(l)* stream capacity ratio (*r*)

APPENDIX M – SURVEY: COLLINS HEAT EXCHANGER, SHELL SIDE, SINGLE WRAP, PRESSURE DROP AND HEAT TRANSFER CORRELATIONS

General Nomenclature (for this appendix):

Variable	Units	Description
d_o	L	*Outside diameter of tube*
d_f	L	*Diameter of fin-tube (to tip of fin); also, the coil pitch*
h_f	L	*Height of fin,* $= (d_f - d_o)/2$
D_c	L	*Coil diameter (coil axis to tube center)*
D_m	L	*Mandrel diameter,* $= D_c - d_f$
n	L^{-1}	*Fin density (number of fins per unit length along tube)*
t	L	*Fin thickness*
A_c	L^2	*Flow cross-sectional area*
A_s'	L	*Heat transfer surface area per length along coil axis*
L	L	*Coil axial length,* $= N_c \cdot d_f$
N_c		*Number of coils*
D_h	L	*Hydraulic diameter,* $= 4r_h$
r_h	L	*Hydraulic radius*
G	$M/(TL^2)$	*Mass flux*
ρ	M/L^3	*Fluid density*
C_p	$L^2/(T^2\theta)$	*Fluid specific heat at constant pressure*
μ	M/(TL)	*Fluid dynamic viscosity*
k	$ML/(T^3\theta)$	*Fluid thermal conductivity*
Eu		*Euler number (stagnation pressure)*
Re		*Reynolds number*
f		*Fanning friction factor,* $= \zeta/(L/r_h)$
ζ		*Flow resistance,* $= \Delta p/Eu$
Nu		*Nusselt number*
Δp	$M/(LT^2)$	*Pressure drop*
h	$M/(T^3\theta)$	*Heat transfer coefficient*
j_H		*Colburn 'j' factor*

Units: L, M, T, θ – length, mass, time, temperature, respectively

1. CTI (Pressure Drop and Heat Transfer); refer to Ganni (Design and optimization of helium refrigeration and liquefaction systems 2009, Appendix E)

The following applies to the shell side with a single wrap. For the Euler number (i.e., stagnation pressure), the projected cross-sectional area is used for the mass flux,

$$A_{c(p)} = \pi D_c \cdot \left(d_f - d_o\right) \cdot (1 - n \cdot t) \qquad \text{(Eq. M.1)}$$

This is the free flow cross-sectional area as if the coil had no helix angle, cut through the tube center line (by an imaginary plane perpendicular to the coil axis). The mass flux used for the Euler number is,

$$G_{(p)} = \frac{\dot{m}}{A_{c(p)}} \qquad \text{(Eq. M.2)}$$

and, the Euler number is,

$$Eu_{(p)} = \frac{{G_{(p)}}^2}{2\rho} \qquad \text{(Eq. M.3)}$$

However, the volume averaged flow cross-sectional area is used for the hydraulic radius and the mass flux used for the Reynolds number, that is,

$$A_{c(v)} = \tfrac{1}{4}\pi^2 D_c \cdot \left({d_f}^2 - {d_o}^2\right) \cdot (1 - n \cdot t)/d_f \qquad \text{(Eq. M.4)}$$

This is the annular volume between the circular fins for one coil divided by the fin outside diameter. The heat transfer surface area per unit length along the coil axis (which can also be known as the average heated perimeter) is taken as,

$${A_{s(1)}}' = \pi^2 D_c \cdot \left[\frac{n}{2}\left({d_f}^2 - {d_o}^2\right) + d_o\right]/d_f \qquad \text{(Eq. M.5)}$$

This is (all) the tube surface outside diameter and both sides of the fin faces; so, it includes the fin base area (which it should not) and does not include the fin tip area (which it should). It also treats the coil length as, πD_c. So, the hydraulic radius is,

$$r_{h(1)} = \frac{A_{c(v)}}{{A_{s(1)}}'} \qquad \text{(Eq. M.6)}$$

The Reynold's number is found as,

$$Re_{(1)} = \frac{G_{(v)} \cdot \left(4r_{h(1)}\right)}{\mu} = \frac{4 \cdot \dot{m}}{\mu \cdot {A_{s(1)}}'} \qquad \text{(Eq. M.7)}$$

where the mass flux used for the Reynolds number is,

$$G_{(v)} = \frac{\dot{m}}{A_{c(v)}} \quad \text{(Eq. M.8)}$$

This is used for correlating the friction factor and the Nusselt number.

$$f_{(1)} = B_{f(1)} \cdot {Re_{(1)}}^{-\nu_{(1)}} \quad \text{(Eq. M.9)}$$

$$Nu_{(1)} = B_{j(1)} \cdot {Re_{(1)}}^{(1-\vartheta_{(1)})} \cdot Pr^{1/3} \quad \text{(Eq. M.10)}$$

where,

$$B_{f(1)} = 2.2;\ \nu_{(1)} = 0.38;\ \text{for, } 25 \leq Re_{(1)} \leq 500 \quad \text{(Eq. M.11)}$$

$$B_{j(1)} = 0.0348\ ;\ \left(1 - \vartheta_{(1)}\right) = 0.87 \quad \text{for, } 20 \leq Re_{(1)} \leq 100 \quad \text{(Eq. M.12)}$$

So, the pressure drop is found by,

$$\Delta p_{(1)} = Eu_{(p)} \cdot \zeta_{(1)} \quad \text{(Eq. M.13)}$$

where,

$$\zeta_{(1)} = f_{(1)} \cdot \frac{L}{r_{h(1)}} \quad \text{(Eq. M.14)}$$

The heat transfer coefficient is found by,

$$h_{(1)} = \frac{Nu_{(1)} \cdot k}{\left(4r_{h(1)}\right)} \quad \text{(Eq. M.15)}$$

Or, alternatively, the Colburn factor,

$$j_{H(1)} = h_{(1)} \cdot \frac{Pr^{\frac{2}{3}}}{C_p \cdot G_{(v)}} = \frac{Nu_{(1)}}{Re_{(1)} \cdot Pr^{\frac{1}{3}}} = B_{j(1)} \cdot {Re_{(1)}}^{-\vartheta_{(1)}} \quad \text{(Eq. M.16)}$$

2. Croft & Tebby (Heat Transfer); refer to Croft and Tebby (The design of finned-tube cryogenic heat exchangers 1970)

The following applies to the shell side with a single wrap. The volume averaged flow cross-sectional area, $A_{c(v)}$, is used for the mass flux, $G_{(v)}$, and hydraulic radius. The heat transfer

surface area per unit length along the coil axis (which can also be known as the average heated perimeter) is taken as,

$$A_{s(2)}{}' = \pi^2 D_c \cdot \left[\frac{n}{2}\left(d_f - d_o\right)^2 + d_o(1 - n \cdot t)\right] \qquad \text{(Eq. M.17)}$$

This is both sides of the fin faces and the tube surface area adjacent to the fins; so, it does not include the fin tip area, $\pi^2 D_c \cdot \left(d_f \cdot n \cdot t\right)/d_f$. It also treats the coil length as, πD_c. So, the hydraulic radius is,

$$r_{h(2)} = \frac{A_{c(v)}}{A_{s(2)}{}'} \qquad \text{(Eq. M.18)}$$

The Reynold's number is found as,

$$Re_{(2)} = \frac{G_{(v)} \cdot \left(4 r_{h(2)}\right)}{\mu} = \frac{4 \cdot \dot{m}}{\mu \cdot A_{s(2)}{}'} \qquad \text{(Eq. M.19)}$$

This is used for correlating the Nusselt number. However, Croft and Tebby do not offer a correlation for the friction factor based upon measurements.

$$Nu_{(2)} = B_{j(2)} \cdot Re_{(2)}{}^{\left(1-\vartheta_{(2)}\right)} \cdot Pr \qquad \text{(Eq. M.20)}$$

where,

$$B_{j(2)} = 0.02771 \; ; \left(1 - \vartheta_{(2)}\right) = 0.80 \qquad \text{(Eq. M.21)}$$

A Reynolds number range is not provided by (Croft and Tebby 1970). But, (Gupta, Kush and Tiwari, Experimental research on heat transfer coefficients from cryogenic cross-counter-flow finned-tube heat exchangers 2009) indicate that this correlation falls within ±10% of their data, which is for low finned height, high fin density tubing; $\left(d_f/d_o\right) = 1.262$, and $n = 26$ fins/in. The approximate Reynolds number range is 500 to 1900. However, their data fit corresponds to using the volume averaged flow cross-sectional area ($A_{c(v)}$) and $A_s{}'$ (instead of $A_{s(2)}{}'$) for the heat transfer surface area for obtaining the hydraulic radius. Also, the finned tubes in (Croft and Tebby 1970) were high fin height and low fin density; $\left(d_f/d_o\right) = 2.313$ and 3.198, and $n = 9$ fins/in

(for both). Following the definitions given by (Croft and Tebby 1970), the heat transfer coefficient is found by,

$$h_{(2)} = \frac{Nu_{(2)} \cdot k}{\left(4r_{h(2)}\right)} \qquad \text{(Eq. M.22)}$$

Or, alternatively, the Colburn factor,

$$j_{H(2)} = h_{(2)} \cdot \frac{Pr^{\frac{2}{3}}}{C_p \cdot G_{(v)}} = \frac{Nu_{(2)}}{Re_{(2)} \cdot Pr^{\frac{1}{3}}} = B_{j(2)} \cdot {Re_{(2)}}^{-\vartheta_{(2)}} \cdot Pr^{2/3} \qquad \text{(Eq. M.23)}$$

3. Gupta, Kush & Tiwari (Pressure Drop); refer to Gupta, et al. (Experimental studies on pressure drop characteristics of cryogenic cross-counter flow coiled finned tube heat exchangers 2010)

The following applies to the shell side with a single wrap. The projected cross-sectional area ($A_{c(p)}$) is used for the mass flux, $G_{(p)}$, associated with both the Euler number, $Eu_{(p)}$, Reynolds number and hydraulic radius. The heat transfer surface area per unit length along the coil axis (which can also be known as the average heated perimeter) is taken as,

$${A_s}' = \pi^2 D_c \cdot \left[\frac{n}{2}\left(d_f - d_o\right)^2 + d_o(1 - n \cdot t) + d_f \cdot n \cdot t\right] / d_f \qquad \text{(Eq. M.24)}$$

This is both sides of the fin faces and the tube surface area adjacent to the fins and the fin tip area. It also treats the coil length as, πD_c. So, the hydraulic radius is,

$$r_{h(3)} = \frac{A_{c(p)}}{{A_s}'} \qquad \text{(Eq. M.25)}$$

The Reynold's number is found as,

$$Re_{(3)} = \frac{G \cdot \left(4r_{h(3)}\right)}{\mu} = \frac{4 \cdot \dot{m}}{\mu \cdot {A_s}'} \qquad \text{(Eq. M.26)}$$

where,

$$G = \frac{\dot{m}}{{A_s}'} \qquad \text{(Eq. M.27)}$$

This is used for correlating the friction factor and the Nusselt number.

$$f_{(3)} = B_{f(3)} \cdot Re_{(3)}{}^{-\nu_{(3)}} \qquad \text{(Eq. M.28)}$$

where,

$$B_{f(3)} = 6.175 \; ; \nu_{(3)} = 0.489 \quad \text{for, } 25 \leq Re \leq 155 \qquad \text{(Eq. M.29)}$$

And, the pressure drop is found by,

$$\Delta p_{(3)} = Eu_{(p)} \cdot \zeta_{(3)} \qquad \text{(Eq. M.30)}$$

where,

$$\zeta_{(3)} = f_{(3)} \cdot \frac{L}{r_{h(3)}} \qquad \text{(Eq. M.31)}$$

4. Gupta, Kush & Tiwari (Heat Transfer); refer to Gupta, et al. (Experimental research on heat transfer coefficients from cryogenic cross-counter-flow finned-tube heat exchangers 2009)

The following applies to the shell side with a single wrap. The authors proposed a heat transfer correlation to account for a 'reasonable' manufacturing gap between the shell and fin-tubing. It is conservative by ~20% if there is no gap. What the authors call the 'free volume concept' or 'porous plug analogy' is used as the free flow area, $A_{c(v*)}$, for the mass flux, $G_{(v*)}$ and is taken as,

$$A_{c(v*)} = \pi D_c \cdot \left\{ {d_f}^2 - \frac{\pi}{4}\left[\left({d_f}^2 - {d_o}^2 \right)(n \cdot t) + {d_o}^2 \right] \right\} / d_f \qquad \text{(Eq. M.32)}$$

This is a rectangular volume that is πD_c long and a cross section of ${d_f}^2$, subtracting the volume of the tube and fins, then divided by the axial distance, d_f.

So, the mass flux used for the Reynolds number is,

$$G_{(v*)} = \frac{\dot{m}}{A_{c(v*)}} \qquad \text{(Eq. M.33)}$$

The tube outside diameter (i.e., fin root diameter), d_o, is used in the Reynold's number, and is found as,

$$Re_{(4)} = \frac{G_{(v*)} \cdot d_o}{\mu} \qquad \text{(Eq. M.34)}$$

This is used for correlating the Nusselt number, which is found as,

$$Nu_{(4)} = B_{j(4)} \cdot Re_{(4)}^{\left(1-\vartheta_{(4)}\right)} \cdot Pr^{1/3} \qquad \text{(Eq. M.35)}$$

where,

$$B_{j(4)} = 0.19 \; ; \left(1 - \vartheta_{(4)}\right) = 0.703 \;\; \text{for, } 500 \leq Re_{(4)} \leq 1900 \qquad \text{(Eq. M.36)}$$

Also, the author's results indicate that several other correlations (by others) adequately fit their experimental data (within +/- 20%) using the same definition for the free flow area, $A_{c(v*)}$, in the mass flux, $G_{(v*)}$, and d_o in the Reynold's and Nusselt numbers. One is by Zukauskas (Heat transfer and flow over finnned tubes 1989),

$$B_{j(5)} = 1.04 \; ; \left(1 - \vartheta_{(5)}\right) = 0.4 \;\; \text{for, } 1 \leq Re_{(5)} \leq 500 \qquad \text{(Eq. M.37)}$$

The other is from the (ESDU 73031 2000),

$$B_{j(6)} = 0.742 \; ; \left(1 - \vartheta_{(6)}\right) = 0.431 \;\; \text{for, } 10 \leq Re_{(6)} \leq 300 \qquad \text{(Eq. M.38)}$$

Both of these were developed for staggered plain tube bundles. Also, the Prandtl number exponent in the Nusselt number, although not precisely 1/3, was close (i.e., 0.36 for (Zukauskas 1989), and 0.34 for (ESDU 73031 2000)); so, it was taken (here) as 1/3. The heat transfer coefficients, $h_{(5)}$ and $h_{(6)}$, and the Colburn factors, $j_{H(5)}$ and $j_{H(6)}$, are found using the same expressions as for $h_{(4)}$ and $j_{H(4)}$, respectively. Another is by (PFR Engineering Systems 1976),

$$Nu_{(7)} = B_{j(7)} \cdot Re_{(7)}^{\left(1-\vartheta_{(7)}\right)} \cdot A_r^{\,-0.17} \cdot Pr^{1/3} \qquad \text{(Eq. M.39)}$$

where,

$$A_r = 1 + n \cdot (d_f - d_o) \cdot \left[\frac{1}{2}(d_f + d_o) + t\right]/d_o \qquad \text{(Eq. M.40)}$$

This is the ratio of the tube and fin surface area to the plain tube surface area (as if there were no fins). And,

$$B_{j(7)} = 0.194 \; ; \left(1 - \vartheta_{(7)}\right) = 0.633 \;\; \text{for, } 1000 \leq Re_{(7)} \leq 40000 \qquad \text{(Eq. M.41)}$$

This was developed for radial high finned in-line tube bundles. The heat transfer coefficient, $h_{(7)}$, is found using the same expressions as for $h_{(4)}$. Or, alternatively, the Colburn factor,

$$j_{H(7)} = B_{j(7)} \cdot {Re_{(7)}}^{-\vartheta_{(7)}} \cdot {A_r}^{-0.17} \qquad \text{(Eq. M.42)}$$

Also, another is from the EDSU 84016 (Low-fin staggered tube banks: heat transfer and pressure loss for turbulent single-phase crossflow 2000),

$$Nu_{(8)} = B_{j(8)} \cdot {Re_{(8)}}^{\left(1-\vartheta_{(8)}\right)} \cdot Pr^{0.33} \cdot \Phi \qquad \text{(Eq. M.43)}$$

where,

$$B_{j(8)} = 0.292 \qquad \text{(Eq. M.44)}$$

$$\left(1 - \vartheta_{(8)}\right) = 0.585 + 0.0346 \cdot \ln\left(d_f/s_f\right) \qquad \text{(Eq. M.45)}$$

$$s_f = \left(\frac{1 - n \cdot t}{n - 1}\right) \qquad \text{(Eq. M.46)}$$

$$\Phi = \left(\frac{s_f}{d_f}\right)^{1.115} \cdot \left(\frac{s_f}{h_f}\right)^{0.257} \cdot \left(\frac{t}{s_f}\right)^{0.666} \cdot \left(\frac{d_f}{d_o}\right)^{0.473} \cdot \left(\frac{d_f}{t}\right)^{0.772} \qquad \text{(Eq. M.47)}$$

s_f is the 'fin spacing'. The Reynold's number range for this correlation is not given. This was developed for radial low finned staggered tube bundles in cross flow. The heat transfer coefficient, $h_{(8)}$, is found using the same expressions as for $h_{(4)}$. Or, alternatively, the Colburn factor,

$$j_{H(8)} = B_{j(8)} \cdot {Re_{(8)}}^{-\vartheta_{(8)}} \cdot \Phi \qquad \text{(Eq. M.48)}$$

APPENDIX N – CORIOLIS MASS FLOW STATISTICAL DATA

Table N.1. Coriolis mass flow meter – test # and start/stop times for measurement

Test #	Heat (Nominal) [W]	Intermediate Pressure (Nominal) [atm]	Date	Time Designation [hh:mm]	Start Time [hh:mm]	Time Duration [hh:mm]
1	30	2.7	30-Dec-2014	15:21	15:00	00:26
2	40	2.7	29-Dec-2014	14:38	14:25	00:16
3	60	2.7	28-Dec-2014	01:01	00:55	00:06
3	60	2.7	29-Dec-2014	17:22	17:05	00:20
4	60	2.7	29-Dec-2014	10:28	10:20	00:09
6	80	2.7	20-Dec-2014	14:23	14:20	00:05
7	80	2.7	29-Dec-2014	19:49	19:35	00:18
8	100	2.7	29-Dec-2014	21:33	21:15	00:21
9	120	2.7	30-Dec-2014	13:15	13:00	00:18
10	40	1.3	30-Dec-2014	17:40	17:25	00:19
11	60	1.3	27-Dec-2014	22:09	22:00	00:10
12	60	1.3	30-Dec-2014	19:15	19:05	00:10
13	80	1.3	31-Dec-2014	10:40	10:30	00:13
14	100	1.3	31-Dec-2014	12:10	12:00	00:15
15	60	1	27-Dec-2014	19:10	18:55	00:17
16	60	0.8	27-Dec-2014	16:24	16:20	00:05
17	60	0.6	27-Dec-2014	13:11	12:45	00:27
18	40	0.5	01-Jan-2015	14:14	14:05	00:12
19	60	0.5	01-Jan-2015	17:03	16:55	00:10
20	80	0.5	01-Jan-2015	20:25	20:20	00:08
21	100	0.5	01-Jan-2015	21:53	21:45	00:11
22	60	0.4	26-Dec-2014	13:43	13:35	00:16
23	40	0.3	07-Feb-2015	15:25	15:10	00:20
24	60	0.3	07-Feb-2015	21:00	20:40	00:24
25	30	0.2	02-Jan-2015	19:20	19:10	00:12
26	40	0.2	31-Dec-2014	14:48	14:30	00:22
27	40	0.2	02-Jan-2015	20:53	20:45	00:12
28	40	0.2	02-Jan-2015	16:05	15:55	00:14
29	60	0.2	23-Dec-2014	20:05	19:55	00:13
30	60	0.2	26-Dec-2014	17:20	17:05	00:17
31	60	0.2	31-Dec-2014	17:25	17:20	00:09
32	80	0.2	20-Dec-2014	20:20	20:15	00:05
33	80	0.2	31-Dec-2014	19:36	19:30	00:10
34	100	0.2	31-Dec-2014	21:44	21:35	00:12
35	60	0.12	26-Dec-2014	20:51	20:40	00:13
36	40	0.1	03-Jan-2015	15:38	15:30	00:13
37	60	0.1	03-Jan-2015	23:45	23:40	00:10
38	80	0.1	03-Jan-2015	20:50	20:45	00:08
39	100	0.1	03-Jan-2015	18:30	18:25	00:08
40	40	Low	17-Jan-2015	16:05	15:40	00:35
41	60	Low	17-Jan-2015	19:15	19:05	00:19
42	80	Low	17-Jan-2015	22:00	21:50	00:15
43	100	Low	18-Jan-2015	01:15	01:00	00:17

Table N.2. Coriolis mass flow meter – test # and mass flow statistics

Test #	Heat (Nominal)	Intermediate Pressure (Nominal)	*Coriolis Mass Flow Rate (CFI2465) [g/s]*			
	[W]	[atm]	Min	Mean	Max	Sigma
1	30	2.7	1.573	1.629	1.717	0.024
2	40	2.7	2.009	2.068	2.154	0.027
3	60	2.7	3.267	3.363	3.432	0.038
3	60	2.7	2.952	3.037	3.131	0.041
4	60	2.7	3.196	3.288	3.375	0.035
6	80	2.7	4.434	4.517	4.546	0.025
7	80	2.7	3.825	3.943	4.071	0.060
8	100	2.7	4.836	4.909	5.018	0.038
9	120	2.7	5.458	5.500	5.563	0.021
10	40	1.3	1.929	1.978	2.044	0.021
11	60	1.3	3.338	3.386	3.437	0.021
12	60	1.3	2.763	2.809	2.843	0.016
13	80	1.3	3.643	3.741	3.826	0.040
14	100	1.3	4.481	4.652	4.747	0.050
15	60	1	3.259	3.356	3.447	0.042
16	60	0.8	3.340	3.407	3.449	0.025
17	60	0.6	3.400	3.505	3.649	0.044
18	40	0.5	1.864	1.919	2.009	0.027
19	60	0.5	2.656	2.757	2.814	0.041
20	80	0.5	3.563	3.609	3.658	0.022
21	100	0.5	4.519	4.558	4.592	0.015
22	60	0.4	3.203	3.305	3.403	0.037
23	40	0.3	1.339	1.442	1.571	0.046
24	60	0.3	2.254	2.370	2.520	0.039
25	30	0.2	1.462	1.513	1.565	0.023
26	40	0.2	1.901	1.957	2.012	0.020
27	40	0.2	1.827	1.881	1.946	0.024
28	40	0.2	1.868	1.911	1.958	0.017
29	60	0.2	3.300	3.371	3.439	0.033
30	60	0.2	3.220	3.304	3.404	0.038
31	60	0.2	2.672	2.716	2.776	0.018
32	80	0.2	4.545	4.627	4.746	0.049
33	80	0.2	3.524	3.574	3.644	0.022
34	100	0.2	4.474	4.513	4.547	0.015
35	60	0.12	3.242	3.309	3.439	0.037
36	40	0.1	1.838	1.908	1.968	0.032
37	60	0.1	2.731	2.781	2.823	0.021
38	80	0.1	3.685	3.735	3.784	0.021
39	100	0.1	4.637	4.671	4.697	0.015
40	40	Low	2.204	2.275	2.347	0.023
41	60	Low	3.120	3.197	3.256	0.022
42	80	Low	4.091	4.143	4.204	0.020
43	100	Low	4.963	5.000	5.040	0.014

APPENDIX O – SUB-ATMOSPHERIC BOIL-OFF TESTS

Tests were conducted to measure the static heat in-leak into the helium liquid vessel, while maintaining it at a sub-atmospheric pressure. Two of these tests, which were quite typical, are included in this appendix along with the detailed calculations.

Referring to Figure O.1, the following code was used to obtain the "Slope" (see below) of the helium vessel liquid level (CLL2473):

myget -c CLL2473 -b '2015-01-06 03:00' -e '2015-01-06 07:00' | awk '{print $1, $2, $3}' | /usr/csite/pubtools/R/bin/Rscript -e 't=read.table("stdin"); x=as.POSIXct(paste(t[,1],t[,2])); y=t[,3]; model=lm(y~x); plot(x,y); abline(model); model'

Slope = -1.906e-03 %/sec

The following are the archiver valves for the helium vessel liquid level (CLL2473) values at the start and end times (shown below) and the calculated "Slope' using a 'straight-line':

	yyyy-mm-dd	*hh:mm:ss*	CLL2473 [%]
Start:	2015-01-06	03:01:07	69.214
End:	2015-01-06	06:58:48	41.7037

Slope = -1.929E-03 %/sec

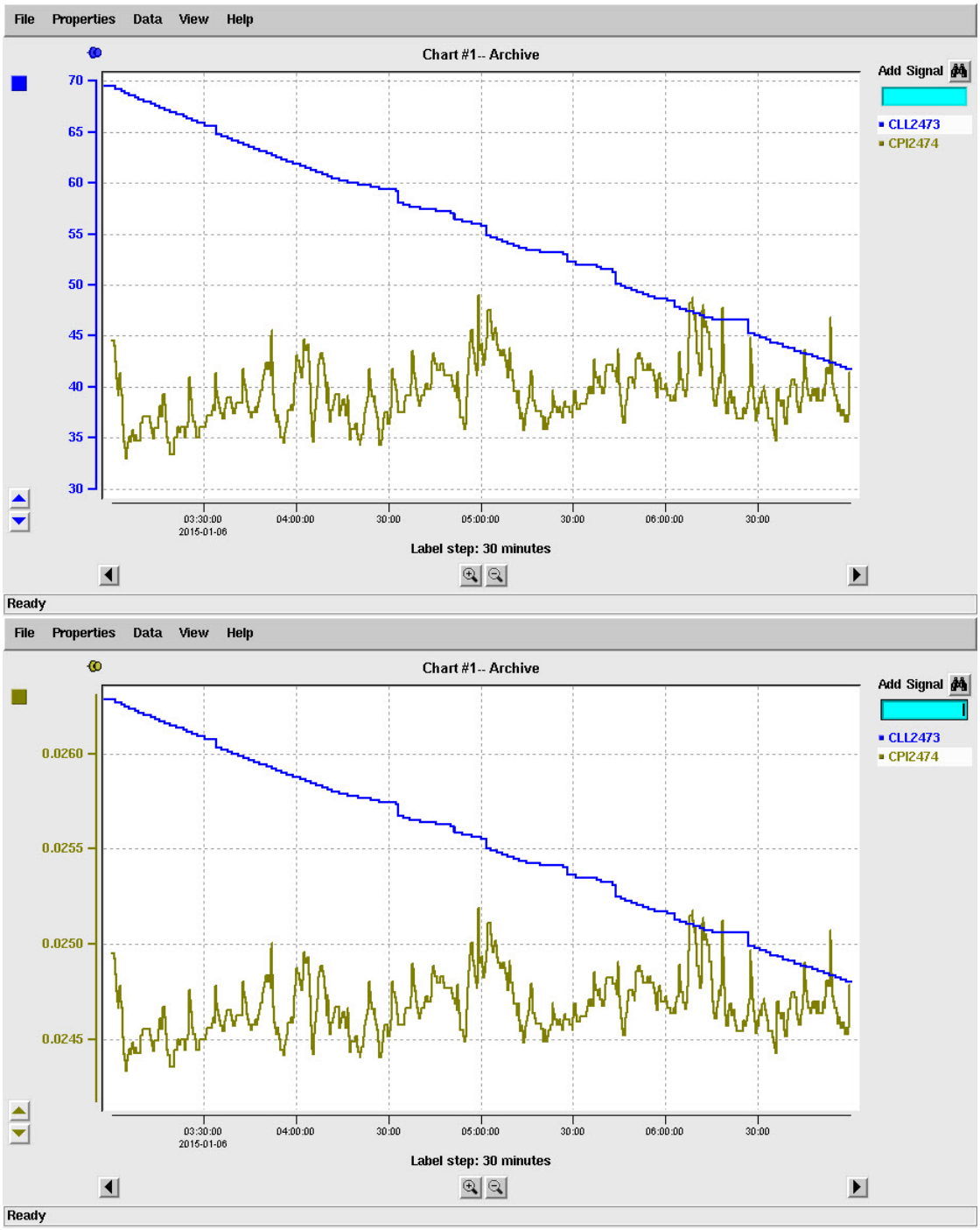

Figure O.1. Boil-off test A: 6-Jan-2015 03:00 to 07:00, vessel liquid level and pressure vs. elapsed time[27]

[27] *x*-axis is time in increments of 30 minutes; "blue" line on the *y*-axis (which is slowly decreasing) is the liquid level (CLL2473) as measured by the AMI super conducting probe (discussed in Chapter 2) and is in 5% increments; "dark yellow" line on y-axis is the helium vessel vapor pressure (CPI2474) and is in 0.0005 atm increments.

The following is the archiver command line code and output data for the helium vessel pressure (CPI2474 [atm]) over the period used to calculate the liquid level slope:

myStats -b '2015-01-06 03:00' -e '2015-01-06 07:00' -l CPI2474 -u

	(Min.)	(Avg.)	(Max.)	(Std. Dev.)
CPI2474	0.0243322	0.0246704	0.0251884	0.000150845

Table O.1 is the detailed calculation of the heat in-leak using the 'straight-line' slope (i.e., -1.929E-3 %/sec) of the liquid level between archiver start and end dates:

Table O.1. Boil-off test A: 6-Jan-2015 03:00 to 07:00, vessel heat in-leak calculation

HX Test - Vessel Boil-Off (no supply flow)			
ΔL	27.51%	[-]	*Fractional change in liquid level for specified time*
Δt	3.961	[h]	*Time for change in liquid level*
ℓ	28	[in]	*SC probe active length*
d	5.834	[in]	*Vessel inside diameter*
V_t	12.265	[ℓ]	*Cylindrical volume for entire SC probe active length*
ΔV	3.374	[ℓ]	*Change in liquid volume*
p	0.025	[atm]	*Pressure in vessel*
T_{sat}	1.926	[K]	*Saturation temperature*
ρ_ℓ	145.5	[g/ℓ]	*Saturated liquid density*
ρ_v	0.6544	[g/ℓ]	*Saturated vapor density*
ρ_r	0.004496	[-]	*Ratio of vapor to liquid density*
Δm	488.9	[g]	*Change in total mass*
w	0.034	[g/s]	*Make-up mass rate*
Δm_ℓ	491.1	[g]	*Change in liquid mass*
w_ℓ	0.03444	[g/s]	*Liquid mass evaporation rate*
λ	23.44	[J/g]	*Latent heat*
q	0.8073	[W]	*Heat in-leak (evaporating the liquid)*

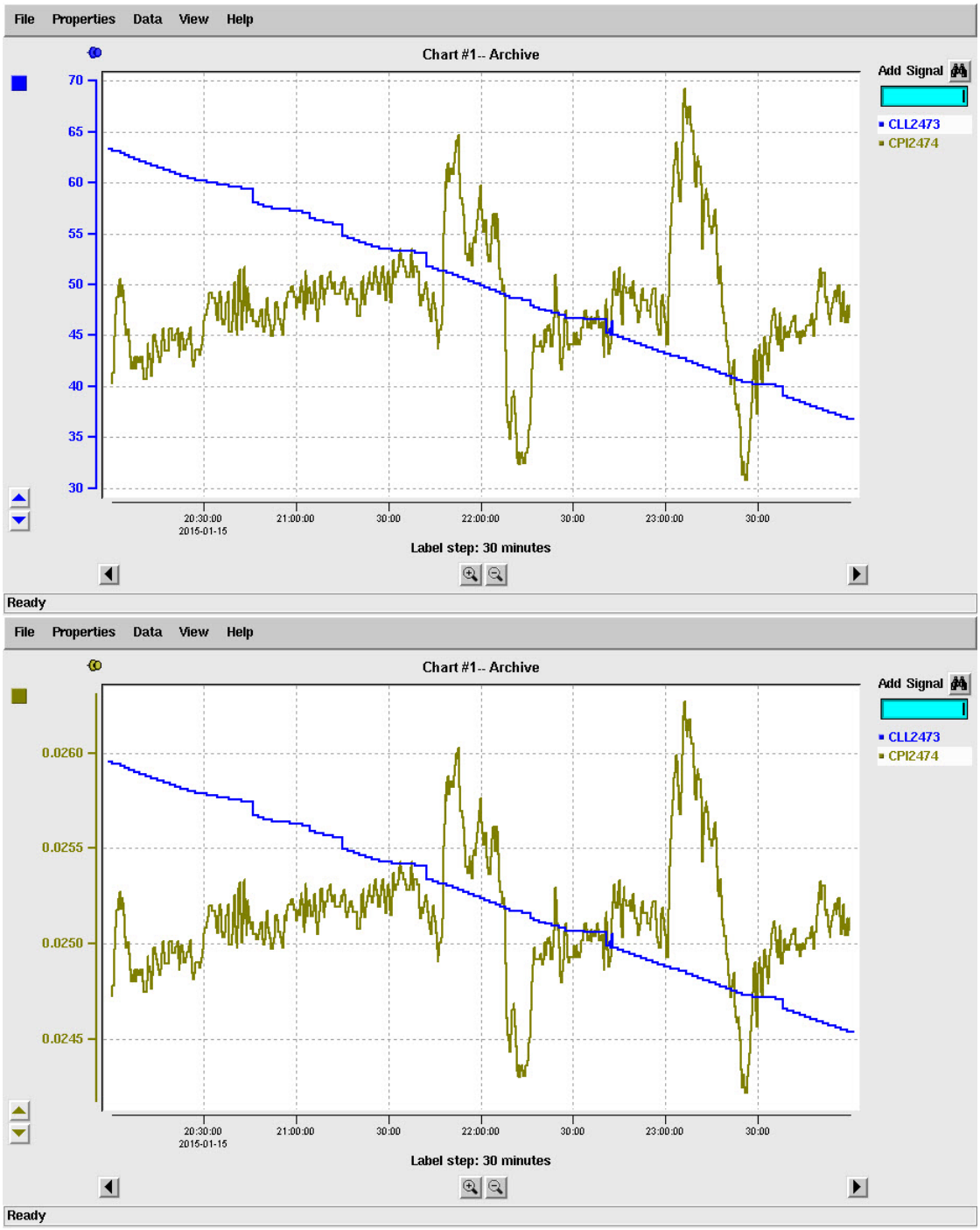

Figure O.2. Boil-off test B: 15-Jan-2015 20:00 to 00:00, vessel liquid level and pressure vs. elapsed time[28]

[28] *x*-axis is time in increments of 30 minutes; "blue" line on the *y*-axis (which is slowly decreasing) is the liquid level (CLL2473) as measured by the AMI super conducting probe (discussed in Chapter 2) and is in 5% increments; "dark yellow" line on y-axis is the helium vessel vapor pressure (CPI2474) and is in 0.0005 atm increments.

Referring to Figure O.2, the following code was used to obtain the “Slope” (see below) of the helium vessel liquid level (CLL2473):

myget -c CLL2473 -b '2015-01-15 20:00' -e '2015-01-16 00:00' | awk '{print $1, $2, $3}' | /usr/csite/pubtools/R/bin/Rscript -e 't=read.table("stdin"); x=as.POSIXct(paste(t[,1],t[,2])); y=t[,3]; model=lm(y~x); plot(x,y); abline(model); model'

Slope = -1.854e-03 %/sec

The following are the archiver valves for the helium vessel liquid level (CLL2473) values at start and end times (shown below) and the calculated “Slope’ using a ‘straight-line’:

	yyyy-mm-dd	*hh:mm:ss*	CLL2473 [%]
Start:	2015-01-15	20:00:14	63.1427
End:	2015-01-15	23:59:16	36.7474

Slope = -1.840E-03 %/sec

The following is the archiver command line code and output data for the helium vessel pressure (CPI2474 [atm]) over the period used to calculate the liquid level slope:

myStats -b '2015-01-15 20:00' -e '2015-01-16 00:00' -l CPI2474 -u

	(Min.)	(Avg.)	(Max.)	(Std. Dev.)
CPI2474	0.0242173	0.025132	0.0262687	0.000318686

Table O.2 is the detailed calculation of the heat in-leak using the ‘straight-line’ slope (i.e., -1.840E-3 %/sec) of the liquid level between archiver start and end dates:

Table O.2. Boil-off test B: 15-Jan-2015 20:00 to 00:00, vessel heat in-leak calculation

HX Test - Vessel Boil-Off (no supply flow)			
ΔL	26.40%	[-]	*Fractional change in liquid level for specified time*
Δt	3.984	[h]	*Time for change in liquid level*
ℓ	28	[in]	*SC probe active length*
d	5.834	[in]	*Vessel inside diameter*
V_t	12.265	[ℓ]	*Cylindrical volume for entire SC probe active length*
ΔV	3.237	[ℓ]	*Change in liquid volume*
p	0.025	[atm]	*Pressure in vessel*
T_{sat}	1.932	[K]	*Saturation temperature*
ρ_ℓ	145.6	[g/ℓ]	*Saturated liquid density*
ρ_v	0.6649	[g/ℓ]	*Saturated vapor density*
ρ_r	0.004568	[-]	*Ratio of vapor to liquid density*
Δm	469.1	[g]	*Change in total mass*
w	0.033	[g/s]	*Make-up mass rate*
Δm_ℓ	471.2	[g]	*Change in liquid mass*
w_ℓ	0.03286	[g/s]	*Liquid mass evaporation rate*
λ	23.44	[J/g]	*Latent heat*
q	0.7702	[W]	*Heat in-leak (evaporating the liquid)*

APPENDIX P – TEST DATA, SCREEN SNAP-SHOTS AND SELECTED GRAPHS

Note: All tests in this appendix are order by their test # designation. The nominal heat [W], nominal intermediate pressure [atm], test date [dd-mmm-yy], and designated test time [hh:mm] are also provided.

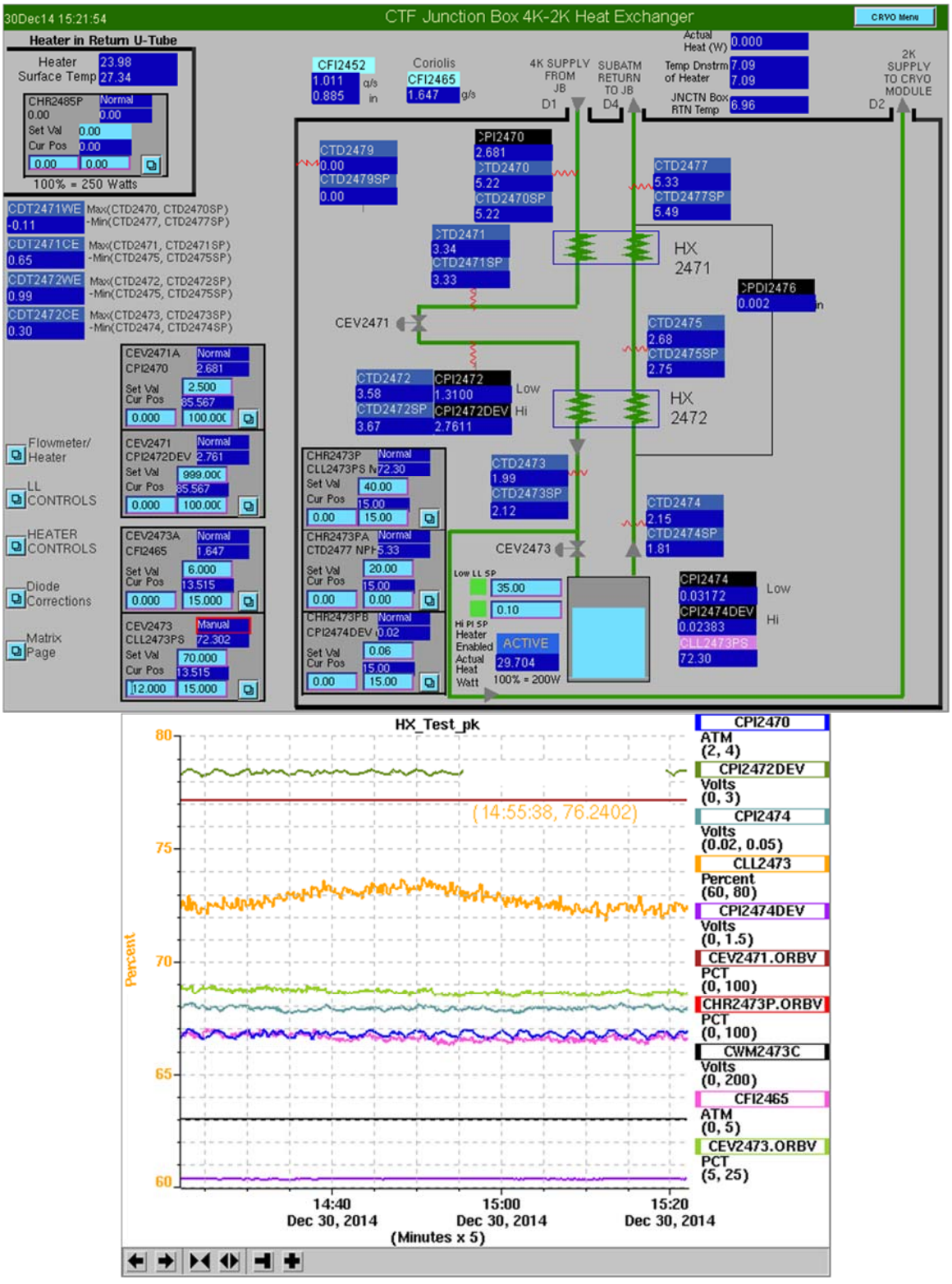

Figure P.1. Data, test #1: 30 W 2.7 atm 30-Dec-14 15:21

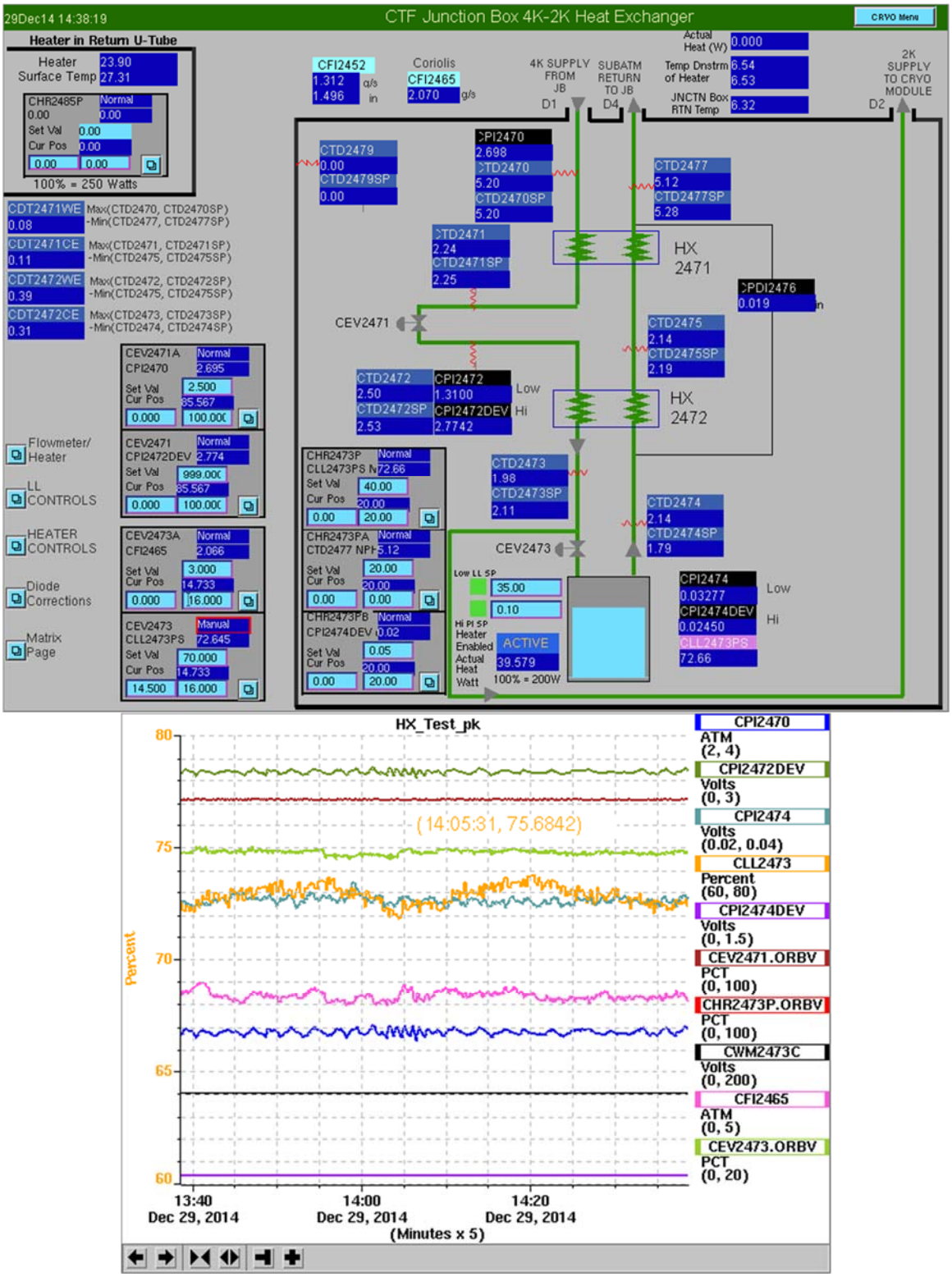

Figure P.2. Data, test #2: 40 W 2.7 atm 29-Dec-14 14:38

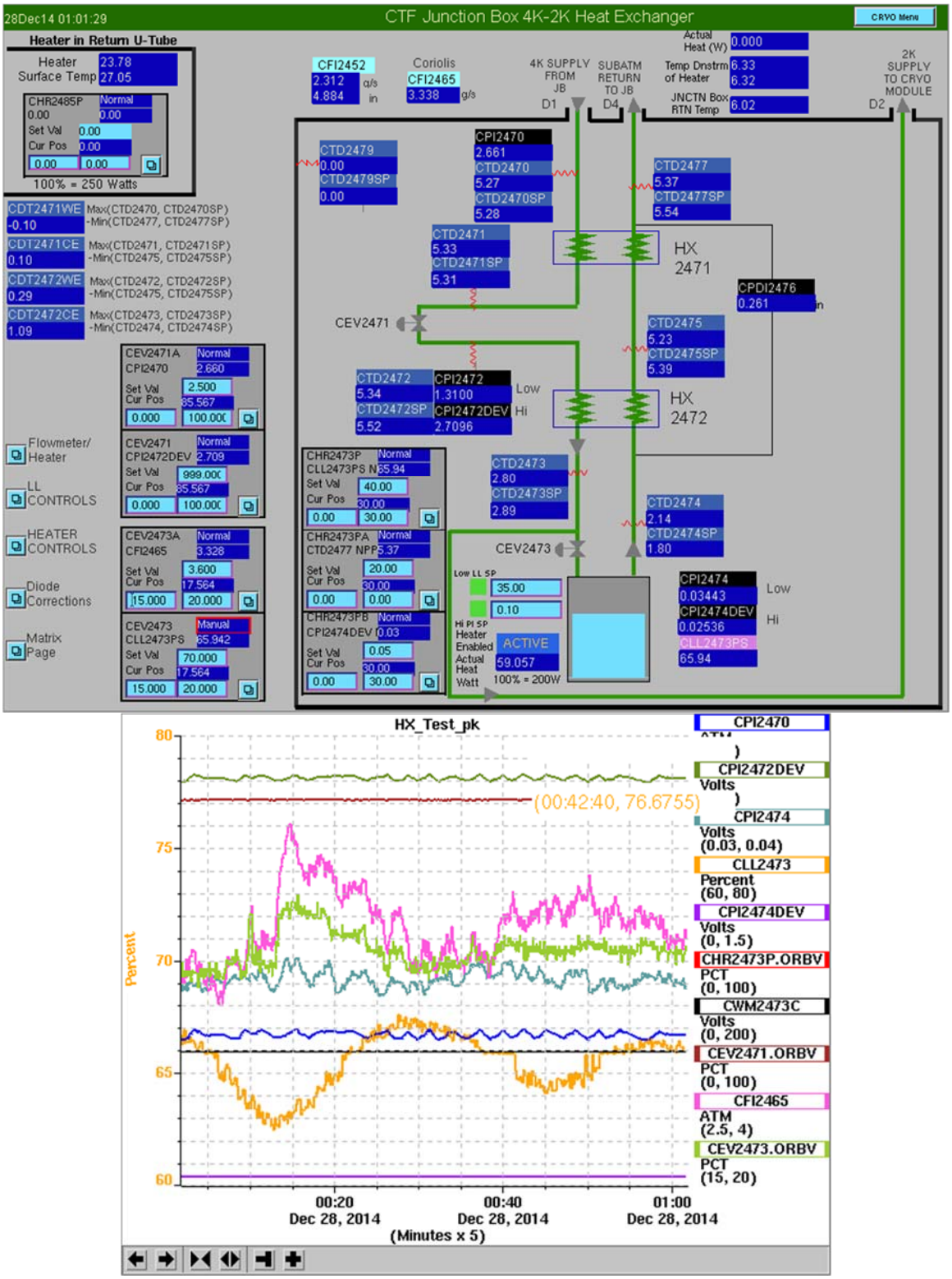

Figure P.3. Data, test #3: 60 W 2.7 atm 27-Dec-14 01:01

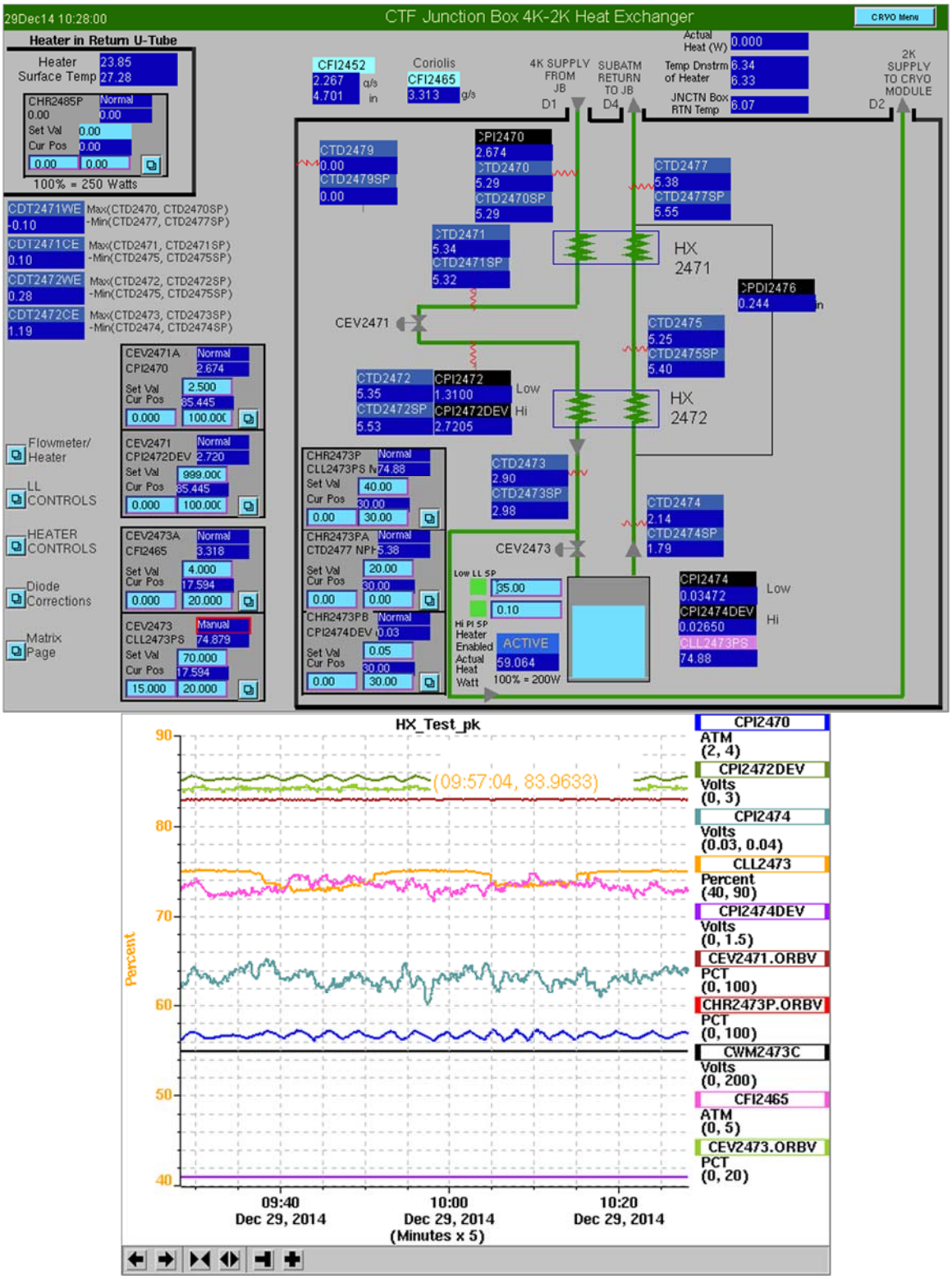

Figure P.4. Data, test #4: 60 W 2.7 atm 29-Dec-14 10:28

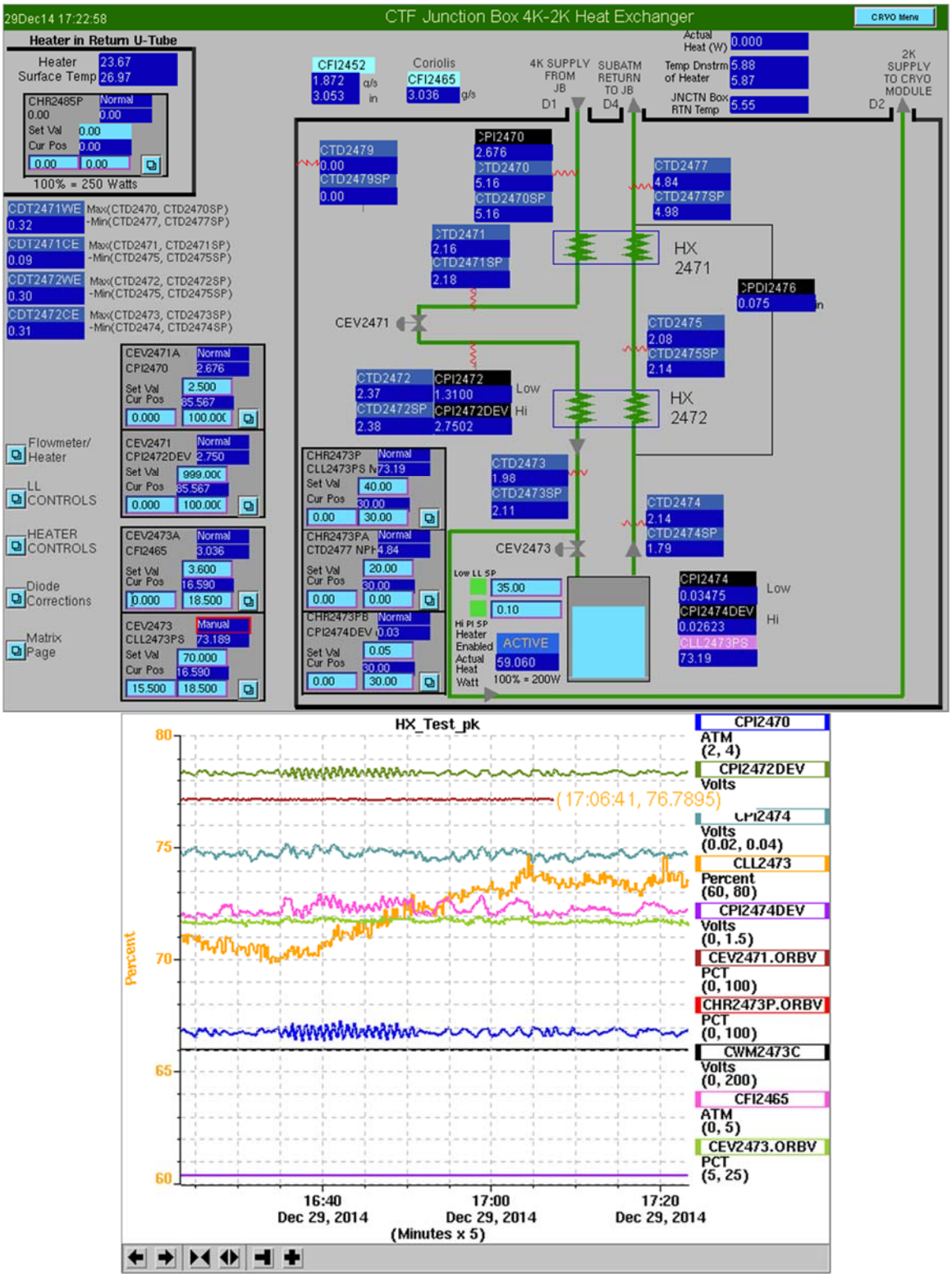

Figure P.5. Data, test #5: 60 W 2.7 atm 29-Dec-14 17:22

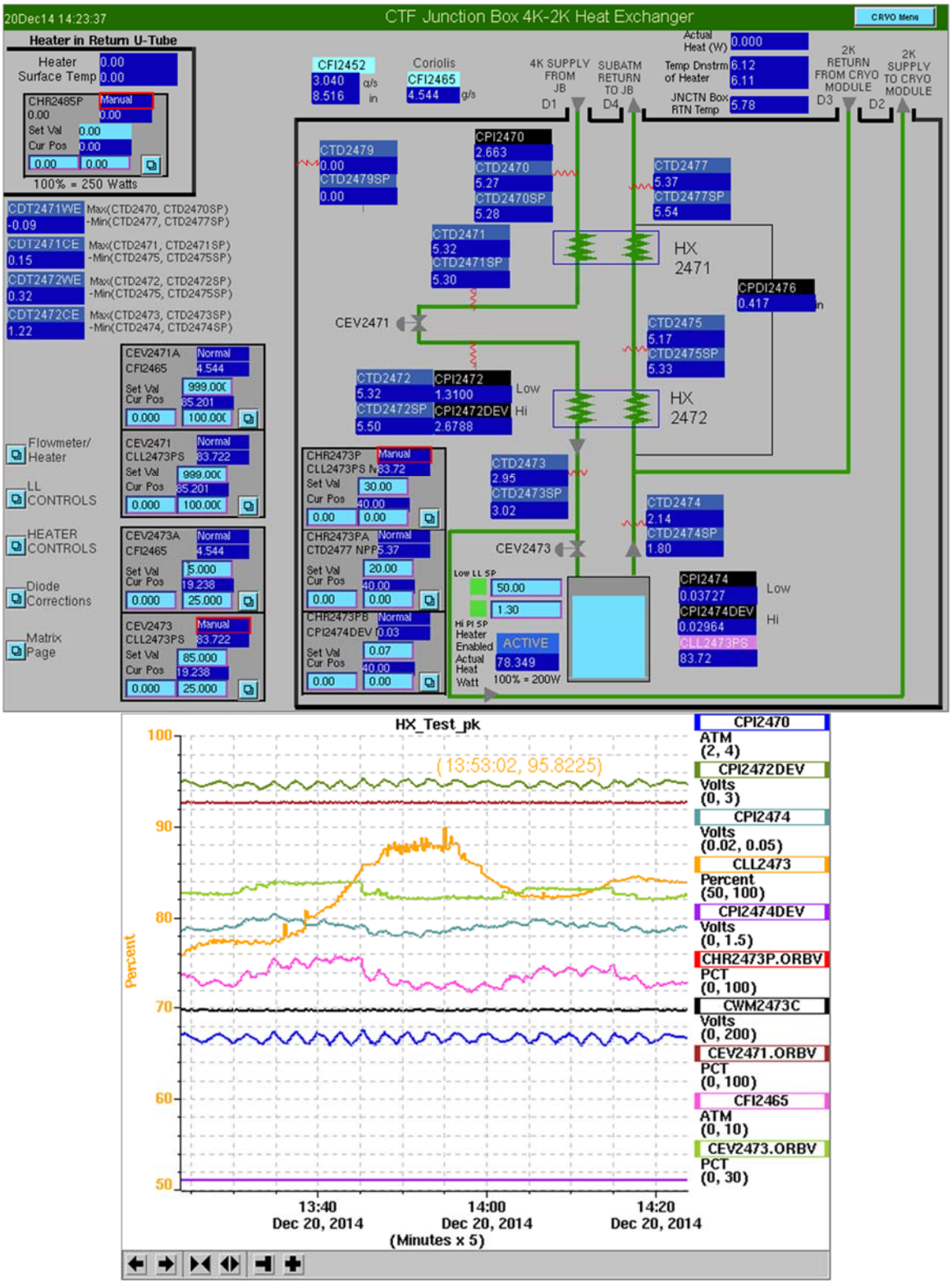

Figure P.6. Data, test #6: 80 W 2.7 atm 20-Dec-14 14:23

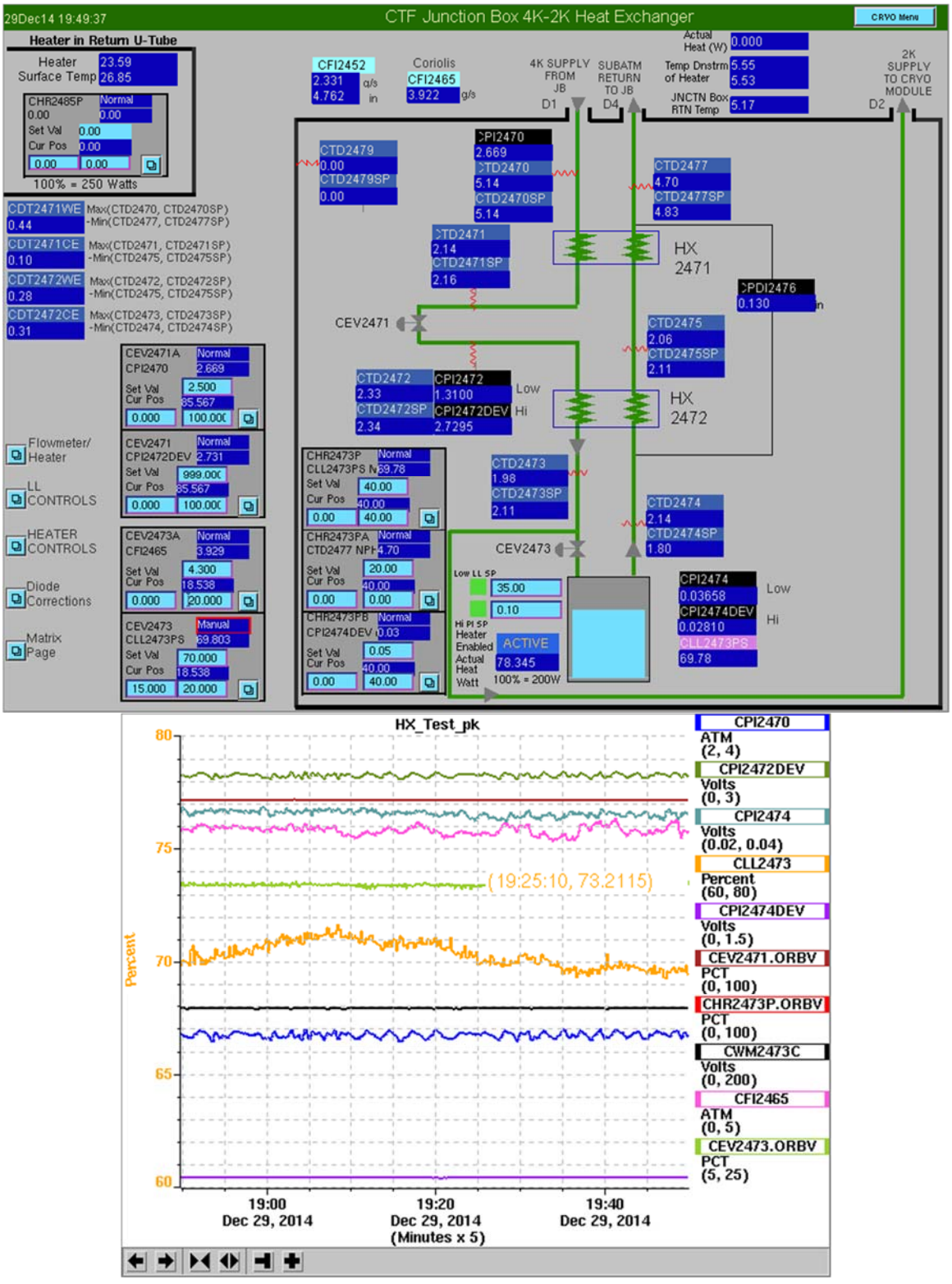

Figure P.7. Data, test #7: 80 W 2.7 atm 29-Dec-14 19:49

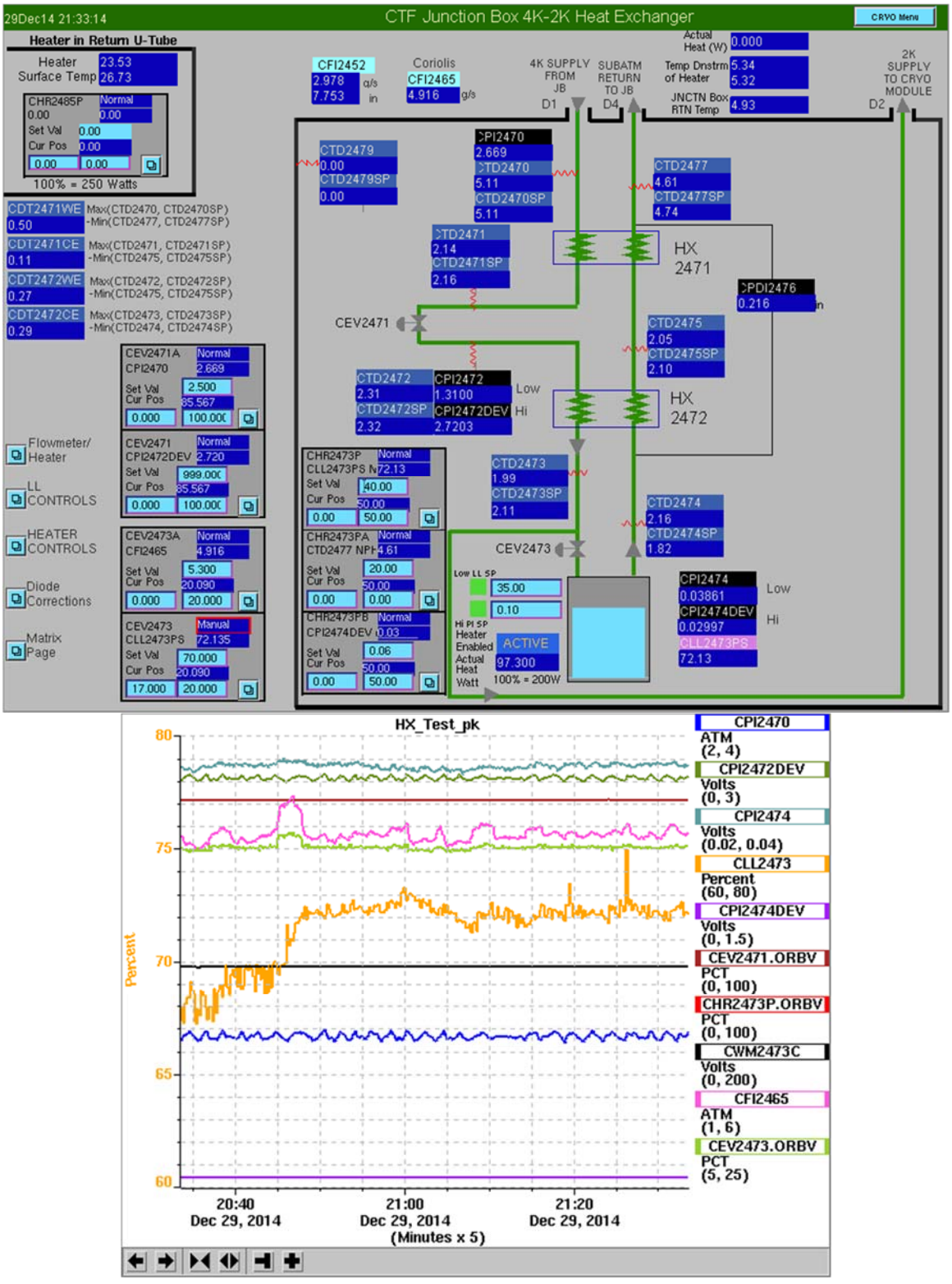

Figure P.8. Data, test #8: 100 W 2.7 atm 29-Dec-14 21:33

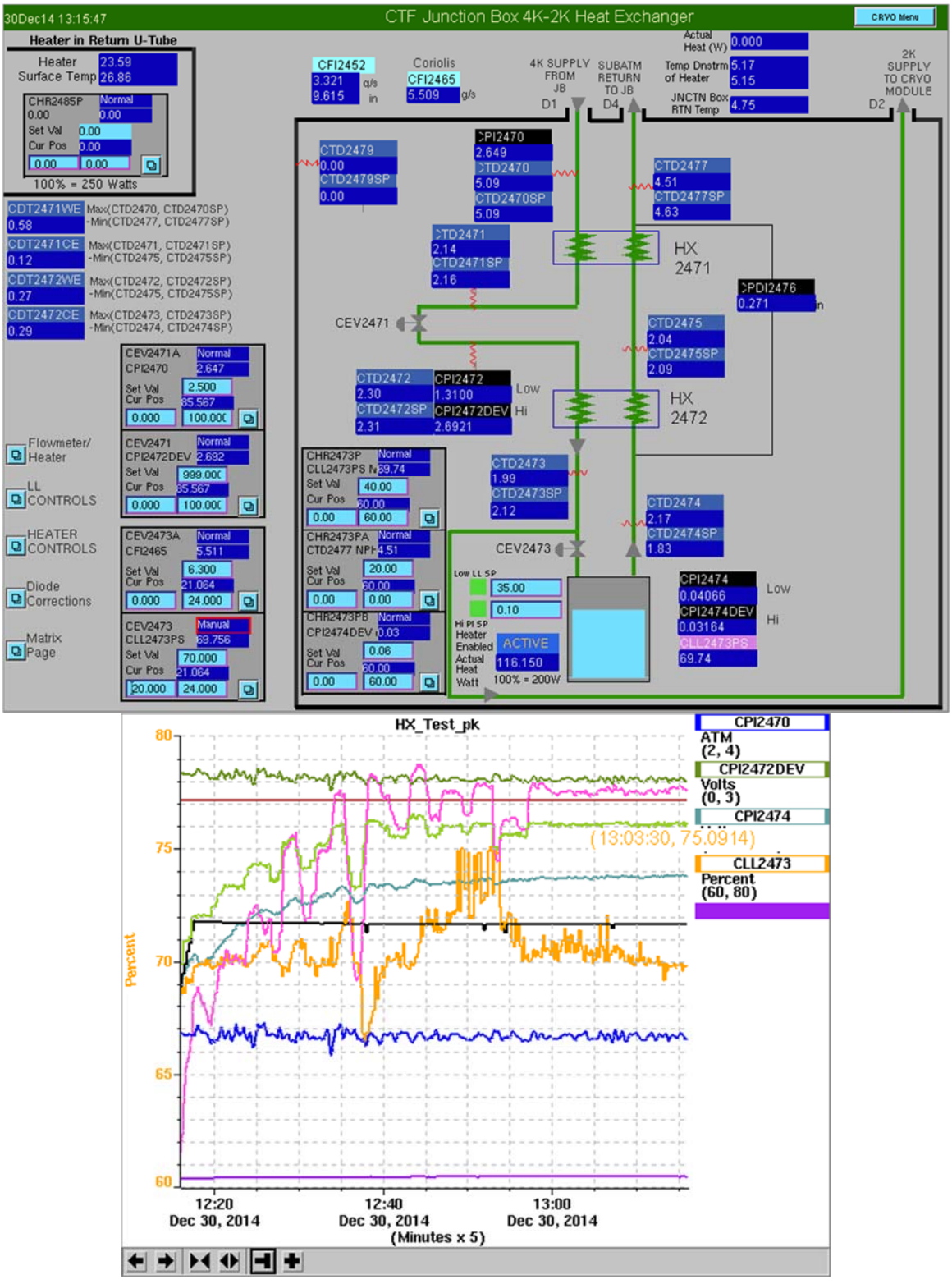

Figure P.9. Data, test #9: 120 W 2.7 atm 30-Dec-14 13:15

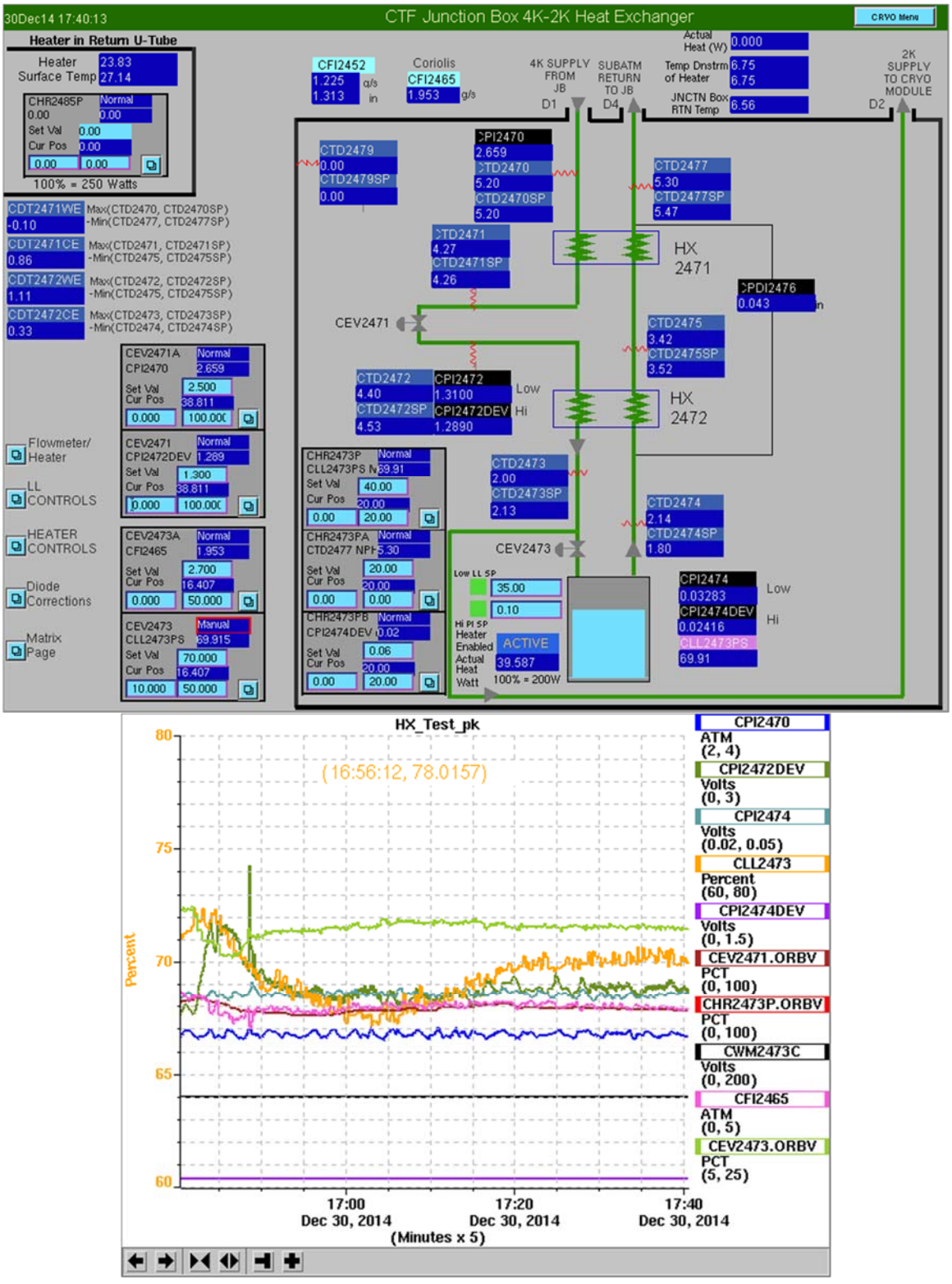

Figure P.10. Data, test #10: 40 W 1.3 atm 30-Dec-14 17:40

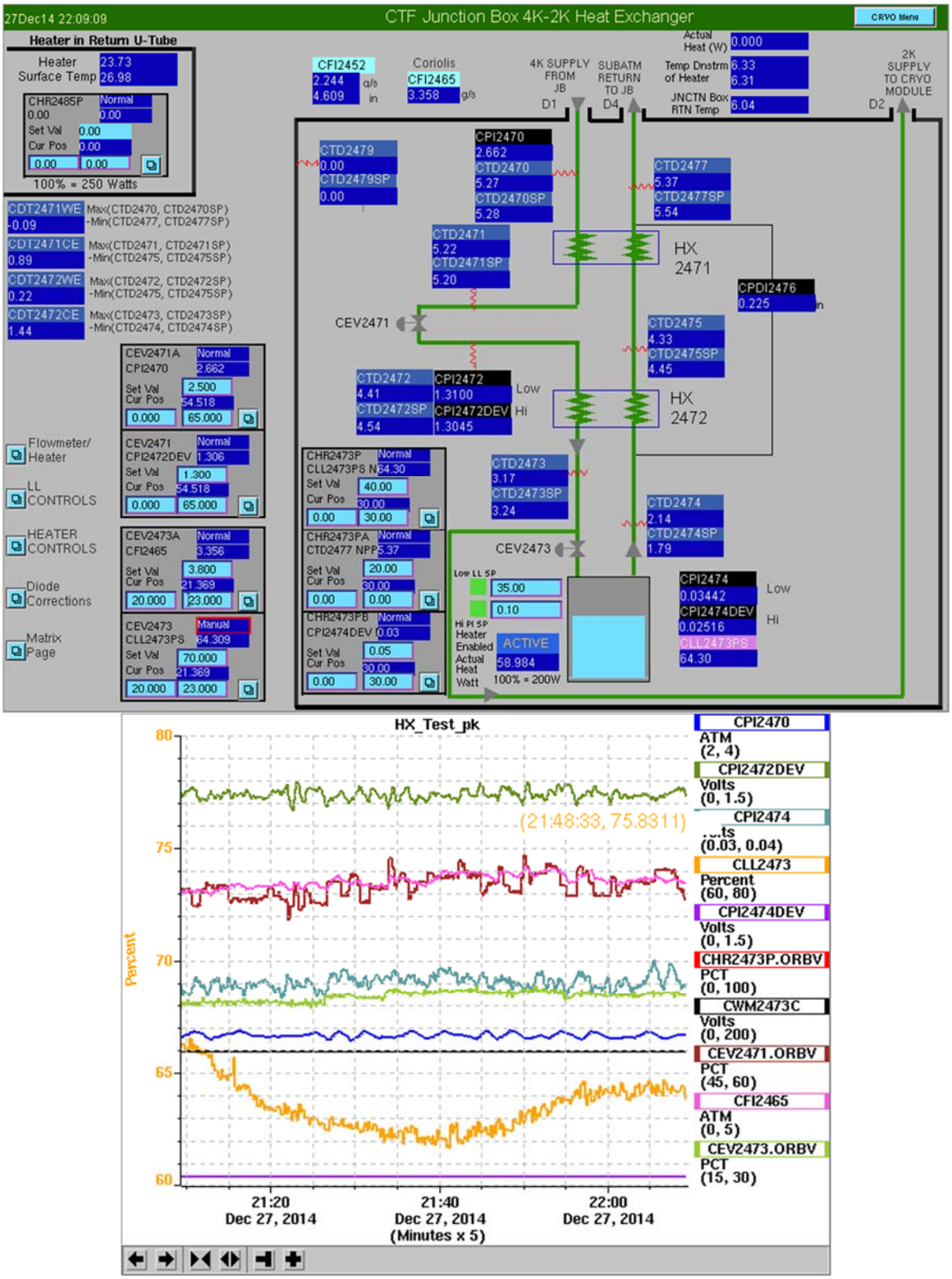

Figure P.11. Data, test #11: 60 W 1.3 atm 27-Dec-14 22:09

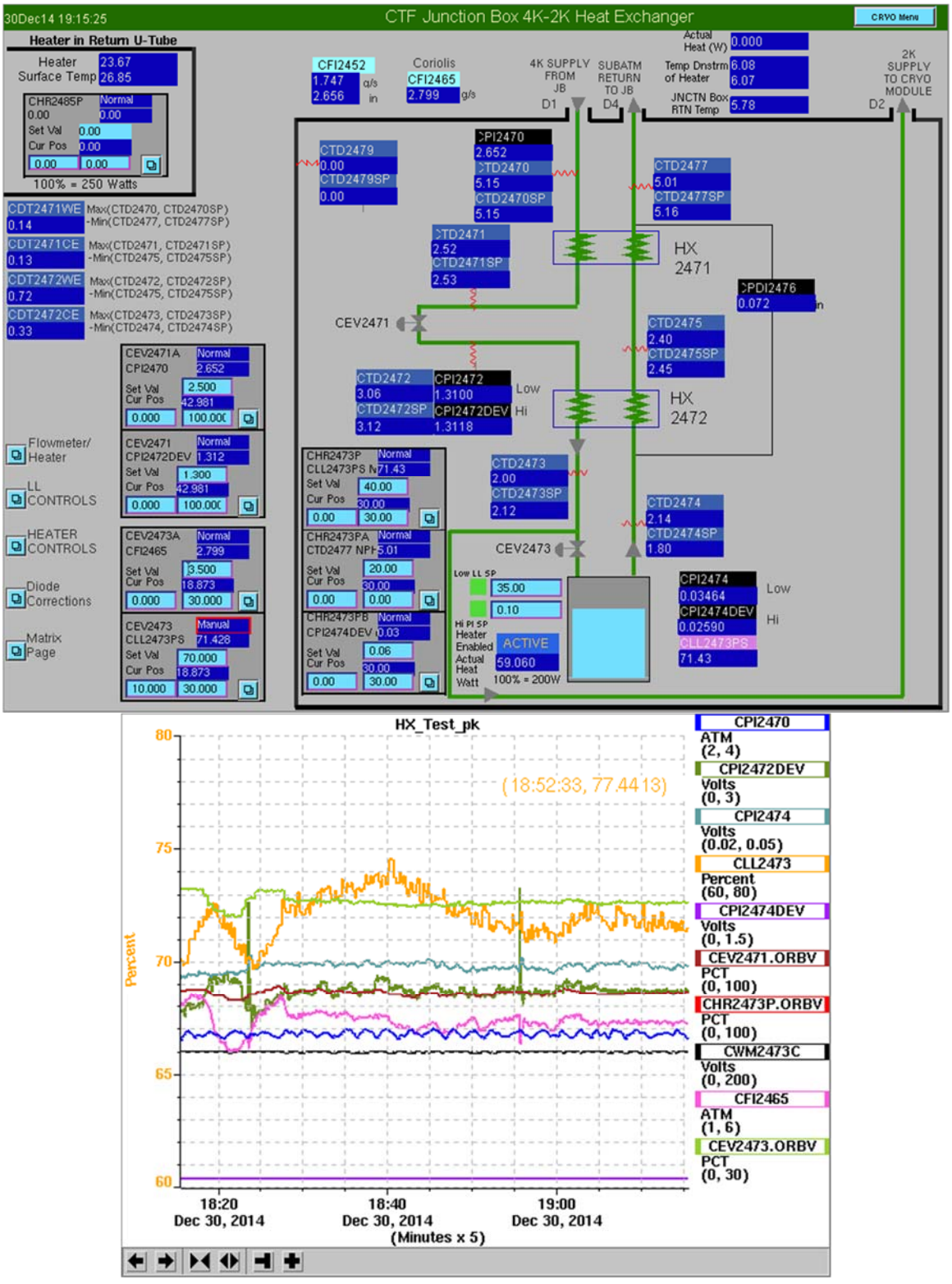

Figure P.12. Data, test #12: 60 W 1.3 atm 30-Dec-14 19:15

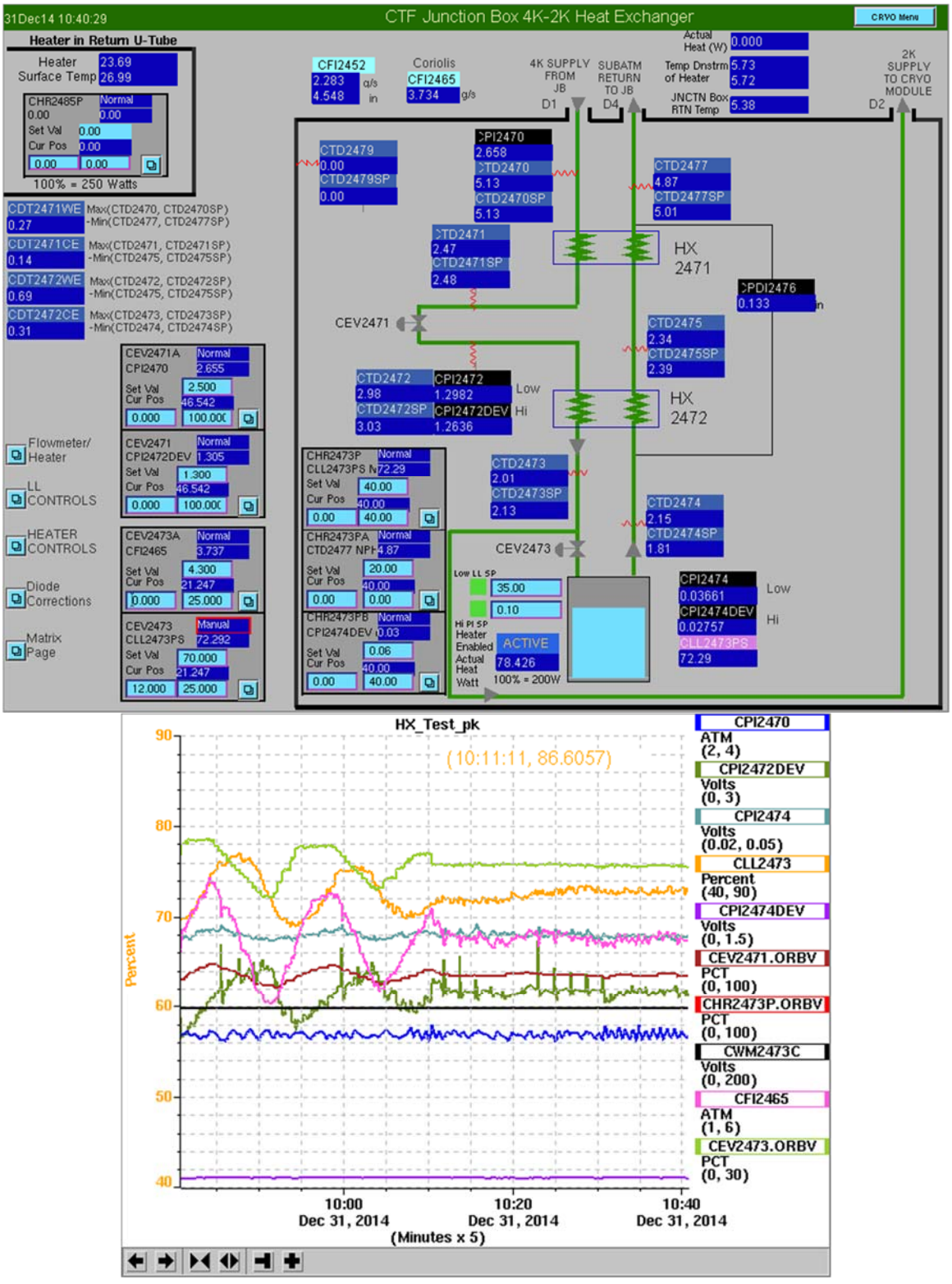

Figure P.13. Data, test #13: 80 W 1.3 atm 31-Dec-14 10:40

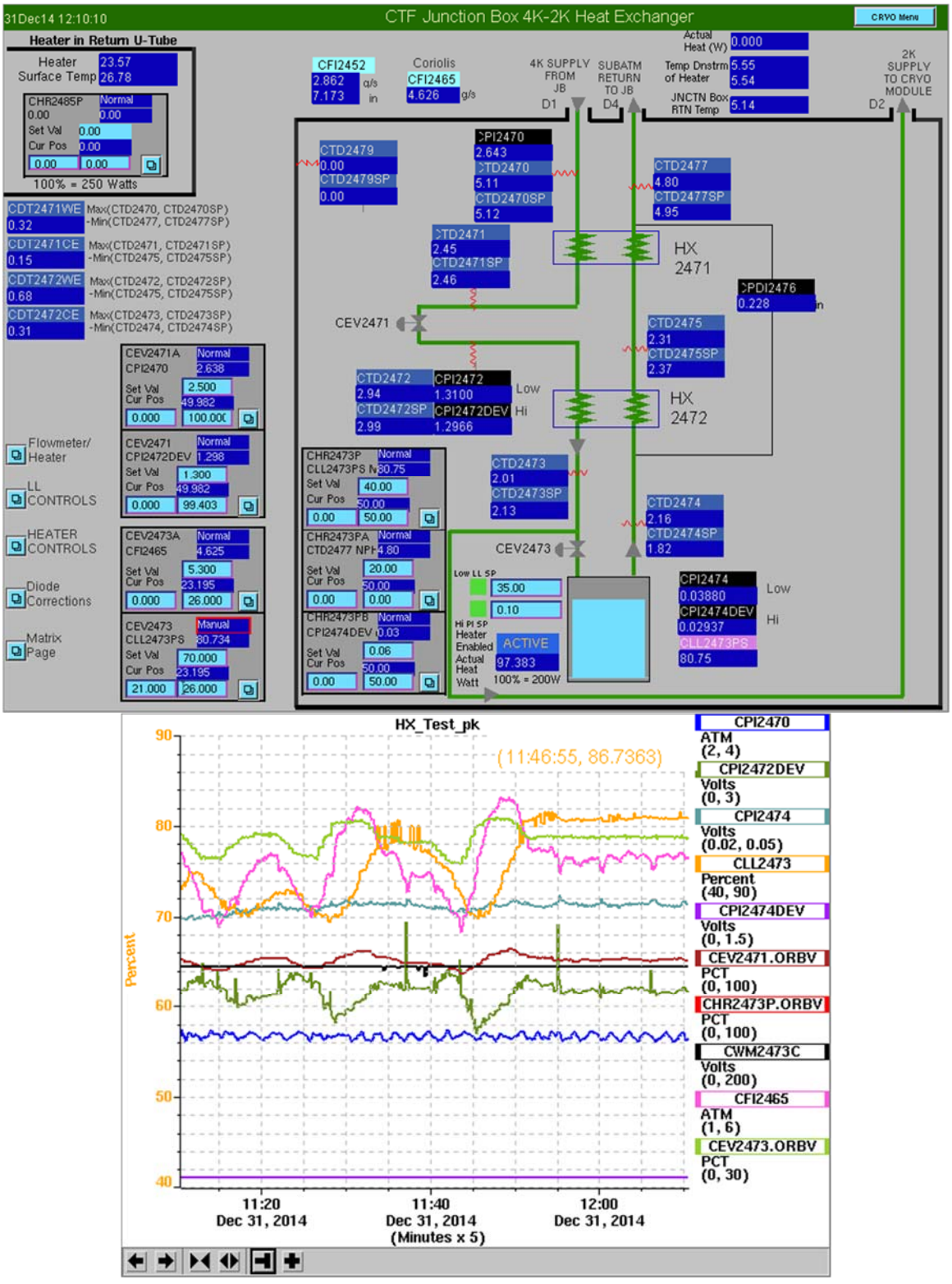

Figure P.14. Data, test #14: 100 W 1.3 atm 31-Dec-14 12:10

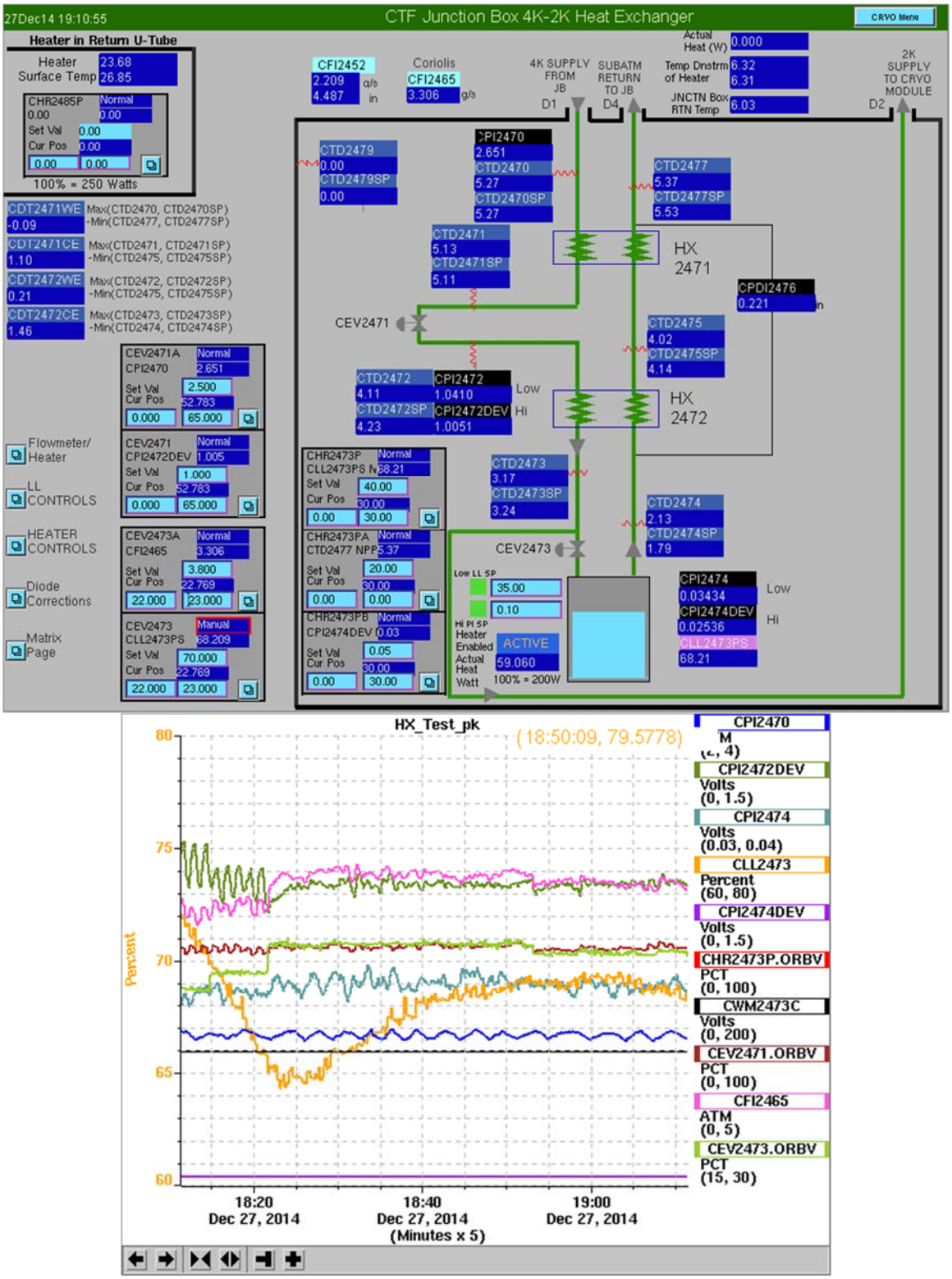

Figure P.15. Data, test #15: 60 W 1 atm 27-Dec-14 19:10

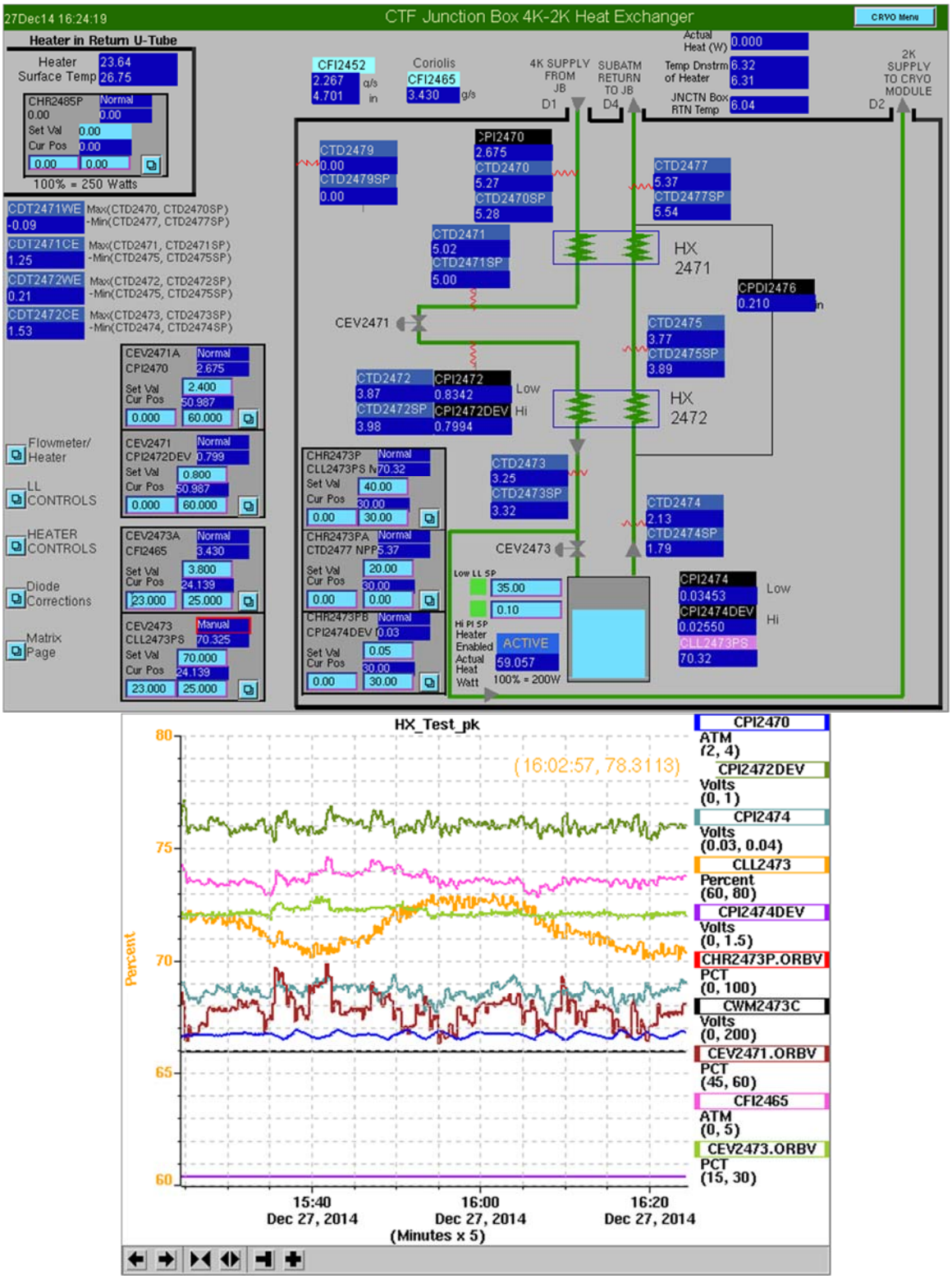

Figure P.16. Data, test #16: 60 W 0.8 atm 27-Dec-14 16:24

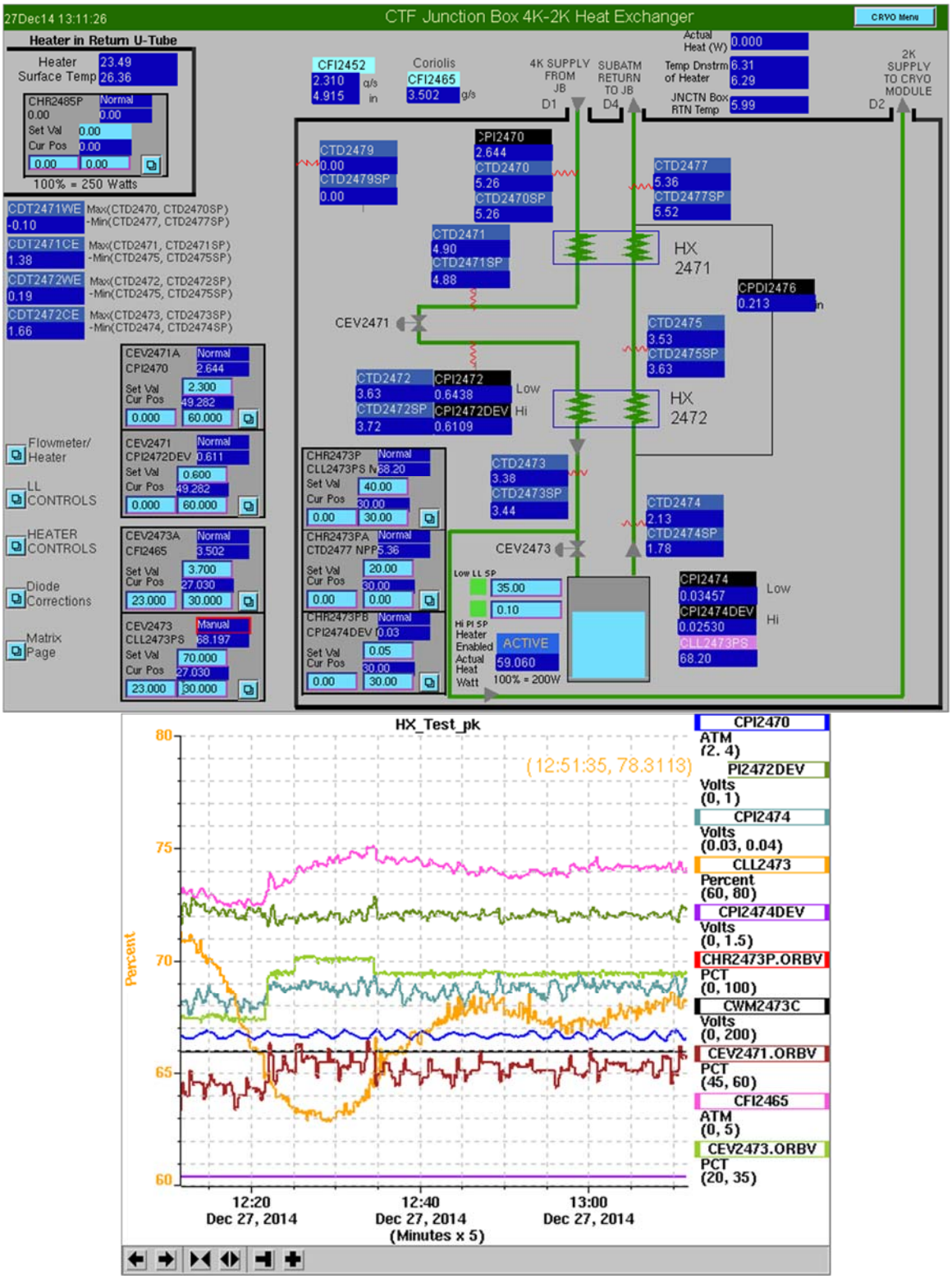

Figure P.17. Data, test #17: 60 W 0.6 atm 27-Dec-14 13:11

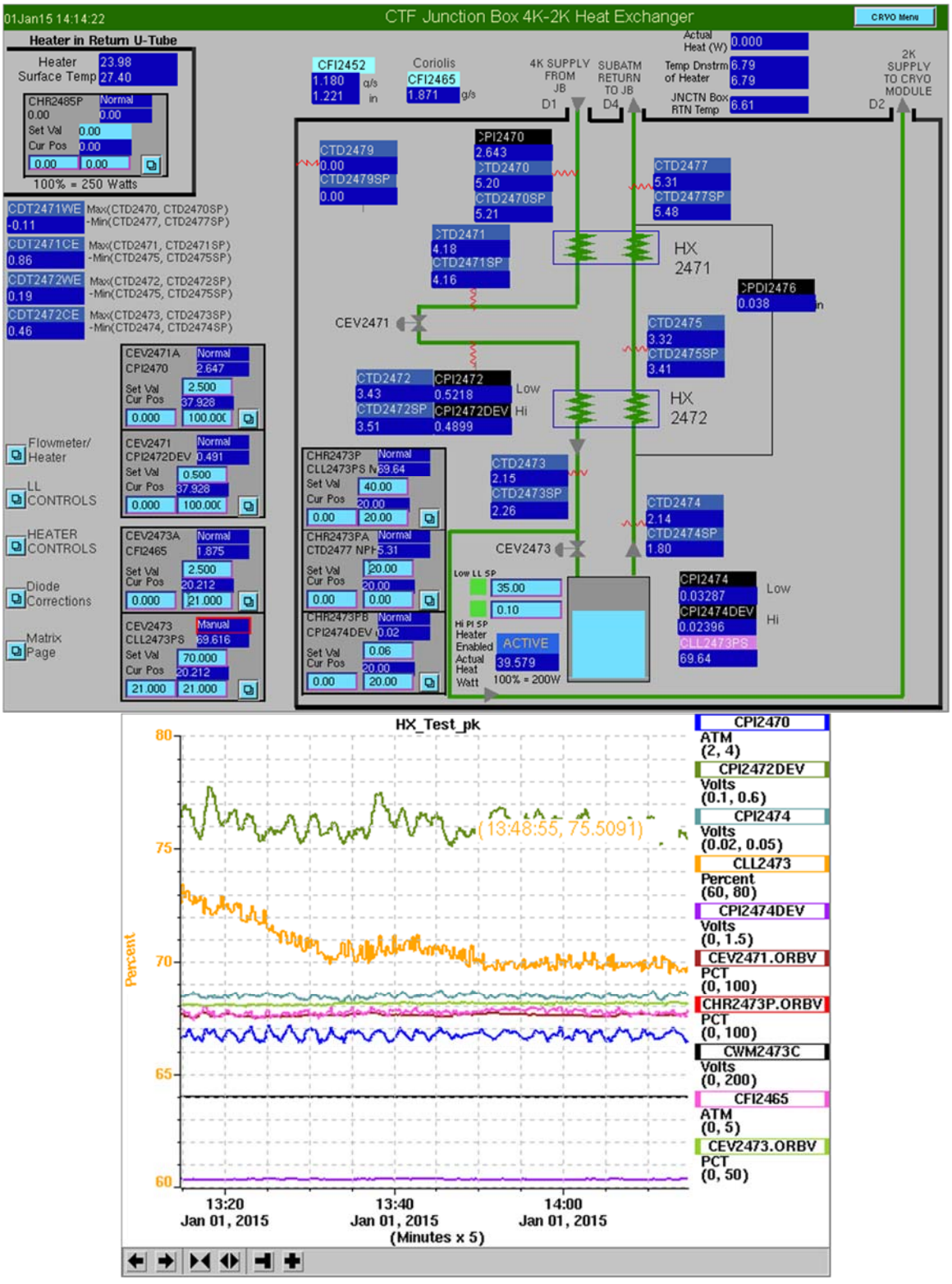

Figure P.18. Data, test #18: 40 W 0.5 atm 01-Jan-15 14:22

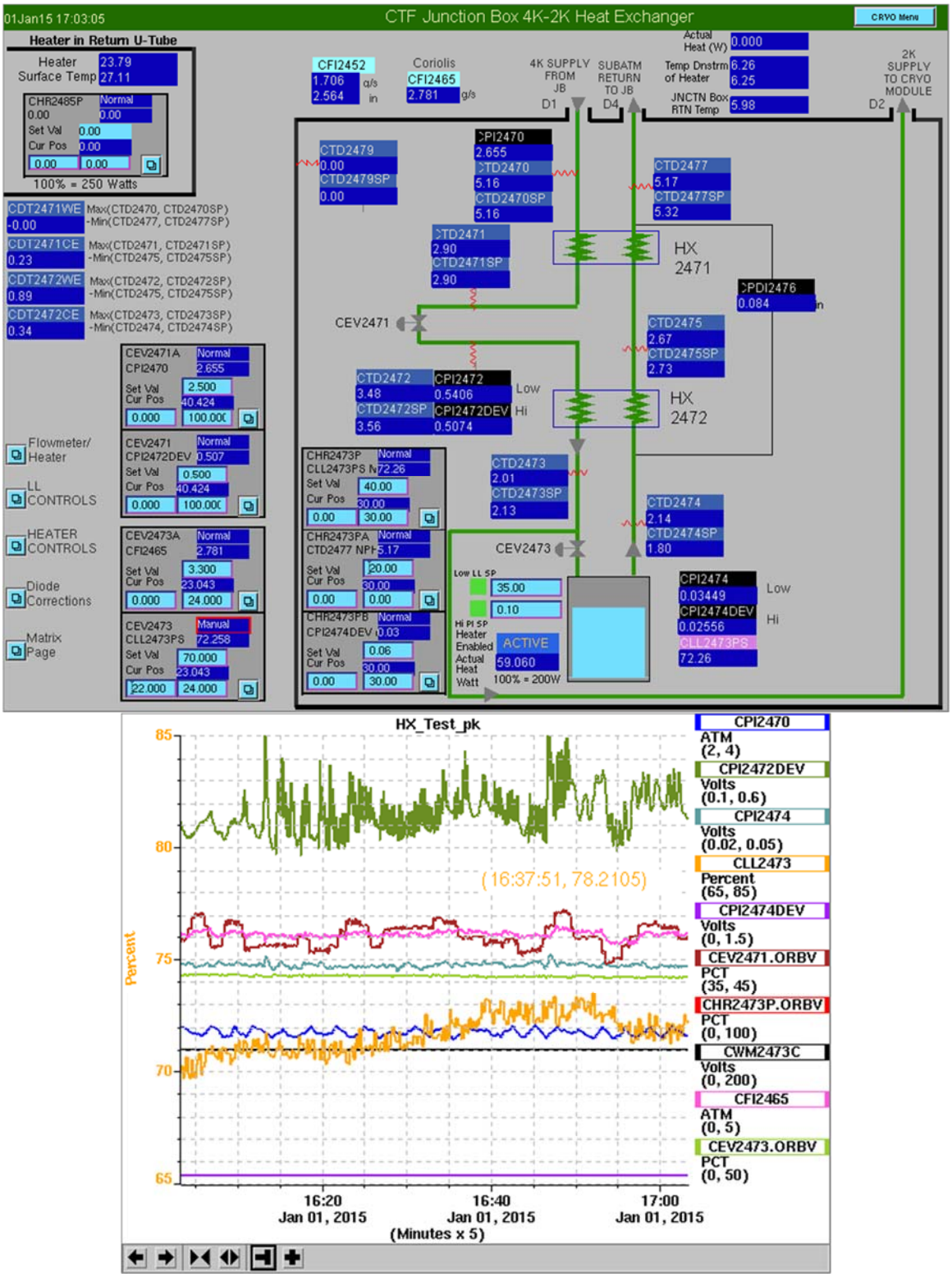

Figure P.19. Data, test #19: 60 W 0.5 atm 01-Jan-15 17:03

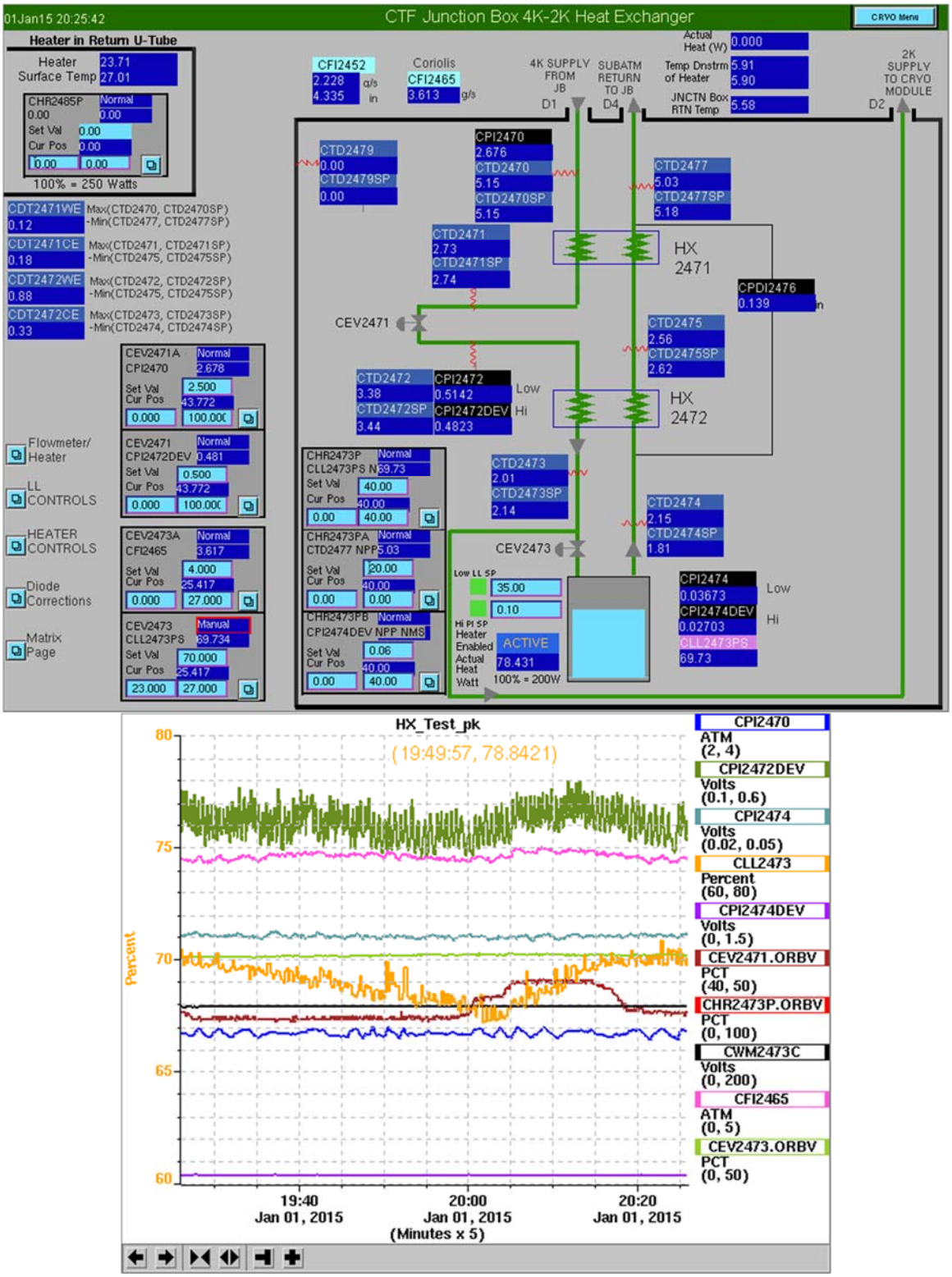

Figure P.20. Data, test #20: 80 W 0.5 atm 01-Jan-15 20:25

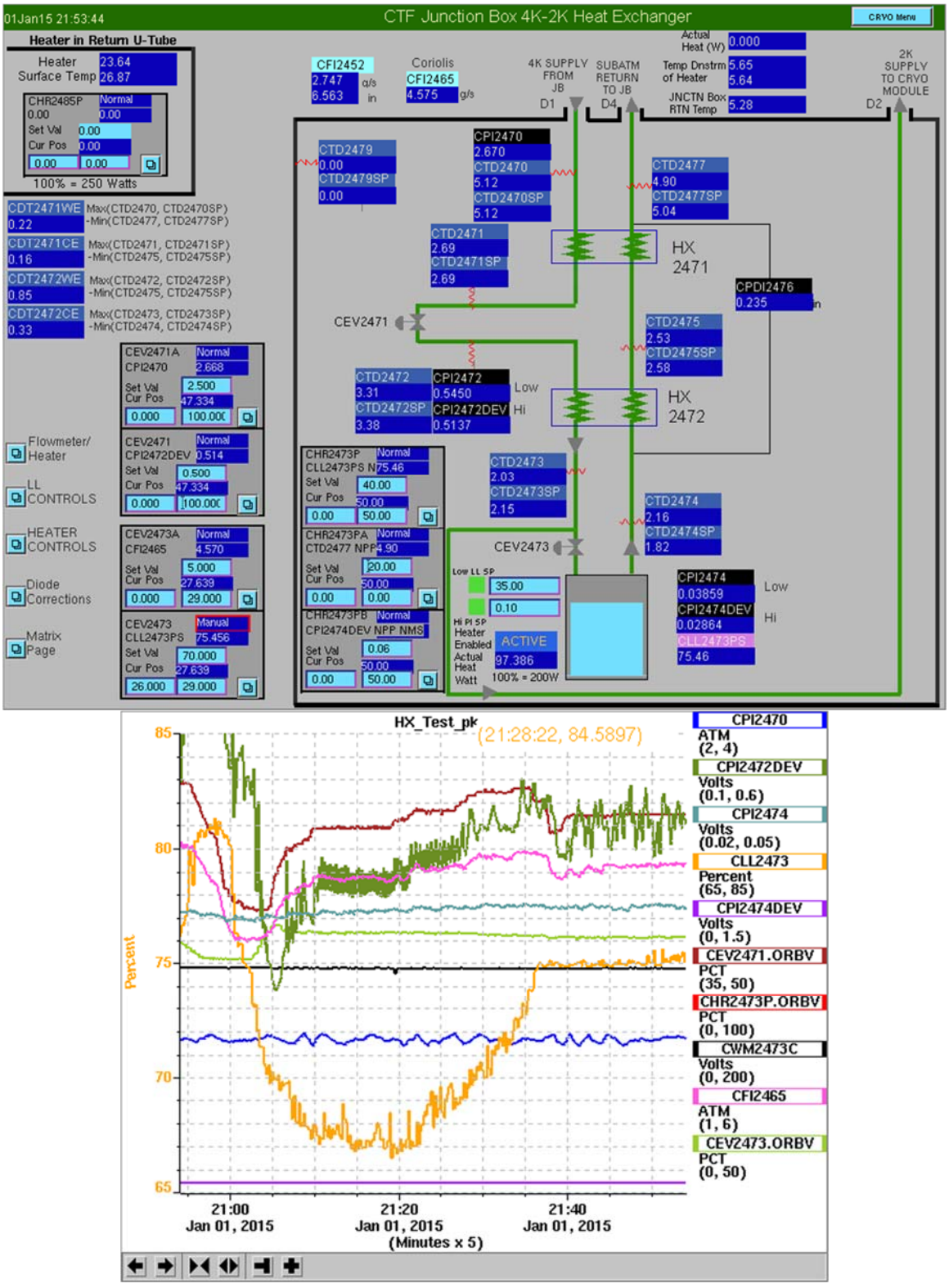

Figure P.21. Data, test #21: 100 W 0.5 atm 01-Jan-15 21:53

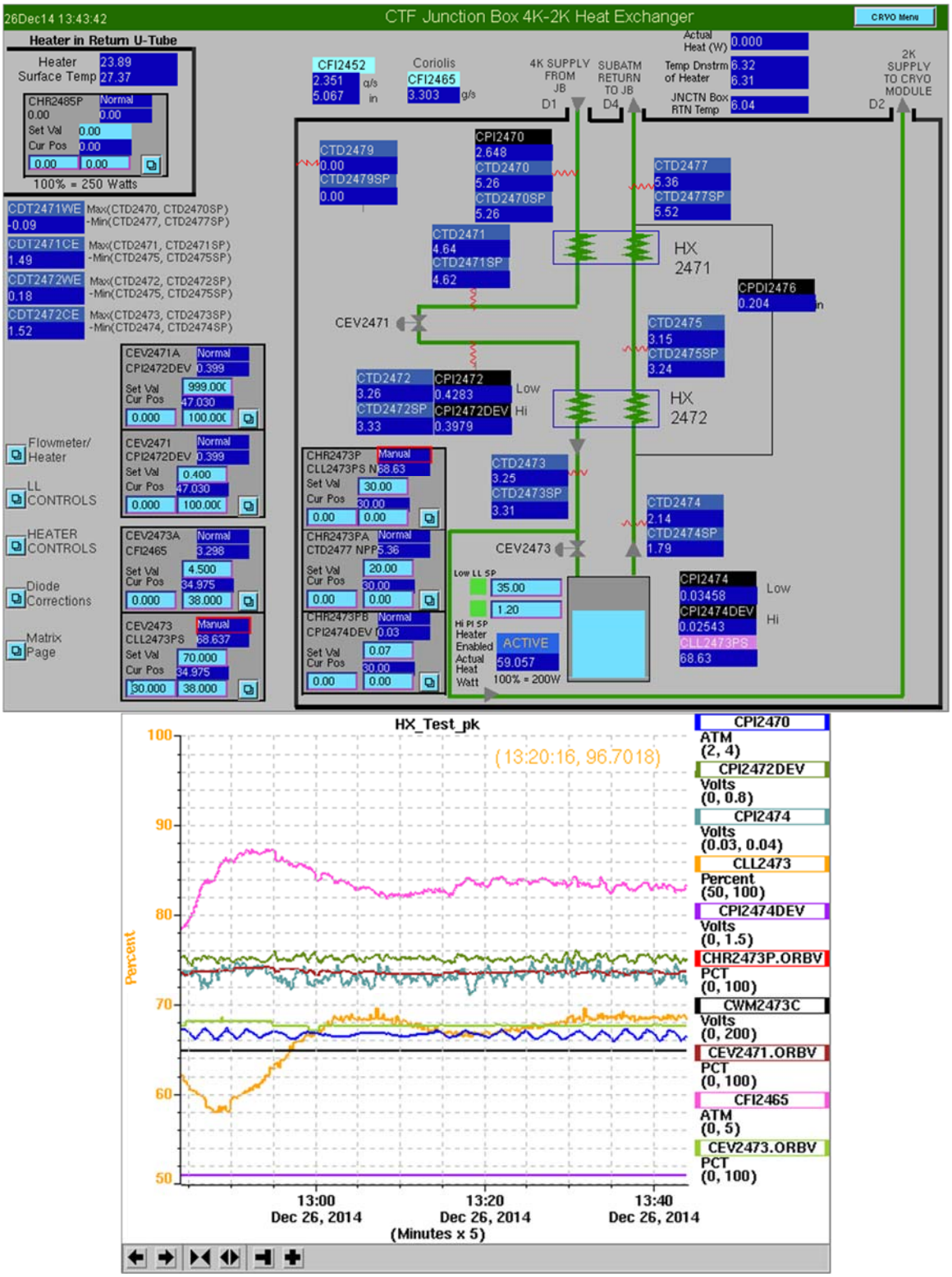

Figure P.22. Data, test #22: 60 W 0.4 atm 26-Dec-14 13:43

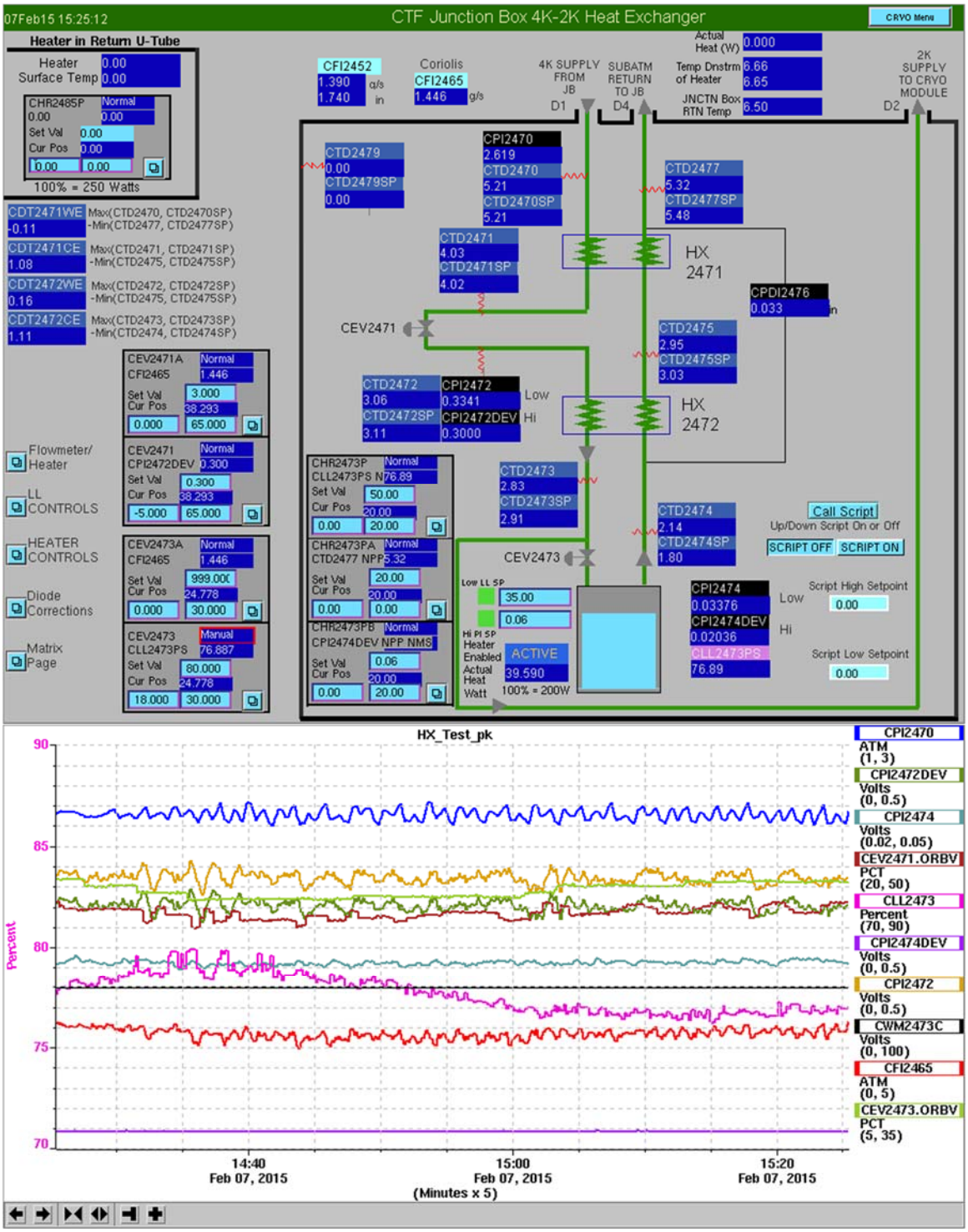

Figure P.23. Data, test #23: 40 W 0.3 atm 07-Feb-15 15:25

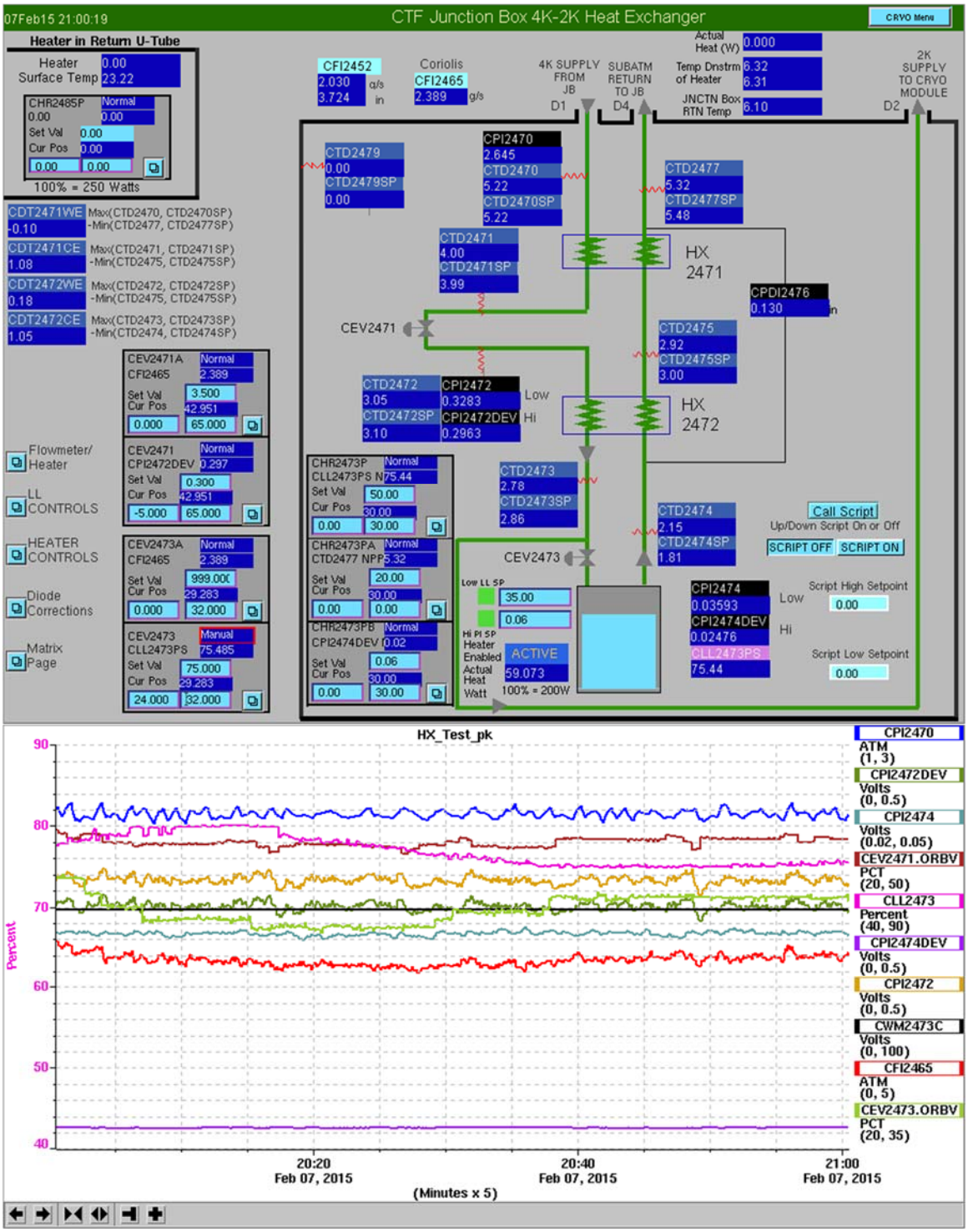

Figure P.24. Data, test #24: 60 W 0.3 atm 07-Feb-15 21:00

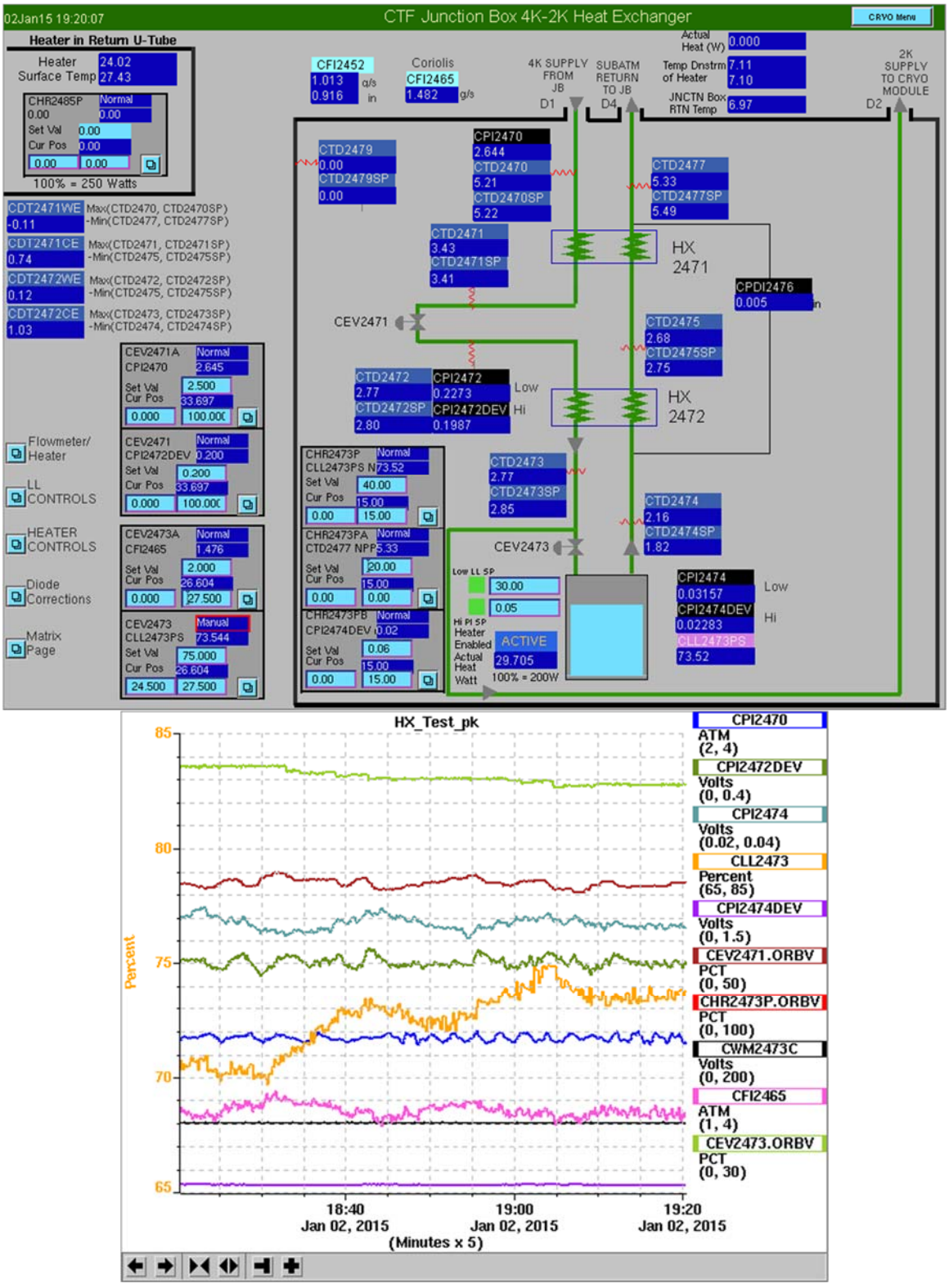

Figure P.25. Data, test #25: 30 W 0.2 atm 02-Jan-15 19:20

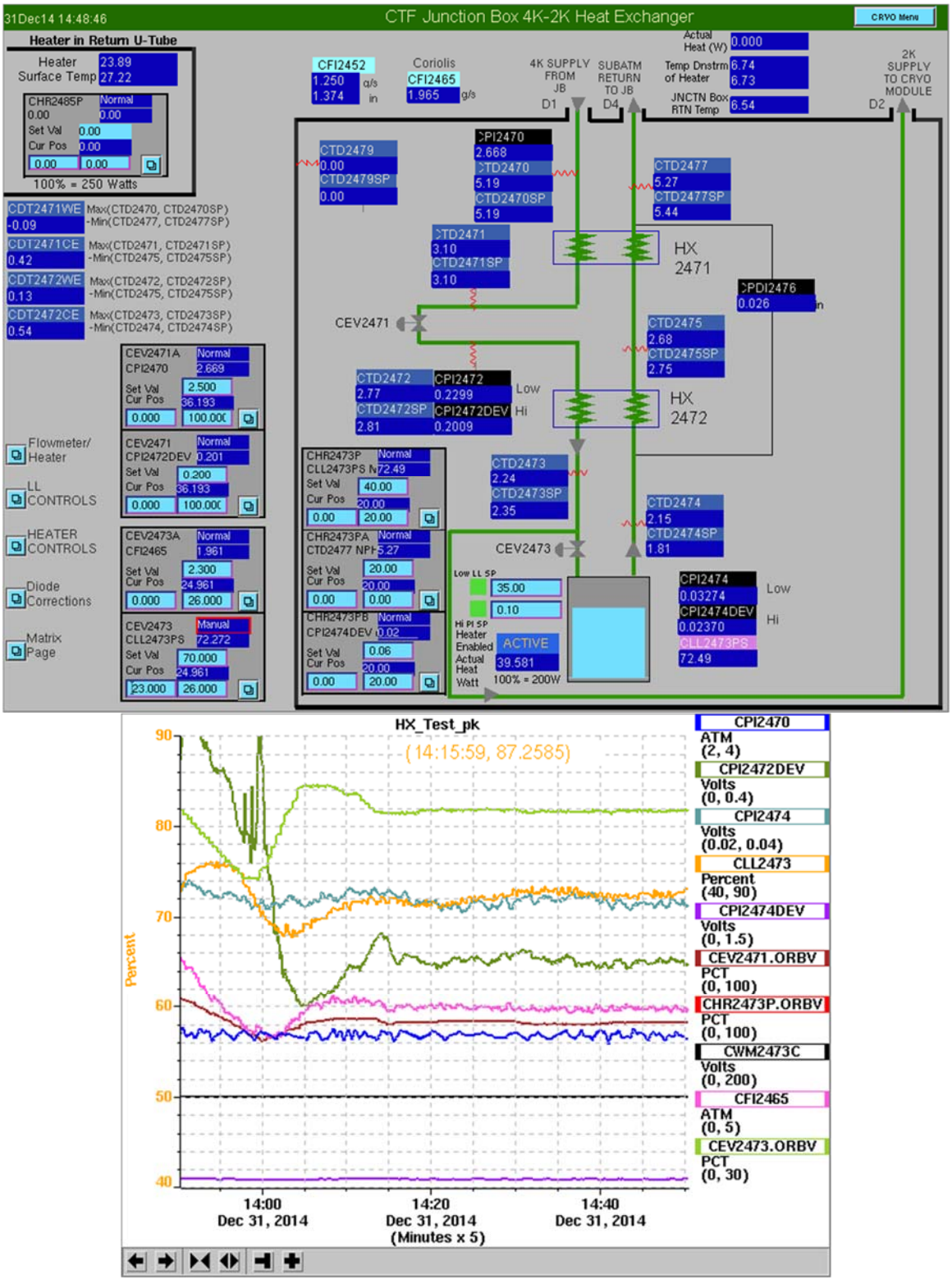

Figure P.26. Data, test #26: 40 W 0.2 atm 31-Dec-14 14:48

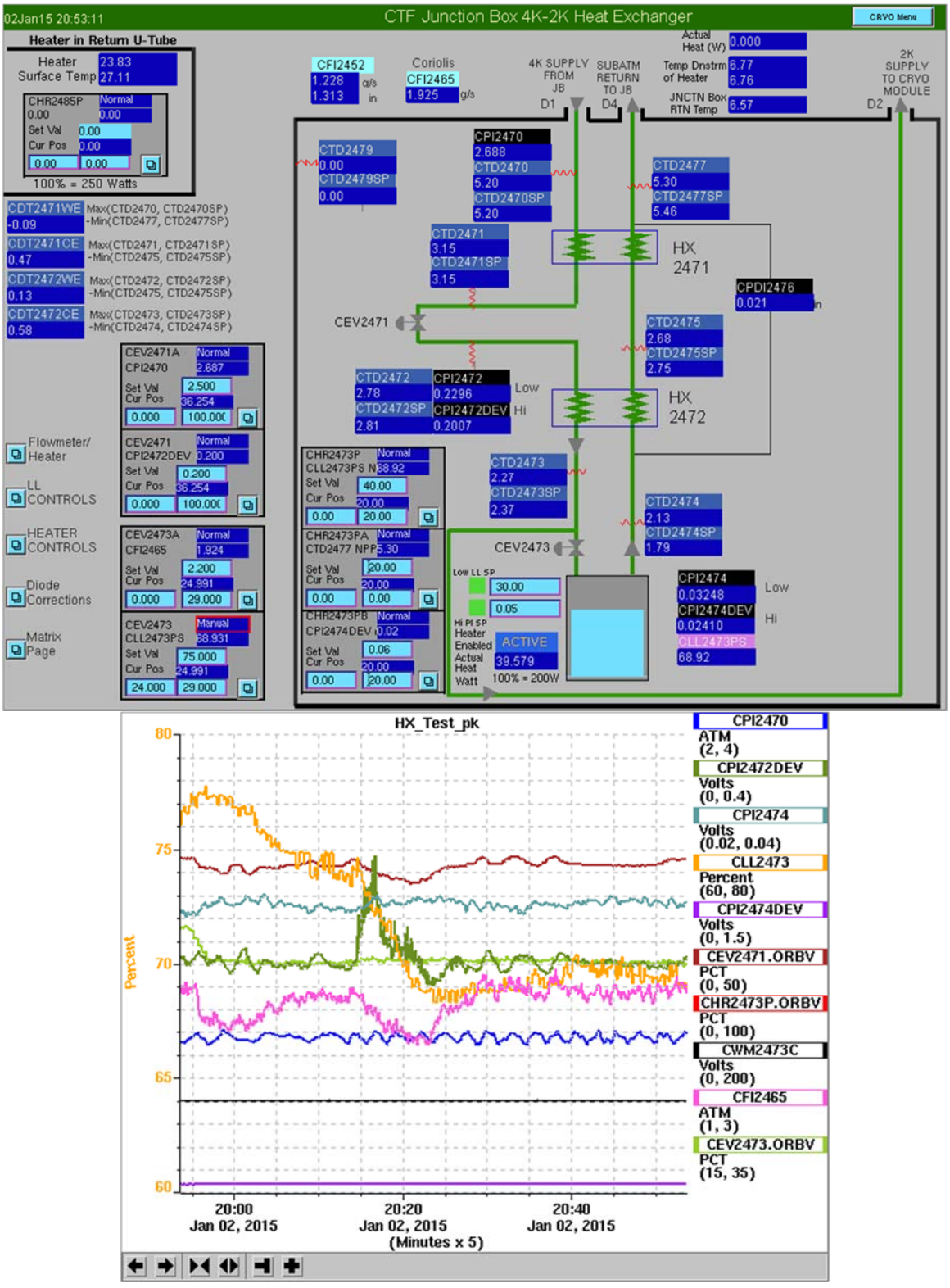

Figure P.27. Data, test #27: 40 W 0.2 atm 02-Jan-15 20:53

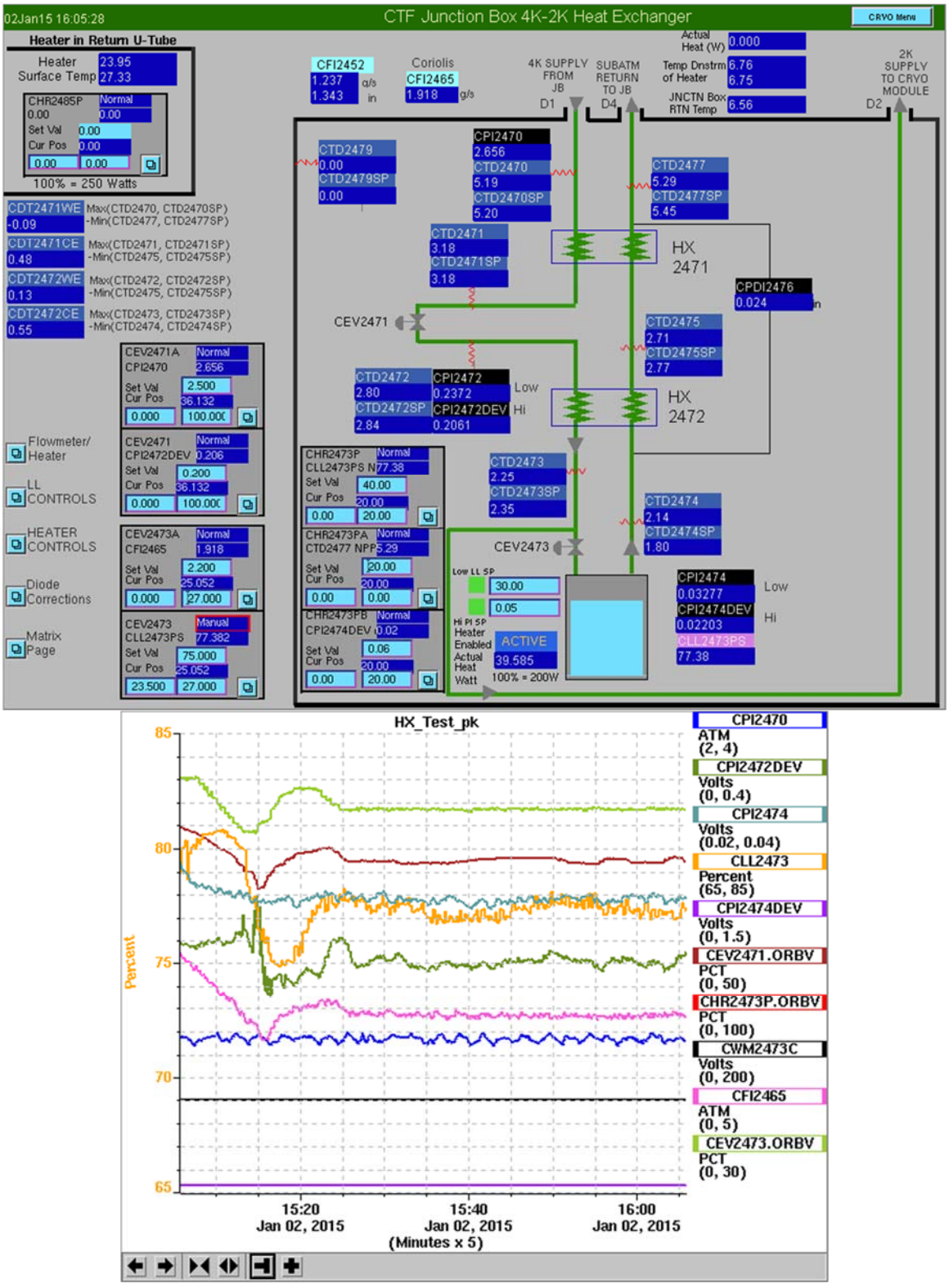

Figure P.28. Data, test #28: 40 W 0.2 atm 02-Jan-15 16:05

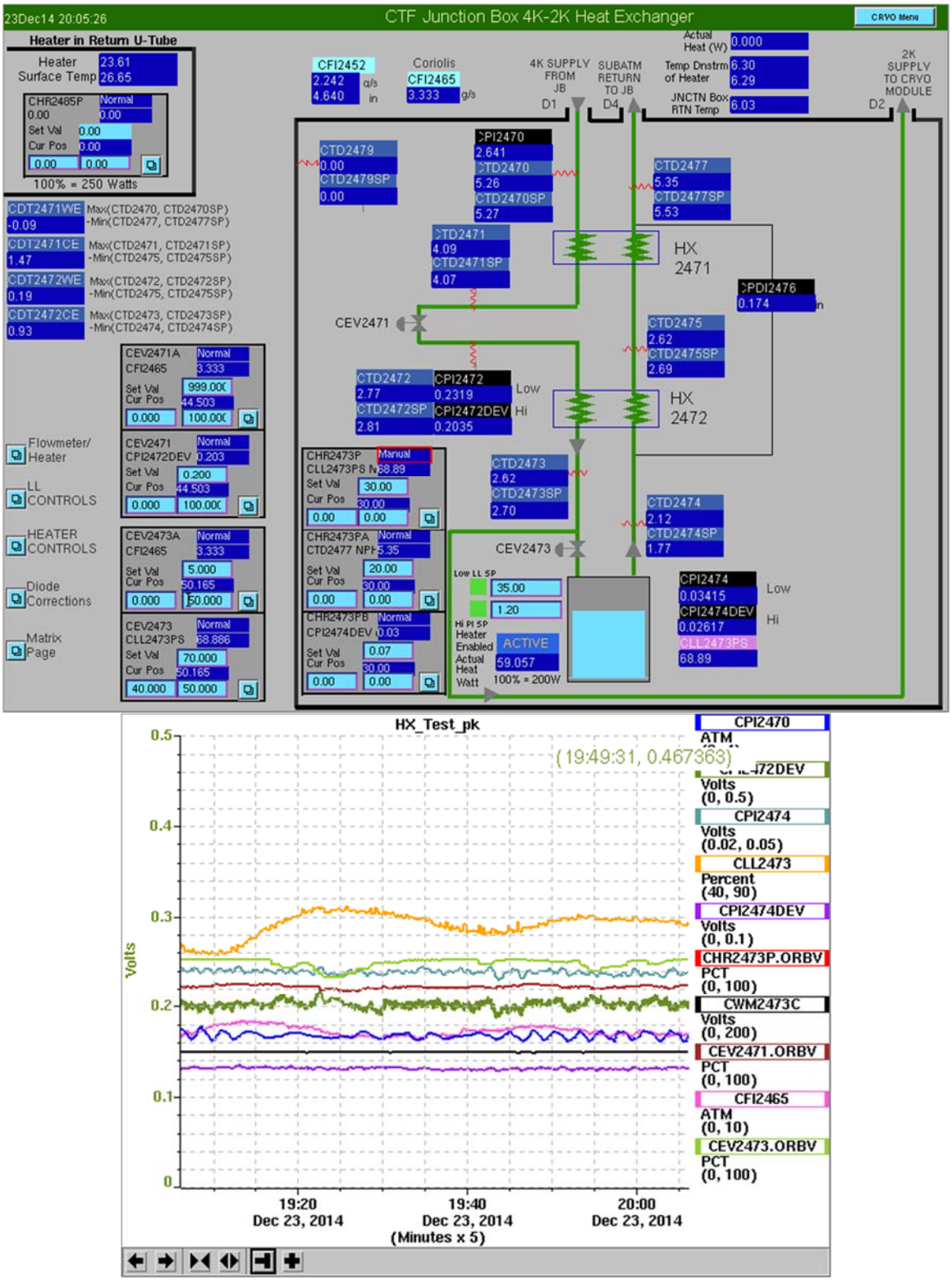

Figure P.29. Data, test #29: 60 W 0.2 atm 23-Dec-14 20:05

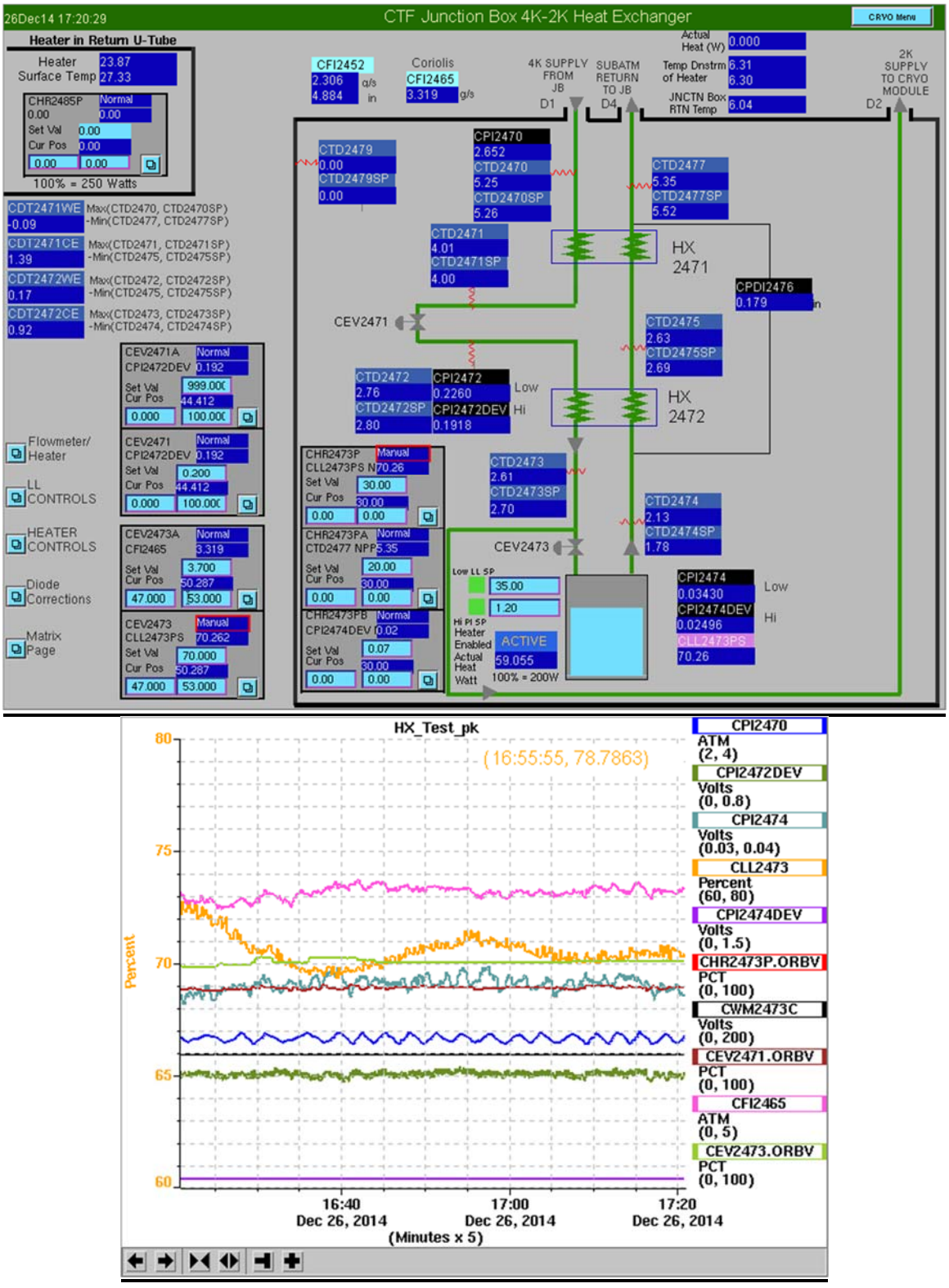

Figure P.30. Data, test #30: 60 W 0.2 atm 26-Dec-14 17:20

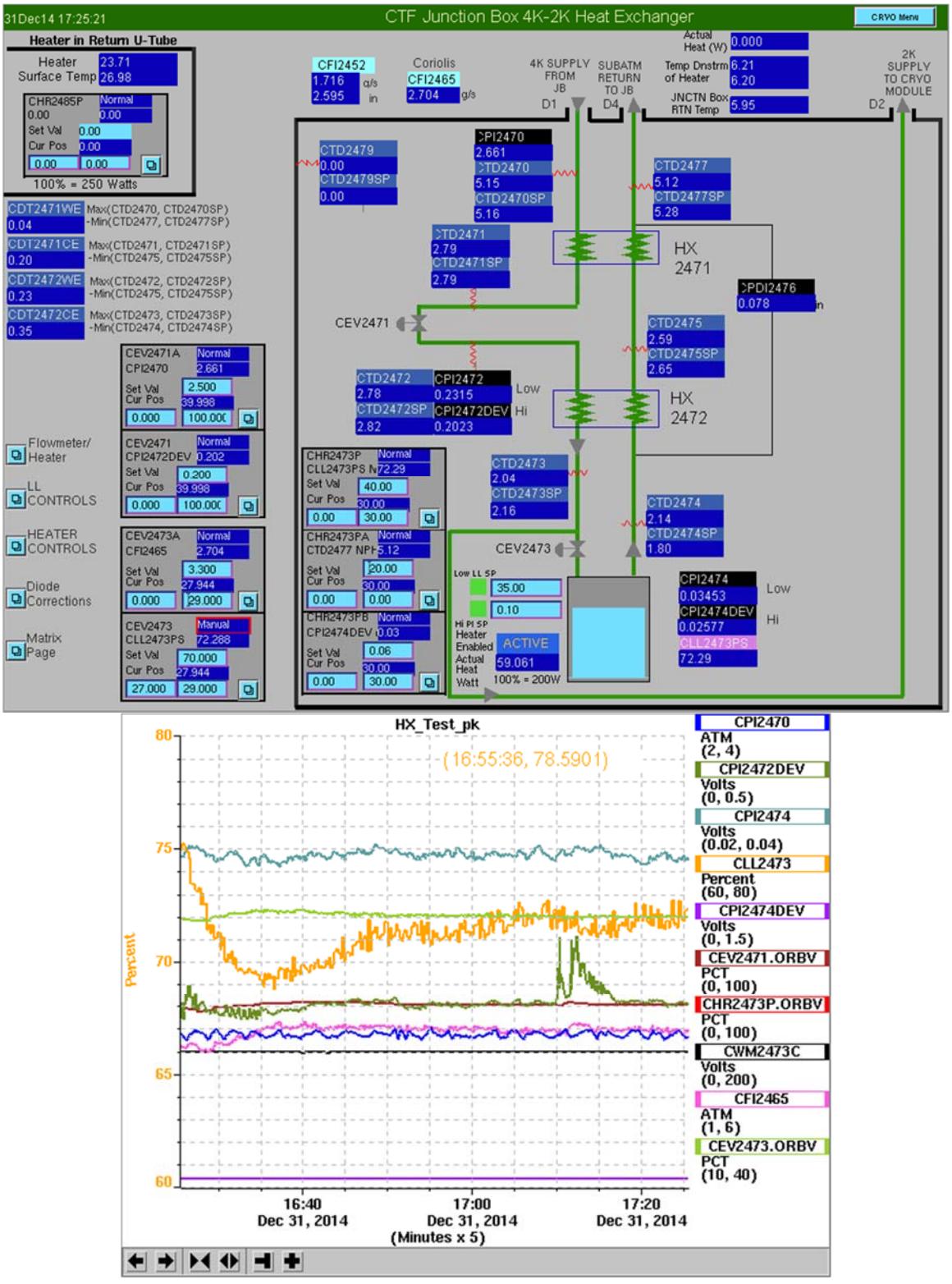

Figure P.31. Data, test #31: 60 W 0.2 atm 31-Dec-14 17:25

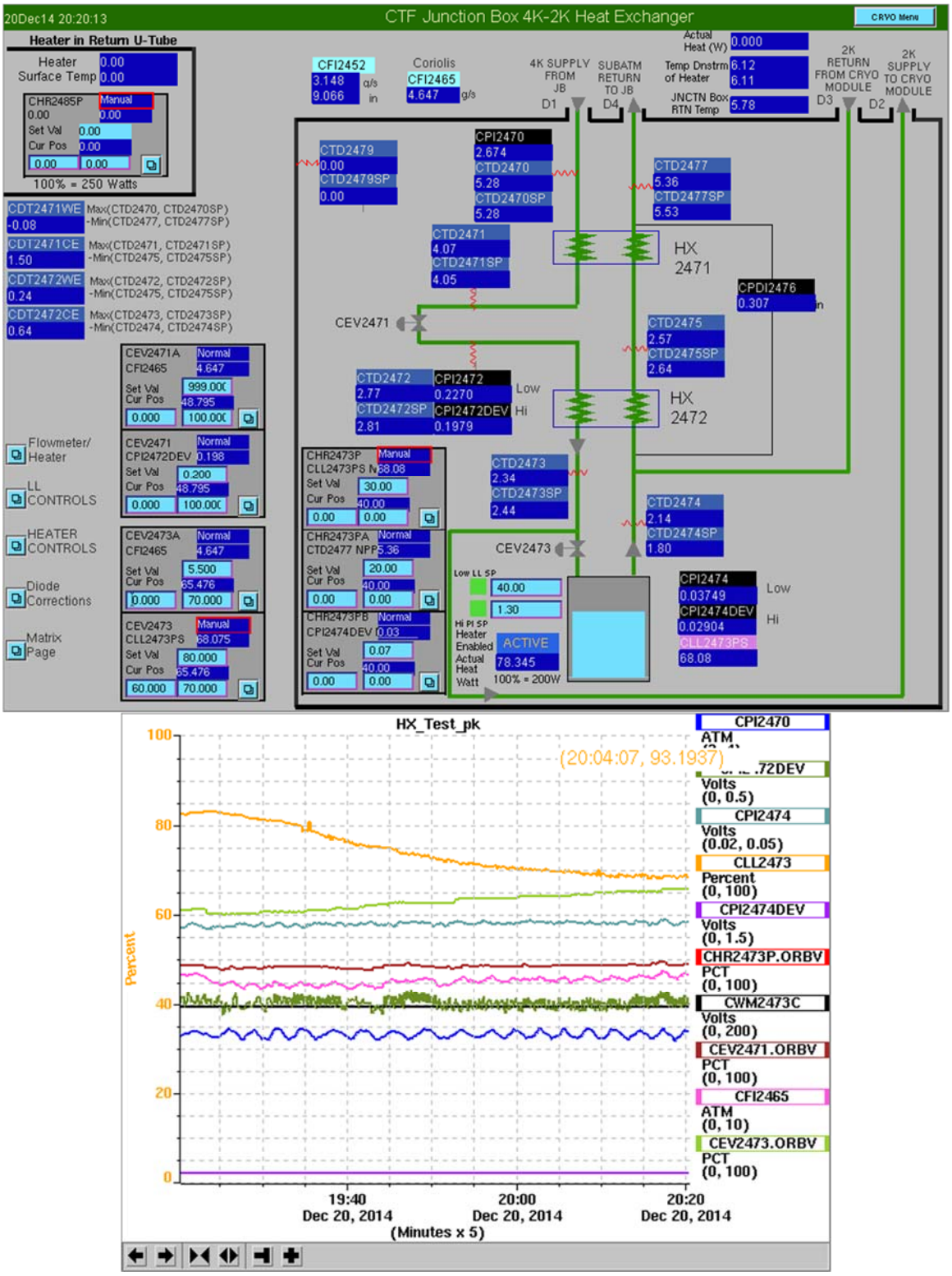

Figure P.32. Data, test #32: 80 W 0.2 atm 20-Dec-14 20:20

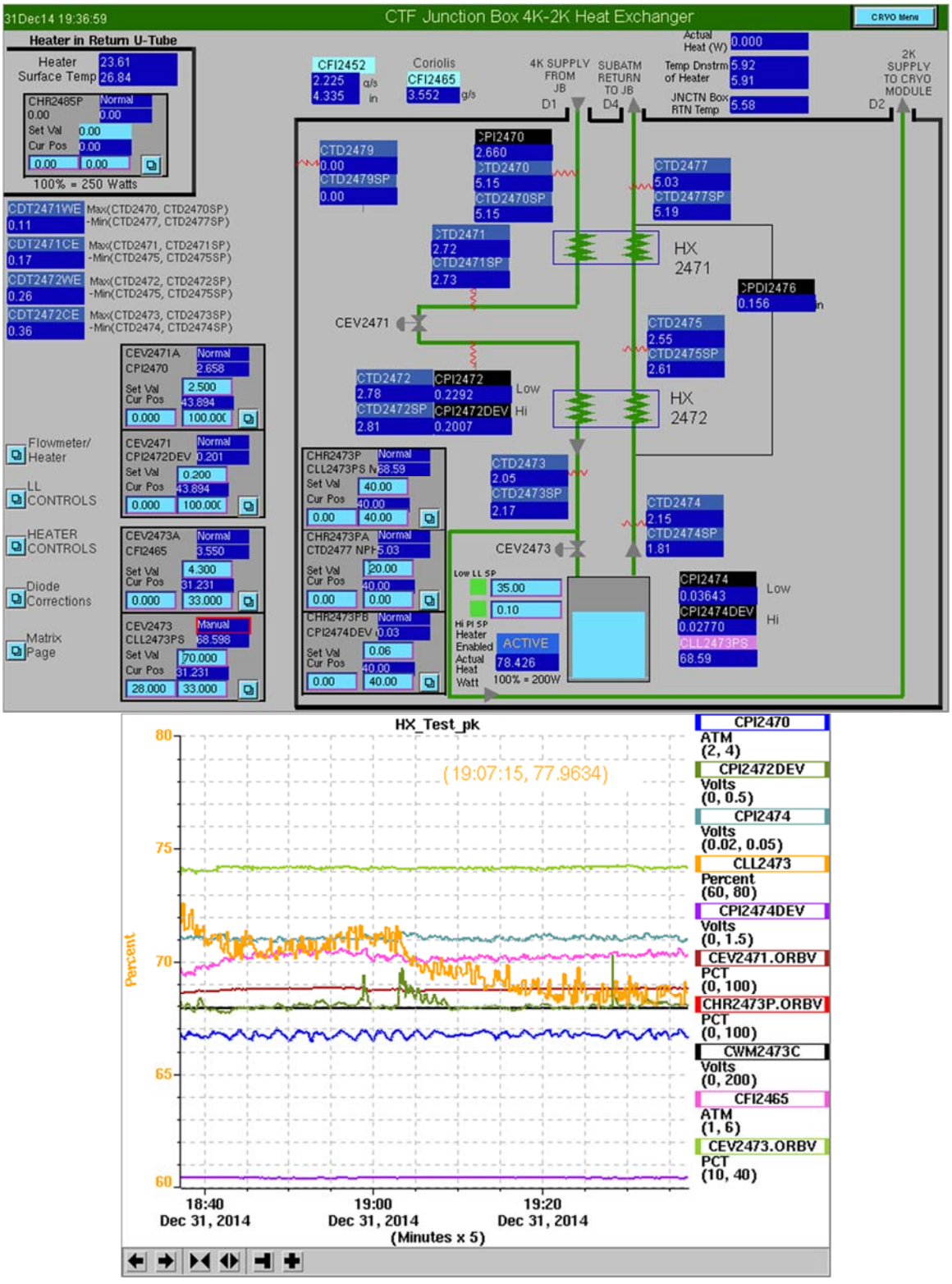

Figure P.33. Data, test #33: 80 W 0.2 atm 31-Dec-14 19:36

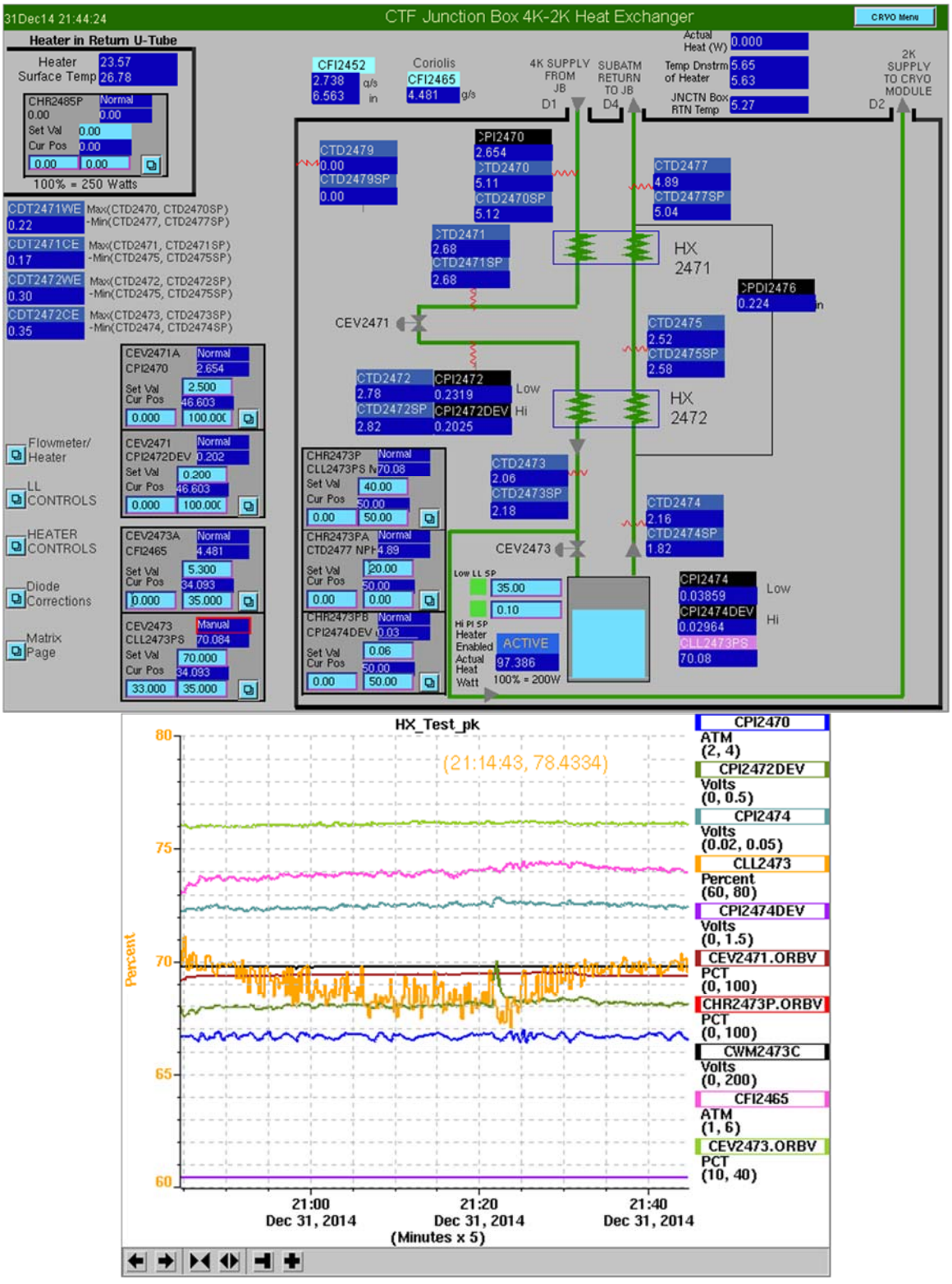

Figure P.34. Data, test #34: 100 W 0.2 atm 31-Dec-14 21:44

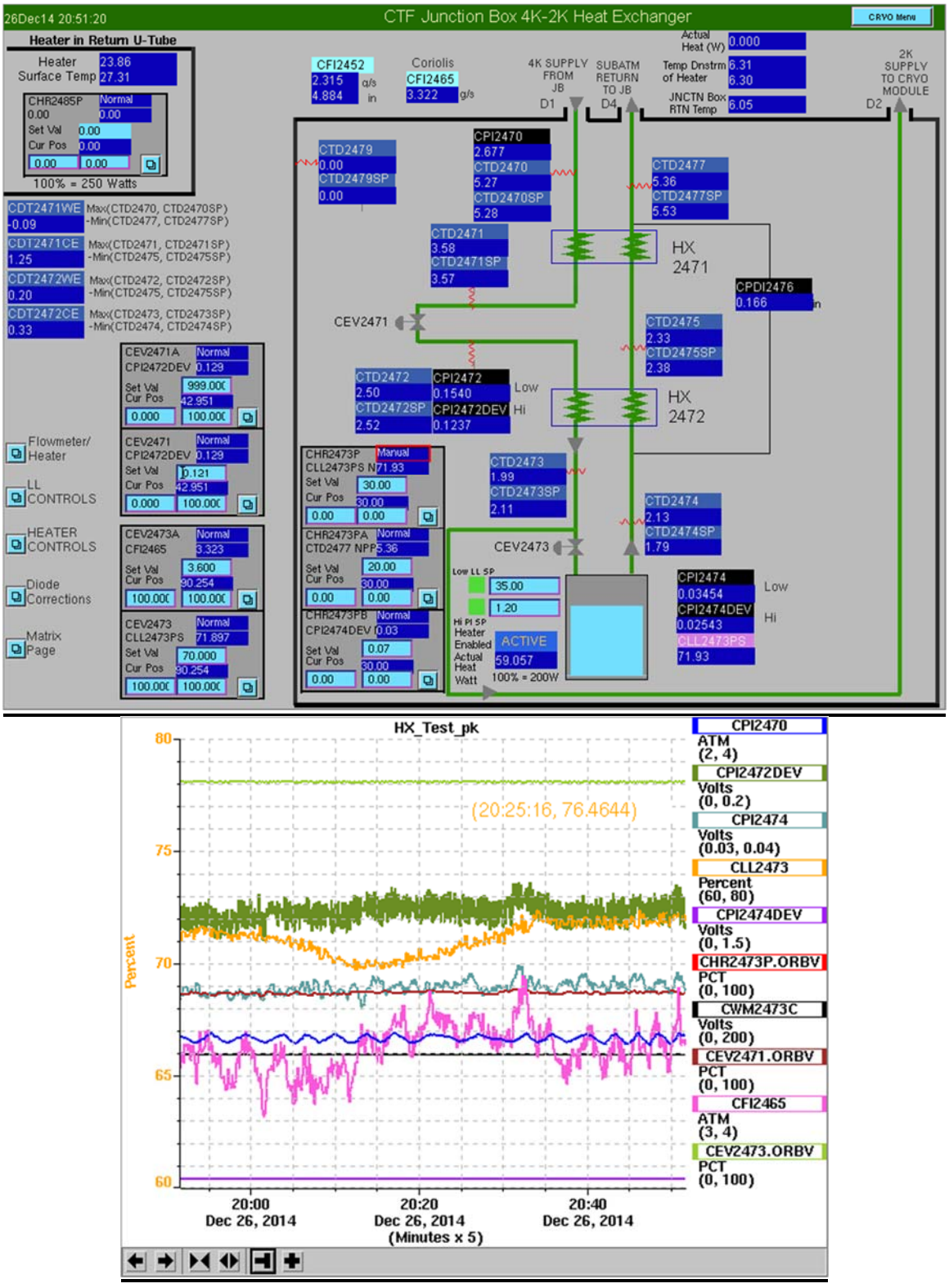

Figure P.35. Data, test #35: 60 W 0.12 atm 26-Dec-14 20:51

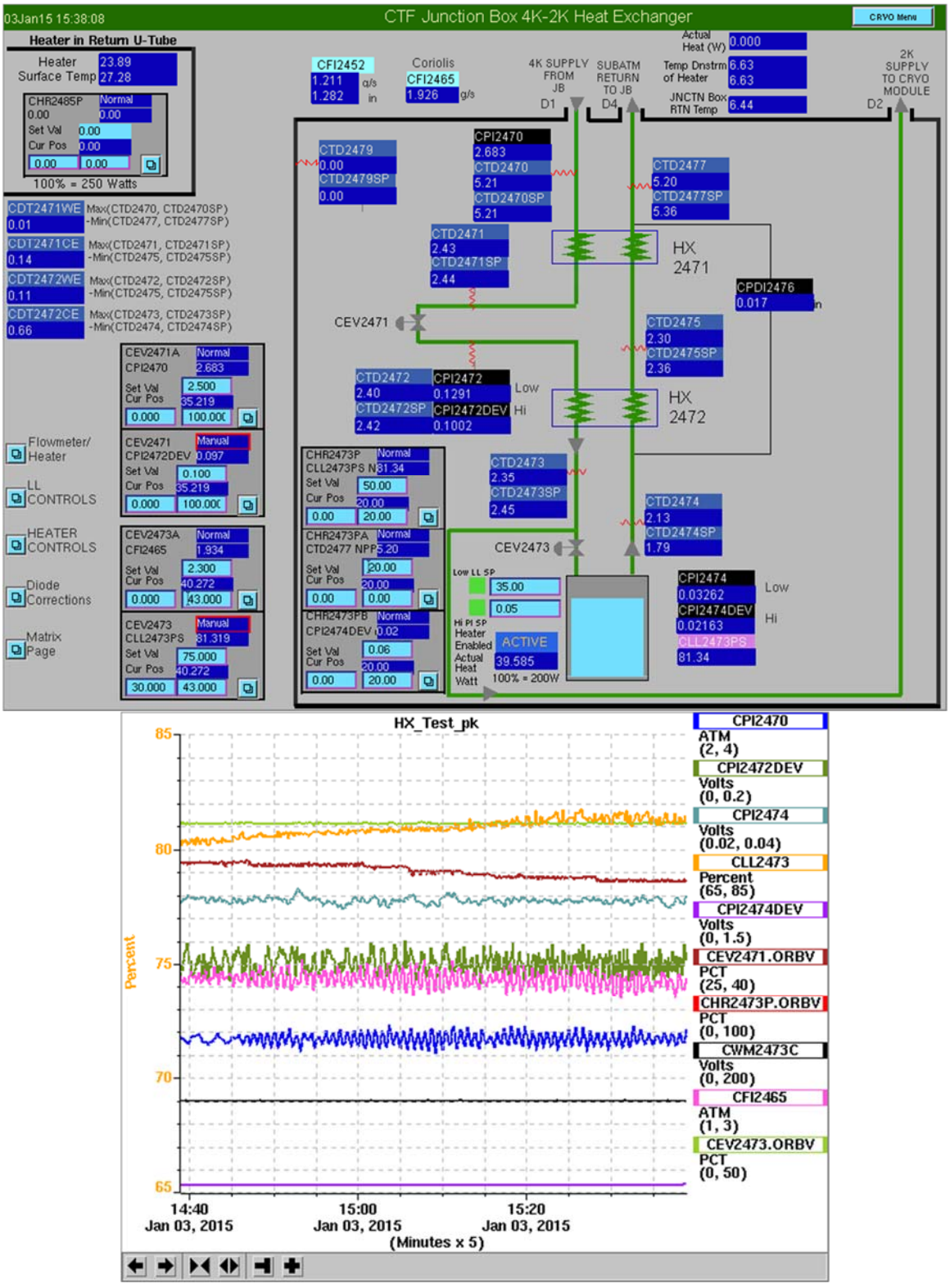

Figure P.36. Data, test #36: 40 W 0.1 atm 03-Jan-15 15:38

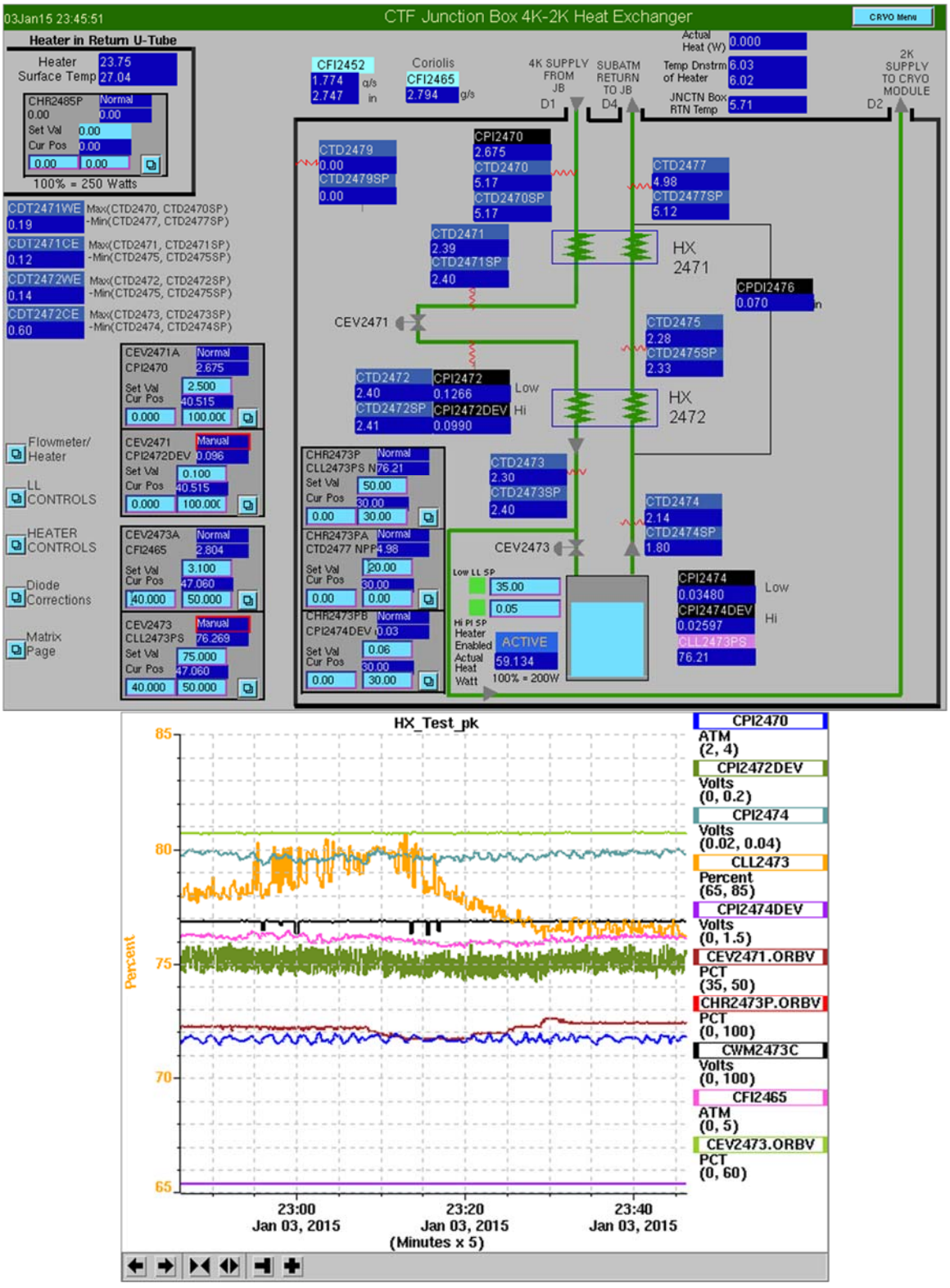

Figure P.37. Data, test #37: 60 W 0.1 atm 03-Jan-15 23:45

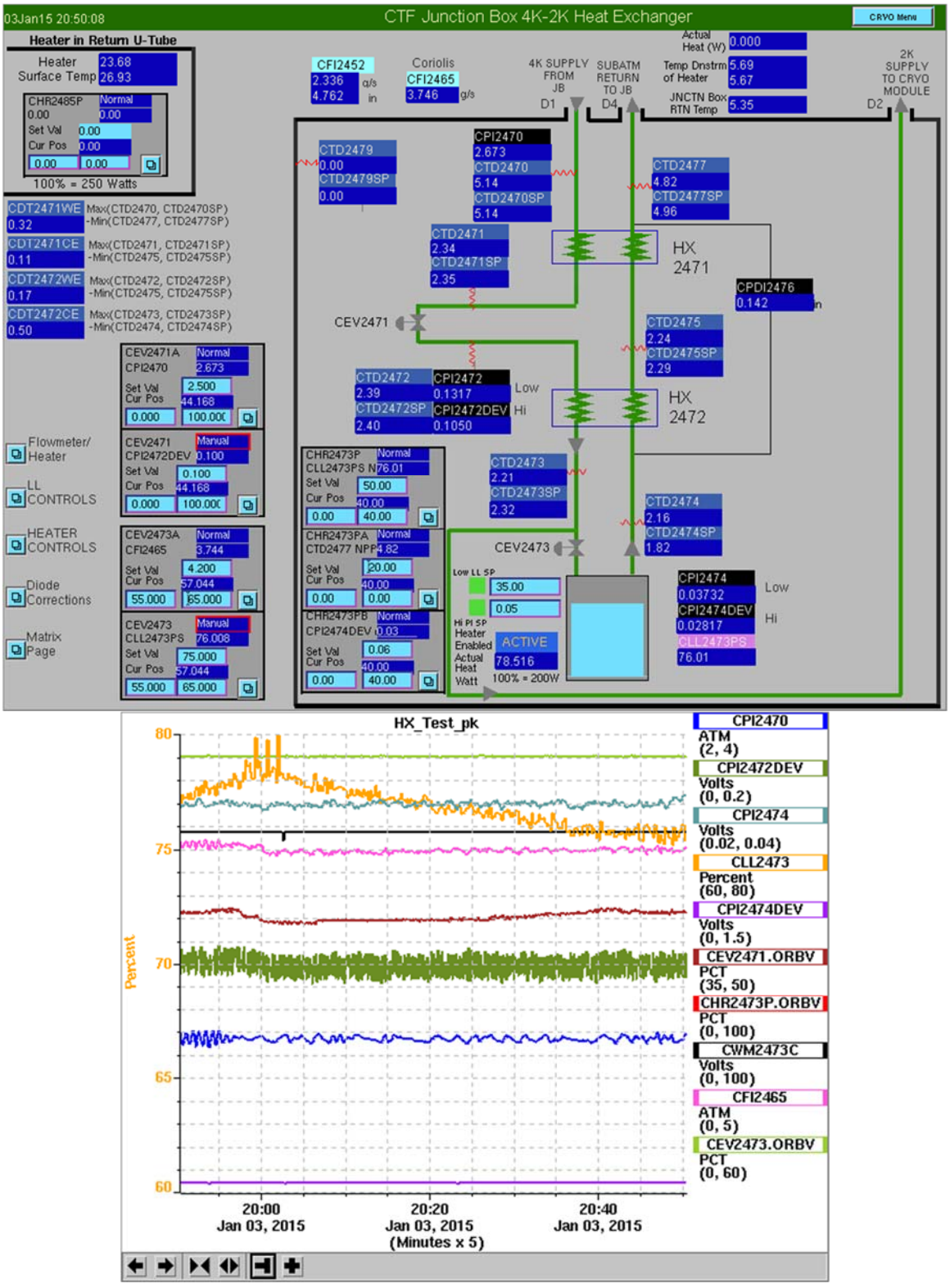

Figure P.38. Data, test #38: 80 W 0.1 atm 03-Jan-15 20:50

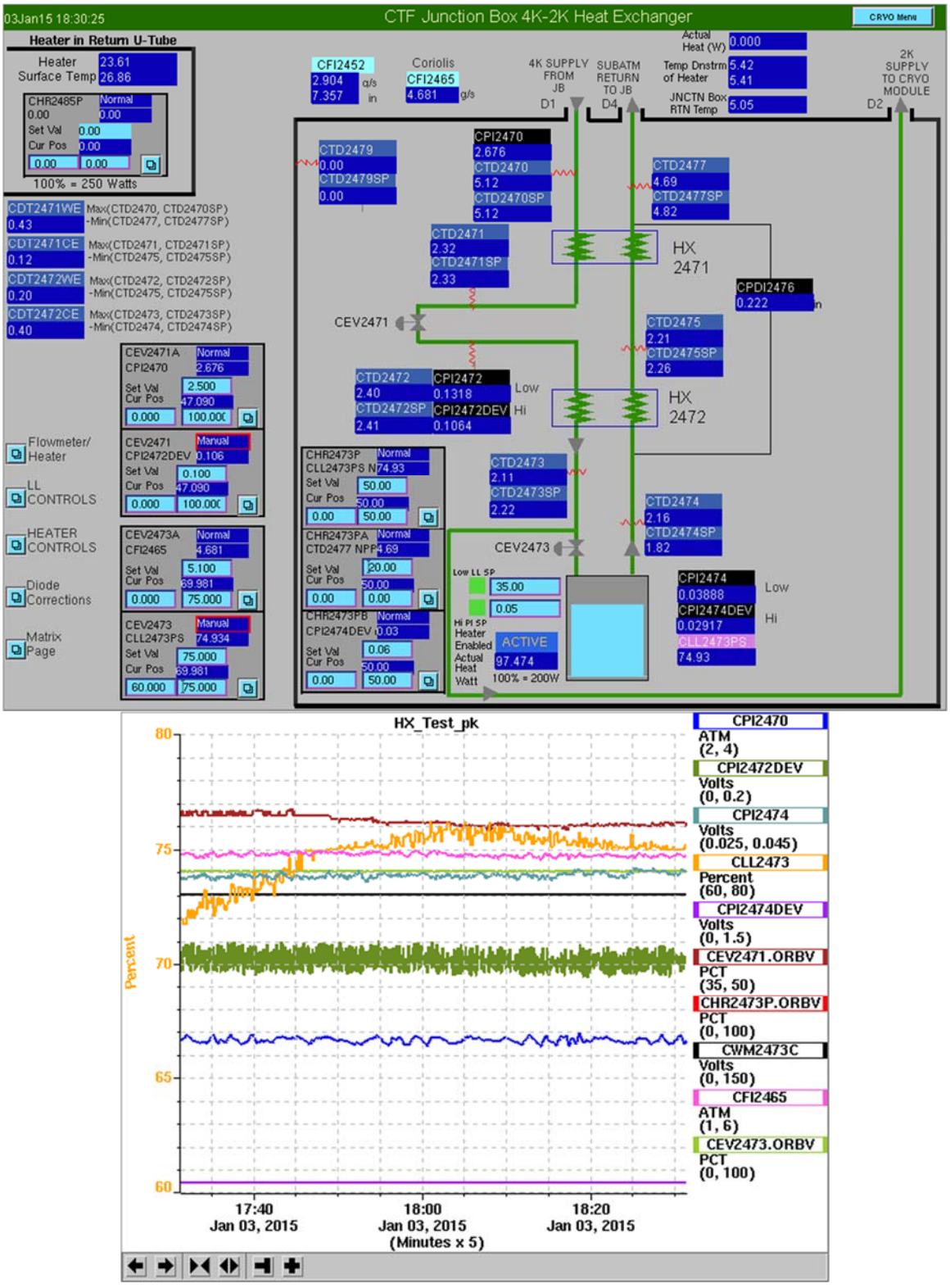

Figure P.39. Data, test #39: 100 W 0.1 atm 03-Jan-15 18:30

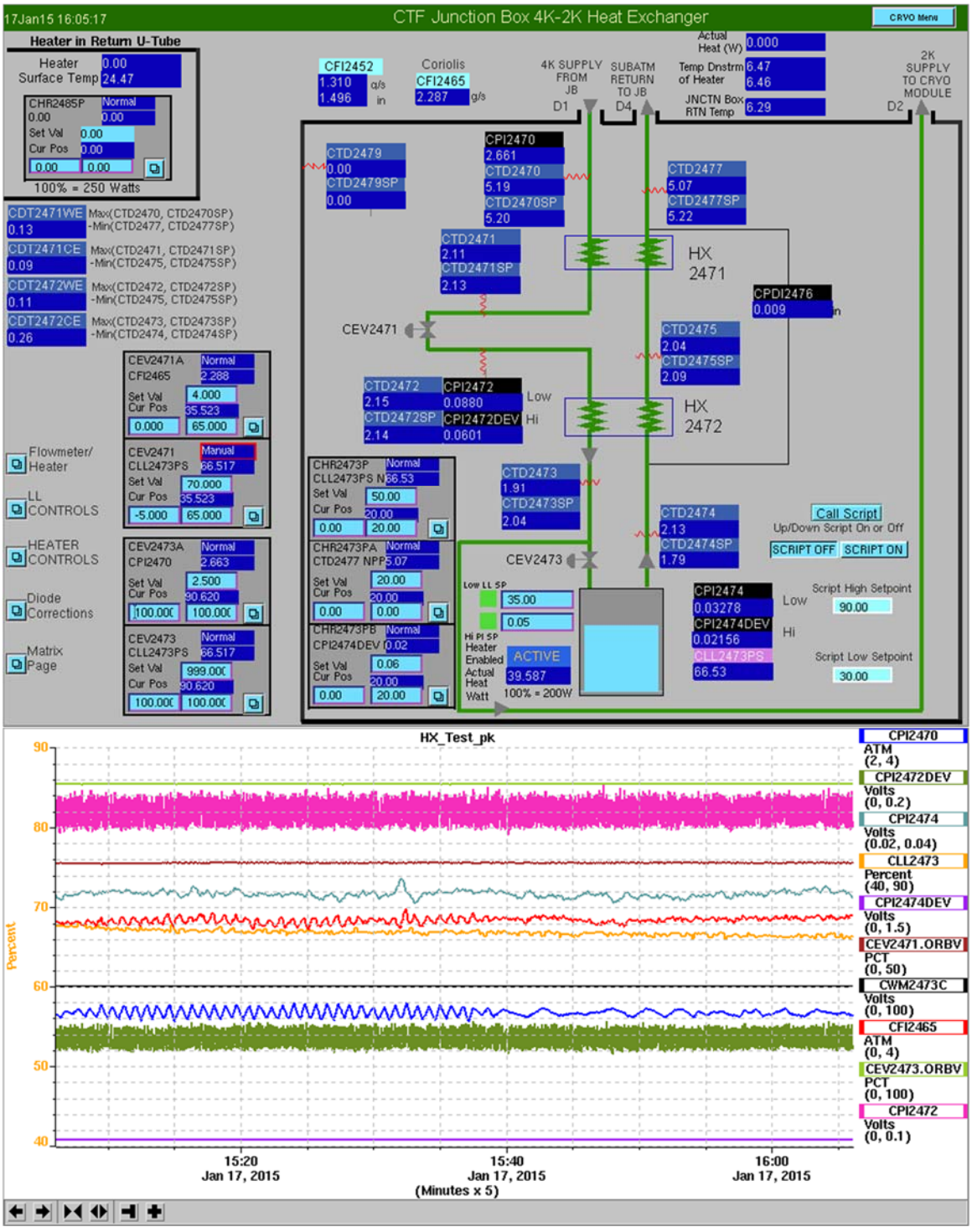

Figure P.40. Data, test #40: 40 W Low 17-Jan-15 16:05

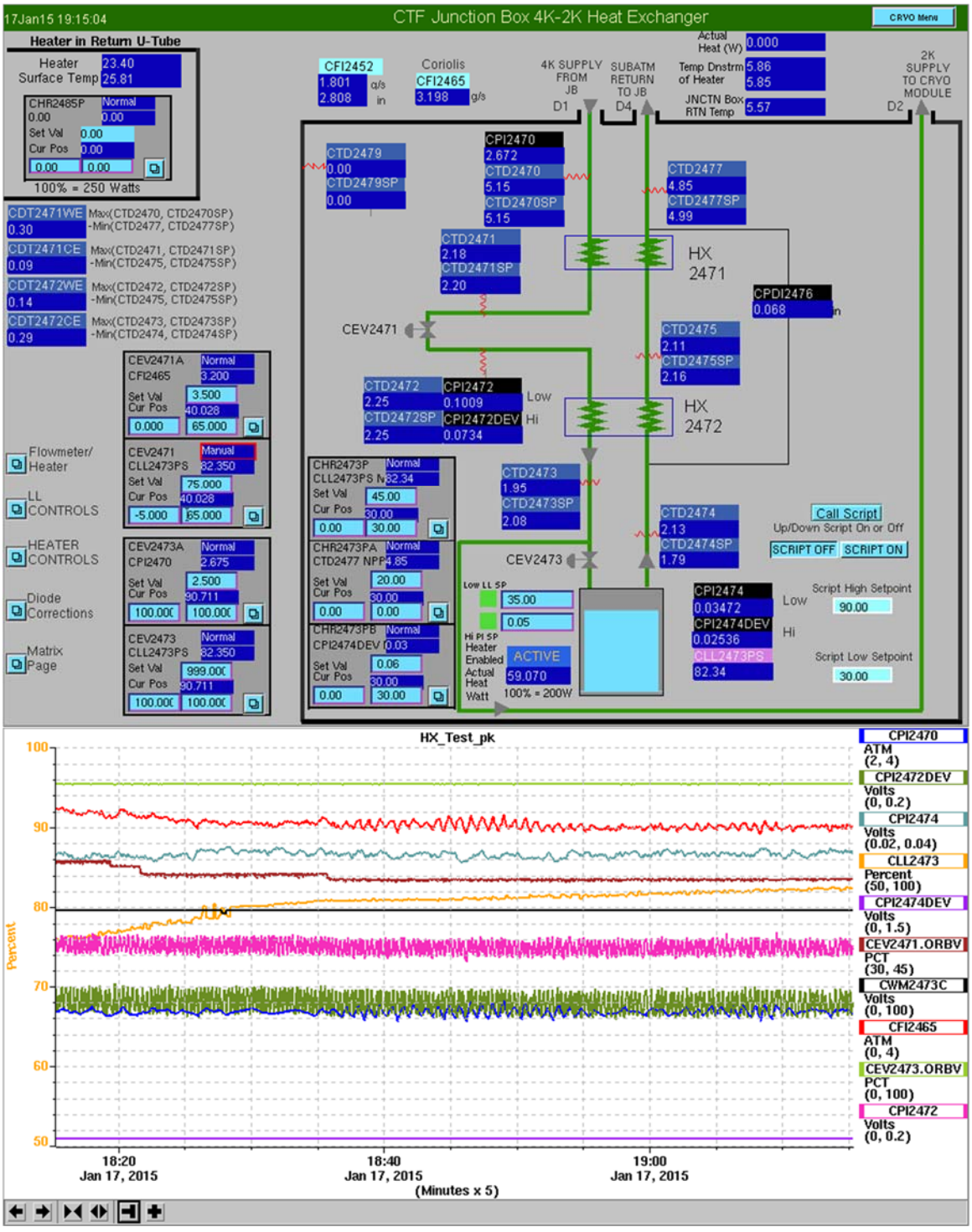

Figure P.41. Data, test #41: 60 W Low 17-Jan-15 19:15

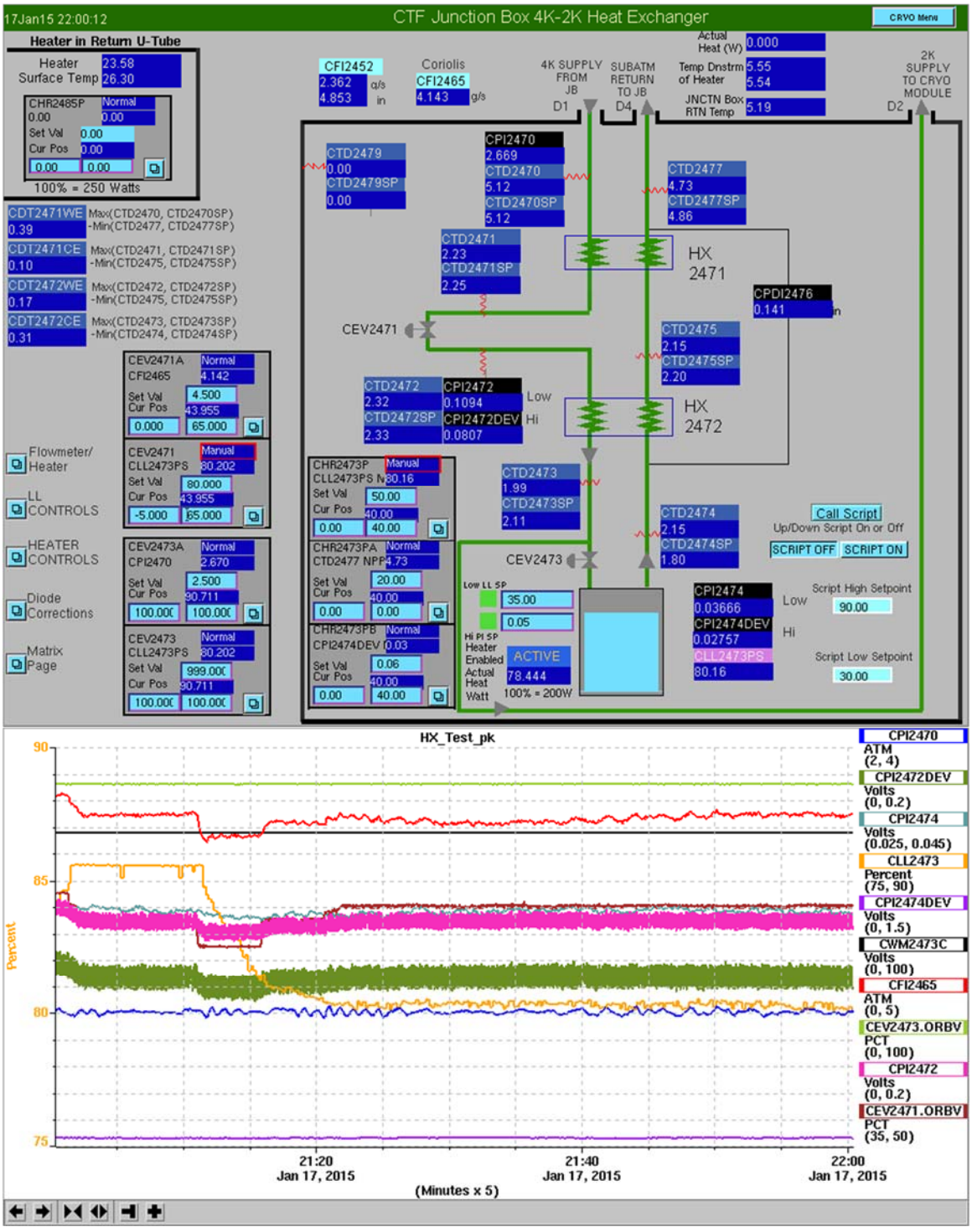

Figure P.42. Data, test #42: 80 W Low 17-Jan-15 22:00

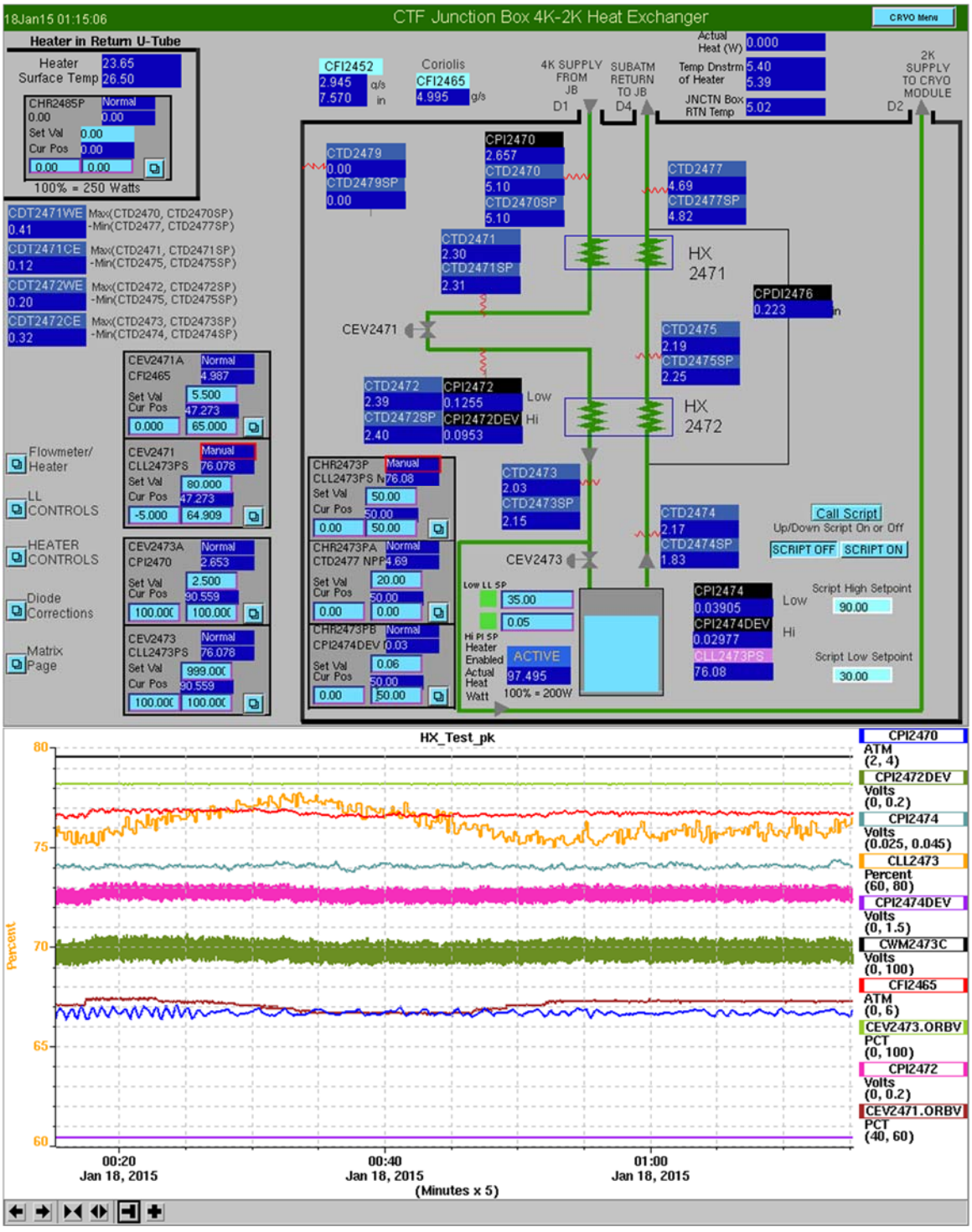

Figure P.43. Data, test #43: 100 W Low 17-Jan-15 01:15

APPENDIX Q – PROCESS MODEL OUTPUT FOR ALL TESTS

This appendix contains the output of the process model for all of the tests, sequentially per test number and one page per test. The output structure is explained in Chapter 3.

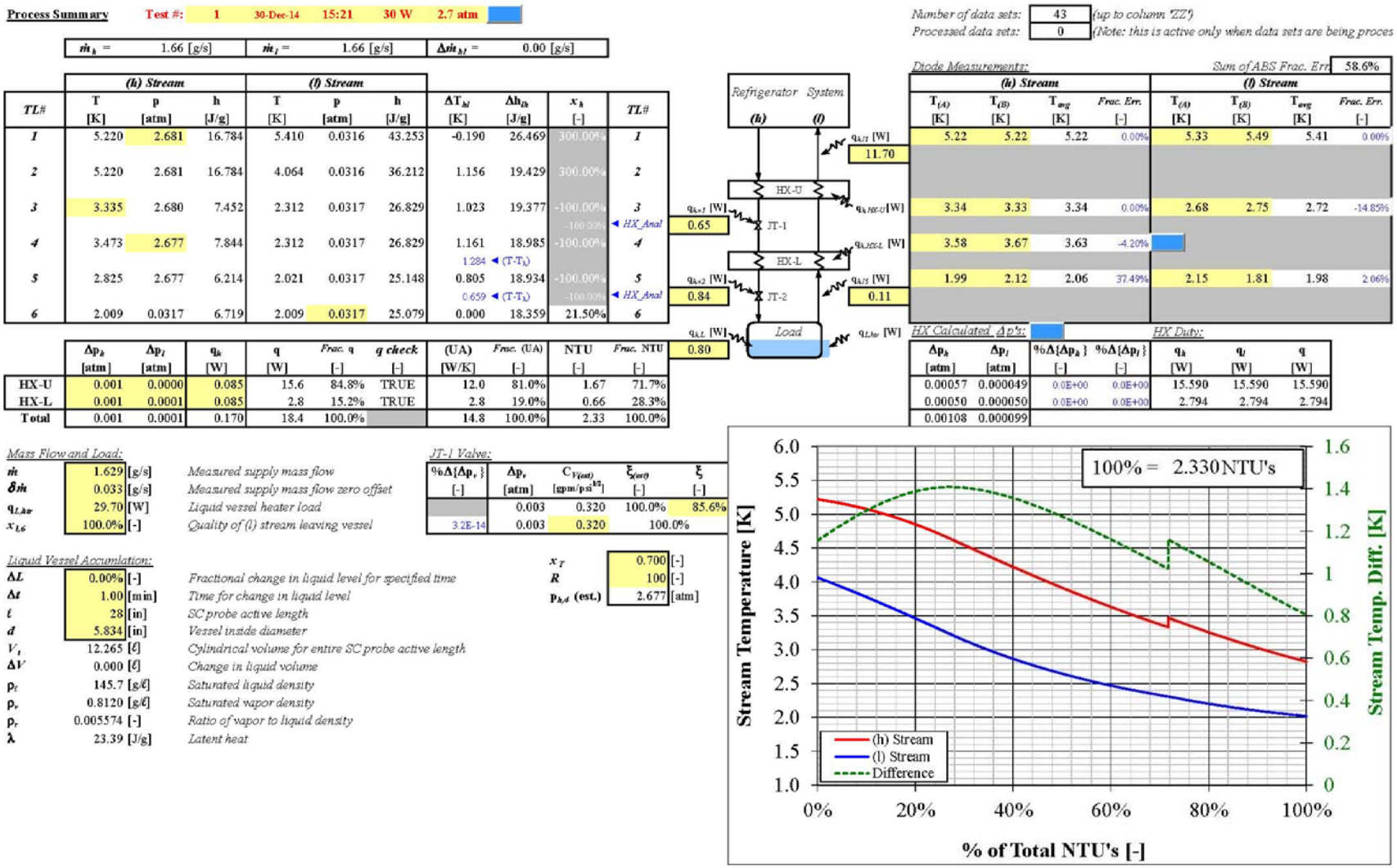

Figure Q.1. Process model output, test #1: 30 W 2.7 atm 30-Dec-14 15:21

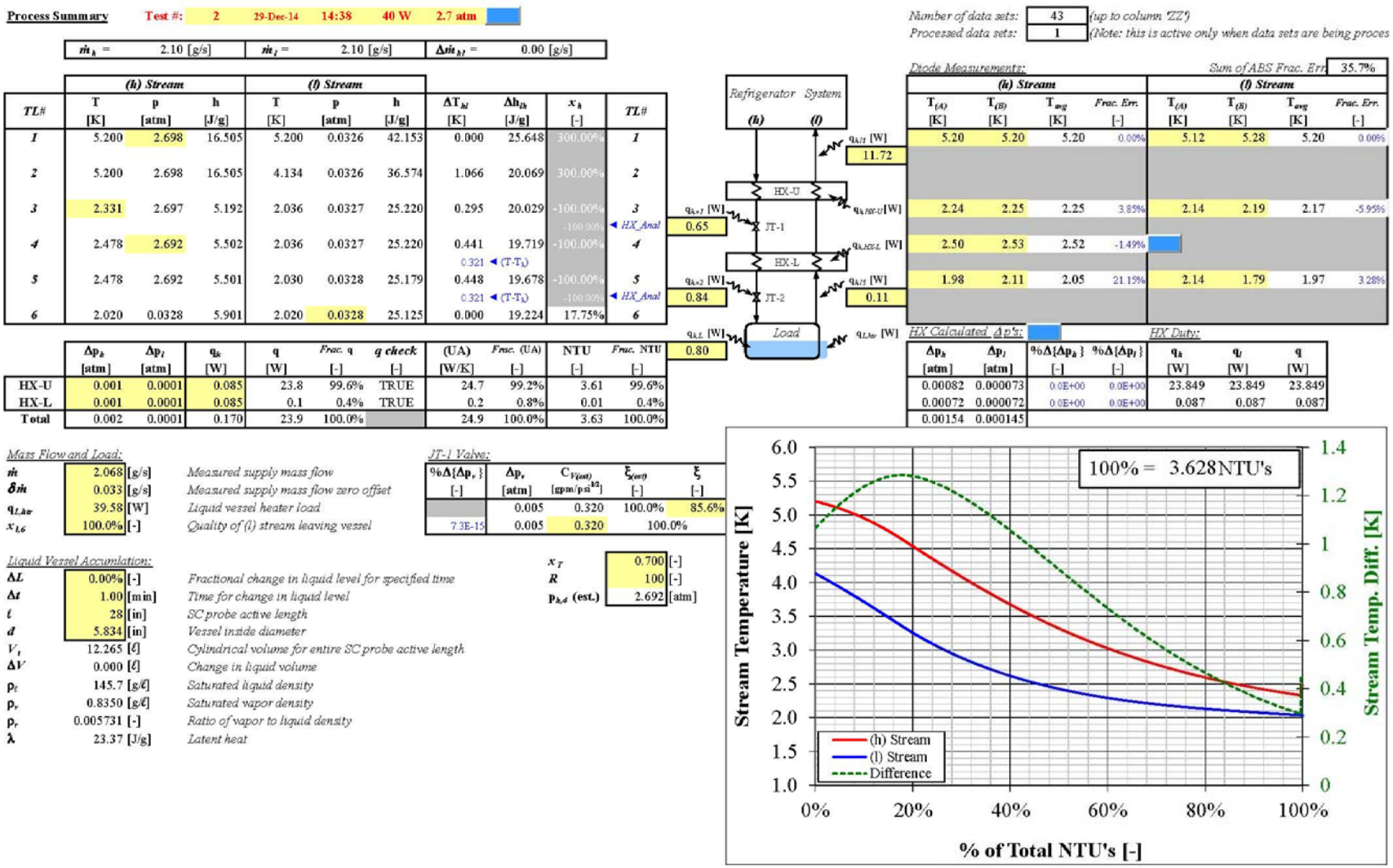

Figure Q.2. Process model output, test #2: 40 W 2.7 atm 29-Dec-14 14:38

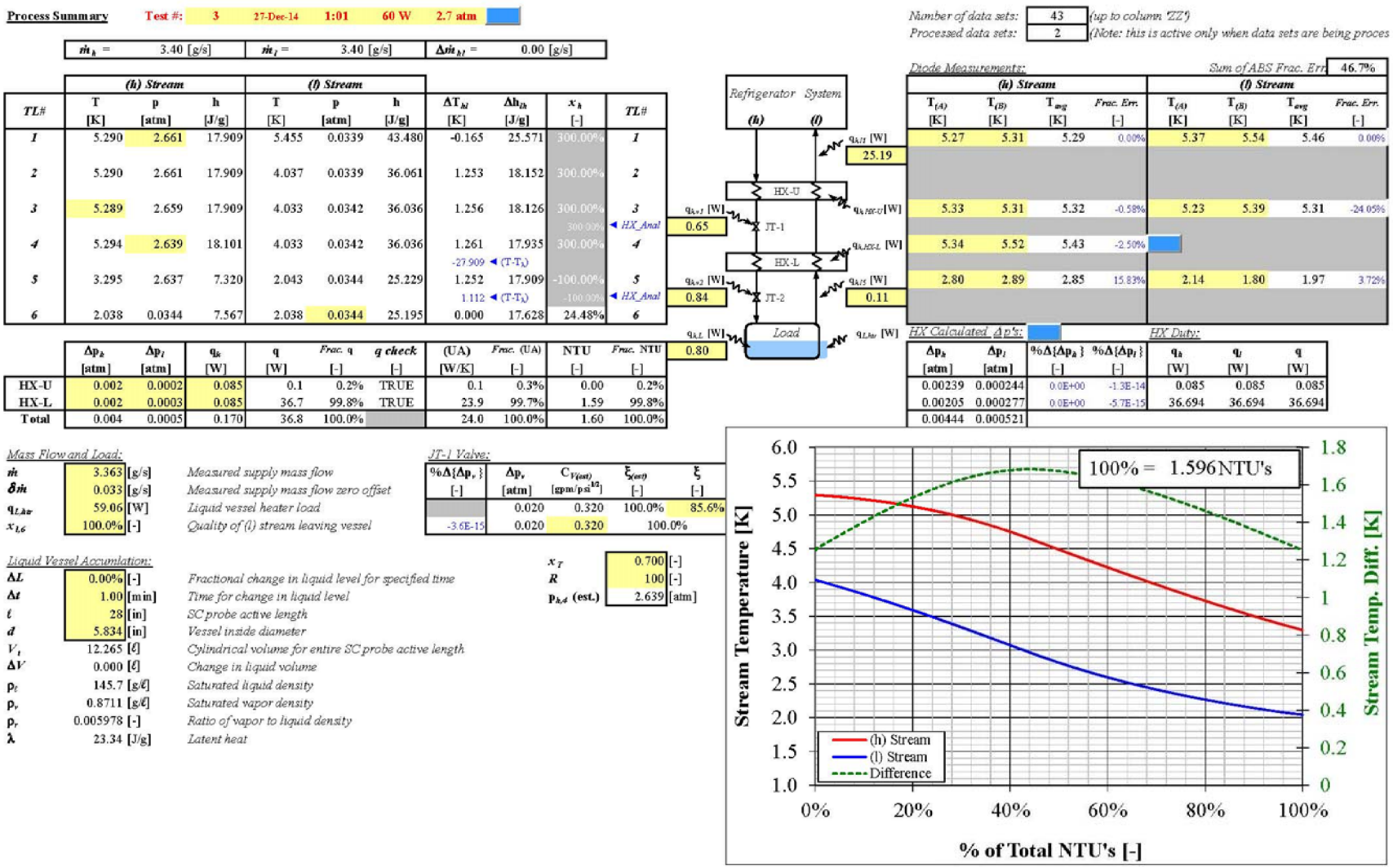

Figure Q.3. Process model output, test #3: 60 W 2.7 atm 27-Dec-14 01:01

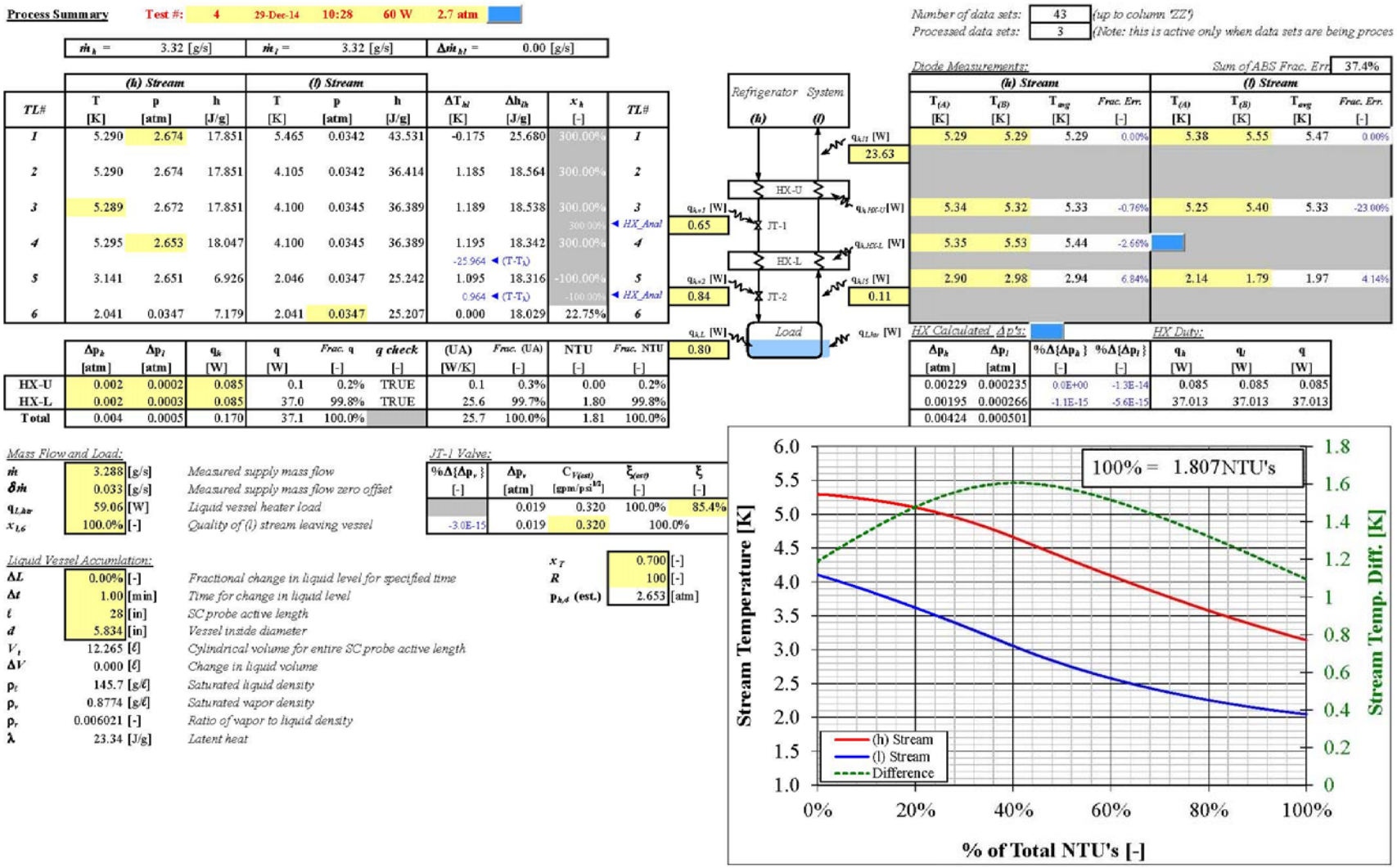

Figure Q.4. Process model output, test #4: 60 W 2.7 atm 29-Dec-14 10:28

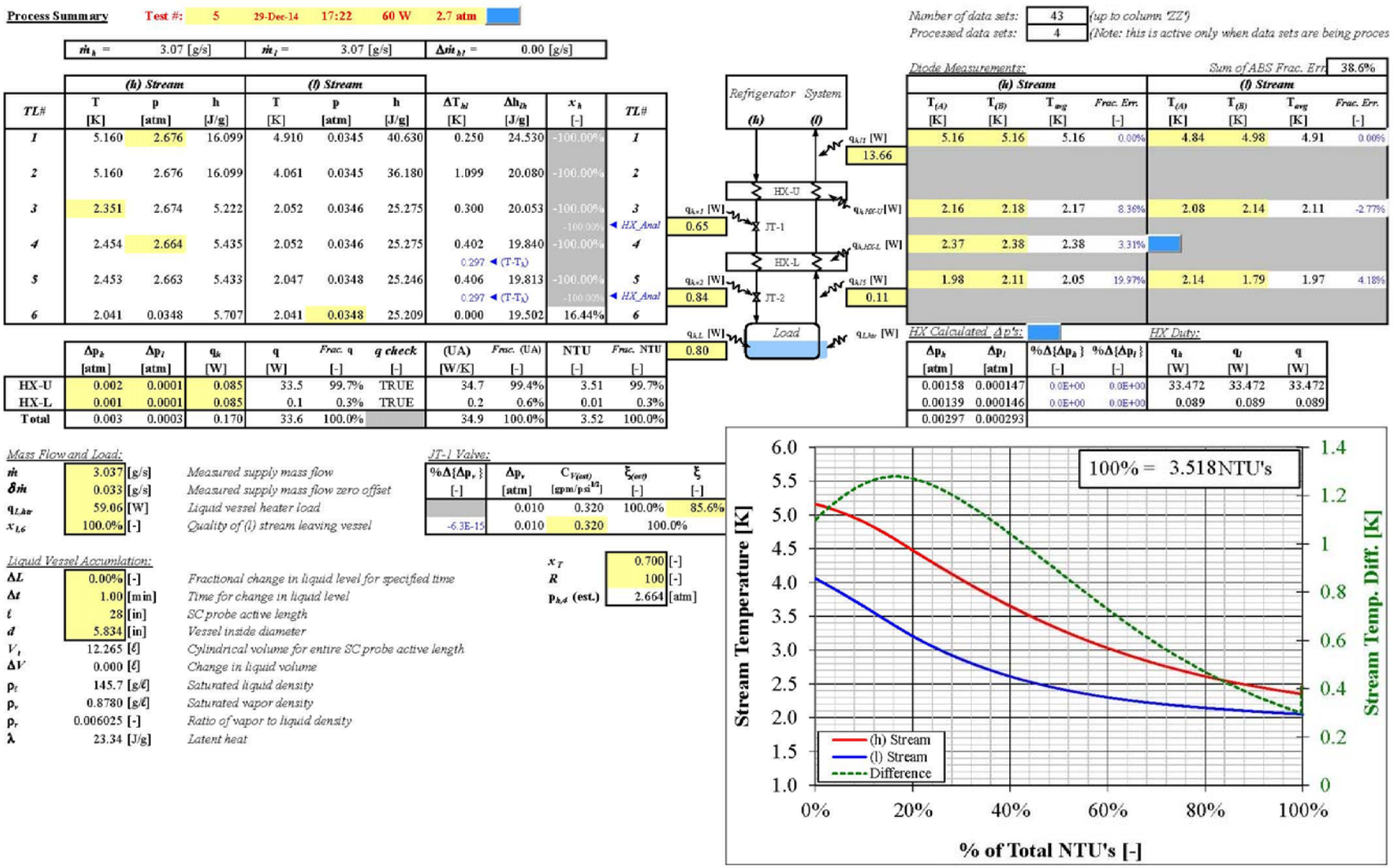

Figure Q.5. Process model output, test #5: 60 W 2.7 atm 29-Dec-14 17:22

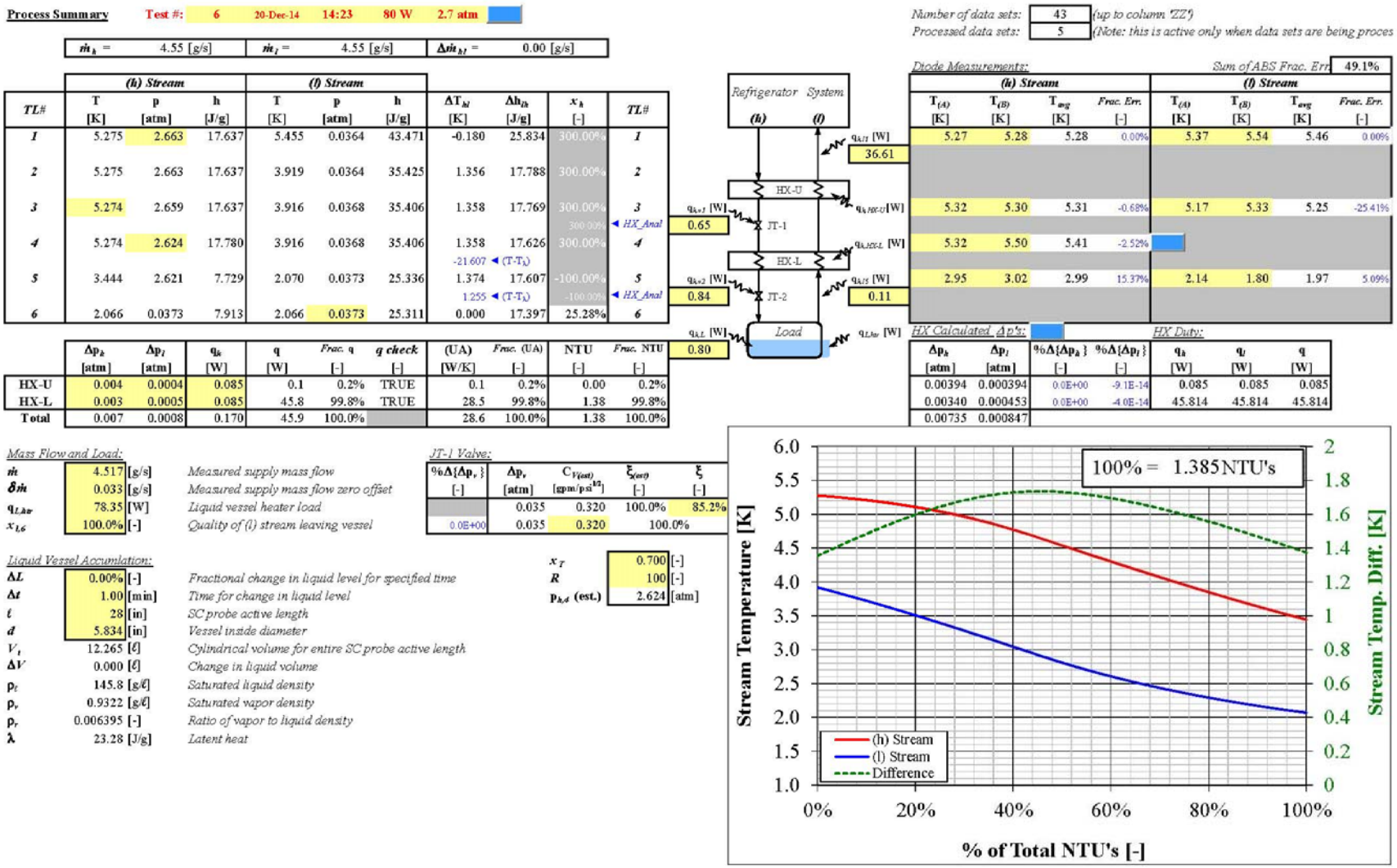

Figure Q.6. Process model output, test #6: 80 W 2.7 atm 20-Dec-14 14:23

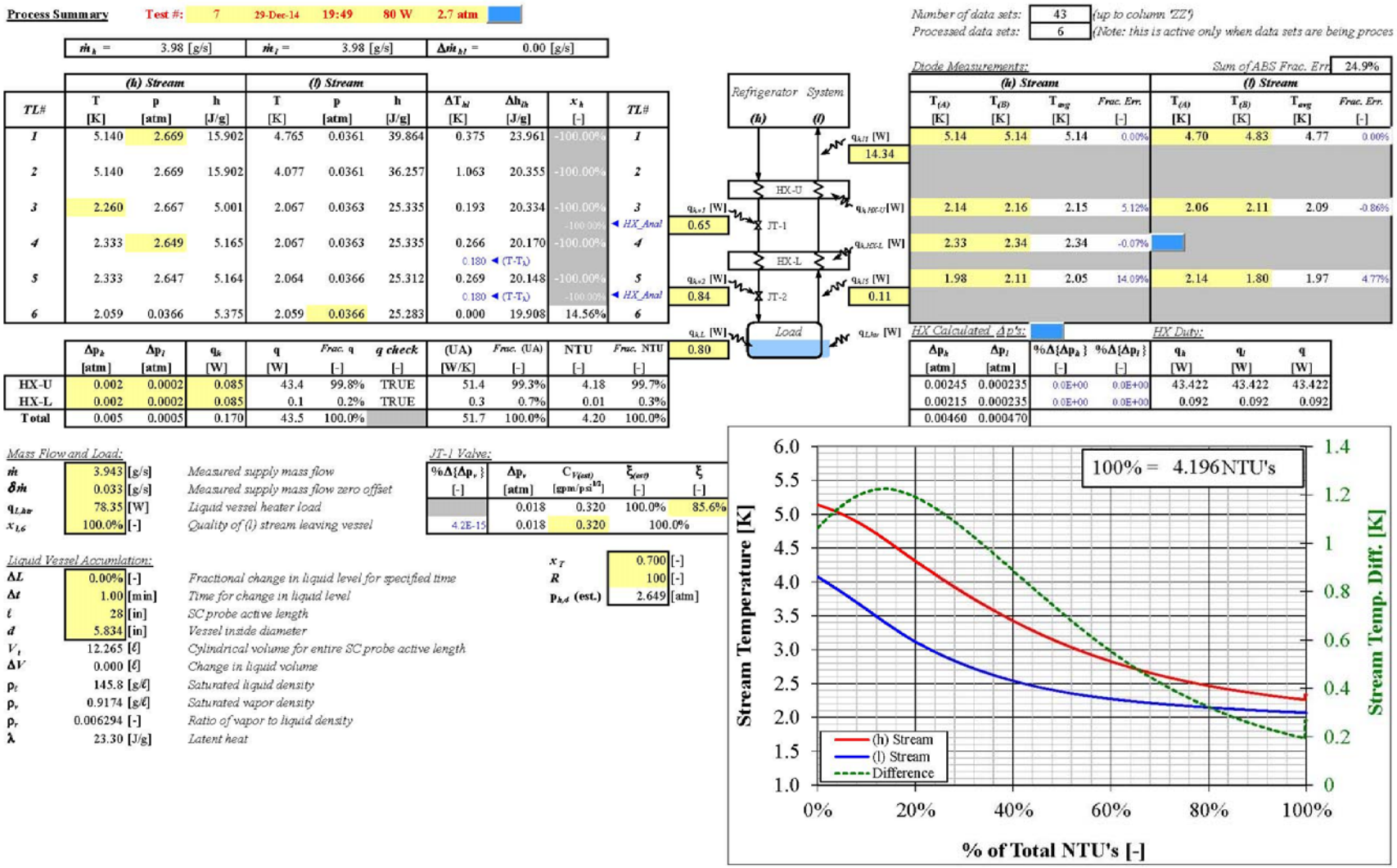

Process Summary	Test #:	7	29-Dec-14	19:49	80 W	2.7 atm

Number of data sets: 43 (up to column 'ZZ')
Processed data sets: 6 (Note: this is active only when data sets are being proces

$\dot{m}_h$ = 3.98 [g/s] | $\dot{m}_l$ = 3.98 [g/s] | $\Delta\dot{m}_{hl}$ = 0.00 [g/s]

TL#	(h) Stream T [K]	(h) Stream p [atm]	(h) Stream h [J/g]	(l) Stream T [K]	(l) Stream p [atm]	(l) Stream h [J/g]	ΔT_{hl} [K]	Δh_{lh} [J/g]	x_h [-]	TL#
1	5.140	2.669	15.902	4.765	0.0361	39.864	0.375	23.961	-100.00%	1
2	5.140	2.669	15.902	4.077	0.0361	36.257	1.063	20.355	-100.00%	2
3	2.260	2.667	5.001	2.067	0.0363	25.335	0.193	20.334	-100.00%	3
									-100.00% ◄ HX_Anal	
4	2.333	2.649	5.165	2.067	0.0363	25.335	0.266	20.170	-100.00%	4
							0.180 ◄ (T-T$_h$)			
5	2.333	2.647	5.164	2.064	0.0366	25.312	0.269	20.148	-100.00%	5
							0.180 ◄ (T-T$_h$)		-100.00% ◄ HX_Anal	
6	2.059	0.0366	5.375	2.059	0.0366	25.283	0.000	19.908	14.56%	6

	Δp_h [atm]	Δp_l [atm]	q_k [W]	q [W]	Frac. q [-]	q check [-]	(UA) [W/K]	Frac. (UA) [-]	NTU [-]	Frac. NTU [-]
HX-U	0.002	0.0002	0.085	43.4	99.8%	TRUE	51.4	99.3%	4.18	99.7%
HX-L	0.002	0.0002	0.085	0.1	0.2%	TRUE	0.3	0.7%	0.01	0.3%
Total	0.005	0.0005	0.170	43.5	100.0%		51.7	100.0%	4.20	100.0%

$q_{h,l1}$ [W] 14.34
$q_{h,HX-U}$ [W]
$q_{h,l2}$ [W] 0.65
$q_{h,HX-L}$ [W]
$q_{h,l3}$ [W] 0.11
$q_{h,L}$ [W] 0.80
$q_{L,hx}$ [W]

Diode Measurements:

	(h) Stream $T_{(A)}$ [K]	(h) Stream $T_{(B)}$ [K]	(h) Stream T_{avg} [K]	(h) Stream Frac. Err. [-]	(l) Stream $T_{(A)}$ [K]	(l) Stream $T_{(B)}$ [K]	(l) Stream T_{avg} [K]	(l) Stream Frac. Err. [-]
	5.14	5.14	5.14	0.00%	4.70	4.83	4.77	0.00%
	2.14	2.16	2.15	5.12%	2.06	2.11	2.09	-0.86%
	2.33	2.34	2.34	-0.07%				
	1.98	2.11	2.05	14.09%	2.14	1.80	1.97	4.77%

HX Calculated Δp's:

Δp_h [atm]	Δp_l [atm]	%Δ{Δp_h} [-]	%Δ{Δp_l} [-]
0.00245	0.000235	0.0E+00	0.0E+00
0.00215	0.000235	0.0E+00	0.0E+00
0.00460	0.000470		

HX Duty:

q_h [W]	q_l [W]	q [W]
43.422	43.422	43.422
0.092	0.092	0.092

Mass Flow and Load:

$\dot{m}$	3.943	[g/s]	Measured supply mass flow
$\delta\dot{m}$	0.033	[g/s]	Measured supply mass flow zero offset
$q_{L,hx}$	78.35	[W]	Liquid vessel heater load
$x_{l,6}$	100.0%	[-]	Quality of (l) stream leaving vessel

JT-1 Valve:

%Δ{Δp_v} [-]	Δp_v [atm]	$C_{V(set)}$ [gpm/psi$^{1/2}$]	$\xi_{(set)}$ [-]	ξ [-]
	0.018	0.320	100.0%	85.6%
4.2E-15	0.018	0.320	100.0%	

x_T	0.700	[-]	
R	100	[-]	
$p_{h,4}$ (est.)	2.649	[atm]	

Liquid Vessel Accumulation:

ΔL	0.00%	[-]	Fractional change in liquid level for specified time
Δt	1.00	[min]	Time for change in liquid level
ℓ	28	[in]	SC probe active length
d	5.834	[in]	Vessel inside diameter
V_t	12.265	[ℓ]	Cylindrical volume for entire SC probe active length
ΔV	0.000	[ℓ]	Change in liquid volume
ρ_l	145.8	[g/ℓ]	Saturated liquid density
ρ_v	0.9174	[g/ℓ]	Saturated vapor density
ρ_r	0.006294	[-]	Ratio of vapor to liquid density
λ	23.30	[J/g]	Latent heat

Figure Q.7. Process model output, test #7: 80 W 2.7 atm 29-Dec-14 19:49

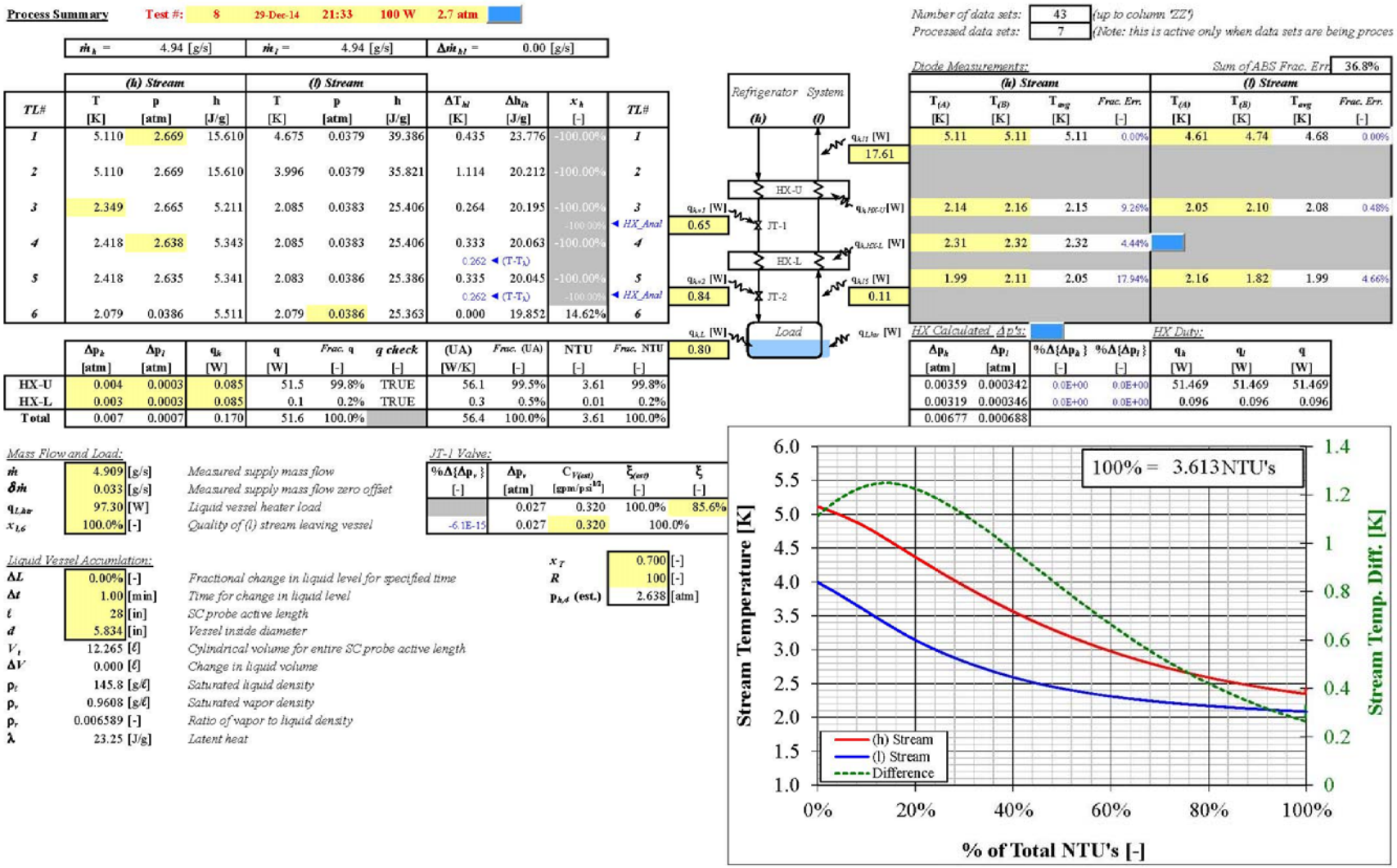

Figure Q.8. Process model output, test #8: 100 W 2.7 atm 29-Dec-14 21:33

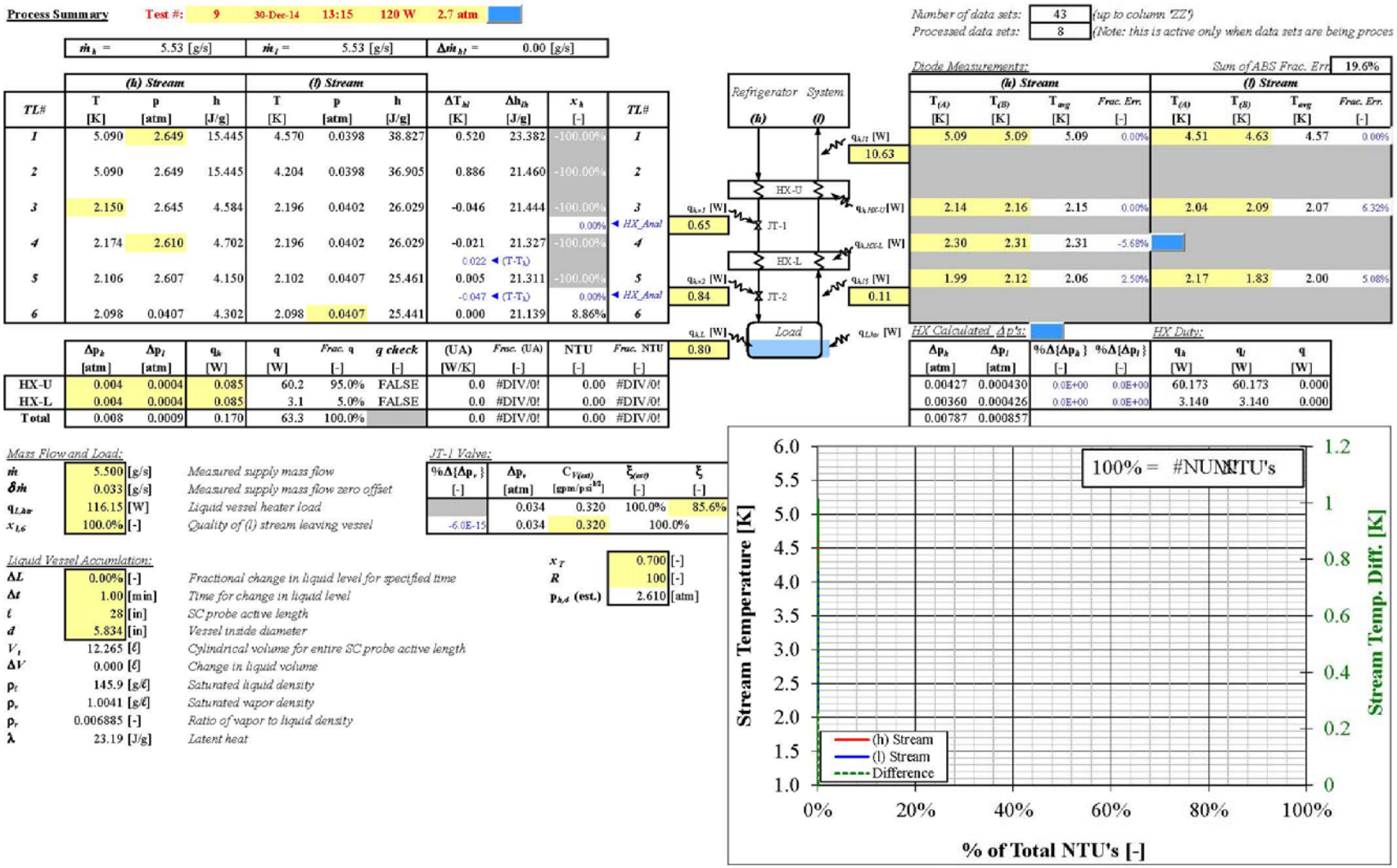

Figure Q.9. Process model output, test #9: 120 W 2.7 atm 30-Dec-14 13:15

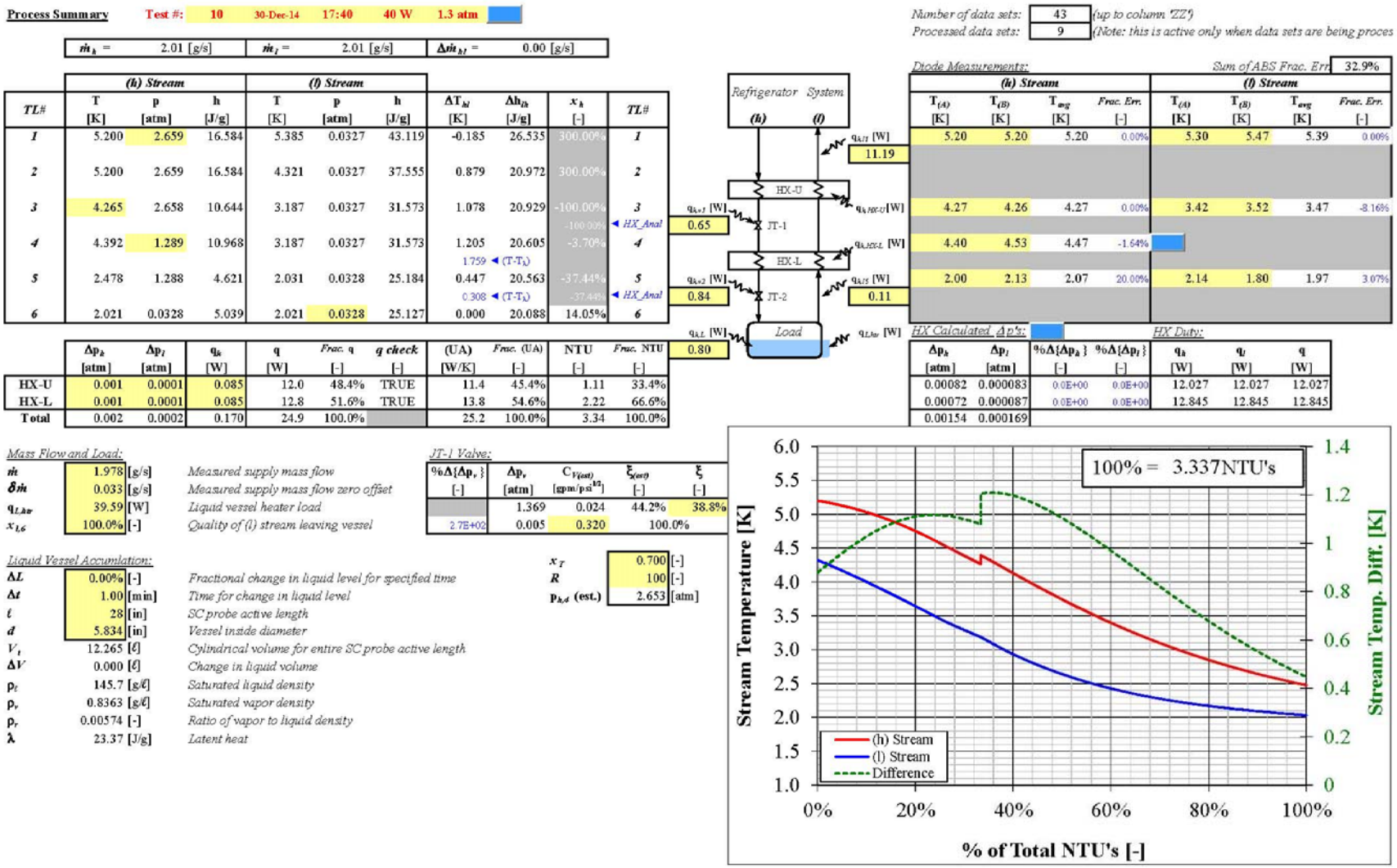

Figure Q.10. Process model output, test #10: 40 W 1.3 atm 30-Dec-14 17:40

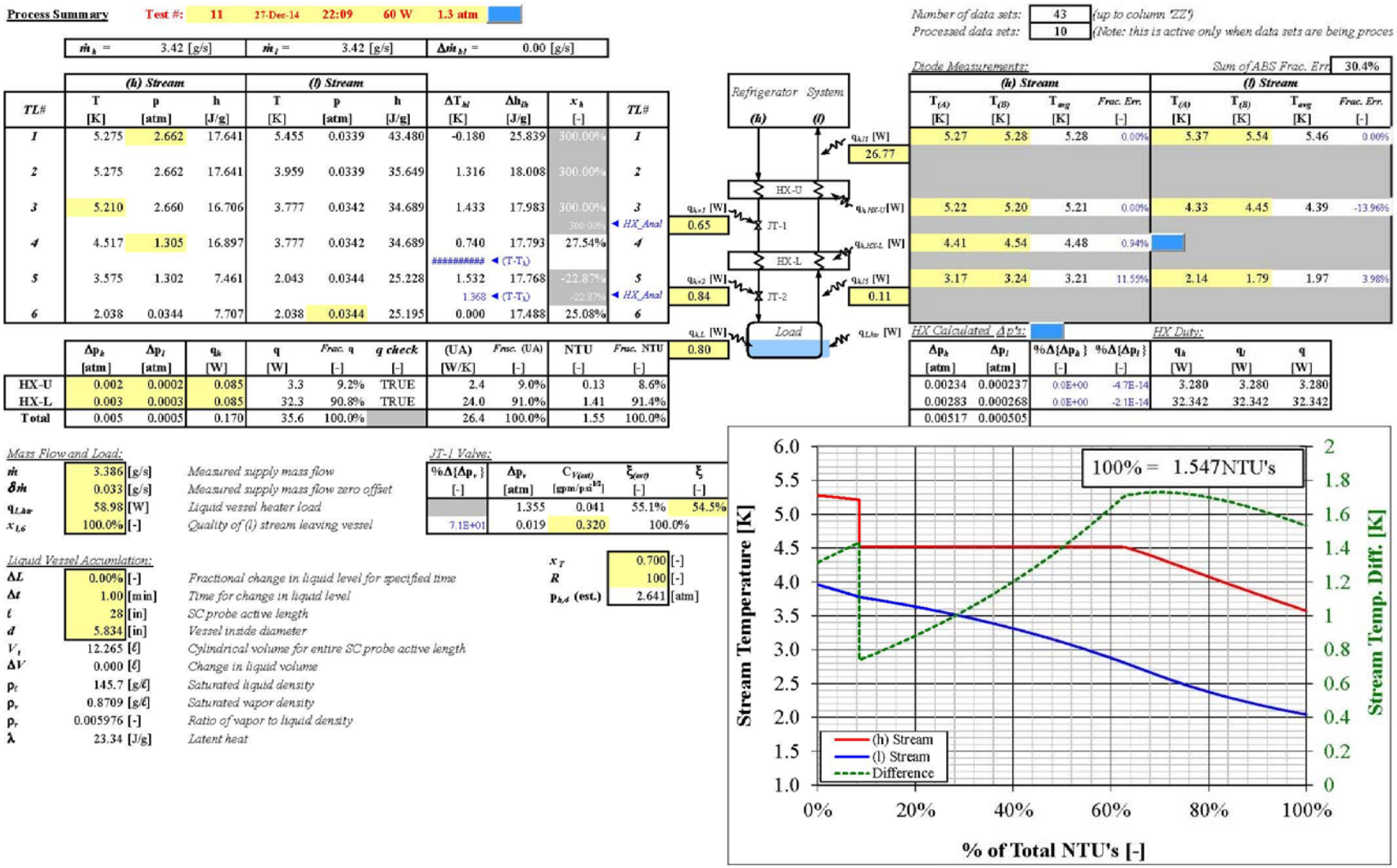

Figure Q.11. Process model output, test #11: 60 W 1.3 atm 27-Dec-14 22:09

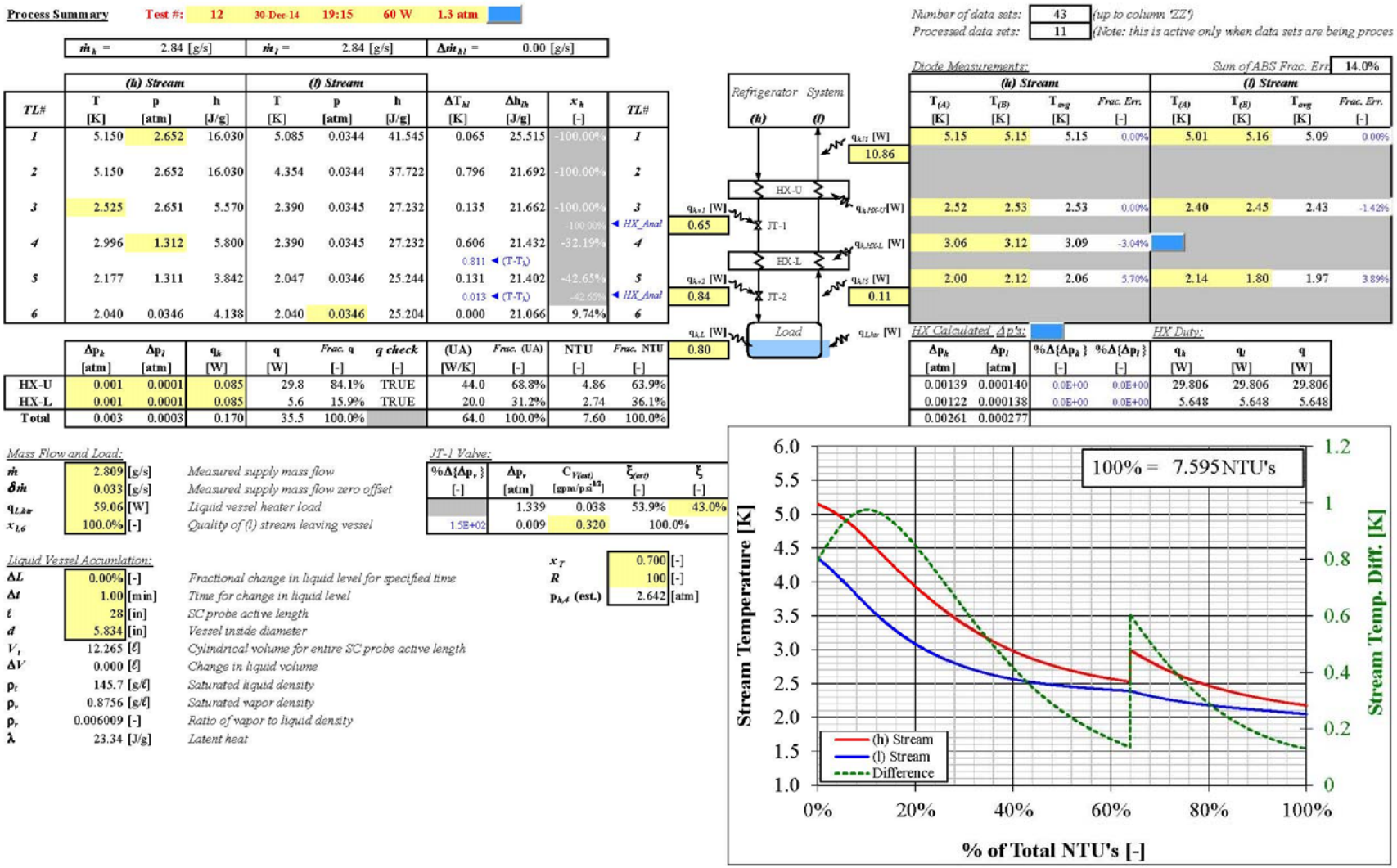

Figure Q.12. Process model output, test #12: 60 W 1.3 atm 30-Dec-14 19:15

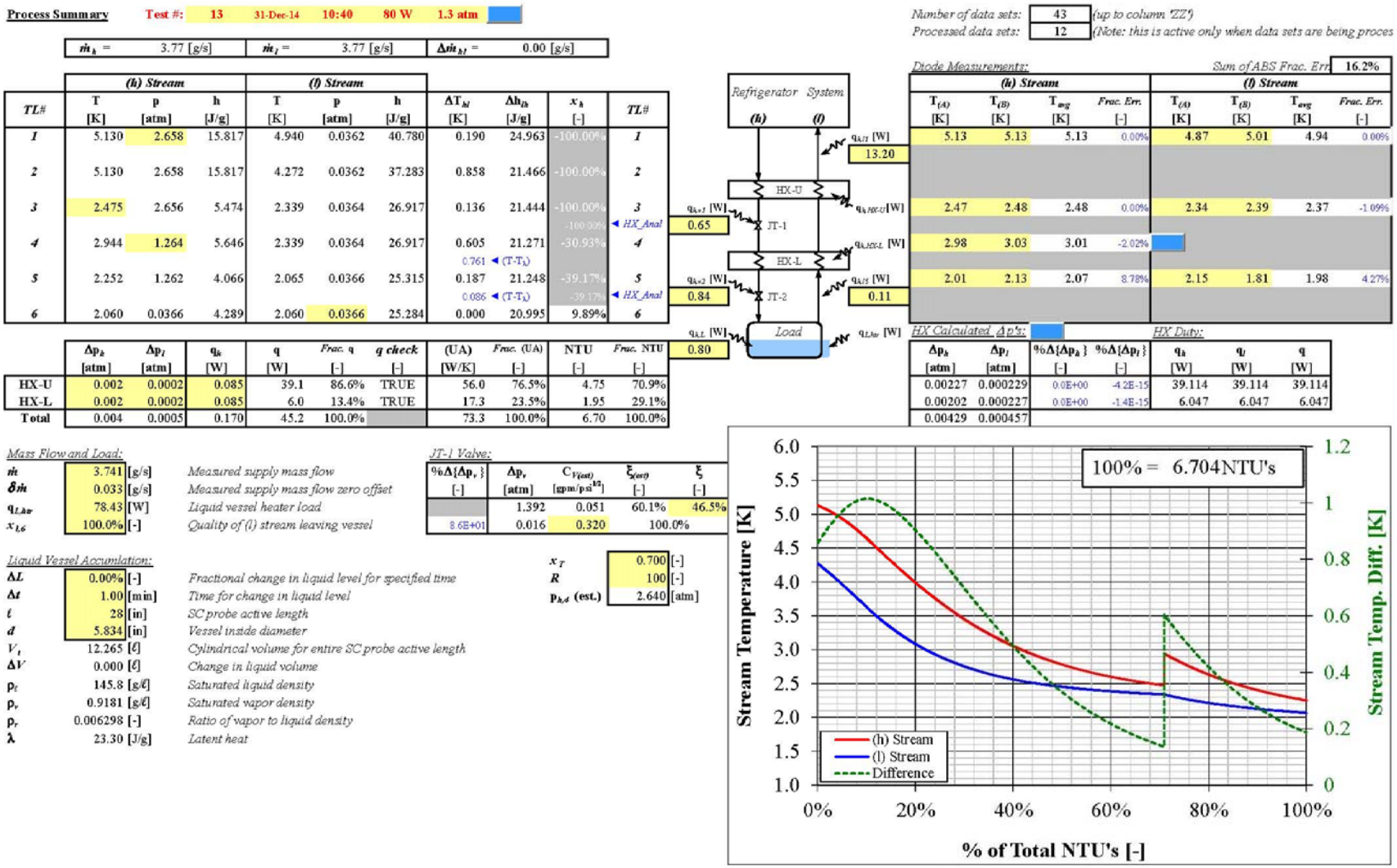

Figure Q.13. Process model output, test #13: 80 W 1.3 atm 31-Dec-14 10:40

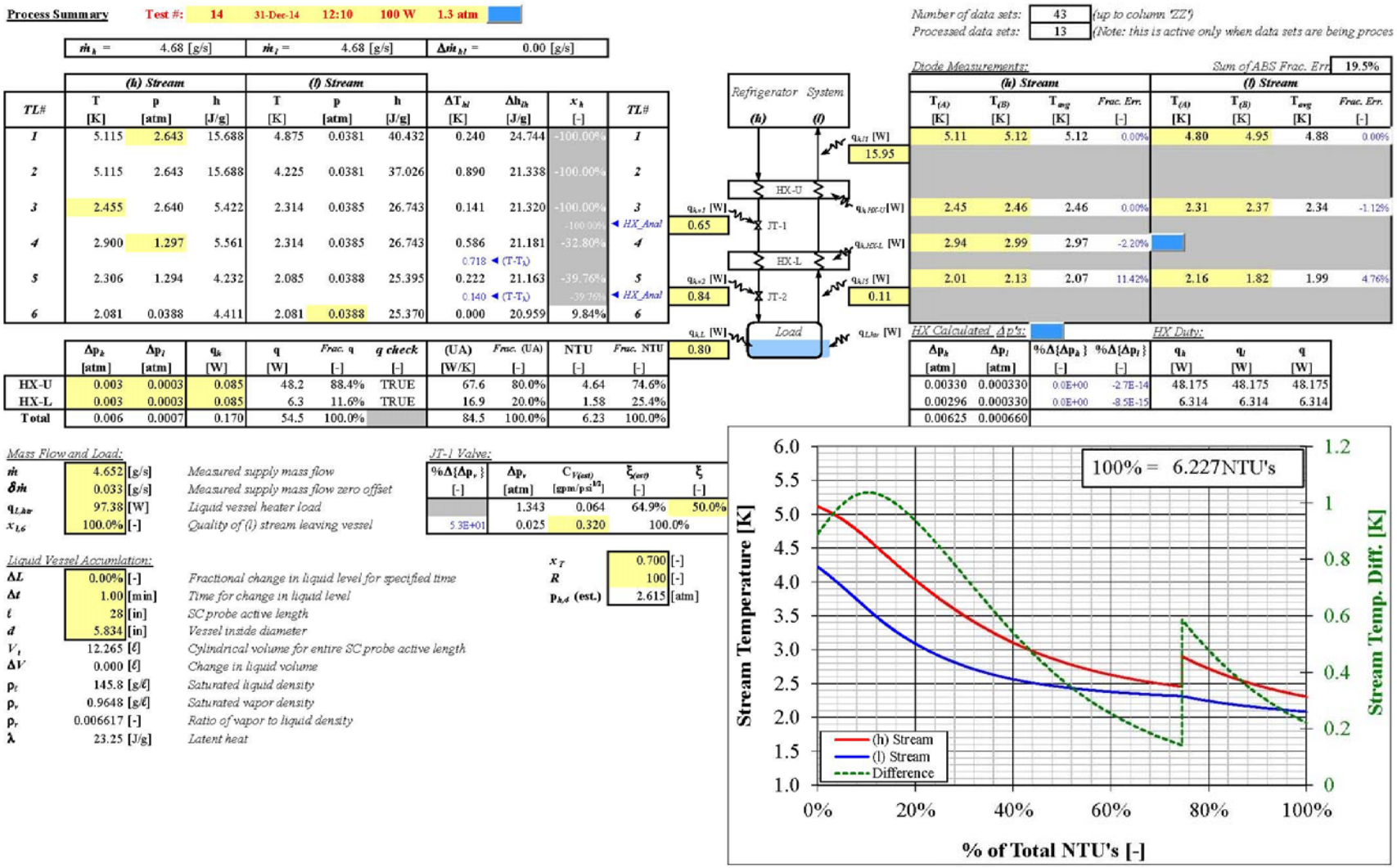

Figure Q.14. Process model output, test #14: 100 W 1.3 atm 31-Dec-14 12:10

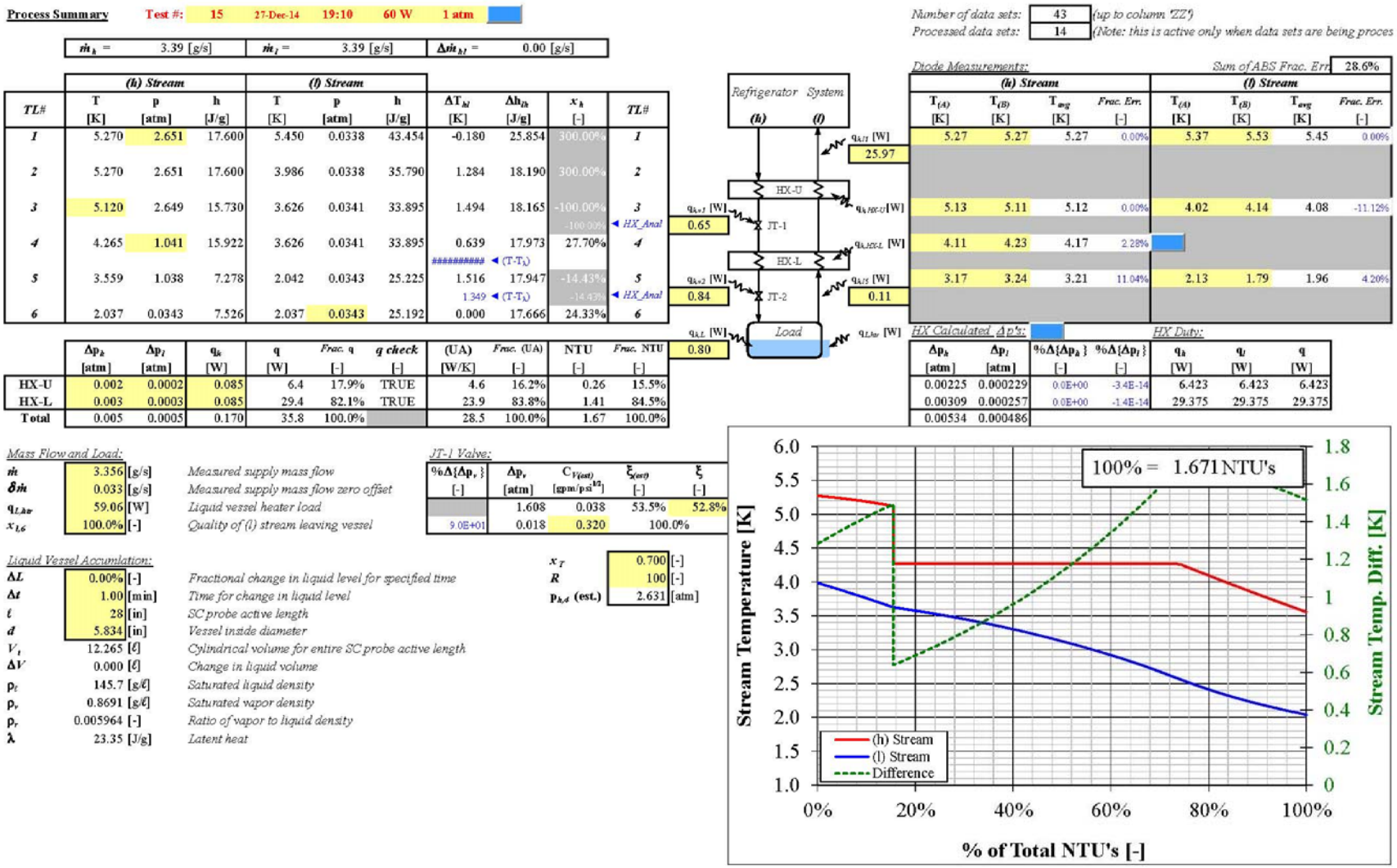

Figure Q.15. Process model output, test #15: 60 W 1 atm 27-Dec-14 19:10

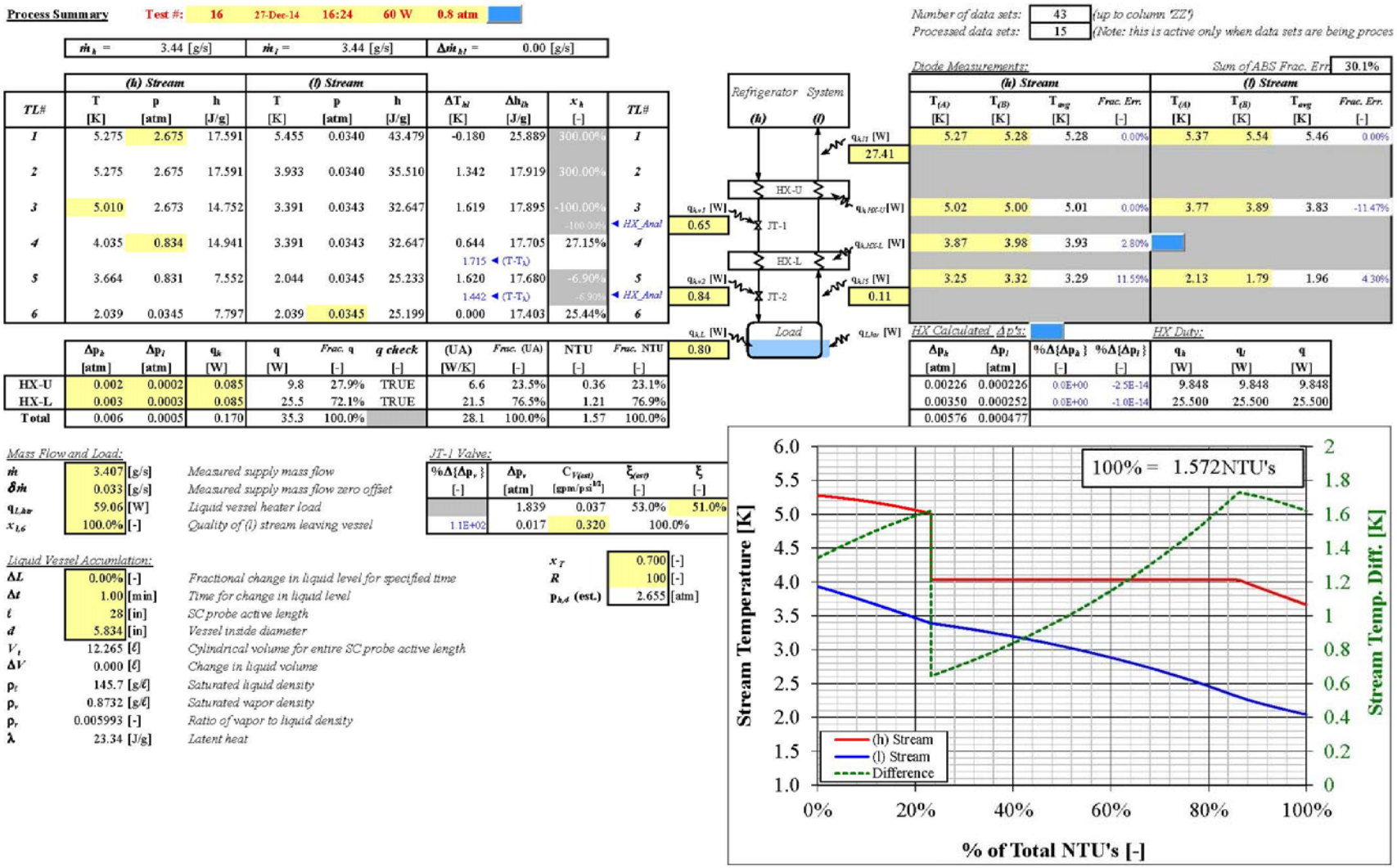

Figure Q.16. Process model output, test #16: 60 W 0.8 atm 27-Dec-14 16:24

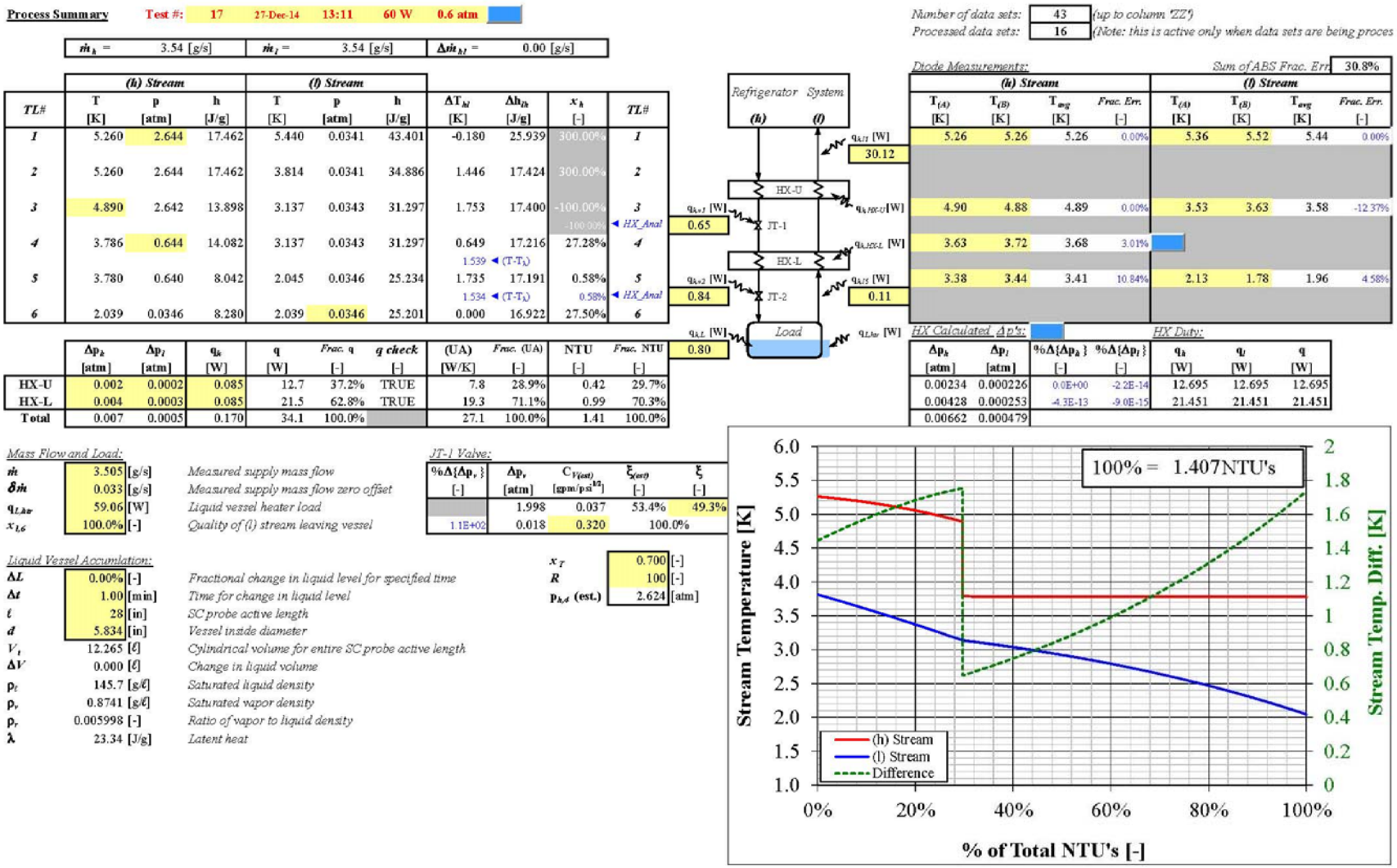

Figure Q.17. Process model output, test #17: 60 W 0.6 atm 27-Dec-14 13:11

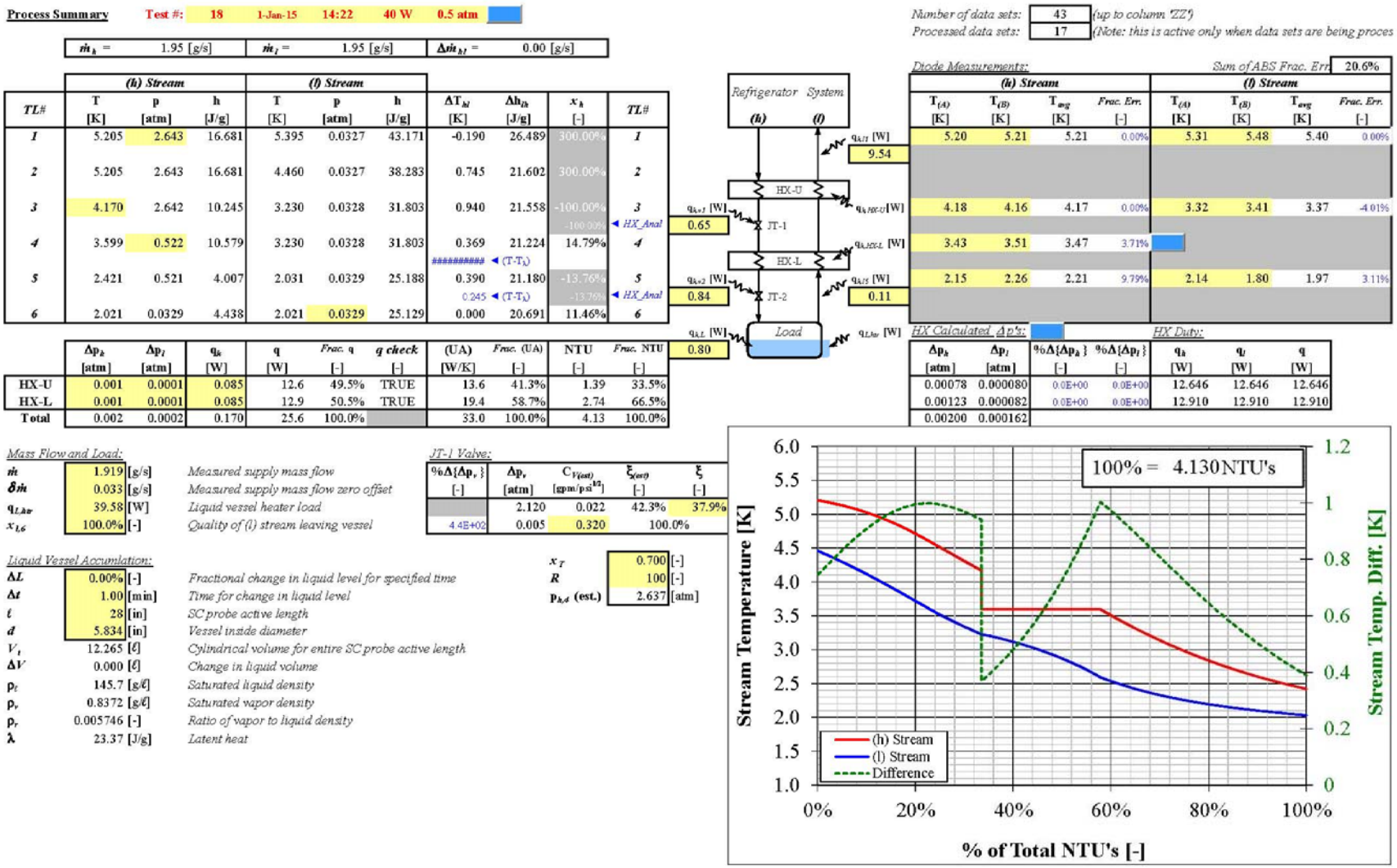

Figure Q.18. Process model output, test #18: 40 W 0.5 01-Jan-15 14:22

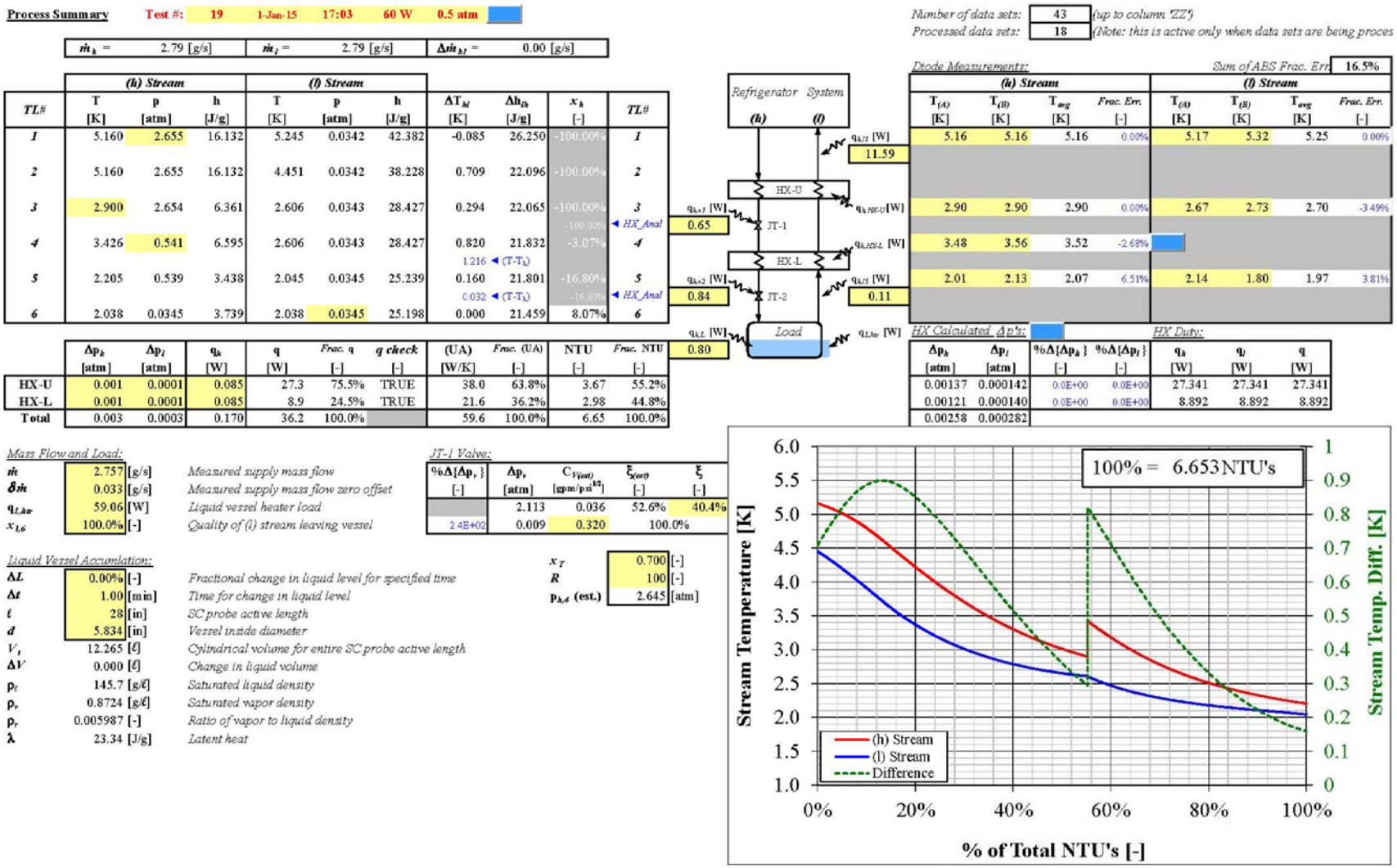

Figure Q.19. Process model output, test #19: 60 W 0.5 atm 01-Jan-15 17:03

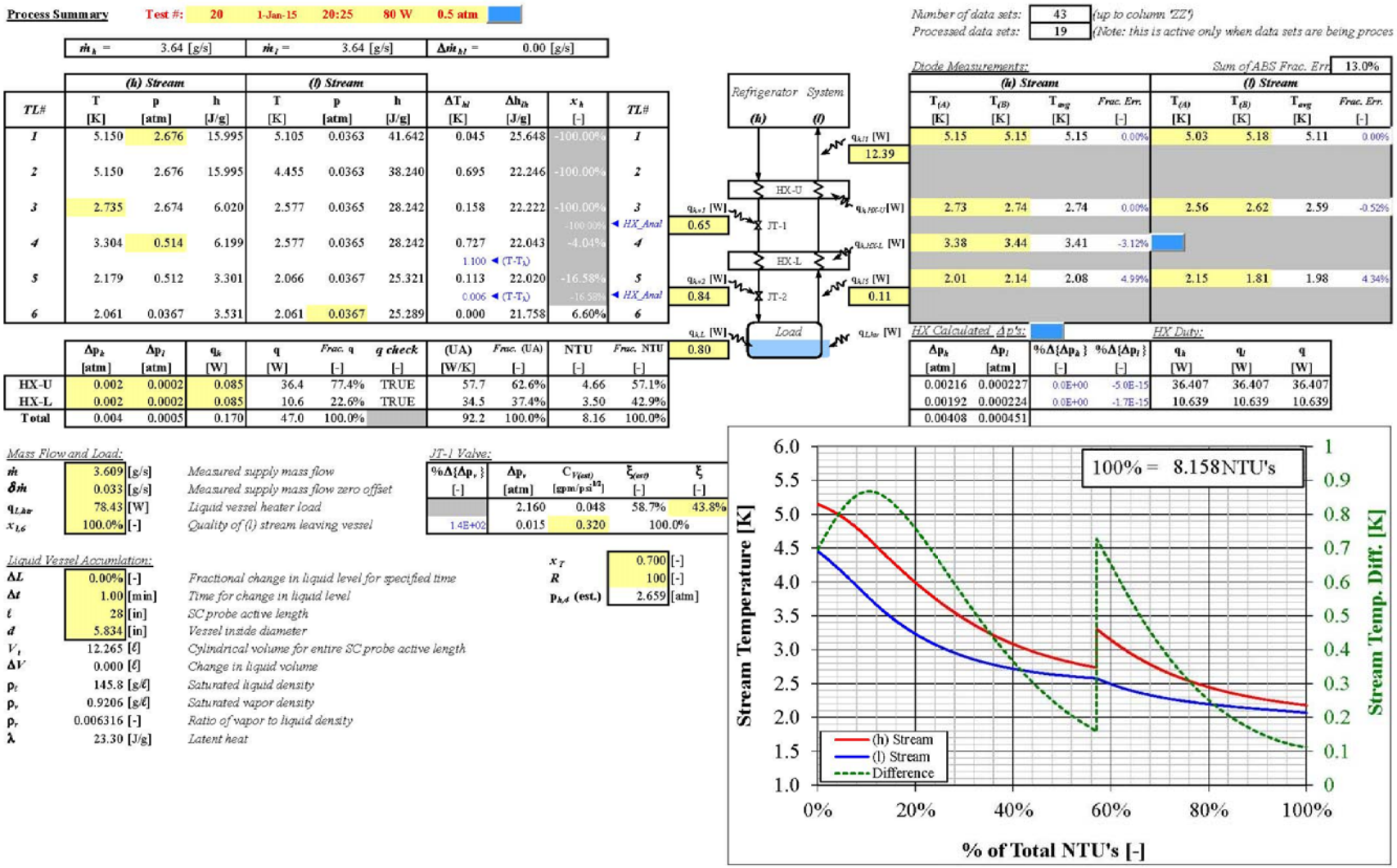

Figure Q.20. Process model output, test #20: 80 W 0.5 atm 01-Jan-15 20:25

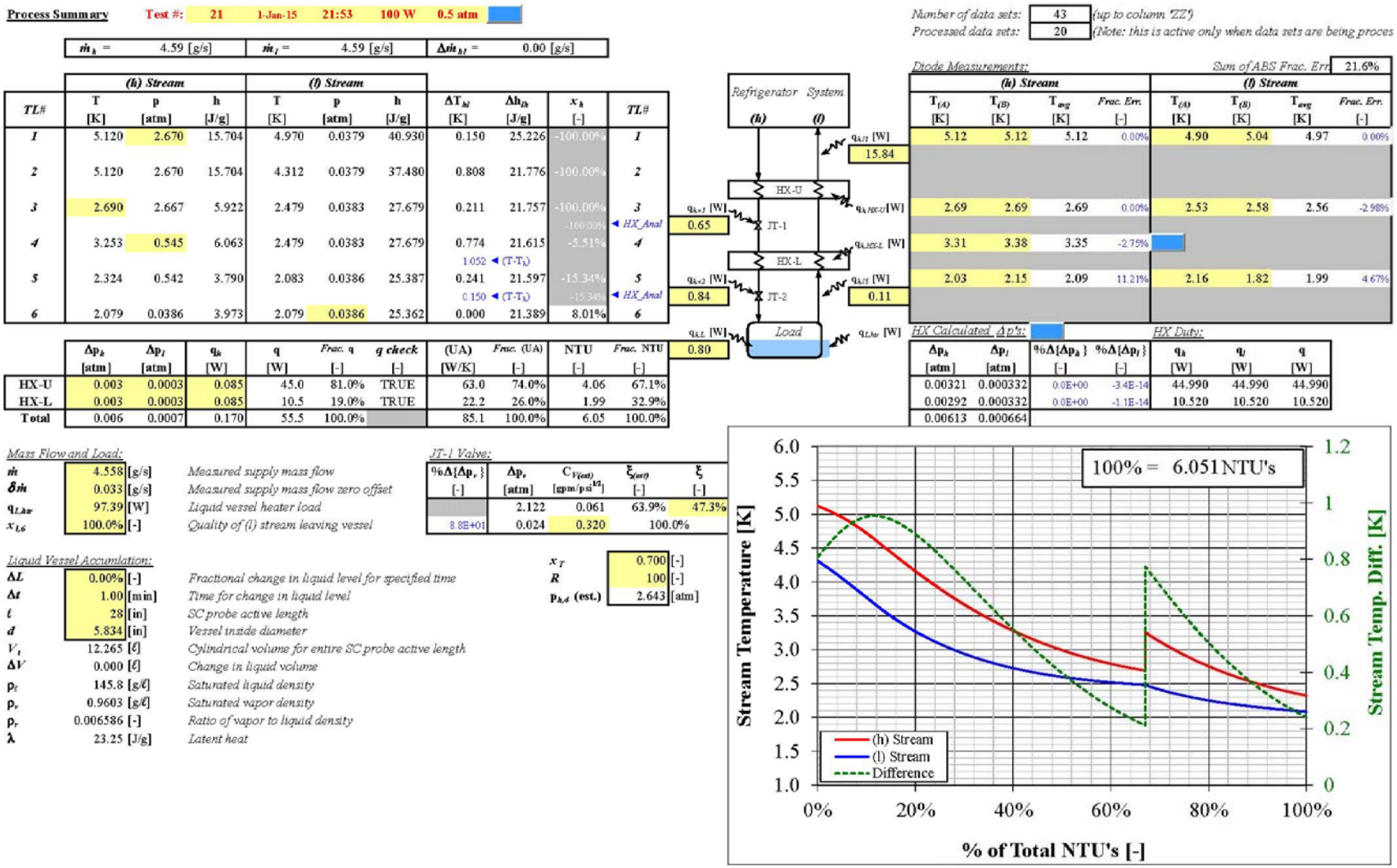

Figure Q.21. Process model output, test #21: 100 W 0.5 atm 01-Jan-15 21:53

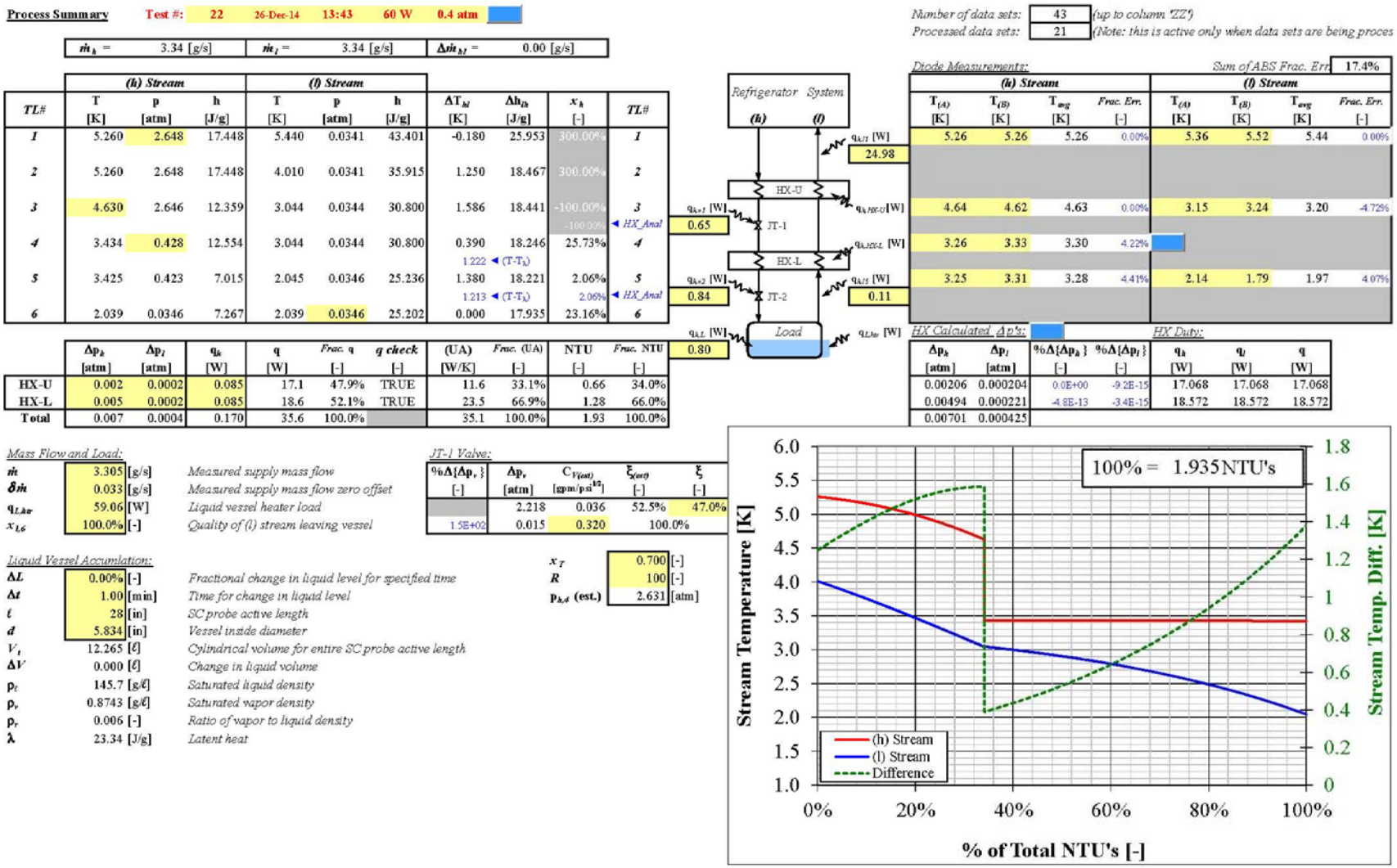

Figure Q.22. Process model output, test #22: 60 W 0.4 atm 26-Dec-14 13:43

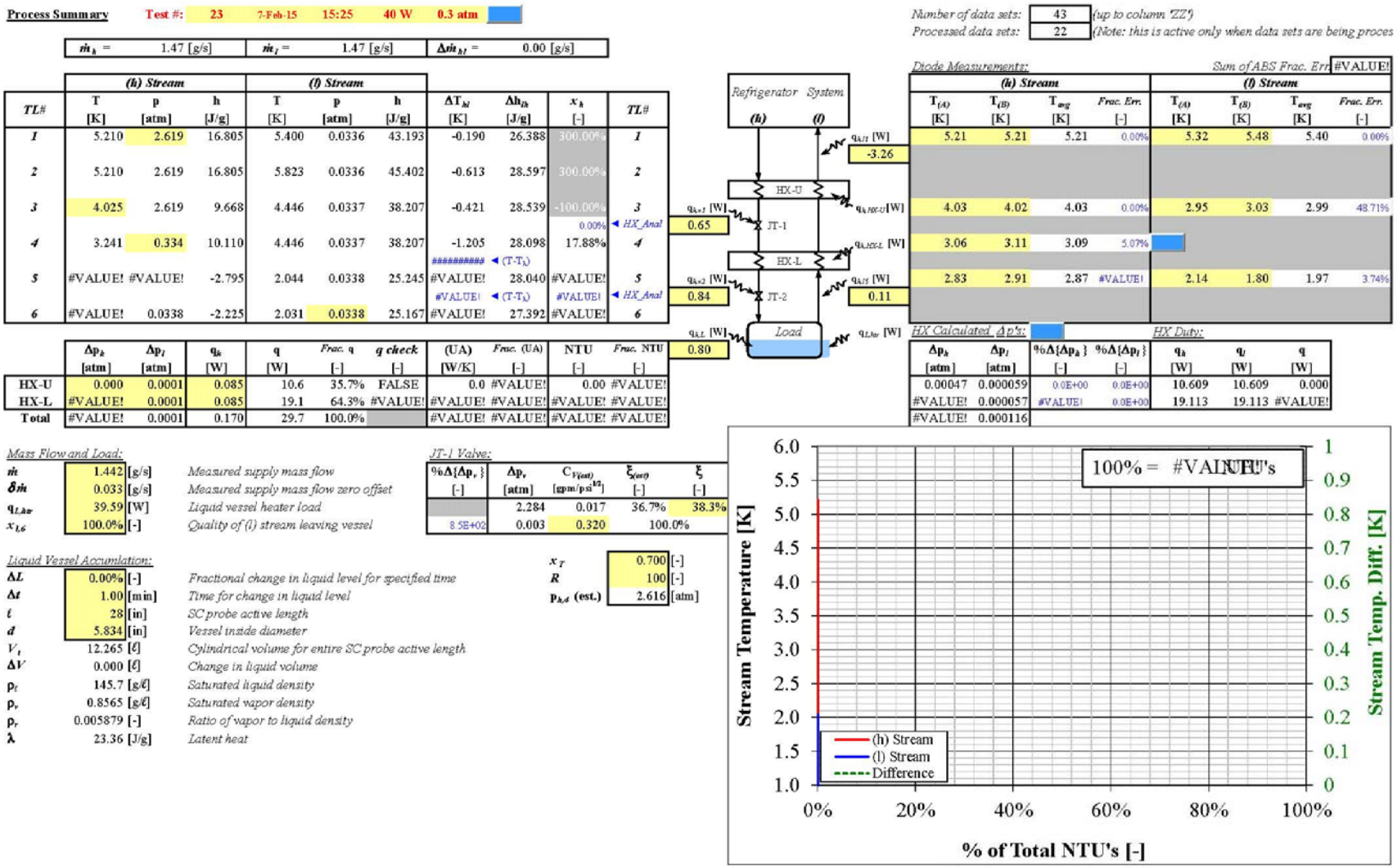

Figure Q.23. Process model output, test #23: 40 W 0.3 atm 07-Feb-15 15:25

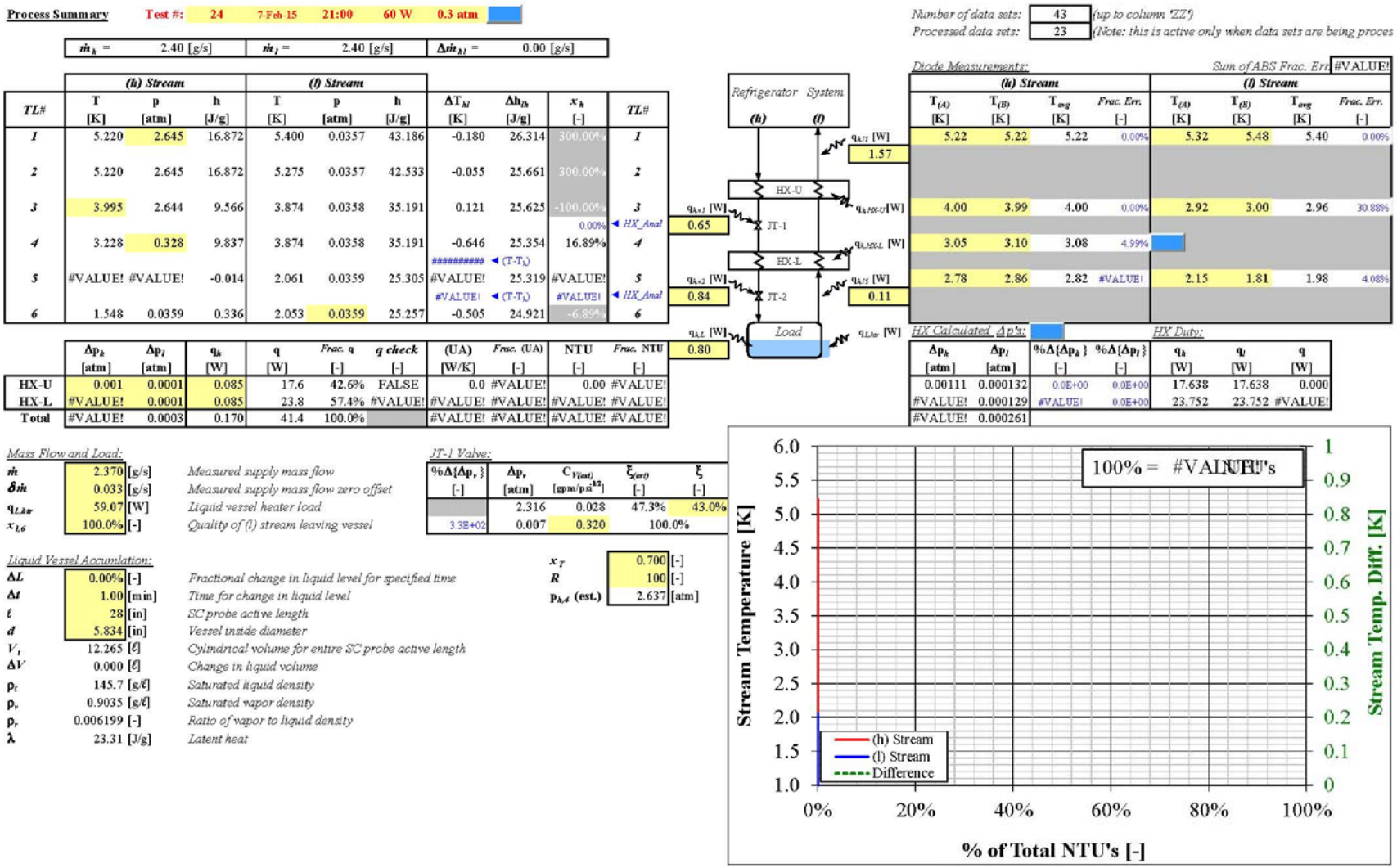

Figure Q.24. Process model output, test #24: 60 W 0.3 atm 07-Feb-15 21:00

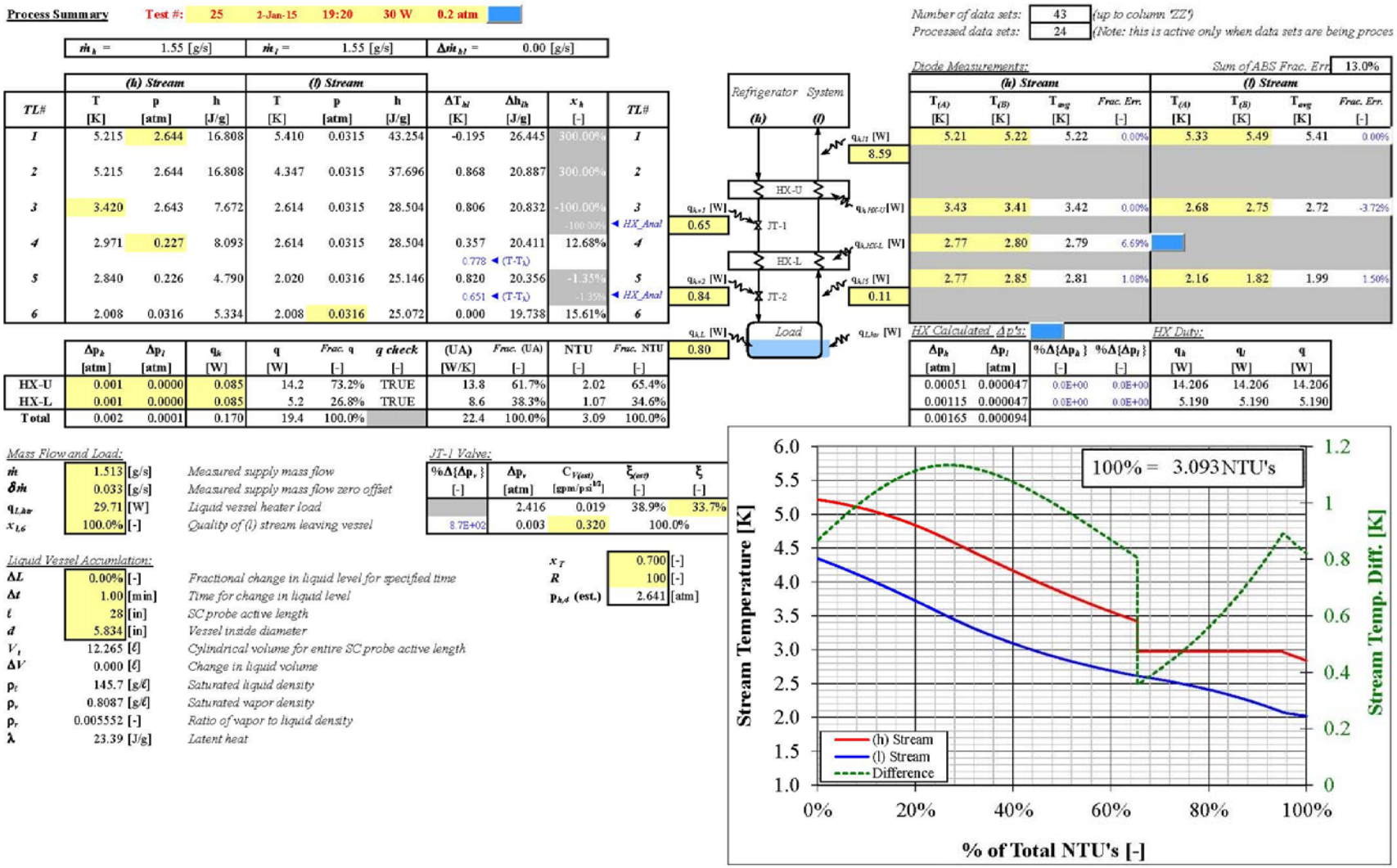

Figure Q.25. Process model output, test #25: 30 W 0.2 atm 02-Jan-15 19:20

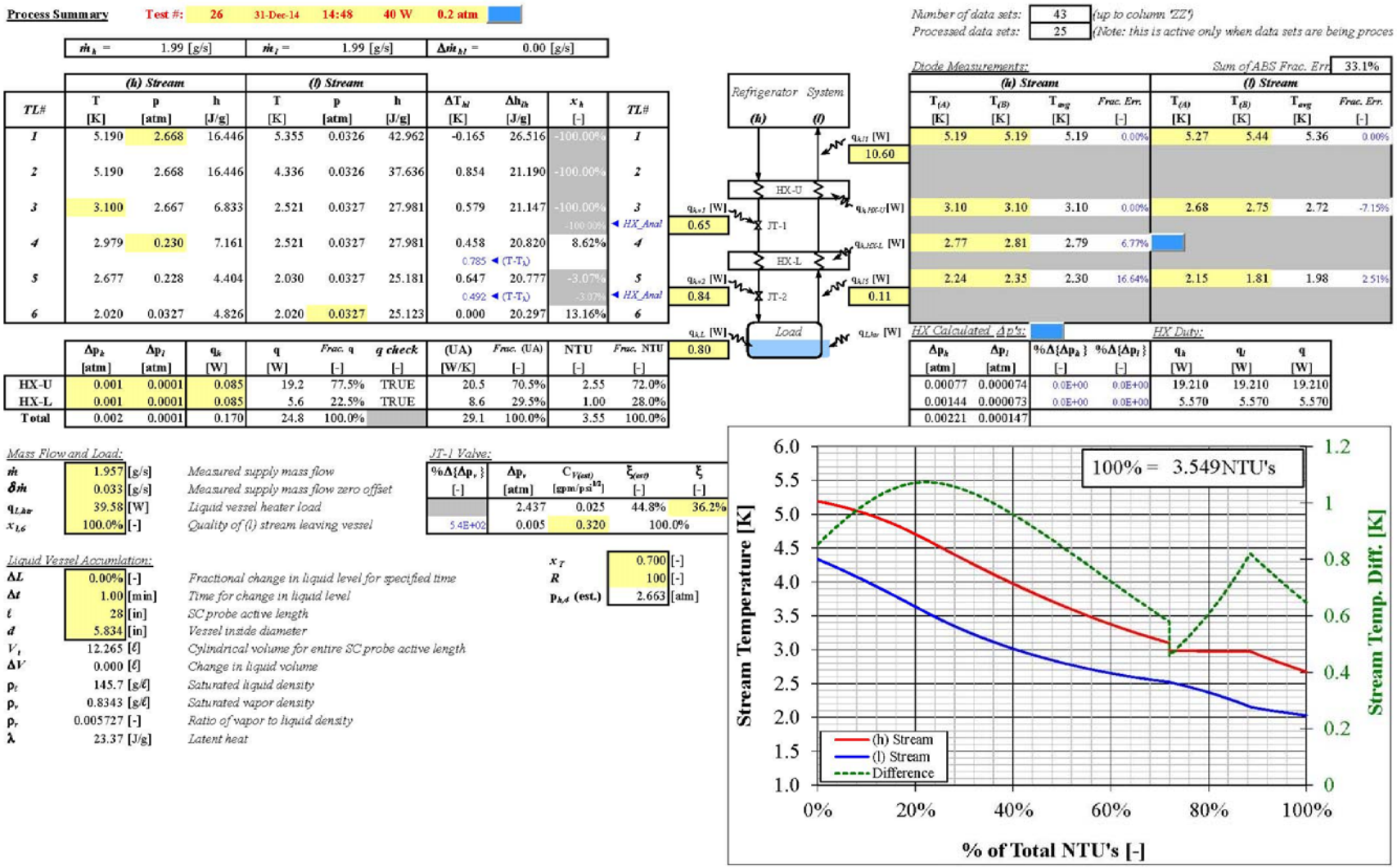

Figure Q.26. Process model output, test #26: 40 W 0.2 atm 31-Dec-14 14:48

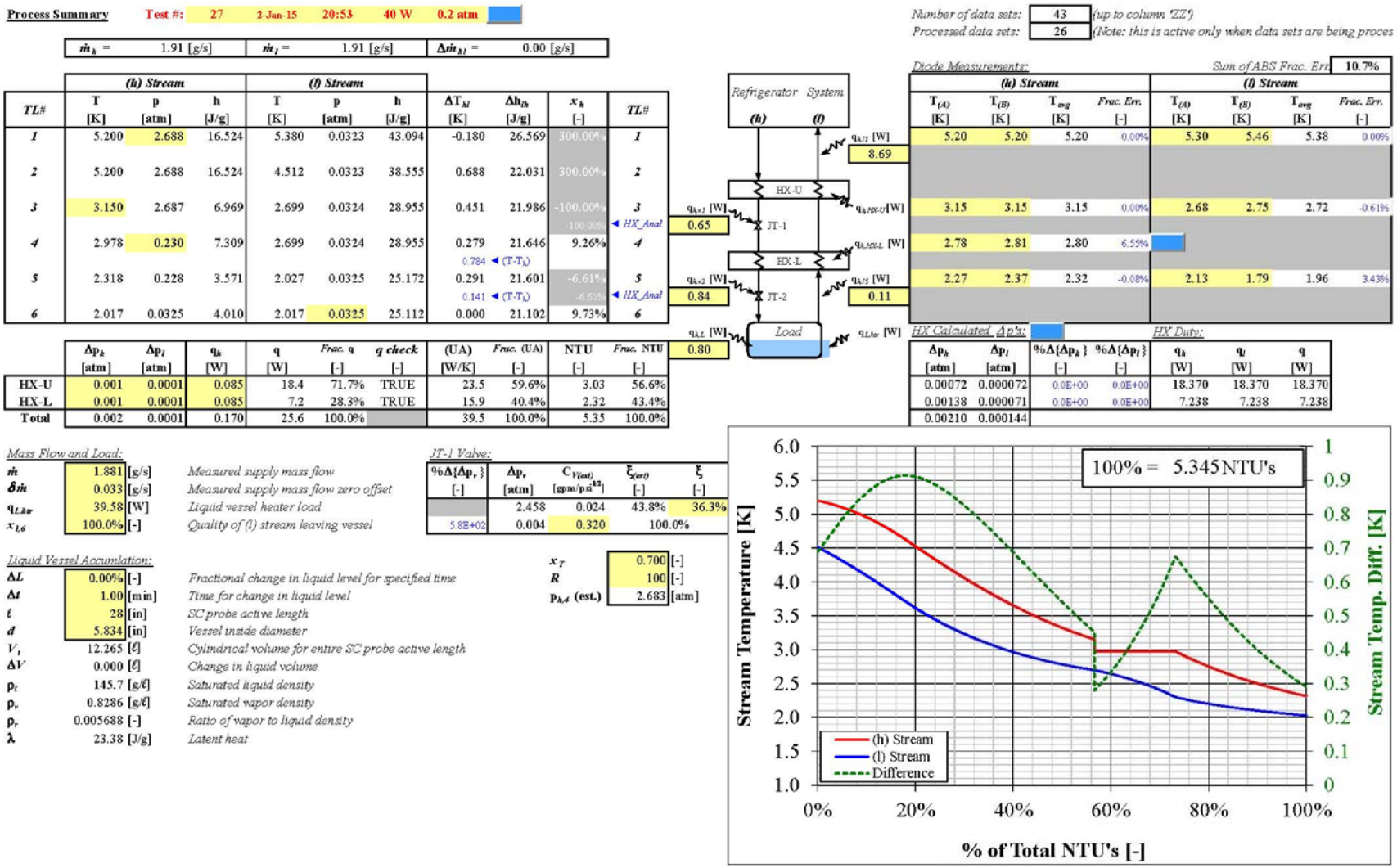

Figure Q.27. Process model output, test #27: 40 W 0.2 atm 02-Jan-15 20:53

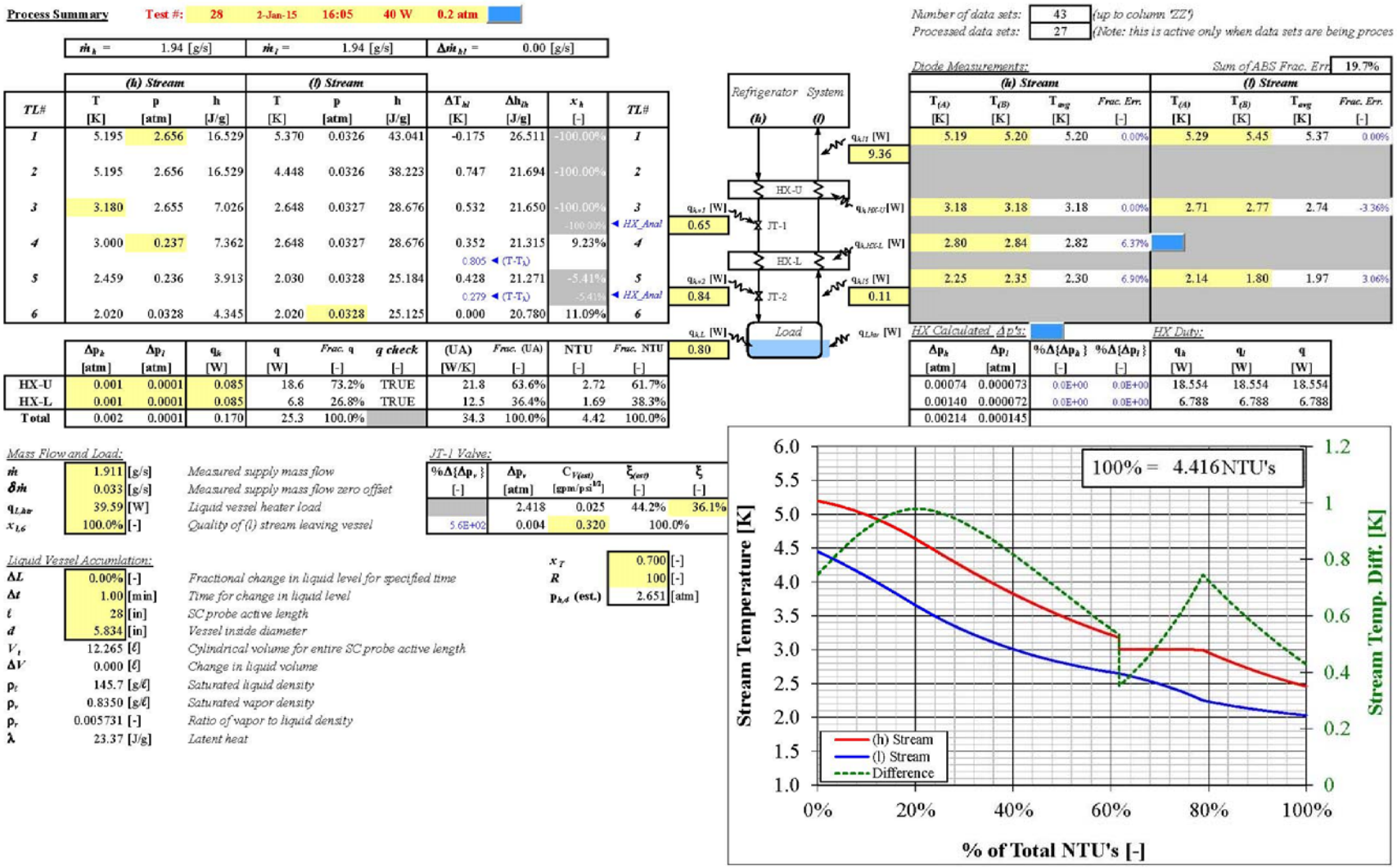

Figure Q.28. Process model output, test #28: 40 W 0.2 atm 02-Jan-15 16:05

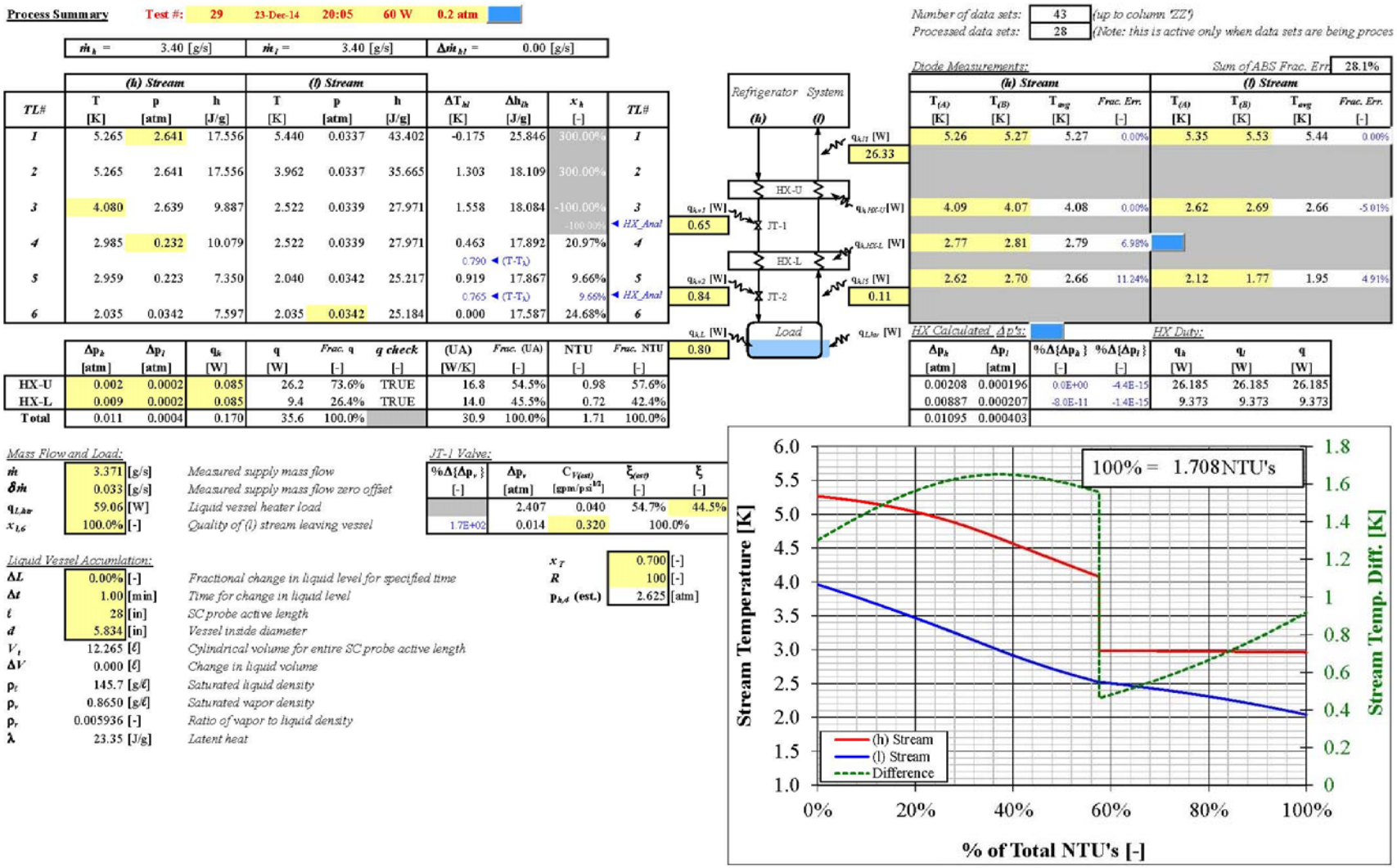

Figure Q.29. Process model output, test #29: 60 W 0.2 atm 23-Dec-14 20:05

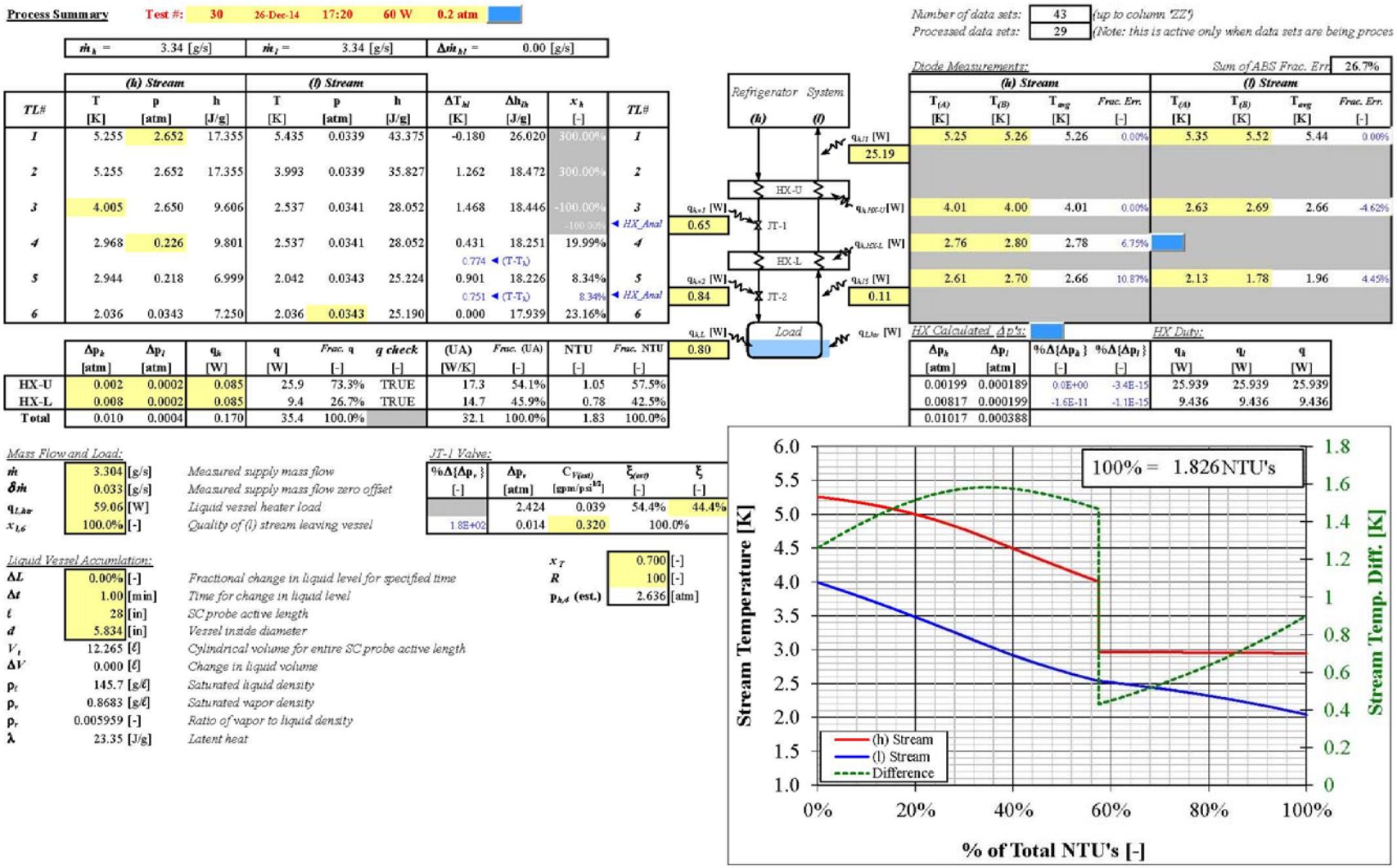

Figure Q.30. Process model output, test #30: 60 W 0.2 atm 26-Dec-14 17:20

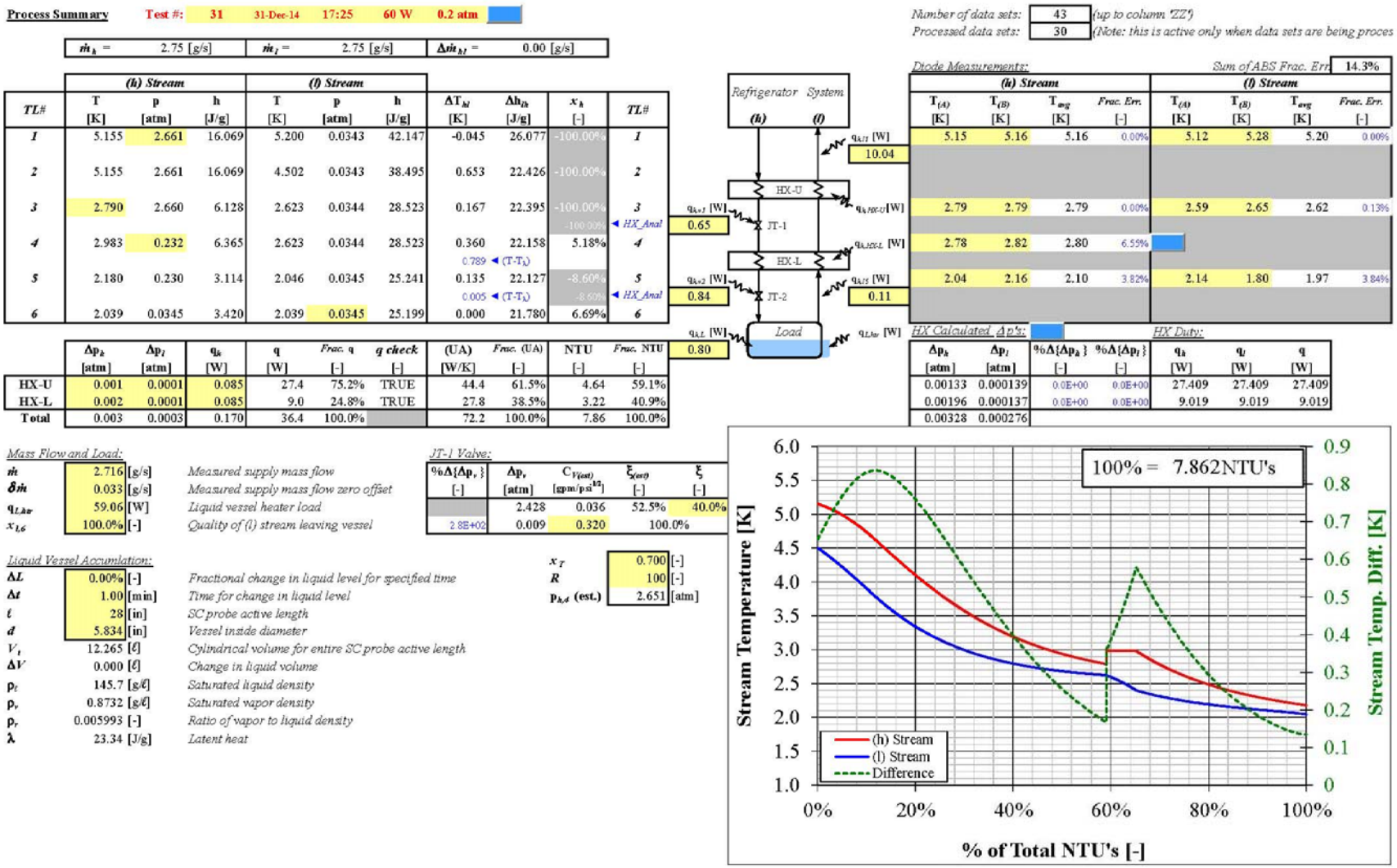

Figure Q.31. Process model output, test #31: 60 W 0.2 atm 31-Dec-14 17:25

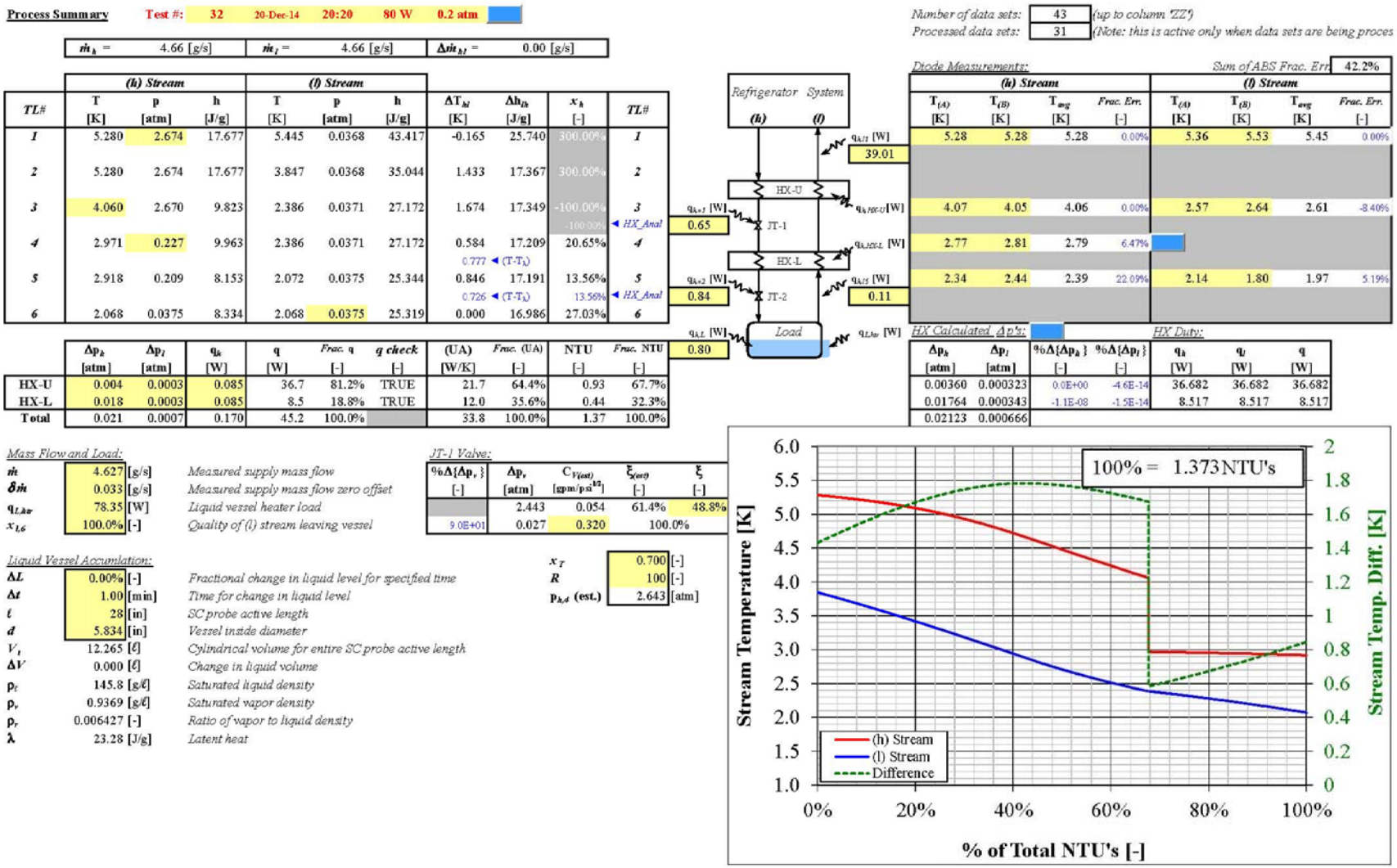

Figure Q.32. Process model output, test #32: 80 W 0.2 atm 20-Dec-14 20:20

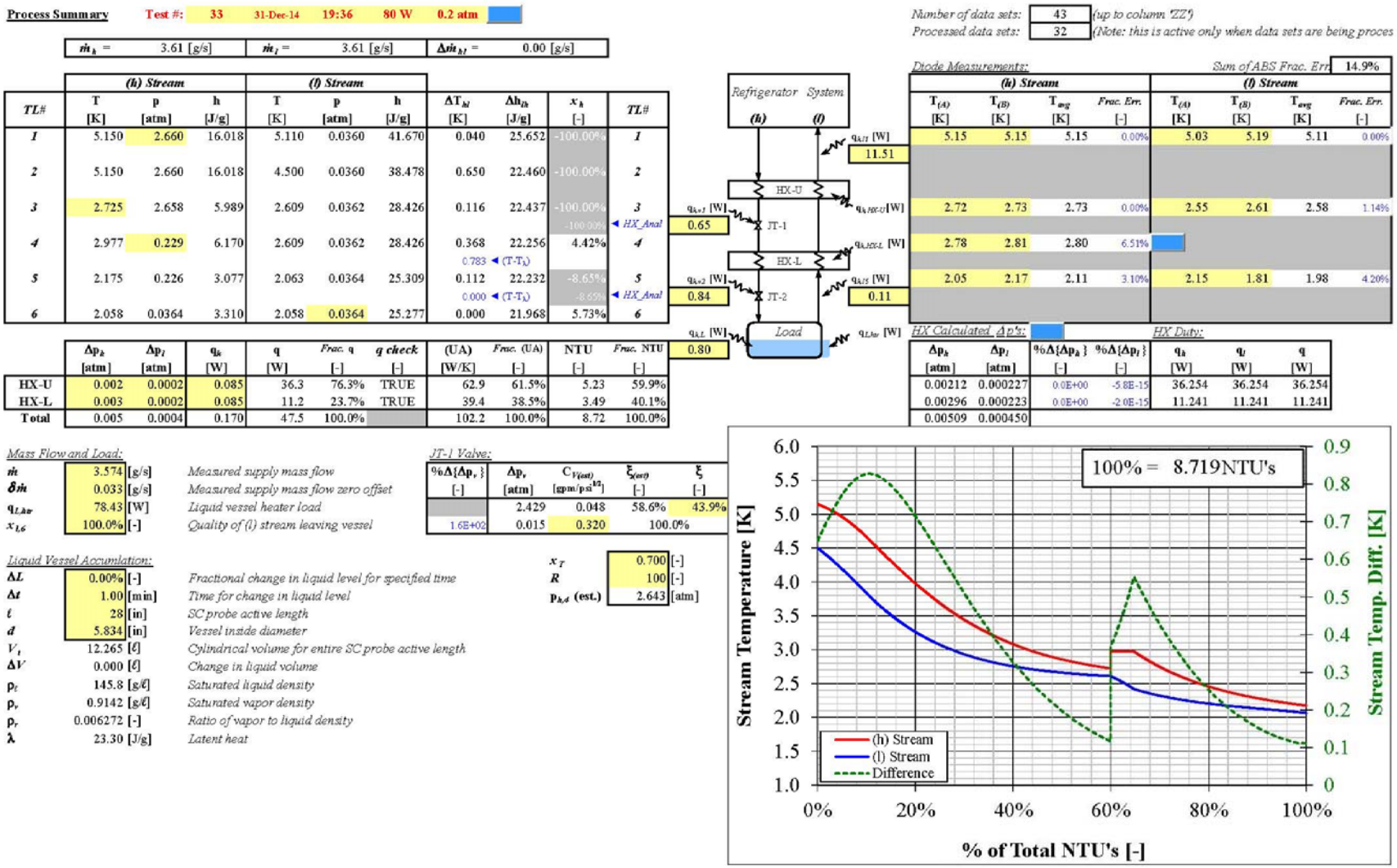

Figure Q.33. Process model output, test #33: 80 W 0.2 atm 31-Dec-14 19:36

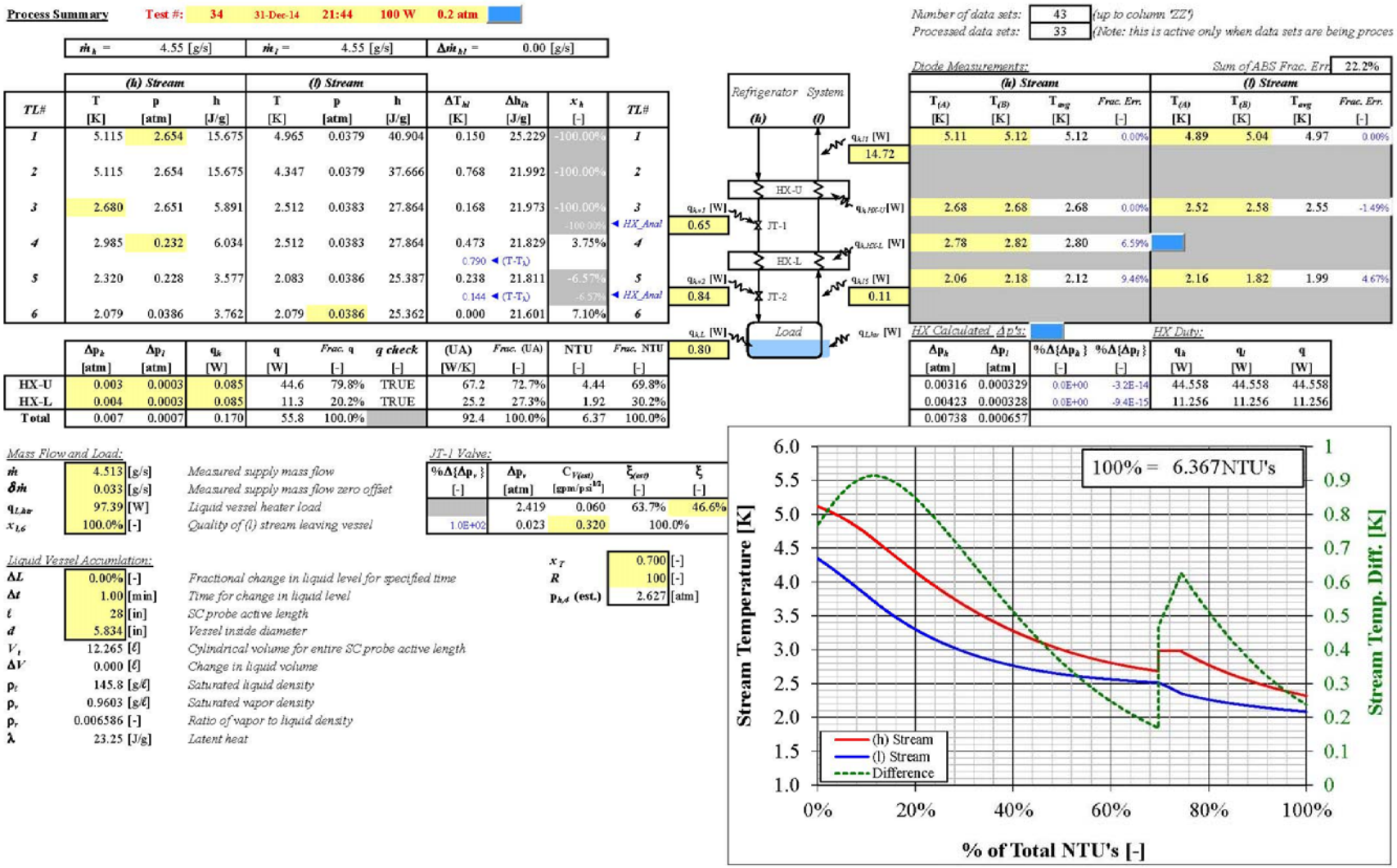

Figure Q.34. Process model output, test #34: 100 W 0.2 atm 31-Dec-14 21:44

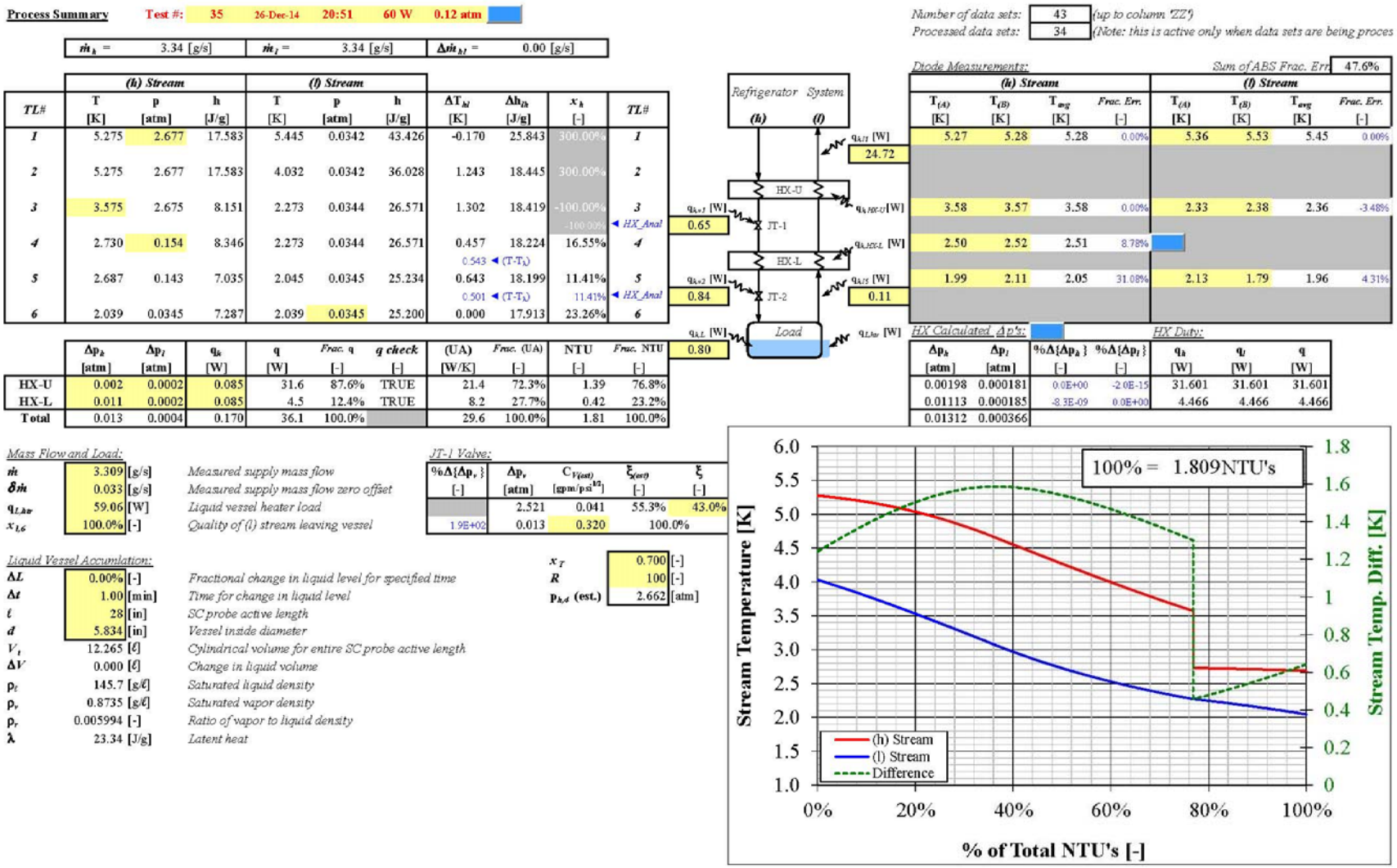

Figure Q.35. Process model output, test #35: 60 W 0.12 atm 26-Dec-14 20:51

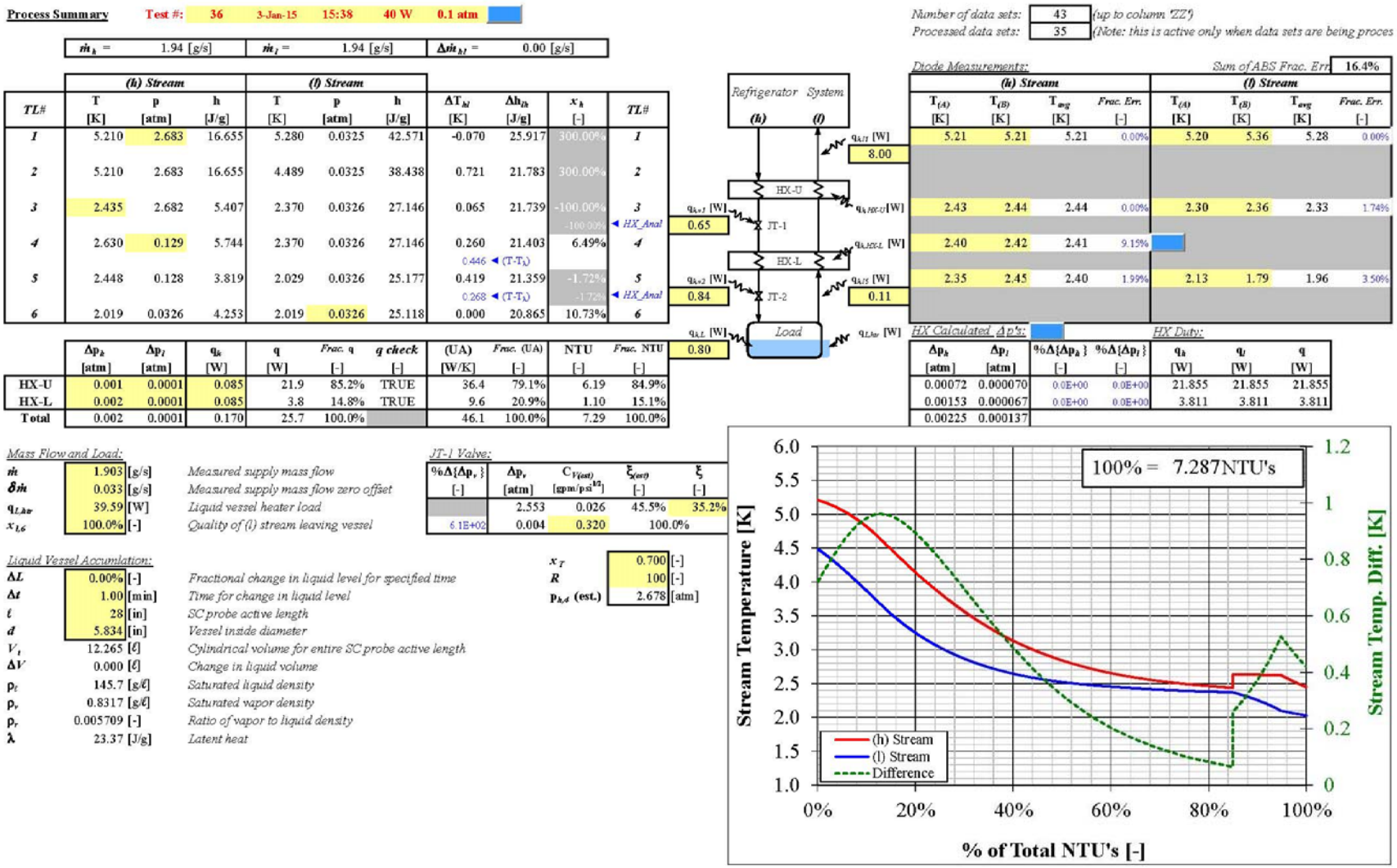

Figure Q.36. Process model output, test #36: 40 W 0.1 atm 03-Jan-15 15:38

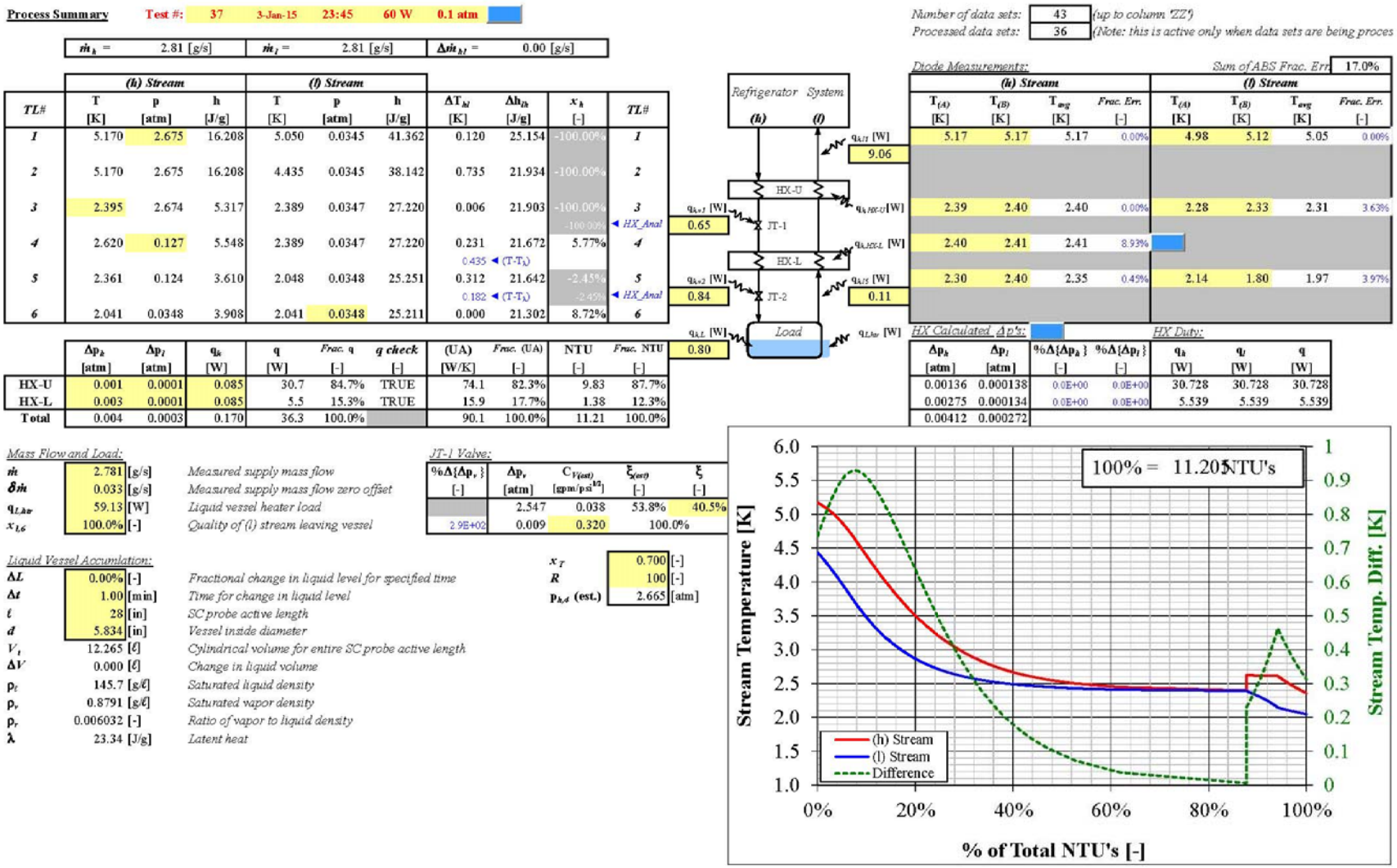

Figure Q.37. Process model output, test #37: 60 W 0.1 atm 03-Jan-15 23:45

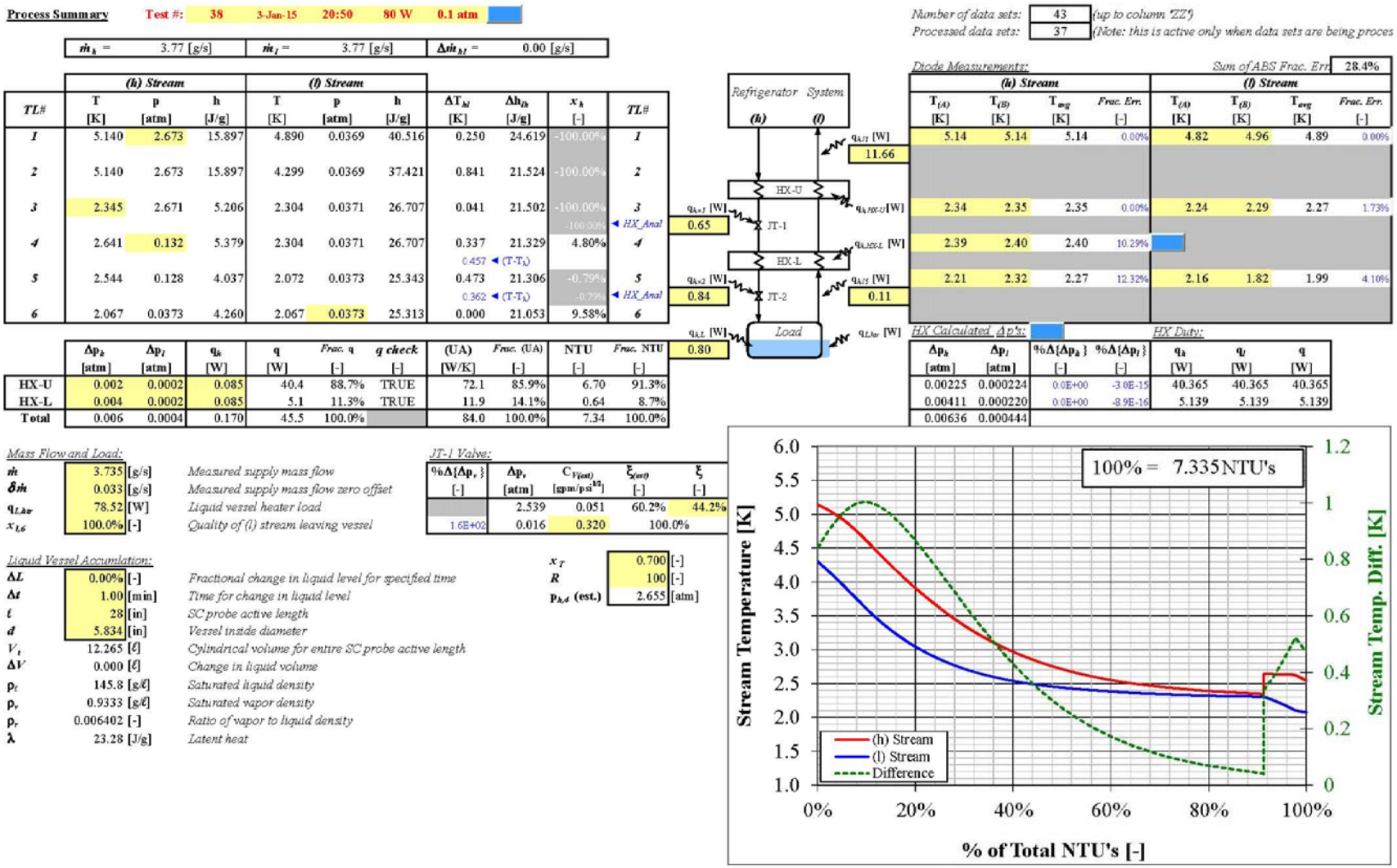

Figure Q.38. Process model output, test #38: 80 W 0.1 atm 03-Jan-15 20:50

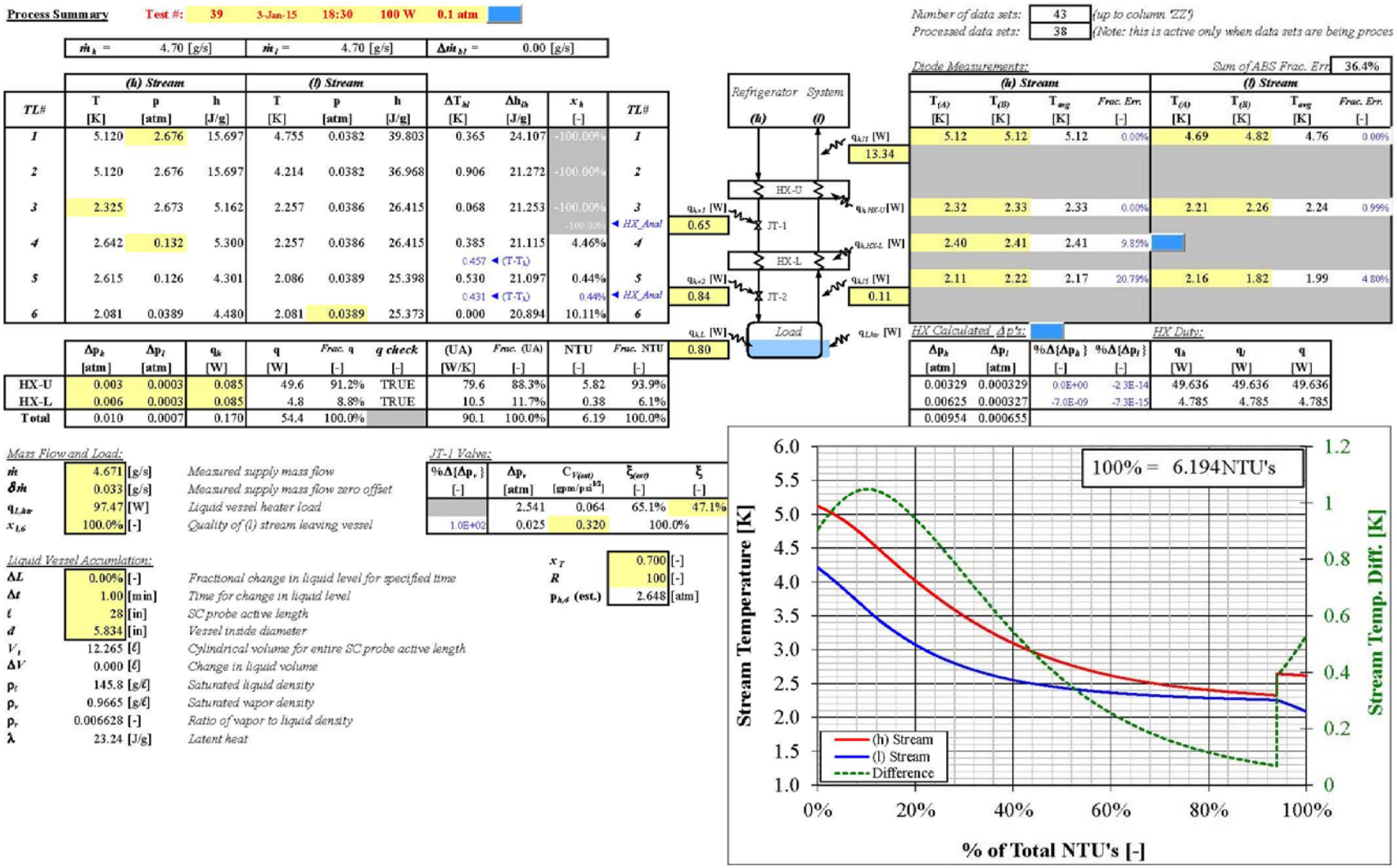

Figure Q.39. Process model output, test #39: 100 W 0.1 03-Jan-15 18:30

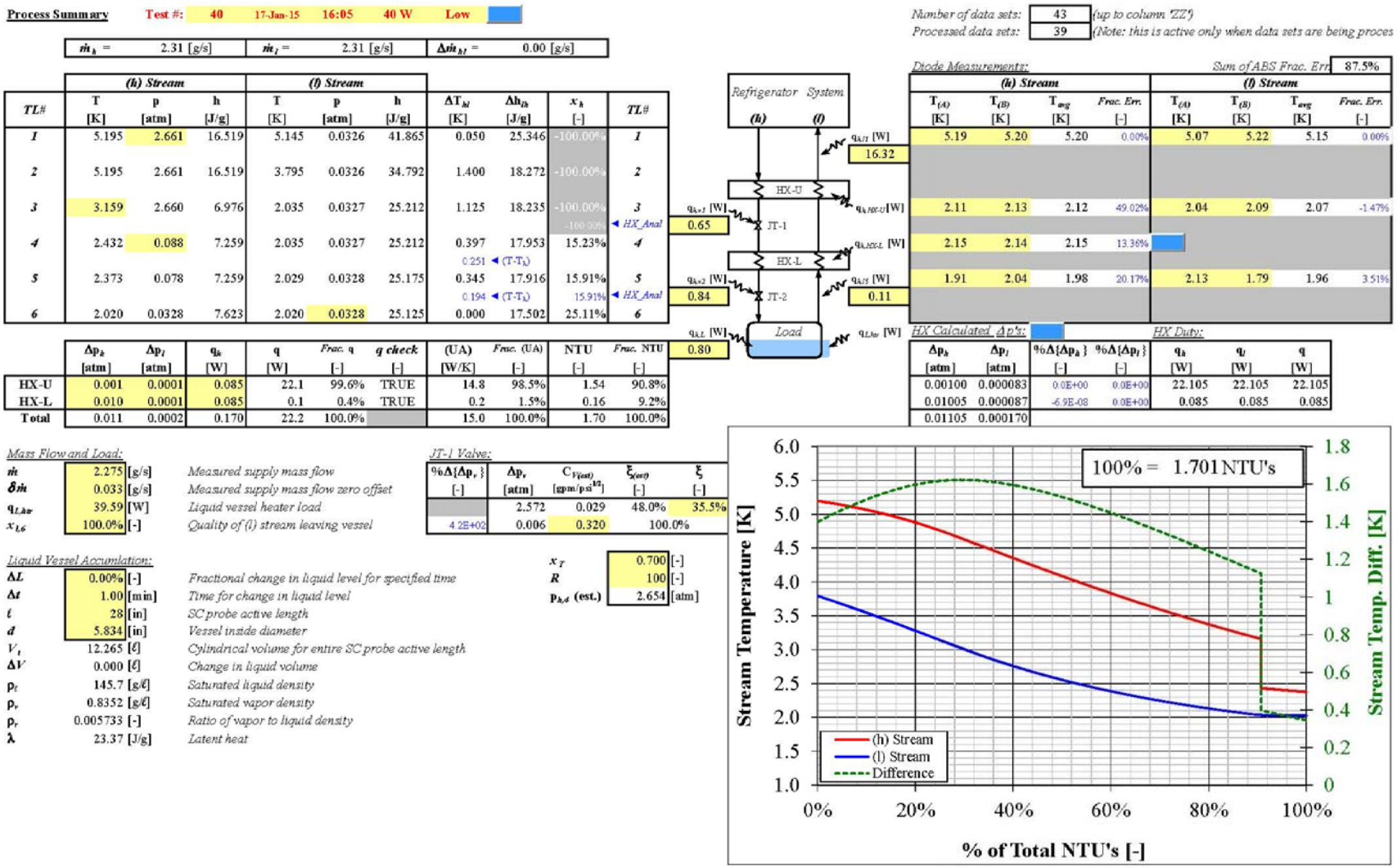

Figure Q.40. Process model output, test #40: 40 W Low 17-Jan-15 16:05

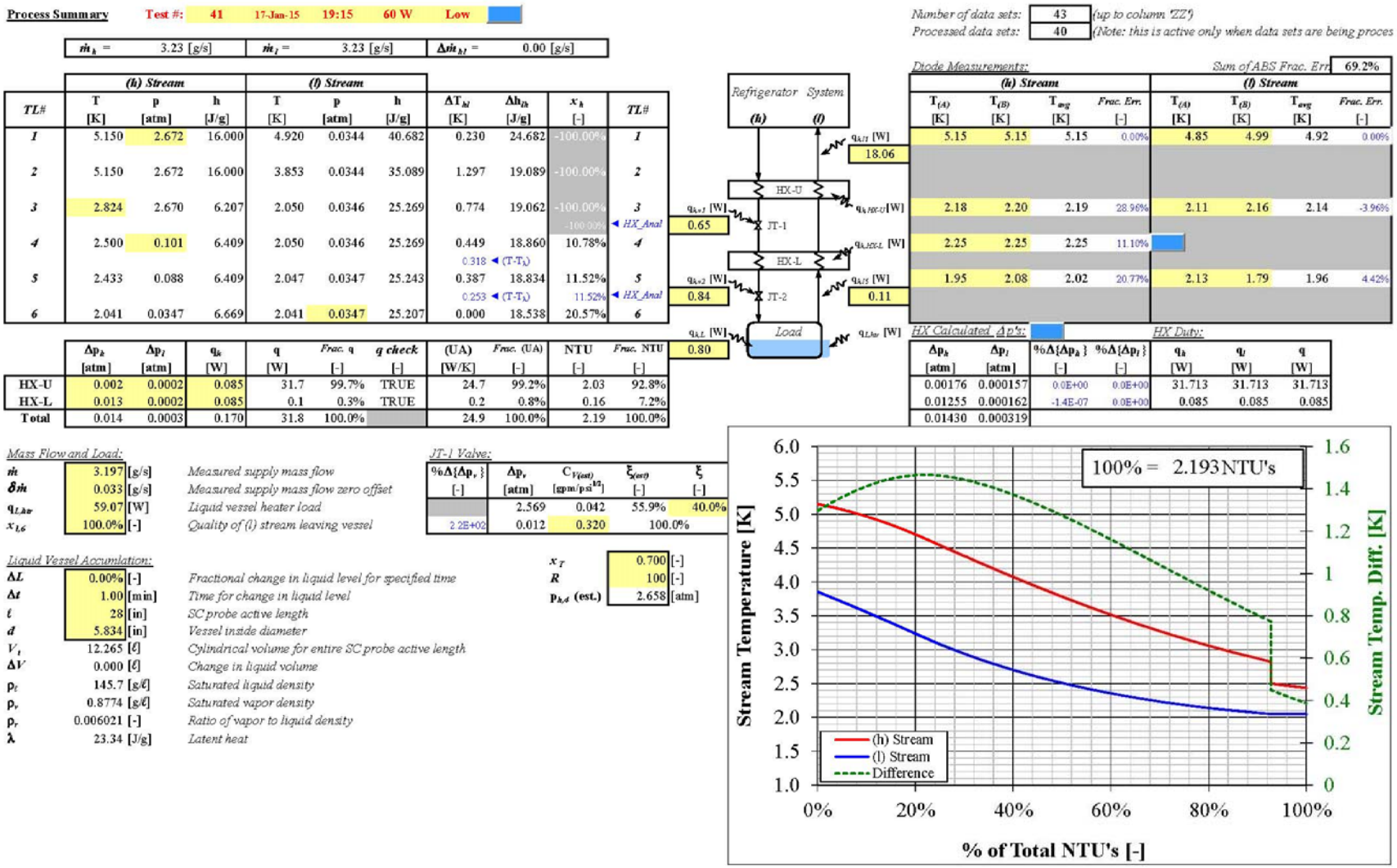

Figure Q.41. Process model output, test #41: 60 W Low 17-Jan-15 19:15

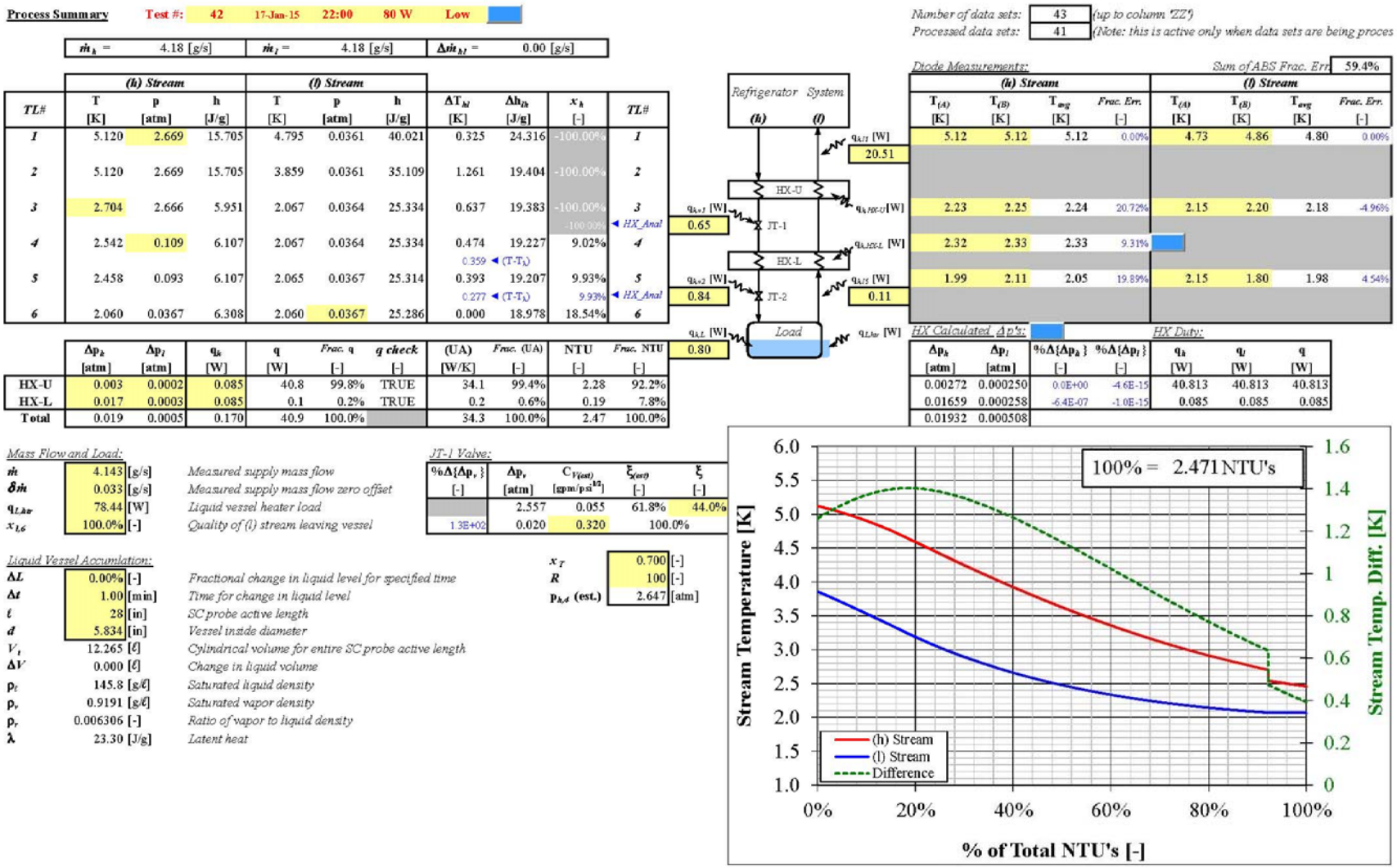

Figure Q.42. Process model output, test #42: 80 W Low 17-Jan-15 22:00

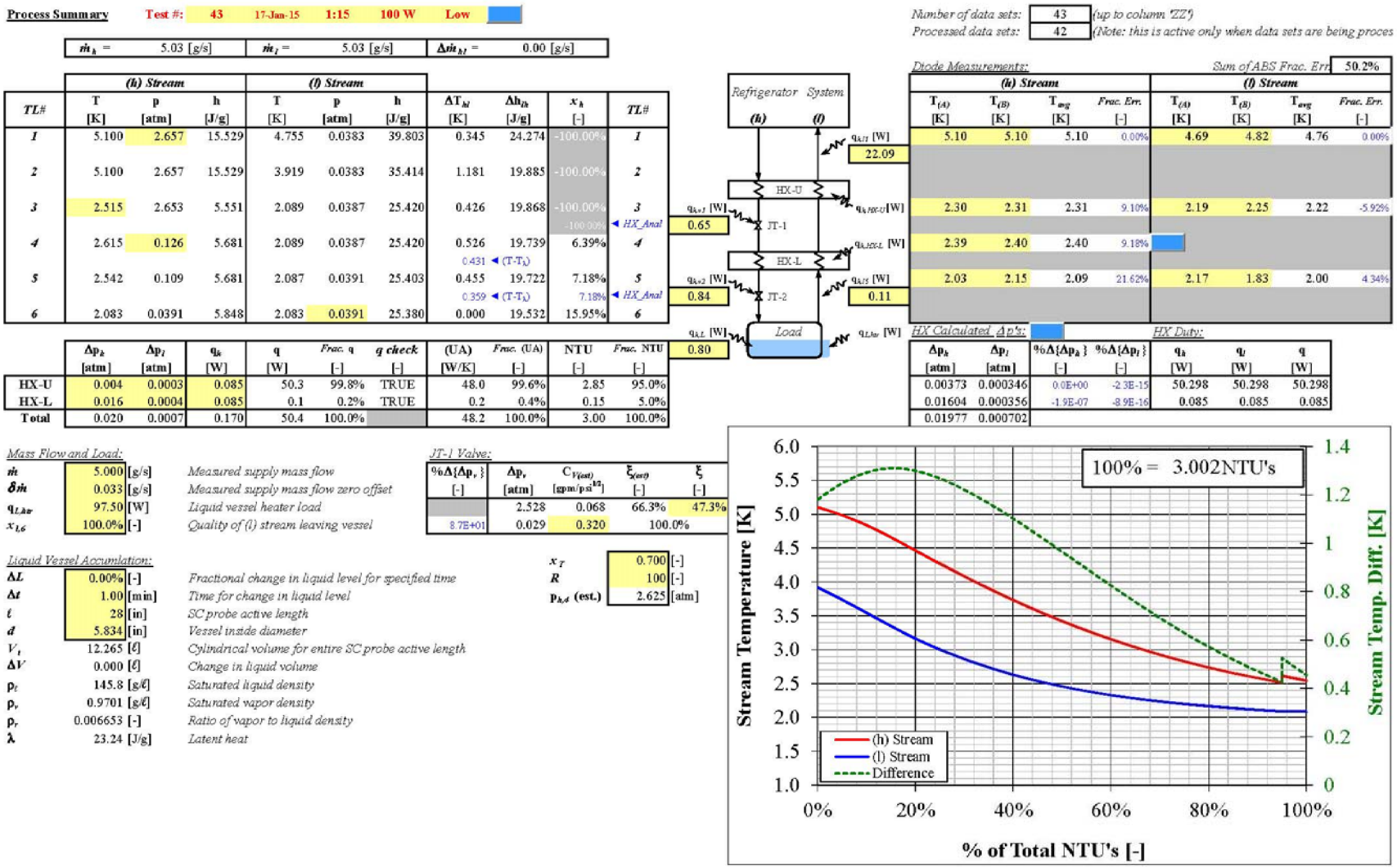

Figure Q.43. Process model output, test #43: 100 W Low 17-Jan-15 01:15

APPENDIX R – DATA COMPARISON OF SELECTED LOW PERFORMING TESTS

The following table compares the process model output for a low performing test (i.e., #'s 3, 4, 6, 11, 22, 29, 30, 32, and 35) to a corresponding better performing test (i.e., #'s 5, 5, 7, 12, 19, 31, 31, 33, and 37, respectively). This is discussed in Chapter 4. Note that, for example, "22:19" means the ratio of test #22 to test #19. Variable nomenclature follows process model output (see Appendix Q) and described in Chapter 3.

Table R.1. Data comparison of selected low performing tests

Test Point #			3	5	3 : 5	4	5	4 : 5
Date			27-Dec-14	29-Dec-14		29-Dec-14	29-Dec-14	
Snap-Shot Time			1:01	17:22		10:28	17:22	
Nominal Heat			60 W	60 W		60 W	60 W	
Nom. Int. Pressure			2.7 atm	2.7 atm		2.7 atm	2.7 atm	
$\dot{m}$	[g/s]	Measured	3.363	3.037	10.7%	3.288	3.037	8.3%
$T_{h,1}$	[K]	Measured (Avg.)	5.290	5.160	2.5%	5.290	5.160	2.5%
$T_{l,1\ (meas)}$	[K]	Measured (Avg.)	5.455	4.910	11.1%	5.465	4.910	11.3%
$T_{h,3}$	[K]	Calculated	5.289	2.351	124.9%	5.289	2.351	124.9%
$T_{h,3\ (meas)}$	[K]	Measured (Avg.)	5.320	2.170	145.2%	5.330	2.170	145.6%
$T_{l,3}$	[K]	Calculated	4.033	2.052	96.6%	4.100	2.052	99.9%
$T_{l,3\ (meas)}$	[K]	Measured (Avg.)	5.310	2.110	151.7%	5.325	2.110	152.4%
$T_{h,4}$	[K]	Calculated	5.294	2.454	115.8%	5.295	2.454	115.8%
$T_{h,4\ (meas)}$	[K]	Measured (Avg.)	5.430	2.375	128.6%	5.440	2.375	129.1%
$T_{h,5}$	[K]	Calculated	3.295	2.453	34.3%	3.141	2.453	28.0%
$T_{h,5\ (meas)}$	[K]	Measured (Avg.)	2.845	2.045	39.1%	2.940	2.045	43.8%
$T_{l,5}$	[K]	Calculated	2.043	2.047	-0.2%	2.046	2.047	0.0%
$T_{l,5\ (meas)}$	[K]	Measured (Avg.)	1.970	1.965	0.3%	1.965	1.965	0.0%
$\Delta T_{hl,2}$	[K]	Calculated	1.253	1.099	13.9%	1.185	1.099	7.8%
$\Delta T_{hl,3}$	[K]	Calculated	1.256	0.300	318.9%	1.189	0.300	296.4%
$\Delta T_{hl,4}$	[K]	Calculated	1.261	0.402	213.7%	1.195	0.402	197.2%
$\Delta T_{hl,5}$	[K]	Calculated	1.252	0.406	208.2%	1.095	0.406	169.5%
$p_{h,1}$	[atm]	Measured	2.661	2.676	-0.6%	2.674	2.676	-0.1%
$p_{h,4}$	[atm]	Measured	2.639	2.664	-0.9%	2.653	2.664	-0.4%
$p_{l,6}$	[atm]	Measured	0.0344	0.0348	-0.9%	0.0347	0.0348	-0.1%
$\Delta p_{l,HX\text{-}U}$	[in. H_2O]	Calculated	0.099	0.060	66.4%	0.096	0.060	60.4%
$\Delta p_{l,HX\text{-}L}$	[in. H_2O]	Calculated	0.113	0.060	89.4%	0.108	0.060	81.7%
$\Delta p_{l,HX\ (calc)}$	[in. H_2O]	Calculated	0.212	0.119	77.9%	0.204	0.119	71.0%
$\Delta p_{l,HX}$	[in. H_2O]	Measured	0.261	0.075	248.0%	0.244	0.075	225.3%
$x_{h,4}$	[-]	Calculated	300.0%	-100.0%		300.0%	-100.0%	
$x_{h,5}$	[-]	Calculated	-100.0%	-100.0%		-100.0%	-100.0%	
$\Delta h_{lh,6}$	[J/g]	Calculated	17.63	19.50	-9.6%	18.03	19.50	-7.6%
$q_{L,htr}$	[W]	Measured	59.06	59.06	0.0%	59.06	59.06	0.0%
$q_{HX\text{-}U}$	[W]	Calculated	0.09	33.47	-99.7%	0.09	33.47	-99.7%
$q_{HX\text{-}L}$	[W]	Calculated	36.69	0.09	41353.7%	37.01	0.09	41713.6%
$q_{HX,tot}$	[W]	Calculated	36.78	33.56	9.6%	37.10	33.56	10.5%
$(UA)_{HX\text{-}U}$	[W/K]	Calculated	0.1	34.7	-99.8%	0.1	34.7	-99.8%
$(UA)_{HX\text{-}L}$	[W/K]	Calculated	23.9	0.2	10821.3%	25.6	0.2	11592.7%
$(UA)_{HX,tot}$	[W/K]	Calculated	24.0	34.9	-31.3%	25.7	34.9	-26.5%
$NTU_{HX\text{-}U}$	[-]	Calculated	0.004	3.507	-99.9%	0.004	3.507	-99.9%
$NTU_{HX\text{-}L}$	[-]	Calculated	1.591	0.011	14753.1%	1.802	0.011	16718.6%
$NTU_{HX,tot}$	[-]	Calculated	1.595	3.518	-54.7%	1.806	3.518	-48.7%

Table R.1. Continued

Test Point #			6	7	6 : 7	11	12	11 : 12
Date			20-Dec-14	29-Dec-14		27-Dec-14	30-Dec-14	
Snap-Shot Time			14:23	19:49		22:09	19:15	
Nominal Heat			80 W	80 W		60 W	60 W	
Nom. Int. Pressure			2.7 atm	2.7 atm		1.3 atm	1.3 atm	
$\dot{m}$	[g/s]	Measured	4.517	3.943	14.6%	3.386	2.809	20.5%
$T_{h,1}$	[K]	Measured (Avg.)	5.275	5.140	2.6%	5.275	5.150	2.4%
$T_{l,1\ (meas)}$	[K]	Measured (Avg.)	5.455	4.765	14.5%	5.455	5.085	7.3%
$T_{h,3}$	[K]	Calculated	5.274	2.260	133.4%	5.210	2.525	106.3%
$T_{h,3\ (meas)}$	[K]	Measured (Avg.)	5.310	2.150	147.0%	5.210	2.525	106.3%
$T_{l,3}$	[K]	Calculated	3.916	2.067	89.4%	3.777	2.390	58.0%
$T_{l,3\ (meas)}$	[K]	Measured (Avg.)	5.250	2.085	151.8%	4.390	2.425	81.0%
$T_{h,4}$	[K]	Calculated	5.274	2.333	126.0%	4.517	2.996	50.8%
$T_{h,4\ (meas)}$	[K]	Measured (Avg.)	5.410	2.335	131.7%	4.475	3.090	44.8%
$T_{h,5}$	[K]	Calculated	3.444	2.333	47.6%	3.575	2.177	64.2%
$T_{h,5\ (meas)}$	[K]	Measured (Avg.)	2.985	2.045	46.0%	3.205	2.060	55.6%
$T_{l,5}$	[K]	Calculated	2.070	2.064	0.3%	2.043	2.047	-0.2%
$T_{l,5\ (meas)}$	[K]	Measured (Avg.)	1.970	1.970	0.0%	1.965	1.970	-0.3%
$\Delta T_{hl,2}$	[K]	Calculated	1.356	1.063	27.6%	1.316	0.796	65.4%
$\Delta T_{hl,3}$	[K]	Calculated	1.358	0.193	603.7%	1.433	0.135	965.0%
$\Delta T_{hl,4}$	[K]	Calculated	1.358	0.266	410.1%	0.740	0.606	22.1%
$\Delta T_{hl,5}$	[K]	Calculated	1.374	0.269	410.4%	1.532	0.131	1070.9%
$p_{h,1}$	[atm]	Measured	2.663	2.669	-0.2%	2.662	2.652	0.4%
$p_{h,4}$	[atm]	Measured	2.624	2.649	-0.9%	1.305	1.312	-0.6%
$p_{l,6}$	[atm]	Measured	0.0373	0.0366	1.9%	0.0344	0.0346	-0.6%
$\Delta p_{l,HX\text{-}U}$	[in. H_2O]	Calculated	0.161	0.096	67.5%	0.096	0.057	69.1%
$\Delta p_{l,HX\text{-}L}$	[in. H_2O]	Calculated	0.184	0.096	92.8%	0.109	0.056	95.1%
$\Delta p_{l,HX\ (calc)}$	[in. H_2O]	Calculated	0.345	0.192	80.2%	0.206	0.113	82.0%
$\Delta p_{l,HX}$	[in. H_2O]	Measured	0.417	0.130	220.8%	0.225	0.072	212.5%
$x_{h,4}$	[-]	Calculated	300.0%	-100.0%		27.5%	-32.2%	
$x_{h,5}$	[-]	Calculated	-100.0%	-100.0%		-22.9%	-42.6%	
$\Delta h_{lh,6}$	[J/g]	Calculated	17.40	19.91	-12.6%	17.49	21.07	-17.0%
$q_{L,htr}$	[W]	Measured	78.35	78.35	0.0%	58.98	59.06	-0.1%
$q_{HX\text{-}U}$	[W]	Calculated	0.09	43.42	-99.8%	3.28	29.81	-89.0%
$q_{HX\text{-}L}$	[W]	Calculated	45.81	0.09	49944.5%	32.34	5.65	472.6%
$q_{HX,tot}$	[W]	Calculated	45.90	43.51	5.5%	35.62	35.45	0.5%
$(UA)_{HX\text{-}U}$	[W/K]	Calculated	0.1	51.4	-99.9%	2.4	44.0	-94.6%
$(UA)_{HX\text{-}L}$	[W/K]	Calculated	28.5	0.3	8236.1%	24.0	20.0	19.9%
$(UA)_{HX,tot}$	[W/K]	Calculated	28.6	51.7	-44.8%	26.3	64.0	-58.8%
$NTU_{HX\text{-}U}$	[-]	Calculated	0.002	4.184	-99.9%	0.132	4.856	-97.3%
$NTU_{HX\text{-}L}$	[-]	Calculated	1.382	0.012	11896.3%	1.413	2.736	-48.4%
$NTU_{HX,tot}$	[-]	Calculated	1.384	4.196	-67.0%	1.545	7.593	-79.6%

Table R.1. Continued

Test Point #			22	19	22 : 19	29	31	29 : 31
Date			26-Dec-14	1-Jan-15		23-Dec-14	31-Dec-14	
Snap-Shot Time			13:43	17:03		20:05	17:25	
Nominal Heat			60 W	60 W		60 W	60 W	
Nom. Int. Pressure			0.4 atm	0.5 atm		0.2 atm	0.2 atm	
$\dot{m}$	[g/s]	Measured	3.305	2.757	19.9%	3.371	2.716	24.1%
$T_{h,1}$	[K]	Measured (Avg.)	5.260	5.160	1.9%	5.265	5.155	2.1%
$T_{l,1\ (meas)}$	[K]	Measured (Avg.)	5.440	5.245	3.7%	5.440	5.200	4.6%
$T_{h,3}$	[K]	Calculated	4.630	2.900	59.7%	4.080	2.790	46.2%
$T_{h,3\ (meas)}$	[K]	Measured (Avg.)	4.630	2.900	59.7%	4.080	2.790	46.2%
$T_{l,3}$	[K]	Calculated	3.044	2.606	16.8%	2.522	2.623	-3.9%
$T_{l,3\ (meas)}$	[K]	Measured (Avg.)	3.195	2.700	18.3%	2.655	2.620	1.3%
$T_{h,4}$	[K]	Calculated	3.434	3.426	0.2%	2.985	2.983	0.0%
$T_{h,4\ (meas)}$	[K]	Measured (Avg.)	3.295	3.520	-6.4%	2.790	2.800	-0.4%
$T_{h,5}$	[K]	Calculated	3.425	2.205	55.3%	2.959	2.180	35.7%
$T_{h,5\ (meas)}$	[K]	Measured (Avg.)	3.280	2.070	58.5%	2.660	2.100	26.7%
$T_{l,5}$	[K]	Calculated	2.045	2.045	0.0%	2.040	2.046	-0.3%
$T_{l,5\ (meas)}$	[K]	Measured (Avg.)	1.965	1.970	-0.3%	1.945	1.970	-1.3%
$\Delta T_{hl,2}$	[K]	Calculated	1.250	0.709	76.3%	1.303	0.653	99.5%
$\Delta T_{hl,3}$	[K]	Calculated	1.586	0.294	438.8%	1.558	0.167	834.5%
$\Delta T_{hl,4}$	[K]	Calculated	0.390	0.820	-52.5%	0.463	0.360	28.4%
$\Delta T_{hl,5}$	[K]	Calculated	1.380	0.160	763.9%	0.919	0.135	582.6%
$p_{h,1}$	[atm]	Measured	2.648	2.655	-0.3%	2.641	2.661	-0.8%
$p_{h,4}$	[atm]	Measured	0.428	0.541	-20.8%	0.232	0.232	0.2%
$p_{l,6}$	[atm]	Measured	0.0346	0.0345	0.3%	0.0342	0.0345	-1.1%
$\Delta p_{l,HX\text{-}U}$	[in. H_2O]	Calculated	0.083	0.058	43.4%	0.080	0.057	41.2%
$\Delta p_{l,HX\text{-}L}$	[in. H_2O]	Calculated	0.090	0.057	57.5%	0.084	0.056	51.4%
$\Delta p_{l,HX\ (calc)}$	[in. H_2O]	Calculated	0.173	0.115	50.4%	0.164	0.112	46.3%
$\Delta p_{l,HX}$	[in. H_2O]	Measured	0.204	0.084	142.9%	0.174	0.078	123.1%
$x_{h,4}$	[-]	Calculated	25.7%	-3.1%		21.0%	5.2%	
$x_{h,5}$	[-]	Calculated	2.1%	-16.8%		9.7%	-8.6%	
$\Delta h_{lh,6}$	[J/g]	Calculated	17.93	21.46	-16.4%	17.59	21.78	-19.3%
$q_{L,htr}$	[W]	Measured	59.06	59.06	0.0%	59.06	59.06	0.0%
$q_{HX\text{-}U}$	[W]	Calculated	17.07	27.34	-37.6%	26.19	27.41	-4.5%
$q_{HX\text{-}L}$	[W]	Calculated	18.57	8.89	108.8%	9.37	9.02	3.9%
$q_{HX,tot}$	[W]	Calculated	35.64	36.23	-1.6%	35.56	36.43	-2.4%
$(UA)_{HX\text{-}U}$	[W/K]	Calculated	11.6	38.0	-69.4%	16.8	44.4	-62.1%
$(UA)_{HX\text{-}L}$	[W/K]	Calculated	23.4	21.6	8.7%	14.0	27.8	-49.5%
$(UA)_{HX,tot}$	[W/K]	Calculated	35.1	59.6	-41.1%	30.8	72.2	-57.3%
$NTU_{HX\text{-}U}$	[-]	Calculated	0.659	3.673	-82.1%	0.984	4.643	-78.8%
$NTU_{HX\text{-}L}$	[-]	Calculated	1.273	2.976	-57.2%	0.723	3.214	-77.5%
$NTU_{HX,tot}$	[-]	Calculated	1.932	6.650	-71.0%	1.707	7.857	-78.3%

Table R.1. Continued

Test Point #			30	31	30 : 31	32	33	32 : 33
Date			26-Dec-14	31-Dec-14		20-Dec-14	31-Dec-14	
Snap-Shot Time			17:20	17:25		20:20	19:36	
Nominal Heat			60 W	60 W		80 W	80 W	
Nom. Int. Pressure			0.2 atm	0.2 atm		0.2 atm	0.2 atm	
$\dot{m}$	[g/s]	Measured	3.304	2.716	21.6%	4.627	3.574	29.5%
$T_{h,1}$	[K]	Measured (Avg.)	5.255	5.155	1.9%	5.280	5.150	2.5%
$T_{l,1\ (meas)}$	[K]	Measured (Avg.)	5.435	5.200	4.5%	5.445	5.110	6.6%
$T_{h,3}$	[K]	Calculated	4.005	2.790	43.5%	4.060	2.725	49.0%
$T_{h,3\ (meas)}$	[K]	Measured (Avg.)	4.005	2.790	43.5%	4.060	2.725	49.0%
$T_{l,3}$	[K]	Calculated	2.537	2.623	-3.3%	2.386	2.609	-8.6%
$T_{l,3\ (meas)}$	[K]	Measured (Avg.)	2.660	2.620	1.5%	2.605	2.580	1.0%
$T_{h,4}$	[K]	Calculated	2.968	2.983	-0.5%	2.971	2.977	-0.2%
$T_{h,4\ (meas)}$	[K]	Measured (Avg.)	2.780	2.800	-0.7%	2.790	2.795	-0.2%
$T_{h,5}$	[K]	Calculated	2.944	2.180	35.0%	2.918	2.175	34.1%
$T_{h,5\ (meas)}$	[K]	Measured (Avg.)	2.655	2.100	26.4%	2.390	2.110	13.3%
$T_{l,5}$	[K]	Calculated	2.042	2.046	-0.2%	2.072	2.063	0.4%
$T_{l,5\ (meas)}$	[K]	Measured (Avg.)	1.955	1.970	-0.8%	1.970	1.980	-0.5%
$\Delta T_{hl,2}$	[K]	Calculated	1.262	0.653	93.2%	1.433	0.650	120.5%
$\Delta T_{hl,3}$	[K]	Calculated	1.468	0.167	780.5%	1.674	0.116	1346.9%
$\Delta T_{hl,4}$	[K]	Calculated	0.431	0.360	19.5%	0.584	0.368	59.0%
$\Delta T_{hl,5}$	[K]	Calculated	0.901	0.135	569.9%	0.846	0.112	653.2%
$p_{h,1}$	[atm]	Measured	2.652	2.661	-0.3%	2.674	2.660	0.5%
$p_{h,4}$	[atm]	Measured	0.226	0.232	-2.4%	0.227	0.229	-1.0%
$p_{l,6}$	[atm]	Measured	0.0343	0.0345	-0.7%	0.0375	0.0364	2.9%
$\Delta p_{l,HX\text{-}U}$	[in. H_2O]	Calculated	0.077	0.057	36.0%	0.131	0.093	42.1%
$\Delta p_{l,HX\text{-}L}$	[in. H_2O]	Calculated	0.081	0.056	45.4%	0.140	0.091	54.1%
$\Delta p_{l,HX\ (calc)}$	[in. H_2O]	Calculated	0.158	0.112	40.7%	0.271	0.183	48.0%
$\Delta p_{l,HX}$	[in. H_2O]	Measured	0.179	0.078	129.5%	0.307	0.156	96.8%
$x_{h,4}$	[-]	Calculated	20.0%	5.2%		20.6%	4.4%	
$x_{h,5}$	[-]	Calculated	8.3%	-8.6%		13.6%	-8.6%	
$\Delta h_{lh,6}$	[J/g]	Calculated	17.94	21.78	-17.6%	16.99	21.97	-22.7%
$q_{L,htr}$	[W]	Measured	59.06	59.06	0.0%	78.35	78.43	-0.1%
$q_{HX\text{-}U}$	[W]	Calculated	25.94	27.41	-5.4%	36.68	36.25	1.2%
$q_{HX\text{-}L}$	[W]	Calculated	9.44	9.02	4.6%	8.52	11.24	-24.2%
$q_{HX,tot}$	[W]	Calculated	35.38	36.43	-2.9%	45.20	47.49	-4.8%
$(UA)_{HX\text{-}U}$	[W/K]	Calculated	17.3	44.4	-61.0%	21.7	62.9	-65.4%
$(UA)_{HX\text{-}L}$	[W/K]	Calculated	14.7	27.8	-47.0%	12.0	39.3	-69.5%
$(UA)_{HX,tot}$	[W/K]	Calculated	32.1	72.2	-55.6%	33.7	102.2	-67.0%
$NTU_{HX\text{-}U}$	[-]	Calculated	1.050	4.643	-77.4%	0.930	5.225	-82.2%
$NTU_{HX\text{-}L}$	[-]	Calculated	0.775	3.214	-75.9%	0.443	3.490	-87.3%
$NTU_{HX,tot}$	[-]	Calculated	1.824	7.857	-76.8%	1.373	8.715	-84.3%

Table R.1. Continued

Test Point #			35	37	35 : 37
Date			26-Dec-14	3-Jan-15	
Snap-Shot Time			20:51	23:45	
Nominal Heat			60 W	60 W	
Nom. Int. Pressure			0.12 atm	0.1 atm	
$\dot{m}$	[g/s]	Measured	3.309	2.781	19.0%
$T_{h,1}$	[K]	Measured (Avg.)	5.275	5.170	2.0%
$T_{l,1\ (meas)}$	[K]	Measured (Avg.)	5.445	5.050	7.8%
$T_{h,3}$	[K]	Calculated	3.575	2.395	49.3%
$T_{h,3\ (meas)}$	[K]	Measured (Avg.)	3.575	2.395	49.3%
$T_{l,3}$	[K]	Calculated	2.273	2.389	-4.8%
$T_{l,3\ (meas)}$	[K]	Measured (Avg.)	2.355	2.305	2.2%
$T_{h,4}$	[K]	Calculated	2.730	2.620	4.2%
$T_{h,4\ (meas)}$	[K]	Measured (Avg.)	2.510	2.405	4.4%
$T_{h,5}$	[K]	Calculated	2.687	2.361	13.8%
$T_{h,5\ (meas)}$	[K]	Measured (Avg.)	2.050	2.350	-12.8%
$T_{l,5}$	[K]	Calculated	2.045	2.048	-0.2%
$T_{l,5\ (meas)}$	[K]	Measured (Avg.)	1.960	1.970	-0.5%
$\Delta T_{hl,2}$	[K]	Calculated	1.243	0.735	69.1%
$\Delta T_{hl,3}$	[K]	Calculated	1.302	0.006	20713.3%
$\Delta T_{hl,4}$	[K]	Calculated	0.457	0.231	98.0%
$\Delta T_{hl,5}$	[K]	Calculated	0.643	0.312	105.8%
$p_{h,1}$	[atm]	Measured	2.677	2.675	0.1%
$p_{h,4}$	[atm]	Measured	0.154	0.127	21.6%
$p_{l,6}$	[atm]	Measured	0.0345	0.0348	-0.7%
$\Delta p_{l,HX\text{-}U}$	[in. H_2O]	Calculated	0.074	0.056	31.2%
$\Delta p_{l,HX\text{-}L}$	[in. H_2O]	Calculated	0.075	0.055	38.0%
$\Delta p_{l,HX\ (calc)}$	[in. H_2O]	Calculated	0.149	0.111	34.6%
$\Delta p_{l,HX}$	[in. H_2O]	Measured	0.166	0.070	137.1%
$x_{h,4}$	[-]	Calculated	16.5%	5.8%	
$x_{h,5}$	[-]	Calculated	11.4%	-2.5%	
$\Delta h_{lh,6}$	[J/g]	Calculated	17.91	21.30	-15.9%
$q_{L,htr}$	[W]	Measured	59.06	59.13	-0.1%
$q_{HX\text{-}U}$	[W]	Calculated	31.60	30.73	2.8%
$q_{HX\text{-}L}$	[W]	Calculated	4.47	5.54	-19.4%
$q_{HX,tot}$	[W]	Calculated	36.07	36.27	-0.6%
$(UA)_{HX\text{-}U}$	[W/K]	Calculated	21.4	74.1	-71.1%
$(UA)_{HX\text{-}L}$	[W/K]	Calculated	8.2	15.9	-48.6%
$(UA)_{HX,tot}$	[W/K]	Calculated	29.6	90.0	-67.1%
$NTU_{HX\text{-}U}$	[-]	Calculated	1.389	9.830	-85.9%
$NTU_{HX\text{-}L}$	[-]	Calculated	0.418	1.374	-69.5%
$NTU_{HX,tot}$	[-]	Calculated	1.808	11.204	-83.9%

APPENDIX S – MODIFIED PROCESS MODEL PARAMETERS FOR TEST #29

This appendix contains the process model output for test #29 (60 W 0.2 atm 23-Dec-14 20:05) modified for:

(a) Filling (liquid) in the vessel

(b) Additional heat load into liquid vessel (temperature at (*h*, 3) matched)

(c) Additional heat load into liquid vessel (temperature at (*h*, 5) matched)

This is discussed in Chapter 4.

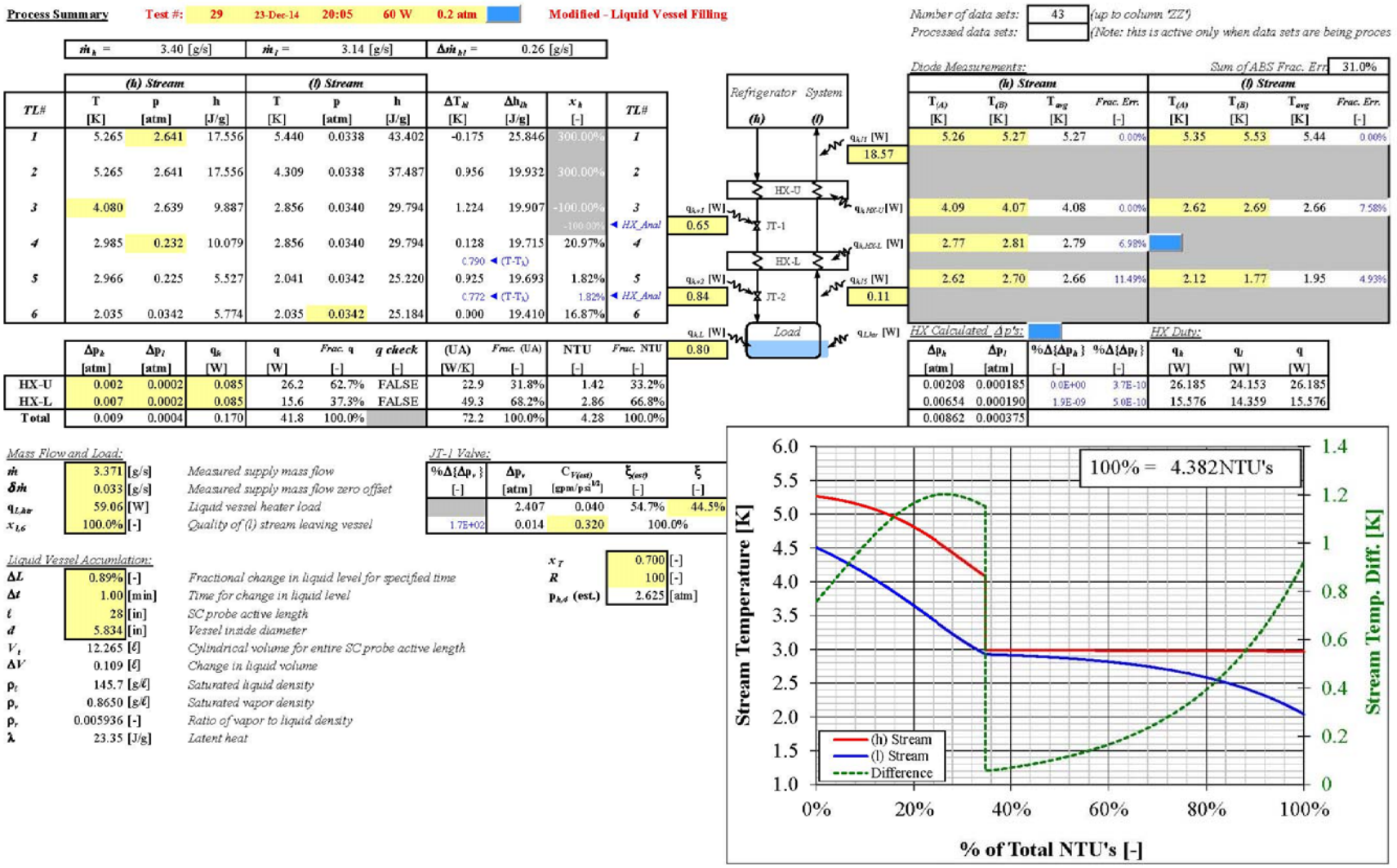

Figure S.1. Process model output, test #29 – modified for vessel filling

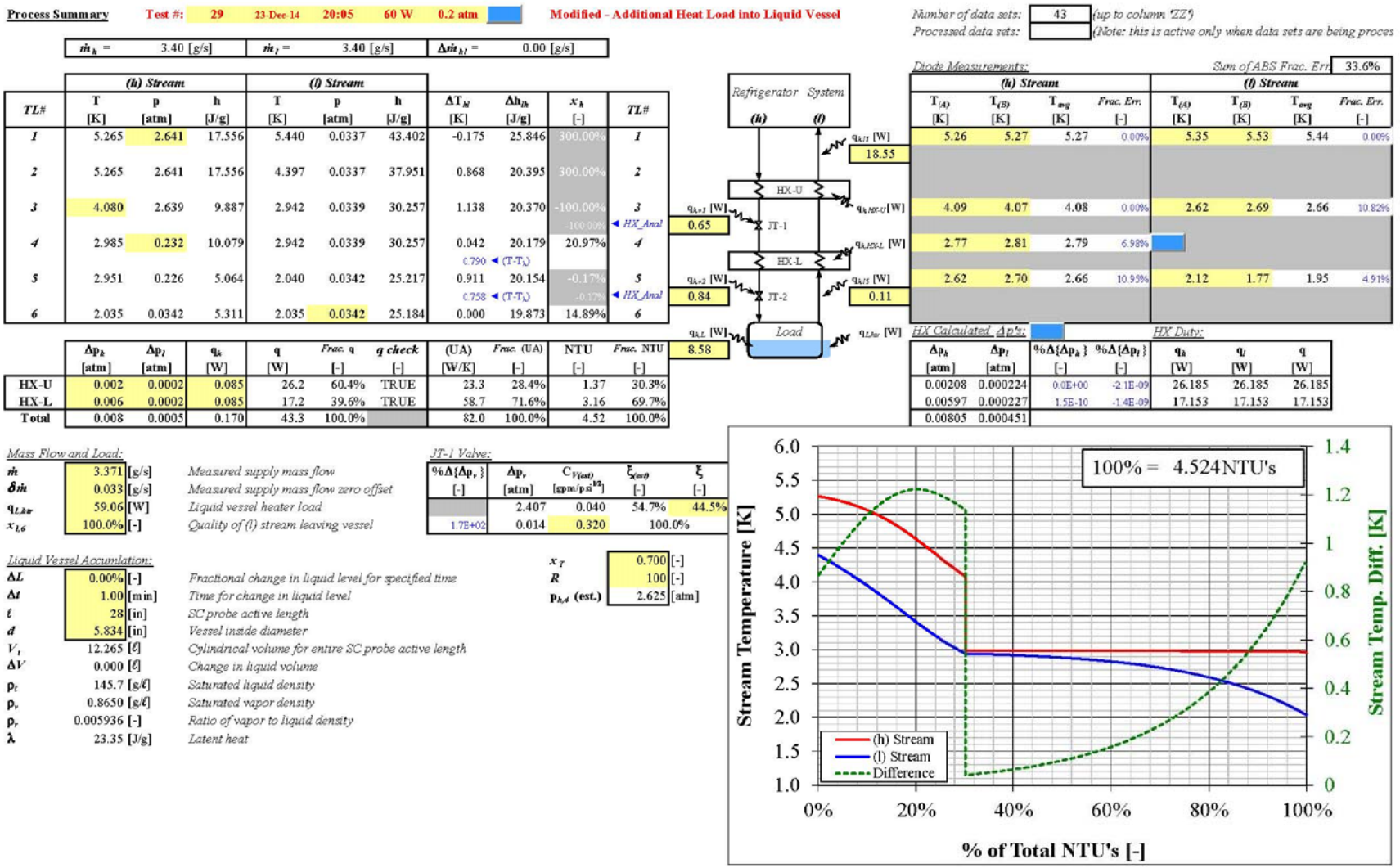

Figure S.2. Process model output, test #29 – modified for additional heat load into vessel and matching temperature (*h*, 3)

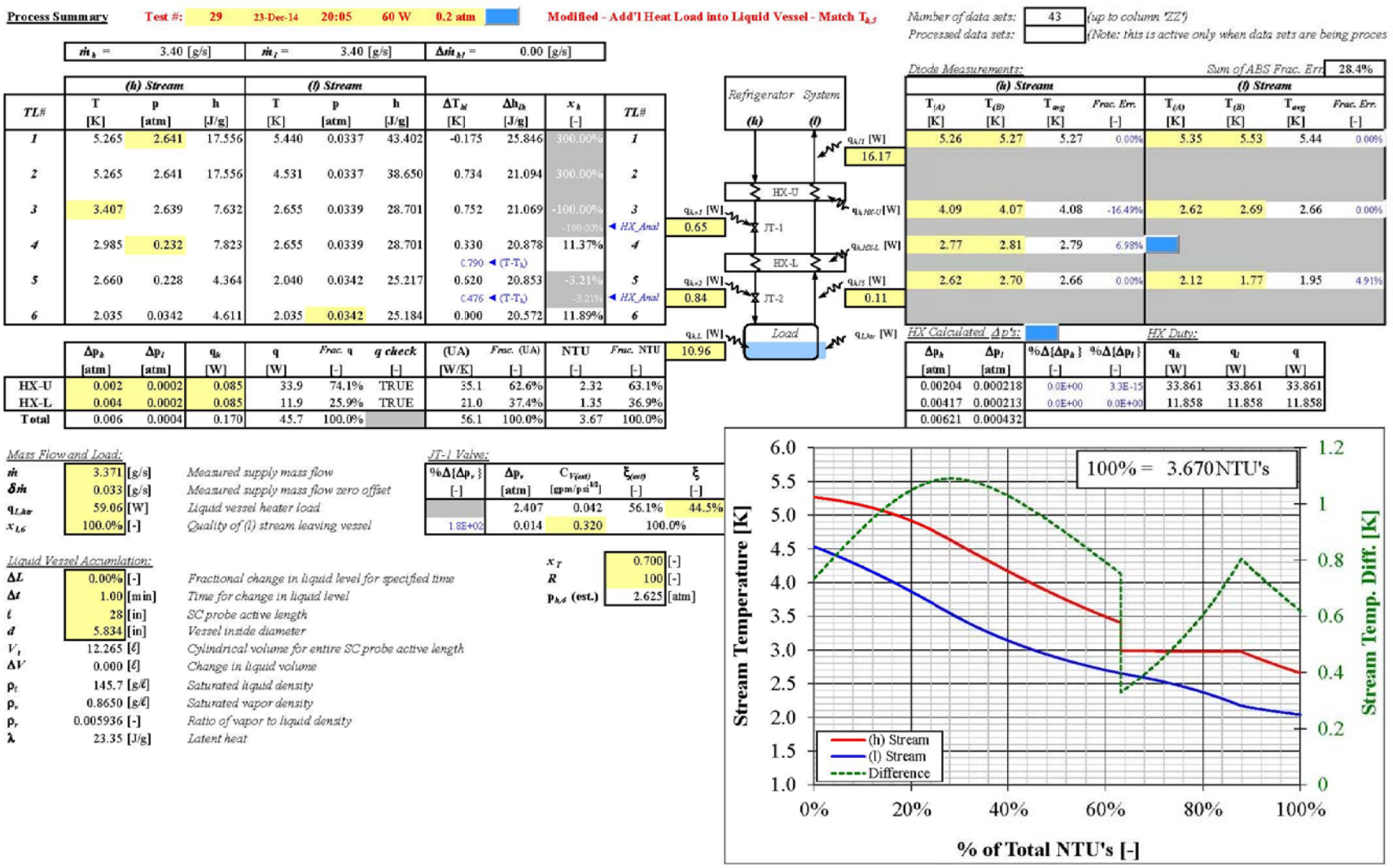

Figure S.3. Process model output, test #29 – modified for additional heat load into vessel and matching temperature (*h*,5)

VITA

PETER N. KNUDSEN
Facility for Rare Isotope Beams, Michigan State University
640 South Shaw Lane, East Lansing, Michigan 48824
Phone: (517) 908-7194, Email: knudsen@frib.msu.edu

EDUCATION:

Colorado State University, *Fort Collins, Colorado*, B.S. Mechanical Engineering, Fall 1990, Magna Cum Laude, GPA 3.84
Old Dominion University, *Norfolk, Virginia***,** M.S. Mechanical Engineering, Spring 2008, GPA 4.00
Old Dominion University, *Norfolk, Virginia***,** Ph.D Mechanical Engineering, Fall 2016, GPA 4.00

EXPERIENCE:

Mechanical Engineer, Cryogenic Systems (Present Position: Senior Cryogenic Process Engineer), *August 2016 to Present*; Employer: Facility for Rare Isotope Beams (FRIB), Michigan State University (MSU), East Lansing, Michigan

- Lead process engineer for helium refrigeration system at MSU FRIB. Lead engineer for process cycle studies, development of 4.5 K cold box specifications and the 2K cold compressor specifications and the 2-K cold box design.

Mechanical Engineer, Cryogenic Systems (Ending Position: Senior Staff Engineer), *July 2000 to August 2016*; Employer: Thomas Jefferson National Accelerator Facility (TJNAF), Newport News, Virginia

- Lead process engineer for helium refrigeration system upgrade for 12 GeV project at TJNAF. Performed process cycle studies and participated in team to develop cold box specifications.
- Process analyst for helium shield refrigerator for NASA-JSC vacuum chamber modifications for testing the James Webb Telescope. Performed process cycle studies and worked with selected vendor for review of cold box design. Participated in team performing process analysis on modifications to convert vacuum chamber forced flow nitrogen shield to thermo-siphon.
- Process analyst and lead TJNAF engineer for Brookhaven National Laboratory (BNL) refrigerator upgrade. Cooperatively with BNL, characterized existing plant performance, performed modified plant simulations, developed major component specifications and designed new cold boxes. Upgrade resulted in power reduction from 9.2 MW to less than 5 MW for the same cryogenic load.
- Lead design engineer for Spallation Neutron Source (SNS) helium cryogenic plant compressor, storage and purifier systems.

Cryogenics and Gases Systems Design Engineer (Ending Position: GS-13), *March 1993 to July 2000*, Employer: NASA at J. F. Kennedy Space Center (KSC), Florida

- Lead project design engineer and lead piping system design engineer for modifications to a facility, which provides high pressure helium supply to the STS orbiters at the launch pads
- Lead thermal cooling, vacuum, and pneumatic systems design engineer for a simulator and related ground support equipment used in support of the International Space Station.

Shuttle Fluid Systems Engineer (Ending Position: GS-11)**,** *February 1991 to March 1993,* Employer: NASA at J. F. Kennedy Space Center, Florida

AWARDS: Certificate of Appreciation presented by Johnson Space Center Director (2008); White House Closing the Circle Award for Leadership in Federal Environmental Stewardship, Cryogenic Refrigeration System Improvements, Washington DC, 2007; DOE Office of Science Pollution Prevention and Environment Stewardship P2 'Best in Class Award', 2006**;** NASA Performance Award, 1993-1994, 1995-1996, 1996-1997, 1997-1998, 1998-1999; Certificate of Appreciation presented by Kennedy Space Center Director (1998)

MEMBERSHIPS: Cryogenic Association of America, Tau Beta Pi, Phi Kappa Alpha